THE ROLLING RESISTANCE OF ARTICULATED DUMP TRUCKS ON HAUL ROADS

BY

GRAEME SCOTT WOOD (B.Eng.)

THESIS SUBMITTED TO THE UNIVERSITY OF EDINBURGH FOR THE DEGREE OF DOCTOR OF PHILOSOPHY

1994

DEPARTMENT OF CIVIL AND ENVIRONMENTAL ENGINEERING
UNIVERSITY OF EDINBURGH

Declaration

I declare that this thesis was written by me, and that the work described was carried out by myself unless otherwise acknowledged.

Abstract of Thesis

The accurate estimation of velocity of articulated dump trucks has been a problem to highway engineers for a long time. The literature published by agricultural, military, and civil engineers, on the subject of rolling resistance has been critically examined. This review indicated that no practical means has been established for predicting the performance of this type of vehicle with respect to classical soil mechanics. A two-dimensional model has been developed, based on classical soil mechanics theory, enabling the rut depth on a haul road to be estimated from the information contained in the site investigation report.

A large amout of site monitoring was undertaken on chalk and clay haul roads, the findings of which were compared with the theoretical model. The results were also used to develop equations relating rolling resistance to the various soil and physical parameters. Reasons for discrepancies between the measured results and the theoretical estimation were investigated. A subsequent theory regarding the deterioration of the haul roads in terms of effective stress is presented, backed up with experimental data. Practical remedies for haul road deterioration problems are also discussed.

Acknowledgements

The author wishes to thank Professor M.C. Forde, Head of the Department of Civil and Environmental Engineering at the University of Edinburgh for placing the departmental facilities at his disposal. The author is also grateful to Professor M.C. Forde for his supervision, encouragement and constructive criticism throughout the duration of the project. The contributions of Dr. D.A. Ponniah as a second supervisor, and Mr. J.R. Osborne, of Tarmac Construction Ltd., as industrial sponsor, are also gratefully acknowledged.

The author would like to thank the following fellow students for their helpful discussions and assistance: Dr. C.A. Fairfield, now at the Department of Civil and Transportation Engineering, Napier University, for many long and fruitful discussions on the behaviour of soils, Messrs. Dunn, and Smith, of Tarmac and the University of Edinburgh, for their assistance in taking site readings, observations, and knowledge of earthmoving operations, and Mr. C. Lambton, formally at the University of Edinburgh, for site, laboratory, and mental assistance. The help from all the site personnel that were involved in the project is also acknowledged.

Thanks are due to the technical staff of the Department of Civil and Environmental Engineering, particularly Mr. I. Fowler, and Mr. R. Paton, at the Department of Civil and Transportation Engineering, Napier University, for their invaluable assistance. Thanks also go to Mr G. Brown and Mr. F. Johnston for the preparation of the photographic material.

The author wishes to thank Ms. M. Foley for her help, patience, encouragement and for reading the manuscript. He is also indebted to his parents and brother for their continual support, and to his colleagues in the Department of Civil and Environmental Engineering for their sociability and friendship.

The financial support for this work has been provided by the Science and Engineering Research Council, Case Award No. 91564505, and Tarmac Construction Ltd., Wolverhampton, and is gratefully acknowledged.

Table of Contents

The text is divided into chapters and sections. Sections are numbered decimally within each chapter; the number given to figures indicate to which chapter they belong, but are not related to the section numbers. Figures, tables, and plates are situated at the end of each chapter and are in the order noted above.

Notation

a	constant
a	regression coefficient
a_n	graphical intercept
B	modulus of deformation due to the cohesive component of the soil
B	number of blows in MCV test
b	regression coefficient
b	width of running gear
C	cone index
C	modulus of deformation due to the frictional component of the soil
C_{RR}	coefficient of rolling resistance
c	apparent soil cohesion
c'	apparent cohesion in terms of effective stress
c_u	undrained shear strength
d	soil deformation
d	wheel diameter
DP	drawbar pull
e_n	average effect of factor n
fitted y	calculated response
g	acceleration due to gravity
G	cone index gradient
G	grade resistance
GVW	gross vehicle weight
h	tyre section height
H	forward thrust
H	gross tractive effort
H	pull
i	slip
I_c	consistency index
j	soil deformation
k	modulus of soil deformation
k_c	soil constant due to cohesion component
k_c'	sinkage modulus
$k\phi$	soil constant due to frictional component
$k\phi'$	sinkage modulus

K	slip constant
K_1	slip parameter
K_2	slip parameter
K_c	constant
K_ϕ	constant
l	length of contact area
l_o	distance of rupture
L	drawbar pull
M	total vehicle mass
MCV	moisture condition value
$MCV_{(V)}$	moisture condition required to travel at velocity v
n	exponent of deformation
n	number of wheels
n	sample size
N	number of driven wheels
N_c	clay mobility number
N_c	Terzaghi's cohesive strength bearing capacity failure constant
N_{cs}	general mobility number
N_q	Terzaghi's bearing capacity solution on a cohesionless soil
N_s	sand mobility number
N_ϕ	Terzaghi's overburden bearing capacity failure constant
NVW	net vehicle weight
p	ground pressure
p	pressure acting on a plate
p_c	carcass stiffness
p_g	ground pressure
p_i	inflation pressure
P	maximum available engine power
P	towed force
Q	shear support force
Q	torque
r	rolling radius of a free rolling tyre on a firm surface
R	rut depth
R	total motion resisting force
R	translational rolling resistance
R^2	correlation coefficient

R_b	bulldozing component of motion resistance
R_c	compaction component of motion resistance
R_n	response at design point n
R_n	rolling resistance
R_O	rolling resistance
R_t	tyre flexing component of motion resistance
s	horizontal shearing strength of running surface
s	sample standard deviation
s_i	standard deviation of coefficient i
t	Student's t-value at 95% confidence level
t	tangential interface stress
T	driving or braking torque
T	input torque
T	tyre width
T_{max}	horizontal component of tangential force
u	pore water pressure
u_o	initial pore water pressure
V	forward velocity of the vehicle
V	hand vane shear strength
V	radial support force
w	corrected moisture content
w_L	liquid limit
w_n	natural moisture content
w_P	plastic limit
W	wheel load
x	input variable
x	measure of the contact length
$\bar{x}$	mean of data
y	response parameter
$\bar{y}$	mean response
z	sinkage
α	angle of approach
β	spissitude
γ	density of soil
δ	tyre deflection

ΔW	contact pressure applied by the wheel
θ	angle
θ_0	forward contact angle
θ_1	rear contact angle
μ	tyre-soil friction
σ	normal interface stress
σ	total normal stress
σ'	effective normal stress
σ'_{nP}	effective normal stress during the n^{th} passage of a wheel
σ'_{nR}	residual effective normal stress after pass n
τ	shear strength
ϕ	angle of shearing resistance
ϕ'	angle of shearing resistance in terms of effective stress
ω	angular velocity of the wheel

Chapter 1 Introduction

The earliest road is attributed to the Egyptian King Cheops, who was said to have constructed a causeway of polished stone, 1km (5 furlongs) long, in about 3000 BC, to facilitate the construction of the Great Pyramid, (Collins et al., 1936). The Incas built highways through the Andes and the Mayans built a network of paved roads in Mexico. From 300 BC the Roman Empire constructed stone highways throughout Europe to support their military campaigns. By early in the fifth century AD the Romans had built thousands of miles of paved roadway in Britain, many of which are still in use today. After the departure of the Roman legions (406 AD), the needs of the people became parochial, the state of the roadways deteriorated and the art of road building was almost forgotten. These early forms of road construction were for the transportation of animals and people. As the speed of the vehicles was slow, the profile of the road was not restricted by visibility or grade, hence were constructed directly on top of existing ground.

The first instance of earthmoving came with the design of the first "modern" roadway, by Trésaguet in France, around 1764. Manual earthmoving, for the preparation of the subgrade, was also used in the subsequent pavement designs of Telford, 1820, and M^{c}Adam, 1822. The earthmoving was carried out by hand, or with the aid of horse drawn scrapers for light work on preploughed sections.

The invention of the petrol engine and motor car around 1886 led to a desired increase in the quality of roads. With the introduction of faster vehicles the road accident rate increased rapidly, reaching two million killed or injured during the period 1926-1935 (Collins et al., 1936). The increase in speed led to the roads being constructed with smoother gradients, better sign posting, and markings. The former remedy for reducing the accident rate demanded a greater amount of earthmoving. In the 1930's the power shovel was introduced for loading carts that ran on rails from the cut face to the embankment, (Collins et al., 1936). Throughout the century technology advanced and earthmoving equipment became sophisticated: with the development of the rigid dump truck and self-loading motorised scraper in the late 1940'^{s}. The articulated dump truck and the backhoe excavator were introduced later in the 1970'^{s}.

Currently, except for very short hauls, under 800m, where scrapers are employed, the majority of earthmoving is carried out by an excavator-dump truck combination. In Britain, articulated dump trucks (ADT) are the most common type of truck used in off-road construction, due to their superior handling and manoeuvrability compared to rigid dump trucks. The ADT was first developed in Scandinavia, to aid with forestry, and its evolution from tractor to current form is shown schematically in figure 1.1.

A typical earthmoving season lasts for approximately eight months of the year, depending on the weather. For contractors and subcontractors it is of vital importance that their tender price for any job is as accurate as possible. Prior to tender, the contractor has to organise the various works and estimate how long each operation will last. On the earthworks side, the type of plant match: excavator -dump truck, or scraper, and the number of vehicles to run the contract efficiently must also be estimated. These decisions are currently made on the basis of the length and gradient of the haul roads, the type of material being transported, and the type of available plant. The estimated speed of the vehicles is all important and the only information available to help the estimator are: the site investigation report, and plant performance data from previous contracts. The production rate of an earthmoving team is currently based on the estimated output of the prime mover, the excavator, or scrapers. The number of vehicles required for an operation is determined by the estimated cycle time of a single vehicle, where a complete cycle is the summation of: loading time, loaded travel time, dump time, empty travel time, and any waiting at the loader. The cycle time is currently estimated simply by the length of the haul road. This method of resourcing an operation, which for the earthmoving on a motorway contract is worth in the region of £1-2M/km, is empirical and is in need of upgrading. Interest in accurate earthmoving estimation is not a fashionable research area and data gained through experience is jealously guarded. The big earthmoving manufacturers now offer a service to resource any contract. Research publications on competitive earthmoving are still minimal, as the information is regarded as precious.

In the United Kingdom under the Institution of Civil Engineers (ICE) 5th and 6th editions of contract, once the contract has started, if it can be quantifiably shown that the vehicles have not been performing as fast as could have been anticipated from the site investigation report, then the moneys lost can be claimed from the

client, unless the deterioration is caused by the weather. With the present empirical method of resourcing it is hard to prove if, and by how much, the vehicles have been slowed down, thereby making difficult the opportunity of an accurate claim. The accurate determination of the decrease in productivity of an earthmoving team was one of the initial aims of the project, and led to an early publication (Staples et al., 1992).

It is evident from the preceding paragraphs that the estimated speed of the vehicles is of primary importance. The parameter which most affects the speed of the vehicles is rolling resistance; which is a combination of all the vehicle and ground factors which retard the progress of the vehicle. Rolling resistance is expressed in terms of percent equivalent grade, which allows it to be added directly to the gradient of the haul road.

The objective of the work carried out for this thesis, was to develop a relationship between the speed of articulated dump trucks on unprepared haul roads and the soil and physical properties of the running surface.

The thesis critically examines some of the literature on the performance of off-road vehicles. Monitoring of articulated dump trucks has been undertaken, on clay and chalk sites, to relate rolling resistance, in terms of percent equivalent grade, to soil and physical properties of the haul roads. A theory for estimating the rut depth from the pre-tender data has been postulated, along with experimental evidence to explain the deterioration of haul roads in terms of effective stress.

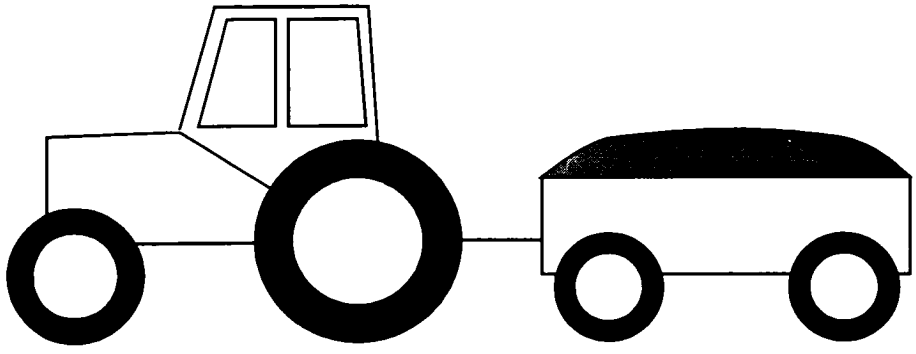

(a) Rear Wheel Drive Tractor with Towed Trailer

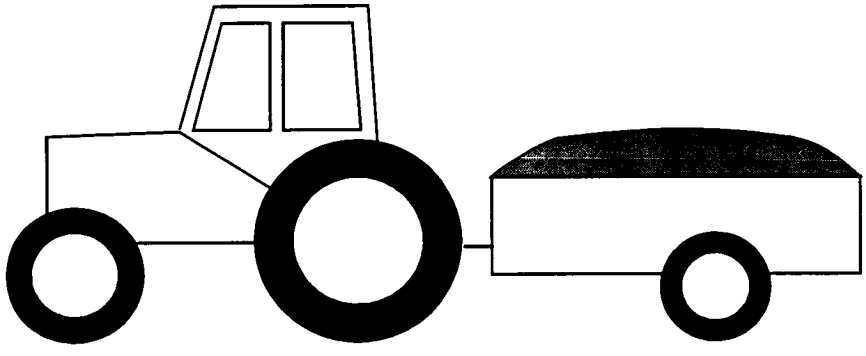

(b) Trailer with Driven Axle

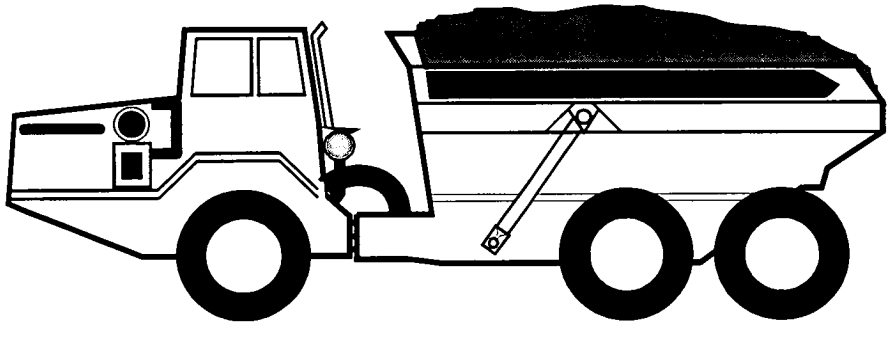

(c) All Axles Driven

Figure 1.1: Evolution of Modern Articulated Dump Truck

Chapter 2 Literature Survey

2.1 Introduction

One of mans' earliest inventions was the wheel. Since the initial concept, there have not been any significant design alterations, but man has demanded different requirements as technology progressed. Initially the wheel was used as a free rolling towed body where the only concern was that the resistance to motion (rolling resistance) was low. As time progressed the wheel was used as a propulsion device and consideration had to be taken of traction forces. The final development was with the invention of the self-propelled, manoeuvrable vehicle, as steering forces developed by the wheel became of interest.

The purpose of the modern day wheel is to support the load imposed by the vehicle and to develop the required forces to drive and steer the vehicle. To achieve efficient designs for any vehicle, the designer must be able to predict the forces acting on the wheels, figure 2.1. In order to calculate the forces it is important to understand the interaction between the wheel and the running surface. The size and shape of the contact area, figure 2.1, are therefore of prime importance, and are determined by the structural properties of both the wheel and in the case of off-road vehicles, the soil.

This chapter aims to follow the historical progression outlined above to describe the methods available for predicting rolling resistance. Tractive and steering forces are outwith the scope of the thesis and therefore will not be discussed in great detail.

The literature on the specific subject of earthmoving on civil engineering haul roads is limited, as the majority of the work on vehicle-soil interaction has been carried out by agricultural, and military engineers, as opposed to civil engineers. The three branches of engineering have different aims, the vehicles are of different design and the condition of the running medium varies considerably. The agricultural engineer generally operates a two-wheel drive agricultural tractor over soil possessing a high air voids content and aims to minimise the compaction of the soil while trying to achieve maximum drawbar pull. The soil is in a very loose

condition to encourage crop growth. The military engineer is concerned with the single and multi-pass agility, and mobility of various combat vehicles across virgin terrain, where vegetation is prevalent. Unlike the agricultural or military terrain, civil engineering haul roads are semi-prepared; being devoid of vegetation and topsoil, and having been compacted heavily by the successive passes of earthmoving plant. The civil engineer in highway construction has been more concerned with the performance of embankments under loading from various types of plant, (Forde, 1975) but does not appear to have considered the achievable speed of vehicles on haul roads, this latter problem being the focus of this thesis. The significance of this problem has increased over the last few years as contracts are being awarded at very low profit margins. As a result of this, contractors require to know exactly: the number of trucks required, and the length of time to complete the contract, both of which are dependent on the speed the trucks can achieve.

The majority of the initial research into the mobility problem was carried out by the military, especially the Americans, after the Second World War, where the immobilisation of combat vehicles was commonplace, (Bekker, 1950). The next section will define the salient terms fully, before moving on to a description of the concepts explaining tyre-soil interaction behaviour.

2.2 Definitions of Wheel and Tyre

For the purpose of this thesis the term *wheel* shall refer to a rigid wheel that shall not deform under loading, and the term *tyre* will refer to a similar structure that shall deform under loading. A *pneumatic tyre*, figure 2.2, is a flexible vessel utilising structural members of high modulus of elasticity, nylon, steel cable, etc., to contain the hoop tension resulting from the inflation pressure. Rubber of low modulus is utilised as a protective cover over the structural members and also forms the tread pattern that provides the traction and wearing medium at the ground interface. Two distinct tyre construction types are available: bias ply, and radial tyres, figure 2.3. The main difference between the two designs is the cord angle, which dictates the cornering characteristics, smoothness of ride, rolling resistance, and wear life of the tyre. Radial ply tyres are normally used on off-road vehicles as the wear life of the tyres under harsh driving conditions is better,

(Wong, 1978). Tyre size nomenclature is derived from the approximate cross section width and rim diameter, with various systems being available. Bias-ply tyres will be described by two numbers, e.g. 23.5-25 where the first number represents the approximate cross sectional width, in inches, and the second number is the rim diameter, also in inches. For radial tyres the designation will be of the form 23.5 R 25, where the numbers define the same dimensions and the R represents radial construction. The term *running gear* will be used to mean any traction device: rigid wheel, pneumatic tyre, or track.

Although all the vehicles monitored on site were equipped with pneumatic tyres it is important from the development of rolling resistance theories to also consider the results of wheel experiments.

2.3 Properties of Pneumatic Tyres

When interacting with the soil the tyre will act in one of two ways: the tyre will act as a rigid wheel if the effective stiffness of the tyre is greater than the maximum normal stress on the soil, i.e. a very stiff tyre operating on a very weak soil, alternatively, if the effective stiffness of the tyre is less than the maximum normal stress then the tyre will deflect, i.e. a tyre running on an undeformable surface. Karafiath et al., (1978), presented a schematic representation of the relationship between soil strength, tyre stiffness, and sinkage as shown in figure 2.4. This figure indicates qualitatively the degree of tyre deflection and sinkage from the qualitative descriptions of tyre stiffness and soil strength. The estimation is found by constructing lines parallel to the sides of the rhombus and the projection of the intersection on the horizontal diagonal indicates the magnitude of the sinkage and tyre deflection. However, this qualitative approach has limited practical use, as it yields no quantitative value of the tyre deflection or sinkage, but it is a useful indicator for checking the validity of any tyre-soil concepts.

2.4 Rolling Resistance Forces

Total rolling resistance is defined (Meyer, 1977) as:

"The resistance to movement of a vehicle provided by the surface on and through which it moves plus, the resistance to movement provided by the internal friction of its moving parts and the energy losses in the traction elements."

The vehicle designer would like to minimise the rolling resistance in order that the energy wasted in overcoming motion resistance forces is as small as possible. Rolling resistance, due to surface effects, is generally split into three components, as detailed in equation 2.1

$$R = R_c + R_b + R_t \qquad (2.1).$$

where: R total motion resisting force
R_c component due to soil compaction
R_b component due to horizontal movement of soil, or bulldozing
R_t component due to the flexing of the tyre.

For a vehicle operating in an off-road condition the components R_c and R_b constitute the greatest percentage of the motion resisting force. The work described in the next sections investigates various methods of predicting the rolling resistance of a vehicle to motion.

2.5 Plate Sinkage Techniques

The concept behind plate sinkage techniques is the assumption that the performance of a wheel is similar to that of a plate being forced into the ground. The following sections briefly describe some of the work that has been carried out in this field.

2.5.1 The work of Bernstein

A semi-empirical approach, to predict the forces on wheels, was first initiated by Bernstein, (1913). Bernstein observed that the rolling resistance acting on a wheel was as a result of the work done in forming a rut. He proposed that the action of a plate being forced into the ground, under a uniformly distributed load, represents

the action of a driven tyre or track, of similar contact area. It is therefore assumed that if there are shear stresses at the running gear-soil boundary, then they do not contribute to the formation of ruts, hence rolling resistance is just a function of the radial stress distribution. The relationship between pressure, p and static sinkage, z, will be of the form in figure 2.5. The general formula describing this relationship, equation 2.2, was proposed by Goriatchkin (1936)

$$p = kz^n \tag{2.2}$$

where: p pressure acting on the plate
k modulus of soil deformation
z sinkage
n exponent of deformation

Bernstein found that n was in the region of 0.5 for an agricultural soil and was independent of plate size. Unfortunately, the value of k varied depending on the size of the rectangular plate. This work has proved to be the basis of extensive theories of rolling resistance and soil deformation at the running gear-soil interface, despite the crude assumptions that a vertically loaded plate will produce the same pressure distribution and act in a similar manner to towed and driven running gears.

2.5.2 The Work of Bekker

In the post World War II years, the military engineer concentrated on developing an understanding of terrain-vehicle interaction. Due to the severe mobility problems during the war, the majority of the wartime research undertaken was hurriedly organised, of a purely empirical nature, and did not focus on any of the fundamental issues. Bekker (1950) emphasised what could be learnt from past experience:

"1. Only a theoretical study of fundamentals may bring a solution to the general problems, because their complexity makes traditional experimental work practically useless.

2. The subject requires a continuous, full-time study by professional personnel.

3. Success in the new study by automotive engineers will depend largely upon training in some branches of science which have not in the past been included in the curricula of automotive engineering courses."

After that publication Bekker continued in the field for the rest of his life, spearheading the American attack on various aspects of the mobility problem. The results of most of his early work have been published in his three books, (Bekker, 1956, 1960 and 1969) and numerous articles. The Bekker approach follows on from the plate penetrating work of Bernstein, relating ground properties to the performance of off-road vehicles.

Bekker used the principles stated by Bernstein, to formulate a theory for predicting the drawbar pull of a vehicle, from an estimation of the rolling resistance and the forward thrust, equation 2.3.

$$DP = H - R \tag{2.3}$$

where: DP drawbar pull
H forward thrust
R resistance to motion

The horizontal thrust is calculated from

$$H = b\int_0^l s\, dx \tag{2.4}$$

where: l length of the contact area
b width of track or wheel
s horizontal shearing strength of the running surface
x measure of the contact length

The horizontal shearing strength of the running surface is calculated from:

$$s = \frac{c + p \tan\phi}{y_{max}} \qquad (2.5)$$

where: c cohesion

ϕ internal angle of friction

p ground pressure

y_{max} maximum value equation 2.6

$$y_{max} = \exp(-K_2 + \sqrt{K_2^2 - 1})K_1 d - \exp(-K_2 - \sqrt{K_2^2 - 1})K_1 d \qquad (2.6)$$

where: K_1 and K_2 slip parameters

d soil deformation

For predicting the resistance to motion in equation 2.3, Bekker applied Bernstein's principle that motion resistance was due to the formation of ruts. However, he proposed that the modulus of soil deformation was composed of two components, one due to each of the cohesive and frictional properties of the soil. Experiments carried out by Bekker showed that Bernstein's pressure-sinkage equation was very sensitive to the dimensions of the loading plate, but repeatable results could be obtained by utilising Bekker's pressure-sinkage relationship of a rectangular plate in a soil, equation 2.7. The plate penetration tests and its theoretical development will be discussed fully in section 2.5.3.

$$p = \left(\frac{k_c}{b} + k_\phi\right) z^n \qquad (2.7)$$

where: p pressure applied to the plate

k_c soil constant due to the cohesion component dependent on plate size

k_ϕ soil constant due to the frictional component dependent on plate size

b plate width

z plate sinkage

n exponent of deformation (for clay $n \approx 0.4$-0.6 and for sand $n \approx 0.6$-1.0)

Knowing the pressure distribution beneath a rigid, rectangular and uniformly loaded area, Bekker went on to propose that the compaction component of rolling resistance could be calculated from the following expression:

$$R_c = \frac{1}{(n+1)(k_c + bk_\phi)^{\frac{1}{n}}} \left(\frac{W}{l}\right)^{\frac{n+1}{n}} \qquad (2.8)$$

where: W wheel load and the other terms are as previously defined.

By considering the geometry of a rigid wheel, diameter d, Bekker derived expressions for the sinkage and compaction component of rolling resistance as:

$$R_c = \frac{1}{(3-n)^{\frac{2n+2}{2n+1}} (n+1)(k_c + bk_\phi)^{\frac{1}{2n+1}}} \left(\frac{3W}{\sqrt{d}}\right)^{\frac{2n+2}{2n+1}} \qquad (2.9)$$

$$z = \left(\frac{3W}{(3-n)(k_c + bk_\phi)\sqrt{d}}\right)^{\frac{2}{2n+1}} \qquad (2.10)$$

Figures 2.6 and 2.7 respectively show how equations 2.9 and 2.10 compare with experimental data, as published by Wills (1966), for a small diameter towed rigid wheel on clay. As can be seen the Bekker equations underestimate the value of rolling resistance and overestimates the degree of sinkage.

Bekker also developed an expression for predicting the motion resistance of pneumatic tyres by assuming that the tyre deflected into the form depicted in figure 2.8. For this case the compaction resistance is estimated by using equation 2.11 to determine the ground pressure.

$$p_g = p_i + p_c \qquad (2.11)$$

where: p_g ground pressure
p_i inflation pressure
p_c carcass stiffness

If the above equation is used to represent the load carried by the flattened portion of the tyre, and is substituted into equation 2.9, then the following equation for the compaction component of rolling resistance is obtained:

$$R_c = \frac{\left[b(p_i + p_c)\right]^{\frac{n+1}{n}}}{(n+1)\left(k_c + bk_\phi\right)^{\frac{1}{n}}} \qquad (2.12)$$

Bekker also considered the bulldozing component of rolling resistance caused by the horizontal displacement of soil. He realised that the components of bulldozing and compaction were difficult to separate mathematically, but produced an equation for the condition of a wheel travelling on a hard surface covered with loose soil, equation 2.13.

$$R_b = \frac{b\sin(\alpha+\phi)}{2\sin\alpha\cos\phi}\left[2zcK_c + \gamma z^2 K_\gamma\right] + \frac{\pi l_o^3 \gamma(90-\phi)}{540} + \frac{c\pi l_o^2}{180} + cl_o^2 \tan\left(45 - \frac{\phi}{2}\right) \qquad (2.13)$$

where: R_b Bulldozing component of rolling resistance

α angle of approach = $\cos^{-1}\left(1 - \frac{2z}{d}\right)$

γ density of soil

l_o distance of rupture = $z\tan^2\left(45 - \frac{\phi}{2}\right)\phi$

K_c constant = $(N_c - \tan\phi)\cos^2\phi$

K_γ constant = $\left(\frac{2N_\gamma}{\tan\phi + 1}\right)\cos^2\phi$

N_c Terzaghi's cohesive strength bearing capacity failure constant (Terzaghi, 1943)

N_γ Terzaghi's overburden bearing capacity failure constant (Terzaghi, 1943)

All the above constants (c, ϕ, k_c, k_ϕ, n, K_1, K_2) are obtained using an instrument developed by Bekker in the mid-1950's, called the bevameter, an acronym for

Bekker value meter. Figure 2.9 shows a schematic view of a bevameter type instrument. Two soil characterisation tests are carried by this instrument; the plate sinkage test, and the ring shear test. These two tests will be discussed fully in the following two sections.

2.5.3 Load Penetration Relationship

As mentioned previously in section 2.5.1, Bekker showed experimentally that equation 2.2, proposed by Goriatchkin (1936), was sensitive to the dimensions of the plate. In order to progress the theory, Bekker considered the work of Taylor (1948) on the settlement of structures. For small settlements, lying on the initial straight portion of figure 2.5, the relationship between applied pressure and settlement could be defined by equation 2.14, which was considered to be independent of the plate dimensions.

$$p = \left(\frac{B}{b} + C\right)z \tag{2.14}$$

where: B modulus of deformation due to the cohesive component of the soil
b width of footing
C modulus of deformation due to the frictional component of the soil.

This equation could not be used directly, as the sinkages caused by off-road transport generally extend into the curvilinear portion of figure 2.5. To combat this Bekker introduced the Bernstein exponent n to the equation, giving:

$$p = \left(\frac{B}{b} + C\right)z^n \tag{2.15}$$

Bekker followed the assumptions of Taylor in that the parameters B and C would remain constant, but changed his notation to k_c and k_ϕ respectively, equation 2.7, the suffices correspond to the Coulomb notation for cohesion and friction. The three parameters, k_c, k_ϕ, and n, are calculated from the results of at least two plate sinkage tests carried out using the bevameter. Graphs of log(pressure) versus

log(sinkage) are plotted for all plate tests completed, that should yield a family of parallel lines, figure 2.10. Comparing the pressure sinkage relationship, equation 2.7, and figure 2.10, it is clear that the intercept a_n will be equal to

$$a_n = \frac{k_c}{b_n} + k_\phi \tag{2.16}$$

where: b_n is the width of plate n.

Assuming k_c and k_ϕ to be constant, simultaneous equations can be constructed for the solution of the unknown parameters. The value of n is then simply the gradient of the log-log plots. Due to non-homogeneities in the soil, the family of lines are not always parallel and solutions for the constants are not always attainable. Published data by Wong (1989) gives ranges of k_c and k_ϕ of 1.16-15.9 and 475-4526 respectively for sand and 6.8-41.6 and 1134-2471 for a clayey loam.

This equation has been used for ongoing research, but the validity of the equation has been questioned by numerous authors, which will be discussed later, including Taylor, (1948) who stated:

> "The expression derived above is of a highly approximate nature..."

And with regard to the coefficients:

> "...if two loading tests were repeated with every effort made to reproduce results as closely as possible, it would be fortunate if the new data should check to within 10 or 20 per cent."

The corresponding difference in sinkage with a 15% variation in the coefficients is approximately threefold. This indicates that the above technique should be treated with extreme caution and the potential errors when extrapolating outwith the bounds of the experiment should be considered. The modification proposed by Bekker to incorporate the non-linear portion of the pressure-sinkage relationship at high sinkages, is thus considered to be potentially erroneous.

2.5.4 The Horizontal Shear Relationship

The second test carried out using the bevameter is the ring shear test, which gives the horizontal shear strength of the soil as per equation 2.5 above.

The object of this test is to relate horizontal shear strength to deformation whilst retaining the Mohr-Coulomb failure criterion, hence the form of equation 2.5 relating shear strength to c, ϕ, p and a displacement parameter y_{max}. The slip parameters K_1 and K_2 are calculated from the shear-displacement curves for various normal loads. A graphical solution for these constants was first proposed by Weiss in 1955, and published by Bekker (1960). This solution was only valid for a brittle soil that exhibits a peak in the shear-deformation curve, figure 2.11. For a plastic material, which has a shear-displacement curve as in figure 2.11, the slip parameters were reduced to a single K-value. The plastic shear curve is fitted to the experimental plot with the equation:

$$\tau = (c + p \tan\phi)\left(1 - e^{\left(\frac{-j}{K}\right)}\right) \qquad (2.17)$$

The K-value is determined from equation 2.17, and is defined by the distance between the ordinate and the point of intersection between the sloped and horizontal portions of the curve, figure 2.11.

Sela (1961) devised another graphical method of determining the slip parameters, that agrees well with that of Weiss, but is equally complicated and graphically involved which is subject to error.

A number of points should be noted with regard to this test. Firstly the soil being tested is on the surface and the depth of soil affected by the bevameter test is likely to be small. In the wheel shear case, the soil sheared may be at some depth below the surface due to sinkage, thus the bevameter test may not take into account any stratification of the soil. If the wheel contact area and the normal load are dissimilar to the plate test, then the pressure bulb will be different, leading to the results being incomparable. Secondly, the parameters for c and ϕ obtained from this part of the test are only valid for the particular test conditions. It may be that

under a wheel load the failure environment may be completely different, e.g. if the rate of shear in the test ring is slower than that under the wheel then errors in the estimation of the soil strength parameters may occur (Casagrande et al., 1951). Finally, the shear plate only shears the plate in a horizontal plane, whereas a treaded or lugged wheel will shear the soil in both the horizontal and vertical planes. This may again lead to discrepancies in the soil strength parameters. The above mentioned points will have varying significance depending on the soil type and state.

2.5.5 Discussion

The Bekker theory of land locomotion is regarded as a very ingenious approach to an exceptionally complex problem. The main criticisms of his work are: the difficulty of estimating the soil parameters, the assumed stress distribution at the running gear-soil interface, and the lack of usage of classical soil mechanics.

2.6 The Work of Reece

Reece (1964, 1965) investigated the validity of the Bekker pressure sinkage equation and found it to be unsatisfactory for five primary reasons:

> "(a) it does not fit experimental work at all well,
> (b) it cannot accommodate the British equation for a clay soil as a special case, ($p=kc$),
> (c) it conflicts with bearing capacity theory,
> (d) it is not dimensionally acceptable because k_c and k_ϕ do not have constant dimensions,
> (e) it is purely empirical and there is no way of calculating k_c, k_ϕ or n."

He also pointed out that the Bekker pressure sinkage relationship is based on a number of assumptions:

(1) It is assumed that the sinkage is small in comparison to the wheel diameter.

(2) The pressure at any depth beneath a plate of any shape is equal to the pressure under the running gear of a vehicle at the same depth. The main difference between the running gear of a vehicle and a flat plate, is that adjacent elements on a horizontal plane are not at the same depth. It is also apparent from bearing capacity theories that the shape of the plate, in relation to the cross-sectional shape of the wheel, is of vital importance.

(3) The principle of superposition can be used in order that the results of two plate penetration tests can be straightforwardly extrapolated to the case of running gear on soil.

He observed that the Goriatchkin equation was of the correct form, but that the Bekker coefficients, k_c and k_ϕ, varied appreciably with plate width. Reece (1964) discussed the work of Terzaghi (1943) and Meyerhof (1951), examining the soil failure beneath strip footings with respect to a pressure sinkage relationship, and suggested the following alteration to the Bekker equation for compact soils:

$$p = \left(ck_c'\right)\left(\frac{z}{b}\right)^n + \left(b\gamma k_\phi'\right)\left(\frac{z}{b}\right)^n \qquad (2.18)$$

where k_c' and k_ϕ' are dimensionless sinkage moduli and are functions of the angle of internal friction. This equation was considered to overcome all the objections to the Bekker equation, detailed above. This relationship was shown to correlate well with plate sinkage tests in both frictional and cohesive soils. It is clear from this equation that the pressure distribution in a cohesive soil is independent of the plate size, but this is not the case for a frictional soil. This equation can therefore be considered an improvement on the Bekker equation and has been verified by an extensive experimental programme carried out by Wills (1966).

2.7 The Work of Onafeko and Reece

Onafeko et al. (1967) investigated radial and shear soil stresses, as well as deformations beneath rigid wheels. This work enabled them to make several conclusions about the Bekker theory. Firstly, they discovered that the radial pressure distribution could not be equated to the pressure beneath a flat plate, which was the basic assumption of the Bekker theory. Both stress distributions

tended to have a peak forward of bottom dead centre that moves forward with increasing slip. Experimental results of pressure distribution under pneumatic tyres and rigid wheels will be discussed fully in chapter 6. Secondly, they discovered that sinkage, and therefore rolling resistance, increased with slip. Slip, equation 2.19, is a measure of travel reduction and is expressed as a percentage.

$$i = \left(1 - \frac{V}{r\omega}\right) \times 100\% \tag{2.19}$$

where: i slip

V forward velocity of the vehicle

r rolling radius of a free rolling tyre on a firm surface

ω angular speed of the wheel

Onafeko (1969) tried to rationalise the concept of rolling resistance for a rigid wheel on a deformable soil. From the statics of a rigid wheel, figure 2.12, he defined the following forces:

$$R = rb\int_{\theta_1}^{\theta_0} \sigma \sin\theta \, d\theta \qquad \text{translational rolling resistance} \tag{2.20}$$

$$H = rb\int_{\theta_1}^{\theta_0} t \cos\theta \, d\theta \qquad \text{gross tractive effort or braking force} \tag{2.21}$$

$$Q = rb\int_{\theta_1}^{\theta_0} t \sin\theta \, d\theta \qquad \text{shear support force} \tag{2.22}$$

$$V = rb\int_{\theta_1}^{\theta_0} \sigma \cos\theta \, d\theta \qquad \text{radial support force} \tag{2.23}$$

$$T = rb\int_{\theta_1}^{\theta_0} t \, d\theta \qquad \text{driving or braking torque} \tag{2.24}$$

Onafeko divided the losses in a wheel into three components: internal, rotational, and translational. The internal loss was due to axle-bearing friction and other mechanical imperfections, together with any deflection in the case of pneumatic tyres. This loss was considered negligible in the case of a rigid wheel, but could be

considerable in a pneumatic tyre with low inflation pressure. Rotational loss was due partly to slip losses, and to that part of the tangential forces, developed by the wheel, which are used to support a proportion of the axle weight. This force Q, equation 2.22, was considered to consume energy, but contributed no useful work in return. Translational loss was due to the horizontal integral of the radial force opposing the wheel's linear motion. The main effect of this force was to reduce the available drawbar pull.

It is thus seen that Onafeko has separated the losses in a driven rigid wheel into rotational and translational losses. However this arbitrary division of losses into components could lead to confusion. There is a danger that translational rolling resistance could be equated to total rolling resistance in calculating drawbar pull. Another problem with this method is that the radial and shear stress distribution at the running-gear soil boundary must be known precisely. Onafeko (1964) claims to have done this for rigid wheels. It is also assumed that the pressure distributions are constant over the whole width of the running gear, which has been shown to be untrue for wheels and tyres on deformable surfaces, (Krick, 1969).

2.8 The Work of Gee-Clough

Gee-Clough (1976) incorporated the effect of slip into a semi-empirical theory for rolling resistance and lift forces, by considering both the normal and shear stresses acting at the boundary of a towed rigid wheel on a purely frictional, or purely cohesive soil. Gee-Clough proposed equation 2.25 to take account of the effects of slip, which is identical to the Bekker equation with the exception of the last term.

$$R_c = \frac{1}{(3-n)^{\frac{2n+2}{2n+1}}(n+1)(k_c + bk_\phi)^{\frac{1}{2n+1}}}\left(\frac{3W}{\sqrt{d}}\right)^{\frac{2n+2}{2n+1}} \frac{1}{(1+i)^{\frac{n}{2n+1}}} \qquad (2.25)$$

Due to the fact that the proposed correcting term for slip will always be greater than unity, Gee-Clough observed that the Bekker equation tends to underestimate rolling resistance. From the results published by Gee-Clough (1976), comparing the two methods of evaluating rolling resistance, figure 2.6, it can be seen that his

amended equation tends to overestimate the measured rolling resistance by as much as the Bekker equation underestimates, for both frictional and cohesive materials. This is partly because the normal and shear stress distributions used by the author do not match measured results, figure 2.13 (Hegedus, 1965, Onafeko et al., 1967, and Krick, 1969) for towed rigid wheels on either a frictional or cohesive material. The experimental distributions are typical in shape, taken from the three references above.

When correcting for sinkage the value proposed by Gee-Clough is worse than that predicted by the original Bekker equation, figure 2.7.

Later experimentation by the same author (Gee-Clough et al., 1978) again compared the Bekker formula with his own for a rigid wheel operating in sand and found that his equation better fitted the measured results. These results should again be treated with care and not extrapolated outwith the test conditions as by his own admission:

> "Although the coefficient of rolling resistance of the 0.025m wide wheel is predicted well by the Gee-Clough equations, this must be regarded as fortuitous since the measured skid of this wheel was considerably in excess of that predicted."

He also plotted the coefficient of rolling resistance (rolling resistance divided by lift force) versus wheel sinkage, for narrow wheels operating in sand, in order to ascertain the intercept values. He found that these intercept values were accurately explained by the relatively simple relationship for shallow sinkage, equation 2.26.

$$C_{RR} = \sqrt{\frac{z}{d}} \qquad (2.26)$$

where: C_{RR} coefficient of rolling resistance.

Whilst considering the effects of slip and deep sinkage upon the rolling resistance of rigid wheels, Gee-Clough proposed an expression by which the soil sinkage parameters could be determined from a single drag measurement taken from a wheel of known dimensions. He pointed out that this method could overcome the

two major drawbacks associated with rolling resistance models based upon the pressure-sinkage relationship. These are: the assumption that soil failure beneath a wheel mimics that of a flat plate, and the difficulty in measuring the Bekker soil sinkage parameters. This led to the invention of the wheel bevameter initiated by Bekker. Pavlics (1961) describes a system based upon a model rigid wheel, while Perdok (1978) used a full size rigid wheel to calculate the soil sinkage parameters by measuring drag for a variety of wheel loads. The advantage of such a piece of apparatus is that the theories on the soil behaviour could be extended to three dimensions, as was established by Wong et al. (1966). The development of the wheel bevameter has been slow, probably due to the realisation that the introduction of such a device would make the pressure-sinkage relationship even more empirical and may not promote a better understanding of the running gear-soil interaction.

2.9 British Theory for Clay

The British approach to the soil-wheel interaction problem, sometimes called the total force method, applied the principles of soil mechanics and was taking place at a similar time to the Bekker approach. This method originated in Britain but subsequent contributions have come from other countries.

2.9.1 The Work of Micklethwaite

Micklethwaite (1944) was concerned with the performance of tracked vehicles during World War II. Although it is not an objective of this thesis to investigate the behaviour of tracks, Micklethwaite's work is of interest as much of it is related to wheels. He considered that the ground bearing pressures under a track would show little difference to that which would result if a length of track was wrapped round each wheel. Although this is an oversimplification, which Micklethwaite himself discussed, it forms his reasoning to investigate the behaviour of wheels prior to tracks.

Micklethwaite first developed an equation relating the sinkage of a wheel to the allowable ground bearing pressure, equation 2.27. He achieved this by introducing

the Mohr-Coulomb failure criterion and Prandtl's (1924) bearing capacity theory. When using the bearing capacity formulae, the contact area is taken as the horizontal projection of the contact area.

$$z = r - \sqrt{r^2 - \left(\frac{W}{nbp}\right)^2} \qquad (2.27)$$

where: z wheel sinkage
r wheel radius
W vehicle weight per metre run of track
n number of wheels
b width of track
p ground bearing capacity

Micklethwaite went on to produce a four quadrant nomograph for calculating the sinkage of any heavy tracked vehicle, with a flexible slack track on clay.

After investigating the tension of the track, Micklethwaite went on to discuss rolling resistance. He applied Bernstein's principle that motion resistance was due to the formation of ruts, and that rolling resistance could be calculated from bearing capacity by determining the work done in forming a rut of unit length and constant depth.

The significance of Micklethwaite's work, in the body of terramechanics research, is that it is a simple attempt to apply the then limited knowledge of soil mechanics to the soil-vehicle interaction problem.

2.10 The Work of Uffelmann

Uffelmann (1961) suggested a simple plastic theory for the rolling resistance of rigid cylindrical wheels operating at small sinkages. In his theoretical approach the wheel is assumed to have:

"1) produced a rut equal to its instantaneous sinkage (plastic deformation without recovery, and

2) a uniform radial pressure, q, over the arc of contact with the soil."

It was then considered that for small angles of sinkage, q could be identified with the surface strip load bearing capacity. By integrating the vertical component of q and equating it to the vertical load W, the sinkage could then be calculated from equation 2.28.

$$z = \frac{W^2}{q^2 b^2 D} \tag{2.28}$$

where: z wheel sinkage
b wheel rim width
D wheel rim diameter

Before progressing to the next stage of Uffelmann's argument, it is of interest to examine the validity of the above relationship. In order to calculate the total vertical load W, figure 2.14, it must be equated with the vertical component of q multiplied by the horizontal component of the contact area. Hence:

$$W = q\,b\cos\left(\frac{\alpha}{2}\right)\sqrt{r^2-(r-z)^2} \tag{2.29}$$

$$= q\,b\sqrt{\frac{2r-z}{2r}}\sqrt{2r-z}\sqrt{z} \tag{2.30}$$

$$W^2 = q^2 b^2 \frac{(2r-z)^2}{2r} z \tag{2.31}$$

Comparing equations 2.28 and 2.31, it is clear that the value of sinkage must be very small in relation to the wheel diameter for equation 2.31 to be valid.

Uffelmann then calculated rolling resistance, assuming that this was entirely due to the work done in compressing down the rut. Thus the rolling resistance per unit length of rut was given as:

$$R = q\,z\,b = \frac{W^2}{q\,b\,D} \tag{2.32}$$

Having defined his interpretation of rolling resistance, Uffelmann went on to consider the case of a driven wheel. For this he assumed that the tangential force was constant along the contact arc and increased with increasing slip to a maximum value equal to the cohesion of the soil. He proposed that the integrated horizontal component of the tangential force would be the tractive soil reaction, T, and at slip stall conditions would have its maximum value of:

$$T_{max} = c\,b\,l \qquad (2.33)$$

where: c soil cohesion
b wheel width
l r sinα
α angle of sinkage

Under critical slip stall conditions, equations 2.32 and 2.33 were equated and the radial pressure was set at the surface bearing capacity value of an ideally rough strip footing, i.e. q = 5.7c. Therefore:

$$\sin\alpha = 5.7(1-\cos\alpha) \qquad (2.34)$$

whence: $\alpha = 20°$, or $\frac{z}{D} = 0.03$

Thus, for a cylindrical rigid wheel of 1.8m diameter, the slip stall failure would occur at a maximum of 54mm, without provision of additional tractive soil reaction. Intuitively this appears to be unreasonable, and the flaw in Uffelmann's argument lies in the step of equating equations 2.32 and 2.33. Equation 2.32 is the work done by the vertical component of the soil-wheel reaction, whereas equation 2.33 is the horizontal component of the soil-wheel tractive reaction. It is not reasonable to equate the horizontal component of one force with the vertical component of another as proposed by Uffelmann.

The theoretical work carried out by Uffelmann with regard to critical sinkage is seen to be invalid. The proposed relationship between sinkage and vehicle parameters has been shown to be applicable only for very low sinkages in relation to wheel diameter. Uffelmann's interpretation of rolling resistance, as described

above, is only the vertical component of rolling resistance and is therefore subject to the aforementioned limitations.

2.11 The work of Heatherington et al.

Heatherington et al., (1978) investigated the use of a predictive technique for towed rigid wheels, of square cross-section, operating in sand. This was based upon the bearing capacity theory of Terzaghi (1943) and equation 2.35 was proposed with the assumption that the rolling resistance of a wheel, is equal to the work done in forming a rut of unit length.

$$\text{Rolling resistance, } R_O = \left(\frac{2W^4}{bd^2\gamma N_q} \right)^{\frac{1}{3}} \qquad (2.35)$$

where: W axle load

b breadth of wheel

d diameter of wheel

γ bulk unit weight of sand

N_q $\dfrac{e^{\left(\frac{3\pi}{2}-\phi\right)\tan\phi}}{2\cos^2\left(\frac{\pi}{4}+\frac{\phi}{2}\right)}$ Terzaghi's bearing capacity solution on a cohesionless soil

ϕ angle of shearing resistance of sand.

Apart from a numerical constant, equation 2.35 could be considered a special case of the general Bekker formula, equation 2.9, with n=1 and $\left(\frac{k_c}{b}+k_\phi\right)=N_q\gamma$. Equation 2.35, was used in their later work (Heatherington et al., 1984), in calculating the decrease in rolling resistance from single to dual wheels.

Later, Heatherington et al. (1981) developed an expression for the rolling resistance of rigid wheels of round cross-section on sand. This equation was derived by considering the sinkage of a sphere into sand, combined with a bearing capacity equation proposed by Terzaghi. This approach is calculated assuming that no rut is left in the wake of the wheel and hence would appear to be fundamentally flawed.

All the relationships developed by Heatherington et al. show excellent correlation with their own experimental results, but have not been validated by other authors.

2.12 Finite Element Method

The finite element method, using triangular elements, has been used to try and predict tyre performance (Yong et al., 1976). In this method the tyre is considered as an elastic system and the terrain as a linear elastic material. Input for the solution involves knowing, or estimating the length of the contact patch, the normal and shear stress distribution at the boundary, as well as the load-unload stress-strain relations for the soil. The output is generally given in terms of stress, strain rate, and velocity fields in the terrain, (Boonsinsuk et al., 1984). It should be noted that if the stress distributions at the soil-tyre boundary are known then the performance of the tyre is completely defined and there is no need to use finite elements to determine stress, strain rate and velocity fields (Wong, 1977, 1984).

A further problem with applying the finite element technique to this study is the assumption that the soil is an elastic medium. In the majority of off-road conditions the terrain normally undergoes large plastic deformations and does not behave elastically, therefore specific soil models would have to be utilised.

2.13 Empirical Techniques

Empirical techniques have the advantage of being developed for a specific problem via a series of experiments and observations. The major disadvantage of empiricism is that the results cannot be extrapolated to other situations with confidence.

2.13.1 Direct Measurement of Vehicle Parameters

The first reported vehicle performance tests were carried out in America by agricultural engineers, comparing the performance of tractors fitted with steel rim and pneumatic tyres (Zink et al., 1934, Jones, 1934, McKibben et al., 1939). In these early experiments the term rolling resistance was taken to mean:

> "...the power consumed in moving the tractor over the ground at the test speed." (Zink et al., 1934)

and was measured by pulling the test tractor with another tractor, the power being recorded by a dynamometer, located in the hitching mechanism. Pulling the tractor at different speeds enabled charts of rolling resistance versus speed to be constructed on specific materials. These early tests sealed the demise of steel wheels, as the rolling resistance of pneumatic tyres was approximately half that of the steel wheels (Zink et al., 1934, Jones, 1934, Wileman, 1934). This vast decrease in rolling resistance led to greater efficiency of operations. Unfortunately, measuring rolling resistance in this way does not take into account any effects of the tyre being driven.

With the knowledge that a marked decrease in rolling resistance can lead to substantial savings, McKibben et al. (1939b) describe apparatus for measuring rolling resistance directly: this apparatus consisted of an instrumented rig, in which a fifth wheel is attached to an extra live axle of a working tractor. Connecting the test wheel to a dynamometer gives the motion resisting force of the wheel, dividing this rolling resistance by the applied load gives a rolling resistance coefficient. This normalising technique allows a comparison to be made between different wheels and driving conditions. With the apparatus constructed, McKibben systematically proceeded to research the effects of varying tyre parameters, concluding: (i) on firm soil, as the inflation pressure is increased the rolling resistance decreases, whereas the opposite is true for soft soils, (McKibben et al., 1940), (ii) increasing the diameter of a tyre lowers the rolling resistance, (McKibben et al., 1940b), (iii) wheels operating in tandem on soft soils had a lower rolling resistance than the equivalent wheels in single or dual arrangements, due to the front wheel compacting the soil ahead of the rear wheel, (McKibben et al., 1940c), (iv) the difference in rolling resistance between a treaded and smooth

tyre was negligible on all four different driving conditions tested (McKibben et al., 1940d), (v) comparison of the rolling resistance of two pneumatic tyres, on seventeen field conditions, with two penetrometers, giving maximum penetration only, gave correlation coefficients in excess of 0.9, (McKibben et al., 1940e). Cone techniques for determining rolling resistance and tractive performance are discussed more fully in section 2.13.3.

After this initial interest in rolling resistance the topic was dropped in favour of tractive efficiency and drawbar pull prediction for various tyres.

The major drawback of the fifth wheel technique is that although the rolling resistance of individual wheels, in different driving conditions, can be fairly easily determined, the rolling resistance of an entire vehicle cannot be ascertained.

2.13.2 Work at the National Institute of Agricultural Engineers (N.I.A.E.)

The N.I.A.E. (1960) split motion resistance into two components: slip, and rolling. They considered rolling resistance to be a horizontal force opposing motion and was defined as:

> "...the equivalent loss of tractive force necessary to account for the remainder of the total losses".

By equating the work input to the work output and the work done against rolling resistance and slip, the following simple expression, equation 2.36, for rolling resistance was derived.

$$R_n = \frac{T}{r} - L \qquad (2.36)$$

where: R_n rolling resistance
T input torque
r rolling radius
L drawbar pull

This definition of rolling resistance requires the measurement of drawbar pull, torque and rolling radius and does not lend itself to analytical determination.

2.13.3 The Cone Penetrometer

The cone penetrometer, developed by the US Army Corps of Engineers, is a simple device for estimating the strength of a fine grained soil, (Knight et al., 1961, Knight et al., 1962). A right circular, 30° apex angle cone of base area 323mm^2, is penetrated into the soil at a uniform velocity of approximately 30mm/s normal to the surface. The soil cone index is the force per unit base area. Five to seven readings should be taken in an area to give a good statistical average of the cone index. There are several advantages of the cone penetrometer over the bevameter: the cone is rapid to perform, the results are quicker and simpler to interpret, the apparatus is manually transportable, and the output can be correlated with terms that define tyre performance.

Figures 2.15 (a and b) show ideal plots of soil penetration resistance versus depth to top of cone, for cohesive and frictional soils respectively. The cone index terms, C and G, in equations 2.39 and 2.40 respectively are calculated from the plots of cone index versus depth. For a cohesive soil, C is the average cone index over the required depth and for a frictional soil, G is the gradient of the cone index versus depth graph, measured in the first 150mm penetration.

For fine-grained soils a remoulding test can be carried out to estimate if the soil will be capable of supporting 50 passes of a specific vehicle. The remoulding test (Knight et al., 1961) is carried out by placing a sample of soil in a mould 101.6mm diameter and 152.4mm high, and subjecting it to 100 blows of a 1.14kg hammer dropped through a height of 0.3m. The cone penetrometer is then used to measure the cone index of the remoulded sample. The ratio of the remoulded cone index to the original cone index is called a remoulding index. The product of a cone index on a similar soil and the remoulding index is called the rating cone index, and is a measure of the soils response to repetitive loads, such as multiple vehicle passes.

A vehicle cone index is obtained using vehicle weight, dimensions, engine, and transmission factors in a series of equations and graphs (U.S. Army, 1968). The vehicle cone index is representative of the minimum rating cone index required for

50 passes of the specific vehicle. A comparison of the vehicle cone index and the rating cone index will determine whether the vehicle will be mobile or not in a particular soil.

Relatively recent advances in technology have resulted in the progressive evolution of cone design. The first step was to develop an electronic recording penetrometer (Carter, 1967, Hendrick, 1969, and Prather et al., 1970). An integrating penetrometer, (Carter, 1969) was developed to omit the manual estimation. With the development of microchip technology and data logging techniques more advanced penetrometers were developed. One of the first (Phillips et al., 1983) required two people to record profiles, but later with micro technology this problem was overcome (Woodruff et al., 1984, Olsen, 1987, and Rawitz et al., 1991).

Over the years the cone penetrometer has been used in the specific studies of root propagation (Farrell et al., 1966), compaction under tractor wheels (Smith et al., 1985, Jakobsen et al., 1989), and in relationships with fundamental soil properties (Ayers et al., 1982, Mulqueen et al., 1977, Karafiath et al., 1978, Rohani et al., 1981, and Elbanna et al., 1987). Rohani et al., (1981) developed a series of equations between the shear strength and stiffness of the soil. Unfortunately these relationships only hold for homogenous, frictional soils. Their theory calculates the cone index from a knowledge of the cohesion, friction angle, and stiffness of the soil, however, the inverse process is more difficult due to the number of unknowns. Nomographs for this inverse process were proposed by Hettiaratchi et al., (1987) for a drop cone test. Mulqueen et al., (1977) carried out a series of experiments to relate cone penetration to shear strength. The following limitations were noted about the cone:

"(i) the relative proportions of shear, compressive and tensile strengths reflected by the cone index vary with moisture content,
(ii) as soil moisture increases, cone index becomes increasingly insensitive to shear strength or compressive strength changes,
(iii) the formation of soil bodies and compaction zones ahead of the probe effectively change the probe geometry and so penetration force no longer reflects the original properties of the soil,
(iv) engagement of the shaft of the penetrometer by soil sometimes prevents attainment of the limit force as well as modifying the penetration force versus depth curve."

A warning was given, cautioning the use of the cone penetrometer in the field, where moisture content, bulk density, shear strength, and structural state vary rapidly with depth. The limitations listed above, particularly (iii) and (iv), can result in the cone index measured at a particular point to be different from the true cone index at that depth.

2.13.4 Mobility Number Methods

Freitag (1965) used dimensional analysis to produce two dimensionless numerics, one each for sand and clay soils. These numerics were then used to predict vehicle performance and rolling resistance of pneumatic tyres.

The tyre and soil parameters are shown in table 2.1 and the Buckingham pi terms in table 2.2. The selection of these variables was a result of compromise since, for example, the pneumatic tyre was represented by a treadless torus, and tyre deflection rather than inflation pressure was used to represent tyre flexibility. Freitag simplified the tyre-soil interaction problem by considering purely frictional soils ($c=0$), and purely cohesive soils ($\phi=0$), separately. In addition to this, the soil cone index was used as a measure of soil condition. As a result of the simplifications the fundamental relationships were reduced to:

$$\text{Clay: } \frac{H}{W}, \frac{P_T}{W}, \frac{Q}{dW}, \frac{z}{d} = f\left(\frac{Cd^2}{W}, \frac{b}{h}, \frac{\delta}{h}\right) \tag{2.37}$$

$$\text{Sand: } \frac{H}{W}, \frac{P_T}{W}, \frac{Q}{dW}, \frac{z}{d} = f\left(\frac{Gd^3}{W}, \frac{b}{h}, \frac{\delta}{h}\right) \tag{2.38}$$

from which the clay and sand mobility numbers in equations 2.39 and 2.40 respectively were formulated.

$$\text{Clay mobility number, } N_c = \frac{Cbd}{W}\left(\frac{\delta}{h}\right)^{\frac{1}{2}} \tag{2.39}$$

$$\text{Sand mobility number, } N_s = \frac{G(bd)^{\frac{3}{2}}}{W}\left(\frac{\delta}{h}\right) \tag{2.40}$$

where C and G are as defined in section 2.13.3 and figure 5.9, all the other parameters are defined in table 2.1.

2.13.5 Amendments to the Mobility Number Equations with Respect to Rolling Resistance Estimation

Turnage (1972), after an extensive programme of testing on a wide range of military tyres, introduced a term to take account of the dimensions of the tyre, the amended equation is given below:

$$\text{Clay mobility number, } N_c = \frac{Cbd}{W}\left(\frac{\delta}{h}\right)^{\frac{1}{2}} \frac{1}{\left(1+\frac{b}{2d}\right)} \qquad (2.41)$$

Wismer et al., (1973) used a similar approach to that of Freitag and developed single wheel numeric, equation 2.42. The single numeric was developed rather than different equations for each soil condition, as it was considered that the difference in results between the equations for the two classes was less than the uncertainty in the predictions of either.

$$\text{General mobility number, } N_{cs} = \left(\frac{Cbd}{W}\right) \qquad (2.42)$$

For a cohesive-frictional, or partially saturated soils, the plot of cone index versus depth is not constant. It was therefore proposed by Wismer et al. (1974) that the value of C should be taken as the average cone index on the 150mm layer centred on maximum tyre sinkage. From a series of experiments carried out by the American army, the general mobility number was related to the rolling resistance of a towed normally inflated tyre, operating on soils "which are not highly compactible" by the following equation:

$$C_{RR} = \frac{1.2}{N_{cs}} + 0.04 \qquad (2.43)$$

where C_{RR} is the coefficients rolling resistance. It can be seen from equation 2.43, that if the tyre were operating on a firm surface, the rolling resistance would be in the region of 4% of the wheel load. For a driven wheel, the rolling resistance was considered to be identical to that for a towed wheel, despite the fact that the pressure distribution at the boundary will be completely different.

The experimental results given by the authors on various tyres at a constant slip rate of 20% shows, by their own admission, "considerable data scatter". The reason for this data spread is considered to be the arbitrary method of calculating the cone index of the ground.

An examination of mobility number methods was also carried out by Dwyer et al. (1974, 1975). The work carried out at the National Institute of Agricultural Engineering, Silsoe, England, was to develop a handbook of agricultural tyres giving dimensions and tractive performance details. Tests were carried out on numerous tyres at various inflation pressures and the performance parameters related to the mobility number of Turnage (1972). Problems were encountered when relating rolling resistance, traction and efficiency to the sand mobility number (Dwyer et al. 1974), but the authors considered the correlation with the clay mobility number to be a success. The relationship between rolling resistance and clay mobility number was quoted as:

$$C_{RR} = 0.26e^{-0.2N_c} + 0.03 \qquad (2.44)$$

The minimum value of rolling resistance in this case is assumed to be 3% equivalent grade compared with the value of 4% by Wismer et al. (1973). The error bounds on this equation were ± 0.05 at the 95% confidence interval, or $\pm 5\%$ equivalent grade. On a surface with an actual rolling resistance of 8% equivalent grade, this error would lead to an estimated maximum velocity of between 12 and 48km/h for a loaded Volvo BM A35 articulated dump truck on a flat haul road, which is obviously unacceptable.

After further experimentation using a wider range of driven agricultural tyres and conditions, Dwyer et al. (1975) stated that the coefficient of rolling resistance could be expressed as:

$$C_{RR} = \frac{0.2}{N_c} + 0.07 \pm 0.05 \qquad (2.45)$$

where N_c is the clay mobility proposed by Turnage, equation 2.41.

The error in this equation is again similar to their previous work and therefore deemed to be of little practical use for the prediction of earthmoving vehicles operating on firm surface conditions. It is of interest to note that the minimum rolling resistance is 7% equivalent grade compared with the previous estimation of 3% especially as the maximum mobility number is greater by 25% in the latter work. The reason for this discrepancy is not apparent as all the same testing equipment was employed throughout.

Later, Dwyer (1984) defined a ground pressure index equal to the inverse of the clay mobility number multiplied by the cone index. However, this ground pressure parameter was not an advancement of the subject, as the new equation for rolling resistance, equation 2.46, is in exactly the same form as his previous equation.

$$\frac{R}{W} = 0.29\frac{G}{C} + 0.05 \qquad (2.46)$$

where $\frac{R}{W}$ is equivalent to C_{RR} and $\frac{G}{C}$ is equivalent to N_C.

Gee-Clough et al. (1978) reanalysed the data recorded at the National Institute of Agricultural Engineering for driven tractor tyres of diameters between 1.45 and 1.75m on ploughed soil. The purpose of this was to construct empirical relationships between mobility number and: coefficient of traction, and rolling resistance. Their results yielded equation 2.47.

No confidence intervals are given on the data, but at a mobility number of 6 the rolling resistance for radial-ply tyres ranges from 3-15% equivalent grade and for bias-ply tyres from 5-20% equivalent grade. The radial-ply tyres yield a lower minimum coefficient of rolling resistance, that is possibly due the fact that radial tyres have an advantage over bias-ply tyres at low loads and corresponding inflation pressures, allowing greater deflection. This advantage decreases as the loading increases, so that at high loads and therefore high inflation pressures, both tyres adopt similar characteristics. This is similar to the findings of Gee-Clough et al. (1977).

Grez et al. (1987) used equations 2.43 and 2.47 to estimate the rolling resistance of an implement cart on both a sand and a clay soil. Rolling resistance was measured directly in the soil bins by a "traction measurer". In the majority of cases, the measured rolling resistances were significantly lower than the estimated values calculated from the predictive equations. The main reasons for this discrepancy are: that the tyres used by Grez et al. were of a much smaller diameter and aspect ratio than those intended to be used in the formulae, and, more fundamentally, they assumed that the rolling resistance of a driven wheel is equal to that of a towed wheel. The first point confirms the reservations expressed by Wismer et al. (1974) and Gee-Clough et al. (1978) about the general applicability of their respective equations.

2.13.6 Problems with the Cone Penetrometer and Mobility Numerics

Reece et al. (1981), used the mobility numbers of Turnage to predict the drawbar performance of a smooth tyre in both frictional and cohesive soils. It was found that although the clay mobility number produced good correlation, the sand numeric, equation 2.40, was inadequate to define the behaviour of the material. This development initiated an in-depth study into the sand numeric by Turnage (1984). The author carried out further experimentation and reanalysed his earlier data to refine the predictive model. Unfortunately, the conclusion of the study was that the sand would have to be characterised by performing a particle size distribution, and cone penetration tests at a variety of moisture contents. This lengthy procedure would annul the advantage of using the cone penetrometer on a frictional material.

It is evident from the findings of Turnage (1978) that it is potentially dangerous to extrapolate developed theories from one soil type to another. Kogure et al. (1985) tried to develop a mathematical model to extrapolate cone indices across a complete site from a finite sample and stated that it was:

> "...readily apparent that a great deal of personal judgement is involved in determining soil trafficability. For example, the current procedure does not explicitly state what cone index measurement (mean, median, smallest, largest, or other) should be used for comparison with the vehicle cone index."

He also stated that it was well known that the results of cone penetration tests show large variations.

Freitag (1987), proposed a soil classification system defined by two numbers; the first is the moisture content at a penetration resistance of 40Pa, which is considered to be the minimum strength to support an average person walking. The other value is the decrease in moisture content associated with a 10-fold increase in the penetration resistance. This method would require a relatively extensive testing procedure and relies on a good relationship between moisture content and cone index, which is not apparent from the given results.

Upadhyaya et al. (1989) concluded after a series of traction experiments on radial-ply tyres, that cone index was not an accurate predictor of the soil condition for traction prediction, reporting (Upadhyaya et al., 1993) mean cone indices of 284kPa, with a standard deviation of 157.

2.13.7 Discussion on the Cone Penetrometer

From the findings of various authors outlined above it is clear that there is no definitive relationship between cone index and rolling resistance. The mobility numbers, developed by the U.S. army, are an excellent concept to simplify the mobility problem, but their inherent empiricism makes extrapolation from one set of tests conditions to another potentially erroneous.

2.14 Work Carried out by Civil Engineers into Earthmoving

As explained earlier, relatively little research has been completed by civil engineers on the subject of the mobility problem and even less has dealt with the specific topic of rolling resistance. The following sections detail the work completed in the field of off-road vehicle engineering.

2.14.1 The Work of Norman

Interference by wet weather is the principal cause of loss of output on earthmoving sites in the U.K. (Norman, 1965). In light of this the Federation of Civil Engineering Contractors proposed that research into the operation of earthmoving plant in wet weather should be one of the first topics to be investigated by the then Civil Engineering Research Association. As the duration of the contract was only two years the potential scope of the project was limited.

The main factors affecting both the production of a given haul, and the length of the construction season are: the type of plant employed, the soil type, the operational technique adopted, and the weather. The effects of wet weather on the earthmoving production were determined statistically by analysing the output of over 40 fleets operating on more than 30 sites. It was found that, during the summer earthmoving season, the amount of rainfall in a month was the dominant weather factor. For each particular fleet a linear relation was established between the percentage loss of output and rainfall. The slope of this relation was termed the "susceptibility" of a plant-soil combination, which is basically the percentage loss of output per inch of rain, per month.

The condition of the haul road was considered to be defined by rolling resistance, expressed in terms of percent equivalent grade. Vehicle manufacturers publish data relating rolling resistance to vehicle speed for each type of machine, by measuring the travel speed on site the rolling resistance can be ascertained relatively easily. This definition of rolling resistance will be discussed fully in the next chapter, and is the method specified in the ICE works construction guide (Horner, 1981).

Norman (1965) related the susceptibility of the soil to rolling resistance and found that rolling resistance was very sensitive at low soil susceptibility values and that a minimum value of rolling resistance for each haul road could be defined. From the work carried out, it is not clear exactly when the rolling resistance was measured. This could be critical, as the rolling resistance of the haul road changes depending on the strength of the material and the speed the driver is willing to travel.

Although the conclusions drawn by Norman were tentative, the report should enable the estimator to make a reasonably accurate estimate of the number of days each month when work will be possible and an indication of the potential outputs on these days. The report should also be used by the project manager who could compare the actual productivity with Norman's predicted output and thus review the efficiency of the working fleet.

Although the work of Norman contributes very little to the field of wheel-soil interaction, his method of calculating rolling resistance from the speed of the plant is easy to perform in a working environment, where interference with operations must be kept to a minimum. This method has therefore been adopted for the remainder of this thesis and a fuller description of the method is contained in the next chapter.

2.14.2 Work Carried out at the Transport Research Laboratory (TRL)

Farrar et al. (1975), investigated the first pass rut depth left behind towed and motorised scrapers on a total of 27 sites, on 9 different motorway contracts, in Britain. Vehicles were split into three categories: towed, small, and medium scrapers. The in-situ strength of the soil was determined by hand shear vane tests and characterised by the moisture content and plastic limit. Large variations were noted with the results of the hand shear vane, consequently a poor relationship between rut depth and vane shear strength was reported. Rut depth was also correlated with the ratio of moisture content to plastic limit, but the results of this correlation were inconclusive. Nevertheless, approximate guidelines are given for the maximum ratio of moisture content to plastic limit and the minimum vane shear strength required for the efficient running of scrapers, on cohesive fills. These

guidelines are split into two soil categories: 50% or more silt and clay, and less than 50% silt and clay.

Several points should be noted about the method of testing reported in this report. Firstly the moisture content has not been corrected for any material greater than 425μm, which can only have a moisture content equal to the absorbency of the individual particles. The ratio of moisture content to plastic limit can be misleading, depending on the plasticity index of the material, e.g. consider two soils with moisture contents and Atterberg limits as per table 2.3. For these two soils the ratio of moisture content to plastic limit are equal, but the consistency indices, equation 2.50, of the London and Lothian clay will be 0.88, and 0.73 respectively. Using Whyte's (1982) relationship between consistency index and undrained shear strength, equation 2.51, the resulting undrained shear strength for the London and Lothian clays will be 66 and 35kN/m^2 respectively. This represents almost a halving of the shear strength of the material. The work carried out by Farrar et al. is thus considered to be of limited applicability.

$$\text{Consistency Index, } I_c = \frac{w_L - w}{w_L - w_P} \qquad (2.50)$$

where: w_L liquid limit
w_P plastic limit
w corrected moisture content.

$$\text{Undrained shear strength, } c_u = 1.6e^{(4.23 I_c)} \qquad (2.51)$$

Following the development of the moisture condition apparatus, (Parsons, 1976), the amount of research into the performance of earthmoving plant increased (Parsons, 1977, Parsons et al., 1982, Parsons et al., 1988). Parsons et al., (1982) related moisture condition value (MCV) to rut depth, speed of vehicle, and limiting speed of vehicles. The purpose of this report was to increase the amount of data on the performance of earthmoving machinery on British soils as:

> "There is very little information available in the literature on the performances of these various types of machine in the more difficult soil conditions that often occur in the United Kingdom." (Parsons et al., 1982)

Twenty-five sites were studied and the results split into vehicle categories. The results relating to rut depth were as varied as in the previous report, since the readings were taken after the first pass of a vehicle in a freshly graded section of haul road. This method of estimation is prone to error, as the rut may simply be due to the displacement of the loose graded material.

The grade was shown to have an effect on the travelling velocity of certain types of plant and these vehicles alone were corrected for speed. Nevertheless, speed, separated for loaded and empty vehicles, was plotted against MCV, for all the machine types. This plot was linearly extrapolated back to zero velocity to estimate the moisture condition value at the point of immobilisation. The validity of this extrapolation must be questioned as all site managers would cease operations prior to this scenario occurring. A general linear regression equation was developed, equation 2.52, to estimate the MCV required to enable a vehicle to travel at a certain velocity.

$$MCV_{(V)} = 15.8 - 0.35V + (0.054V - 0.783)N + (0.031V - 0.399)T - \\ - (0.00084V + 0.00184)P + (0.113 - 0.003V)M \qquad (2.52)$$

where: $MCV_{(V)}$ minimum moisture condition value required
V vehicle velocity (km/h)
N number of driven wheels
T tyre width (inches)
P maximum available engine power (kW)
M total vehicle mass (tonnes)

This regression equation was developed from the immobilisation MCV extrapolated for each vehicle, with the various vehicle parameters. Since all the equations were assumed to be linear, the MCV required for any velocity was easily formulated. During validation of equation 2.52 it was found to be invalid for articulated dump trucks and should only be applied to rigid dump trucks and motorised scrapers.

Parsons et al. (1988), carried out tests on soils close to the limits of trafficability of on- and off-road earthmoving plant. Tests were completed on three different soils

in a bin. The results of this study were to supersede those from Parsons et al. (1982) relating single pass rut depth to MCV, and incorporate the parameter rolling resistance. Rolling resistance was calculated in a similar manner to that of Zink et al. (1934), where the vehicle was towed over a flat test track with a dynamometer housed in the hitching mechanism. This assumes that a vehicle towed at 4km/h, will have an identical rolling resistance as a self-propelled one, independent of velocity. The vehicles were tested in four different soil conditions defined by MCV'S of approximately 6,7,8, and 9, and at three different levels of payload: full, half full, and empty. These low MCV values, representing a relatively wet, weak soil, yielded a minimum first pass rolling resistance of 14% equivalent grade, the description of which, according to Caterpillar (1993) would be:

> "Rutted dirt roadway, soft under travel, no maintenance, no stabilisation, 200mm tire penetration and flexing."

The empirical relationships between first pass rut depth and MCV, equation 2.53, and rolling resistance and MCV, equation 2.54, were found to be very encouraging with correlation coefficients in excess of 0.85.

$$\text{Rut Depth, } z = a\,e^{-kB} \tag{2.53}$$

where: $a = 0.00193\frac{D}{n}\left(\frac{W}{bD}\right)^{1.4}$

$k = 0.515$

$B = 10^{\frac{MCV}{10}}$

$$\text{Rolling Resistance, } R_0 = 0.0154\,n^{-0.717}\left(\frac{W^2}{bD}\right)e^{-0.4113} + 0.05W \tag{2.54}$$

where: n number of axles

W total mass

b nominal wheel width

D wheel diameter

The authors caution against using the above equations if any of the vehicle parameters has a value outside the range tested. It is noteworthy that the constant term at the end of equation 2.54, the internal component of rolling resistance caused by transmission losses, etc., has a value of 5% equivalent grade. This value of internal rolling resistance is 2.5 times that quoted by manufacturers (Terex, 1981, VME, 1989, Caterpillar, 1993). This increase in rolling resistance would reduce the maximum velocity of a Volvo BM A35, 6x6, articulated dump truck, on a level haul, from 49 to 30 km/h.

On combining the new results with previous data from Parsons et al. (1982) an updated version of equation 2.52 was developed as below:

$$MCV_{(V)} = 10.7 + 0.057V + (0.052V - 1)N + (0.55V - 7.5)T - \\ - (0.0009V + 0.0041)P + (0.0076 - 0.000038V)M \qquad (2.55)$$

with the nomenclature as before. Equation 2.55 was considered valid for all types of vehicle tested, but is valid only for the velocity range investigated, which was limited to soils close to the limit of trafficability of the plant. In the majority of earthmoving conditions the soil is a lot drier, therefore stronger, and the plant is capable of travelling at much faster velocities. The relationship between earthmoving plant and this type of soil condition has never been investigated.

2.15 Discussion

It is evident from the preceding sections that the definition of rolling resistance changes depending on the author and the purpose of the research. It is therefore important to state clearly which definition is being utilised. Most of the research, in this field, has been undertaken by agricultural or military engineers. The outcome of this are that: the work has not been orientated towards civil engineering soil mechanics, the documentation and description of soils has lacked the required detail, the specific topic of civil engineering earthmoving has been overlooked, and little experimentation has been carried out on civil engineering haul road conditions.

Many approaches on the mobility problem have been made, but, except by direct measurement, none of them consider the vehicle as a complete identity, concentrating only on a single wheel. The majority of the available techniques require considerable instrumentation of either the soil and/or the vehicle, which is exceptionally expensive and time consuming if a fleet of vehicles is to be tested.
Some of the theoretical methods described above are based on assumptions that are unrealistic and the solution procedures are not conducive to practical results. Furthermore some of the theoretical methods, such as finite elements, have not been validated in the field. As expressed by Wong (1989):

> "... the theoretical methods currently available have not been developed to a point which can be considered practically useful for the performance prediction of tires in the field.

The primary conclusion to be drawn from this literature survey is that no general theory for rolling resistance exists which is of direct value to the engineer interested in the performance of earthmoving vehicles on civil engineering haul roads. It would be folly to extrapolate existing semi-empirical theories to that of the earthmoving scenario as the majority of the experimentation has been carried out on towed, small diameter rigid wheels. The most promising method of measuring rolling resistance in the field would appear to be that adopted by Norman (1965), discussed fully in the next chapter, and is in fact the approach adopted in this thesis. The methodology proposed by the Transport Research Laboratory, Crowthorne, was considered to be well founded and a similar technique was attempted in order to predict the performance of earthmoving plant on different soil conditions.

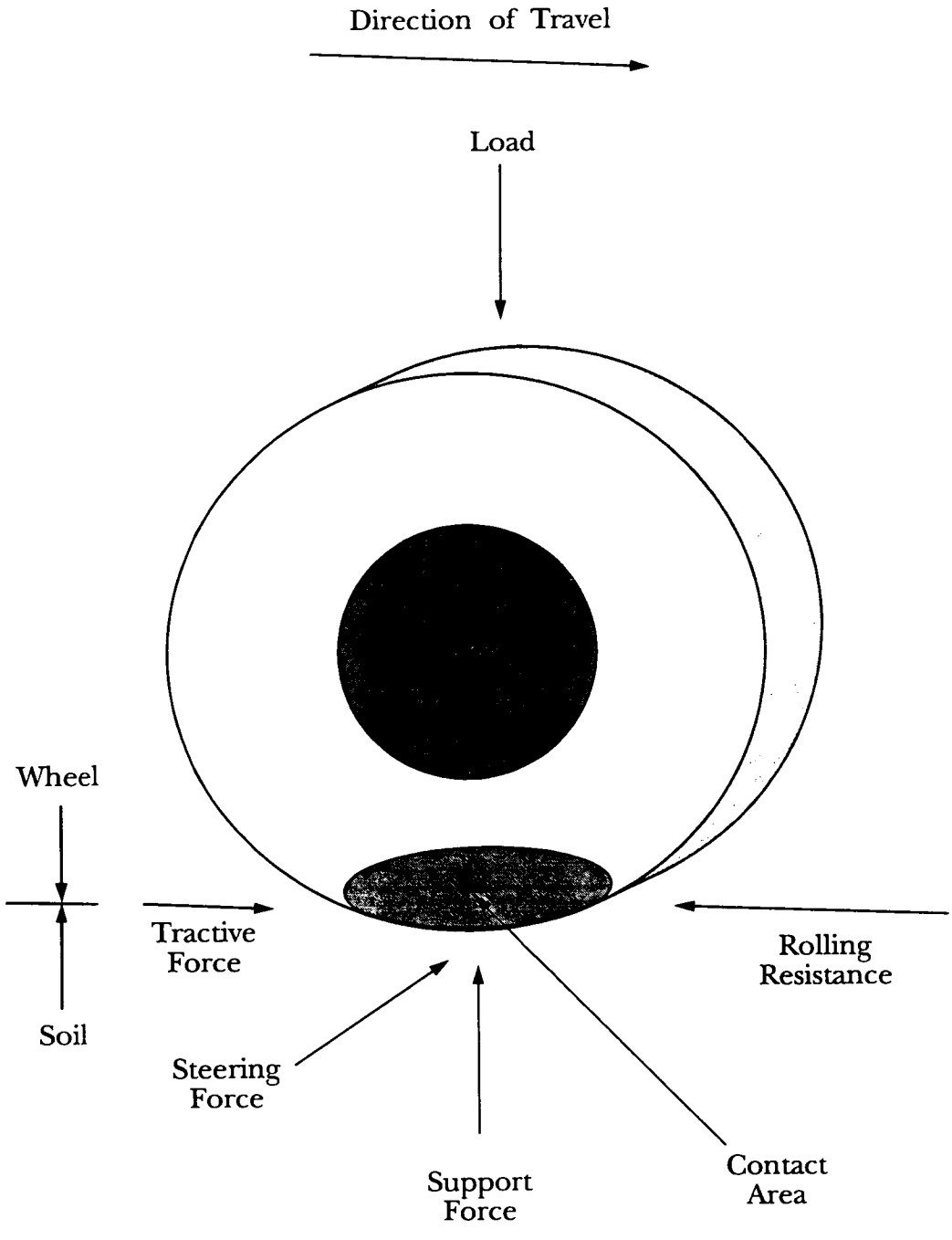

Figure 2.1: Forces Acting on a Wheel Operating on Soil

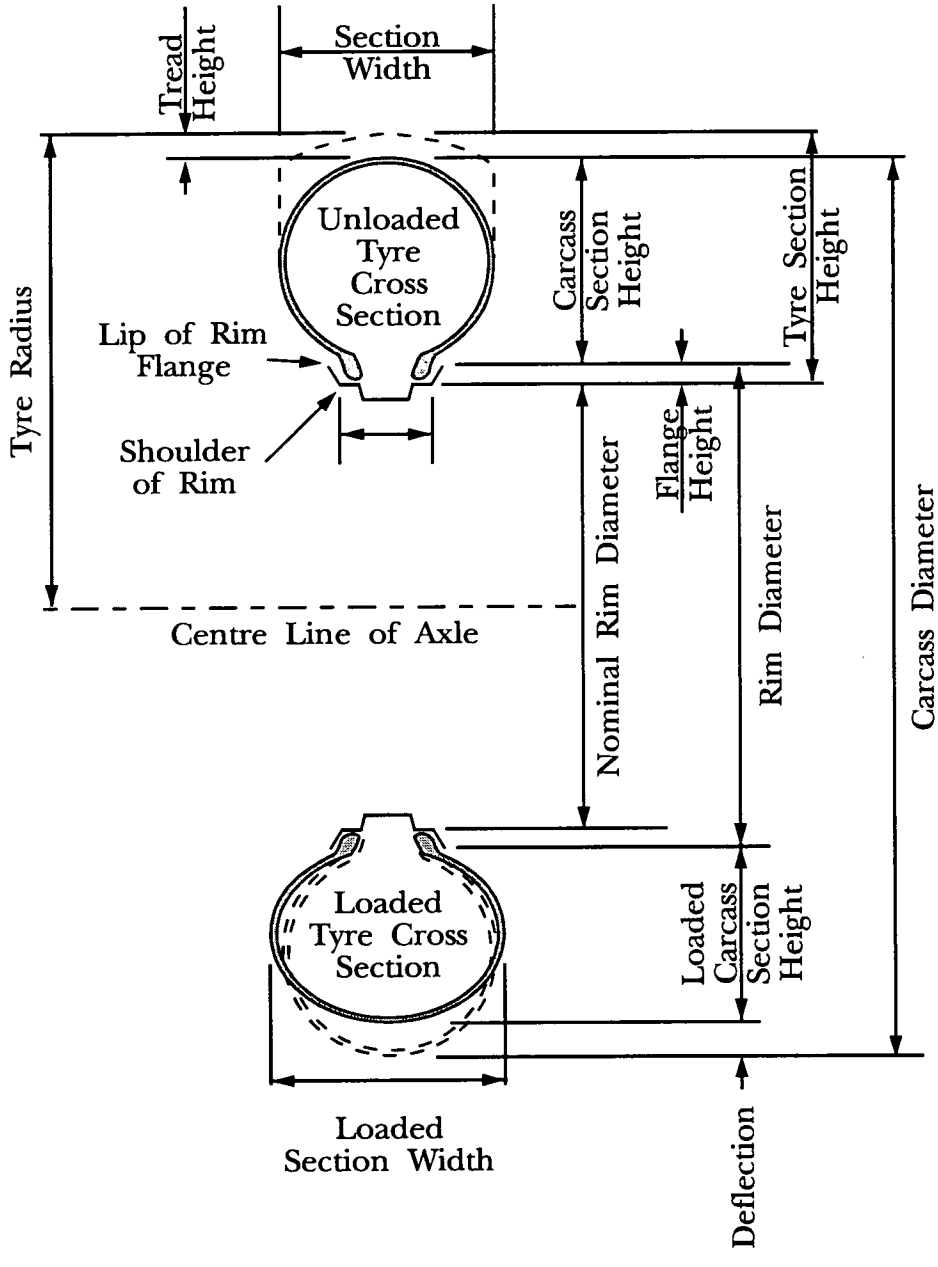

Figure 2.2: Some Pneumatic Tire Dimensional Factors (after Meyer, 1977)

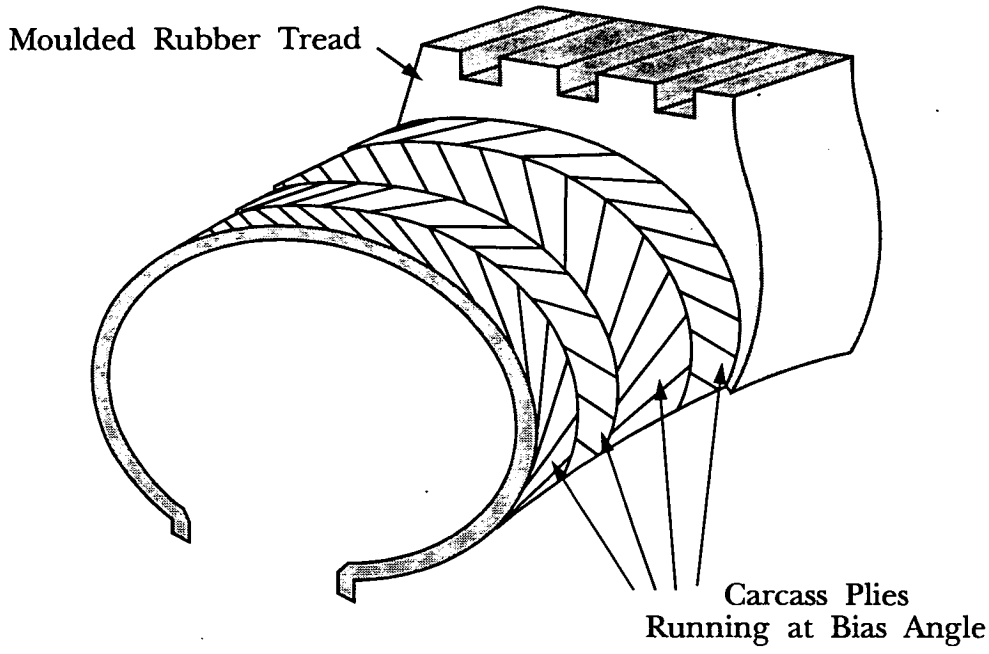

(a) Bias-ply Tyre Construction

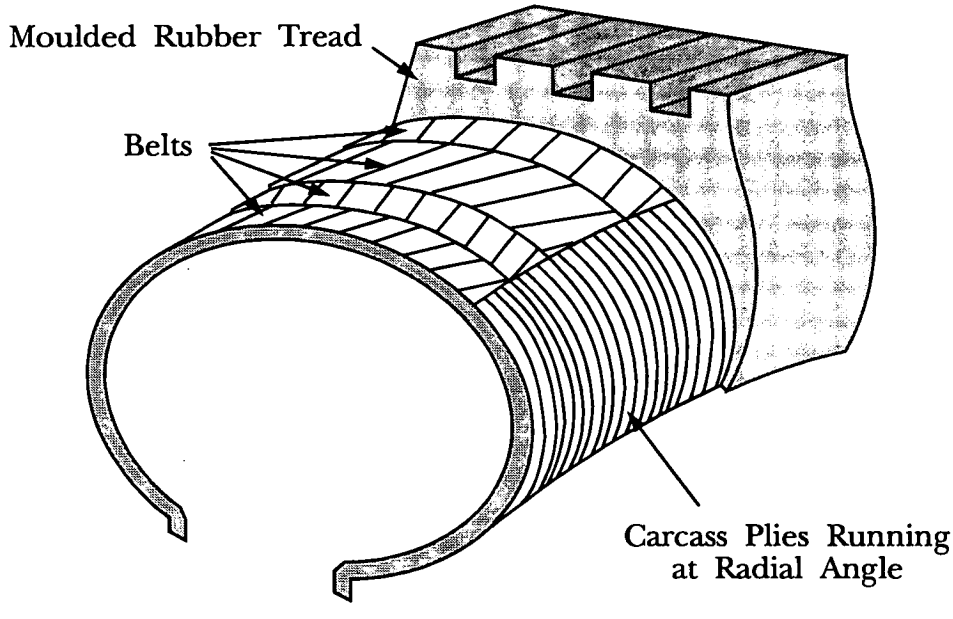

(b) Radial-ply Tyre Construction

Figure 2.3: Schematic Representation of Two Forms of Tyre Construction

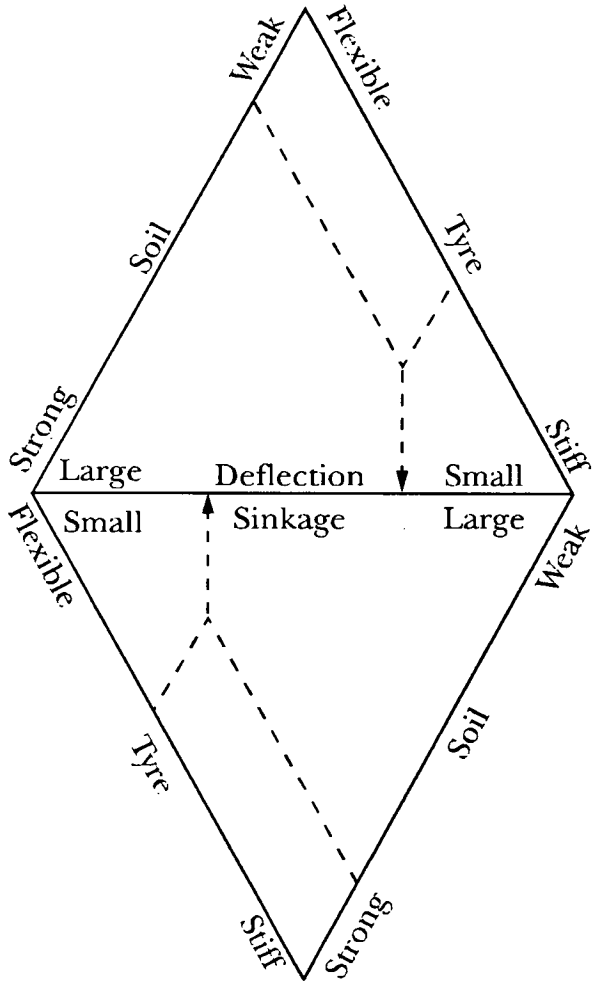

Figure 2.4: Schematic Representation of Tyre-Soil Behaviour (after Karafiath and Nowatzki, 1978)

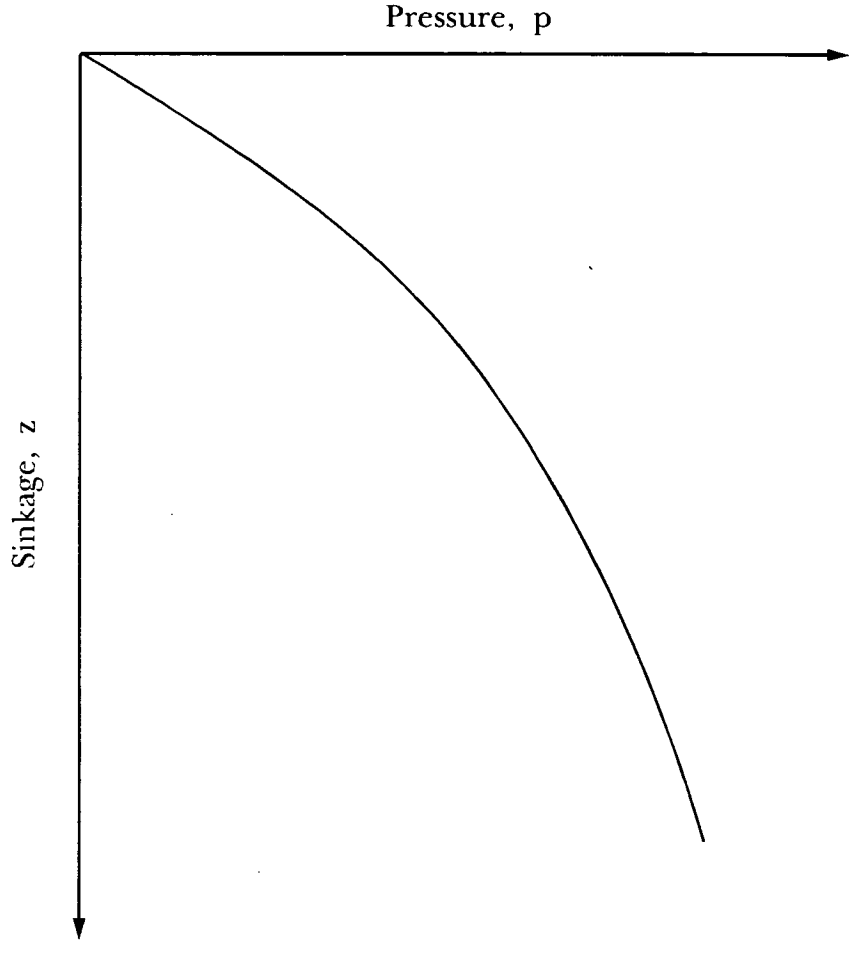

Figure 2.5: Relationship Between Static Sinkage and Pressure

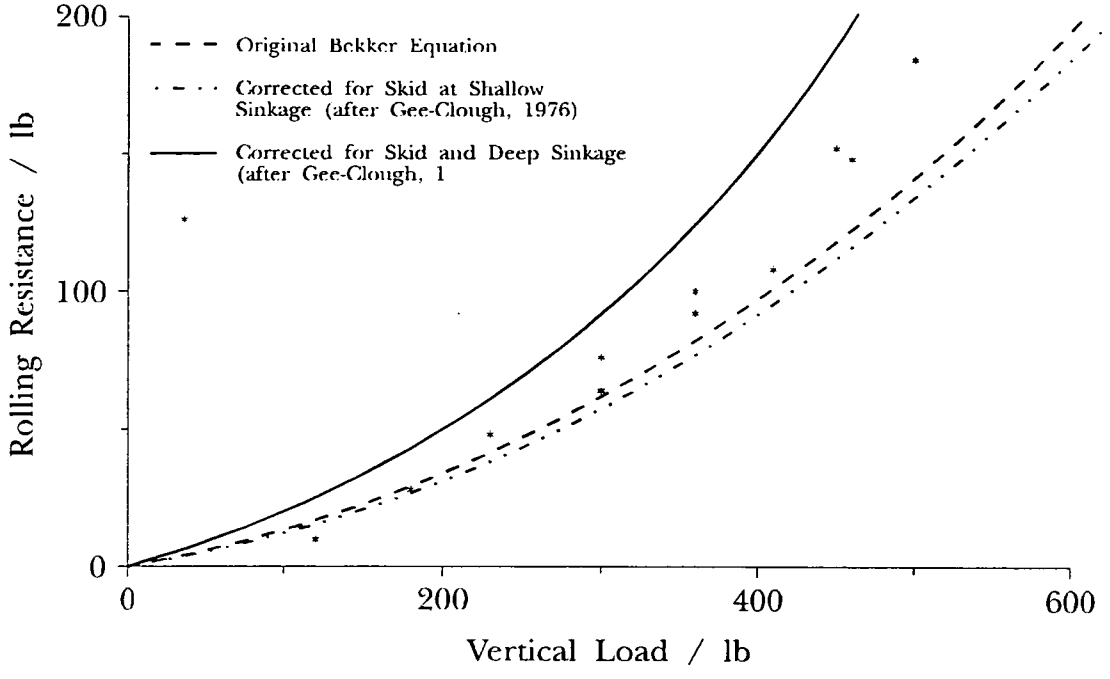

Figure 2.6: Comparison of Measured and Predicted Values of the Rolling Resistance of a 20" x 3" Rigid Wheel on Clay

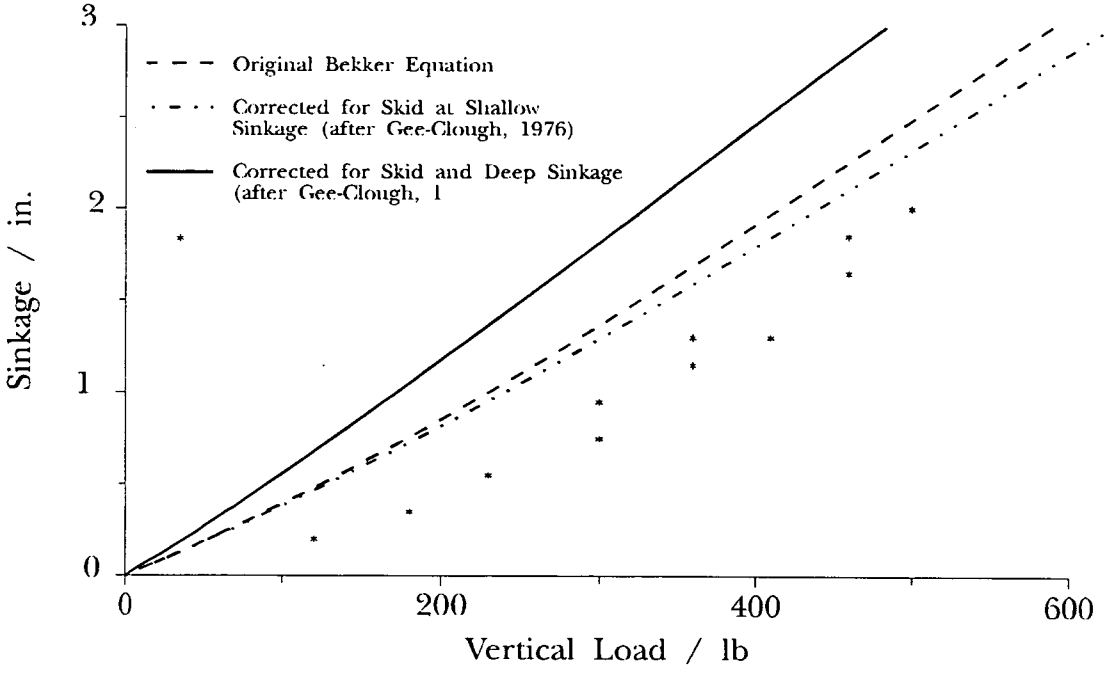

Figure 2.7: Comparison of Measured and Predicted Values of the Sinkage of a 20" x 3" Rigid Wheel on Clay

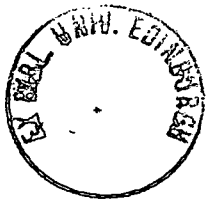

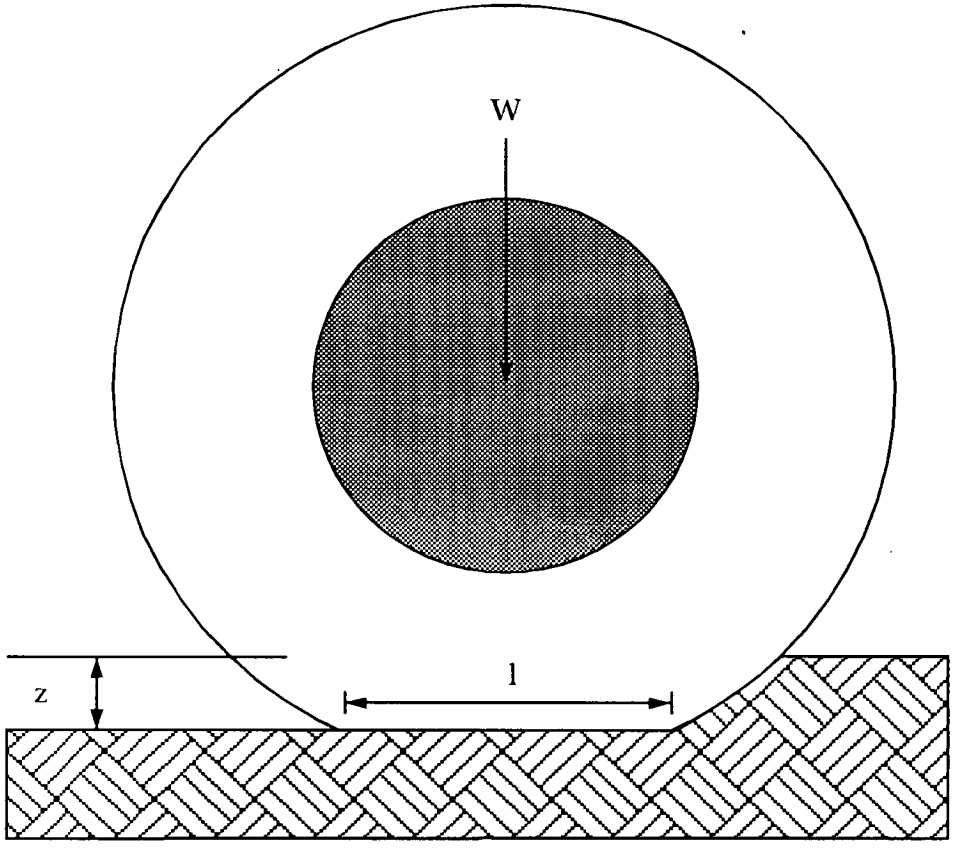

Figure 2.8: Pneumatic Tyre Deformation in Soft Soil, as Proposed by Bekker

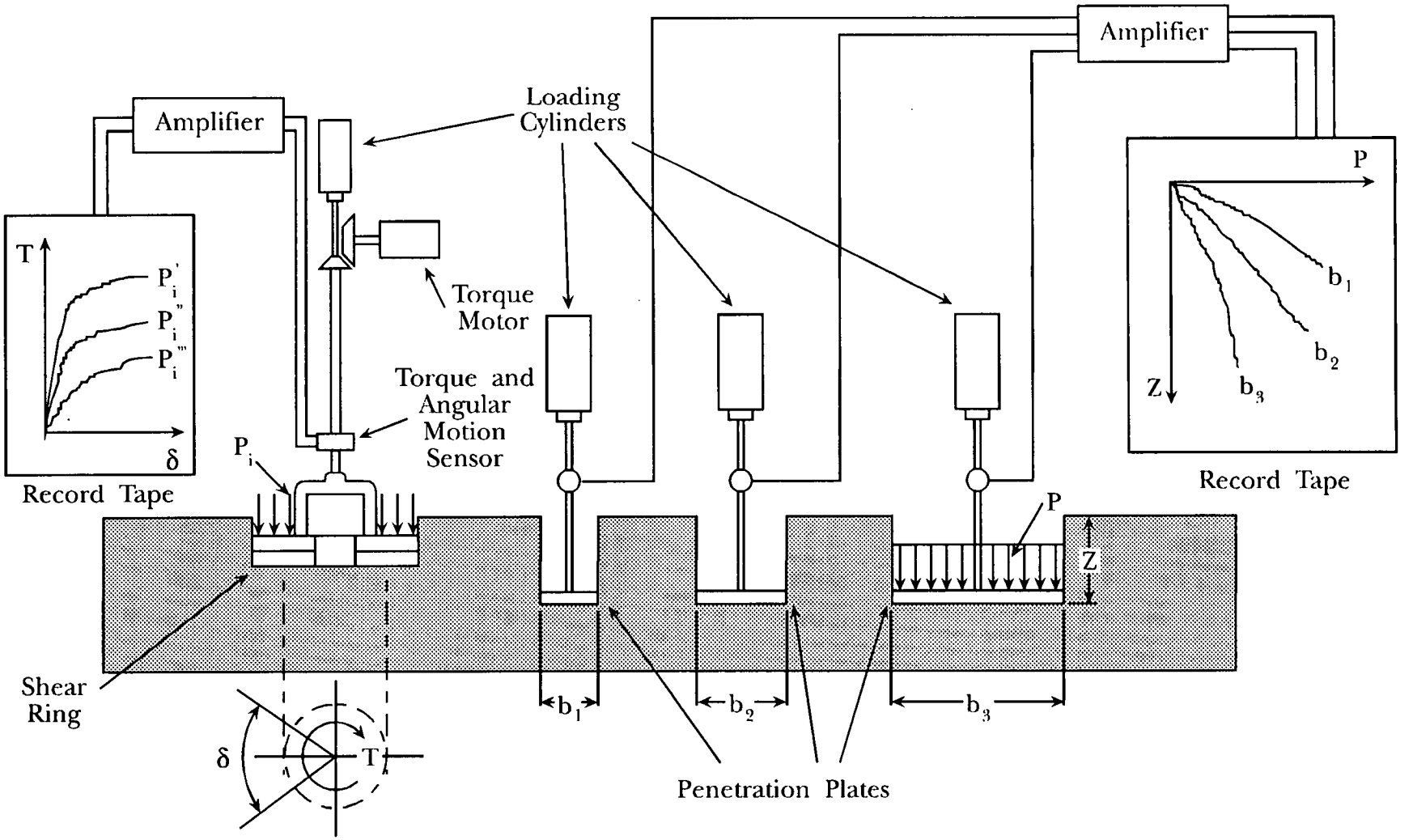

Figure 2.9: Schematic View of a Bevameter Type Instrument

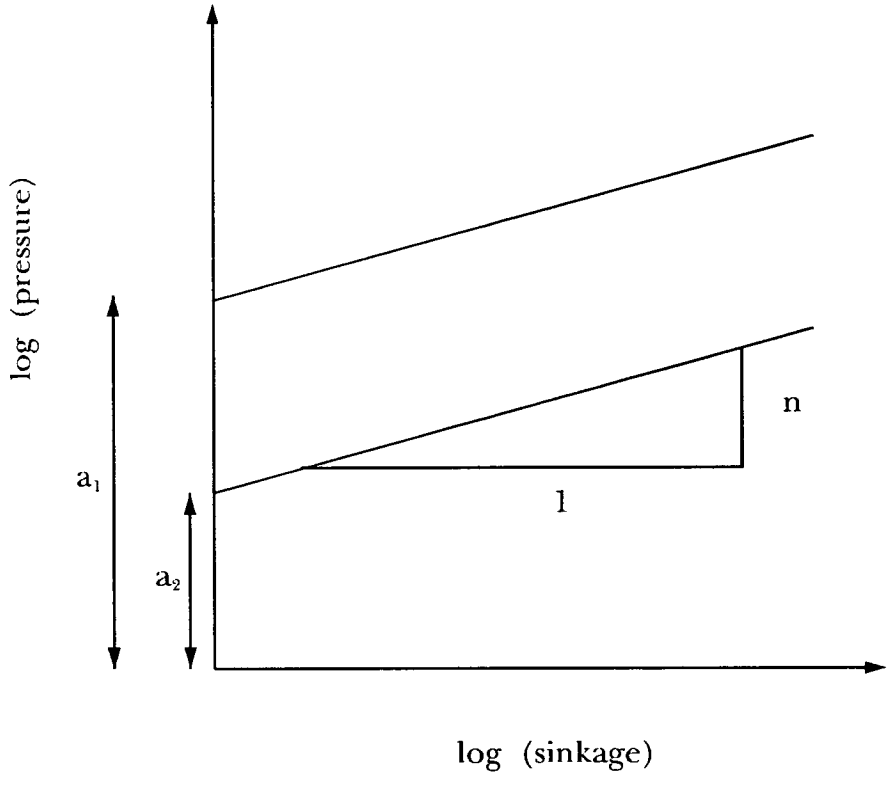

Figure 2.10: Graphical Method for Calculating Sinkage Moduli and Exponent

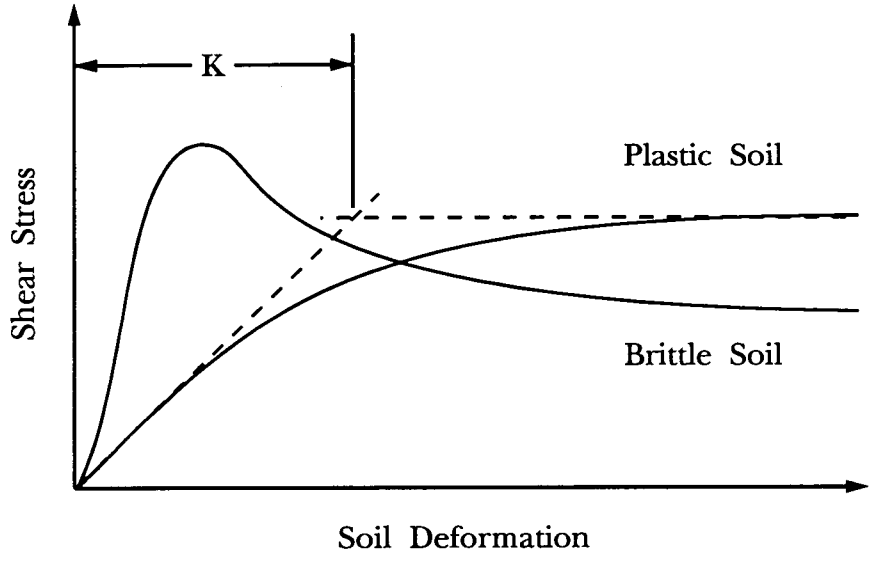

Figure 2.11: Idealised Shear Stress - Deformation Graphs for both Brittle and Plastic Soil Masses

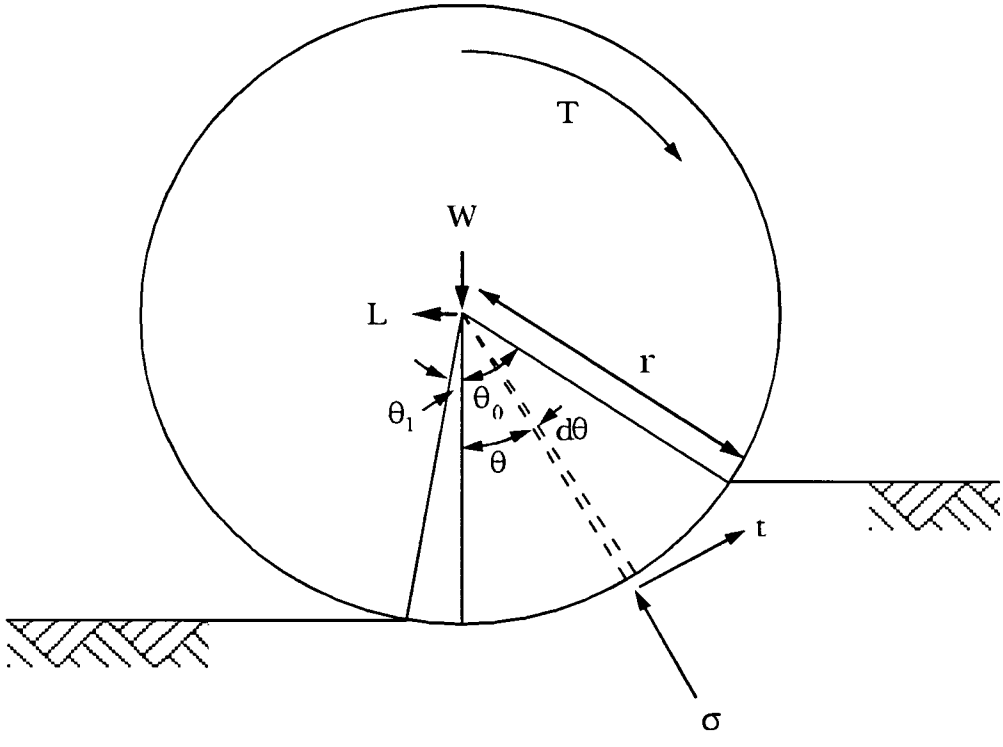

Figure 2.12: Statics of a Rigid Wheel on Deformable Soil (after Onafeko, 1969)

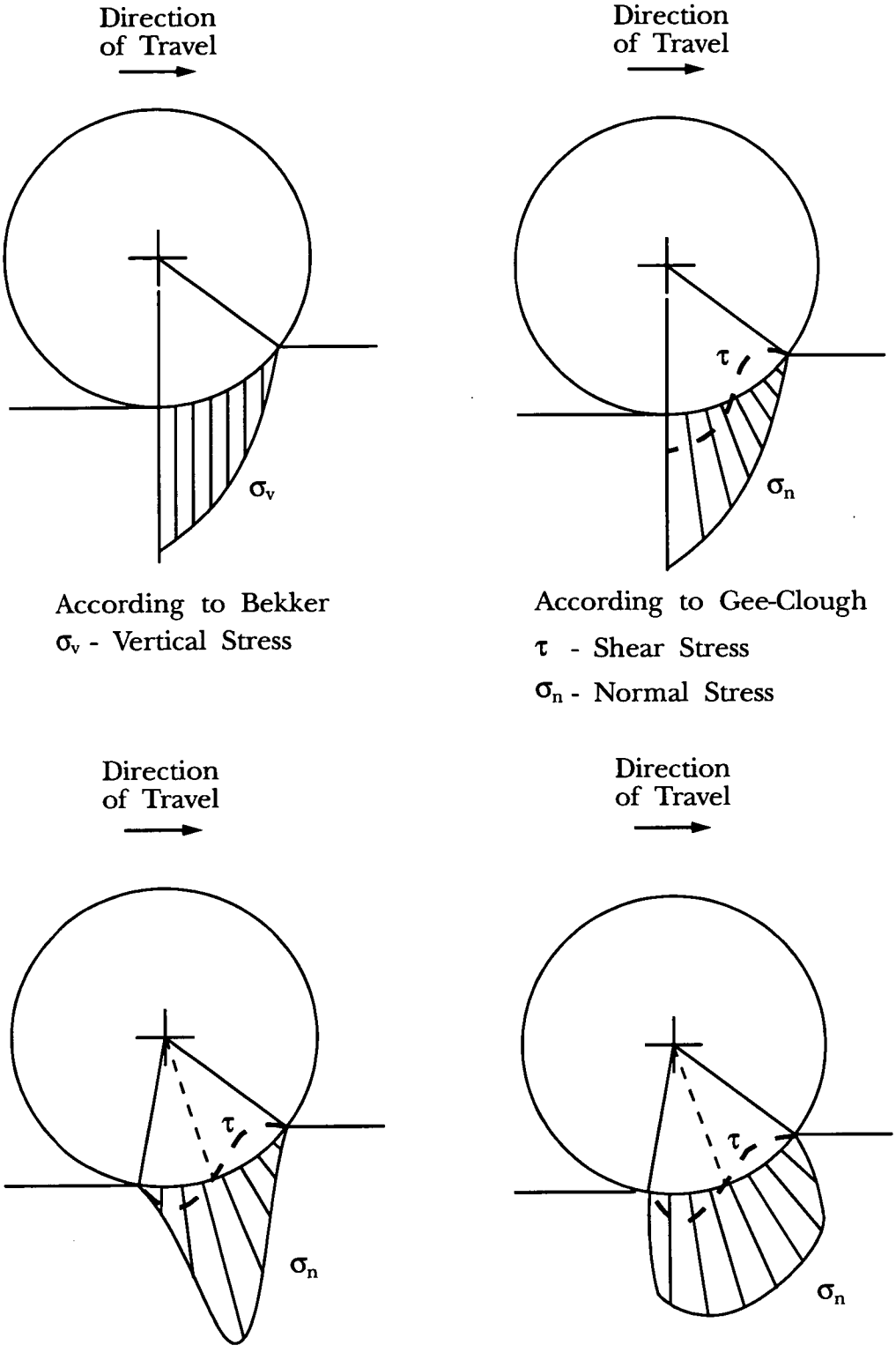

According to Bekker
σ_v - Vertical Stress

According to Gee-Clough
τ - Shear Stress
σ_n - Normal Stress

Experiments in Sand

Experiments in Clay

After Hegedus, 1965, Onafeko et al., 1967, and Krick, 1969.

Figure 2.13: Distribution of Interface Stresses Beneath Towed Rigid Wheels

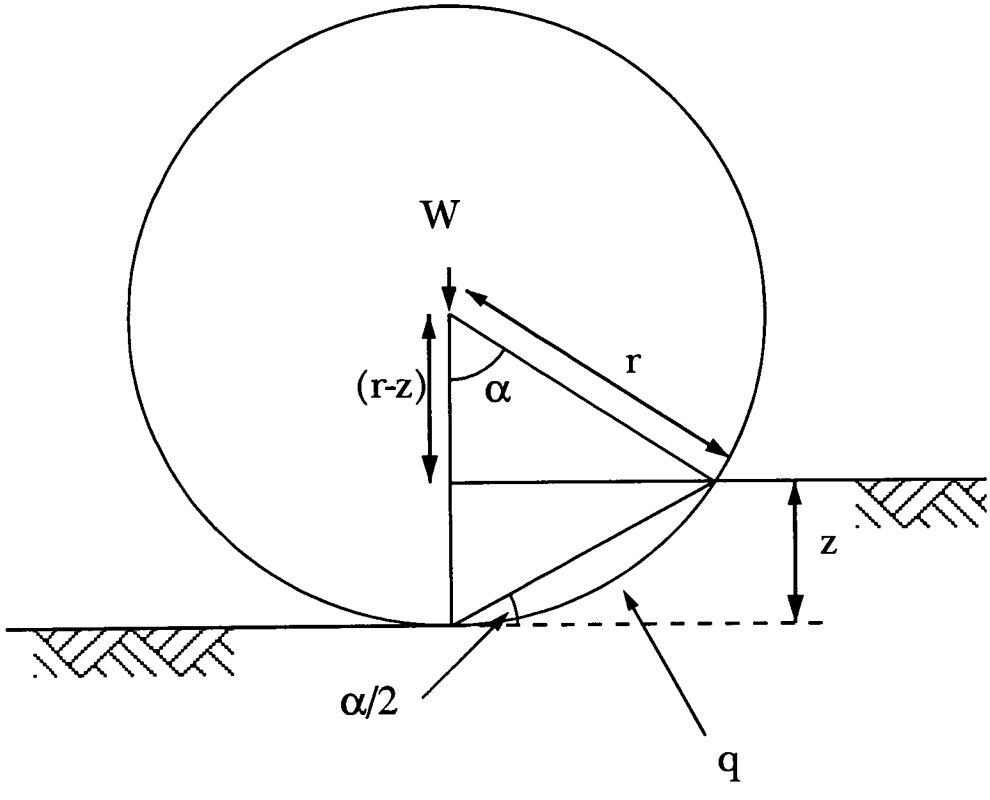

Figure 2.14: Schematic View of Wheel for Uffelmann's Theory

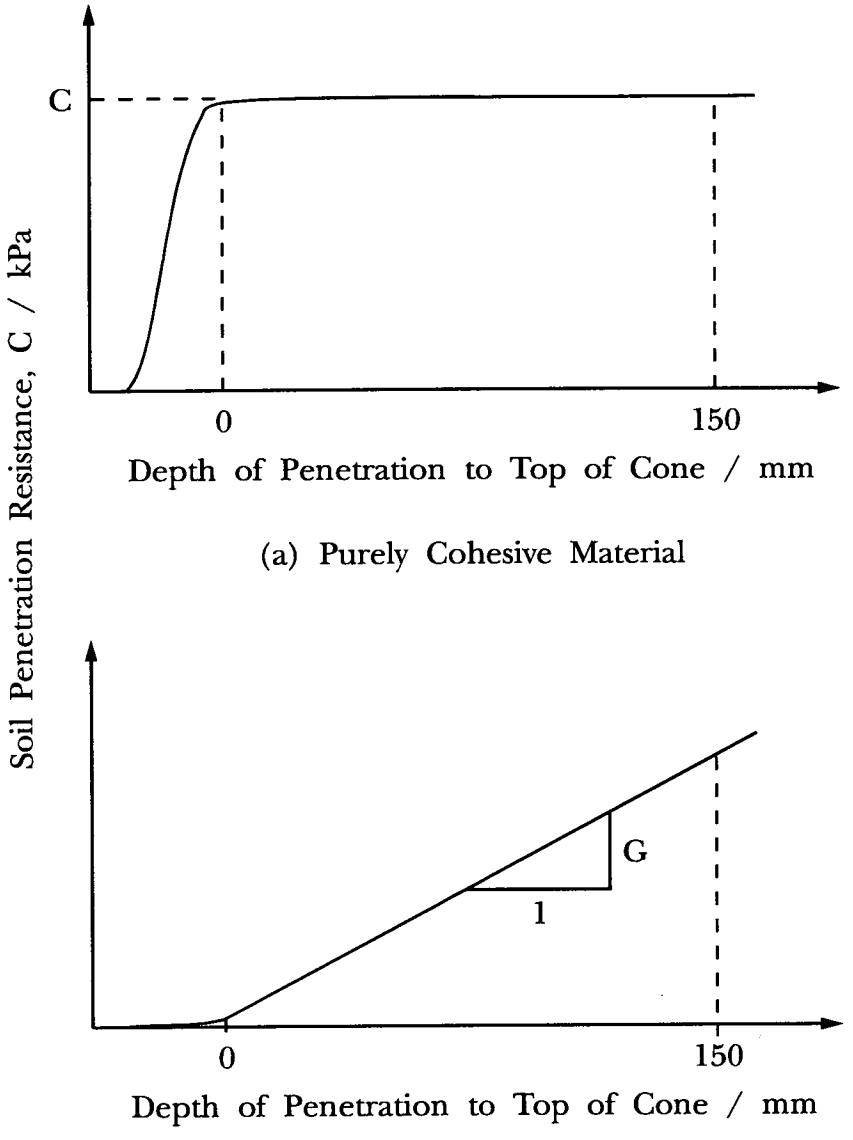

Figure 2.15: Ideal Plots of Soil Penetration Resistance versus Depth to Top of Cone, in a Purely Cohesive and Purely Frictional Material.

Variable	Symbol	Dimensions
Independent Variables		
Tyre		
Diameter	d	L
Section width	b	L
Section height	h	L
Deflection	δ	L
Soil		
Friction Angle	ϕ	-
Cohesion	c	FL^{-2}
Specific weight	γ	FL^{-3}
Spissitude	β	FTL^{-2}
System		
Load	W	F
Translational Velocity	V	LT^{-1}
Slip	i	-
Tyre-soil friction	μ	-
Acceleration due to gravity	g	LT^{-2}
Dependent Variables		
Pull	H	F
Towed Force	P_T	F
Torque	Q	FL
Sinkage	z	L

Table 2.1: Tyre-Soil System Variables Identified by Freitag

$\pi_1 = \frac{H}{W}$	$\pi_8 = \frac{b}{d}$
$\pi_2 = \frac{P_T}{W}$	$\pi_9 = \frac{h}{d}$
$\pi_3 = \frac{Q}{dW}$	$\pi_{10} = \frac{d}{h}$
$\pi_4 = \frac{z}{d}$	$\pi_{11} = \frac{cd^2}{W}$
$\pi_5 = \mu$	$\pi_{12} = \frac{\gamma d^3}{W}$
$\pi_6 = \phi$	$\pi_{13} = \frac{\beta V d}{W}$
$\pi_7 = i$	$\pi_{14} = \frac{gd}{V^2}$

Table 2.2: Buckingham Pi Terms used by Freitag

	Plastic Limit /%	Liquid Limit /%	Moisture Content /%	$\frac{\text{Moisture Content}}{\text{Plastic Limit}}$	Consistency Index	Undrained Shear Strength / kN/m^2
London Clay	30	80	36	1.20	0.88	66
Lothian Clay	20	35	24	1.20	0.73	35

Table 2.3: Parameters used for Example

Chapter 3 Rolling Resistance

3.1 Introduction

This chapter will investigate various definitions of rolling resistance used in practice and how this parameter affects the velocity of the vehicles using three different methods of calculation. There are two methods of calculating rolling resistance in order to estimate the performance of the vehicles, firstly using one of the methods described in the previous chapter relating rolling resistance to various input parameters. Secondly, empirical tables constructed through experience can be used to estimate the value of rolling resistance. From the civil engineering point of view the first method is impractical as either the soils test work required is too specialised or the input parameters are unknown without a significant amount of vehicle instrumentation, which is uneconomic when working at such low profit margins.

The theoretical development of rolling resistance has been discussed in the previous chapter. The remainder of this chapter will therefore deal solely with the empirical determination of rolling resistance.

3.2 Definition of Rolling Resistance

The Volvo performance handbook, (VME, 1989) describes rolling resistance concisely by:

> "When driving, energy is absorbed by the deformation of tyres and ground. An example of this is rutting. The restraining effect this has on the vehicle is called rolling resistance".

Rolling resistance is therefore a measure of the force that must be overcome to roll, or pull, a wheel over the ground surface. The deeper the tyre penetrates into the soil, the higher the value of rolling resistance. This can be thought of as the wheel having to continually climb out of a rut. The rolling resistance is affected by various factors including: soil type, moisture content, condition of the running surface, wheel loading, dimensions of the tyre, tyre construction and pressure,

internal friction, and the driver. Each of these factors will be dealt with in turn for vehicles travelling on a typical civil engineering haul road:

- Soil type - all other factors being similar, a vehicle travelling on a sand will cause the soil to fail in a different manner than a clay soil.

- Moisture Content - as the moisture content of a soil increases the undrained shear strength of the soil decreases, therefore the wheel causes a larger rut increasing the rolling resistance.

- Conditions of the Ground - if the ground is very hard and smooth the vehicle will travel quickly at a low rolling resistance, however if there are obstructions on the haul road then these will slow the driver-vehicle system, effectively increasing the rolling resistance.

- Wheel Loading - if the tyre pressure remains the same, then as the mass of the vehicle increases the tyre penetration will increase, augmenting the value of rolling resistance.

- Dimensions of the Tyre - the dimensions of the tyre dictate the pressure distribution at the tyre-soil boundary. Hence, if either the width, or diameter of the tyre increase, the ground contact pressure will decrease, significantly reducing the resulting rolling resistance, (McKibben et al., 1940b).

- Tyre Construction and Pressure - tyre construction; radial or bias ply, and carcass stiffness, have been shown to have a minimal effect on rolling resistance, (Gee-Clough et al., 1977). The inflation pressure of the tyre has an effect on the rolling resistance, (McKibben et al., 1940, Yong et al., 1978), on hard ground a high inflation pressure is desired to minimise the contact area, but on a soft soil it is more efficient to lower the inflation pressure in order to reduce the contact pressure and hence lower the tyre penetration.

- Internal Friction - this is caused by losses within the driving mechanism of the vehicle and can only be kept at a minimum via a stringent maintenance procedure.

- Driver - no two operators react to identical driving conditions in a similar manner. A younger driver is apt to be slightly more careless increasing the speed, decreasing the apparent rolling resistance of the driver-vehicle system. Vibrations, transmitted through the vehicle to the driver, caused by the condition of the haul road and the speed of the vehicle also cause variations in the speed, and hence rolling resistance. As the driver gets tired, the reaction time, along with the speed of the vehicle decreases, increasing the apparent rolling resistance.

Clearly, from this discussion on the factors affecting rolling resistance, the driver can have a major effect on the rolling resistance. This is not normally considered when estimating the rolling resistance of a section of haul road. At the present time all the tables giving estimates of the rolling resistance assume an *average operator*, and in the main do not differentiate between the various types of plant that have completely different types of running gear (tyres or tracks).

Vehicle manufacturers quote values of rolling resistance in percent equivalent grade; grade resistance is caused by the vehicle having to lift itself as it travels forward, uphill grades have positive grade resistance. Calculation of grade resistance is calculated by dividing the change in height by the corresponding change in the horizontal direction, this can be calculated using a theodolite or a clinometer and should never be estimated by eye.

Initially rolling resistances were calculated as a force, as the difference between the thrust, and the power available at the drawbar for towing, (McKibben et al., 1939b). Knowing the mass of the vehicle it is easy to convert from resistance as a force to a percentage of gross vehicle weight. Since grade and rolling resistances can be expressed in the same units they can be added giving a value of total resistance, equation 3.1.

$$\text{Total Resistance} = \text{Grade Resistance} + \text{Rolling Resistance} \qquad (3.1)$$

Air resistance is another retarding force on the vehicle. This is normally ignored in the case of earthmoving vehicles, as they do not travel at a fast enough rate to generate a significant resisting force.

From experience, manufacturers have produced rolling resistance tables, tables 3.1 and 3.2. Comparing the two charts it is clear that there is a wide range in rolling resistance for vehicles travelling in off-road conditions. The descriptions are of use only after the ground has been trafficked. Unfortunately, this is of limited use to the estimator, who needs to calculate the performance of the vehicles prior to commencement of operations. On the whole the Volvo and Caterpillar rolling resistance tables are in agreement except in the relationship between tyre sinkage and rolling resistance. Specific categories also show large discrepancies, for example *loose sand and gravel* in table 3.1 has a range of 15-30% whereas table 3.2 gives a single value of 10% for the same category of road material. It shall be shown later that these differences have a great effect on the expected speed of travel of the vehicles.

The rolling resistance charts give a rough indication of the quality of the haul road, but does not show how fast the vehicle will be able to negotiate a particular stretch of haul road. Presently the velocity of the vehicles can be estimated in one of two ways, the manufacturers' specification sheets, or by the use of a computer program. For the studies reported herein, two computer programs were available: Accelerator, developed by Accelerator Inc., Fort Myers, and Vehsim developed at Caterpillar Inc., Peoria.

3.3 Manufacturers' Specification Sheets

The manufacturers' specification sheets give the basic information on the vehicle, including: engine details, gear ratios and corresponding maximum speeds, braking systems employed, dimensions, weights, rimpull and retardation charts, and lists of standard and optional equipment. These sheets indicate how to calculate velocity using rimpull charts, figure 3.1. Rimpull is a term used to designate the tractive force between the driving pneumatic tyres and the running surface, but is limited by traction. Rimpull is measured in units of mass, or force and is generally given in the manufacturers' specifications, but can also be calculated from equation 3.2 (Peurifoy et al., 1985), or 3.3 (VME, 1989).

$$\text{Rimpull(kg)} = \frac{\text{constant x engine power(kW) x efficiency}}{\text{speed (km / h)}} \qquad (3.2)$$

for the metric system of units the constant equals 367.

$$\text{Rimpull(kg)} = \frac{\text{GVW(kg) x Total Resistance(\%)}}{100} \qquad (3.3)$$

where: GVW is the gross vehicle weight.

To calculate velocity using the manufacturers' specification sheets, figure 3.1, the mass of the truck and the total resistance of the driver-vehicle-terrain system must be estimated. The velocity is calculated as follows; from the value of total resistance on the right hand side of figure 3.1, follow the diagonal line until it intersects the required mass of the vehicle, normally net vehicle weight (NVW), or gross vehicle weight (GVW). From this point, read horizontally to the left until the graph of rimpull versus speed is intersected, then read down to give the vehicle speed.

When the vehicle is travelling on long steep negative slopes, exceeding -5% total resistance, the vehicle's retarder, or exhaust brake, will be in operation and the velocity should be estimated using a retardation chart, figure 3.2. The exhaust brake is used on longer slopes as the wheel brakes can experience fading due to overheating.

The major drawback of the rimpull and retardation charts is that only the maximum attainable velocity is ascertained, therefore the acceleration characteristics of a vehicle cannot be determined easily. This makes the estimation of travel time and productivity exceptionally difficult.

Other charts published by the various manufacturers include: travel times at different total resistances, travel times through curves with varying lengths and radii, and traversability at different coefficients of traction and total resistance. These charts are produced for each vehicle in both the empty and fully loaded conditions and are modifications of the basic rimpull and retardation charts.

3.4 Computer Programs

Two computer programs: Accelerator, (Accelerator, 1987) and Vehsim, (Caterpillar, 1987) were available for estimating vehicle performance. These two programs have essentially the same input parameters, but calculate the acceleration of the vehicle in different ways. Vehsim uses computerised rimpull charts whereas Accelerator calculates the vehicle performance from the weight to power ratio. The following sections will describe and discuss the two programs.

3.4.1 Vehsim

The Vehsim computer package was developed by W.C. Morgan at Caterpillar Incorporated, Peoria, USA. This package was developed solely for the earthmoving market and is menu driven. Vehsim allows estimations to be made for velocities, travel times, production rates, and costings.

The program has six main menus: haulers, courses, simulate, display, print, and other. The *haulers* and *courses* menus define which vehicles and courses will be used in the simulation and allows additions and modifications to be made to existing data bases. The *simulate* menu allows a list of all vehicle-course combinations to be viewed and the subsequent simulations to be computed. The *display* menu allows the output of the analysis to be viewed, the *print* menu allows various reports to be printed, and the *other* menu is for customising the program and file management.

The required vehicle input parameters are shown in figure 3.3, and as can be seen does not contain a substantial amount of detailed specifications. As the program calculates the performance from computerised rimpull curves, the main sections for the subsequent analyses are the gear shifting velocities and the velocity-rimpull characteristics. These values define the speed when the vehicle should change gear, and the amount of pull corresponding to each velocity. The program linearly interpolates between the entered values. From the computerised velocity-rimpull curve the road power can be calculated for any combination of these two, using equation 3.2. Knowing power and velocity, the accelerating force can be calculated from fundamental mechanics, equation 3.4, the vehicle acceleration is then

calculated by dividing the accelerating force by the mass, equation 3.5. As the vehicle accelerates or the haul road profile changes, the vehicle's velocity will change, slightly altering the available road power, the force available for acceleration, therefore the computer program must continually update the performance of the vehicle.

$$\text{Force(kN)} = \frac{\text{Power(kW)}}{3.6 \text{ x Velocity(km/h)}} \qquad (3.4)$$

the constant on the denominator it to maintain consistency in the units.

$$\text{Acceleration}(m.s^{-2}) = \frac{\text{Force(N)}}{\text{Vehicle mass(kg)}} \qquad (3.5)$$

Once the required vehicles have been defined the courses must be entered as segments of the complete haul route. These segments should be as constant in grade and curvature as practical. Provisions for loader type and any known obstructions that will cause time delays can be easily incorporated. The length, grade, rolling resistance, and curvature, if any, must be entered for each section of the haul road. The only guidance given on the value of rolling resistance to use is in a form similar to that given in table 3.2.

Discussions with the author of the software (Morgan, 1993) on the subject of rolling resistance were informative. At the time of the meeting the table of rolling resistance coefficients that Caterpillar published, and had published for many years, was a simplified version of table 3.2. This table was used by members of the company to estimate the rolling resistance for any consultancy contracts, for input into the Vehsim software. The results of the project to that date were presented to members of the company dealing with earthmoving on a day to day basis and the feedback on the advancement of the project was very positive. Discussion on the recorded values of rolling resistance followed and particular interest was shown in the results concerning the effect of grade and haul road condition on the apparent rolling resistance, sections 4.6, 5.6.1 and 5.6.7. Possibly, for this reason, the updated version of the rolling resistance factor table, (Caterpillar, 1993), table 3.2, has an extra three rolling resistance categories,

splitting the old 10-20% bracket for a "soft muddy, rutted roadway, no maintenance", (Caterpillar, 1992).

3.4.2 Accelerator

The Accelerator system was developed by R.D. Pugh for estimating the speed of any wheeled vehicle on any ground condition, and is being further developed by him for VME. The program is based around four separate but interconnected screens: vehicle, test, road, and job. The *vehicle* screen, figure 3.4, is used to describe the vehicle's power, weight, tyres, and other relevant configuration data. The *test* screen is basically a spreadsheet where each line is a separate enquiry into the performance of the vehicle in the vehicle screen. The *road* screen is a worksheet for constructing haul road profiles and for initiating travel time calculations. Finally the *job* screen shows a summary of the travel time calculations, and its subsidiary automatic job control screen can be used to automate a series of different vehicles on different haul roads. The four screens are all interrelated and it is simple to switch between the various screens.

The Accelerator software computes vehicle performance using the vehicle's average weight to power ratio, figure 3.4. This ratio is a measure of how much power is available to overcome motion resistance. Accelerator assumes that the available road power does not change significantly over the range of operating velocities. A rimpull option is available in the secondary vehicle screen to estimate the average road power. Corresponding velocities and rimpull data are entered from the vehicle specification sheets and the program calculates the available road power using equation 3.2. Once several points have been entered, the average road power stabilises, and this can then be entered in the vehicle screen, figure 3.4. The algorithm the program uses for calculating the performance of the vehicle is assumed to be similar to that used in the Caterpillar program, as explained in the previous section.

The haul roads are again constructed in segments and details of the length, grade, curvature, and rolling resistance, of each section are required. For estimating the rolling resistance of each section, the author gives a chart similar to tables 3.1 and 3.2. Rolling resistance was discussed with the author, (Pugh, 1993) and for

estimating purposes a value would be used from experience, but he would not be able to accurately estimate the rolling resistance of the articulated dump trucks from information contained within a site investigation report. Having researched in this field for several years he had never seen a more practical detailed method of estimating rolling resistance than tables similar to tables 3.1 and 3.2. It was therefore his belief that the initial findings of the project were very interesting and exceedingly valuable to the field of knowledge on this subject.

3.5 Comparison of the Three Methods of Estimating Velocity

The simplest way to compare the three methods of calculating travel speed of the plant was to increase the rolling resistance of a section of haul road and monitor the velocity responses. For the analysis the grade resistance was kept at 0%, i.e. a flat haul road, and the rolling resistance was increased. In all three methods grade resistance is assumed not to cause secondary effects on the rolling resistance of the vehicles, see sections 4.6 and 5.6.1, therefore this analysis is akin to increasing the total resistance.

Figure 3.5 shows the relationship between total resistance and maximum attainable velocity, for a 75% loaded Volvo BM A25 6x6 articulated dump truck. When estimating rolling resistance from the speed of the vehicles, it must be assumed that the vehicles are travelling at their maximum possible velocity, otherwise the value of rolling resistance could be calculated as anything beneath the velocity total resistance curve. Figure 3.5 shows that the Vehsim software takes no account of the vehicles retarder when travelling on steep downhill grades. When the total resistance is positive all three methods show similar trends with Accelerator giving slightly lower velocities than the other methods. Both the handbook and Vehsim are not smooth graphs as they take into account gear changes. This result was consistent for other vehicle types and also when the machines were operating under fully loaded and empty conditions.

It can be seen from figure 3.5, that the maximum attainable velocity of the vehicle is very sensitive when the total resistance is low, for example, a change in total resistance from 3-4% causes a reduction in speed from 43-32 km/h for a 75% loaded Volvo BM A25 using Accelerator. Only once the total resistance increases

beyond 15% does the slope of the graph begin to flatten by any significant amount. Examining the Volvo table of rolling resistance coefficients, tables 3.1, it is evident that the bands in rolling resistance represents an unacceptably large range in velocities. Comparing the information in tables 3.1 and 3.2 with figure 3.5, it is evident that even a small difference in the estimated value of rolling resistance could result in a large difference in the estimated velocity of the vehicle, especially when the resulting total resistance is low.

It was decided to use the Accelerator software for all future analysis. Vehsim was rejected on the grounds that the program took no account of the retarder when the vehicle was travelling downhill, giving wildly inaccurate results. Calculating the speed of the vehicles using the manufacturers' handbook was also discarded as the method was considered clumsy, and somewhat inaccurate when reversing the process to acquire the rolling resistance from the velocity of the vehicle. Also, as the findings of this thesis are going to be used in the estimation of the performance of articulated dump trucks, it would have been useless relating any findings to a rolling resistance that could only estimate maximum attainable velocity and not be used directly to estimate performance.

3.6 Effect of Mass on the Velocity versus Rolling Resistance Relationship

From the initial considerations of what affects rolling resistance, it was stated that vehicle mass was a significant factor. Using Accelerator, the maximum attainable velocity was estimated for a range of rolling resistance at four values of rated payload: zero, 50%, 75%, and full rated payload, figure 3.6. This figure shows for all masses of vehicle that maximum attainable velocity is most very sensitive at lower levels of total resistance. For estimating purposes, the mass of the vehicle is important if the total resistance is known, for example at an estimated total resistance of 5% a loaded Volvo BM A25 could travel at between 22.2 and 31.1km/h depending on the payload, figure 3.6.

From an estimation of the density of the material to be hauled and the volume capacity of the truck, the mass of the payload could be estimated. The volume capacity of the truck is given in the manufacturers' specification sheets for two cases; struck and heaped. The struck volume is defined as the actual volume

enclosed within the walls of the body, as restricted in figure 3.7(a). The heaped body volume of the hauler is the sum of the struck body volume and the volume enclosed by four surfaces inclined at 2:1 from the upper edges of the sides and ends of the body, figure 3.7(b). For all vehicles tested, this turned out to be in the region of 75%, therefore a full payload was impractical and all calculations were carried out assuming the 75% payload.

Knowing the estimated mass of each type of truck, a set of graphs similar to that in figure 3.6 were developed for each type of vehicle encountered, in both the loaded and empty conditions. From the measurement of the vehicles speed on site, an estimation of the apparent rolling resistance for each section could be ascertained using the set of graphs.

3.7 Summary

The above sections contain a discussion on the practical definition of rolling resistance for civil engineering usage and the factors affecting this parameter. Empirical tables of rolling resistance factors have been devised through experience by manufacturers and have been shown to be inconsistent, which could lead to erroneous performance predictions. The primary function of the manufacturers is to sell vehicles and the accurate determination of rolling resistance factors is not a primary goal of these companies. It would therefore be naïve for companies to formulate performance estimations based upon these figures, which were developed on different soil conditions to those found in Britain.

Three practical methods of calculating velocity from a value of rolling resistance have been discussed and for reasons explained in the previous sections the Accelerator method will be adopted for the remainder of the thesis.

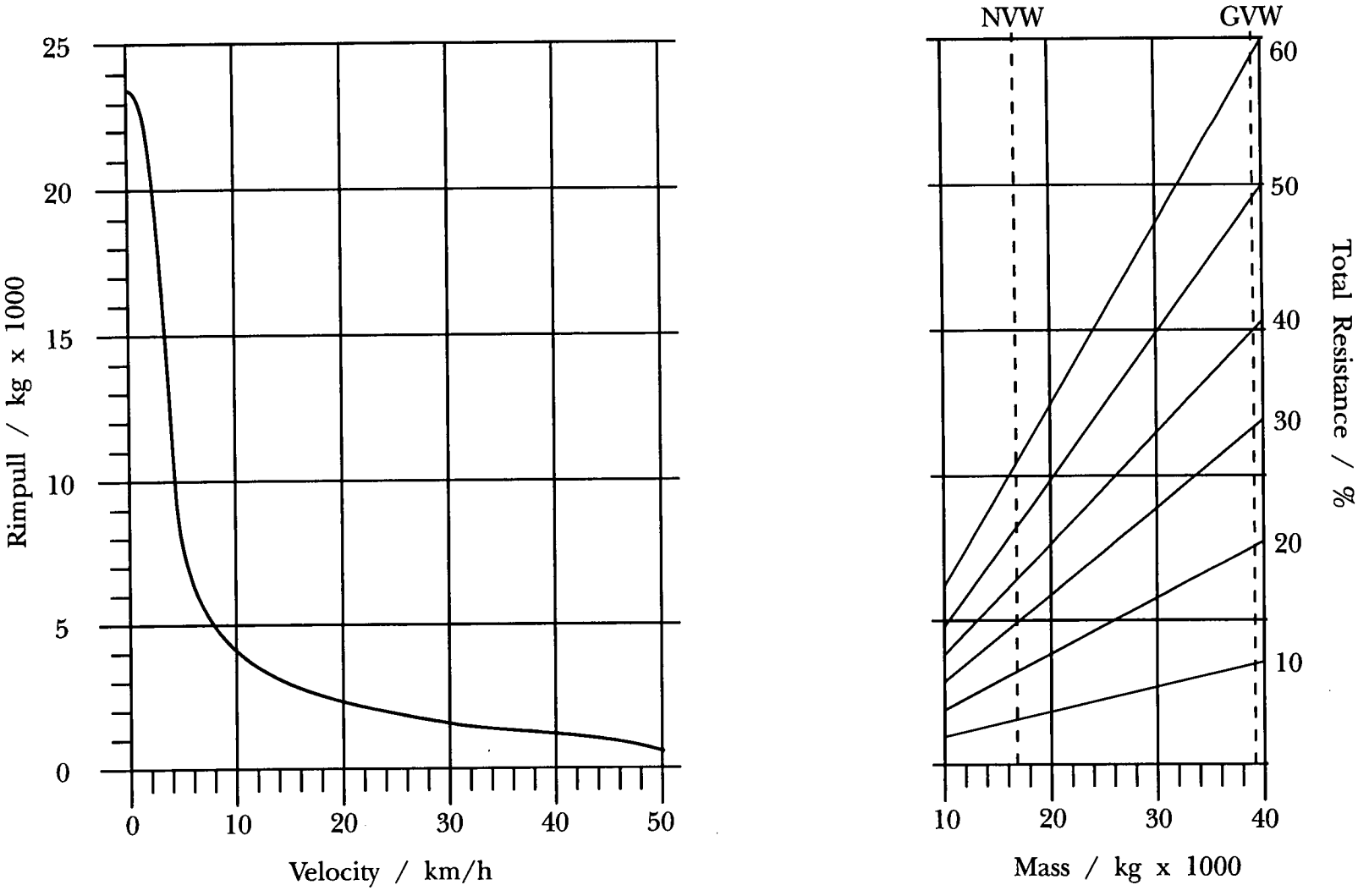

Figure 3.1: Rimpull Chart for Volvo BM A25 6x6 Articulated Dump Truck

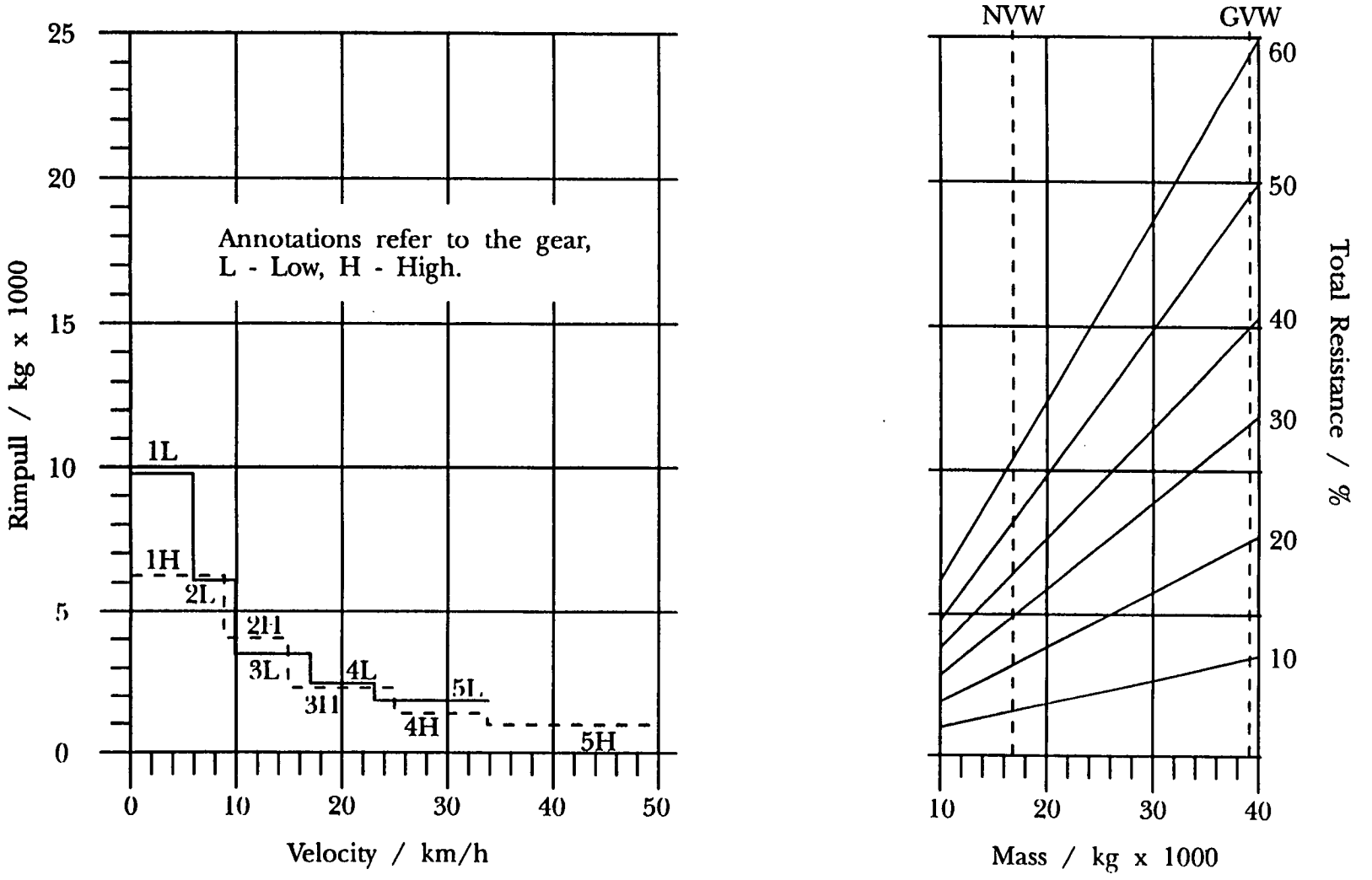

Figure 3.2: Retardation Chart for Volvo BM A25 Articulated Dump Truck

CATERPILLAR INC.
VEHICLE SIMULATION ANALYSIS

MACH CODE	MODEL	ENGINE	HP	TRANSMISSION	FWD GEARS	CAPACITY	TIRES
V001	A25	TD 71K	240	ZF 5 HP 500	10	22.5	23.5RA25

PAYLOAD 22,500 EMPTY WEIGHT 16,900 SORT 16

NO.	SHIFTING VELOCITIES (KPH)	ROTATING MASS (CONSTANT)
1	6.00000	0.27000
2	9.00000	0.17000
3	9.40000	1.00000
4	15.00000	0.08000
5	15.40000	0.38000
6	22.00000	0.07000
7	25.00000	0.18000
8	31.00000	0.05000
9	36.00000	0.11000
10	51.00000	0.09000
11	0.00000	0.00000
12	0.00000	0.00000
13	0.00000	0.00000
14	0.00000	0.00000
15	0.00000	0.00000
16	0.00000	0.00000

NO.	VELOCITY COORDINATES (KPH)	RIMPULL COORDINATES (KILO)
1	0.00000	26,000
2	2.00000	15,900
3	3.00000	10,600
4	4.00000	8,550
5	5.00000	7,199
6	6.00000	6,300
7	8.00000	5,200
8	10.00000	4,600
9	12.00000	4,050
10	14.00000	3,550
11	16.00000	3,050
12	18.00000	2,800
13	20.00000	2,600
14	25.00000	2,000
15	30.00000	1,800
16	35.00000	1,700
17	40.00000	1,400
18	45.00000	1,200
19	50.00000	650
20	51.00000	0
21	0.00000	0
22	0.00000	0
23	0.00000	0
24	0.00000	0
25	0.00000	0
26	0.00000	0
27	0.00000	0
28	0.00000	0
29	0.00000	0
30	0.00000	0
31	0.00000	0
32	0.00000	0

Figure 3.3: Vehicle Input Parameters for the Vehsim Computer Program

Vehicle : Volvo BM A25 6x6 Nbr: 35
Description : Articulated Dump Truck
Data Source : Volvo Bm Performance Manual
Test Data :

PRIMARY SCREEN

Powertrain Efficiency	85.0 pct	Height	315.0*cm
Avg. Power Percent	74.5 pct	Width	249.0*cm
Pct. Effectiveness	63.4 pct	Coverage	100.0*pct
Net Engine Power	188.0*kW	Frontal Area	7.84 sq.m.
Avg. Road Power	119.1 kW	Drag Coefficient	0.900*
		Drag Factor	7.06
Empty Weight	16900*kg		
Payload	22500*kg	Tire Pressure	345 kPa
Loaded Weight	39400 kg	Tire RoRes at 0 km/h	0.83 pct
Weight / Avg Power	330.75 kg/kW	Number of Tires	6
Max. Road Power	159.8 kW	BSFC Rate	0.243 g/W-hr
Weight / Max Power	246.51 kg/kW	Fuel Density	0.84 g/cc
		Ignition (S or D)	Diesel
		Accessory Losses	13.2 kW
Time: Sec or Min	Min		
Start-up Time	0.00	Braking Rate	0.100 g-s
Motion Resistance	0.00 pct	Lateral g-s	0.100 g-s

SECONDARY SCREEN

--Average Power Percent---			--------Gearing---------			--Dynamic Weight Transfer-	
Net Power (kW)		188.0	Tire Revs/km		0	Weight Distribution	
@ r/min		0	Axle Ratio		0.000	Front Pct.	29.2
Net Torque (N-m)		0	Auxiliary Ratio		1.000	Rear Pct.	70.8*
@ r/min		0	Top Speed by Gear			Wheelbase (cm)	500.0
Gear Ratios:	1	0.000		1	0.0	Center of Gravity	
	2	0.000	(km/h	2	0.0	above ground (cm)	157.5
(Lock	3	0.000	at	3	0.0	Drive: Front, Rear,	
Selections)	4	0.000	Net kW	4	0.0	or 4-Wheel	Rear
	5	0.000	r/min)	5	0.0	4-Wheel Drive Split,	
	6	0.000		6	0.0	Pct to Rear	0.0
Power Slope			Redline r/min		0		
kW / 100 r/min		0.00	Redline Top Speed		51.0*		
Pct Engine Speed						Downhill:	
at Gear Change		0.00				Accel or Coast	Coast
			------Productivity------			Retarder kW	188.0
Avg Power Percent		74.53	Payload Units		Lb		
			Payload kg/Unit		0	Price	0
			Vehicle Cost/Hour		0.00	Date	

Figure 3.4: Vehicle Input Parameters for the Accelerator Computer Program

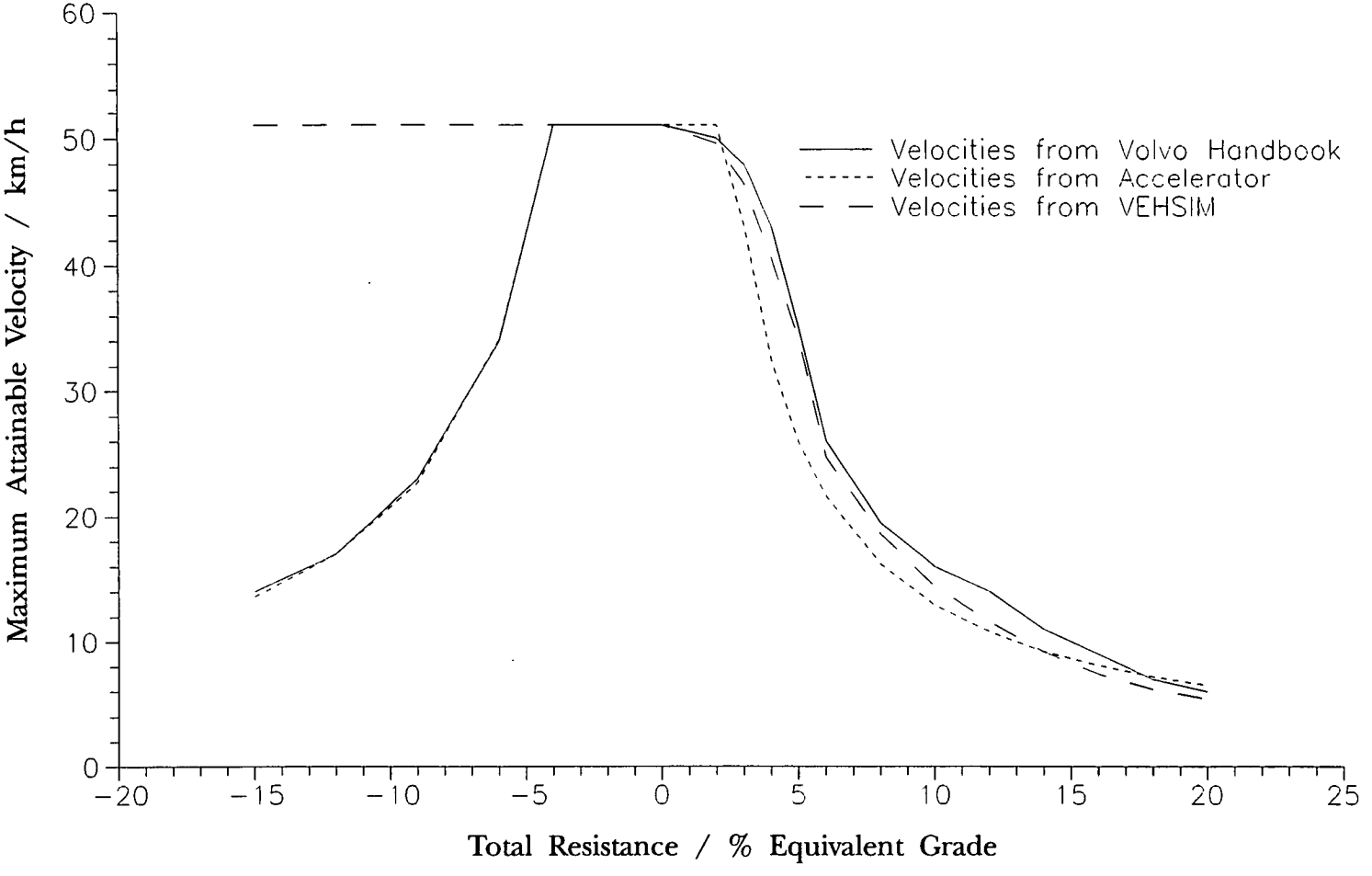

Figure 3.5: Maximum Attainable Velocity versus Total Resistance for a Partially Loaded (75%) Volvo BM A25 6x6 Articulated Dump Truck.

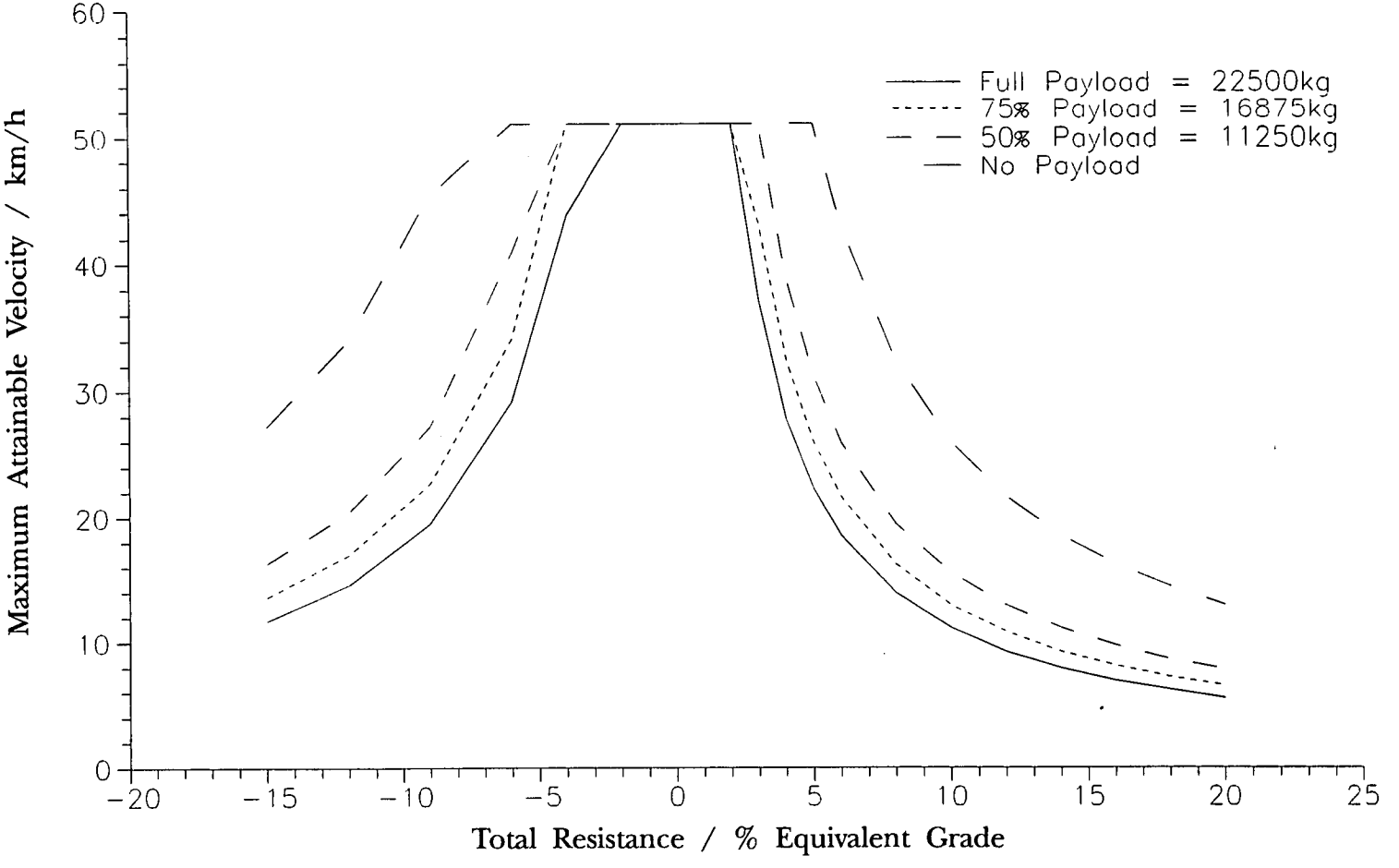

Figure 3.6: Maximum Attainable Velocity versus Total Resistance for a Volvo BM A25 Articulated Dump Truck under Various Loading Conditions, Velocities Calculated Using the Accelerator Software.

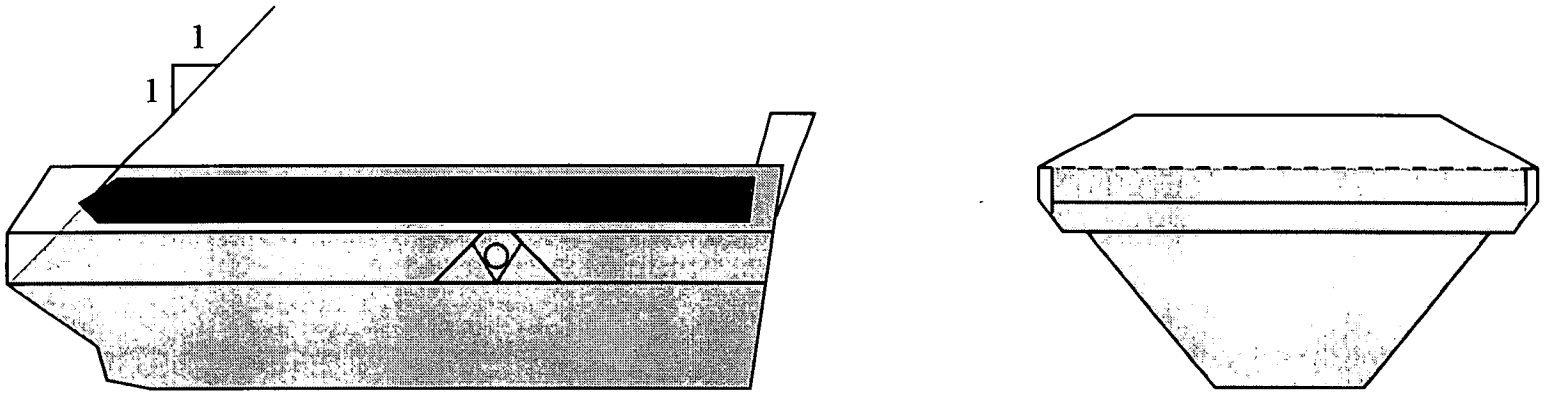

(a) Struck Capacity

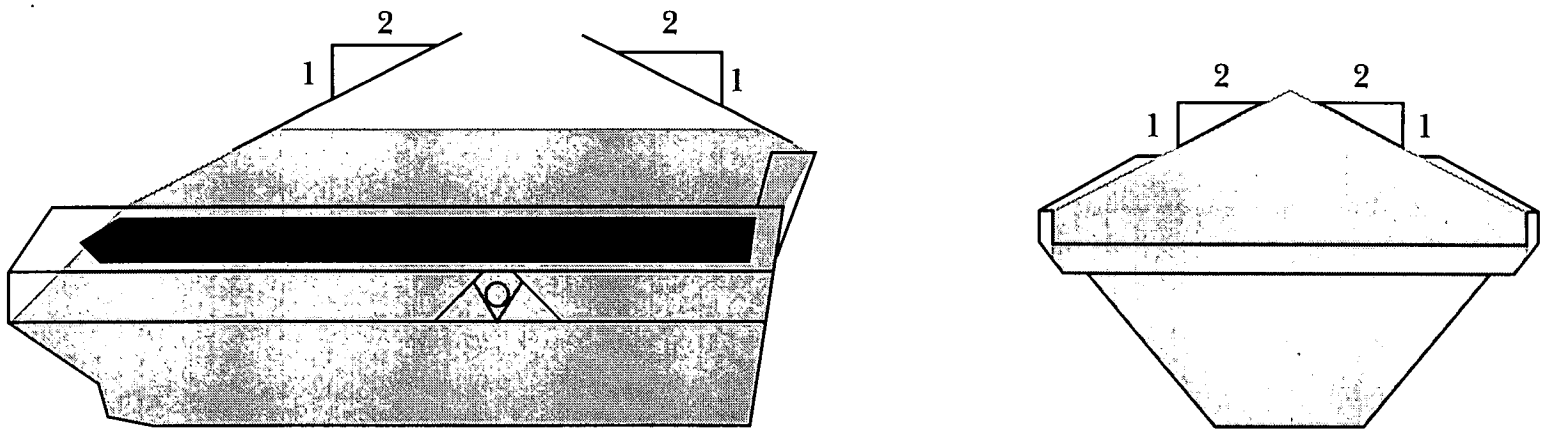

(b) Heaped Capacity

Figure 3.7: Calculation of Body Volume for both Struck and Heaped Capacties as per Specifications

Surface Type	Rolling Resistance / Equivalent Grade	Sinkage of tyres / mm
Concrete, dry	2	-
Asphalt, dry	2	-
Macadam	3	-
Gravel road, compacted	3	-
Dirt road, compacted	3	40
Dirt road, firm rutted	5	60
Stripped arable land, firm, dry	6	80
Earth back-fill, soft	8	100
Stripped arable land, loose, dry	12	150
Woodland pastures, grassy banks	12-15	150-180
Sand or gravel, loose	15-30	180-350
Dirt road, deeply rutted, porous	16	200
Stripped arable land, sticky wet	10-20	120-250
Clay, loose, wet	35	400
Ice	2	-

Table 3.1: Volvo BM Rolling Resistance Table (after VME, 1989)

Surface Condition	Rolling Resistance / % Equivalent Grade
A very hard, smooth roadway, concrete, cold asphalt or dirt surface, no penetration or flexing.	1.5
A hard smooth stabilised surfaced roadway without penetration under load, watered, maintained.	2.0
A firm, smooth rolling roadway with dirt or light surfacing, flexing slightly under load or undulating, maintained fairly regularly, watered.	3.0
A dirt roadway, rutted or flexing under load, little maintainance, no water, 25mm penetration or flexing.	4.0
A dirt roadway, rutted or flexing under load, little maintainance, no water, 50mm penetration or flexing.	5.0
Rutted dirt roadway, soft under travel, no maintainance, no stabilisation, 100mm tyre penetration or flexing.	8.0
Loose sand or gravel.	10.0
Rutted dirt roadway, soft under travel, no maintainance, no stabilisation, 200mm tyre penetration or flexing.	14.0
Very soft, muddy, rutted roadway, 300mm tyre penetration, no flexing.	20.0

Table 3.2: Caterpillar Table of Rolling Resistance (after Caterpillar, 1993)

Chapter 4 Chalk

4.1 Introduction

No records of the speed of earthmoving plant on chalk haul roads can be found in the literature, but chalk has been widely researched to establish its mechanical and physical properties. The remainder of this section gives a brief outline of how it was formed, the properties of chalk, and its characteristics. The remainder of the chapter studies problems associated with chalk haul roads and possible solutions, also the procedure followed to estimate the speed of articulated dump trucks on a specific chalk site.

Chalk is a soft fine-grained limestone that is deeply weathered caused generally by frost action during the Pleistocene age. The effect of freezing was to produce a mass of crumbly frost shattered rock, weathered to a soft or firm clayey consistency adjacent to fissures and joints. Chalk was deposited during the Upper Cretaceous period, about 70-100 million years ago. It has a wide geographical distribution, being commonly found in Europe (Denmark, England, France, Germany, and Holland). In England chalk can be found eastwards of a line joining Hampshire and South Yorkshire, and attains a maximum thickness of approximately 450m.

During the Upper Cretaceous period most of Europe was submerged and the south of England was in a sub-tropical zone at a latitude of about 40°N, (Hart et al., 1975). It has been postulated (Montford, 1970) that the nearest outcrops of land were covered in deep vegetation, and that this prevented the products of land erosion contaminating the sea. In these conditions deposits came almost exclusively from the dying marine life. Chalk therefore consists almost entirely, up to 98% in upper chalks, of calcium carbonate fragments of microscopic marine shells and planktonic organisms, including calcispheres, rhabdoliths, and coccoliths, which account for over 60% of the chalk mass (Black, 1953). Noel (1970), using a scanning electron microscope estimated that there are the remains of approximately 25 million of these fossilised creatures in every square centimetre of chalk.

The unique characteristics of chalk stem from the fact that little to no recrystallation has taken place. Because of this fact many of the shells remain hollow and the void ratio can be relatively high, in upper chalks rising to 1.1 with a corresponding bulk density of 1300kg/m^3, (Henry, 1986). A well compacted chalk may have a dry density greater than the in-situ rock mass. Any mechanical disturbance of the cellular structure releases pore water from the near saturated cells. Excess pore water causes dilatency of the silt sized chalk particles creating a material called putty chalk. This process is facilitated by chalk's low plasticity index and lack of absorbency. Drying of putty chalk results in recementation and generally increases the shear strength.

Chalk is particularly susceptible to the effects of frost. Nevertheless the thickness of modern major highways is generally sufficient to protect the underlying chalk from freezing.

4.2 Properties of Chalk

Chalk has a permeability similar to silt, in the region of 10^{-5}mm/s, however intact chalk will have a permeability much greater than this depending on the proportion and spacing of fissures. Shear strength parameters are influenced by disturbance during sampling, testing methods, anisotropy and degree of saturation but commonly, $\phi' \approx 37\text{-}40^\circ$ and $c_u \approx 50\text{-}250$ kN/m^2, (Henry, 1953). Normally there is a reduction in volume of approximately 10% between cut and intact chalk and the corresponding compacted fill. Heavy plant is generally required to crush hard chalk during compaction, but over-compaction of any grade of chalk can cause severe problems, (Reina, 1975, and Anon., 1972).

The breaking down of the chalk blocks tends to decrease permeability and impedes drainage. In the case of saturated soft chalk this degrading may generate excess pore pressures, although these are dissipated comparatively rapidly depending on constituent particle size. When the in-situ moisture content of chalk is almost saturated, the culmination of multiple handling may produce a slurry with negligible strength and is not permitted in the specifications for highway works (Department of Transport, 1991).

4.3 Classification of Chalk

The initial classification of chalk was carried out by Ward et al. (1968) on a middle chalk at Mundford, Norfolk, the basis for the gradings was three-fold, as follows:

- Visual description and classification in situ from inspections in a number of 0.75m diameter boreholes, taking into account hardness, jointing and the degree of weathering.
- Each grade was quantified in terms of load deformation behaviour at three locations, by 0.9m diameter plate bearing tests.
- At one of these locations, load-deformation behaviour was studied in a large scale loading test, for which a water tank, 18.3m diameter and 4500 tonnes maximum loaded weight, was employed. This test was required because of the very large size of the proton accelerator to be erected and the small allowable tolerance on differential settlements.

The Mundford classification ranked chalk into five categories, giving a brief description of the fracture spacing, an approximate range of Young's modulus, approximate bearing stress, as well as the creep properties of the material. A sixth category was introduced by Wakeling (1970), which covered extremely weak structureless chalk containing small intact lumps. A general table of the amended Mundford scale is given in table 4.1. Although the original authors caution the interpolation of this scale to other sites, this is still one of the most widely used classification systems in Britain. The classification of chalk from SPT results should be treated with caution, as the results of the test can be influenced by the presence of fissures and the formation of putty chalk during driving. Although the Mundford classification is inappropriate for earthworks, as large strains are being considered, this system is still used on earthworks contracts therefore warrants inclusion in this thesis, but the inappropriateness of the scheme should be noted.

Another classification systems utilised in Britain is the one developed at TRL, (Ingoldby et al., 1977) and is the method specified by the Department of Transport (1991a). It is calculated from a knowledge of the saturated moisture content of the intact chalk and the chalk crushing value. It splits the chalk into four grades

according to the type of excavation plant being used and the season of operation, summer or winter, figure 4.1. This table is slightly out of date now as it includes information on the utilisation of scrapers, whereas chalk in Britain should be "excavated by a shovel-loader which excavates, swings and unloads without moving the chassis or undercarriage", (Department of Transport, 1991), unless specified by the engineer..

The saturated moisture content (BSI, 1990) of the sample is calculated from the dry density of a 300-500ml sample of chalk using a specific gravity for the chalk particles of 2.7, and in Britain is similar to the in situ moisture content. The chalk crushing value uses the same apparatus as the moisture condition value test, and measures the degree of crushing of the 10 to 20mm fraction of chalk. Although the saturated moisture content gives an indication of potential temporary instability and sensitivity to crushing, it does not correlate well with the chalk crushing value test (Guy, 1990). A problem with the chalk crushing value test arises from the sample selection of material lying in the 10-20mm bracket only. This excludes the influence of the fine material which forms an increasingly significant proportion of the material in the more highly weathered grades and the blockier chalk of hard unweathered chalk.

This method of chalk classification was discussed at the evening meeting of the British Geological Survey on 1/12/93 at the Institution of Civil Engineers headquarters in London. This meeting was to discuss both the forthcoming CIRIA report, chalk in general, and how the properties of chalk relate to different engineering problems in Britain. A speaker for TRL indicated that future classification schemes would relate dry density and natural moisture content, discontinuing the use of the chalk crushing value test. Suitability on site would be controlled by the natural moisture content of the material. This revised method of classification would be akin to the French classification scheme, as described in the next paragraph. Both the revised TRL system and the new scheme devised at CIRIA would be compatible, improving the overall engineering description of chalk.

The French system of classification utilises dry density and natural moisture content (LCPC-SETRA, 1976). The dry density is considered to yield an estimate of the structural strength of the material and the natural moisture content is used to

predict the behaviour of the material during placement. Chalk is then assigned to one of six categories, figure 4.2. Rat et al., (1990), specify for each of the six categories the placement techniques and compactive energy that should be used to produce a sound embankment.

Other methods of classification have been proposed using hardness terminology and dry density (Mortimore, et al., 1990), and degree of saturation and porosity (Guy, 1990). These methods of classification do not recommend any compaction techniques relative to each grade.

No method of chalk classification for acceptability is suitable for estimating the speed of the vehicles on the haul roads, as they are all concerned with the compaction of the material. The ideal specification for this would consider how easily the material degrades as well as the natural and saturated moisture contents. Calculating the moisture content of the material on the haul road is difficult as the blocks normally used for moisture content determination have been reduced to their constituent particle sizes. However, as discussed later, the site layout and the initial construction of the haul roads may have more influence on the speed of the plant than any properties of the material.

4.4 Problems on Haul Roads

The quality of haul roads on chalk are generally very good, there are however certain areas where the contractor should take particular care not to cause unintentional deterioration of the haul road. These points occur where the machines accelerate or decelerate at the same position on each circuit: at the bottom of ramps between benches, before and after tight corners, in the loading and dumping areas, and at constrictions due to other works, for example plant crossings and Bailey bridges.

The deterioration of the chalk is caused by the breakdown of the cellular structure, releasing water into the particle matrix. Being nearly saturated, the silt sized material will be at a moisture content close to its liquid limit. As the material is continually trafficked additional material is broken down releasing more water, after a period of time excess pore water pressures may build up causing a further

decrease in the effective stress of the matrix. This reduction in effective stress leads to a further reduction in shear strength, see analysis in chapter 7. Due to the reasonably low permeability of the chalk the released moisture will not seep to any depth, this leads to a very wet, weak, and slippery top surface which can be removed relatively easily.

4.4.1 Deterioration of the Ramps between Benches

On large excavations in any material it is common to excavate in steps, called benches. The height of a bench is usually in the region of 2.5 - 3m, depending on the size of excavator and the type of material being shifted. Normally ramps are constructed between benches at relatively steep grades of about 15 - 20%. It was observed that soft areas tended to appear towards the foot of the ramps just below the position where the rate of change of curvature was at a maximum, plate 4.1. These soft spots would propagate in size once established and when quite large, 10-15m in length, a second soft spot would appear, approximately 20m downhill from the first, on the horizontal portion of the bench, figure 4.3.

The formation of these soft areas occurs as follows; the vehicles are decelerated prior to reaching the top of the ramp, the driver then maintains a constant velocity down the ramp and then accelerates just after the transition zone between the steep and shallow portions of the ramp. The chalk breaks down to its constituent silt sized particles through the mechanical forces imparted onto the soil from the acceleration of the vehicles at this point. As the chalk is near saturation point the silt matrix will have a moisture content in the region of the saturated moisture content of the intact chalk, about 25-30%. This moisture content will be just below the liquid limit of the matrix, which means that the material will be in a very weak condition. The rate of change in gradient is important as the driver will approach the foot of a ramp slower if the rate of change of slope is great, and then accelerate harder causing a greater deterioration of the haul road. Severe rates of change of gradient should therefore be avoided. When returning to the loading area the driver accelerates hard into the ramp at a similar point as when accelerating from the ramp. As the ramps are generally only one vehicle wide, the chalk is broken down by vehicles travelling in both directions. As the chalk progressively breaks down the surface of the haul road becomes wet and slippery around the soft spot, causing

the drivers to treat the section differently. When descending the ramp the drivers will keep the speed slow coasting through the soft area, then accelerate hard once clear of the poor quality section. Likewise going in the opposite direction the driver will accelerate prior to the soft spot, to avoid accelerating on the wet section and skidding due to lack of traction. Again these points of acceleration will coincide causing the second weak spot, lower than the first soft spot, figure 4.3. Given time these two spots will continue to enlarge merging into one another.

As the material breaks down the moisture in the chalk is released and causes the silt sized particles to take on the characteristics of putty. As this is continually trafficked the pore water pressure in the silt matrix will increase with time, further reducing the effective strength of the matrix. This top layer of the haul road becomes useless as a supporting medium and the speed of the vehicles is dramatically reduced, as it is impossible to produce high traction for accelerating. The problem could be remedied practically in one of three ways, by surcharging the haul road with dry fines, constructing the ramp at a shallower grade, or by grading the surface putty-like layer away revealing a new, solid base for the haul road.

If dry fines are added to the putty chalk, the moisture content of the matrix will decrease, making the material stronger. Fines will do this much more effectively than a blockier material as they will mix easier through trafficking. Chalk recently excavated may not be suitable to use as a surcharging material as it will be near saturated, hence it will not reduce the moisture content of the putty chalk. This material will also degrade in time effectively increasing the depth of the problem. It may not be cost effective to import dry fines for surcharging, and the British climate does not lend itself to drying excess material on site. These remedies may be viable depending on the specific site.

A simpler solution to the problem is to construct the ramps at a shallower grade with a longer transition zone. This would not be any more difficult for the excavator driver, but would take a slightly longer period of time to construct. The advantage of solving the degradation problem in this manner is that not only is the problem of weak material removed, but the drivers will drive faster down a shallower grade, increasing both velocity and productivity.

If the problem of degradation is going to be solved solely by grading, the ramps must be smooth enough to allow the blade of the grader to reach all parts effectively, figure 4.4, especially as the worst breakdown of material occurs near the point of greatest curvature on the ramp. To avoid disturbing the solid material under the putty chalk the grader driver has to be continually altering the depth of the blade, this is a difficult operation to complete accurately. Bulldozing the area is not a good solution as the track grousers will disturb the solid underlying chalk increasing the rate of deterioration in the future.

A final method is to leave the material to dry naturally, increasing the strength of the material, but this will probably not be fiscally viable in the British climate and the relatively small problem pockets could be removed by one or more of the preceding solutions.

4.4.2 Deterioration due to Manoeuvring

The loading and unloading areas rut quite badly, as the vehicles are continually manoeuvring into position under the loader, or positioning in the fill area. The constant demand for high traction to overcome initial friction, combined with breaking and turning forces imparts large shearing forces in the chalk causing the material to degrade rapidly in these areas.

Remedial work in the loading area is very difficult to achieve effectively as interference using other pieces of plant congests this area quickly. This has the effect of reducing productivity dramatically, therefore utilising graders in this situation is impractical. Grading the problem areas during breaks is probably the most effective method, another is to keep altering the section being excavated to allow improvements. On site the latter option is generally impractical as the travel time for the excavator between benches would result in a greater loss in productivity than the potential gain.

The dumping area is another zone where the degrading of the chalk can cause major problems, not only from an earthmoving point of view but from a short term structural standpoint. The layout of dumping areas varies from site to site, therefore it is hard to generalise, nevertheless most dumping areas have a common

point of entry and turning section for the dump trucks. As in the case of the loading area, the constant manoeuvring of machines in a constricted area causes the chalk to break up faster than on the body of the haul roads, where the vehicles are travelling at a reasonably constant velocity. The continually manoeuvring compacting machinery is also present in the dumping area, and the chalk is being very heavily trafficked. Care must be taken not to over compact the soil as this could lead to instability of the embankment.

There are two schools of thought concerning the compaction of chalk. One is to use a high compactive effort, such as that favoured by the Department of Transport, which effectively crushes the chalk and minimises the air voids. The other is to use thicker layers and lower compactive efforts thereby maintaining the rock structure of the material and hence the stability of the fill. This leaves a higher air void content with the increased possibility of settlement. Compaction of chalk is out with the scope of this thesis, but several papers have dealt with this topic, (Privett 1990, Quibel, 1990, Rat et al., 1990 and Clayton 1980). This compaction topic was also discussed at the BGS evening meeting in London. The experts compiling the forthcoming CIRIA report had not come to any firm conclusion as to which method is superior under differing circumstances and were asking the floor for any comments on this topic.

4.4.3 Other Problem Areas

Any other place on the haul road where vehicles are perpetually accelerating or decelerating has the possibility of degrading. These points may occur at plant crossings, constrictions on the haul road due to other works or at Bailey bridges. If these bottlenecks cannot be avoided then the best remedy is to keep trimming the haul road with a grader to remove the layer of putty chalk. Graders on chalk should have very little to do except to maintain these problem areas and to remove any large blocks that have fallen from the body of a dump truck. When grading, the blade of the machine should not penetrate into the solid chalk underlying the putty chalk, as this will degrade the surface by displacing and breaking up the intact chalk blocks, increasing the rate of formation of putty chalk in the future. The presence of graders causes obstructions for the haulers which can travel at faster velocities, especially on steep grades. An analogy for the grader blade can

be drawn with a scraper blade, which are not permitted to excavate chalk, (Department of Transport, 1991) because they cause excessive degradation of the material.

Where the vehicles are travelling unobstructed and at a reasonably constant velocity, the main body of the haul road remains in excellent condition with no rutting and only slight flexing. The surface of the haul road is made of intact chalk blocks infilled with dried putty chalk which gives an exceptionally smooth and strong running layer. As the plasticity index of the putty chalk is very low, if it starts raining the vehicles should stop running almost immediately, as the strength of the material will decrease rapidly. If the wet surface is trafficked prior to halting operations and ruts are created once the material has dried the rolling resistance of the haul road will increase slowing the vehicles down until the ruts are graded.

4.5 Monitoring

The chalk site monitored through the 1993 earthmoving season was the final section of the M3 from Bar End to Compton, through Twyford Down. This 5km stretch of motorway contains 2.7Mm^3 of earthmoving, the majority in a single cut. The earthworks were constructed entirely using a backhoe-dump truck combination, as scrapers are not allowed to be used for transporting class 3 material (Department of Transport, 1991), due to the excessive disturbance this form of excavation causes the material. The excavators on the site were Cat 245's and the haulers were a mixture of Volvo BM A35 and Cat D400D articulated dump trucks. The majority of the loaded hauling was downhill, from the single huge cut, and the maximum grades on the ramps was approximately 25%.

The site contained upper chalk with a large quantity of flint nodules. Using the amended Mundford scale (Wakeling, 1970) the chalk was predominantly classified as grades 3 and 4, with an increasing percentage of grade 2 with depth. Using the on site laboratory results, all carried out to BS1377 (BSI, 1990), the TRL classification (Ingoldby and Parsons, 1977) showed the material to be predominantly class A, with a small portion of class B. The French scheme (LCPC, 1976) indicated the material was classes CR1, CR2 s, m and h and CR3 h, and hardness (Mortimore et al., 1990) to be from medium hard to extremely

soft. From the site laboratory data the average dry density and natural moisture content of the blocks were 1.63Mg/m³ and 23.8% respectively, taken from a sample size of 500. The dry densities ranged from 1.38-2.16Mg/m³ with a standard deviation of 0.14 and the natural moisture contents ranged between 9 and 29 with a standard deviation of 4.5. The natural moisture contents of the tested blocks were all at least 90% of the corresponding saturated moisture contents, which had an average of 24.7%. The relationships from the site laboratory data showed very strong relationships between dry density and saturated and natural moisture contents, figures 4.5 and 4.6, which is the basis for the French system of classification, and possibly the revised TRL specification.

On the main body of the haul roads there was no visible jointing between the blocks as this had been completely filled with chalk fines, leaving after repeat trafficking an exceptionally smooth running surface. Localised degrading of the chalk had occurred at the foot of ramps, in the loading and dumping areas, and at plant crossings. There was also one exceptionally weak section on the haul road where saturated peat was being hauled from a river diversion to tip. As the haulers climbed out of the loading area water drained out the rear of the machine saturating the haul road. This dramatic increase in moisture content on this section of the haul road caused severe rutting and associated problems for the dump trucks. The degree of degradation could have been reduced if the vehicles had been allowed to drain at the side of the loader, but gangers have an ethos of always keeping the vehicles moving, focusing on shot term productivity and dealing with any problems as they occur.

No instrumentation or interference with the operation of the plant was possible, therefore all timings had to be recorded from the side of the haul road. Vehicles were timed over complete sections of varying grade, as long sections of constant grade were not available on this site. A typical section of haul road is shown in figure 4.7. Timings were taken at recognisable positions: at the crest or foot of ramps, at soft spots where drainage channels had been built, at road constrictions, or beside a marker. It was also noted whether it was the front or rear wheel of the vehicle as this becomes more important as the length of the segment decreases. Timings were averaged from at least 10 passes of similar plant. The length and grade of each section was ascertained by surveying the haul road with an electronic theodolite accurate to approximately 3mm in a 100m. All sections were assumed to

have no obstructions and recordings that involved a vehicle that had been delayed by an external factor were removed from the analysis.

4.6 Rolling Resistance and Site Results

No information from previous work was available indicating the rolling resistance of vehicles on chalk. From a visual inspection of the excellent quality of the haul roads, plate 4.2, it was expected that the rolling resistance would be correspondingly low. From the Caterpillar handbook the best description of the haul road would be; "A firm, smooth, rolling roadway with dirt or light surfacing, flexing slightly under load or undulating, maintained fairly regularly, watered - 3%" (Caterpillar, 1993). The Volvo handbook (VME, 1989) for similar conditions gives an identical value for rolling resistance.

The back analysed rolling resistances were assumed to be constant across each timed segment of the section. It was expected that the varying gradient would have an effect on the apparent rolling resistance of the section, but the effect of this could not be estimated at this stage.

Results for downhill grades have always tended to be more operator dependent than corresponding uphill grades. This is because on the uphill grades the speed of the vehicle is primarily governed by the output of the engine, whereas on steep downhill grades the vehicle will travel as fast as the driver is willing to let it, unless an automatic retarder is fitted. The severity of the grade also affects the variability of the timings. There are many factors out with the scope of the project that could affect the speed the driver is willing to travel: amount of experience in the vehicle, health problems, vibration effects, and if the vehicle is not performing as per the manufacturers specifications.

No physical tests were carried out on the chalk, the surface was too strong to use the shear vane or the cone penetrometer and no laboratory testing of the material was undertaken as all the tests carried out on chalk require a 300-500ml lump of chalk, which is difficult to obtain due to the surface being covered in dried putty chalk. Figures 4.7 and 4.8 show the relationship between back analysed rolling resistance, calculated using the Accelerator software, and average gradient over

each section, for the two types of hauler, Volvo BM A35 and Cat D400D articulated dump trucks respectively. The abscissae in the figures are the average gradients for each timed section, any section which had a wide spread of gradients was omitted from the sample, for example sections 1-2 and 5-6, in figure 4.7.

As grade is an input parameter in all the methods of calculating rolling resistance the effect of gradient should be already taken into account. For a loaded Volvo BM A35 travelling down a steep slope, greater than 10%, figure 4.8, the apparent rolling resistance decreases linearly as the gradient becomes shallower, contradicting the expected outcome. The value of rolling resistance is approximately 4% lower than the grade resistance, giving a constant total resistance of approximately 4%. As the slope becomes shallower the apparent rolling resistance stabilises at a value of between 3 and 6% and the total resistance rises linearly. The equation of the linear best fit line shown in figure 4.8, equation 4.1, has a R^2 value of 88%.

$$\text{Apparent Rolling Resistance} = 0.11 - 0.79 \times \text{Grade Resistance} \quad (4.1)$$

This vehicle was never monitored travelling loaded uphill as the dumping areas were at the bottom of the cut. When travelling uphill empty the apparent rolling resistance was constantly recorded below 6% and this value can be seen to decrease slightly as the severity of the slope increases. The linear best fit line for the unloaded portion of the graph is given in equation 4.2 and has a R^2 value of 40%. This value of R^2 is much lower than that for the loaded vehicles due to the inherent variability in the unloaded travel time.

$$\text{Apparent Rolling Resistance} = 4.05 - 0.10 \times \text{Grade Resistance} \quad (4.2)$$

The slope of the graph for this case is as would be expected because the speed of the vehicle is becoming increasingly engine dependent. Similarly if the trucks were hauling uphill loaded then it would be expected that the apparent rolling resistance would again lie in the 2 to 6% bracket. It is impossible however to predict the performance of empty vehicles travelling downhill without further monitoring. These values are in the majority higher than the those expected from the description of the haul roads in the Caterpillar handbook.

Figure 4.9, shows the relationship between apparent rolling resistance and grade resistance for the Cat D400D articulated dump trucks. This graph does not indicate as good a relationship as for the Volvo BM A35 in the previous figure. The majority of the points on the empty uphill portion of the graph lie below 6% apparent rolling resistance, the linear best fit line is given in equation 4.3 with a R^2 value of 64%. As the gradient becomes flatter and then downhill the rolling resistance increases indicating that the grade has a marked effect on driver-vehicle performance.

$$\text{Apparent Rolling Resistance} = 6.86 - 0.22 \times \text{Grade Resistance} \quad (4.3)$$

The loaded results show greater variability, but this can be partly explained by the inexperience of the drivers to a different and far steeper haul road. The two shaded areas in figure 4.8 lie out with a distinct trend, and these points relate to the sections of the haul road in figure 4.7. When monitoring took place this haul road had never been travelled by the Cat D400D plant and the steep sections were longer and steeper than the drivers had previously encountered on this contract.

Figure 4.10 shows the relationship between maximum speed and total resistance, (the sum of grade and rolling resistance) and indicates that if the downhill grade is steep then as the rolling resistance increases the speed of the plant will increase until a value of grade resistance minus 2 to 3% is achieved, at this point the vehicle will be travelling as fast as possible. Thus, the shaded area to the far left of figure 4.8 indicates that the vehicles are travelling slower than would have been anticipated, this could be due to the inexperience of the drivers in descending such severe slopes, as mentioned in the previous paragraph, or the vehicle is deliberately slowed down to avoid overheating. The shaded area above and to the right of the expected trend shows that the vehicles are again travelling slower than would have been anticipated and is caused by the drivers slowing down in preparation for the next descent. Omitting the shaded areas the linear best fit line through the data is given in equation 4.4 and has a R^2 value of 78%. Again the degree of correlation is greater for the loaded vehicles than the empty vehicles for similar reasons as explained earlier.

$$\text{Apparent Rolling Resistance} = 5.48 - 0.33 \times \text{Grade Resistance} \quad (4.4)$$

Both figures 4.8 and 4.9 show that steep downhill grades have the effect of increasing the apparent rolling resistance of the driver-vehicle-terrain system. From an estimating point of view this is exceptionally important as the vehicles are travelling significantly slower than could have been expected from any information available to date.

4.7 Analysis of Smoothing the Gradients

An analysis was carried out using the Accelerator software to quantify the difference in travel time for the vehicles, if shape of the haul road was changed from a combination of ramps and shallow portions to one of uniform gradient. The new haul profile was calculated by taking the extreme surveyed points and joining them linearly, giving both distance and grade. For each machine, an upper and lower bound of apparent rolling resistance was calculated from the graphs of apparent rolling versus grade resistance to give an extreme range of performance. Both sets of data were analysed using identical vehicle parameters as the original analysis.

The results from this analysis can be seen in table 4.2. For the loaded Volvo BM A35 dump trucks, travelling downhill, the decrease in travel time expressed as a percentage of the original time varied between 2.5% and 32.4%. On average the lower and upper bound rolling resistances gave an average time saving of 22.7% and 10.7% respectively. These results would be expected to be similar for vehicles travelling on any material, as the slowing down of the machines in this situation is caused by the driver and not the performance of the engine.

When travelling uphill on a constant grade the vehicles were expected to move slower than on a varying gradient, because they do not have any shallower gradients where they can accelerate prior to the next incline. This effect would be most pronounced on the long hauls which vary frequently in gradient. The results confirm this hypothesis with the greatest increase in time being 28.4% and the largest decrease being 42.4%. On average the upper bound showed an increase in time of 6% and the lower bound a decrease of 5%.

If both effects are combined as would be the case in real life the lower bounds all show a decrease in travel time of between 2.1 and 32.8%, with an average of 12.8%. The upper bound on rolling resistance shows the range varying between a decrease of 23.7% to an increase of 9.5% with an average of a decrease in travel time of 1.3%. This average is kept high by the large 23.7% value, if this is removed then the average drops to an increase in travel time of 1.8%.

Similar results are given for the Cat D400D articulated dump trucks in table 4.3. Travelling downhill loaded, the lower bound analysis yields a range of between 1.6% slower and 41.7% faster, with an average decrease in travel time of 21.3%. The upper bound results actually indicate that the vehicle would move, in the majority, faster than the lower bound solution between 17.6% and 38.5%, with an average of 31%, this is due to the program including automatically a provision for inertial resistance. Travelling uphill the results are similar to the Volvo results, with a lower bound average showing a decreased travel time of 16.8%, whereas the upper bound indicates an increase in time of 4.5%. Combining the times shows that the vehicles will always travel between 2.2 and 31.2% faster, with an upper and lower bound average of 13.8 and 19.6% respectively.

The entry speeds for all sections was assumed to be 20km/h, if this was increased then it is probable that the combined travel time would decrease even further. The corresponding increase in productivity will be substantially lower than the decrease in travel time, as the productivity is dependent not only on the travel time of the vehicles, but also on the average load time, number of trucks, number of passes the excavator requires to fill the vehicle, dump time, spot time, and the variance of these times. However an increase in travel time of around 15% could lead to an increase in productivity of 5-10%.

4.8 Effects of Plant Mixing

The utilisation of different specifications of truck using the same haul road often causes problems. On this site there was a reasonably long haul of approximately 2km where Cat D400D and Volvo BM A35 articulated dump trucks were being loaded at a similar point by three Cat 245 backhoe excavators. On one particular timed section of this haul, figure 4.7, the Volvo trucks were travelling on average

at 26.7km/h compared with 18.2km/h for the Cat D400Ds. This difference in speed causes bunching, as shown in plate 4.3 where two Volvos are stuck behind a Cat D400D and a third Volvo is catching them rapidly. Overtaking was not viable as there were too many blind summits and the haul road was not physically wide enough. This unintentional slowing down of the vehicles can have a secondary negative effect by infuriating the Volvo drivers, which in extreme cases could lead to dangerous driving, or morale problems.

In this case the twelve trucks, six of each, were being loaded on the same bench by two excavators and a third excavator on a lower bench was loading a further four Volvos For maximum productivity the excavators should be permanently loading, but with severe bunching the loader has to wait for the next truck to arrive, in this case just over five minutes, then a convoy of three to five trucks would all return at once. In every case after a long wait at the loader the next vehicle to arrive would be a Cat. The gap between long waits was between 4 to 6 minutes. This behaviour obviously reduces productivity and should be avoided if possible. There is nothing gained by allowing the Volvos to overtake in the dump area as both types of vehicle travel at a similar pace uphill, approximately 22km/h. In any situation with two loaders, if they complete filling two different types of vehicles at approximately the same time then the faster vehicle should always receive priority.

4.9 Conclusions

- The apparent rolling resistance for empty machines travelling uphill on chalk is approximately 4%. Downhill the rolling resistance of the driver-vehicle-terrain system is dependent on the gradient of the haul road. Table 4.4 gives a résumé of the equations relating apparent rolling resistance to grade resistance.

- It is possible to estimate the rolling resistance of certain types of plant on strong, smooth chalk haul roads, enabling better estimates of the time required to complete an operation to be made.

- Grade resistance has a secondary effect on the driver which slows the vehicle down more than expected.

- Graders should not be used on chalk haul roads except to remove debris and to clear putty chalk from the surface without disturbing the underlying strong material.

- Ramps between benches should be as shallow as possible to avoid degrading the chalk at this point and to allow graders to clear the section easier.

- Obstructions on the haul roads should be kept to a minimum.

- The utilisation of different types of plant on the same haul route should be avoided if possible, to prevent bunching.

- Priority should be given to the faster machines, wherever possible, when bunching occurs.

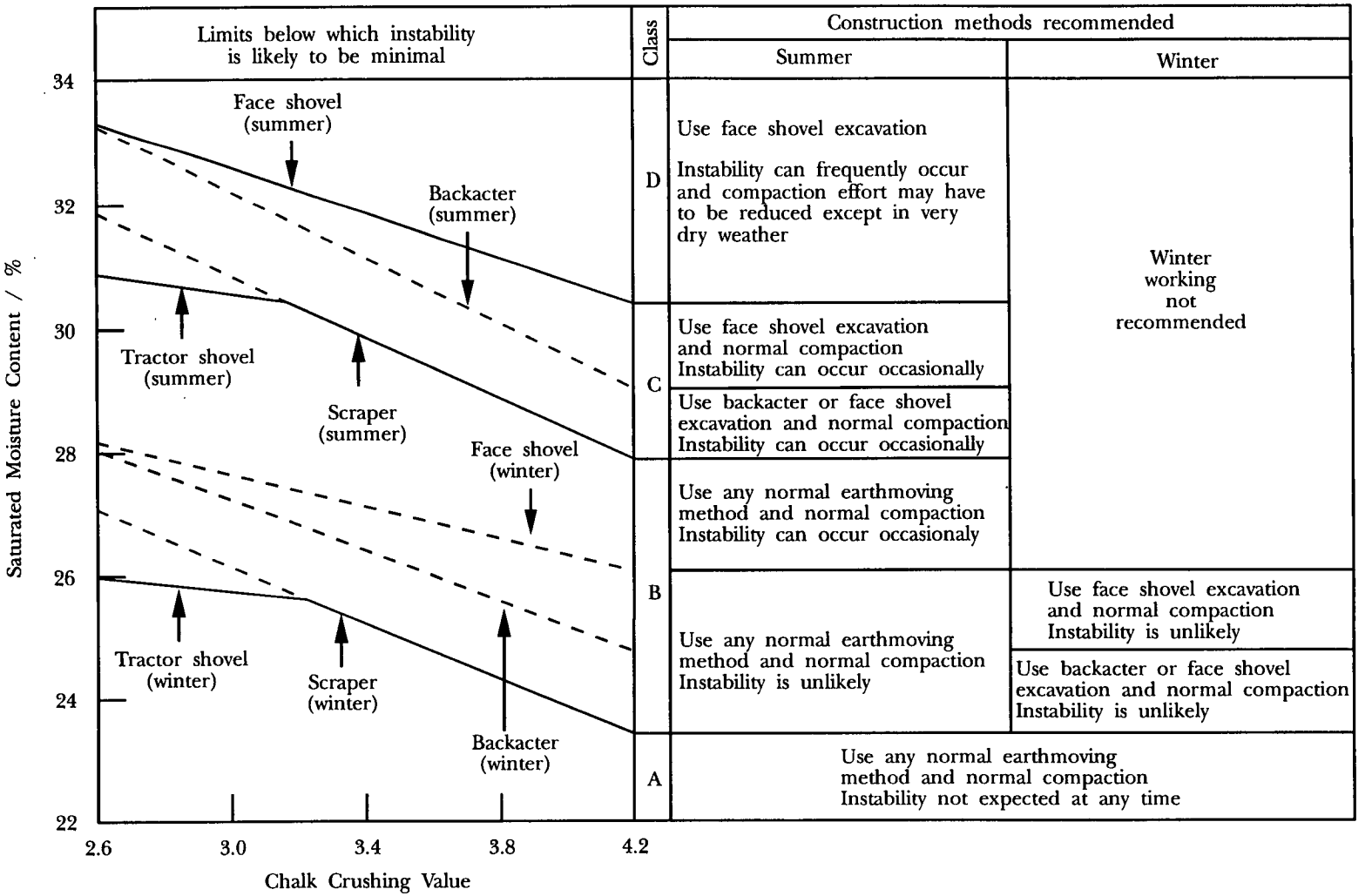

Figure 4.1: TRRL chalk classification scheme with measures required to avoid or minimise instability. (Ingoldby et al., 1977)

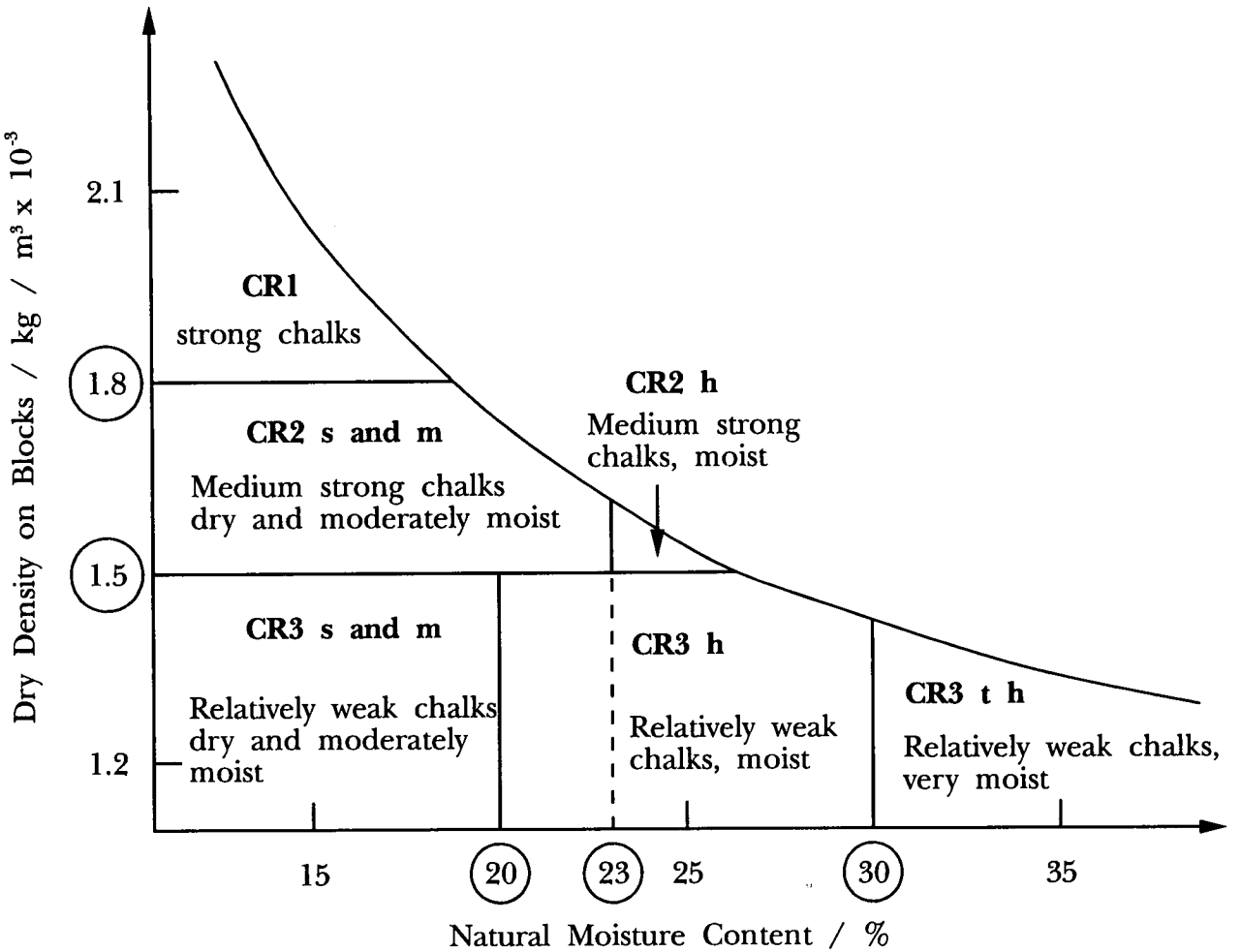

Figure 4.2: French chalk classification scheme (LCPC, 1976)

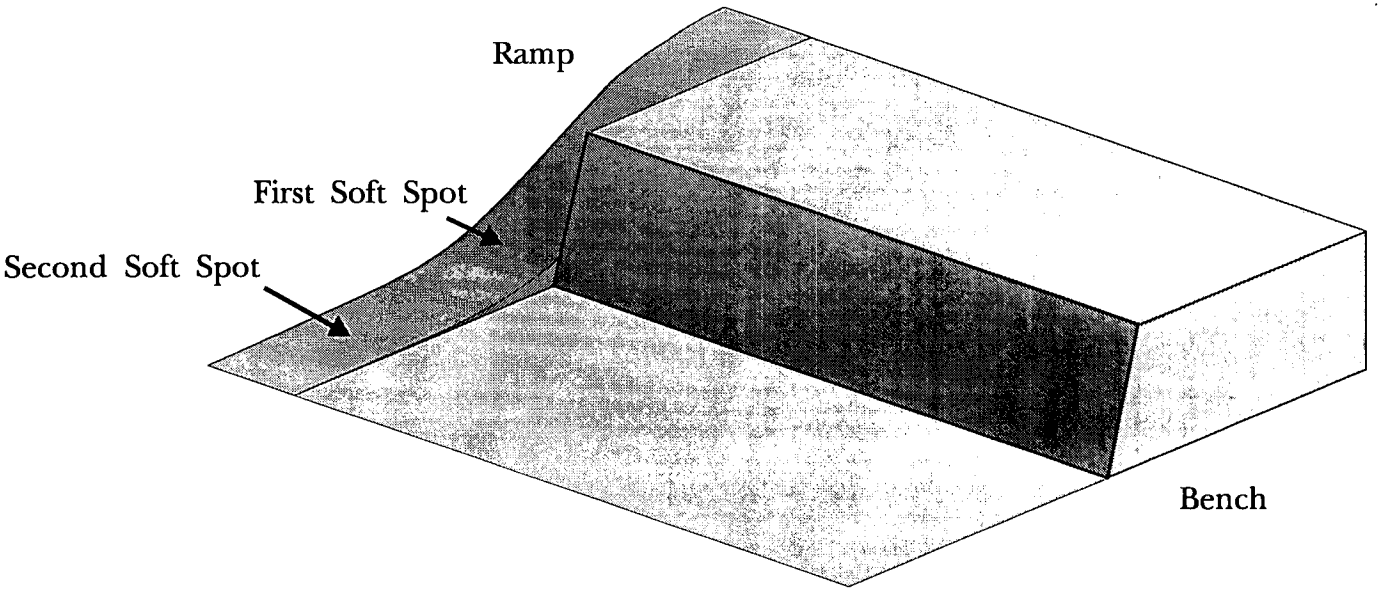

Figure 4.3: Cutting Bench and Ramp

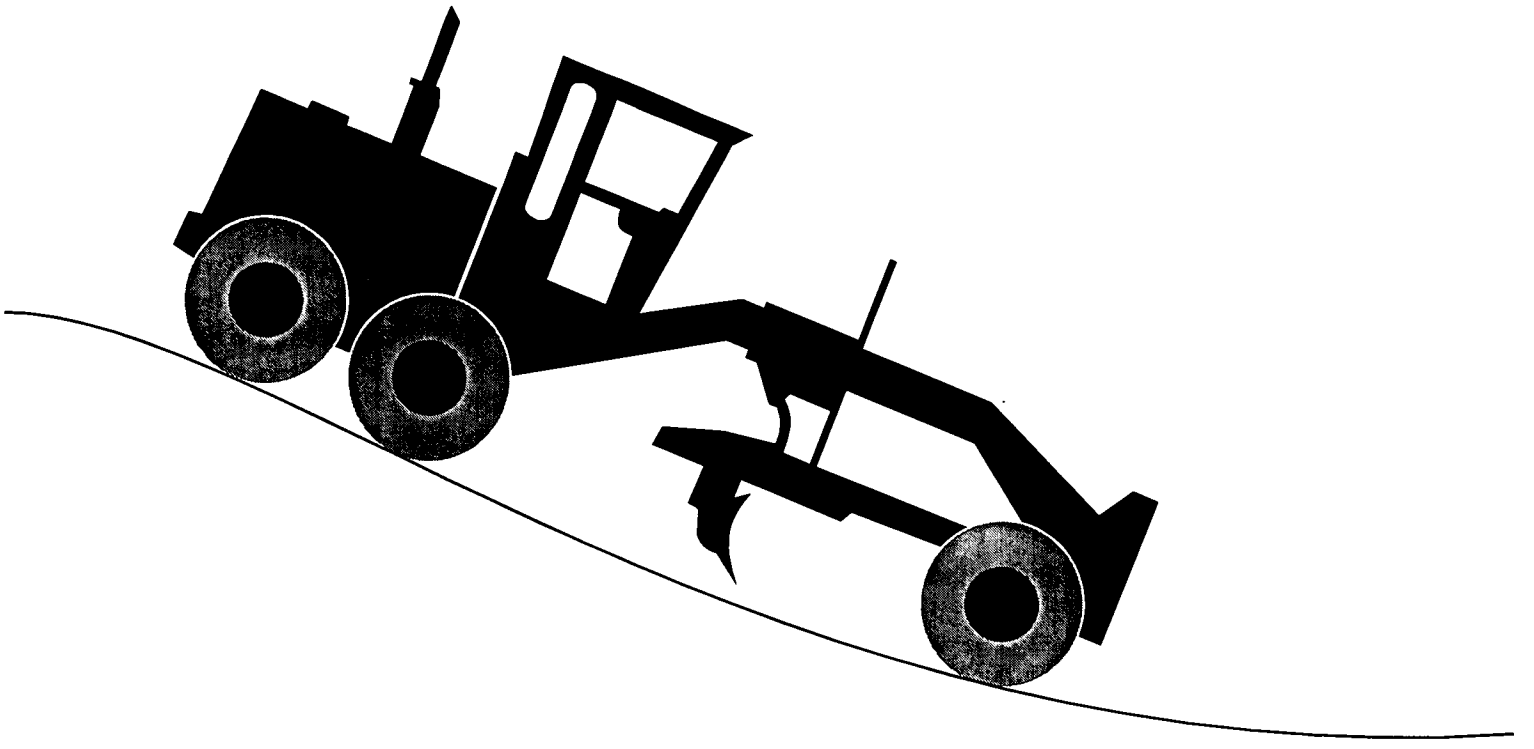

Figure 4.4: Grader Incapable of Grading on Ramps with a High Rate of Change of Curvature

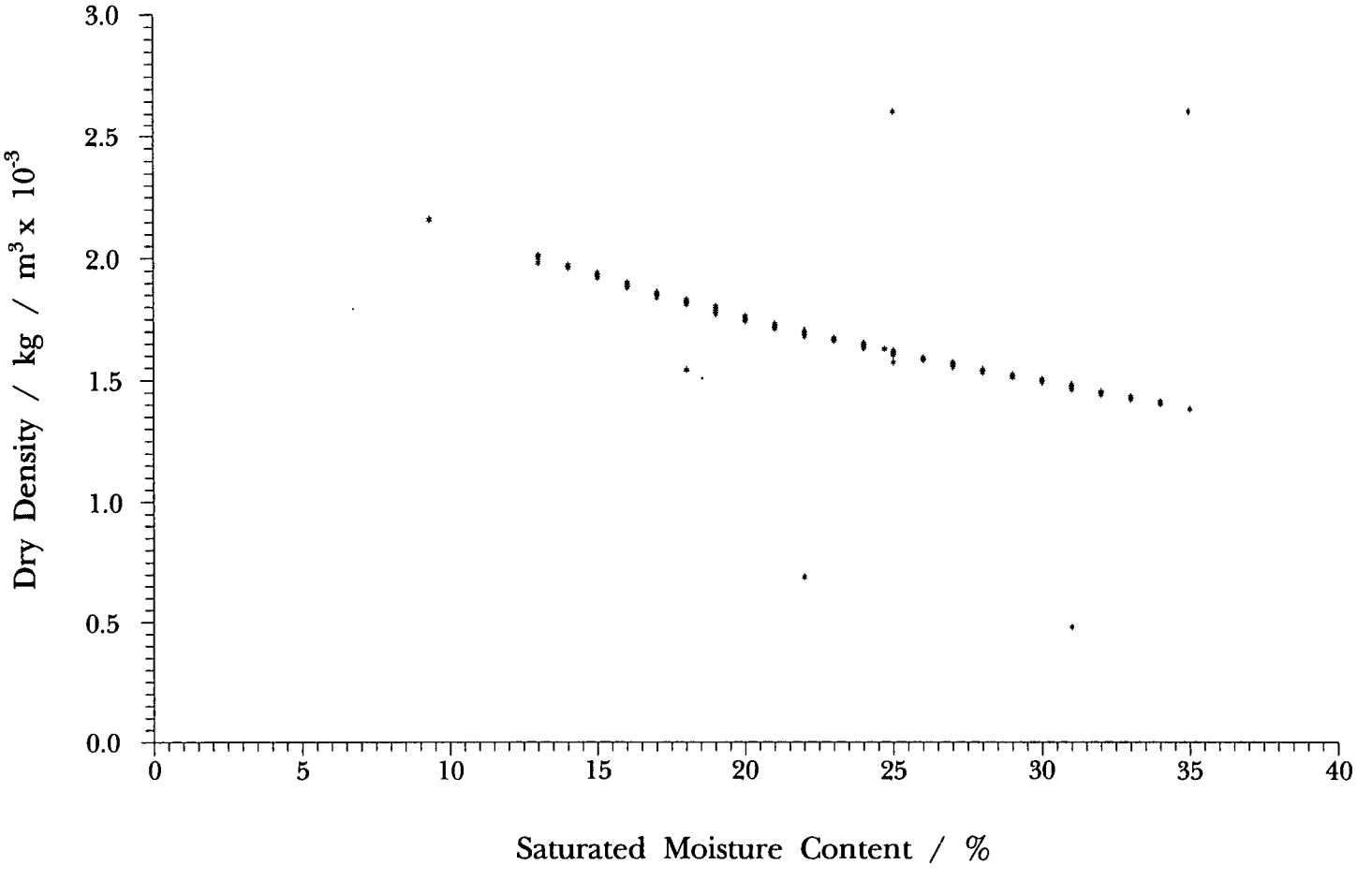

Figure 4.5: Dry Density versus Saturated Moisture Content for the Chalk on the M3 as per Tarmac Lab Data, Sample size of 500

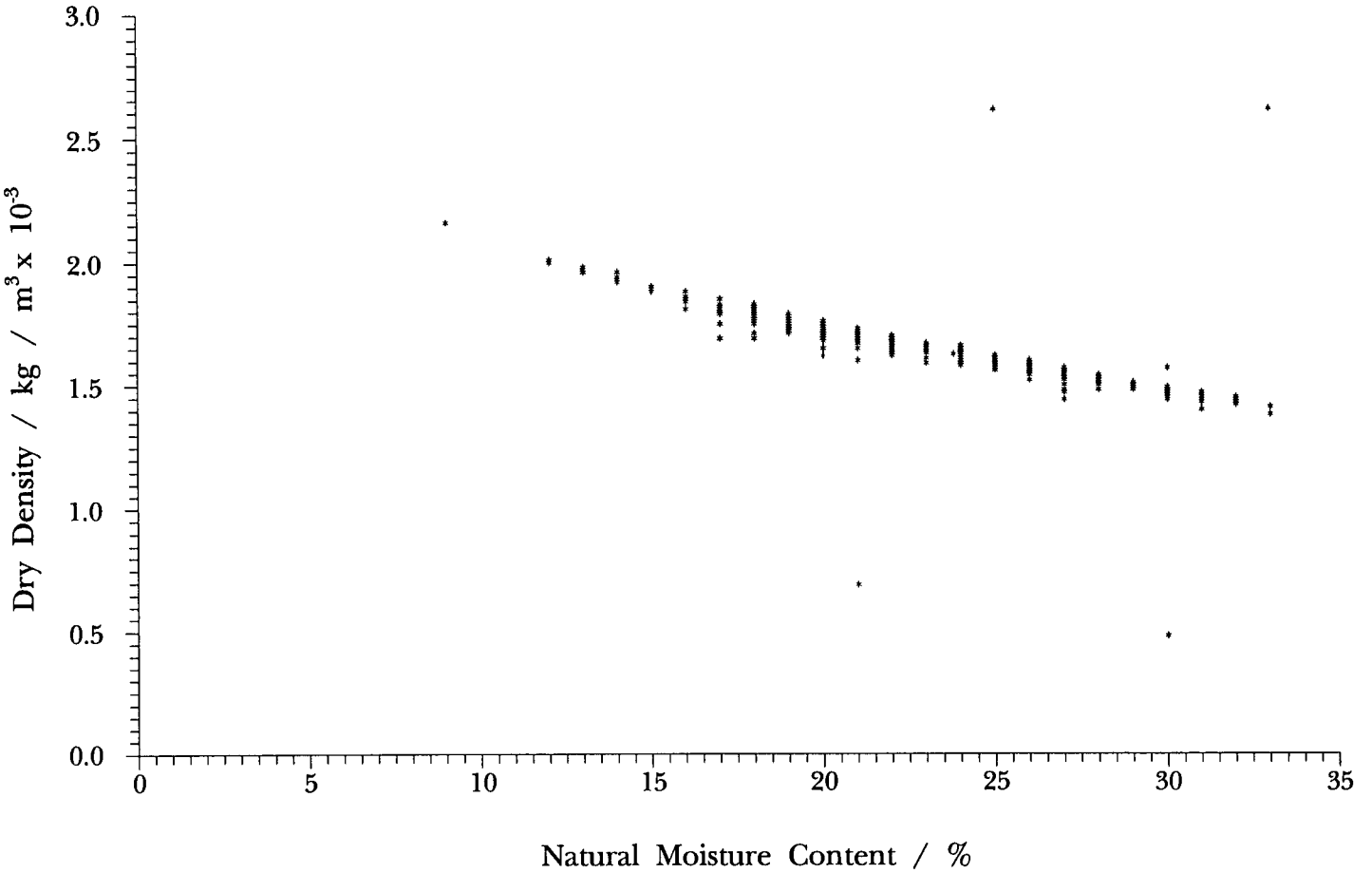

Figure 4.6: Dry Density versus Natural Moisture Content for the Chalk on the M3, as per Tarmac Lab Data, Sample size of 500.

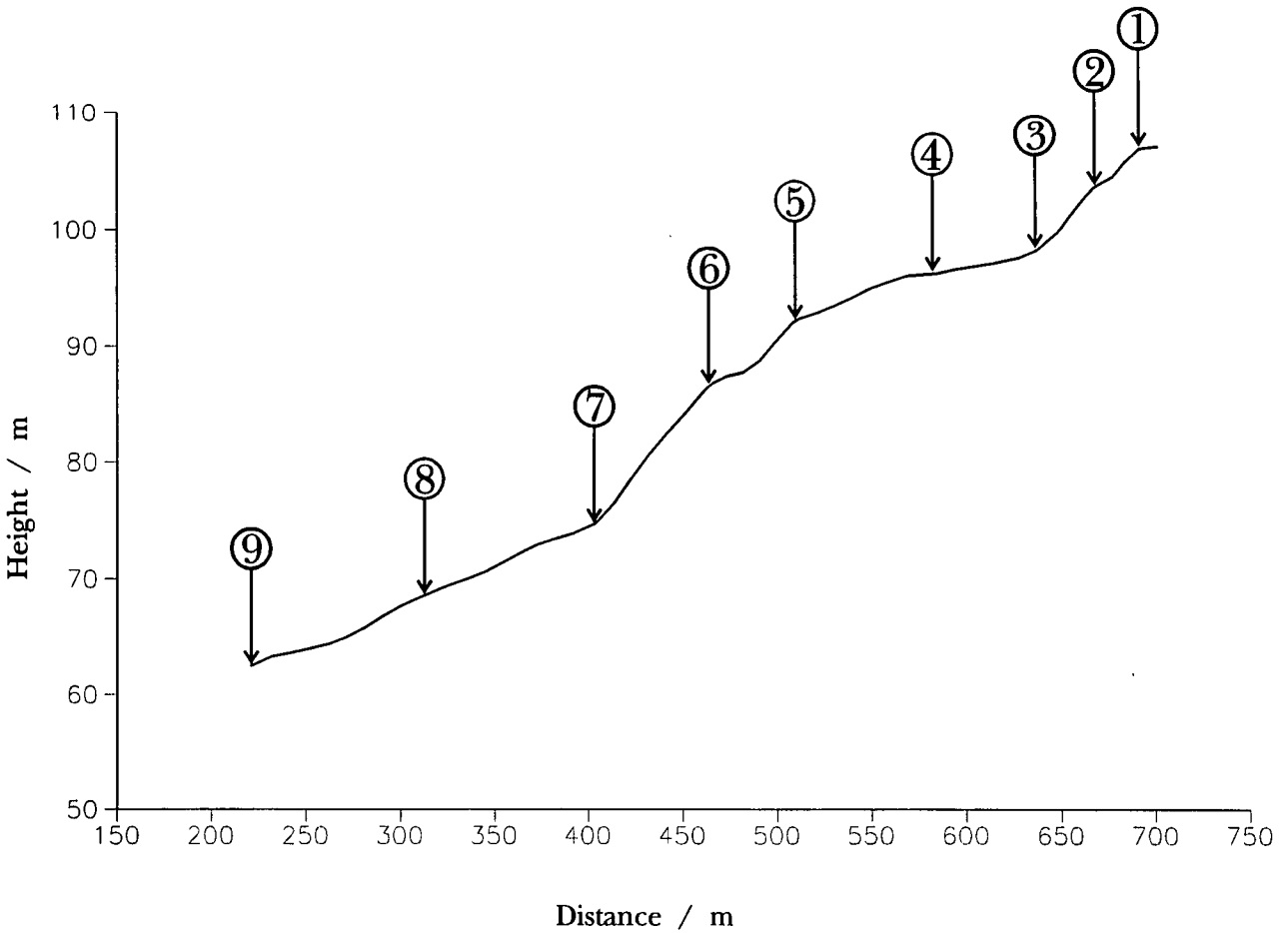

Figure 4.7: Surface Profile for a Section on the M3 with Timing Markers.

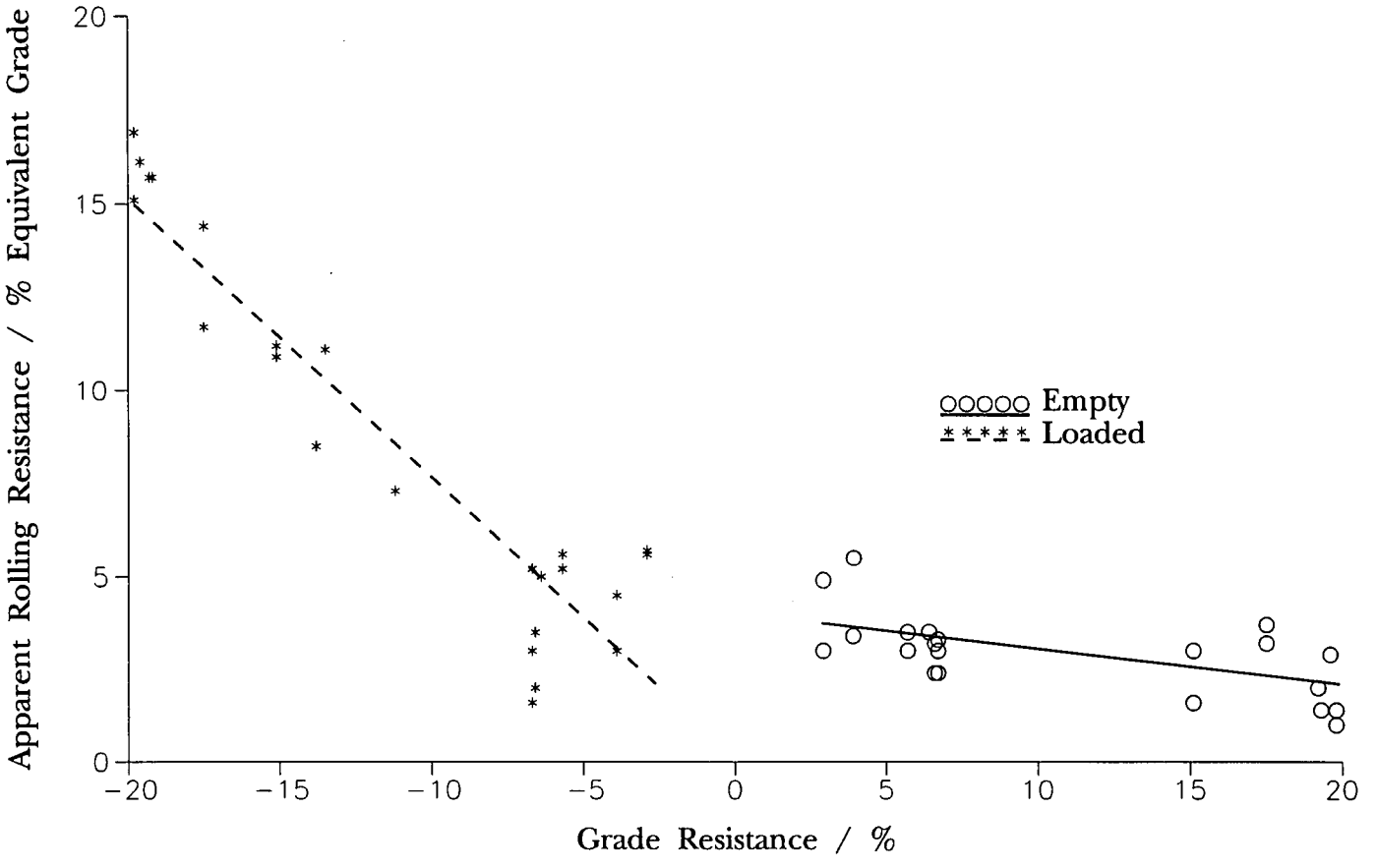

Figure 4.8: Apparent Rolling Resistance versus Grade Resistance for Volvo BM A35 Articulated Dump Trucks on Chalk

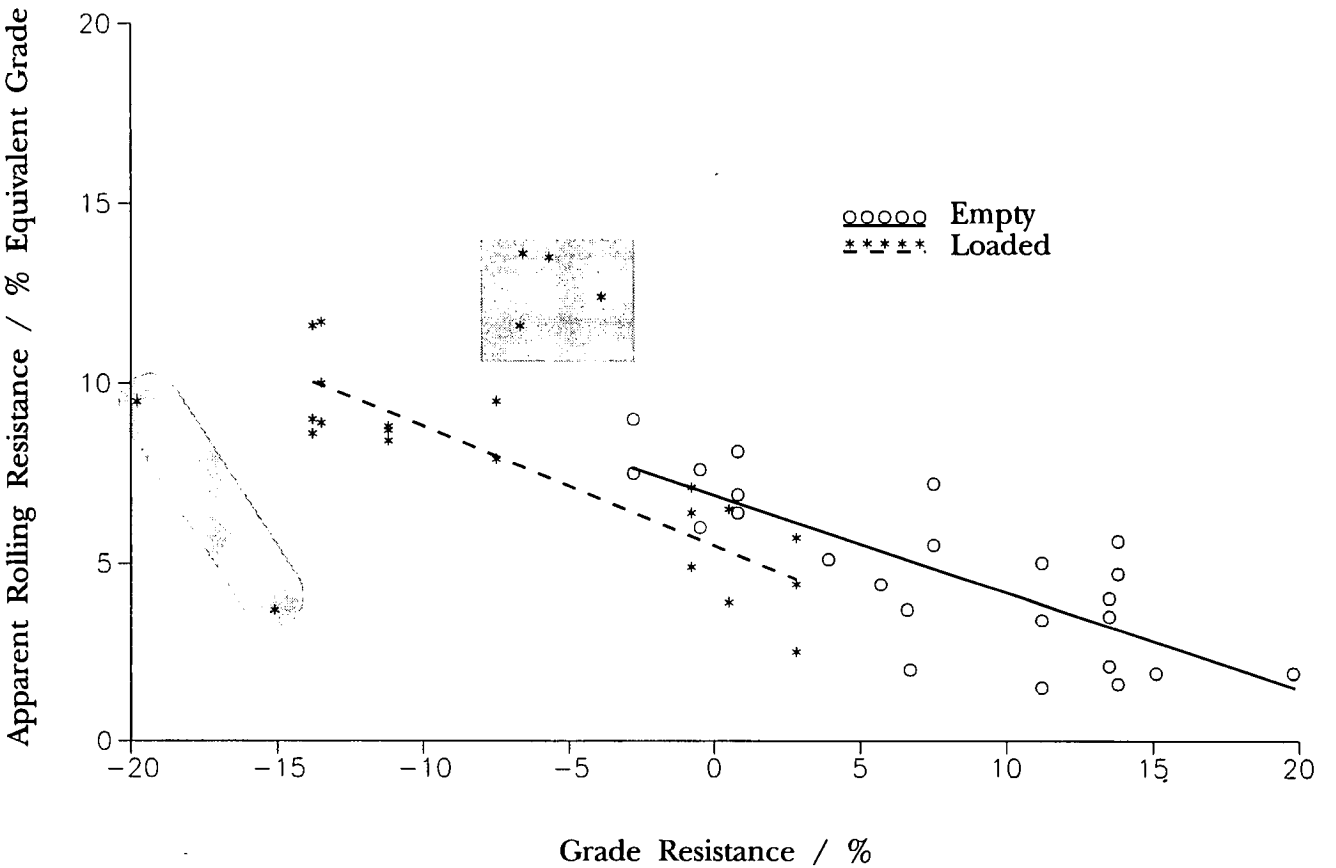

Figure 4.9: Apparent Rolling Resistance versus Grade Resistance for Cat D400D Articulated Dump Trucks on Chalk

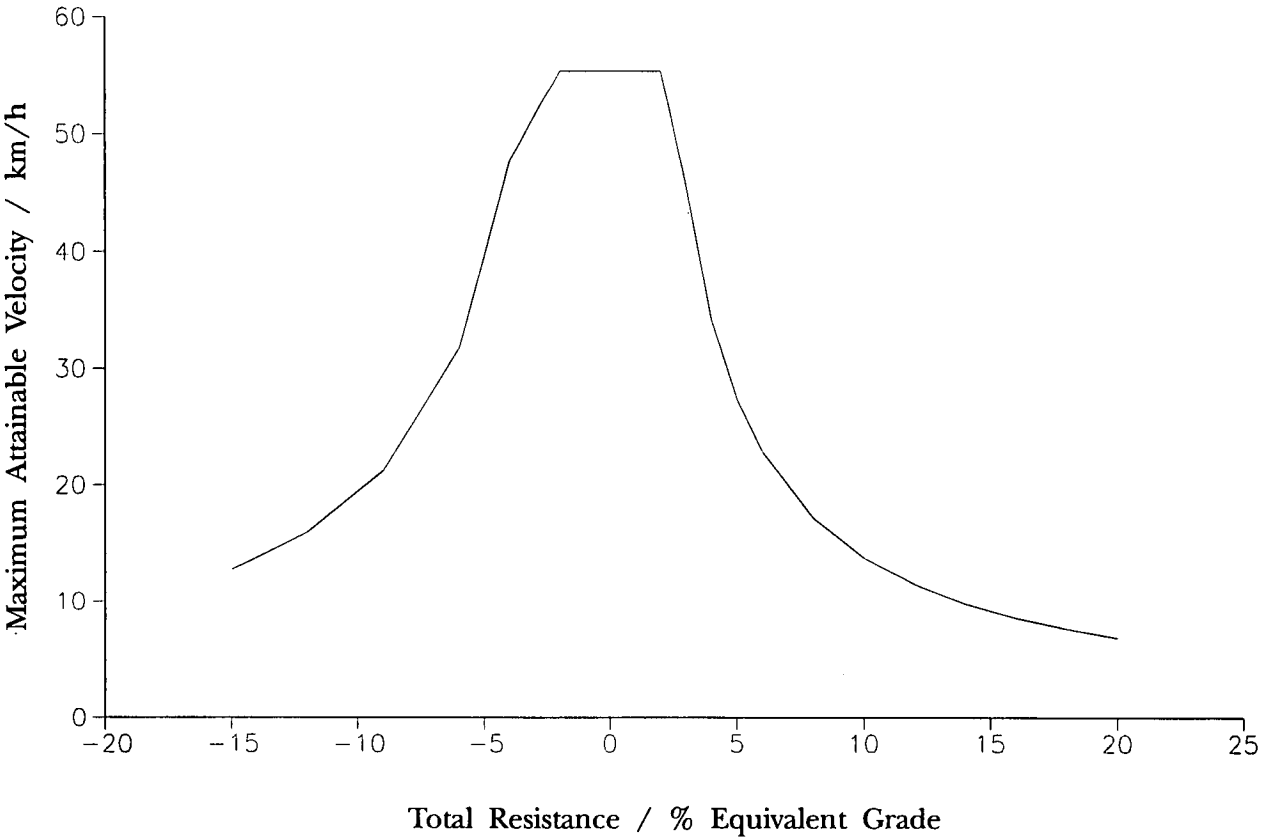

Figure 4.10: Maximum Velocity versus Total Resistance for a Loaded Cat D400D Articulated Dump Truck

Weathering Grade	Description	Approx. Range of Young's Modulus / kN/m^2	Bearing Stress causing "yield" / kN/m^2	SPT	Creep Properties
I	Hard, brittle chalk with widely spaced tight joints	$> 50 \times 10^5$	> 1000	> 35	Negligible Creep for stresses of at least 400 kN/m^2
II	Medium hard to hard chalk with widely spaced tight joints	20×10^5 - 50×10^5	> 1000	25 - 35	Negligible Creep for stresses of at least 400 kN/m^2
III	Medium to hard rubbly to blocky chalk closely spaced, slightly open joints	10×10^5 - 20×10^5	400 - 600	20 - 25	For stress not exceeding 400 kN/m^2 creep is small and terminates in a few months
IV	Friable to rubbly chalk with open joints often infilled with soft remoulded chalk	5×10^5 - 10×10^5	200 - 400	15 - 20	Exhibits Significant Creep
V	Structureless remoulded chalk containing lumps of intact chalk	$< 5 \times 10^5$	< 200	8 - 15	Exhibits Significant Creep
VI	Extremely soft structureless chalk containing small lumps of intact chalk	$< 5 \times 10^5$	< 200	< 8	Exhibits Significant Creep

Table 4.1: Amended Mundford classification correlating grade and the mechanical properties of chalk (after Wakeling, 1970)

Haul Name	Loaded Empty	Original Time /s	New Grade / %	Distance / m	Rolling Resistance / %		New Times / s	
					Lower Bound	Upper Bound	Lower Bound	Upper Bound
Big	L	22.46	-12.8	152.6	8	10.5	16.79	19.95
	E	34.54	+12.8	158.9	2	3.5	33.21	36.34
Shoreford	L	8.8	-14.8	56.6	10	12	7.76	8.54
	E	13.01	+14.8	56.6	1.5	3	12.34	13.34
4-Ramps	L	38.31	-4.6	225.6	2	5.5	25.91	31.98
	E	45.27	+4.6	225.6	3	5	26.1	31.77
Top	L	17.42	-9.1	111.2	4	7	12.98	15.65
	E	22.76	+9.1	111.2	2.5	4	18.69	20.88
Big	L	24.03	-11.4	203.3	6.5	8.5	21.40	23.43
	E	37.66	+11.4	203.3	2	3.5	39.02	43.01
Top	L	17.12	-9.1	111.2	4	7	12.98	15.65
	E	17.94	+9.1	111.2	2.5	4	18.69	20.88
Long	L	63.95	-9.3	473.9	4.5	7.5	45.67	51.04
	E	77.47	+9.3	483.5	2.5	4	82.59	92.72
Long	L	59.09	-9.3	473.9	4.5	7.5	45.67	51.04
	E	72.22	+9.3	483.5	2.5	4	82.59	92.72

Table 4.2: Results of the Analysis from Smothing the Haul Road for Volvo BM A35 Dump Trucks

Haul Name	Loaded Empty	Original Time /s	New Grade / %	Distance / m	Rolling Resistance / %		New Times / s	
					Lower Bound	Upper Bound	Lower Bound	Upper Bound
4-ramps	L	40.14	-4.6	225.6	6	8	29.38	24.67
	E	43.73	+4.6	225.6	4.5	7	28.32	35.31
4-ramps	L	35.96	-4.6	225.6	6	8	29.38	24.67
	E	35.61	+4.6	225.6	4.5	7	28.32	35.31
3-ramps	L	25.02	-4.8	181.2	6	8	25.41	20.61
	E	25.79	+4.8	181.2	4.5	7	23.24	28.82
long	L	93.75	-9.3	473.9	8	10	54.65	59.71
	E	77.92	+9.3	483.5	2.5	6	76.66	98.58

Table 4.3: Results of the Analysis from Smoothing the Haul Road for Cat D400D Dump Trucks

Vehicle	Loaded / Empty	Equation	Gradient Range		R^2
			Min.	Max.	
Volvo BM A35	Loaded	$R_o = 0.11 - 0.76 \times G$	-19.8	-2.9	88
	Empty	$R_o = 4.05 - 0.10 \times G$	2.9	19.8	40
Cat D400D	Loaded	$R_o = 5.48 - 0.33 \times G$	-13.8	2.8	78
	Empty	$R_o = 6.86 - 0.27 \times G$	-2.8	19.8	64

R_o - Apparent Rolling Resistance
G - Grade Resistance

Table 4.4: Equations of Apparent Rolling Resistance for Chalk

Plate 4.1

Plate 4.2

Plate 4.3

Chapter 5 Clay Site

5.1 Introduction

Monitoring and soil testing on a clay site was carried out on the A1/M1 link contracts 2 and 3, during the 1992 earthmoving season and early into the 1993 season. Combined, these contracts were 28km in length, with a total volume of soil to be moved of 3 million cubic metres. The earthworks were constructed using predominantly a backhoe/dump truck combination, although there were also a small number of scraper operations. The dump trucks were primarily a mixture of Cat D400D, Volvo BM A25 6x6, Volvo BM A30 6x6 and Volvo BM A35 articulated dump trucks and the excavators were a combination of Caterpillar 235 and 245.

5.2 Description of Soil from Site Investigation Report

The site investigation was carried out by five companies over a period of 11 years. From these reports the soil was typically a brown silty clay with, in the majority of cases, over 80% passing the 425μm sieve. Average Atterburg limits were w_L = 47% and w_P = 22%. The clay at depth was dark grey with over 95% passing the 425μm sieve with similar liquid and plastic limits.

5.3 Quality of Haul Roads

The haul roads were generally in good condition although flexing was apparent under most sections of the haul roads during prolonged periods of trafficking. This was considered to be caused by a lowering in effective stress due to an increase in pore water pressures in the multipass situation, see chapter 7. The material forming the haul roads was generally dry of the plastic limit, remoulded and well compacted. Rut depths were minimal, but increased if trafficked soon after rainfall. During long dry spells a layer of loose dry material tended to accumulate on the surface with trafficking. Work halted during prolonged periods of rain to preserve the condition of the haul roads and they were left to dry adequately prior

to re-trafficking. The decision to recommence trafficking came from the works manager whose decision was founded solely on experience.

5.4 Site Monitoring

The objective of the site monitoring was to establish a relationship between one or more of the soil parameters, and/or grade resistance, and apparent rolling resistance, back analysed using the available computer programs and specification sheets. Once established the relationship would enable the estimator to price a contract at tender stage with greater accuracy.

All monitoring carried out on the site had to be undertaken from the side of the haul road as no instrumentation of, or interference with, the operation of the plant was possible. Timings of vehicles were taken over 60m stretches of the haul road, where the vehicles could be assumed to be travelling at a steady velocity on a constant grade with no obstructions. Timings were taken by two people signalling and using a stop watch, figure 5.1 and averaged from at least 10 passes of a similar type of dump truck. If any vehicle was significantly delayed then the timing was removed from the analysis, as the average time would dramatically augment, increasing the apparent rolling resistance. Each section was surveyed using an electronic theodolite to ascertain its length and gradient accurately. Four soil samples were taken at 20m intervals along the section and the following soil tests were carried out at each point: moisture content, moisture condition value, MCV, cone penetrometer, and shear vane. Along with these tests a series of plastic and liquid limits, particle size distributions, both wet sieving and hydrometer methods, and multistage triaxial tests were carried out on a representative sample of the material.

From the knowledge of the timings and gradients for each section of the haul road, it was possible to use the charts developed using the Accelerator software to back analyse the apparent rolling resistance. These would then be compared with the soil and physical conditions at these points.

5.5 Laboratory Soils Testing

The laboratory testing can be split into two sections: classification of the material, and multistage undrained triaxial shear tests. All tests were carried out in accordance with the relevant sections of BS1377, (BSI, 1990).

5.5.1 Classification Tests

From the soil samples taken on the haul roads the average plastic and liquid limits were 20% and 50% respectively, each taken from a sample size of 46. Variation throughout the site was minimal and dependent on the depth of the haul road from the original ground level and to a lesser degree the position along the site. The envelope of particle size distributions is shown in figure 5.2, this was derived from 23 wet sieving and hydrometer tests, with a minimum of 88% passing the 425μm sieve. Wet sieving was carried out by washing the material through all sieves prior to drying, then dry sieving. The particle size distribution again varied along the length of the haul road and also in vertical profile. Small pockets of coarser material where found on the haul road, but insufficient trafficking on this material meant that no firm conclusions could be drawn.

Comparing these results with the site investigation data indicates that the soil has a slightly wider plasticity index, hence would be slightly less susceptible to moisture content change. All classification tests were carried out in accordance with the relevant parts of BS1377, (BSI, 1990).

5.5.2 Multistage Undrained Triaxial Shear Tests

The multistage undrained triaxial shear tests were carried out using 100mm diameter remoulded samples. The tested sample can be assumed to replicate the field conditions as the material can be considered to be remoulded having been heavily trafficked, maintained using a grader causing severe disturbance to the surface layers, then recompacted as the plant continues to traffic.

The sample was broken up and passed through a 5mm sieve and oven dried before mixing to the required moisture content. It was then sealed in a polythene bag and the moisture content allowed to equilibrate for at least 24 hours. The sample was then compacted into a mould in ten equal layers using a consistent number of blows of a 2.5kg hammer. The surface of each layer was indented, ensuring keying between layers, extruded and placed into a membrane for testing. During testing the axial strain was held constant at 2% per minute and the cell pressure was increased from ½ to 2 to 3kPa. Each increase was made as the deviator stress - axial strain curve approached a constant, or when the axial strain reached 16 or 18% respectively. Towards the end of the third increment, or at 20% axial strain, the confining pressure was reduced to the original value for a further 2% axial strain, in order to compare with the initial portion of the graph, figure 5.3. The load and displacement readings were recorded directly using low voltage displacement transducers at 10 second intervals. The voltages were recorded using a microlink data recorder which transferred the digitised data directly into a microsoft Excel spreadsheet running in the Windows environment. The spreadsheet was constructed to post the results into the relevant cells, perform all the calibration and correction factors, and plot the deviator stress - strain curve in real time. It was therefore easy to see when the increments of cell pressure should be applied.

Each multistage triaxial test yielded three Mohr's circles as in figure 5.4, one for each cell pressure. This enabled the undrained soil parameters to be established in a single test, rather than repeating the procedure on three samples where it was difficult to achieve similar moisture contents and degrees of compaction.

The sample was assumed to be near saturated, and this is confirmed in that the maximum angle of internal friction was measured at below 3°. This small angle of friction is inherent to the testing procedure, (Anderson, 1974). Hand vane shear strengths, using a 19mm pilcon hand vane, were taken in each end of the sample after testing. Four moisture contents were taken from the sample, one prior to the test and three after the test, one from each end and one from the centre, all of these values showed less than a 2% variation.

There is a strong relationship between the multistage undrained triaxial shear strength and hand vane shear strength, taken in the sample after the completion of

the test, figure 5.5. This relationship has a correlation coefficient of 0.955. The shear vane is a quick and useful test to do at this stage as it can be used to characterise the soil and be utilised easily and rapidly in the field. The cluster of values at the high end of the graph is because the hand vane can only read to a maximum of 174kN/m^2.

Shear strengths have been related to soil plasticity data by various workers (Skempton et al., 1952, and Whyte, 1982). In this context consistency index, equation 5.1, has been found to be a useful normalising concept when relating moisture content to the plasticity of the soil.

$$\text{Consistency Index, } I_c = \frac{w_L - w}{w_L - w_P} \tag{5.1}$$

where: w_L liquid limit
w_P plastic limit
w corrected moisture content.

Where the corrected moisture content, equation 5.2, is the correction to the natural moisture content assuming the fraction $> 425\mu m$ has an absorption moisture content of 4%.

$$\text{Corrected moisture content} = \frac{100\%.w_N - \%>425\mu m.4\%}{\%<425\mu m} \tag{5.2}$$

where w_N natural moisture content

The results of the multistage triaxial tests show good correlation between undrained shear strength and consistency index, figure 5.6, with an R^2 value of 97.4% on equation 5.3, also between hand vane shear and consistency index, figure 5.7.

$$c_u = 0.79\exp(4.94 I_c) \tag{5.3}$$

These graphs show that the soil is very susceptible to changes in moisture content, dropping from an undrained shear strength of 110kN/m^2 at the plastic limit, to a value of around 40kN/m^2 at a consistency index of 0.80, this was considered to be caused by the relatively high medium silt content, figure 5.2, making the soil, moisture content susceptible. This relationship was compared with similar site investigation data, figure 5.8, and equation 2.51 postulated by Whyte (1982), figure 5.9, which indicates excellent correlation, R^2 = 96.9%. From figure 5.8, it is evident that there is significantly more variation in the site investigation data, which would make any subsequent detailed analysis with this information almost impossible.

In general terms it is clear that unless the quality of site investigation reports improve then the use of the data contained within them becomes limited, especially for detailed analysis. The shift in emphasis towards design and construct projects should result in contractors demanding more detailed, research quality standard, site investigation reports. This will increase the cost of the investigation, but the information contained within should be accurate and thus reduce the risks taken (Blockley, 1993, and Whyte, 1994).

5.6 Site Testing and Results in Relation to Rolling Resistance

The following sections contain all the individual relationships of rolling resistance with: grade resistance, moisture condition value, cone index, hand vane shear strength, consistency index, and rut depth.

5.6.1 Grade Resistance versus Velocity and Rolling Resistance

The calculation of apparent rolling resistance was undertaken, as described earlier in chapter 3, by using the Accelerator software. This program was designed to normalise the effects of grade resistance, therefore it was expected that grade resistance would not have a secondary effect on the apparent rolling resistance of the plant. Figure 5.10(a-j) shows the relationship between grade resistance and velocity, and apparent rolling resistance, for the various articulated dump trucks monitored. The trends in these graphs are similar for all types of vehicle: for an

empty vehicle the apparent rolling resistance decreases at an average rate of 0.70% per percent increase in gradient; and for the loaded vehicles the apparent rolling resistance decreases at an average rate of 0.51% per percent increase in grade. There are two possible explanations for this phenomenon: the Accelerator computer package is not correcting properly for grade resistance, or the gradient of the haul road is having a secondary effect on the performance of the operator-vehicle-terrain system. The former reason was considered less likely as the software does not have a secondary correction for the effect of grade on the driver and the three methods of calculating rolling resistance: Accelerator, Vehsim, and the performance charts, all give similar results. It was considered therefore that the gradient of the haul road does have a secondary effect on rolling resistance. For the subsequent chapters the apparent rolling resistances have not been normalised to the value at zero grade resistance, but an example of the effect of this fact is shown in each section. All of the results were not normalised for the simple reason that if the computer program Accelerator, or any of the other methods are going to be used in conjunction with the findings of this thesis then, for simplicity, the user will not want to apply a correction factor to the input rolling resistance, for each change in grade resistance, on each section of the haul road.

Each point on figure 5.10 (a-j) is an average of at least ten passes of similar plant. Figure 5.11 shows identical data to figure 5.10(b) for a loaded Cat D400D articulated dump truck travelling uphill, with the 95% confidence intervals for apparent rolling resistance about each point. Only one graph is shown with error bars for clarity. The confidence limits were calculated using equation 5.4.

$$\text{limits} = \bar{x} \pm t.\left(\frac{s}{\sqrt{n}}\right) \tag{5.4}$$

where: $\bar{x}$ mean of the data

s sample standard deviation

n sample size

t value from the Student's T-table corresponding to 95% confidence and (n-1) degrees of freedom.

The smaller error bands in figure 5.11 were generally associated with a greater number of readings. The error bars for grade are the maximum and minimum gradients for each 10m segment within a section. This shows that all the data is explained by the least squares best fit line.

Figure 5.11 also shows 95% confidence and prediction intervals for the regression between the two variables: grade resistance and the average apparent rolling resistance, as described in section 5.7.3. The 95% prediction interval would be used for estimating the apparent rolling resistance for a single pass of a vehicle on a haul road of specified gradient, whereas the 95% confidence interval would be the average apparent rolling resistance over the duration of an operation.

A single graph of the 95% confidence bounds and intervals will be given for each of the single factor interactions with apparent rolling resistance, simply to show the basic trend. The graphs for all cases are not shown as a more detailed multiple regression analysis is carried out in section 5.7.4.

5.6.2 Moisture Condition Value versus Rolling Resistance

The moisture condition value (MCV) test developed at TRL (Parsons, 1976, and SDD, 1989) is being used extensively on road sites for determining the acceptability of fill material. The benefits of this test are that it is relatively quick to complete and it gives an almost instantaneous result. These reasons make the MCV an ideal method for estimating and monitoring the speed of the plant, both at the tender and construction stages of an operation. The moisture condition apparatus can be utilised to characterise a soil with respect to moisture content, therefore if this parameter alters on site the effect on velocity hence productivity should be calculable.

On site, the MCV test was carried out immediately after taking the four samples and returning to the lab. Figure 5.12(a-j) shows the relationship between apparent rolling resistance, back analysed using Accelerator and MCV, for a variety of articulated dump trucks split into both uphill and downhill grades. These figures can be split into four main sections: loaded uphill, loaded downhill, empty uphill, and empty downhill. The gradients of the sections were all quite shallow, generally

below 5%, it was therefore assumed that there would be no severe secondary effects of grade resistance on the apparent rolling resistance, as recorded with the chalk, compare with section 4.6. Several of these graphs do not have sufficient data to derive any firm conclusions, but in general, as the MCV increases, the soil becomes drier and stronger, the average apparent rolling resistance decreases slightly. The apparent rolling resistances plotted are calculated from the average times of at least ten passes of a similar type of dump truck, and each point will have an upper and lower limit and be normally distributed.

Combining the graphs for all the vehicles on each of the four categories of haul road, it can be seen that the apparent rolling resistance for each case is relatively constant. At any single value of MCV the apparent rolling resistance could vary by approximately 5%. For loaded vehicles the average apparent rolling resistance lies between 3 and 7% for uphill grades and between 6 and 9% for downhill grades. The apparent rolling resistance increases when the vehicles are empty and lies between 6 and 10%, and 9 and 12% for uphill and downhill grades respectively. The reasons for this increase in apparent rolling resistance from uphill to downhill grades could be caused by vibration effects on the driver, or subconscious psychological effects in the knowledge that the operation is over resourced and therefore would have to wait at the loading area. When returning to the loader the driver is apt to decrease the speed below the maximum attainable to ensure that the vehicle is not driving in a strained condition, hence overheating the engine.

The uphill grades tend to have a lower apparent rolling resistance as the driver is more likely to attack these sections at a faster speed and keep the accelerator fully deployed throughout the ascent. It is not possible to relate the spread in apparent rolling resistance to a corresponding range in velocity as the difference on a shallow grade will be different to that on a steep slope.

Figure 5.13 (a and b) shows the same data as figure 5.12 (e and f) except that the apparent rolling resistance has been corrected for grade in accordance with figure 5.10 (e and f) respectively. This has the effect of bringing both the uphill and downhill data points into alignment. As explained previously, this correction could be performed for all vehicles, but when utilising computer programs or specification sheets for estimating the apparent rolling resistance, a correction

would have to be made to the gradient of each section of the haul road. This would be a waste of time as well as a possible source of error.

From the evidence of the data held in figure 5.12 (a-j) it could be assumed that the apparent rolling resistance does not vary with moisture condition value, for each of the four categories of hauling on relatively shallow grades. Using moisture condition value as the sole estimator of apparent rolling resistance, could lead to sizeable errors in the estimation of the velocity of vehicles on site. This can be emphasised by figure 5.14 which shows the 95% bounds for each average point, and the 95% confidence and prediction intervals for a loaded Cat D400D travelling uphill. The error bars for MCV are the maximum and minimum of the four readings for each section. This shows a surprisingly large range considering the low variation in moisture content along the section.

5.6.3 Notes on the Moisture Condition Value Test

Several limitations can be noted about the MCV test on this silty clay. Firstly there is not one single value of MCV for an individual sample, this depends on how the sample is broken up and placed in the mould for testing. If the sample has bulked too much to fit in the mould then some initial compaction is required in order to fit the fabric disc to the top of the sample. If the sample is very dry then the test does not appear to be sensitive enough to pick up variations in the moisture content, as the dry material does not compact easily and maintains a high air voids content. This could relate to large decreases in shear strength.

The moisture content apparatus works on the principle that there is a direct relationship between maximum bulk density, compactive effort and moisture content, and that shear strength is a measure of acceptability. Knowing, from the multistage triaxial testing, section 5.5.2, that there is a relationship between shear strength and consistency index, figure 5.15 was plotted, showing the relationship between MCV and consistency index. This figure shows the information from the site investigation report along with the work carried out on site. Both sets of results show that there is a distinct trend, but there is a large data spread, e.g. taking a MCV value of 14 the consistency index varies from 0.9 to 1.3 from laboratory data and from 0.6 to 1.6 from the site investigation data. This figure

would tend to indicate that there is a weak relationship between the MCV and the undrained shear strength of a material.

It has been shown by Parsons et al. (1988) that the repeatability and reproducibility of a moisture condition value test on a heavy clay is ± 0.8 and ± 1.6 respectively, which agrees with the measured results.

Characterisation of a soil can also be undertaken using the MCV apparatus by varying the moisture content of a sample. The moisture content along each individual section varied slightly, therefore a graph of moisture content versus MCV for each section could be constructed. Most of these graphs displayed the characteristic linear decrease in MCV as the moisture content increased, but several show anomalies, including increasing MCV with increasing moisture content and no apparent trend in the data. These results cast doubts on the accuracy of the test with respect to moisture content, especially in the everyday work environment where the utmost care may not be taken in relation to the accuracy of the testing procedure. BS 1377: Part 4 (BSI, 1990) states the procedure for sample preparation and placement in the mould, this arbitrary method is carried out by placing the soil "as loosely as possible in the clean dry mould" and states that, "the soil may be pushed into the mould if necessary". This specification may contribute to the lack of consistency in the reported results. As indicated in BS1377: Part 4 (BSI, 1990):

> "If the soil is not placed in its loosest condition the reproducibility of the test may be affected.".

Perhaps the use of a higher mould could alleviate some of these preparatory problems. Assuming the soil is placed in its loosest condition this will only be the MCV for the material that passes a 20mm sieve, if the material is further reduced in size then the MCV would not give the same answer, as the initial packing state would be considerably different. This is a major drawback of the test for research purposes.

5.6.4 Cone Index versus Rolling Resistance

The cone penetrometer was developed by the American army to determine if an area of ground was passable for military vehicles, giving a go / no go response, (ASCE, 1985). From its inception it has been used to predict the performance of vehicles in both frictional and cohesive materials (Freitag, 1965, and Wismer et al., 1972). Agricultural engineers have related the cone index to performance parameters such as drawbar pull and thrust, but all researchers have reported large variations in the results, see section 2.13.3.

Various types of cone penetrometer exist, but the one used in this study was the MEXE cone penetrometer, which had a cone 25mm high and a 30° tip angle attached via connecting rods to a calibrated spring, figure 5.16. The cone is pushed into the ground at a steady rate and readings taken at calibrated depths. The cone gives outputs as in figure 5.17, showing the average cone index at four points along a section; each line is an average of six readings of similar variation. The data shows no constant trend and it was therefore considered impossible to try to accurately predict the speed of the plant from these data.

One of the major problems with the cone is that it is influenced dramatically by the presence of particles of relatively large diameter, greater than 2mm. When encountering a stone the cone attempts to push it, blunting its point and shearing a far larger area of soil, hence reporting a higher, misleading result. Keeping the cone moving at a constant pace is another problem difficult to combat without employing some mechanical device, which would have been impractical for use on heavily trafficked haul roads. When passing from a strong material through to a weaker substratum the cone has a tendency to accelerate making accurate data recording difficult.

5.6.5 Hand Vane Shear versus Rolling Resistance

The hand held shear vane has been used since 1918 for the rapid determination of the undrained shear strength of saturated clays. The vane is generally of cruciform shape with the height of the vane equal to twice its width, figure 5.18, and works on the principal of shearing the soil along a specified cylindrical boundary.

Knowing the length of the plane it is relatively simple to correlate applied torque to undrained shear strength. The torque is measured on a calibrated spring attached to the vane via extension rods.

The vane should not be used on laminated soils or a material with a large stone content, as any stone traversing the shearing plane will increase the torque required to fail the soil, thus yielding an artificially high reading for the vane shear strength of the material. BS 1377: Part 9 (BSI, 1990) limits the use of shear vanes to weak cohesive materials.

The vane used on site was a 19mm diameter, 38mm high shear vane, with a maximum reading of 188kN/m^2, before correction. This was used to measure the surface vane shear strength of the haul road. The rate of shear was kept constant at approximately 60°/s, opposed to the 6°/min recommended in BS 1377: Part 9 (BSI, 1990). The shear rate was kept high as it was more akin to wheel loading and the time available to take a reading was limited by the continual trafficking of the haul road. At least three readings were taken at each of the four points within a section, these were averaged to give an overall value for each section. The measured vane shear strengths were corrected in accordance with Bjerrum (1973). This empirical correction factor is applied because the undrained shear strength measured by the vane is generally greater than the average strength mobilised along a failure surface in the field. This discrepancy was found to increase as the plasticity index of the soil increased, and attributed to rate and anisotropic effects.

Figure 5.19 (a-j) shows the relationship between apparent rolling resistance and hand vane shear strength for a variety of articulated dump trucks travelling both uphill and downhill, loaded and empty. As with the MCV results several of the graphs do not contain enough information to formulate any definite conclusions, but consistent trends are visible. Several of the figures contain a cluster of points at the upper limit of vane shear strength, this is due to the limitation of the apparatus only reading to a corrected value of 174kN/m^2. Any point at this value of shear strength could move to the right of the graph by some indeterminable amount. In the majority of cases the graphs show the expected trend, in that as the shear strength of the soil increases the apparent rolling resistance decreases. There is a clear split in the value of rolling resistance between the uphill and downhill grades, the uphill grades showing lower apparent rolling resistances by approximately 2%.

ensure the correct value for the plastic limit is determined. The main problem with the test is that it is heavily operator dependent, as every operator applies a different pressure and considers the sample to have failed at a different stage. The required length of time to carry out the test is very dependent on who is completing the test. For research quality work only four complete tests were possible in one day, whereas the length of time spend on each plastic limit test on site was considerably less. For a site investigation company who charge in the region of £10 for both a liquid and plastic limit test, they can not afford to carry out the testing at research quality speed. This is probably a major cause of the wide variation in the graph of consistency index versus undrained shear strength, figure 5.8.

Figure 5.22 (a-j) shows the relationship between rolling resistance and consistency index for various articulated dump trucks. As indicated previously, the downhill grades have a higher apparent rolling resistance than the uphill grades, for similar reasons as explained for the MCV test. Experimentally the consistency index has the advantage over the hand vane shear method in that there is no restriction on the extent of the data range. Another advantage is that consistency indices can be calculated from the information given in the site investigation report, making initial predictions possible at the tender stage. The accuracy of any estimation relies wholly on accurate input, and as has been shown in figure 5.8, site investigation data can be misleading.

For on site checking a value for the consistency index could be estimated from the corrected moisture content of the soil of a previously tested material, as the Atterburg limits for a particular soil should not change considerably, but the corrected moisture content would take at least 24 hours to determine accurately. This should not be a problem for routine monitoring of the velocity of the plant.

Most of the graphs in figure 5.22 show the expected trend with lowering apparent rolling resistance as the consistency index increases, i.e. the soil becomes drier. These graphs show a better correlation than any of the previous soil property relationships, indicating that the consistency index of the sample is a superior single variable method of estimating the apparent rolling resistance of the driver-vehicle-terrain system. This is indicated graphically in figure 5.23, showing the 95% confidence bounds for apparent rolling resistance and 95% confidence and prediction intervals for a loaded Cat D400D articulated dump truck travelling

uphill. The errors on consistency index assume that the Atterberg limits and the moisture content were correct to $\pm 1\%$.

The graph for the empty Cat D400D shows rolling resistance increasing slightly, this may be due to the different suspension systems between the Caterpillar and Volvo trucks, or simply an anomaly in the field results. Any decrease in empty speed, caused by an increase in apparent rolling resistance, will be compensated by a corresponding increase in velocity of the loaded trucks. This increase in speed is more important to the overall productivity, as the vehicle generally travels in a laden condition for a greater proportion of the complete cycle time.

The graphs for the Volvo BM A25 6x6 articulated dump trucks show a wider data spread than the other vehicles. The reasons for this cannot be explained, but it may stem from the fact that there are insufficient results to form any firm conclusions.

Figure 5.24 (a and b) compare the best fit relationships of rolling resistance and consistency index for three types of articulated dump truck Cat D400D, Volvo BM A30 and Volvo BM A35, in both the loaded and empty states. As would have been expected, all vehicles show similar characteristics in the loaded state, figure 5.24a, especially on downhill grades where the best fit lines of apparent rolling resistances are almost coincident. The Caterpillar machine shows the same trend as the Volvo machines on the uphill grades but at a slightly greater value of apparent rolling resistance. The reasons for this are unclear as the machines or drivers could not be instrumented. Unloaded there is no information available on the Volvo machines travelling uphill, but the trend would be expected to be parallel to the downhill grades, as in all the previous cases, and about 2% equivalent grade lower. The Volvo machines experience a higher apparent rolling resistance at lower values of consistency index, but this decreases as consistency index increases, unlike the Caterpillar vehicle. The difference for this discrepancy is considered to lie in the different suspension methods between the two machines, causing two completely different dynamic responses at the driver position. Further work instrumenting the driver and the machine would be needed before any firm conclusions can be drawn on the relationship between the smoothness of the haul road and the speed that the driver is willing to travel.

The apparent rolling resistance was again corrected for grade resistance and plotted against consistency index, figure 5.25. As previously this has brought the results for the two driving conditions together and tightened the data spread. Clearly from this result the gradient of the haul road has a marked effect on the speed the driver is willing to travel.

5.6.7 Rut Depth versus Rolling Resistance

The rut depth was taken by placing a rule across the rut and measuring from the rule to the rut bottom. Calculating the rut depth in this manner does not take into account any heaving of the material at the side of the rut or any elastic recovery of the material after the passage of the vehicle. Measurements were recorded at each of the four points along the section, and the average value for the section calculated. Average rut depths were plotted against apparent rolling resistance for all vehicle types, figure 5.26 (a-j), with an estimated error of $\pm$25mm.

For any driving condition the results generally show that as the rut depth increases the apparent rolling resistance increases slightly. Several of the individual graphs have an insufficient number of points to draw any firm conclusions. The results for the empty machines tend to have quite a wide spread in data, and the trends are not so well defined. This is partly due to the problem of the empty vehicles not having their own haul road and travelling in the same tracks as the loaded vehicles, which cause larger ruts.

As in the previous sections the apparent rolling resistance when travelling downhill is greater than the vehicles travelling uphill. Figure 5.27 (a and b) shows equivalent graphs to figure 5.26 (e and f), except that the apparent rolling resistance has been corrected for grade resistance. This has the effect of bringing the results for the uphill and downhill conditions closer together, nearer to the expected trend for these graphs.

At this stage rut depths can only be used as an estimator of rolling resistance after the commencement of the contract, see chapter 6. It is therefore of relatively little importance to the estimator, but could be useful as a quick monitoring method on site. Figure 5.28 shows the 95% confidence bounds and 95% confidence and

prediction intervals for a loaded Cat D400D articulated dump truck travelling uphill. From this graph it can be seen that rut depth can be an excellent estimator for apparent rolling resistance, with in this case a correlation coefficient of 0.81.

5.7 Regression Analysis

Regression analysis is a statistical method used to determine the relationship between two or more variables. As the results reported in the previous sections can be assumed to be approximately linear, simple linear regression was used as an initial estimate. Using the method of least squares the equation of the best fit line through these points can be ascertained relatively easily.

5.7.1 Theory

Although the majority of the regression work carried out was with multiple input variables, the simplest way of understanding regression analysis is to consider a single input variable and the response, as this can easily be displayed graphically in Cartesian form. The basic theory can then be easily expanded to incorporate a greater number of input variables.

The assumptions relating to regression analysis are as follows:

1. In the underlying population the relationship between the input and response should be a straight line. At each value of the input parameter a mean of the output can be calculated and the averages of all the outputs must, at least approximately, lie in a straight line.

2. For each value of input, the variation in the population of responses should be approximately the same. This variance is usually called the variance of the response about the regression line, and is denoted by σ^2. Correspondingly σ is called the standard deviation of the response about the regression line.

3. For each input value, the distribution of the response in the population should be approximately normal.

4. The response that are obtained should be approximately independent.

These conditions have been approximately met by the monitoring carried out on site and assumed to be true for the data sets.

The simple regression theory is best illustrated with an example. Figure 5.29 shows the relationship between apparent rolling resistance and grade resistance for all loaded vehicles travelling downhill, studied on the A1M1 link. All vehicles have been grouped together as the difference between the various vehicles was slight, and in the majority of cases there was an insufficient number of data points to complete an accurate regression. As can be seen from figure 5.29, the relationship is approximately linear. Several linear best fit lines could be drawn through the data, but the one depicted is the least squares best fit line, i.e. where the sum of the squares of the deviations from the best fit line has been minimised. The method for finding the best fit line is best illustrated with an example. Using the data for figure 5.29, the spreadsheet in figure 5.30 was constructed. The data for both grade and apparent rolling resistance, R_o, are displayed under their relevant headings. The other information held in the main section of this figure are necessary parameters for estimating the equation of the best fit line, establishing if the factors are statistically significant, and to allow confidence and prediction intervals to be calculated. The column entitled 'fitted y' is the estimated value of rolling resistance at the corresponding grade from the linear best fit line equation. If the equation of the best fit line is assumed to be of the form:

$$y = a + b.x \tag{5.5}$$

then from general statistics (Larson, 1982);

$$b = \frac{\Sigma(x - \bar{x}).(y - \bar{y})}{\Sigma(x - \bar{x})^2} \tag{5.6}$$

and;

$$a = \bar{y} - b.\bar{x} \tag{5.7}$$

where: y response parameter
x input variable
$\bar{y}$ average observed response
$\bar{x}$ average observed input value
a, b coefficients

The values of the coefficients are shown underneath the primary section. This small section also contains a parameter entitled 's'. This is the standard deviation of the response about the regression line, and is an estimate of the standard deviation, σ. This value is calculated using equation 5.8, has n-2 degrees of freedom and is used in all subsequent significance and confidence interval equations.

$$s = \sqrt{\frac{\Sigma(y - \textit{fitted } y)^2}{n-2}} \tag{5.8}$$

where: s standard deviation of the response about the regression line
fitted y the calculated response using equation 5.5
n the number of data points.

The standard deviation of the coefficients a and b are given in the small secondary section of the spreadsheet, alongside the value of a and b, and are calculated using equations 5.9 and 5.10.

$$s_a = \sqrt{\frac{s^2 . \Sigma x^2}{n . \Sigma(x - \bar{x})^2}} \tag{5.9}$$

$$s_b = \sqrt{\frac{s^2}{\Sigma(x - \bar{x})^2}} \tag{5.10}$$

where: s_i standard deviation of coefficient i

It is important to know whether there is evidence of statistical significance between the input parameters and the response. This is carried out by testing the relationship against a null hypothesis, e.g. coefficient b=0. This value is found using equation 5.11. The result is posted in the spreadsheet, under the heading 't-ratio', alongside the coefficient and the standard deviation of the coefficient. This value has to compared with the general Student's *t*-distribution function with the required significance level and number of degrees of freedom, as found in most statistics' books, (Larson, 1982, and Chatfield, 1983). If the calculated value is

greater than that in the table, then the coefficient is statistically significant as a predictor for the output.

$$t = \frac{\text{Coefficient - hypothesised value (=0)}}{\text{Estimated Standard Deviation of the coefficient}} \qquad (5.11)$$

The R-squared value also given in this small section is a measure of the correlation between the input and the response. This value is the square of the normal correlation coefficient. This is calculated from equation 5.12, and can be thought of as the fraction of the variation in the response that is explained by the fitted equation. It is normally expressed as a percentage and the higher the value the better the correlation.

$$R^2 = 1 - \frac{\Sigma(y - \textit{fitted } y)^2}{\Sigma(y - \bar{y})^2} \qquad (5.12)$$

5.7.2 Residuals

The 'Residuals' column, at the right hand side of the first section in figure 5.30, is the difference between the observed response and the estimated value from the regression equation. The residuals are used to check whether the linear best fit is an inadequate model to the response. If the residuals are plotted against the input variable, figure 5.31, and the points are scattered around the zero residual line then the linear equation is an adequate predictor. If the points follow a trend, e.g. at low values of input the residuals are high, as the input value increases the residual value decreases and then increases again, then a polynomial or logarithmic regression should be considered.

5.7.3 Confidence and Prediction Intervals

Confidence and prediction intervals are used to predict what will happen in the future. The confidence interval is used as an estimate of the population mean of all responses at any given input value, and is given by equation 5.13. Whereas the prediction interval is the estimator for a single output. Since dealing with a single

value rather than an average, greater uncertainty would be expected and therefore a wider interval anticipated, as can be seen from figures 5.11, 5.14, 5.20, 5.23, and 5.28. The equation for the prediction interval is given by equation 5.14.

$$\text{Confidence Interval} = \text{fitted y} \pm \text{t.(st.dev.fit)} \tag{5.13}$$

$$\text{Prediction Interval} = \text{fitted y} \pm \text{t.}\sqrt{(\text{st.dev.fit})^2 + s^2} \tag{5.14}$$

where: st.dev.fit standard deviation of the fitted response calculated using equation 5.15

t Student's t value at the appropriate significance level and number of degrees of freedom, input at the top of the spreadsheet in figure 5.30.

$$\text{st.dev.fit} = s.\sqrt{\frac{(x-\bar{x})^2}{\Sigma(x-\bar{x})^2} + \frac{1}{n}} \tag{5.15}$$

These calculations can be seen in the bottom section of figure 5.30, where the 'predict' headed column is the input values on which the prediction is to be based, 'fit' is the calculated value for the apparent rolling resistance from the regression equation, and the other columns are as described above. The important values from the estimators point of view are the 95% confidence intervals, as this would be the range of the expected average rolling resistance over the duration of an operation. The 95% prediction interval would be applicable if only one or two readings were taken of the vehicles on site. As can be seen from figure 5.30, the range of apparent rolling resistance between the 95% confidence intervals increases from a minimum value of 0.8% at the average value of grade resistance to a value of 2.27% at a grade resistance of -6%. This is shown graphically in figure 5.32 along with the 95% prediction intervals.

From simple linear regression it is relatively simple to extend the theory to introduce a greater number of input variables. All the parameters have similar meanings, but graphical representation becomes impossible when there are more than two input variables.

5.7.4 Analysis

The multiple regression analysis carried out was to establish equations for apparent rolling resistance with five input variables: grade, consistency index, moisture condition value, vane shear strength, and rut depth. All possible combinations of these five input factors were considered. Initially the analysis dealt with individual types of vehicle travelling in the four main conditions: loaded uphill, loaded downhill, empty uphill, and empty downhill, but it was soon discovered that there was an insufficient number of points to carry out the analysis satisfactorily. It was therefore decided to simplify the analysis by combining all the vehicle types together. Hence six driving conditions were defined for all vehicles: all empty, all empty uphill, all empty downhill, all loaded, all loaded uphill, and all loaded downhill. These conditions were regressed against all possible combinations of the five input variables.

As well as the regression analysis, correlation coefficients between all six parameters were calculated to establish whether any two variables were dependent. The results of the correlation analysis were conclusive in that the highest degree of correlation was consistently between moisture condition value and vane shear strength with an average correlation coefficient of 0.748. This indicates that moisture condition value is a reasonable indicator of hand vane shear strength. Second to this was the correlation between apparent rolling resistance and grade resistance, closely followed by all conditions containing the factor consistency index. The worst correlation was between moisture condition value and apparent rolling resistance, with an average correlation coefficient of 0.121.

The regression analysis showed that the multiple regression with the highest R^2 value was the five factor interaction, with an average value of 70% for all six driving conditions. The coefficients for each of the five parameters and the constant term are shown in table 5.1, e.g. the equation for any truck travelling uphill empty would be as in equation 5.16;

$$R_0 = 12.3-0.588G-1.30Ic+0.300MCV-0.0335V-0.00648R. \qquad (5.16)$$

where: R_0 Apparent Rolling Resistance (% Equivalent Grade)
G Grade Resistance (%, uphill grades positive)

Ic	Consistency Index
MCV	Moisture Condition Value
V	Hand Vane Shear Strength (kN/m^2)
R	Rut Depth (mm)

It would be dangerous to extrapolate for values of apparent rolling resistance outwith the data limits, which can be ascertained from the data contained within the previous sections.

One drawback from this formula is that at the time of tender the rut depth on the haul road is unknown. For this reason the four factor regression equation, omitting the factor rut depth, has also been calculated and is shown in table 5.2. As site investigation reports seldom hold all of this information at any single point, tables 5.3-5.6 give regression equations for all two factor regressions containing grade, except rut depth, and the single factor regression with just grade. The coefficients do not always have the expected sign, for example the coefficients for moisture condition value have a positive sign that would indicate that as the moisture condition value increased, the ground becomes drier, the apparent rolling resistance would increase. This is caused by the somewhat flat nature of the apparent rolling resistance versus moisture condition value graphs, figure 5.12 (a-j). The other anomalies in the regression analysis are most likely a function of considering all the vehicles and interactions at once, where a single stray result can completely alter the relationship.

For an estimator, it would be useful to know the range of average apparent rolling resistances for a given set of input conditions. Using the average values for each of the five parameters, on the six driving conditions, 95% confidence intervals were calculated for each of the regression equations and can be seen in table 5.7. When monitoring an individual operation for a short period of time the spread in data will be greater than the average for the complete operation. Prediction intervals have been calculated for the various regression analyses and the results can be seen in table 5.8. Both tables 5.7 and 5.8 show the range in confidence and prediction intervals to be similar for all the different regression equations, at the average values. Care must be taken not to extrapolate outwith the data limits defined by the graphs in the preceding sections.

Relating the confidence and prediction intervals to the velocity of the vehicle shows how accurate the prediction would be. For example an empty vehicle travelling downhill, and using the five factor regression, with average input values, has a 95% confidence interval for apparent rolling resistance of 10.4-11.2%. This corresponds for a Volvo BM A25 6x6 articulated dump truck to a range in maximum speed from 26 to 29km/h. The corresponding prediction interval for apparent rolling resistance is 8.4-13.2%, which relates to a maximum velocity range of 22.5-36km/h.

5.7.5 Validation of Regression Equations

When the regression equations were calculated three sets of data were omitted from the analysis as there were only a few data values for each of the vehicle types. The makes of vehicles had all been incorporated into the analysis, but the vehicles came from different subcontractors. These vehicles generally worked in conjunction with the various other subcontractors on the operations. The input parameters for the five factor regression analysis for these extra sections are given in table 5.9. The predicted apparent rolling resistances were calculated using the relevant equations from table 5.1, and the results are given in table 5.10.

Comparing the predicted rolling resistances with the rolling resistances back analysed using Accelerator, shows excellent correlation between the two. The majority of the predicted values lie within the 95% confidence interval, and all the estimated rolling resistances lie within the 95% prediction interval. The corresponding velocities for both the predicted and actual apparent rolling resistances can also be seen in table 5.10. These show the expected results with the sections on uphill grades having lower velocities than the downhill grades.

The percentage differences in the velocities expressed as a percentage of the predicted velocity can be seen in table 5.11. This table also shows the number of timings taken to formulate the average, and the number of different operator-vehicle combinations. The large percentage changes in velocity are related to the number of timings taken to calculate the average, figure 5.33. This shows that as the number of readings increases the accuracy of the estimation improves. At the lower number of time recordings there is still the possibility of a reasonable

correlation, but the probability is much lower. Therefore when monitoring the vehicles on site a minimum of ten recordings should be taken before calculating the average.

The number of vehicles used in the estimation also effects the average, for example if there is only one operator-vehicle combination in operation, then the recorded average is statistically less likely to be similar to the average for a number of drivers over the same section of haul road. For this reason the predicted value of rolling resistance for the single Tarmac Volvo A35 has the greatest inaccuracy of all the validation vehicles. Increasing the number of vehicles used to determine the average travel time generally increases the accuracy of the estimation.

Even for the limited number of results used to validate the five factor regression equation, it is clear that the equations work well for the conditions tested.

5.8 Summary

The experimental work carried out in this chapter is unique apart from a small amount of work carried out at TRL, (Parsons et al., 1982) relating the speed of earthmoving plant to moisture condition value, see section 2.13.2. This work dealt mainly with scrapers and rigid dump trucks, insufficient data was collected for articulated dump trucks. Velocities were corrected for grade using linear regression. Multiple regression was carried out, with four input parameters, on all the results to estimate the MCV required for a particular velocity. The four input parameters were: number of driven wheels, tyre width, available engine power, and total vehicle mass. Unfortunately:

> "In the case of articulated dump trucks a number of obvious anomalies resulted and it is considered that the various formulae should not be used for this type of equipment." (Parsons et al. 1982)

The fundamental approach carried out to the estimation of the speed of earthmoving plant will allow subsequent theories to be developed and tested. The extensive testing has also shown that the apparent rolling resistance of the man-vehicle-terrain system is dependent on the psychological effect of the gradient on the operator as well as the strength of the supporting medium. Unfortunately the

sites monitored did not enable readings to be made when the ground was in a poor weak condition as work always ceased when weather conditions deteriorated. By no means does this invalidate the work, as most earthmoving contracts are completed under these relatively dry conditions. It is in these good driving conditions that small decreases in velocity are not noticed, but the financial repercussions of the plant moving slower could make the difference between the contract making a profit or loss.

Empirical formulae have been developed using a simple linear regression relating the apparent rolling resistance to various combinations of five input parameters: gradient, consistency index, moisture condition value, vane shear strength, and rut depth. The five factor regression equations, having a correlation coefficient in excess of 0.83, will allow estimations to be made prior to tendering and to enable continual monitoring throughout the duration of an earthmoving operation. Simpler regression equations are given as all the information required may not be available at the time of tender. The regression equations have been validated by results that were not included in the formulation of the regression equations, to an acceptable level of accuracy.

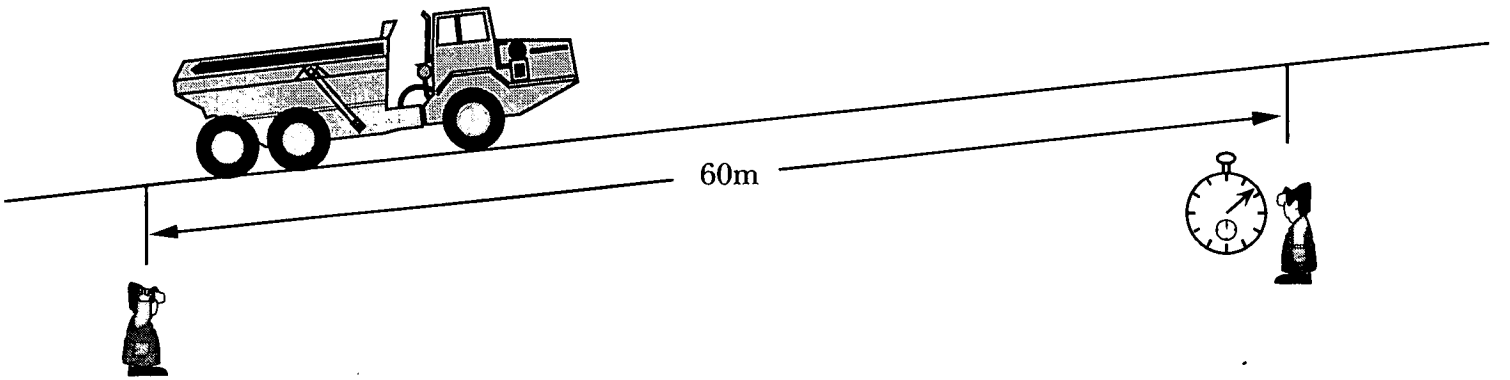

Figure 5.1: Layout of a Section of Haul Road for the Timing of Vehicles

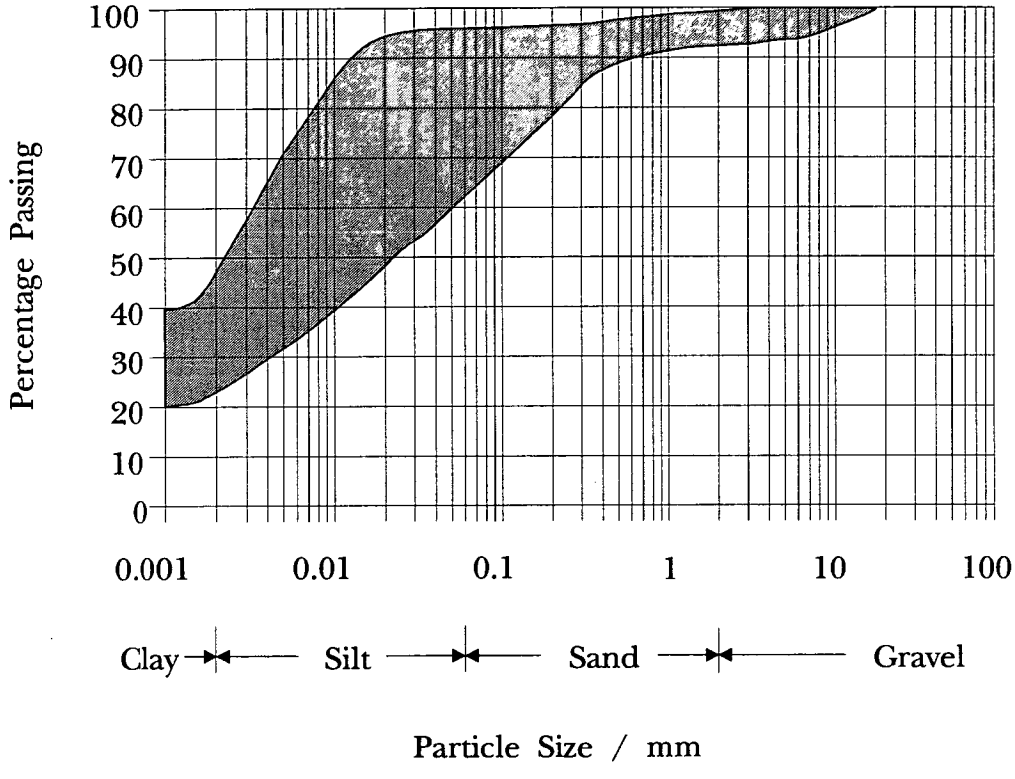

Figure 5.2: Particle Size Distribution Envelope for A1/M1 Link

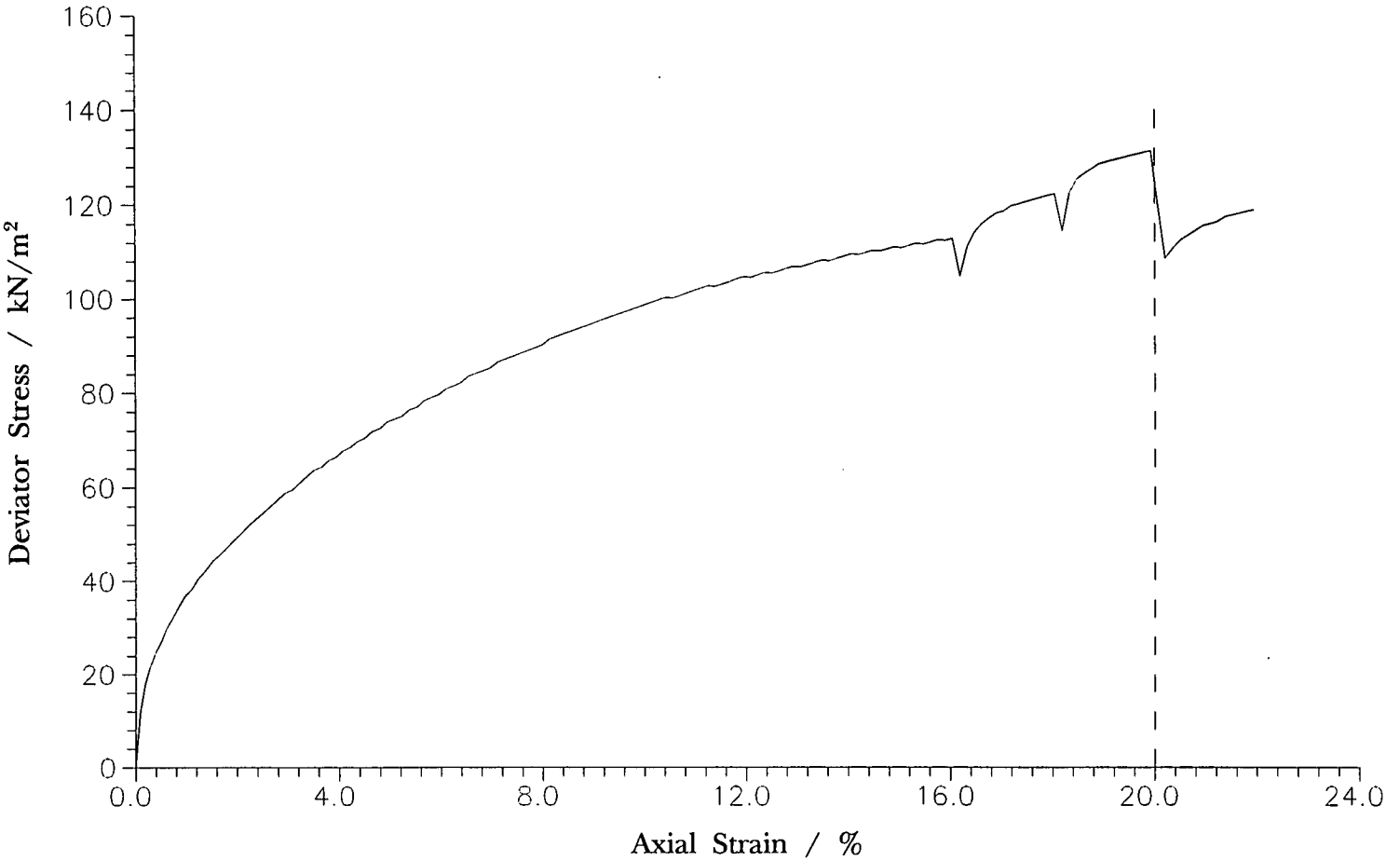

Figure 5.3: Deviator Stress versus Axial Strain for Multistage Undrained Triacial Test, Test 15, Chainage, 10340 9/7/92.

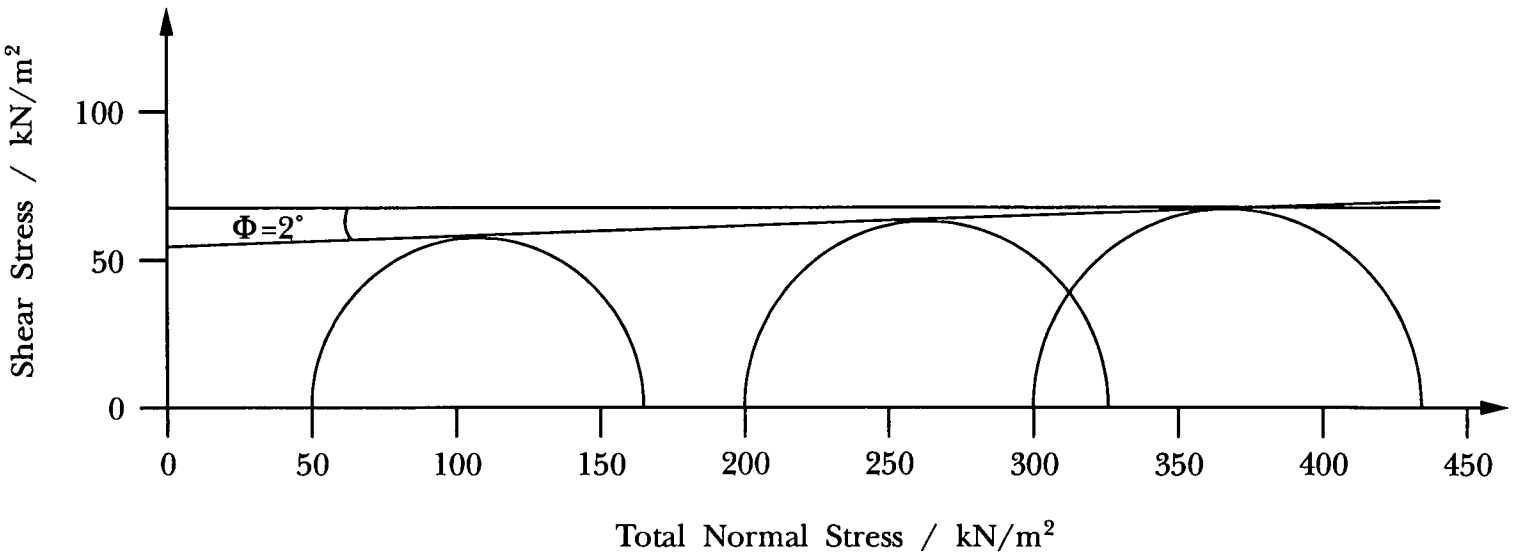

Figure 5.4: Mohr Circles for Quick Undrained Multistage Triaxial Test, Test Number 15, Chainage 10340, 9/7/92.

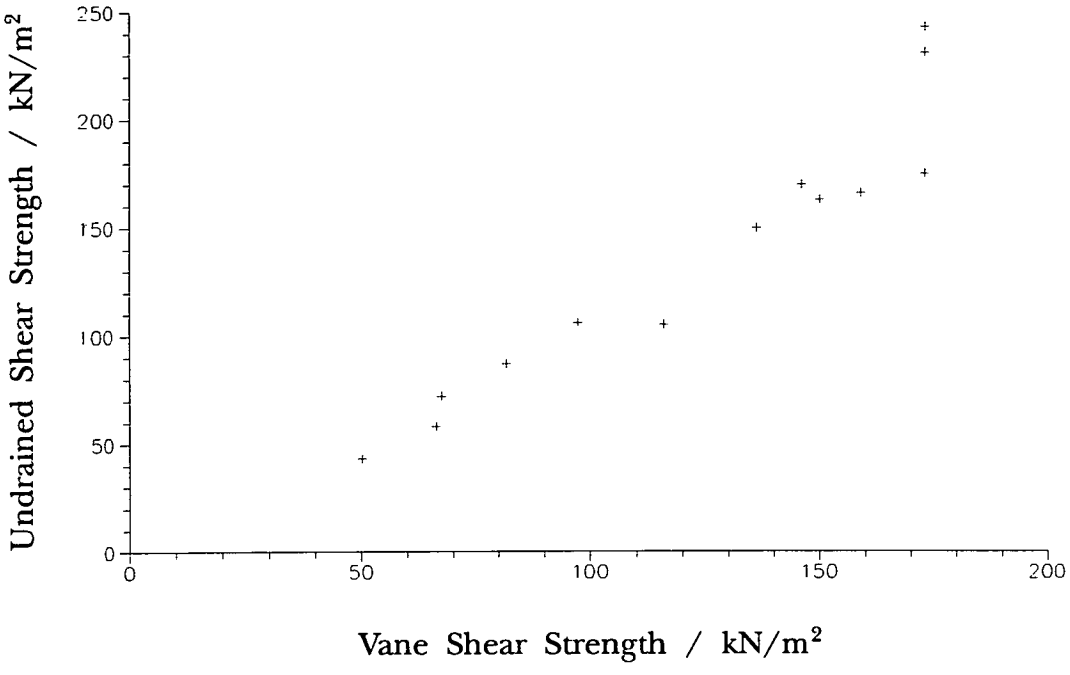

Figure 5.5: Undrained Shear Strength versus Hand Vane Shear Strength from Multistage Undrained Triaxial Tests.

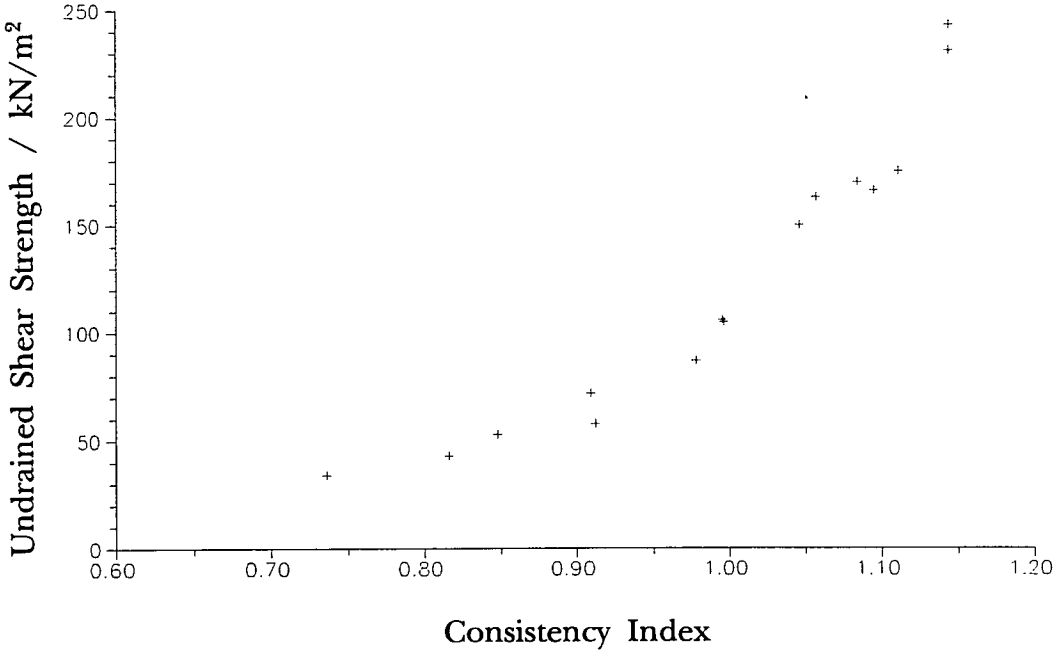

Figure 5.6: Undrained Shear Strength versus Consistency Index from Multistage Undrained Triaxial Tests.

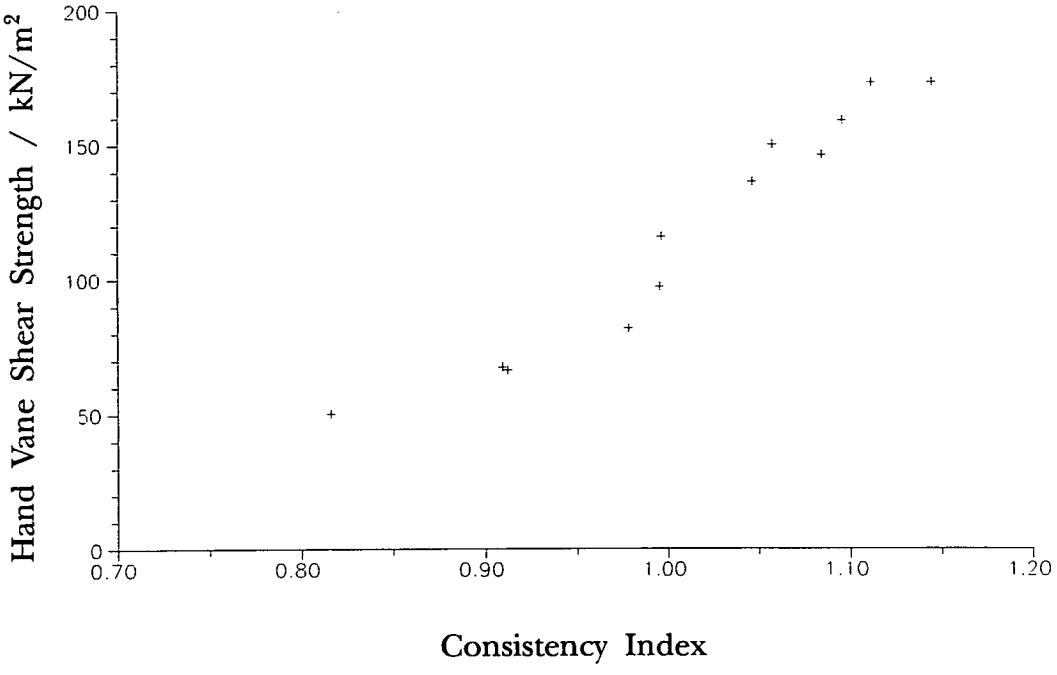

Figure 5.7: Hand Vane Shear Strength versus Consistency Index from Multistage Undrained Triaxial Tests.

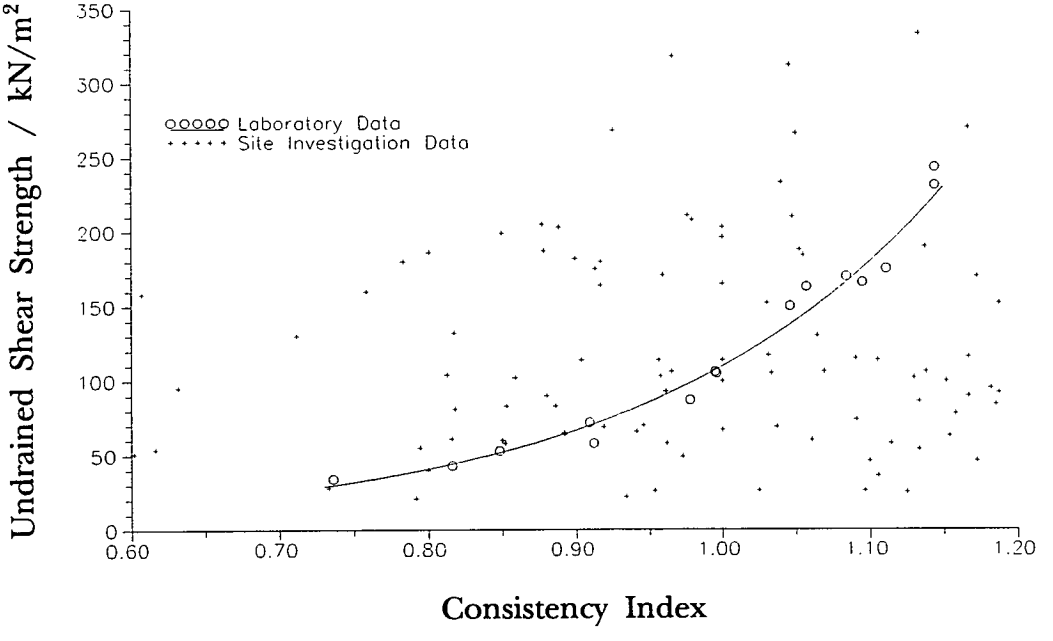

Figure 5.8: Undrained Shear Strength versus Consistency Index for the A1M1 Link, Comparing Site Investigation and Laboratory Data.

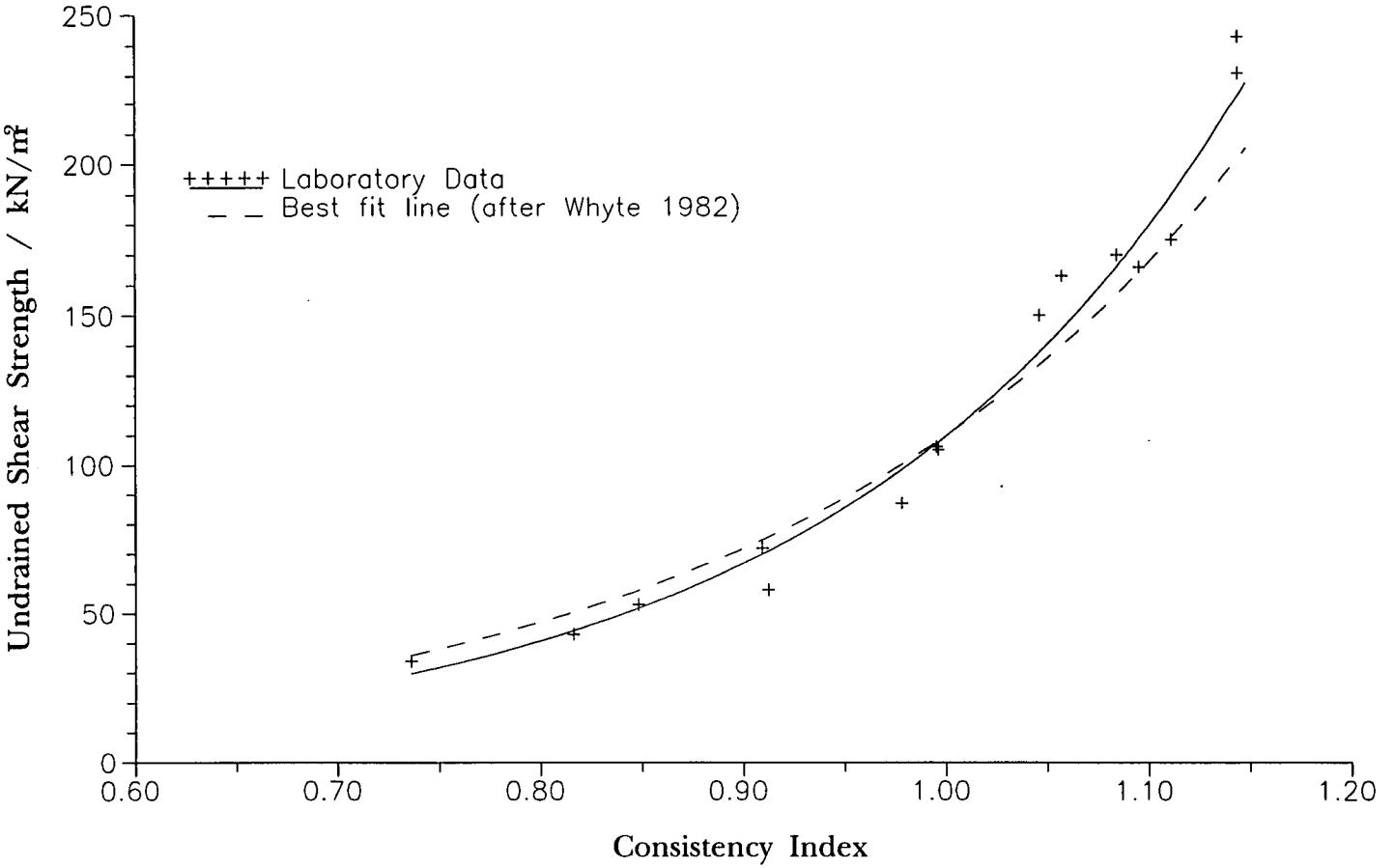

Figure 5.9: Undrained Shear Strength versus Consistency Index, Comparing the A1/M1 Data with that of Whyte, 1982.

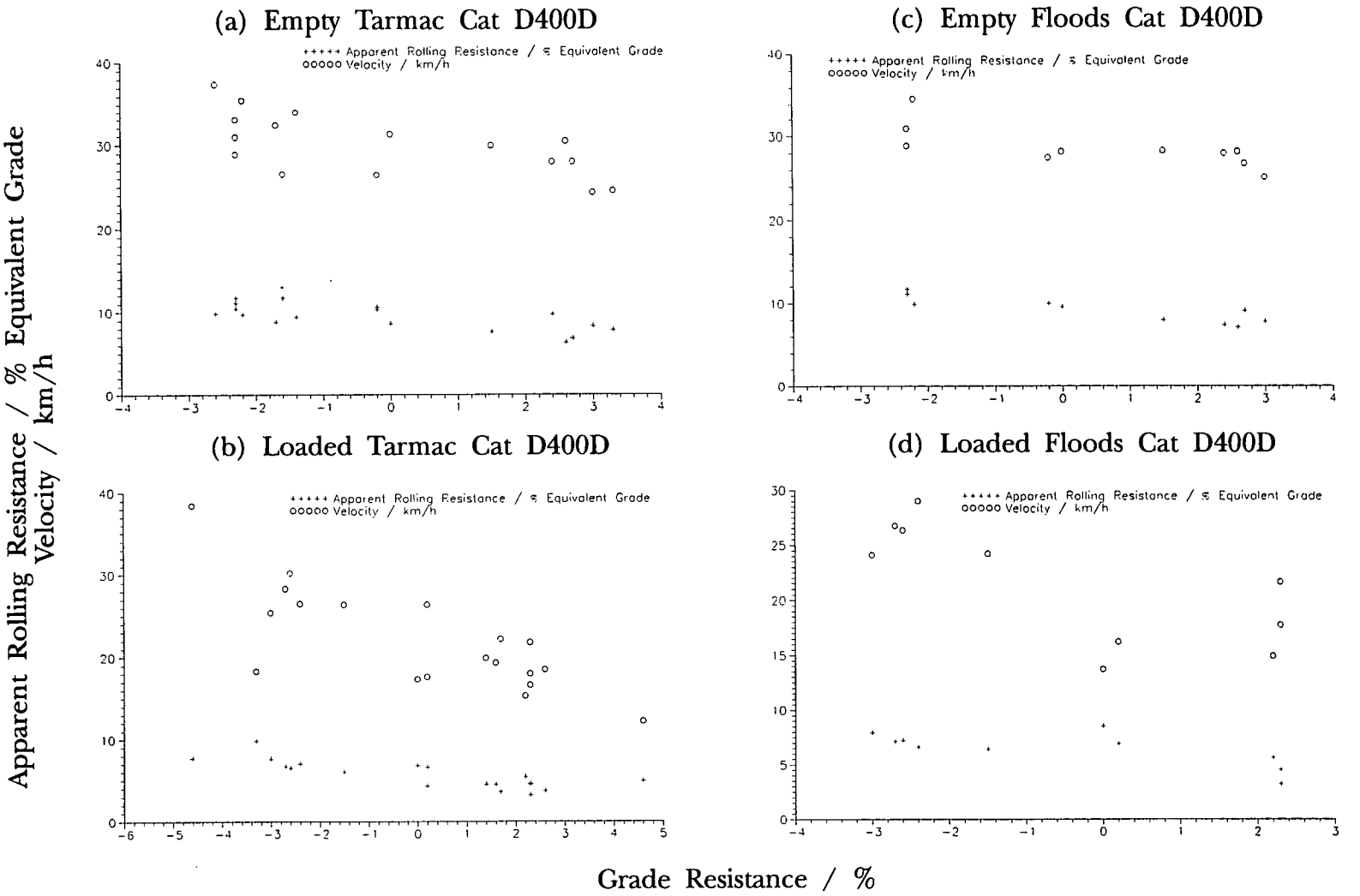

Figure 5.10 (a-d): Apparent Rolling Resistance and Velocity versus Grade Resistance

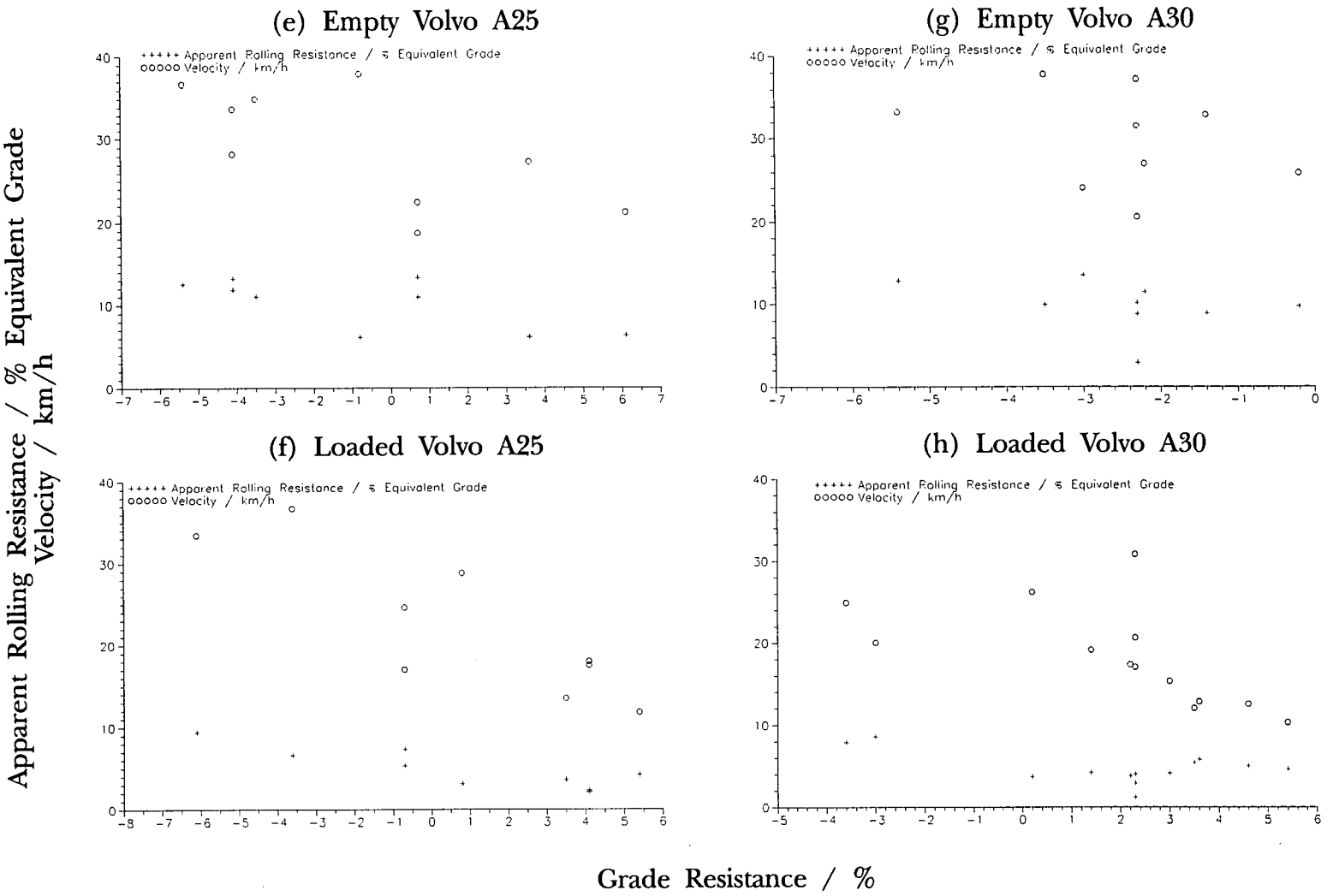

Figure 5.10 (e-h): Apparent Rolling Resistance and Velocity versus Grade Resistance

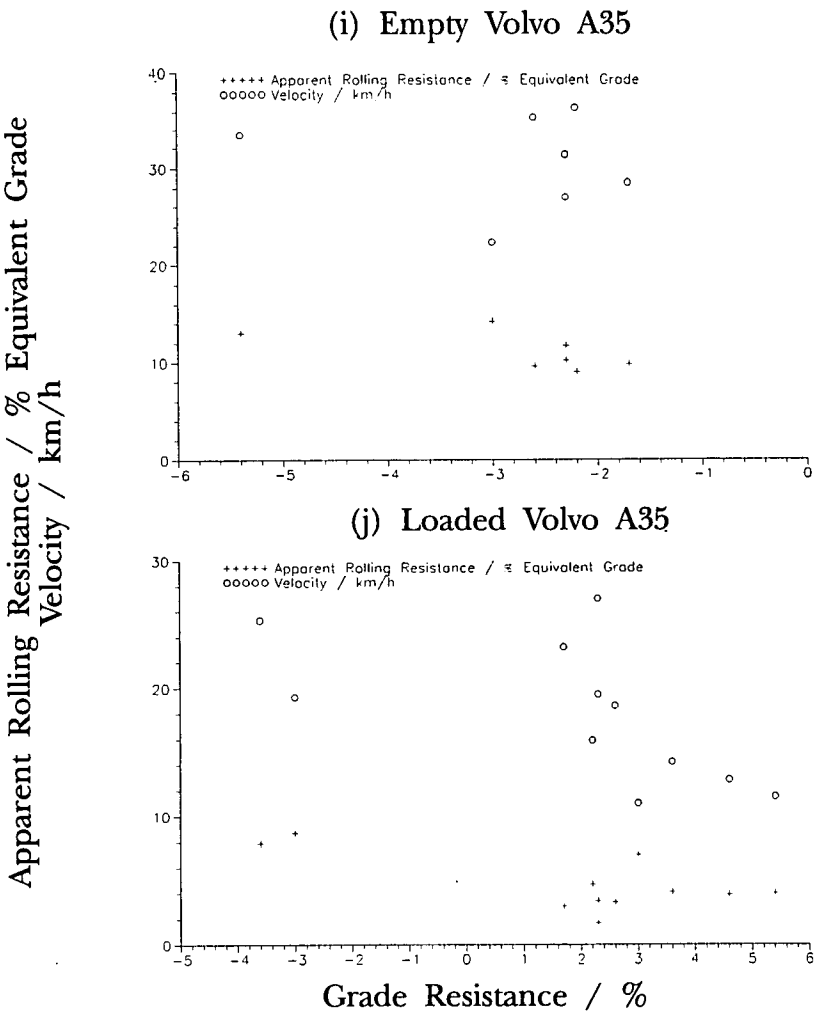

Figure 5.10 (i-j): Apparent Rolling Resistance and Velocity versus Grade Resistance

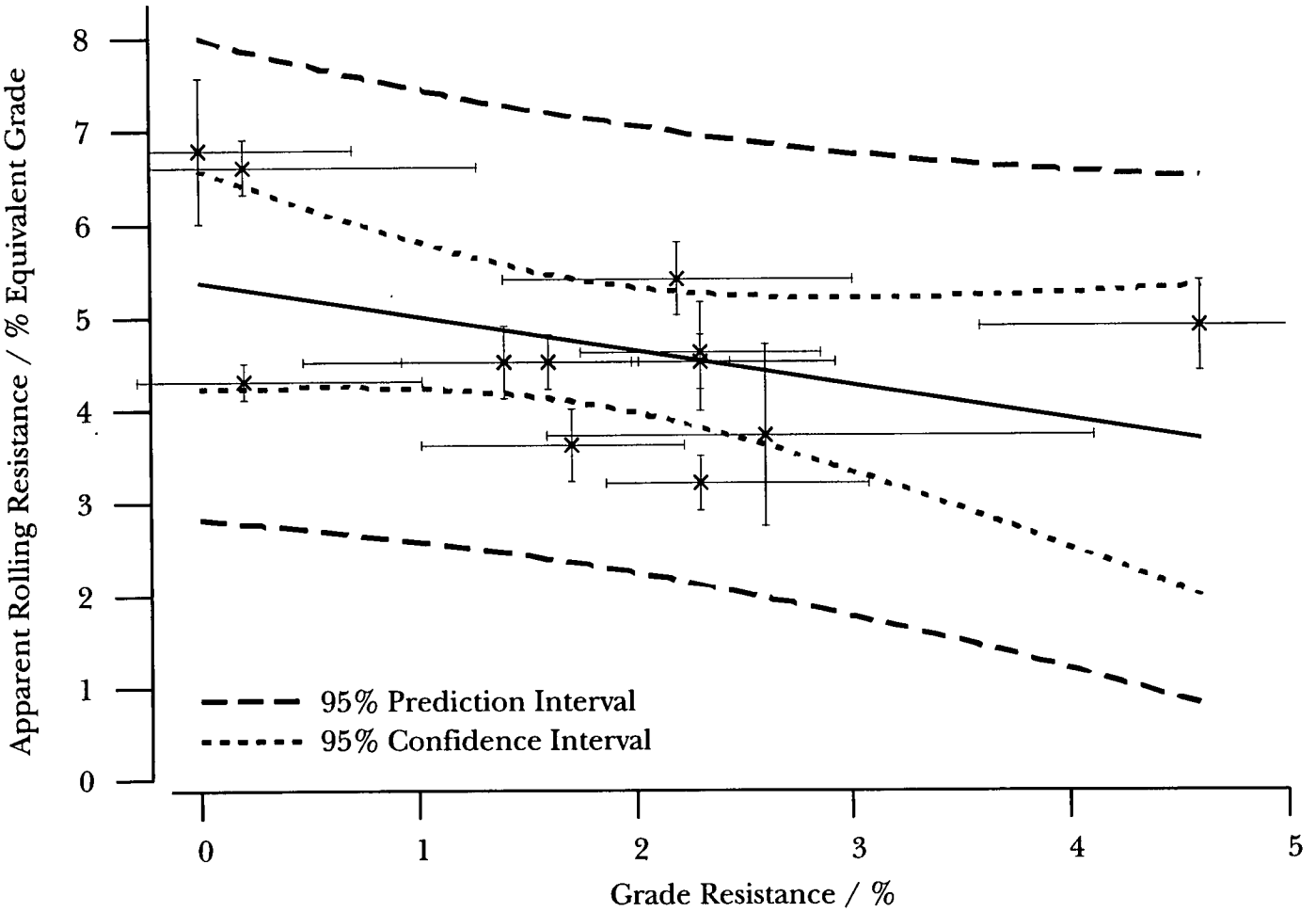

Figure 5.11: Apparent Rolling Resistance versus Grade Resistance for a Loaded Cat D400D Articulated Dump Truck Travelling Uphill showing 95% Confidence and Prediction Intervals

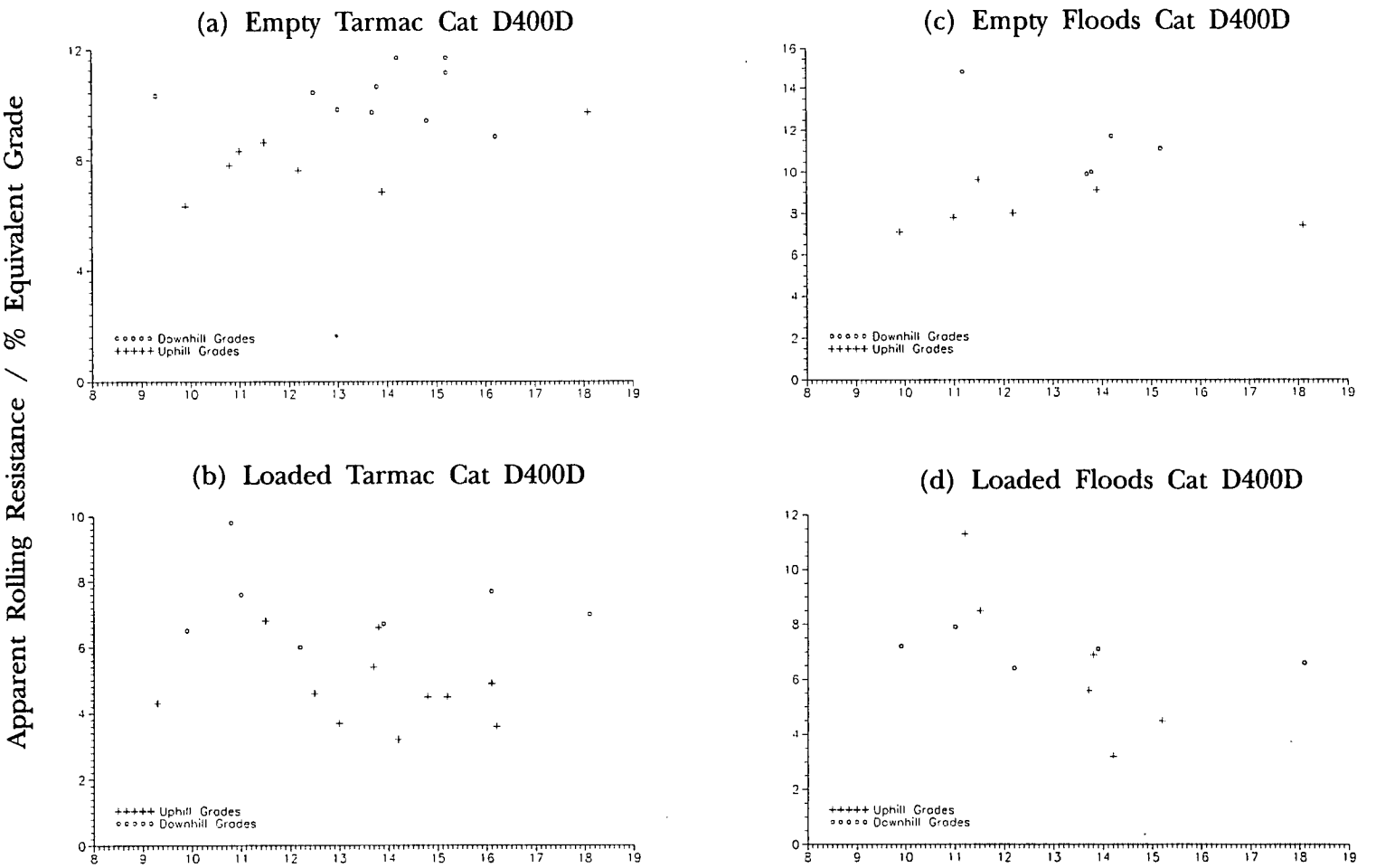

Figure 5.12 (a-d): Apparent Rolling Resistance versus Moisture Condition Value

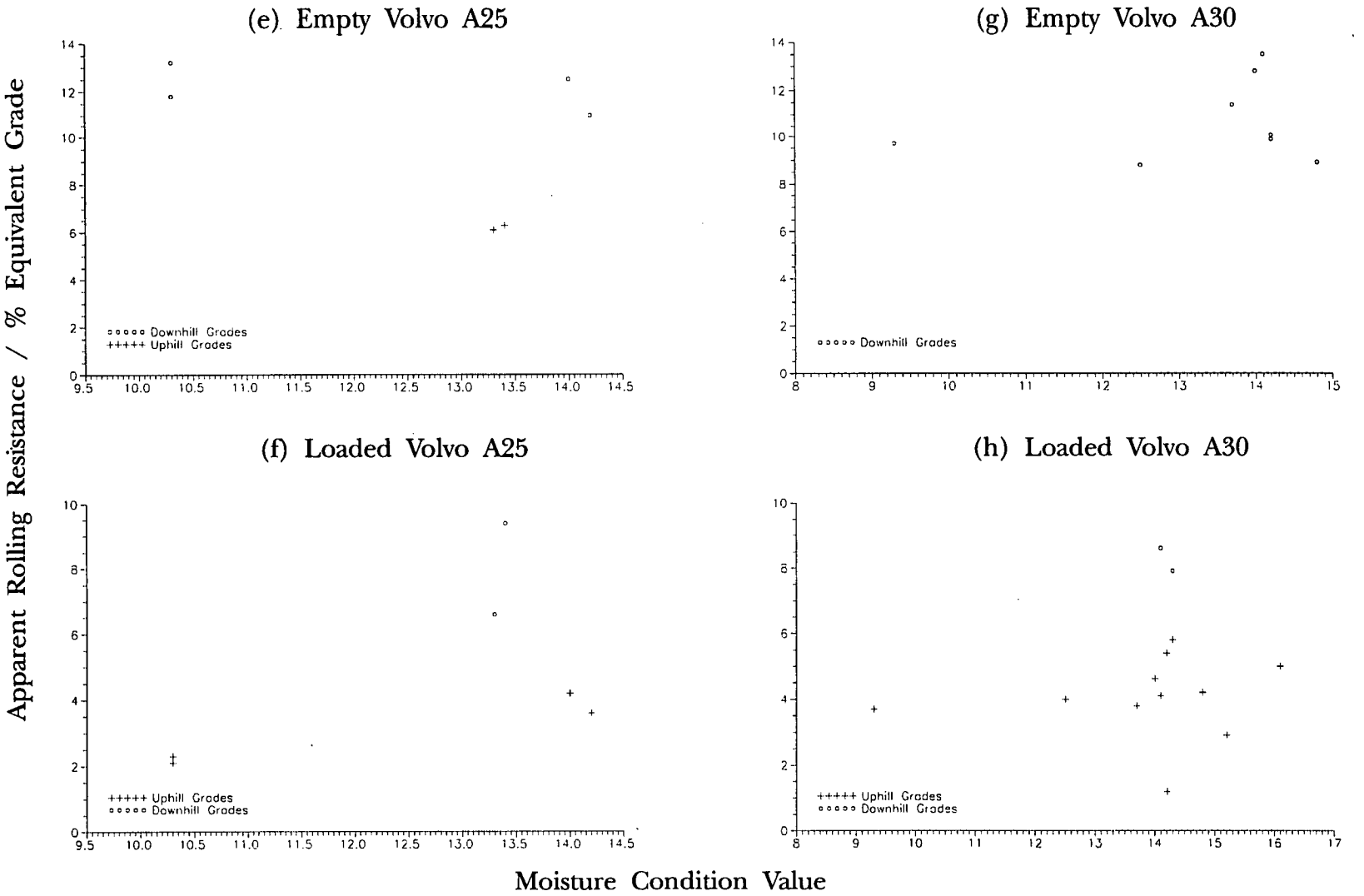

Figure 5.12 (e-h): Apparent Rolling Resistance versus Moisture Condition Value

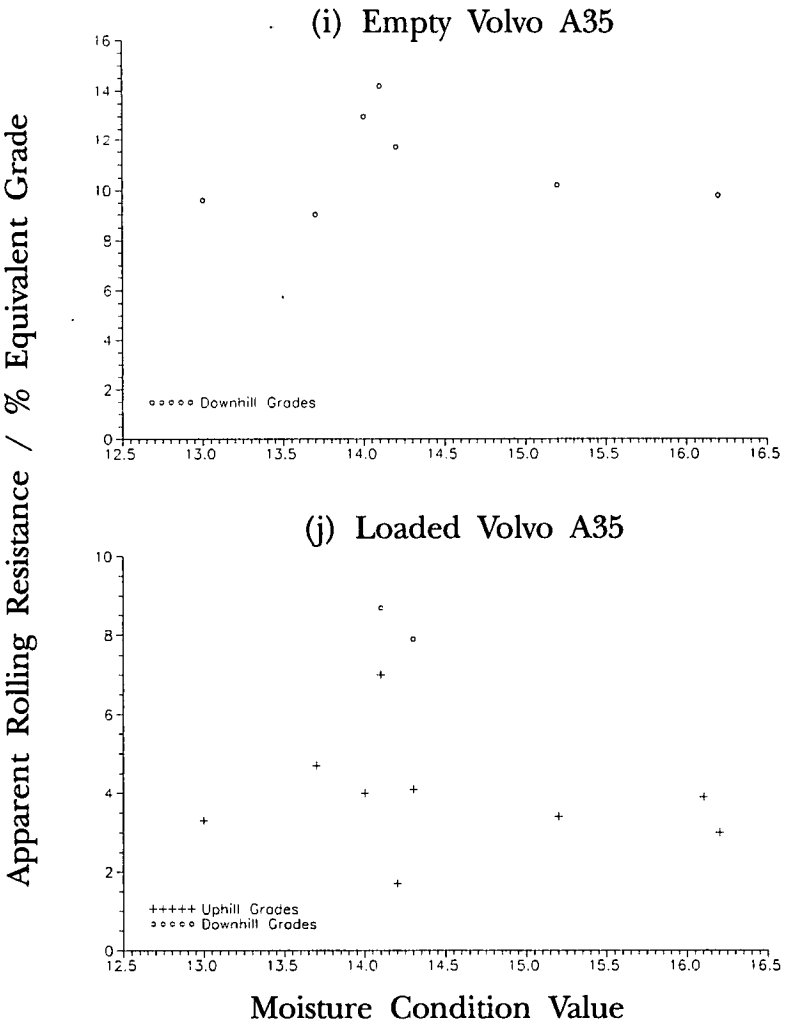

Figure 5.12 (i-j): Apparent Rolling Resistance versus Moisture Condition Value

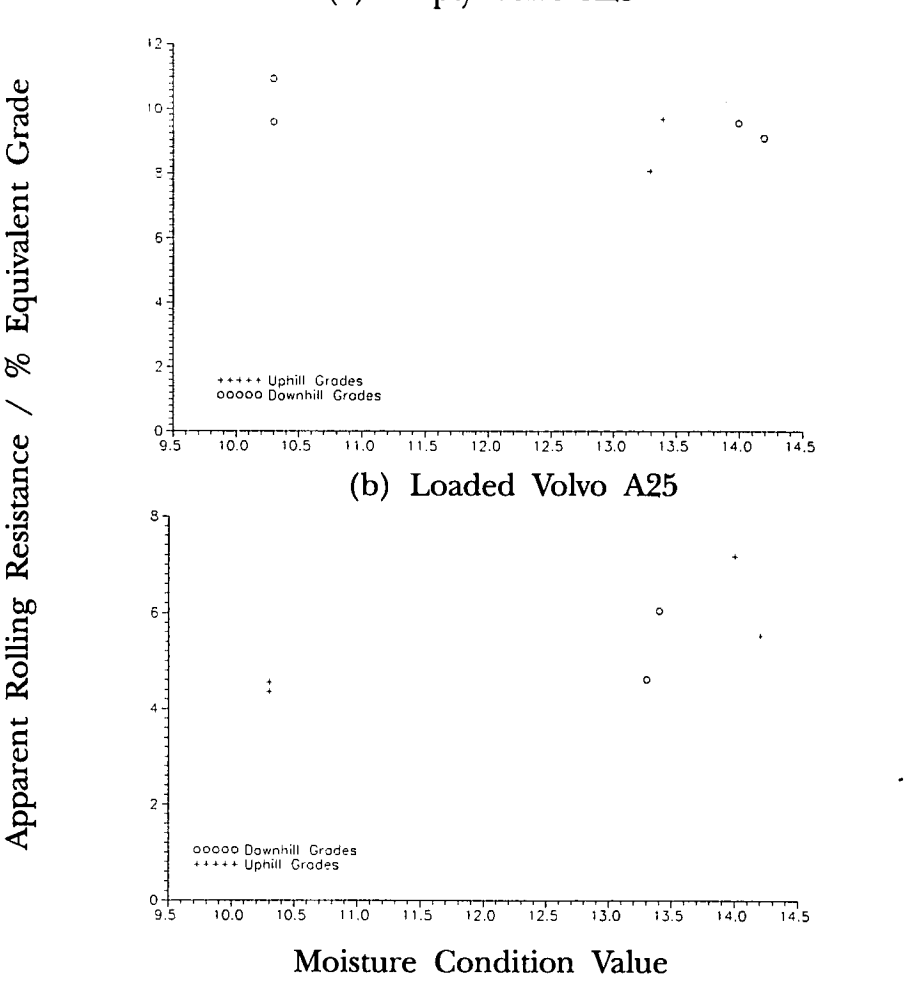

Figure 5.13: Apparent Rolling Resistance Ameded for Grade versus Moisture Condition Value

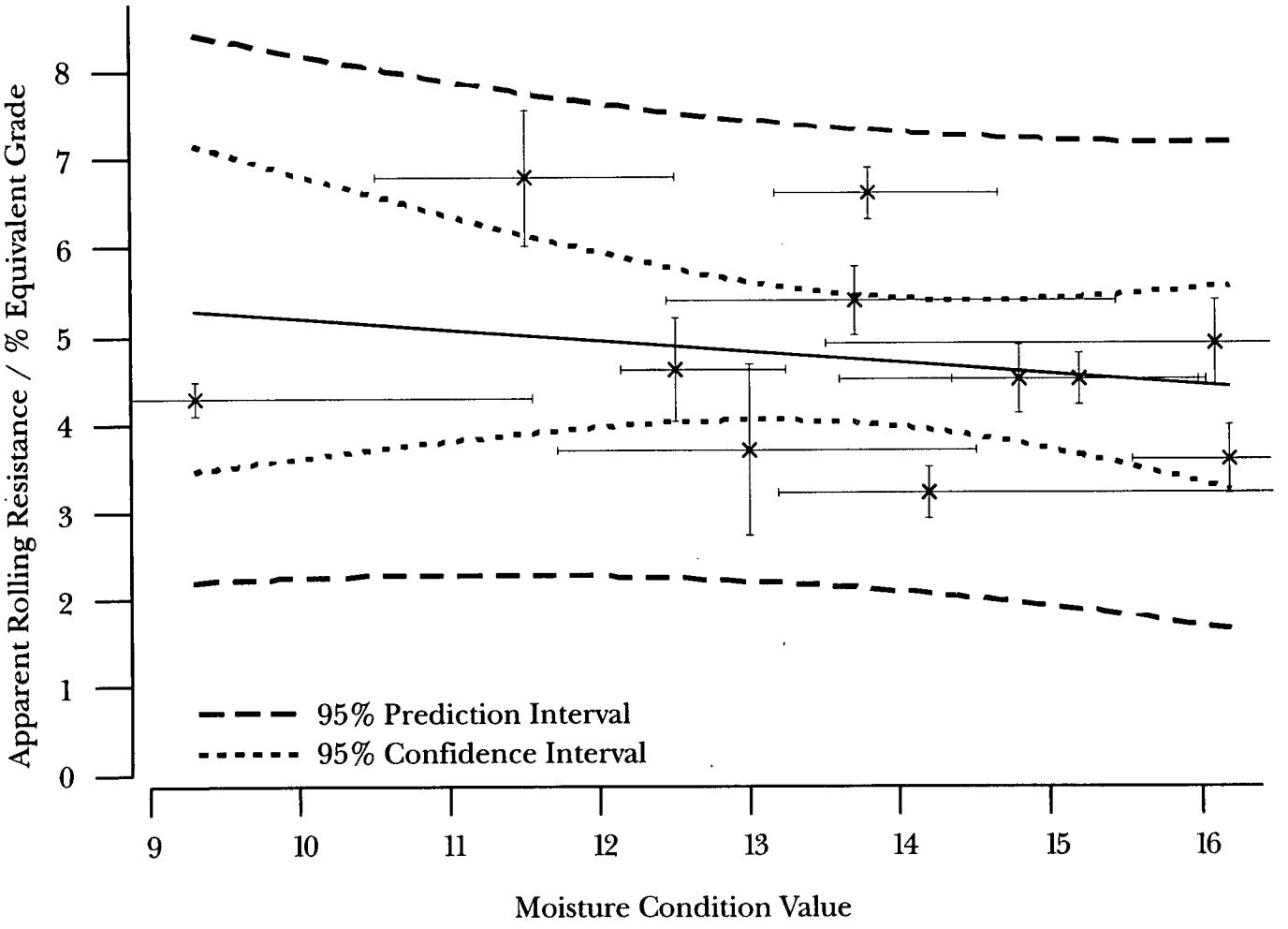

Figure 5.14: Apparent Rolling Resistance versus Moisture Condition Value for a Loaded Cat D400D Articulated Dump Truck Travelling Uphill showing 95% Confidence and Prediction Intervals

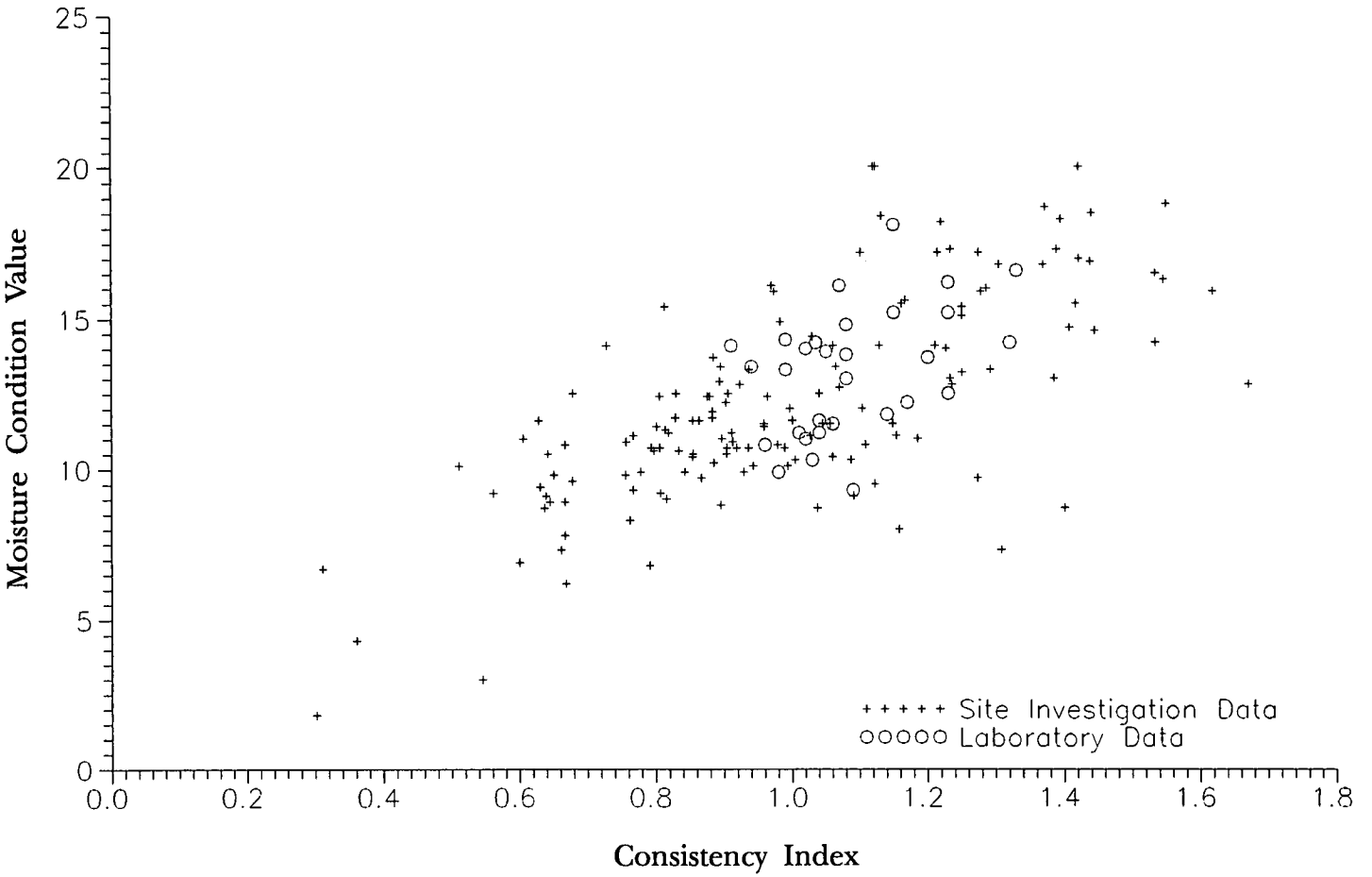

Figure 5.15: Moisture Condition Value versus Consistency Index for both Site Investigation and Laboratory Data from the A1M1 Link.

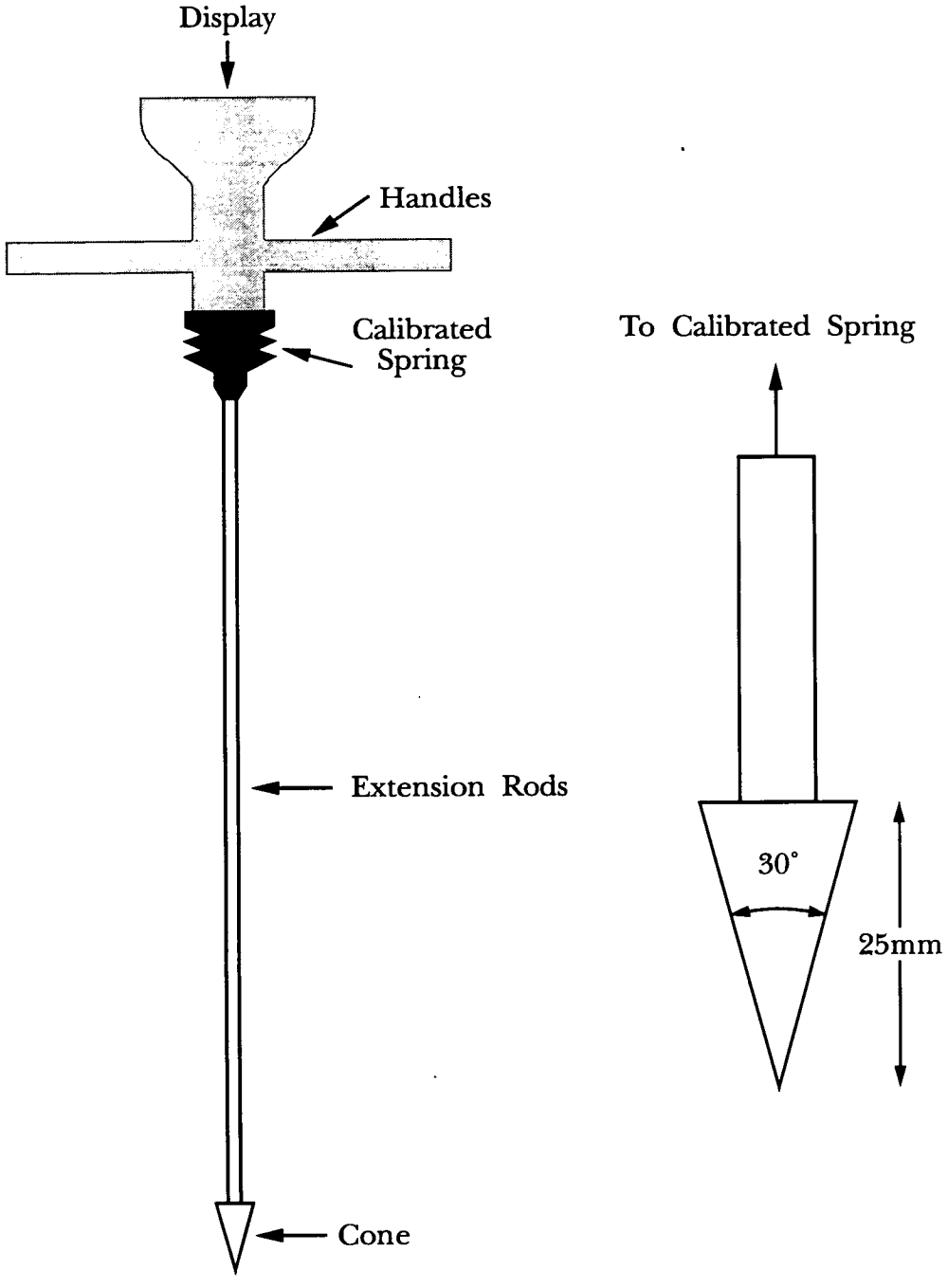

Figure 5.16: MEXE Cone Penetrometer

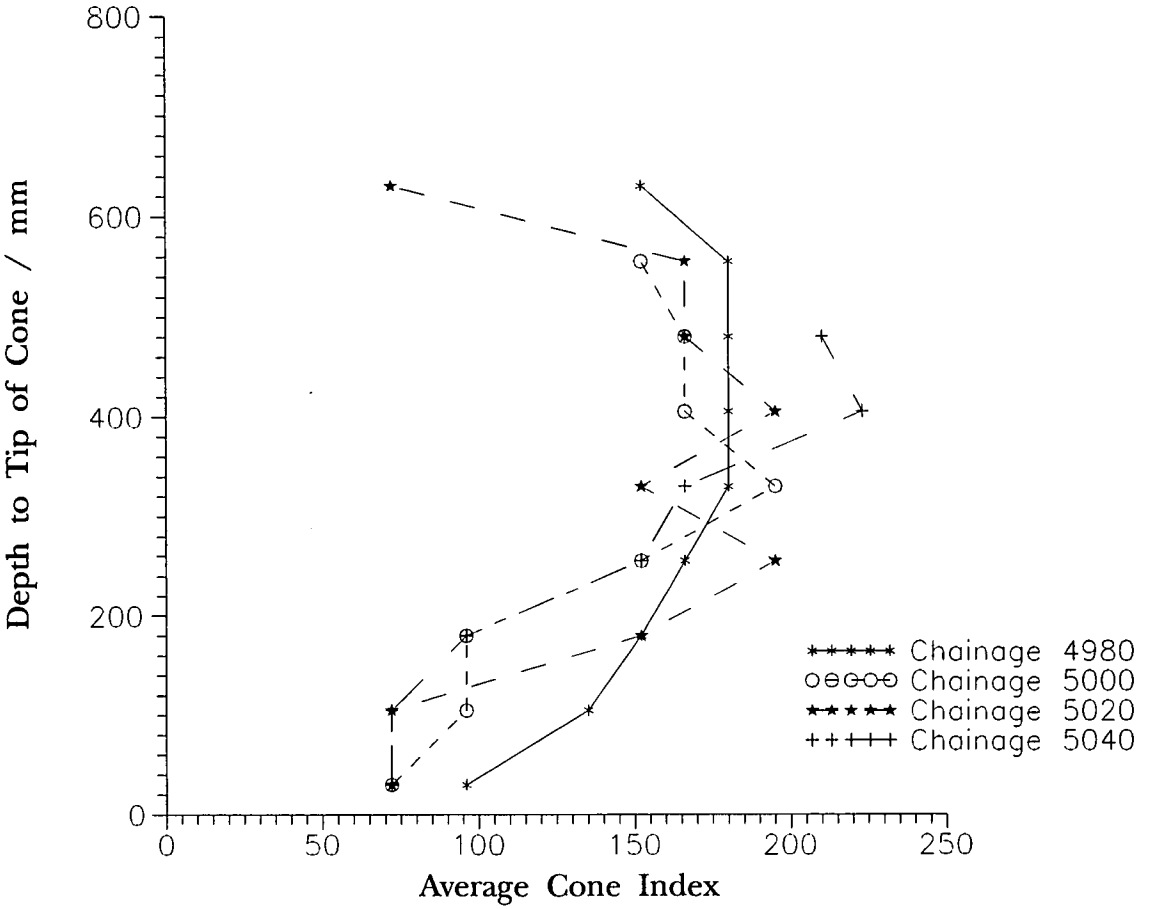

Figure 5.17: Depth versus Average Cone Index for a Typical Section on the A1M1 Link

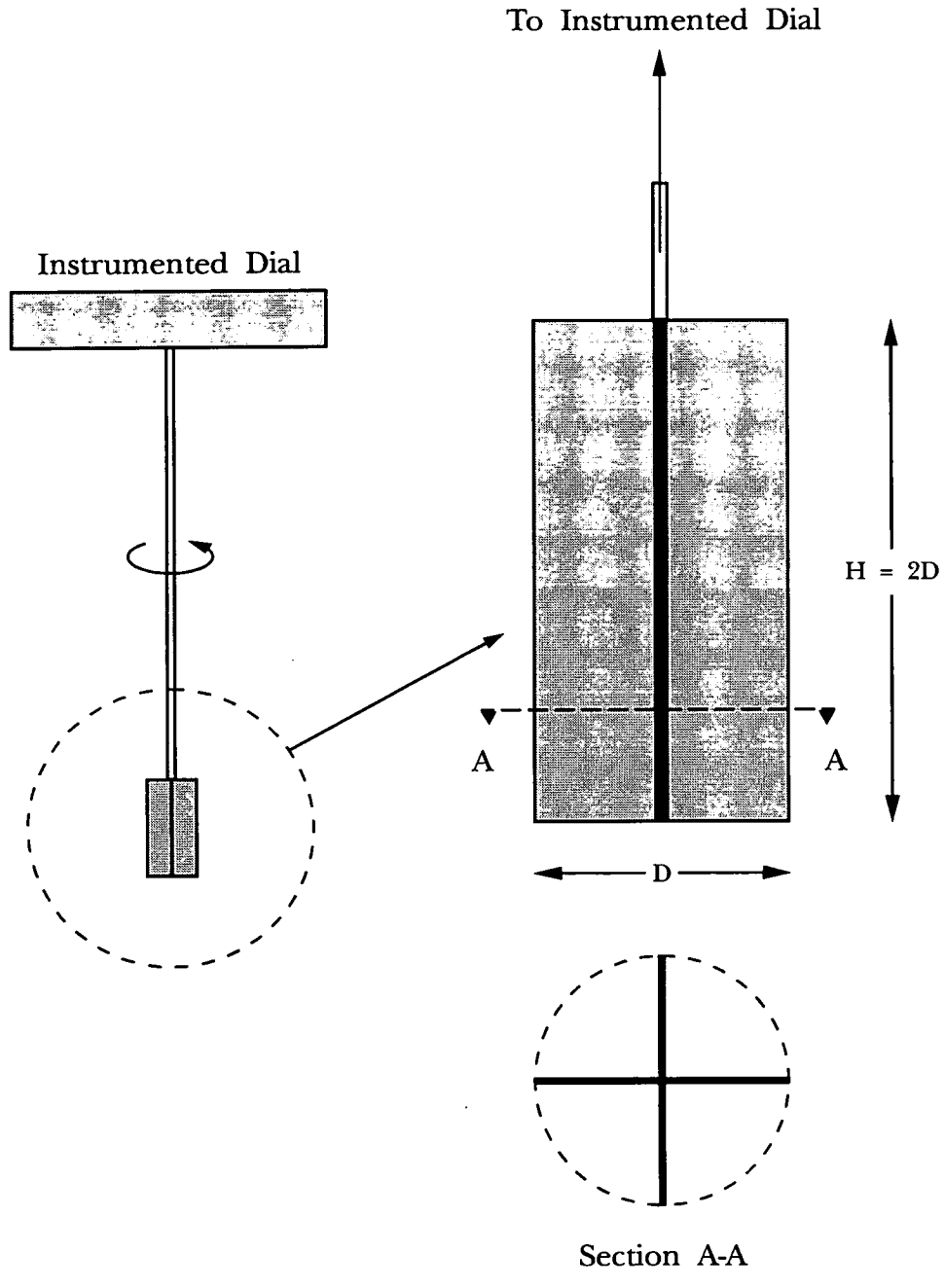

Figure 5.18: Hand Shear Vane Showing Detail of the Vane

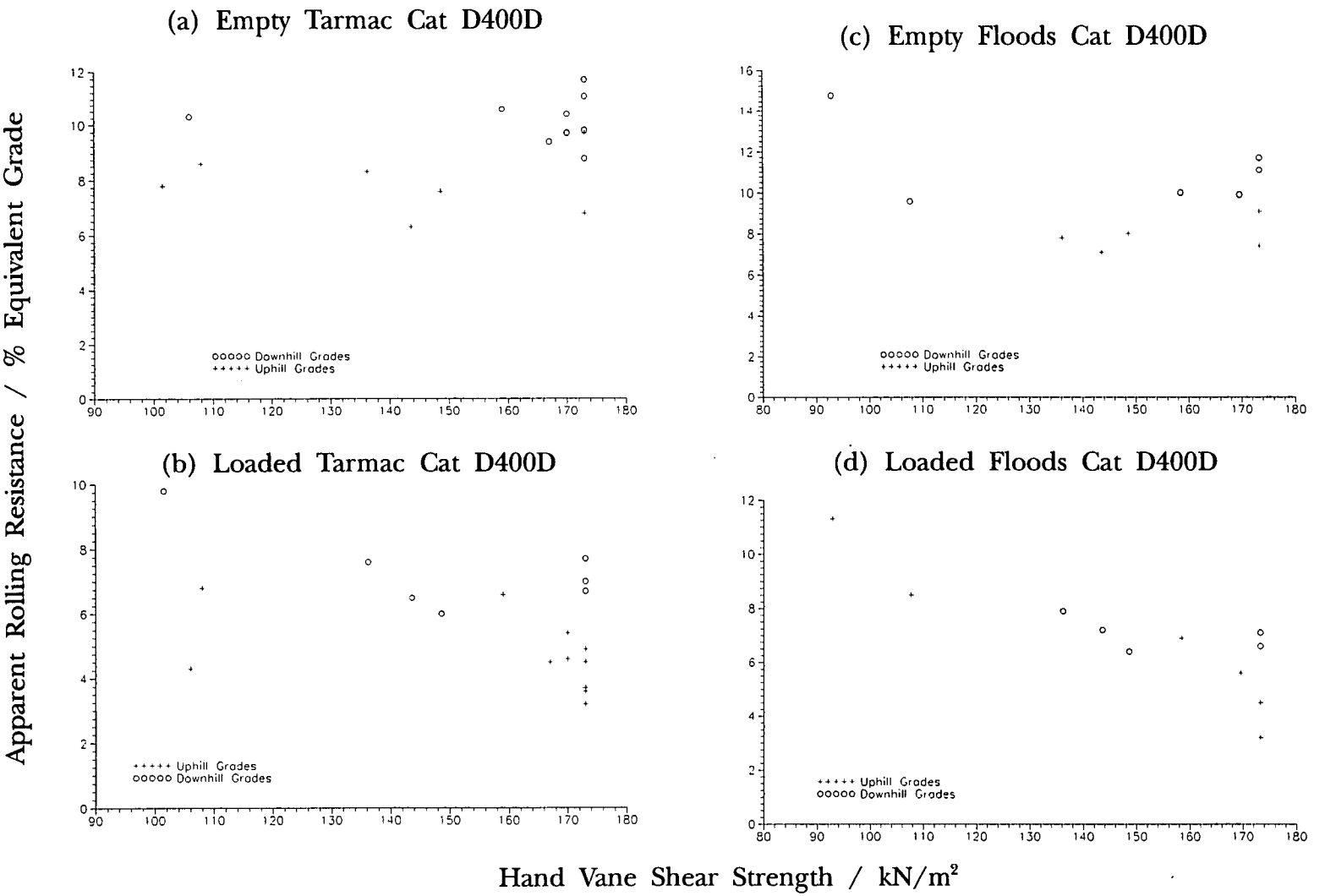

Fifure 5.19 (a-d): Apparent Rolling Resistance versus Hand Vane Shear Strength

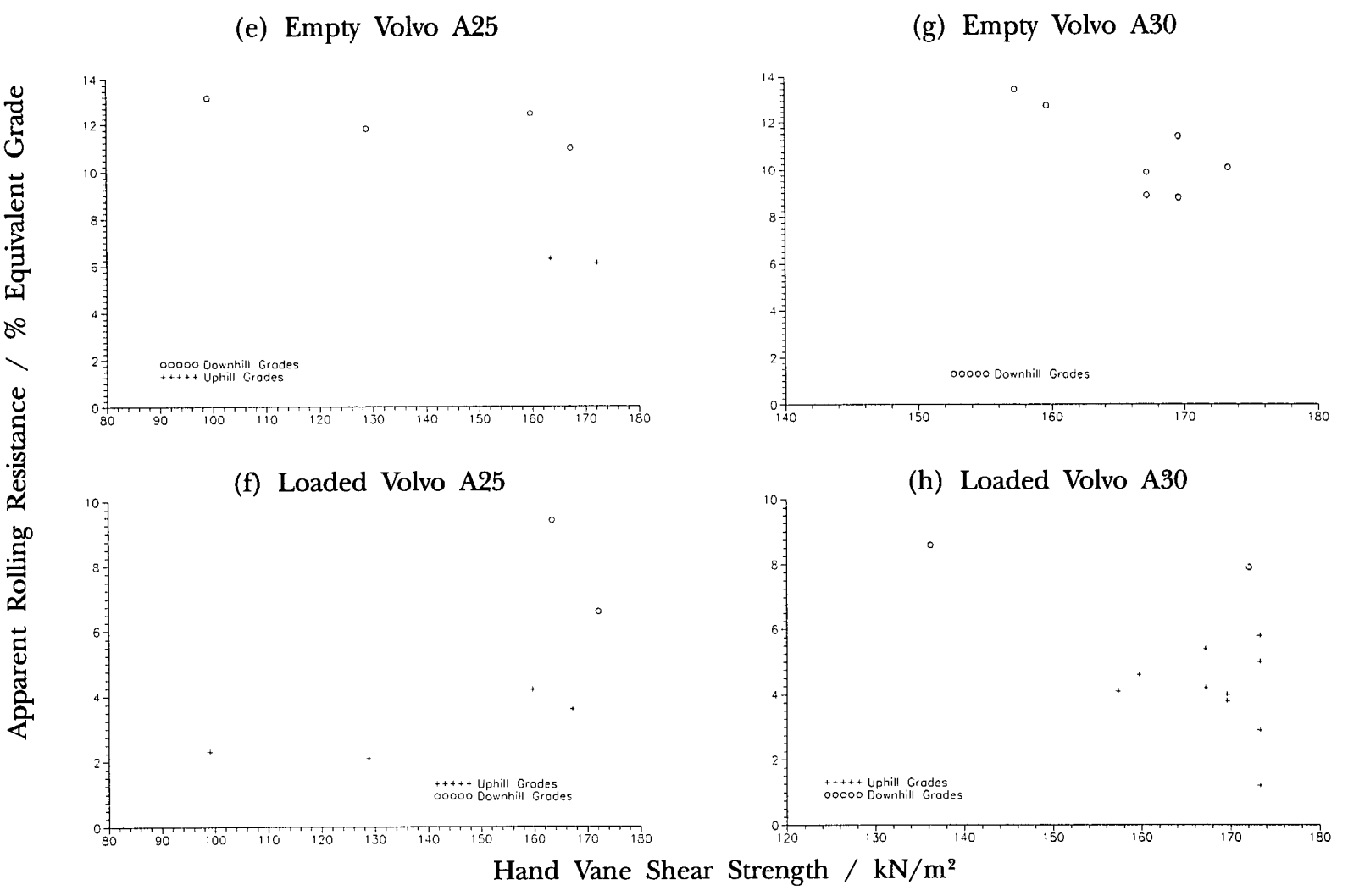

Figure 5.19 (e-h): Apparent Rolling Resistance versus Hand Vane Shear Strength

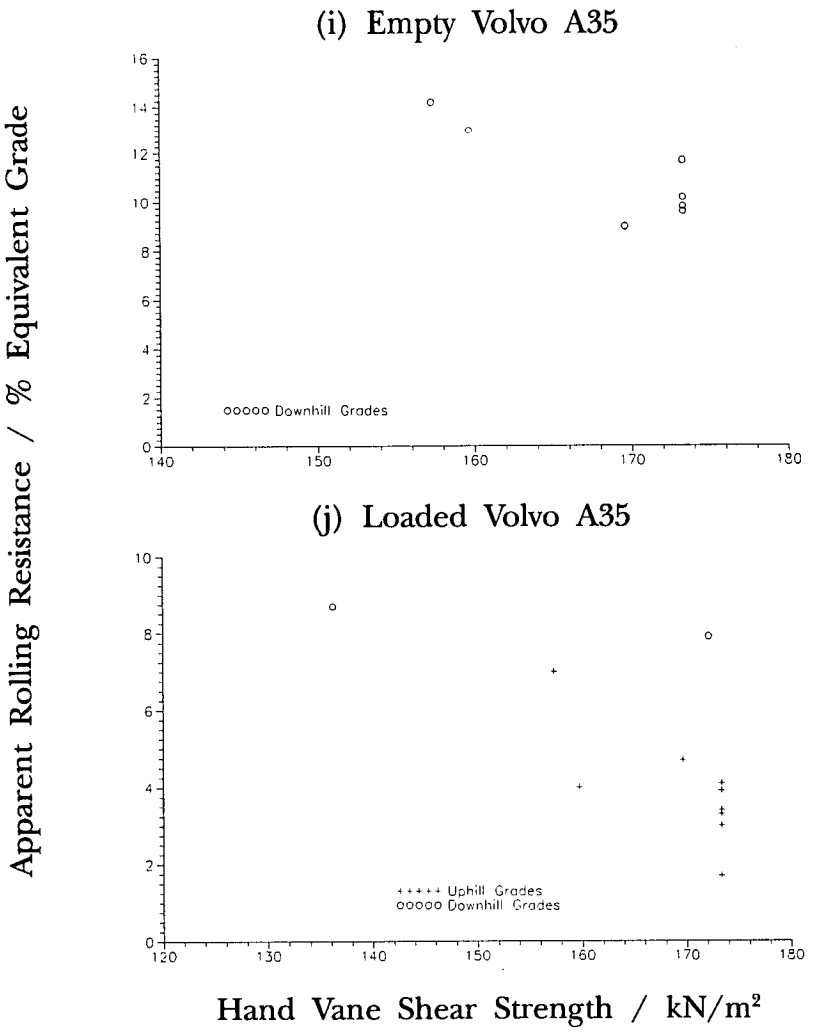

Figure 5.19 (i-j): Apparent Rolling Resistance versus Hand Vane Shear Strength

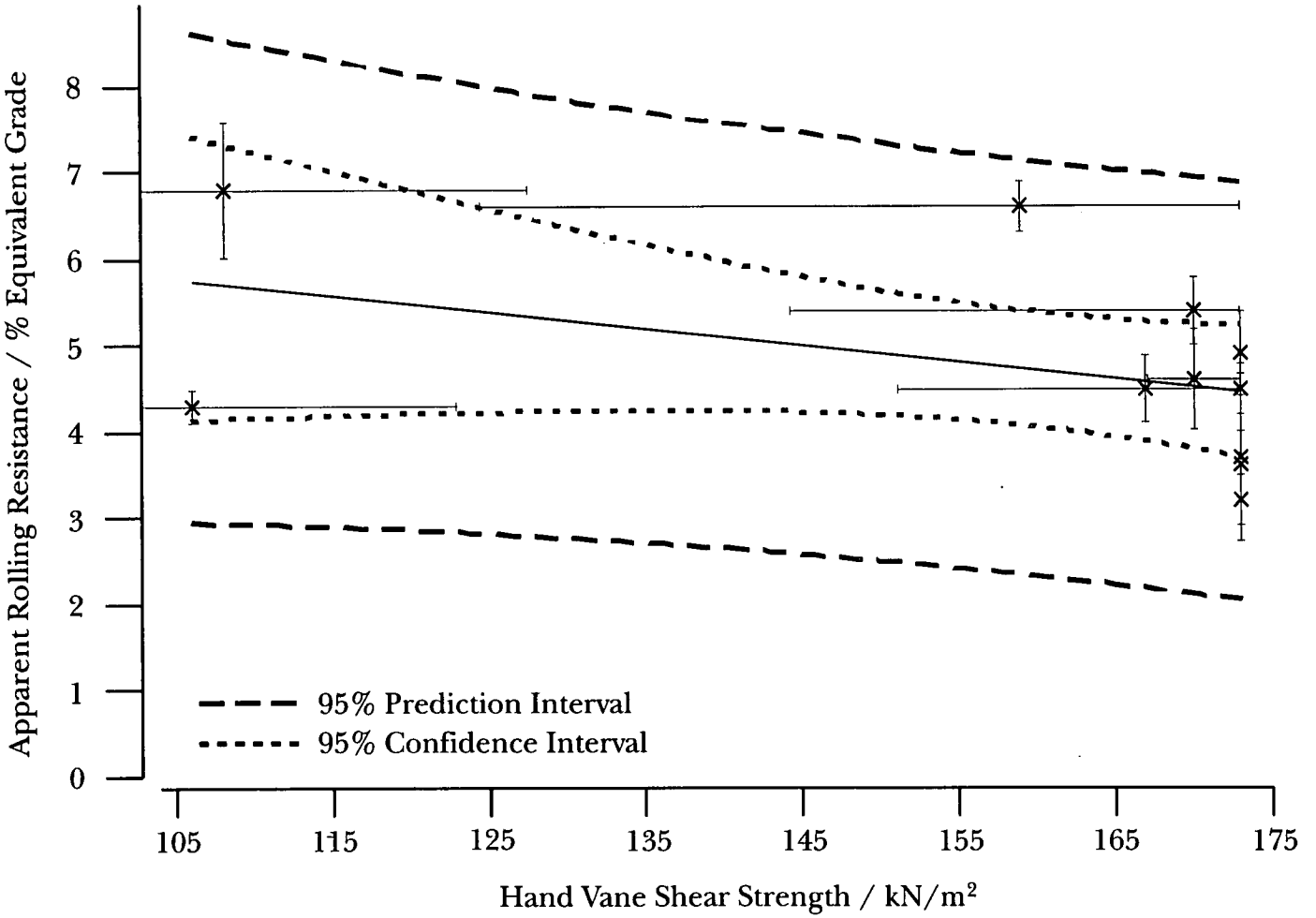

Figure 5.20: Apparent Rolling Resistance versus Hand Vane Shear Strength for a Loaded Cat D400D Articulated Dump Truck Travelling Uphill showing 95% Confidence and Prediction Intervals

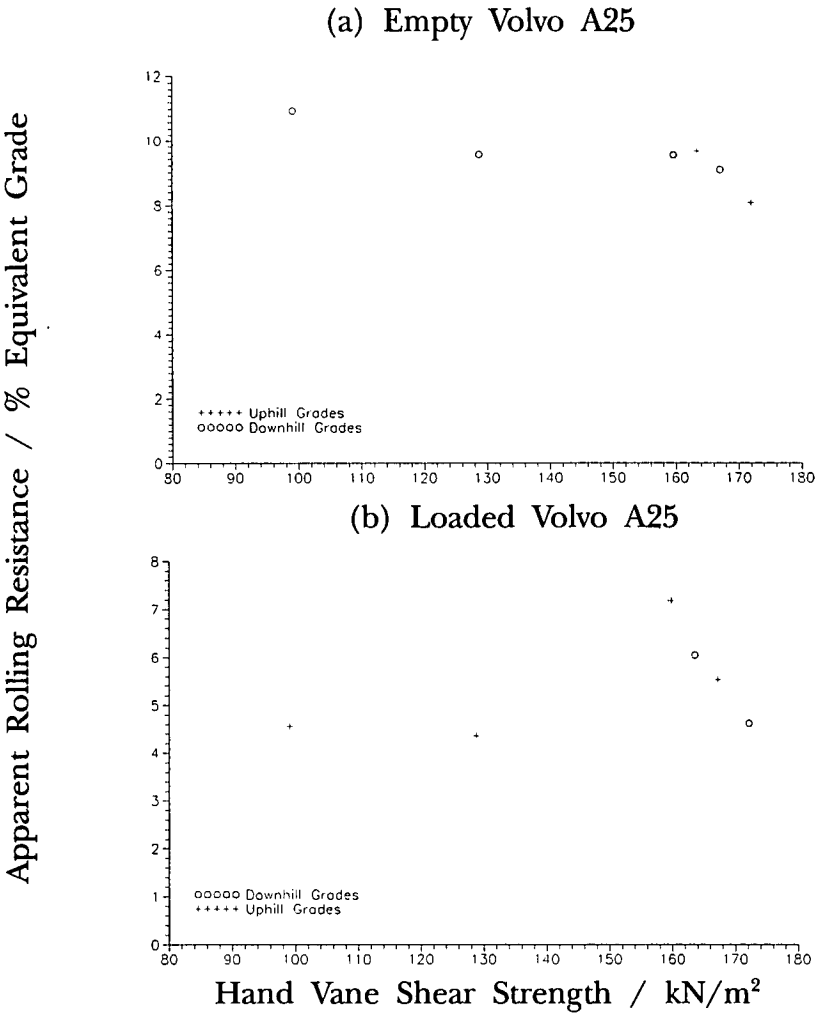

Figure 5.21: Apparent Rolling Resistance Ameded for Grade versus Hand Vane Shear Strength

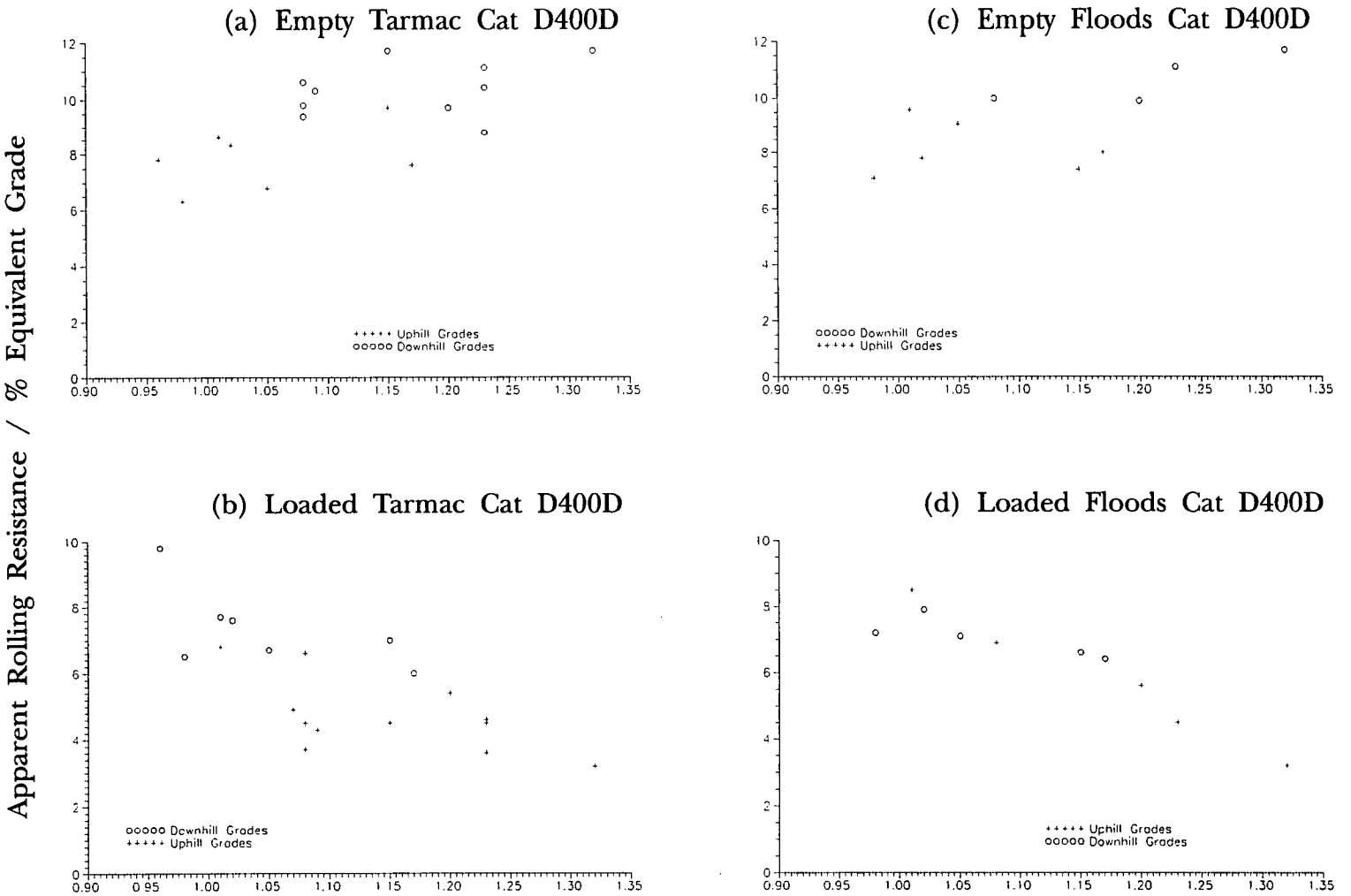

Figure 5.22 (a-d): Apparent Rolling Resistance versus Consistency Index

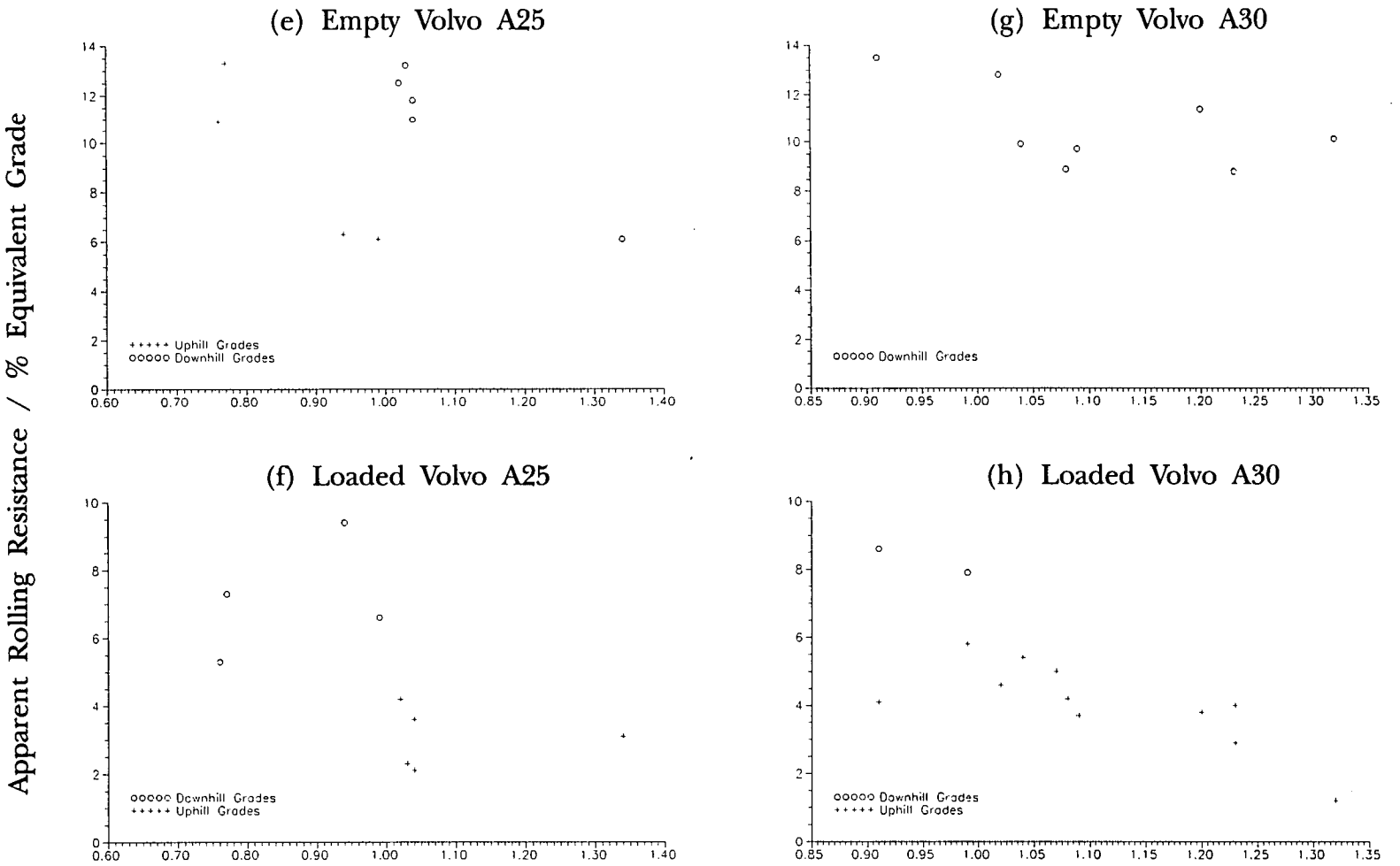

Figure 5.22 (e-h): Apparent Rolling Resistance versus Consistency Index

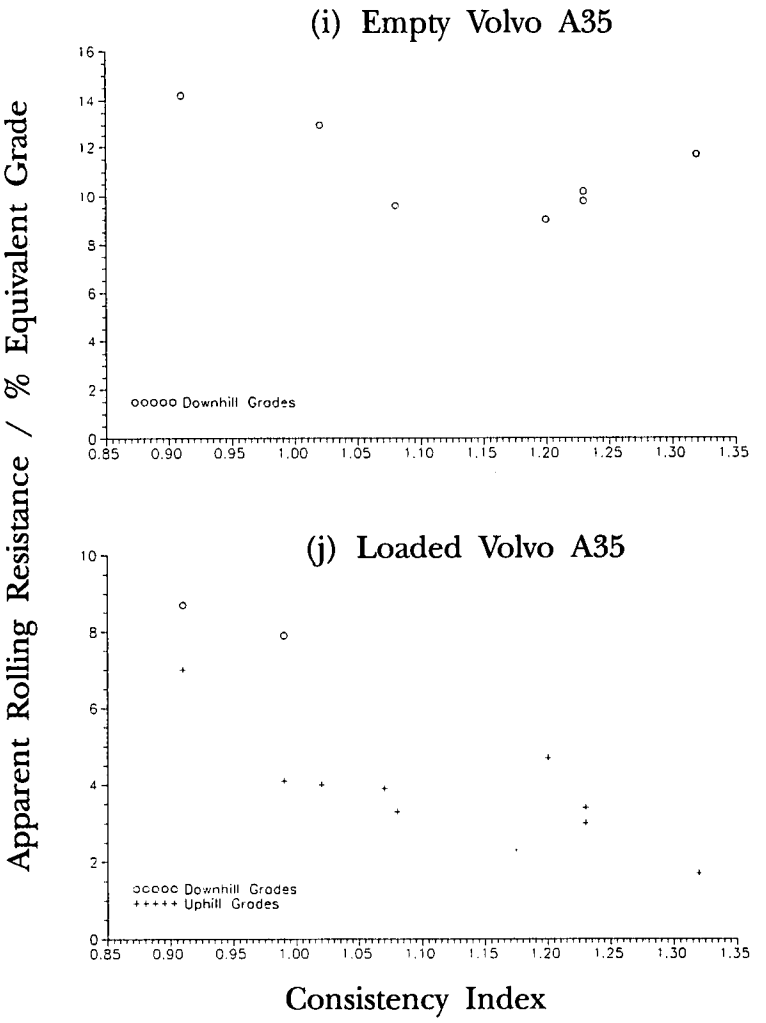

Figure 5.22 (i-j): Apparent Rolling Resistance versus Consistency Index

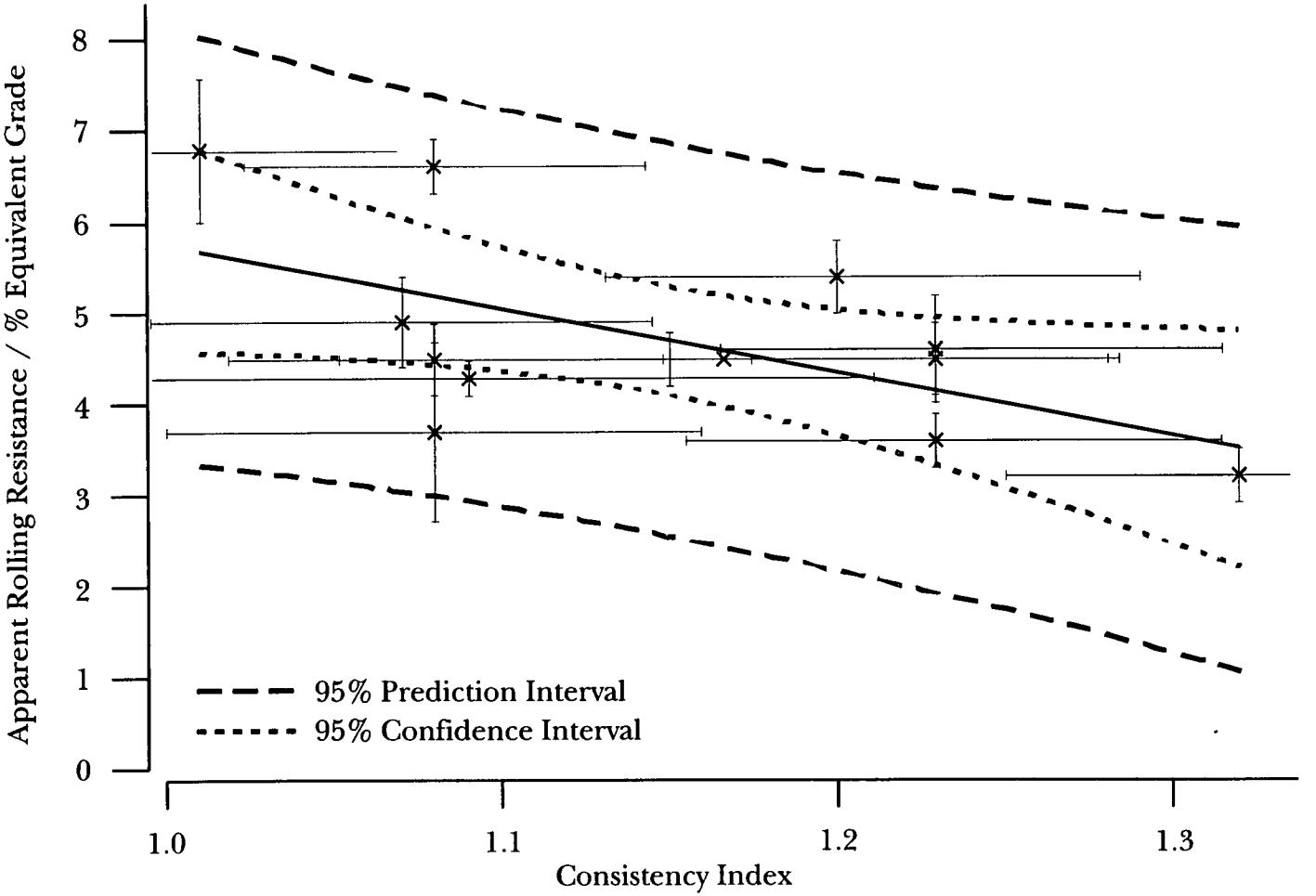

Figure 5.23: Apparent Rolling Resistance versus Consistency Index for a Loaded Cat D400D Articulated Dump Truck Travelling Uphill showing 95% Confidence and Prediction Intervals

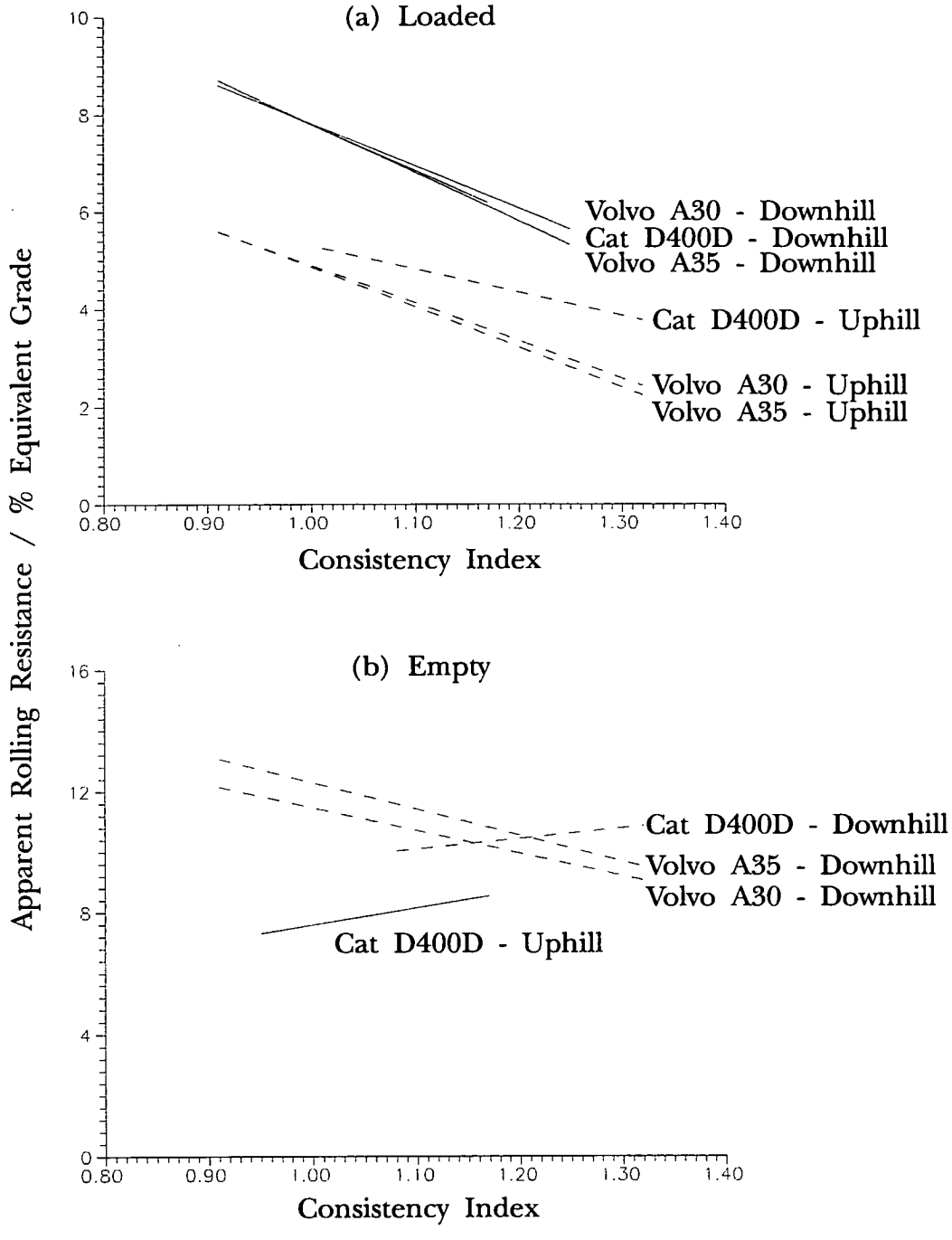

Figure 5.24: Apparent Rolling Resistance versus Consistency Index for Various Vehicles and Driving Conditions from A1M1 Link

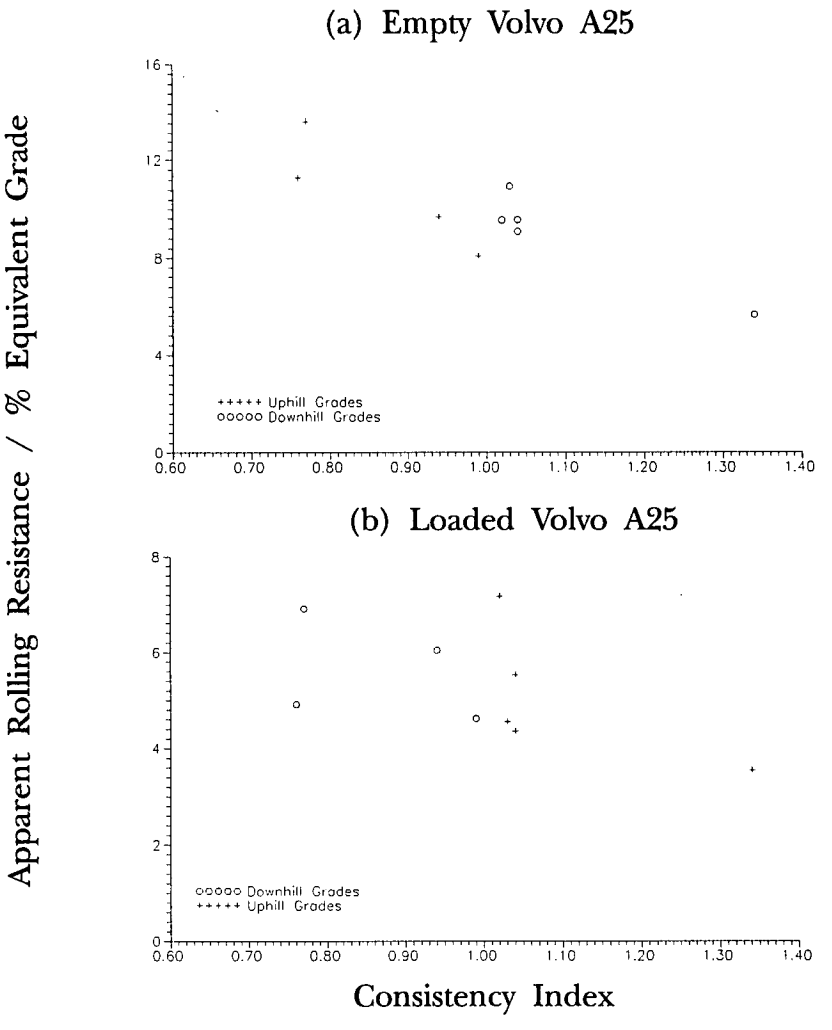

Figure 5.25: Apparent Rolling Resistance Ameded for Grade versus Consistency Index

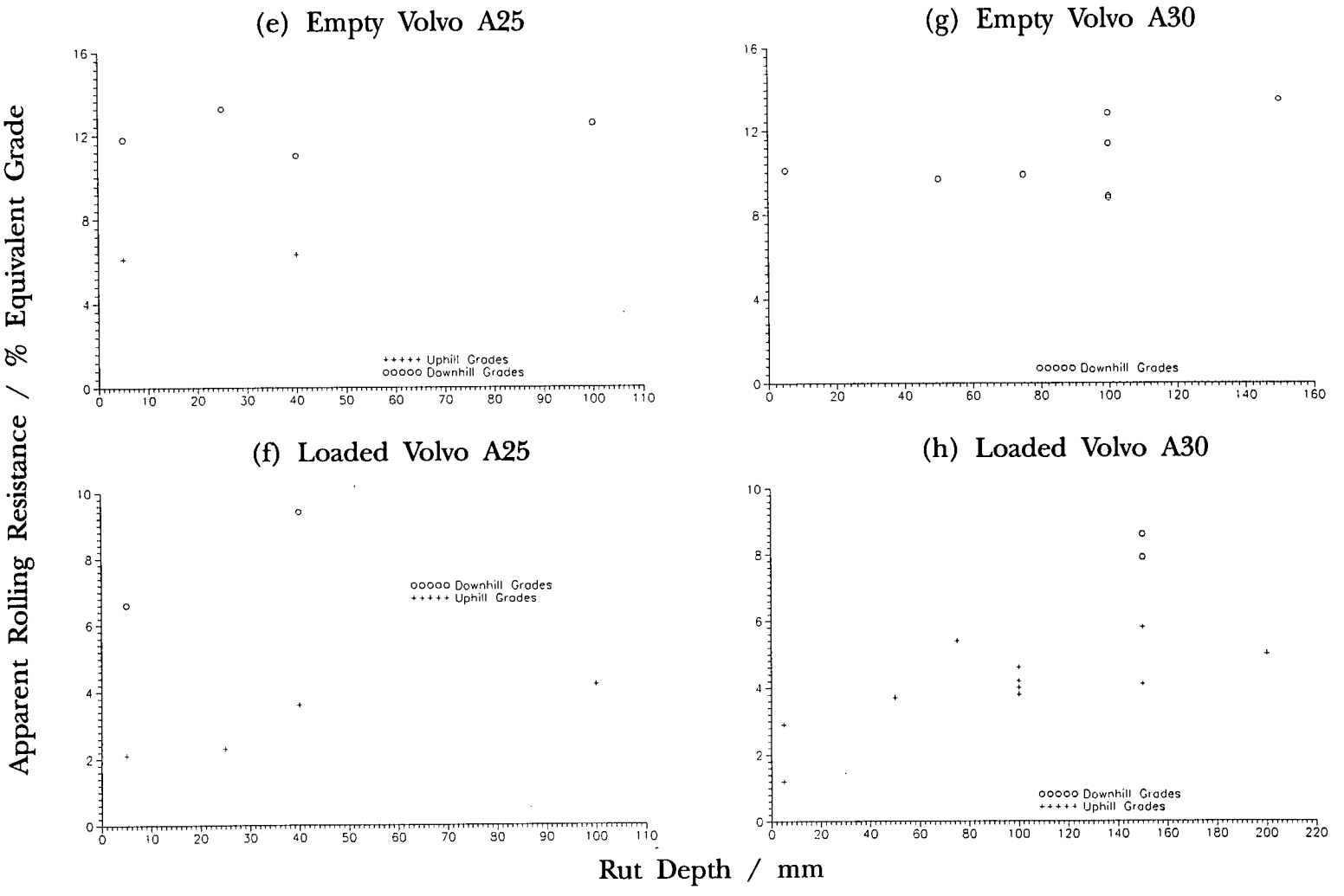

Figure 5.26 (e-h): Apparent Rolling Resistance versus Rut Depth

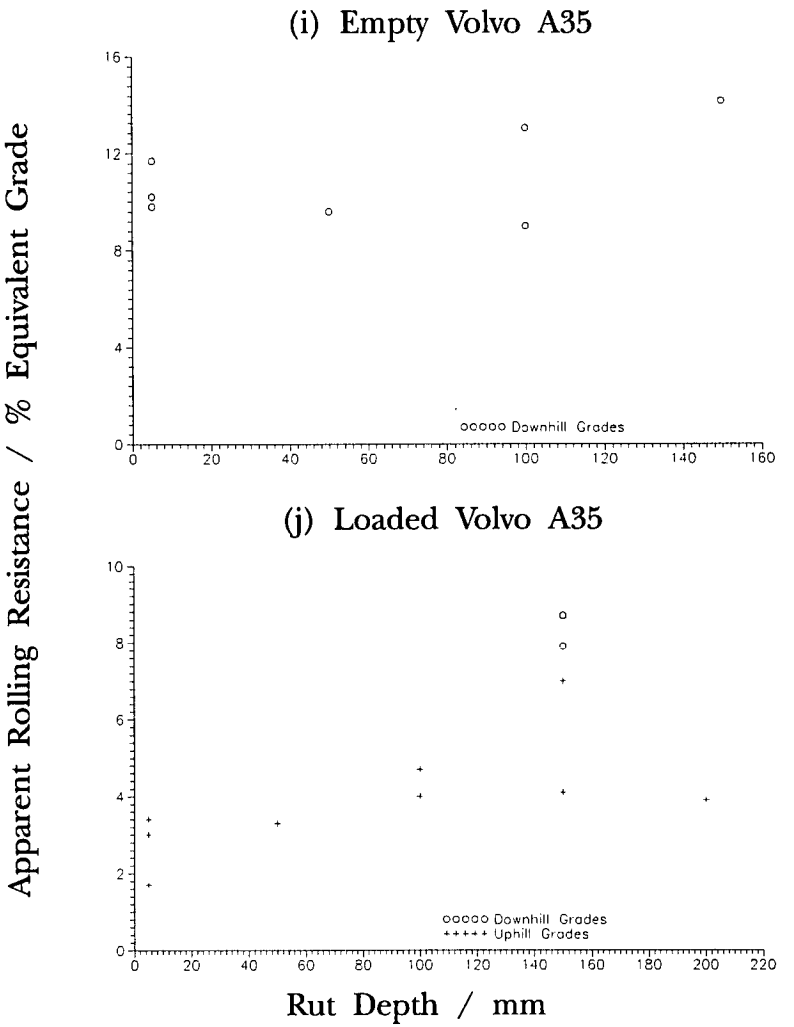

Figure 5.26 (i-j): Apparent Rolling Resistance versus Rut Depth

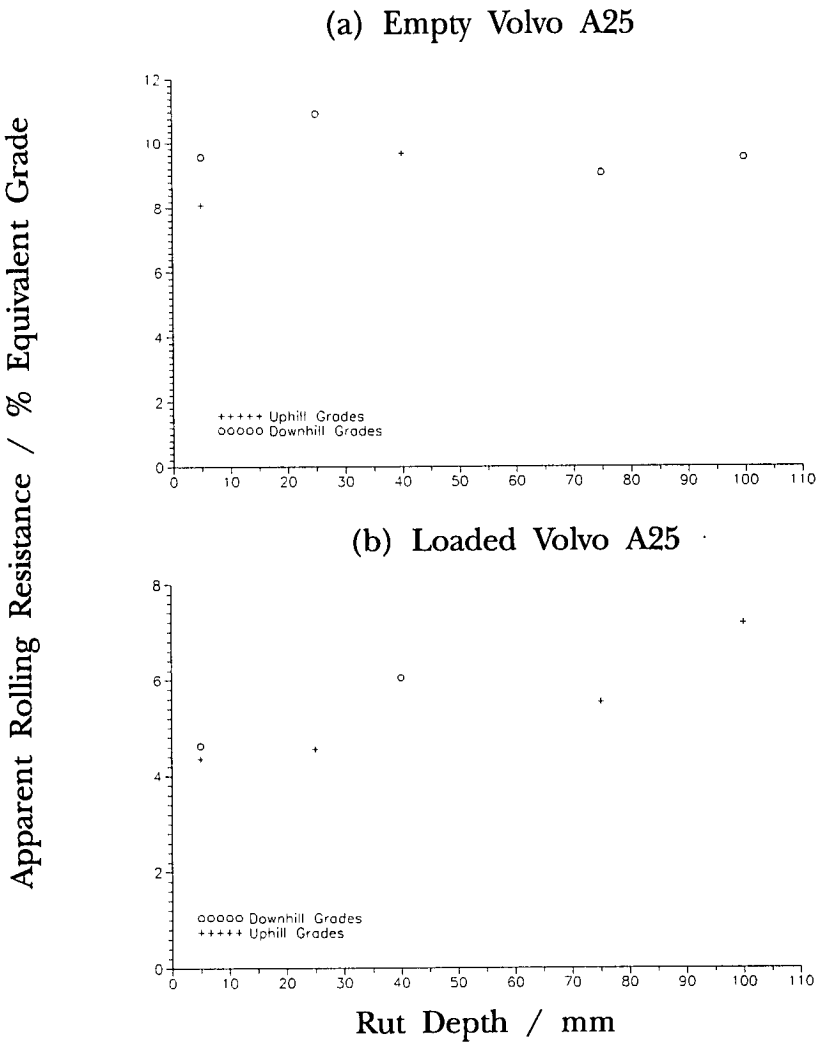

Figure 5.27: Apparent Rolling Resistance Ameded for Grade versus Rut Depth

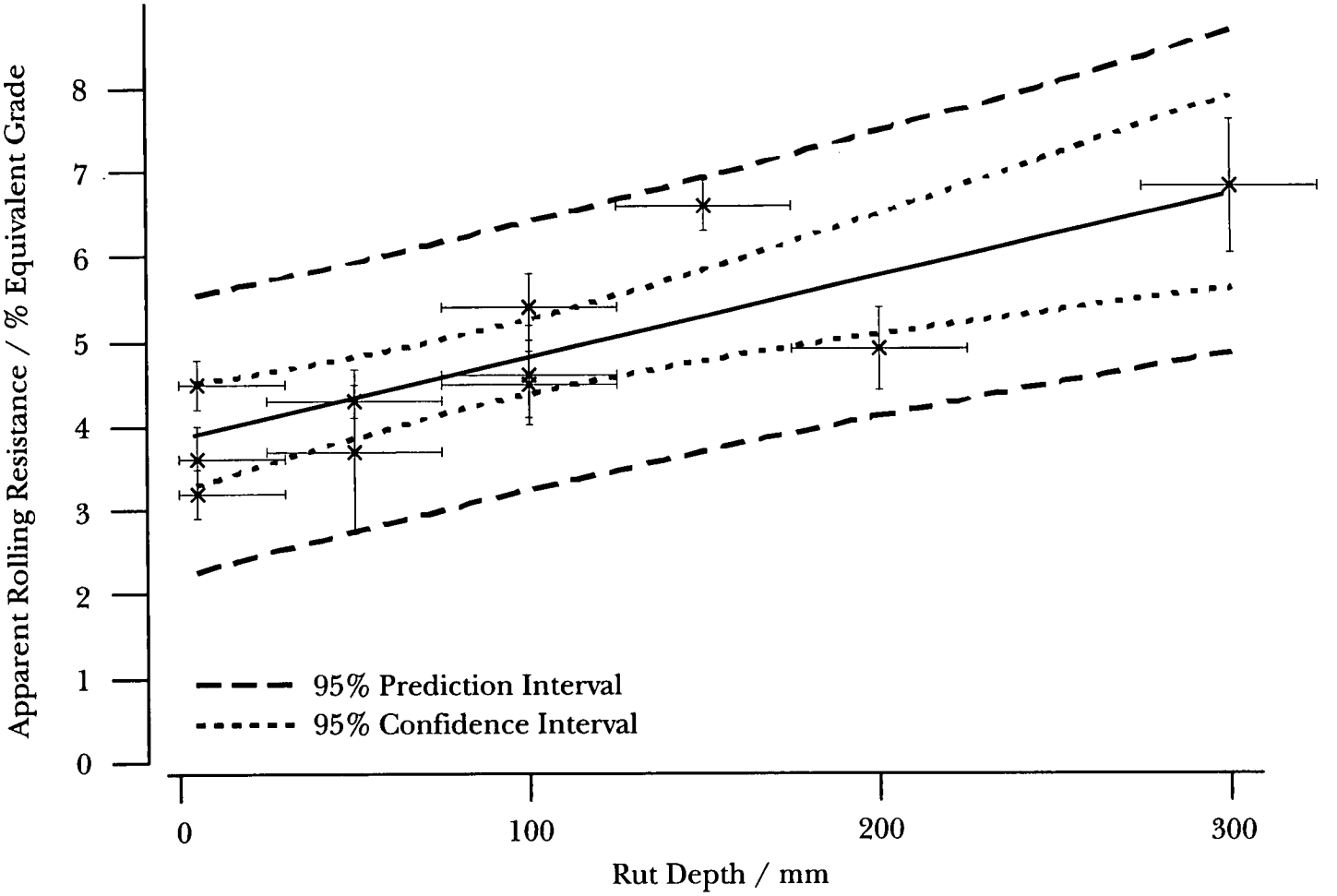

Figure 5.28: Apparent Rolling Resistance versus Rut Depth for a Loaded Cat D400D Articulated Dump Truck Travelling Uphill showing 95% Confidence and Prediction Intervals

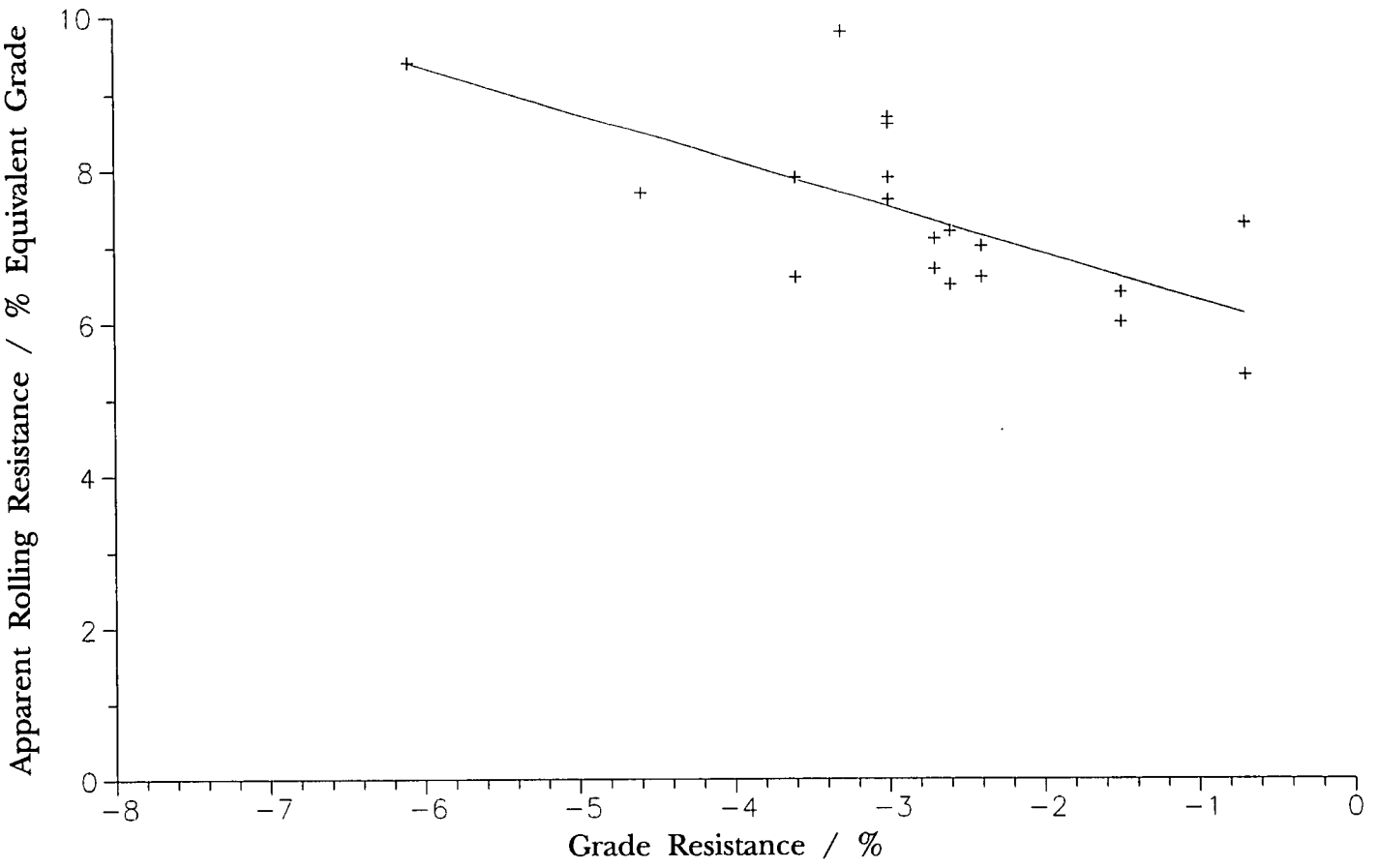

Figure 5.29: Apparent Rolling Resistance versus Grade Resistance for all Loaded Vehicles Travelling Downhill on the A1M1.

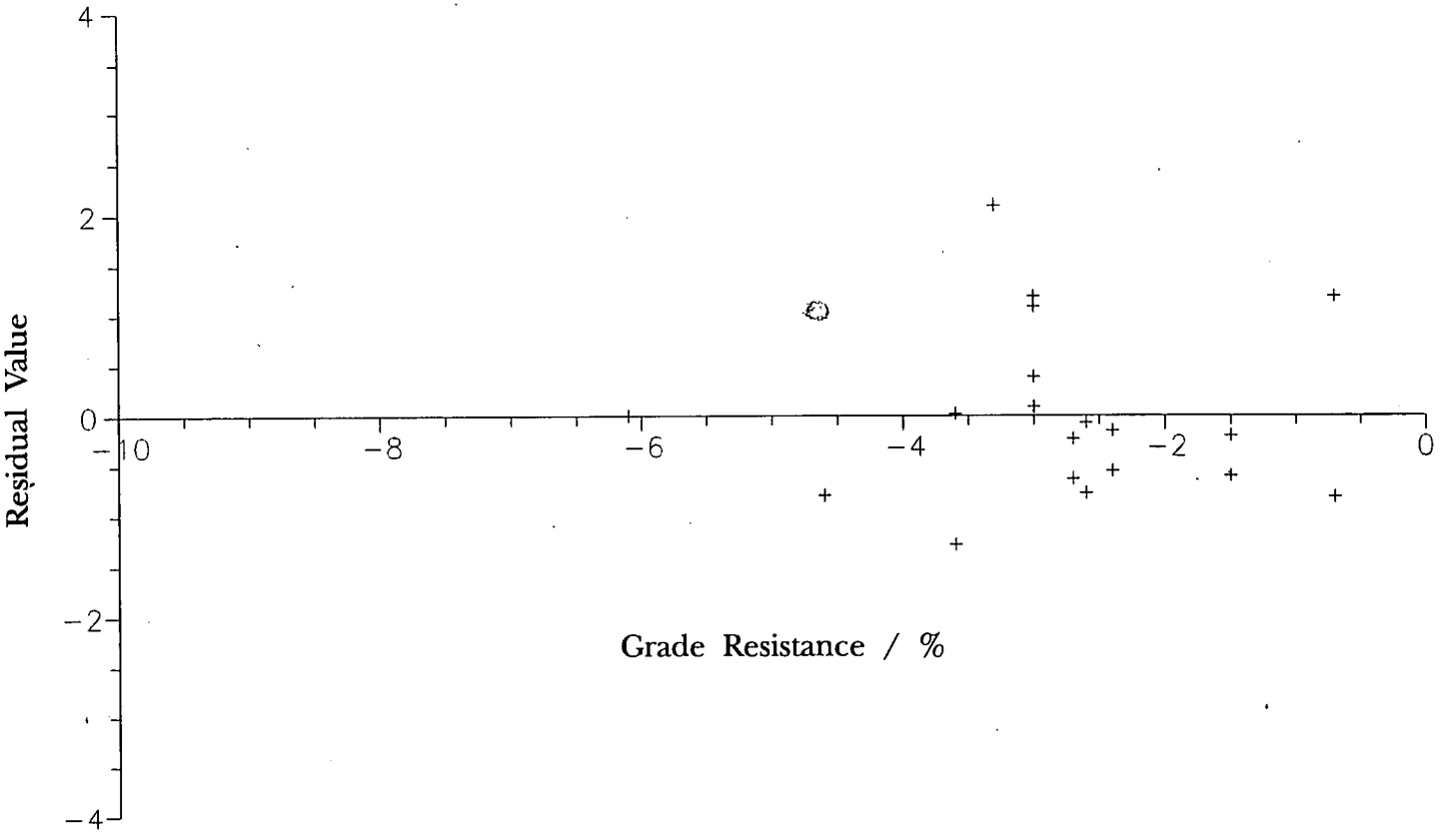

Figure 5.31: Residual Values versus Grade Resistance for the Single Factor Regression between Apparent Rolling Resistance and Grade.

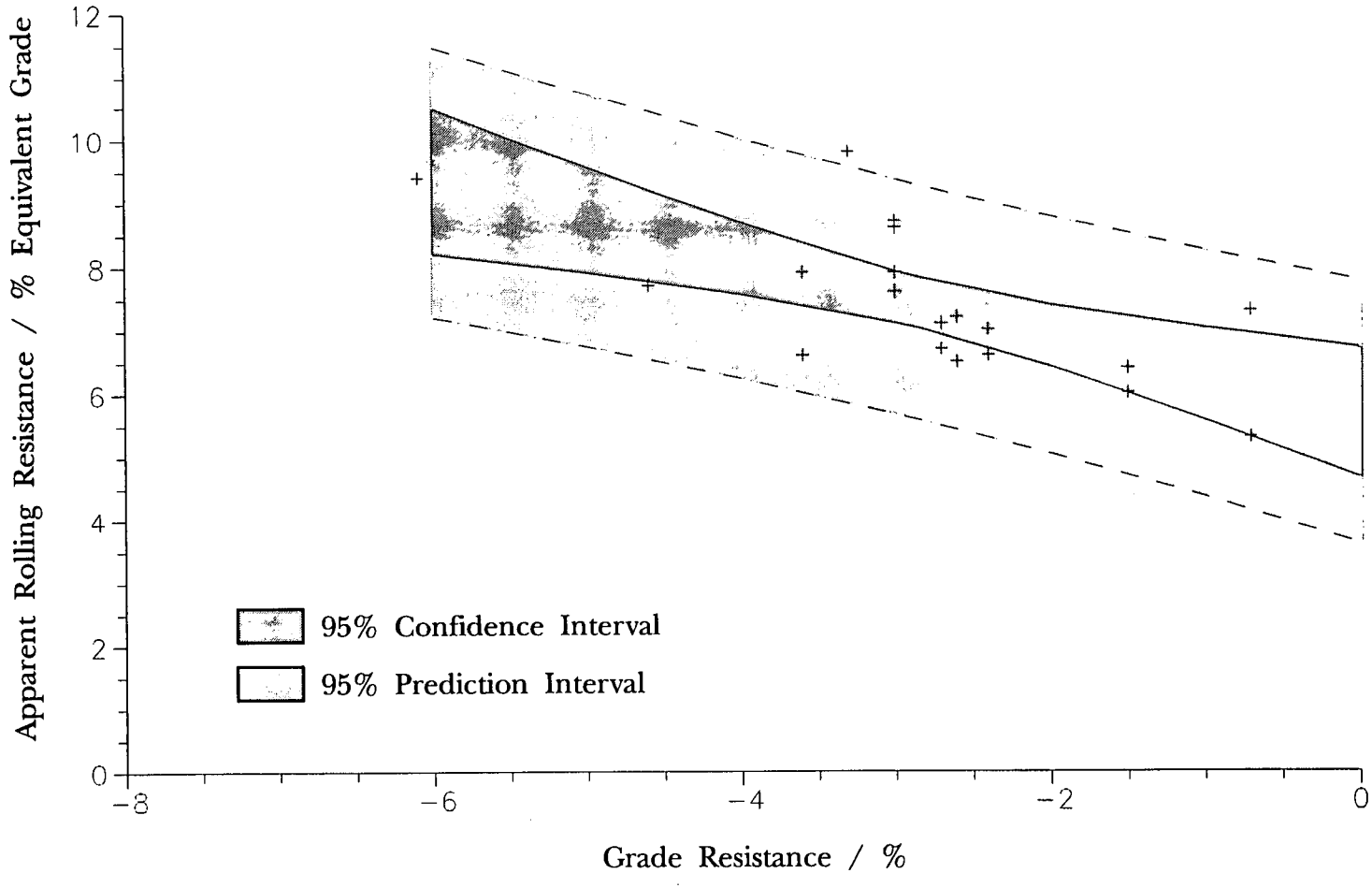

Figure 5.32: Apparent Rolling Resistance versus Grade for all Loaded Vehicles Travelling Downhill on the A1M1, Showing 95% Confidence and Prediction Intervals.

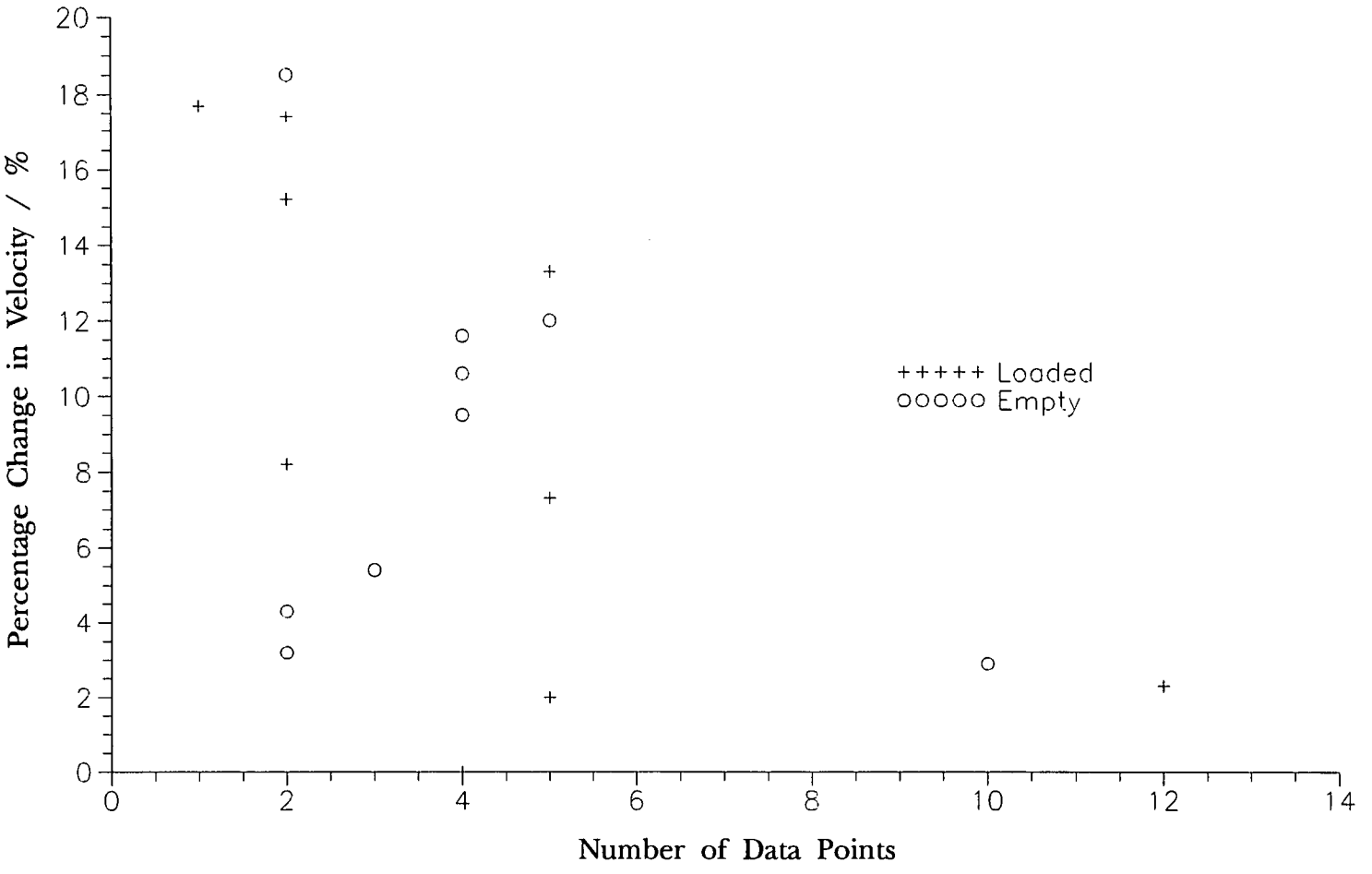

Figure 5.33: Percentage Change in Velocity versus Number of Points for the Various Vehicles used in the Validation of the Five Factor Regression Equations.

Driving Condition	Coefficients for the Parameters						
	Constant	Grade	Consistency Index	Moisture Condition Value	Vane Shear Strength	Rut Depth	R^2 /%
All Empty	12.7	-0.637	-2.30	+0.287	-0.0281	-0.00359	74.3
All Empty Up	12.3	-0.588	-1.30	+0.300	-0.0336	-0.00648	56.8
All Empty Down	11.5	-0.615	-0.35	+0.385	-0.0446	+0.00254	47.6
All Loaded	9.11	-0.477	-4.84	+0.117	-0.0027	+0.00797	82.3
All Loaded Up	6.3	-0.43	-3.87	+0.060	+0.0102	+0.01130	68.4
All Loaded Down	12.5	-0.599	-2.99	+0.197	-0.0409	-0.00023	88.4

Table 5.1: Coefficients for the Parameters in the Five Factor Regression Analysis Relating Apparent Rolling Resistance to Grade, Consistency Index, Moisture Condition Value, Vane Shear Strength and Rut Depth.

Driving Condition	Coefficients for the Parameters					R^2 /%
	Constant	Grade	Consistancy Index	Moisture Condition Value	Vane Shear Strength	
All Empty	11.20	-0.625	-1.62	+0.266	-0.0236	73.2
All Empty Up	7.48	-0.294	+1.27	+0.252	-0.0239	52.2
All Empty Down	12.60	-0.587	-1.38	+0.349	-0.0396	47.3
All Loaded	12.60	-0.447	-7.36	+0.212	-0.0113	76.6
All Loaded Up	12.40	-0.576	-9.09	+0.234	+0.0019	48.4
All Loaded Down	12.40	-0.602	-2.92	+0.196	-0.0408	88.4

Table 5.2: Coefficients for the Parameters in the Four Factor Regression Analysis Relating Apparent Rolling Resistance to Grade, Consistency Index, Moisture Condition Value, and Vane Shear Strength

Driving Condition	Coefficients for the Parameters			
	Constant	Grade	Consistancy Index	R^2 /%
All Empty	14.70	-0.647	-4.92	64.6
All Empty Up	16.70	-0.728	-6.67	57.2
All Empty Down	14.40	-0.579	-4.43	44.7
All Loaded	12.20	-0.446	-6.07	71.9
All Loaded Up	14.20	-0.451	-7.79	42.1
All Loaded Down	8.22	-0.623	-2.57	51.4

Table 5.3: Coefficients for the Parameters in the Two Factor Regression Analysis Relating Apparent Rolling Resistance to Grade, and Consistency Index.

Driving Condition	Coefficients for the Parameters			
	Constant	Grade	Moisture Condition Value	R^2 /%
All Empty	8.95	-0.603	+0.0278	68.8
All Empty Up	7.38	-0.487	+0.1260	42.2
All Empty Down	10.40	-0.631	-0.0840	35.2
All Loaded	5.42	-0.531	+0.0236	59.4
All Loaded Up	4.41	-0.320	+0.0530	9.5
All Loaded Down	6.42	-0.673	-0.0710	44.7

Table 5.4: Coefficients for the Parameters in the Two Factor Regression Analysis Relating Apparent Rolling Resistance to Grade, and Moisture Condition Value.

Driving Condition	Coefficients for the Parameters			
	Constant	Grade	Vane Shear Strength	R^2 /%
All Empty	10.70	-0.621	-0.0089	69.8
All Empty Up	9.10	-0.451	-0.0014	34.6
All Empty Down	12.30	-0.636	-0.0185	41.0
All Loaded	7.39	-0.512	-0.0105	60.6
All Loaded Up	6.25	-0.264	-0.0078	10.4
All Loaded Down	9.97	-0.763	-0.0310	77.0

Table 5.5: Coefficients for the Parameters in the Two Factor Regression Analysis Relating Apparent Rolling Resistance to Grade, and Vane Shear Strength.

Driving Condition	Coefficients for the Parameters		
	Constant	Grade	R^2 /%
All Empty	9.40	-0.579	55.2
All Empty Up	10.00	-0.774	39.1
All Empty Down	8.96	-0.720	36.0
All Loaded	5.71	-0.529	58.0
All Loaded Up	4.96	-0.268	7.4
All Loaded Down	5.69	-0.608	44.8

Table 5.6: Coefficients for the Parameters in the Single Factor Regression Analysis Relating Apparent Rolling Resistance to Grade.

	95% Confidence Interval for the Average Values					
Driving Condition	Five Factor	Four Factor	Two Factor Grade and Consistency Index	Two Factor, Grade and Moisture Condition Value	Two Factor, Grade and Vane Shear Strength	Single Factor
All Empty	9.6 - 10.2	9.5 - 10.2	9.6 - 10.3	9.5 - 10.2	9.5 - 10.2	9.5 - 10.3
All Empty Up	7.3 - 8.7	7.1 - 8.5	7.6 - 9.0	7.3 - 8.4	7.3 - 8.4	7.5 - 9.0
All Empty Down	10.4 - 11.2	10.4 - 11.2	10.2 - 11.1	10.4 - 11.2	10.4 - 11.2	10.2 - 11.2
All Loaded	5.1 - 5.6	5.1 - 5.6	5.0 - 5.6	5.0 - 5.7	5.0 - 5.7	5.0 - 5.6
All Loaded Up	4.0 - 4.6	3.4 - 4.6	3.9 - 4.6	3.9 - 4.8	3.9 - 4.8	3.8 - 4.7
All Loaded Down	7.2 - 7.8	7.2 - 7.7	7.0 - 7.8	6.9 - 7.8	7.1 - 7.6	7.0 - 7.8

Table 5.7: 95% Confidence Intervals for the Regression Analyses Given in Tables 5.1-5.6, all Intervals are Calculated on Average Values.

Driving Condition	95% Prediction Interval for the Average Values					
	Five Factor	Four Factor	Two Factor Grade and Consistency Index	Two Factor, Grade and Moisture Condition Value	Two Factor, Grade and Vane Shear Strength	Single Factor
All Empty	7.7 - 12.0	7.7 - 12.0	7.4 - 12.4	7.5 - 12.1	7.6 - 12.1	7.1 - 12.7
All Empty Up	5.7 - 10.2	5.6 - 10.0	5.4 - 11.1	5.7 - 10.0	5.6 - 10.1	5.0 - 11.5
All Empty Down	8.4 - 13.2	8.4 - 13.1	8.1 - 13.3	8.3 - 13.3	8.4 - 13.2	7.9 - 13.4
All Loaded	3.6 - 7.1	3.3 - 7.4	3.1 - 7.5	2.7 - 8.0	2.7 - 7.9	2.7 - 7.9
All Loaded Up	2.5 - 6.1	2.0 - 6.6	2.0 - 6.6	1.4 - 7.3	1.4 - 7.3	1.4 - 7.2
All Loaded Down	6.5 - 8.5	6.5 - 8.4	5.6 - 9.2	5.5 - 9.2	6.2 - 8.5	5.6 - 9.3

Table 5.8: 95% Prediction Intervals for the Regression Analyses Given in Tables 5.1-5.6, all Intervals are Calculated on Average Values.

	Loaded Grade /%	Empty Grade / %	Consistency Index	Moisture Condition Value	Vane Shear / kN/m²	Rut Depth / mm
Cat D400D (McAlpines)	-3.0	3.0	1.02	11.0	136	40
	-2.7	2.7	1.05	13.9	173	5
	-2.6	2.6	0.98	9.9	144	110
	0.2	-0.2	1.08	13.8	158	150
Volvo A35 (Halls)	3.0	-3.0	0.91	14.1	157	150
	5.4	-5.4	1.02	14.0	160	100
Volvo A35 (Tarmac)	-1.5	1.5	1.17	12.2	149	110
	3.5	-3.5	1.04	14.2	167	75
	5.4	-5.4	1.02	14.0	172	100

Table 5.9: Input Parameters for Vehicles not Included in the Regression Analysis

		Rolling Resistance / % Equivalent Grade		Velocity / km/h		95% Confidence Interval for Rolling Resistance / % Equivalent Grade	95% Prediction Interval for Rolling Resistance / % Equivalent Grade
		Predicted	Actual	Predicted	Actual		
Loaded	Cat D400D (McAlpines)	7.8	7.7	24.4	24.9	7.4 - 8.2	6.8 - 8.8
		6.6	6.9	30.1	27.9	6.1 - 7.1	5.5 - 7.6
		7.1	7.0	26.0	26.6	6.7 - 7.6	6.1 - 8.2
		6.2	7.4	18.3	15.4	5.5 - 6.8	4.3 - 8.1
	Volvo A35 (Halls)	5.6	4.3	14.1	16.6	4.9 - 6.4	3.7 - 7.5
		3.6	5.0	13.5	11.7	3.0 - 4.3	1.7 - 5.5
	Volvo A35 (Tarmac)	6.2	5.5	25.8	30.3	5.6 - 6.7	5.1 - 7.3
		4.1	4.8	15.9	14.6	3.7 - 4.6	2.3 - 6.0
		3.7	3.8	13.3	13.2	3.1 - 4.4	1.8 - 5.7
Empty	Cat D400D (McAlpines)	7.7	8.8	25.2	22.8	6.7 - 8.7	5.3 - 10.1
		7.7	9.1	25.9	22.8	6.5 - 8.9	5.2 - 10.1
		7.0	7.3	28.0	27.2	5.9 - 8.0	4.6 - 9.3
		9.9	9.6	27.7	28.6	8.8 - 10.9	7.3 - 12.4
	Volvo A35 (Halls)	11.8	10.9	31.8	35.5	10.8 - 12.8	9.3 - 14.4
		13.0	13.9	36.9	33.0	11.9 - 14.0	10.4 - 15.5
	Volvo A35 (Tarmac)	7.9	7.5	29.8	31.1	6.4 - 9.3	5.3 - 10.5
		11.5	11.1	35.0	36.9	10.8 - 12.2	9.0 - 13.9
		12.4	14.0	40.0	32.6	11.3 - 13.5	9.8 - 15.0

Table 5.10: Comparison of Actual Measured Rolling Resistance and Predicted Values from the Five Factor Regression Analysis.

		Velocity / km/h		Percentage Change in Velocity / %	Number of Different Vehicles in Calculating Average Travel Time	Number of Timings to Calculate Average Travel Time
		Predicted	Actual			
Loaded	Cat D400D (McAlpines)	24.4	24.9	+2.0	3	5
		30.1	27.9	-7.3	3	5
		26.0	26.6	+2.3	4	12
		18.3	15.4	-15.2	2	2
	Volvo A35 (Halls)	14.1	16.6	+17.7	1	1
		13.5	11.7	-13.3	2	5
	Volvo A35 (Tarmac)	25.8	30.3	+17.4	1	2
		15.9	14.6	-8.2	1	2
		13.3	13.2	-0.8	1	4
Empty	Cat D400D (McAlpines)	25.2	22.8	-9.5	3	4
		25.9	22.8	-12.0	4	5
		28.0	27.2	-2.9	4	10
		27.7	28.6	+3.2	1	2
	Volvo A35 (Halls)	31.8	35.5	+11.6	2	4
		36.9	33.0	-10.6	2	4
	Volvo A35 (Tarmac)	29.8	31.1	+4.3	1	2
		35.0	36.9	+5.4	1	3
		40.0	32.6	-18.5	1	2

Table 5.11: Percentage Change in Velocity, as a Function of the Predicted Velocity, the Number of Vehicles and Individual Timings to Calculate the Average Travel Time for the Vehicles used in the Regression Validation.

Chapter 6 Development of Theory of Rolling Resistance

6.1 Introduction

A theory estimating the apparent rolling resistance of a haul road from the information contained within the site investigation report would be desirable for any contractor. This would enable accurate determination of the speed of the plant on site. From this, the productivity and duration for each operation are easily calculated. The initial concept of the theory was to relate the undrained shear strength of the soil to the apparent rolling resistance of the driver-vehicle-terrain system. The relationship could either be formulated empirically, theoretically, or semi-empirically.

A relationship could be constructed empirically by simply building up a data base of haulers, ground conditions, and soil parameters as has been done to some extent on the A1/M1 and the M3 contracts. This data collection exercise would have to continue on different ground conditions and with a full range of operating plant. The downfall of this approach is that it cannot be extrapolated with total confidence to other vehicle-terrain systems. Theoretically, as there is very little information on the interaction between a pneumatic tyre and the soil it would be exceptionally difficult to develop an accurate theory without extensive experiments to validate all the initial assumptions. Even after this, some adjustment would have to be incorporated, for driver variability. The third option available is to construct a semi-empirical theory, utilising collected field results, basic soil mechanics and the limited known data on the interaction between the tyre and the terrain. It is this semi-empirical approach that has been followed in the thesis.

6.2 Fundamental Relationships

The theory was developed around two relationships, that between rut depth and shear strength, and that between rut depth and rolling resistance. The first relationship relies upon the assumption that the truck is invariant, therefore the only way that the rut depth could increase is for the running material to

decrease in strength. This could occur by the material becoming wetter or by the pore water pressure increasing, see chapter 7. The latter effect could be significant in a narrow, heavily trafficked area, where the time between loadings is insufficient for the excess pore pressures to dissipate.

In reality the vehicle is a variable and can accelerate causing the load distribution to alter, increasing the dynamic load, hence the deterioration of the haul road. All measurements taken on site assumed that the vehicles were travelling at a constant velocity, therefore this load transfer effect should not affect the theoretical output.

The relationship between rut depth and shear strength requires a knowledge of the normal and shear stress distributions at the tyre-soil boundary; this is discussed in the next section.

The second relationship between rut depth and rolling resistance was first proposed by Caterpillar in the 1950's (Caterpillar, 1993, and Morgan, 1993), and has never been extensively researched. This relationship will be discussed more fully in the section 6.4.

6.3 Pressure Distribution Beneath Pneumatic Tyres

Virtually all of the work carried out in this field of study has been completed by the agricultural engineers, (Burt et al, 1987, Wulfsohn et al., 1992). The main criterion for the tractor operator is to produce the maximum tractive effort with the minimum detrimental effect on the soil structure, especially as the modern day farmer traffics the land more frequently and with heavier equipment. As soil becomes consolidated, the mechanical strength of the soil is increased, the water-holding capacity of the soil mass is lowered, and the moisture infiltration rate is decreased, inhibiting the growth of the crop, (Trabbic et al., 1959). For this reason the inflation pressure of working agricultural tyres is very low, thus spreading the load and reducing compaction. The relatively narrow width of agricultural tractor tyres arises because the vehicles must also work on road so the design of the tyre is a compromise between the two working environments.

Conversely to the agricultural situation, the ideal hauling conditions, from a civil engineering standpoint, are for the material on the haul road to be at as high a dry density as possible, in order that the speed of the plant is not limited by the condition of the soil on the haul road. The demand for high traction is not as necessary in this situation where speed is the essential component, unless the ground conditions are really bad. In poor working conditions contractors would be reluctant to work and would probably improve the quality of the haul road by surcharging it with drier material, or by letting the ground dry naturally.

The relationship between tractive performance and soil properties is complicated and relies upon either integrating and resolving forces at the running gear-soil boundary, (Wong et al., 1967, Onafeko, 1969) by dimensional analysis (Wismer et al., 1973, Turnage 1978), or by empirical formulae derived from instrumentation of a vehicle wheel (VandenBerg et al., 1962, Taylor, 1973, Gee-Clough et al., 1977). For any estimation to be carried out, both the normal and shear pressure distributions at the tyre-soil interface must be known. The pressure distributions vary in three directions and is dependent on: inflation pressure, carcass stiffness, tyre lug pattern, dimensions of the tyre, dynamic load, soil type, and moisture content.

The stress distributions under both a rigid wheel, (Onafeko et al., 1967) and a pneumatic tyre, (Krick, 1969, Wood et al., 1987) have been researched to show the general shape of the distributions, but no general theory exists to describe the pressure distribution under any combination of torque, slip and wheel construction. The following section will describe the work carried out to date on the pressure distribution at the tyre-soil boundary.

6.3.1 Review of Pressure Distribution Literature

The pioneering work carried out in this field of study was by Soehne (Soehne, 1953, 1958) where he relates the stress distribution with depth under pneumatic tyres to the semi-empirical work carried out by Froehlich, (1934) based on the studies of Boussinesq. Deriving formulae for pressure variation with depth

requires the pressure distribution at the tyre-soil boundary and the author describes this for a buffed tyre on three soil conditions: dense, hard, dry cohesive soil; relatively dense, fairly moist, sandy clay, and a wet soil. A buffed tyre is one where the lugs have been removed.

On the dry cohesive soil, akin to the civil engineering haul roads investigated, using a buffed tyre, the maximum normal pressure occurs towards the centre of the loaded area and is only 12.5% greater than the average normal pressure. As the soil becomes wetter the maximum normal stress increases, due to stress concentration around the loading axis, to a value twice that of the average normal pressure. This stress concentration is caused by introverted shear stresses being present in the contact area, causing an increase in the normal stress near the load axis. These stresses are caused by the relative motion of the soil and the rubber which increases as the soil becomes wetter. Another possible reason for the stress concentration is that as the soil becomes wetter the deformation of the soil becomes plastic. This causes the soil to yield at the load area boundary, which again leads to a concentration of pressure under the axis of loading. Soehne (1958) also reported that the maximum contact pressure under the high lugs of a tractor tyre, on a hard dry soil, could be up to five times that of the average pressure, due to the reduced contact area. These stress concentration factors are important for the development of the theory as the greatest pressure the soil encounters must be used in the analysis.

VandenBerg et al. (1962) carried out a series of tests using an under-inflated smooth tyre on various soils. They measured the pressure distributions in the soil and on the tyre surface. With the instruments buried in the soil the direction of the stress was not known as the transducers had a tendency to move, especially in softer soils. They found that the maximum pressure occurred under the periphery of the tyre, where the carcass stiffness was having a marked effect on the pressure distribution. This effect decreased as the tyre pressure increased, as the inflation pressure was transmitting proportionally more of the load. The measured maximum normal pressures were at least twice the value of the average normal pressure which agrees with the work carried out by Soehne except that the maximum pressure occurred at the periphery and not at the centre. This is because Soehne (1958) assumed the stress distribution to be parabolic. Freitag et al., (1965), carried out similar

tests using a smooth tyre on various soils. Tests were carried out on a soft clay and as the inflation pressure was increased from 103 to 413kN/m^2 (15 to 60psi), the peak normal stress tended to move towards the centre longitudinal axis of the tyre, this is in agreement with the findings of VandenBerg and Gill, (1962).

Trabbic et al. (1959) and Reaves et al. (1960), investigated the pressure distribution beneath normally inflated lugged tractor tyres. The former by instrumenting the tyre and the latter instrumenting the soil. Both these papers show that the maximum pressure occurs under the centreline of the tyre, agreeing with the findings of Soehne (1958). The reports show that the lugs have a marked effect on the pressure distribution at the tyre-soil boundary. The results in the Trabbic paper indicate that the maximum stress is approximately three times the average pressure across the tyre width which agrees well with the other results using a lugged wheel.

Krick, (1969) measured both normal and shear stresses on the surface of both a rigid wheel and a lugged pneumatic tyre on a soil described as a "soft sandy loam". Comparing figures 6.1 and 6.2 for the pressure distributions beneath a pneumatic tyre and rigid wheel respectively, it is clear that there are distinct differences. The rigid wheel displays large peak values at the edge of the wheel, whereas the pneumatic tyre has the tendency to smooth the pressure distributions. The published results also show that as the slip of the wheel increases both the circumferential and lateral stress distributions become flatter. The maximum normal stress occurred near the centre of the tyre under the axle, figure 6.1, and the magnitude of the maximum shear stress was approximately 60-70% that of the normal stress. Averaging the normal stresses over the contact length gives the maximum to be about 50% greater than the average, hence agreeing well with the work of Soehne (1958) for a soil with medium moisture content.

Virtually no further work was carried out in this field until the mid-1980's when a team of agricultural engineers from Auburn Alabama carried out a series of tests to determine three dimensional deflection patterns, (Burt et al., 1987a and Burt et al. 1987b) contact stresses, (Wood et al., 1987), and inflation pressure effects (Burt et al., 1982) on the performance of agricultural

tyres. As with Krick they found that the peak normal stresses occurred just before the peak tangential stress. The results given are incomplete therefore it is impossible to ascertain the ratio of tangential stress to maximum normal stress. The maximum normal stress on a lug was found to be approximately twice the average normal stress across the width of the tyre.

All the above papers, independent of the soil type and load, it is indicated that the rear contact angle is approximately 10°, figure 6.1. This figure is also valid for work carried out on rigid wheels, figure 6.2, (Onafeko et al., 1967, Karafiath et al., 1978).

Although a greater amount of research has been carried out on the behaviour of rigid wheels, it was considered necessary to avoid using these stress distributions as they differ significantly from those for pneumatic tyres, compare figures 6.1 and 6.2 (Krick 1969).

Several problems are associated with the applicability of the agricultural engineering results using tractor tyres to that of an earthmoving tyre. Firstly an earthmoving tyre is approximately twice as wide as a conventional tractor tyre, typical sizes being 26.5 R25 and 13 x 38 respectively. The width of the contact area has been known to effect the performance of a tyre since the initial research into tyre performance in the 1930's, (Hurlbut et al., 1937). Tyre size nomenclature is derived from the approximate cross section width and rim diameter with various classification systems available. Generally the first number relates to the cross sectional width of the tyre and the second number to the rim diameter, both in inches. An R in the notation denotes radial construction, see section 2.2.

The lug pattern on the two types of tyres also varies dramatically; the tractor tyre has deep relatively isolated lugs, whereas the pattern on an earthmoving vehicle tyre is similar to a car tyre's tread. These two different patterns will alter the pressure distribution at the tyre-soil boundary as has been described earlier. Even on a hard surface the rut left in the wake of an earthmoving tyre is generally deeper than the tread on the wheel. Therefore it may be assumed that the pressure distribution beneath the tyre will resemble an intermediate case between that of a smooth buffed tyre and a lugged tractor tyre.

The inflation pressure of the two types of tyre under working conditions also varies considerably. Most of the agricultural laboratory testing was carried out with tyres inflated only slightly above the recommended minimum for the load carried, or under inflated, i.e. 70-125kPa. Flotation is not generally required on earthmoving machinery as the haul road conditions are reasonably firm and compaction of the soil is not critical, therefore the inflation pressure is increased dramatically; typical values for a Volvo A35 articulated dump truck on chalk are 350kPa for the front tyres and 500kPa for the rear. The effect of increasing the inflation pressure will be to flatten the stress distribution in both the lateral and longitudinal direction.

The difference in speed between agricultural and earthmoving machinery is another factor which must be taken into account. It is well known that the rate of application of the load has an effect on the shear strength of the soil (Casagrande et al., 1951). Earthmoving vehicles aim to move as fast as possible along the haul roads, generally about 25-30km/h, whereas a working tractor will travel at between 5-10km/h. The speed of testing the agricultural tyres is rarely given, but it is assumed to be slow, both to mimic field conditions and so that the instrumentation can respond to the pressure changes. Sabey et al. (1967) showed that the contact length decreased, by up to 30%, as the speed of the vehicle increased from 0 to 48km/h, depending on the tyre type. Their work involved photographing the contact area of small diameter car tyres passing over a glass plate. This change in contact area will have an effect on the magnitude of the pressure and the distribution over the whole contact area.

Another major consideration is that most of the agricultural testing used a single pass of a tyre in soil bins. The material was generally described as loamy and uncompacted. On site, the earthmoving plant is working in a multipass condition on heavily compacted soils with little organic content. From the work carried out by agricultural engineers it is clear that the bulk density of the soil and the type of soil have a significant effect on the pressure distribution at the running gear-terrain interface. No direct comparison between the bulk density of the soil and the pressure distribution has been carried out, but intuitively as the bulk density increases the contact area will decrease,

changing shape and altering the pressure distribution. Due to the differences in ground conditions and power input between agricultural and civil engineering driving conditions the degree of wheel slip will vary. Krick (1969) showed this to have a marked effect on the tangential stress which increased as the slip increased. The normal stress decreased under similar conditions.

Notwithstanding these differences between the two fields of study the agricultural engineering research does indicate several important trends that can be used for the theoretical estimation of the rolling resistance of earthmoving plant. Firstly the maximum normal stress lies between 1.12 and 1.50 times the average normal stress on a firm to medium cohesive soil, depending on the stiffness. For the following analysis this was called the normal load constant, and as an initial estimate a value of 1.2 was used. Secondly the magnitude of the shear stress ranges between 60% and 70% of the maximum normal stress and occurs at a similar point on the circumference, slightly forward of the axle and near the centreline of the tyre. Maximum values are used in the analysis as every element of soil will, at some instant in time, be subjected to the maximum stress regime.

6.4 Caterpillar Relationship Between Rut Depth and Rolling Resistance

Caterpillar Incorporated developed equation 6.1 (Caterpillar, 1993), in the 1950's, relating rolling resistance to the weight of the vehicle and the degree of tyre penetration

$$Ro = (2\% \text{ of GVW}) + (0.6\% \text{ of GVW per cm tyre penetration}) \quad (6.1)$$

where Ro Rolling Resistance (kg)
GVW Gross Vehicle Weight (kg).

To express rolling resistance in percent equivalent grade, as is required by the various methods for determining operating speed of the plant, equation 6.1 must be divided by the gross vehicle weight. The tyre does not actually have to penetrate the soil for rolling resistance to increase above the minimum, if the road flexes under the wheel load, due to elastic recovery, then the effect is

similar, as the wheel must always be climbing out of an apparent rut. Only on very hard, smooth surfaces with a well compacted base will the rolling resistance approach the minimum. Inflation pressure and tread design are said to cause slight variations in rolling resistance. This effect is found to be minimal and does not significantly effect equation 6.1. This relationship between rolling resistance and tyre penetration was developed on a series of experiments carried out on a single scraper in the 1950's on prepared haul roads (Morgan, 1993). The data from these tests were not available for consultation. No information on the condition of the haul road, the range of rut depths investigated or the type of material trafficked was available. It could not therefore be ascertained whether equation 6.1 was valid for current vehicle specifications, or haul roads conditions in Britain. A linear equation is perhaps not what one would intuitively expect. Nevertheless the equation was used as an initial estimate for the rolling resistance of the soil, knowing the rut depth.

6.5 Spreadsheet Analysis

A spreadsheet was constructed for calculating the required shear strength to support a vehicle leaving a rut of specified depth. A typical spreadsheet is shown in figure 6.3.

6.5.1 Input Parameters

The analysis was simplified so that there were only four basic vehicle input parameters required to estimate the relationship between rut depth and shear strength of the soil. These are: vehicle weight, number of wheels, wheel width, and tyre diameter.

Three parameters pertaining to the tyre have not been included in the analysis: tyre pressure, carcass stiffness, and lug pattern. In the majority of earthmoving situations the tyre pressures will be kept constant for each individual type of plant. Typical inflation values on chalk for a Volvo A35 articulated dump truck are: 350kN/m^2 for the front tyres, and 500kN/m^2 for the rear. These high pressures, being much greater than the shear strength of the soil, tend to cause

the tyre to act more as a rigid wheel. It was therefore considered unnecessary to include tyre pressure as an input variable. The other two parameters, carcass stiffness and lug pattern are also similar for most types of earthmoving plant therefore should not have a significant effect on the analysis.

Three properties describing the interaction between the tyre and the soil are also required; these are: the normal load factor, Poisson's ratio, and the magnitude of the shear stress at the wheel-soil boundary with respect to the maximum applied normal load. These parameters are required to enable Mohr's circles of stress to be constructed, yielding an estimate of the undrained shear strength required to form a rut of a certain depth with the given loading conditions.

6.5.2 Contact Area

The initial step related rut depth to contact area. The theory was based on the geometry for a rigid wheel, as information on the deformation characteristics and contact area of a moving pneumatic tyre have not been researched fully, except for specific tyres of small diameters, (Sabey et al., 1967) and for tractor tyres, (Masuda et al., 1966). With high inflation pressures, as are encountered with earthmoving hauling vehicles, even if the ground is reasonably strong the tyre will act as a rigid wheel. From approximate measurements on site, where the ground conditions were reasonably firm, the contact area of a flexible stationary tyre is similar to that for a rigid wheel, figure 6.4, although the shape is completely different. Therefore, it was assumed for the purposes of this simple analysis that the contact area for a specific rut depth would equal that of a rigid wheel. For each vehicle fitted with a specific size of tyres a range of contact areas can be calculated by varying the rut depth.

The horizontal projection of contact area was assumed to be rectangular in shape. From a visual inspection of the tyre on the running surfaces this was approximately the case, and would definitely be true for a rigid wheel.

The column labelled rut depth in figure 6.3 relates to the height r.d. in figure 6.5, the measured rut depth after the passage of the vehicle, after any elastic

rebound. The rear angle is assumed to be 10° (Karafiath et al., 1978). The forward angle, ø, is calculated from the geometry of the rigid wheel, knowing the diameter of the tyre. The contact area, column 3, figure 6.3, is then a simple multiplication of the circumferential contact length and the wheel width. The tyre penetration, R.D. in figure 6.5, is required for the calculation of rolling resistance as per equation 6.1.

6.5.3 Shear Strength

The average normal static pressure was calculated simply by dividing the weight of the vehicle by the number of wheels and the contact area. For a loaded machine this assumption is acceptable, (VME 1989). The average static load was then multiplied by the normal load constant, initially 1.2, to arrive at the maximum normal load. Assuming a Poisson's ratio for the soil the confining pressure can be estimated. The Poisson's ratio was taken to be 0.45 as an initial estimate, as the soil was considered to be near incompressible. The shear stress on the soil at this point was taken to equal 65% of the maximum normal pressure or 78% of the average static normal pressure. Diagramatically, figure 6.6 shows an element of the soil in a fully loaded condition. From the known stresses Mohrs' circles of stress can be constructed, figure 6.7. The first circle is drawn for the static case with a σ_1 equal to unity and a σ_3 equal to 0.45 times the static normal stress. Applying the normal load constant of 1.2 yields the circle passing through $0.54\sigma_1$ and $1.2\sigma_1$. Then by introducing a shear stress equal to 78% of the static normal pressure, as described earlier, the large Mohrs circle can be drawn, from geometry the maximum value of the circle is $0.85\sigma_1$.

6.5.4 Rolling Resistance

The caterpillar rolling resistance, figure 6.3, is calculated using equation 6.1. The undrained shear strength is calculated using the relationships described in the previous section. The consistency index for this shear strength was calculated using the relationship derived from the multistage quick undrained triaxial tests, equation 6.2, as described in section 5.5.2.

$$c_u = 0.786 \exp(4.94\ I_c) \qquad (6.2)$$

A consistency index corresponding to the caterpillar rolling resistance can be estimated using the relationships determined from the site results, between rolling resistance and consistency index, section 5.6.6. Comparing the theoretical relationships between rolling resistance and consistency index with those derived from the caterpillar equation, figure 6.8 for a loaded Cat D400D articulated dump truck travelling downhill, it can be seen that the theoretical results indicate that apparent rolling resistance is more sensitive to changes in consistency index. The differences between the two lines was considered to be the inapplicability of the Caterpillar equation to modern day vehicles and British haul road conditions. It was therefore decided to amend the caterpillar equation, but to maintain the linearity of the equation.

6.5.5 Amending the Theory

Altering the equation relating rut depth to rolling resistance, column entitled "amended rolling resistance" in figure 6.3, changes the value of the site consistency index. The site consistency index is again calculated using the best fit equations derived in the previous chapter, relating apparent rolling resistance to consistency index for each vehicle in each driving condition. Then by plotting both experimental and theoretical consistency indices versus rolling resistances on the same graph and aligning the two series of data, figure 6.9, the amended rolling resistance - rut depth relationship is ascertained.

This process was carried out for all the vehicles travelling loaded and empty, uphill and downhill and the amended equations are given in table 6.1. It is clear from the results that the degree of tyre penetration does not significantly effect the rolling resistance until large deformations occur. The equations for the Volvo A25 vary considerably from that of the other vehicles. This can be related to the fact that the relationship between rolling resistance and consistency index did not contain a sufficient number of points, c.f. section 5.6.6.

6.6 Comparison of Theory with Measured Rut Depths

On site rut depths were recorded at four points along each section. This was carried out by placing a straight edge over the sides of the rut and measuring

with a steel tape to the base of the rut. This method of measuring rut depth does not take into account any tyre flexing or recovery of the soil and includes any material heaved up above the original surface, by displacement from the rut. An average rut depth for each section was calculated, the error in this average was assumed to be ±25mm.

Figure 6.10 (a-j) shows for the various vehicles the relationship between the measured rut depths, and both the Caterpillar equation, equation 6.1, and the amended equations, table 6.1, relating rut depth to rolling resistance. From figure 6.10, it can be seen that the Caterpillar equation is not a good estimator of apparent rolling resistance from rut depth values, but the amended equations give a reasonably good approximation to the apparent rolling resistance of the driver-vehicle-terrain system. The linearity of the relationship between rut depth and rolling resistance is questionable, but as the trend in the actual data is scattered it was considered unnecessary to try to refine the estimation.

6.7 Comparison Between Rut Depth and Consistency Index

On site it may have been expected that there would be a distinct relationship between the depth of rut and consistency index along a particular section of haul road. Figure 6.11 (a-e) illustrates the site results, both for uphill and downhill grades, along with the theoretical estimation for a loaded machine, using the parameters given in table 6.2. Figure 6.11 (e) includes error bars for both the rut depth and consistency index. The error for the average rut depth was taken as ±25mm and for consistency index as ±1% on three parameters: liquid limit, plastic limit, and moisture content. These graphs clearly show that there is no distinctive trend in the measured data, except perhaps, that as the consistency index decreases the rut depth generally increases. This holds for both the uphill and downhill grades. In the majority of cases the rut depths associated with the downhill grades are lower than those for the uphill grades at a similar value of consistency index, this may be caused by the vehicle driving more into the haul road when travelling uphill, causing larger ruts. The theoretical curves approximate to the measured data reasonably well in the majority of cases, considering the errors in the measurement of rut depth. Unfortunately, in several cases, there was an insufficient number of data points

to draw any firm conclusions as to the applicability of the theory. Previous work (Staples et al., 1992, and Parsons et al., 1982), relating rut depth to soil properties have also resulted in large variations in the reported results.

6.8 Sensitivity Analysis

A sensitivity analysis was carried out using the developed theory to investigate which of the input parameters had the greatest effect on the output rolling resistance.

6.8.1 Introduction

The sensitivity analysis was carried out using the parameters for a loaded Caterpillar D400D articulated dump truck. The initial input values, as in table 6.3, were varied to give an upper and lower bound for each input parameter. The method used to carry out the sensitivity analysis was a factorial design, which allows the inspection of interactive effects between parameters as well as the main variables themselves.

In performing a factorial design, a set number of levels for each parameter are chosen and experimental runs for all combinations are carried out. The simplest form is a 2^k factorial study where only two levels for each factor are calculated, this method was used in the following analysis.

6.8.2 2^k Factorial Design

This method considers all factors, at two levels, which influence the response of a function. The method is more fully explained in Law et al. (1991) and Montgomery (1991). The factorial design requires that two levels for each factor are chosen, and the responses calculated at each of the 2^k possible of factor-level combinations, called design points. Each of the two factor levels are designated using either plus and minus, or 1 and 0 notation. A design matrix is then constructed, as in figure 6.12, showing all possible design points

for a 2^4 factorial design. The more logical the layout of factor levels the easier the calculation of the factor effects and interactions.

The main effect of a factor is the average change in a response due to moving a factor from its lower to upper level while maintaining all other factors constant. This average is taken for all combinations of other factors in the design. For the 2^4 factorial design in figure 6.12, the main effect of factor 1 is therefore:

$$e_1 = \frac{(R_2 - R_1) + (R_4 - R_3) + \ldots + (R_{16} - R_{15})}{8} \tag{6.3}$$

where: e_1 - average effect of factor 1

R_n - response at design point n

Note that at design points one and two, factors 2, 3, and 4 remain fixed, as they do at design points 3 and 4, 5 and 6, etc. The other main effects can be calculated in a similar way ensuring that the other factors remain constant.

By comparison with the design matrix, it can be seen that the main effects can be computed by performing the dot product between the factor matrix and the response matrix, and dividing by 2^{k-1}, which for the 2^4 factorial design is 8.

Interaction effects can be determined in a similar way. For the interaction between factors 1 and 2, each respective entry in the two desired factor matrices would be multiplied together and the resulting matrix would then be used in the dot product with the response matrix. The order of multiplying the factor matrices does not alter the interactive effect, i.e. $e_{12} = e_{21}$. Again this form of calculation is best completed using a spreadsheet.

6.8.3 Effect on Rolling Resistance Using 2^k Factorial design

There are seven input parameters needed to calculate the rolling resistance using the spreadsheet in figure 6.3: vehicle mass, wheel diameter, wheel width, number of wheels, normal load constant, Poisson's ratio, and the tangential to

maximum normal stress ratio. This can be immediately reduced to six factors as the number of wheels will hopefully remain constant. These factors are all assumed to lie within a certain range. For the case of a loaded Cat D400D the upper and lower bounds are given in table 6.3. The parameters pertaining to the vehicle: mass, tyre diameter, and tyre width, all vary over a large range, especially the vehicle mass, which is assumed to range from 50% to full payload. The parameters relating to the soil: normal load constant, Poisson's ratio, and the ratio of tangential to maximum normal stress were the most difficult limits to define, because little research work has been carried out on their evaluation. With six input factors the rolling resistance has to be determined 64 times. To reduce the time consuming determination of calculating the rolling resistance, all the wheel parameters were combined together leaving only four factors, hence only 16 rolling resistance determinations were initially required.

Figure 6.13 shows the design matrix for a 2^4 factorial design on the effect of rolling resistance, the -1 and +1 relate to the lower and upper bounds respectively. There are sixteen design points representing every possible combination of upper and lower bound for the four input parameters. These four effects are: the normal load constant, Poisson's ratio, the ratio of tangential to maximum normal stress, and a wheel constant. The wheel constant combines three effects: the loaded mass of the vehicle, the wheel diameter, and the tyre width. The input upper and lower bounds for each of these effects can be seen in table 6.3. The formula relating rolling resistance to rut depth was then calculated at each design point. For the purpose of the analysis a definite response, rather than a formula, was needed, therefore the rolling resistance was calculated for an arbitrary tyre penetration of 100mm. This value was not critical as the relationship between rolling resistance and rut depth was assumed to be linear. The response matrix for rolling resistance is shown alongside the design matrix in figure 6.13.

Figure 6.14 plots the response against each design point. The plot shows consistently one high point and then one low point. Considering the design matrix in figure 6.13, it can be seen that this pattern follows the changes of factor 1, the wheel constant. This tends to show that an increase in the wheel constant results in a decrease in the rolling resistance. Similarly, the next eight

design points are lower than the first eight. This relates to factor 4, the ratio of tangential to maximum normal stress. These observations are valuable and the effects should be quantified.

The average effect of moving from the lower to upper bound for each design factor was calculated as described above; by performing the dot product of the appropriate factor matrix and the response function. These results are also shown in figure 6.13, alongside the response matrix. The notation for each effect and combination of effects is: prefix "e" for effect, followed by the factor number(s). Figure 6.15 shows the average main and combined effects on the response charted with the effect number. From this it can be concluded that the wheel constant has the greatest overall average effect on rolling resistance, closely followed by the ratio of tangential to maximum normal stress and normal load constant. The Poisson's ratio, as well as all of the interaction effects had very little influence on the average rolling resistance. Since the wheel constant showed the greatest effect on the average rolling resistance, a further 2^3 factorial design exercise was carried out on the parameters making up the wheel constant.

The input bounds for the mass, diameter, and width are shown above the design matrix in figure 6.16. The other input factors, normal load constant, Poisson's ratio and the ratio of tangential to maximum normal stress were all held constant at the base values of 1.2, 0.45, and 0.65 respectively. Figure 6.16 also shows the rolling resistance response matrix at a rut depth of 100mm, as well as the average main effects and interactive effects. Figure 6.17 depicts the response function in terms of each design point. From inspection it would appear that factor 1, vehicle mass, was having the greatest effect on rolling resistance as the values are alternating high and low. This is confirmed by figure 6.18 showing the average effect on rolling resistance by the main and combination effects, by increasing each factor from the lower to higher bound. The interactive effects are again causing very little effect on the rolling resistance response.

These results may not be as expected in that, as the ground pressure increases, e.g. the vehicle mass increases, the rolling resistance decreases. The reasons for this can best be explained through an example. It must first be remembered,

that the equation relating tyre penetration and rolling resistance is determined through the use of the site relationship between consistency index and apparent rolling resistance. It has been assumed that this equation will not alter although the input parameters have changed.

Consider the simplest case, where all the input parameters remain constant apart from the vehicle mass. By using the spreadsheet in figure 6.3 the corresponding equations relating rolling resistance, rut depth, and consistency index were calculated for a loaded Caterpillar D400D articulated dump truck. The loaded masses were 46,000kg and 64,300kg, this corresponds to 50% and full payload respectively. Again these are extreme figures, as it would be uneconomical to perpetually run the vehicles in the former case, and full payload is never actually achieved on site as the load is generally limited by the volume of the truck rather than the mass of the material. Assuming a normal density for a hauling material, approximately 1700kg/m^3, the former case would result in the vehicle running at approximately three quarters volume capacity.

From figure 6.19, showing the relationship between rolling resistance and rut depth, it can be seen that the two equations have similar gradients, but the intercept varies by under 1%, which is almost insignificant in terms of velocity. The heavier machine has the lower rolling resistance which is contrary to what one would expect.

From inspection of figure 6.20 relating consistency index to rut depth, it can be seen that to achieve a rut of constant depth for both loaded conditions the consistency index must be greater, the material stronger, for the heavier vehicle, as would be expected.

The consistency index is related to rolling resistance as shown in figure 6.21. The site consistency index line is a constant, as can be seen, and the theoretical curve is forced to mimic this line, yielding the equation relating rut depth to rolling resistance. The matching of the theoretical results to the site results may not be a valid technique, as the linear relationship between rolling resistance and consistency index will probably change in the field if the vehicle is operating under a different set of working conditions. However the variation in

rolling resistance versus rut depth, figure 6.19, for a loaded Cat D400D travelling downhill, are comparatively minimal compared with the site spread of data, figure 6.10 (b). The theoretical curves do still approximate reasonably well to the site results, and the discrepancies are caused by natural variation in the system.

6.9 Summary

The above sections contain a brief review of the work carried out on the pressure distribution at a pneumatic tyre - soil boundary. It is clear that most of the research has been carried out by agricultural engineers. The result has been that research workers were not involved with the civil engineering aspects of soil mechanics. Hence the approach to soil-tyre interaction has lacked a detailed documentation of soil properties.

Previously developed formulae relating rut depth to rolling resistance have been shown to be inadequate to deal with British conditions for off-road hauling. The newly developed theory, differing from the previous methods, relating rut depth to rolling resistance and consistency index has been shown to match the site observation data well. Practically, the developed formula enables the engineer, knowing the relationship between undrained shear strength and consistency index and the parameters pertaining to the hauling vehicles, to estimate the maximum rut depths that will be encountered during the duration of a contract and therefore the degree of haul road maintenance that is likely to be required. Knowing the rut depth likely to be encountered on the haul road the value can be used in the regression equations developed in chapter 5.

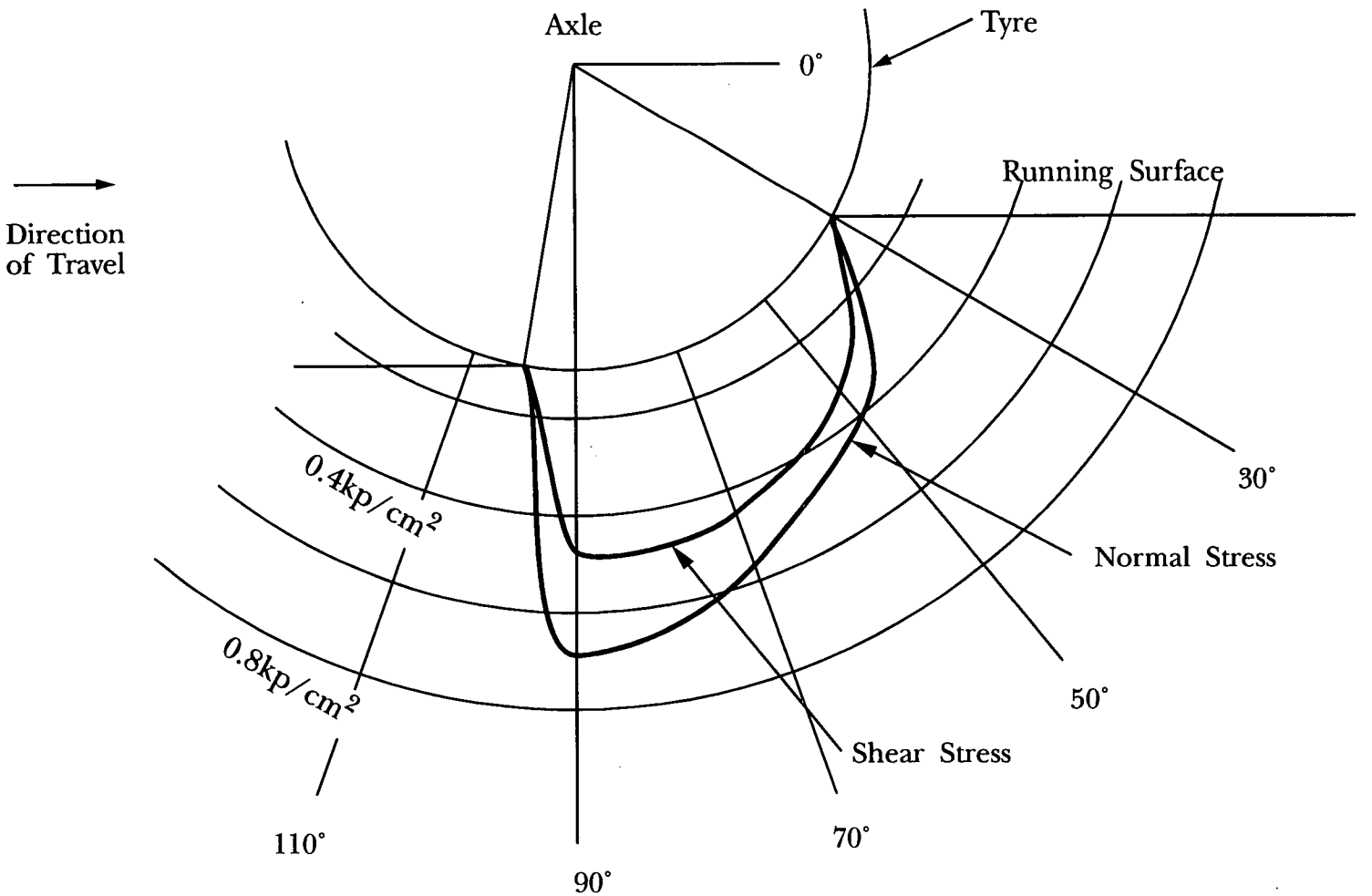

Figure 6.1: Normal and Shear Stress Distribution Under a Test Tyre with 40% Slip, Wheel Load 5345N (545kp), near the centreline of the tyre, Tyre Deflection not Shown, after Krick 1969

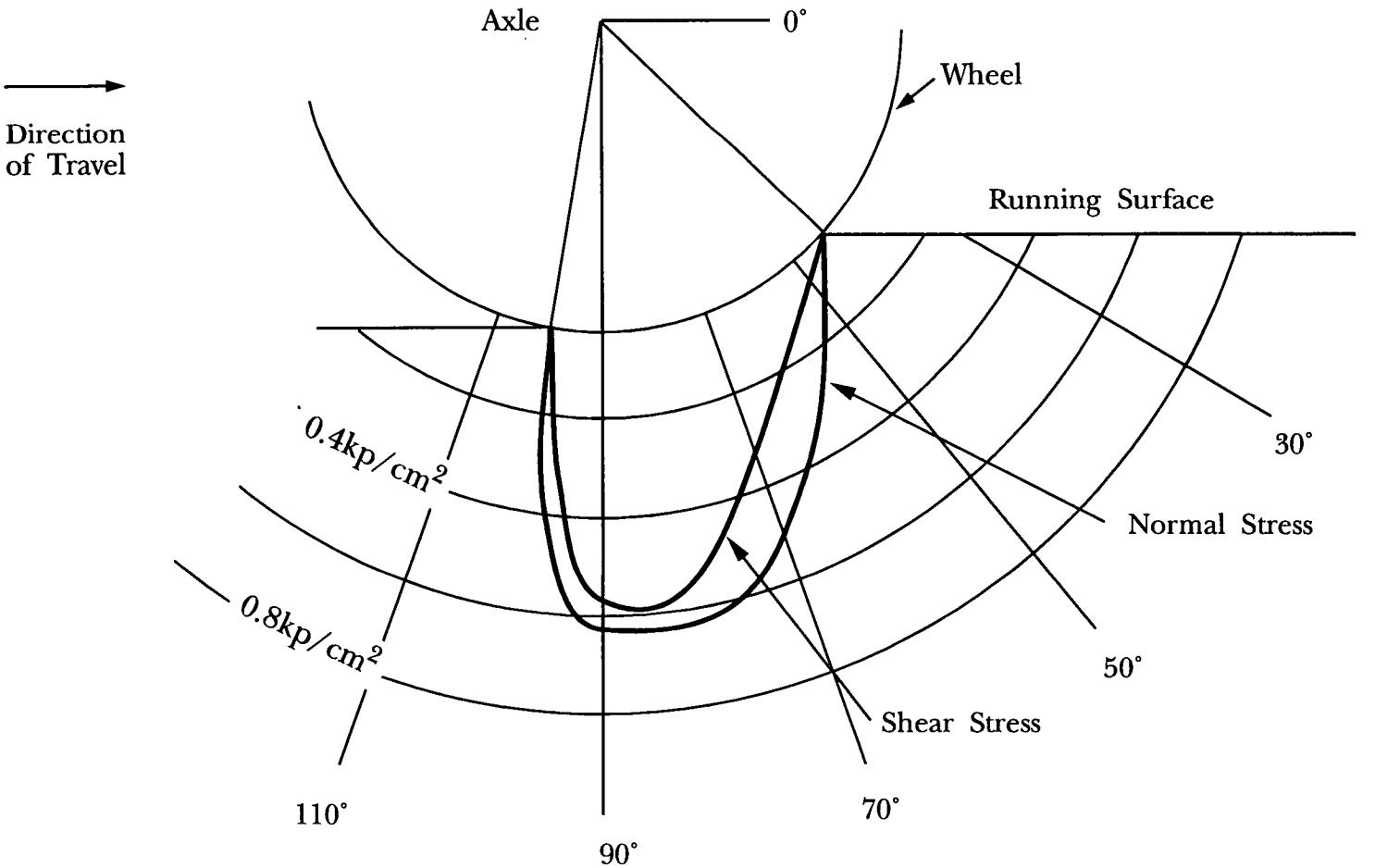

Figure 6.2: Normal and Shear Stress Distribution Under Rigid Wheel with 40% Slip, Wheel Load 4610N (470kp), near the centreline of the wheel, after Krick 1969

Vehicle Type	Cat D400D
Loaded/Empty	Loaded
Vehicle Weight (kg)	55232
Wheel Diameter (m)	1.86
No. of Wheels	6
Wheel Width (m)	0.66

Normal Load Factor	1.2
Poissons Ratio	0.45
Shear/max. normal stress	0.65

Rut Depth / mm	ø / rad	Contact Area per Wheel / m ^{2}	Tyre Penetration / mm	Shear Strength Required / kN/m ^{2}	Caterpillar Rolling Resistance / %	Ic Theory	Amended Rolling Resistance / %	Ic Site
2	0.19	0.22	16	345.1	3.0	1.23	5.9	1.20
5	0.20	0.23	19	329.9	3.1	1.22	5.9	1.20
15	0.25	0.26	29	292.9	3.7	1.20	6.0	1.19
25	0.29	0.29	39	267.6	4.3	1.18	6.0	1.19
50	0.37	0.34	64	227.4	5.8	1.15	6.2	1.17
75	0.44	0.38	89	202.3	7.3	1.12	6.3	1.16
100	0.50	0.41	114	184.6	8.8	1.11	6.4	1.14
125	0.55	0.45	139	171.0	10.3	1.09	6.6	1.13
150	0.60	0.48	164	160.2	11.8	1.08	6.7	1.11
200	0.69	0.53	214	143.7	14.8	1.05	7.0	1.09
250	0.77	0.58	264	131.5	17.8	1.04	7.3	1.06
300	0.85	0.63	314	122.0	20.8	1.02	7.5	1.03
350	0.92	0.67	364	114.2	23.8	1.01	7.8	1.00
400	0.98	0.71	414	107.7	26.8	1.00	8.1	0.97

Figure 6.3 Theoretical Determination of the Relationship Between Rut Depth, Rolling Resistance, and Consistency Index.

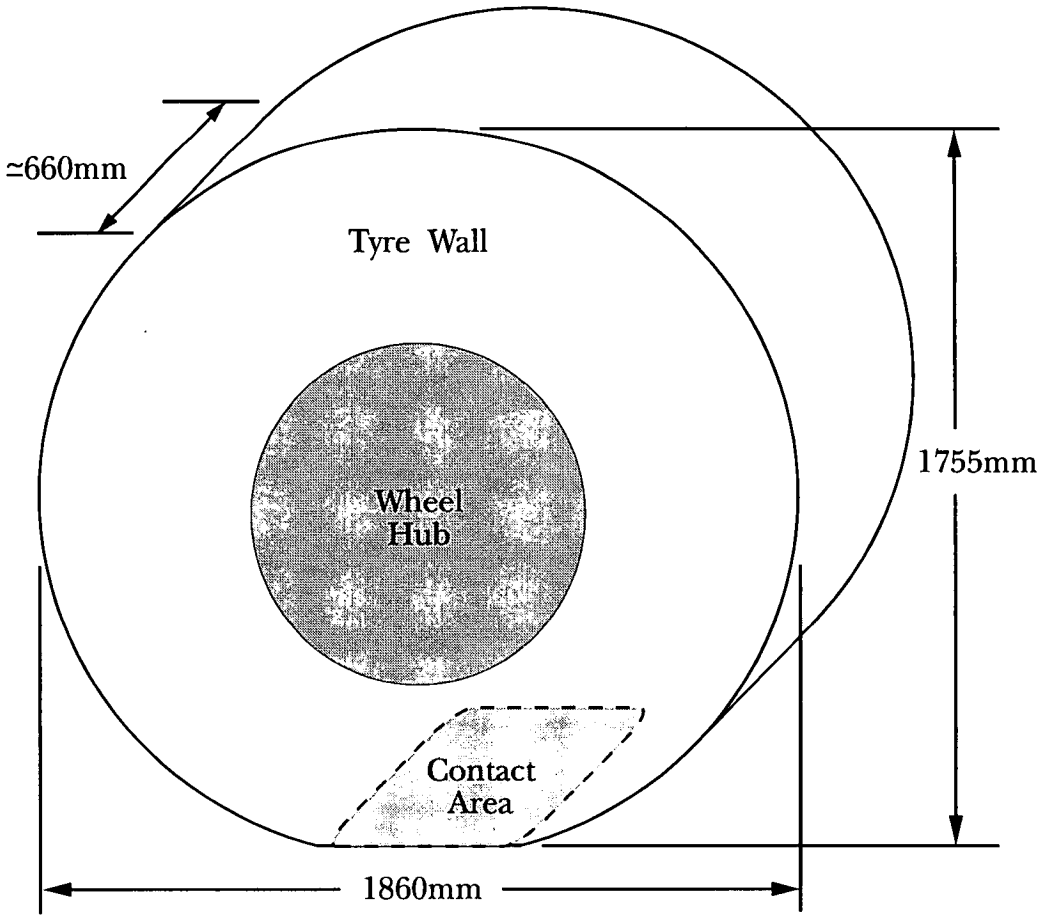

Site Measured Contact Area = $0.33m^2$
Contact Area Assuming Rigid Wheel = $0.34m^2$

Figure 6.4: Tyre Deflection of a Loaded Cat D400D Articulated Dump Truck

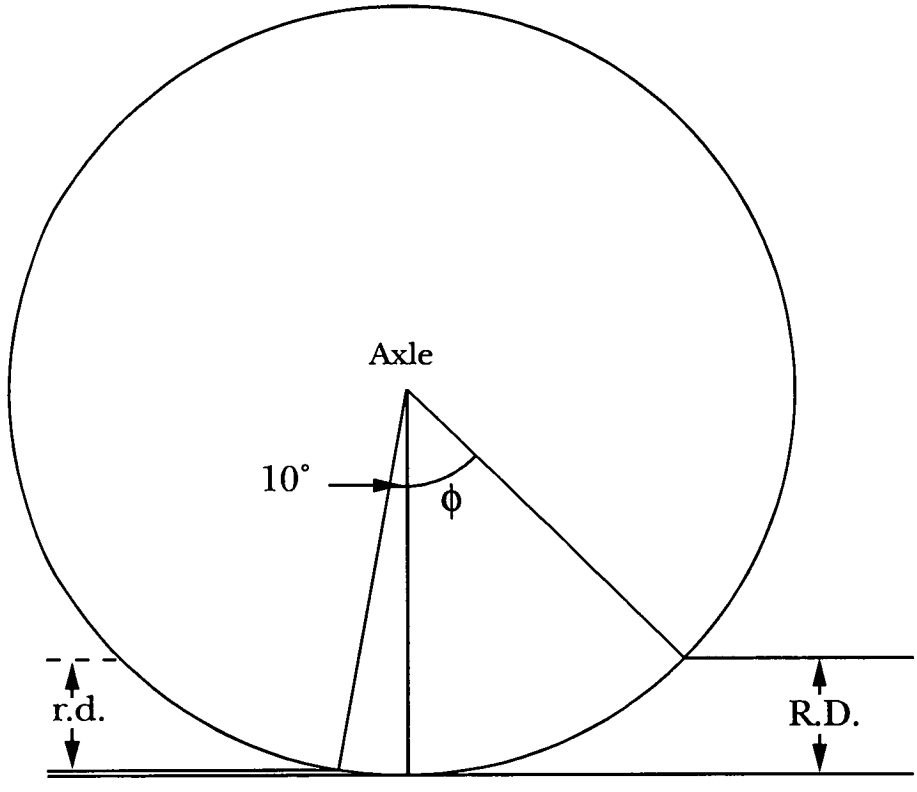

Figure 6.5: Geometry of Wheel

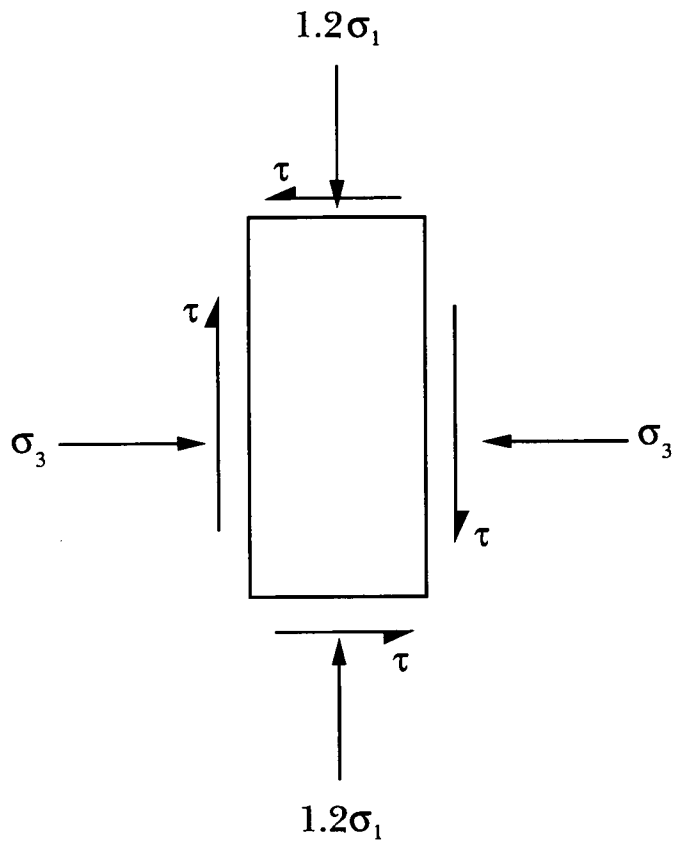

σ_1 = normal stress due to static load

σ_3 = lateral stress = 0.45 $(1.2\sigma_1)$ = $0.54\sigma_1$

τ = shear stress = 0.65 $(1.2\sigma_1)$ = $0.78\sigma_1$

Figure 6.6: Stressed Soil Element at the Tyre-Soil Interface

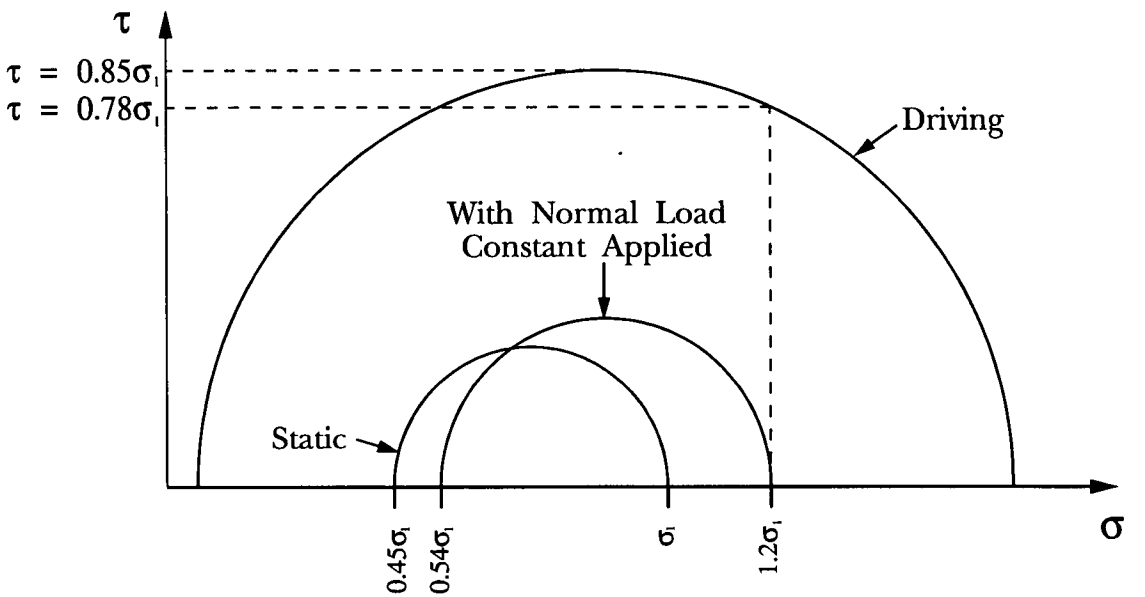

Figure 6.7: Mohr Circle of Stress for the Soil Element in Figure 6.6

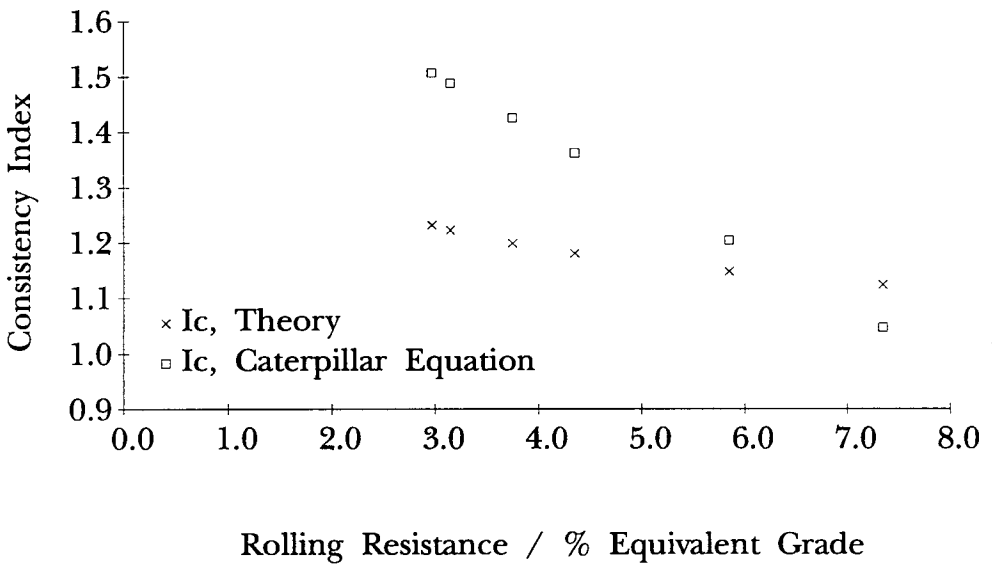

Figure 6.8: Comparison of the Theoretical Relationship Between Consistency Index and Rolling Resistance with the Caterpillar Equation, for a Loaded Cat D400D Dump Truck, Travelling Downhill

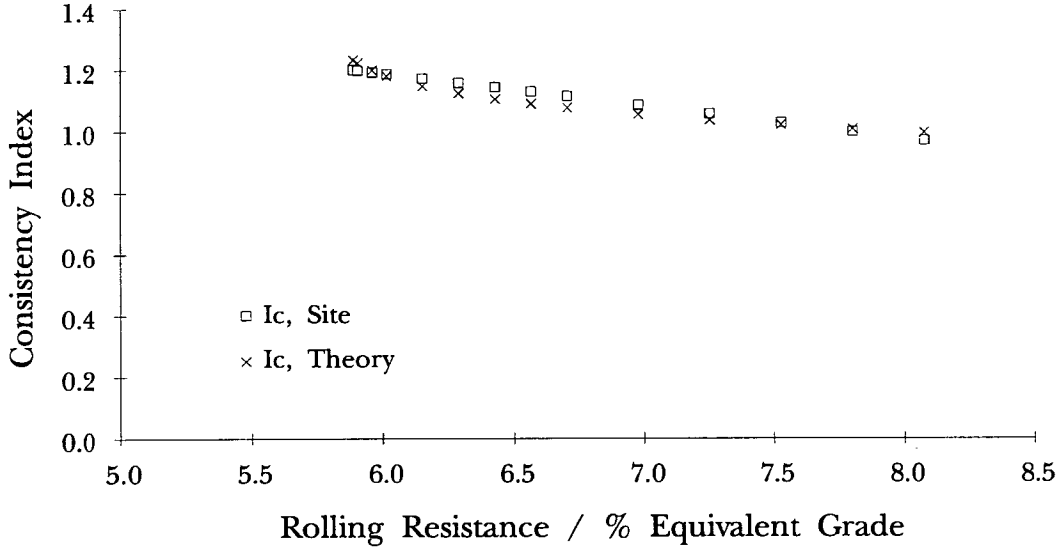

Figure 6.9: Aligning the Theoretic Graph of Consistency Index versus Rolling Resistance with the Experimental Equation, for a Loaded Cat D400D Travelling Downhill

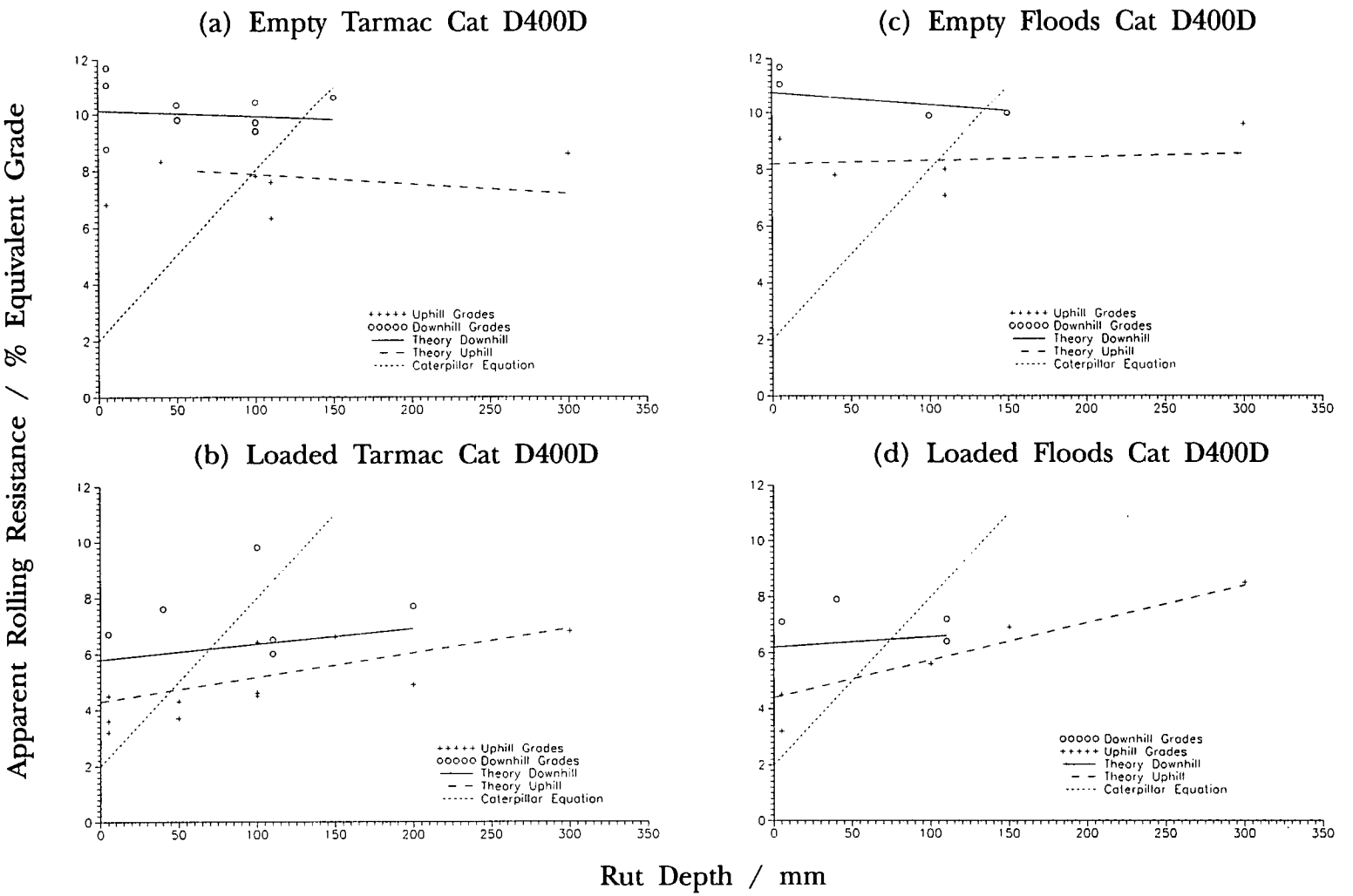

Figure 6.10 (a-d): Apparent Rolling Resistance versus Rut Depth Comparing Theory with Site Measurements

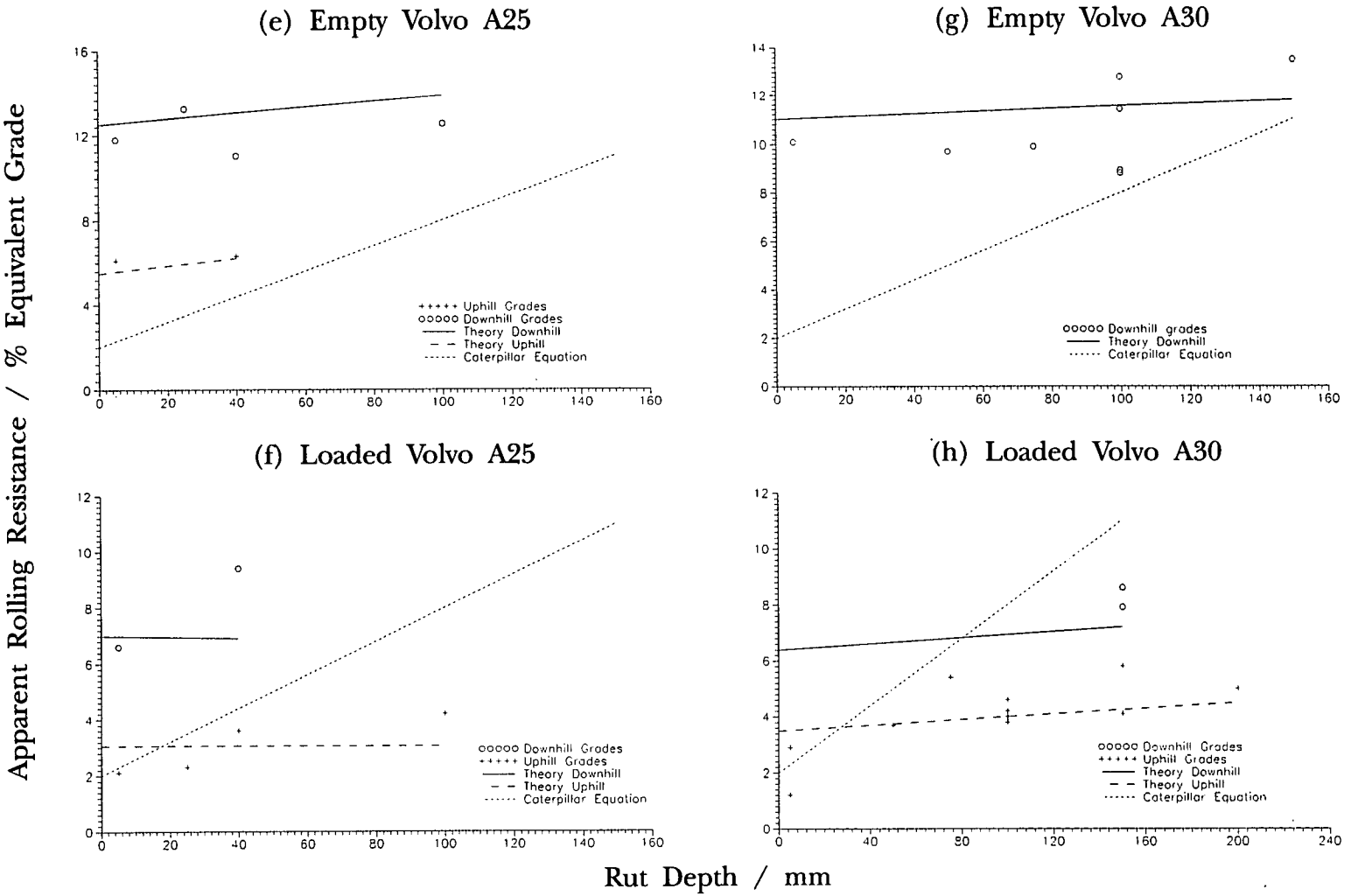

Figure 6.10 (e-h): Apparent Rolling Resistance versus Rut Depth Comparing Theory with Site Measurements

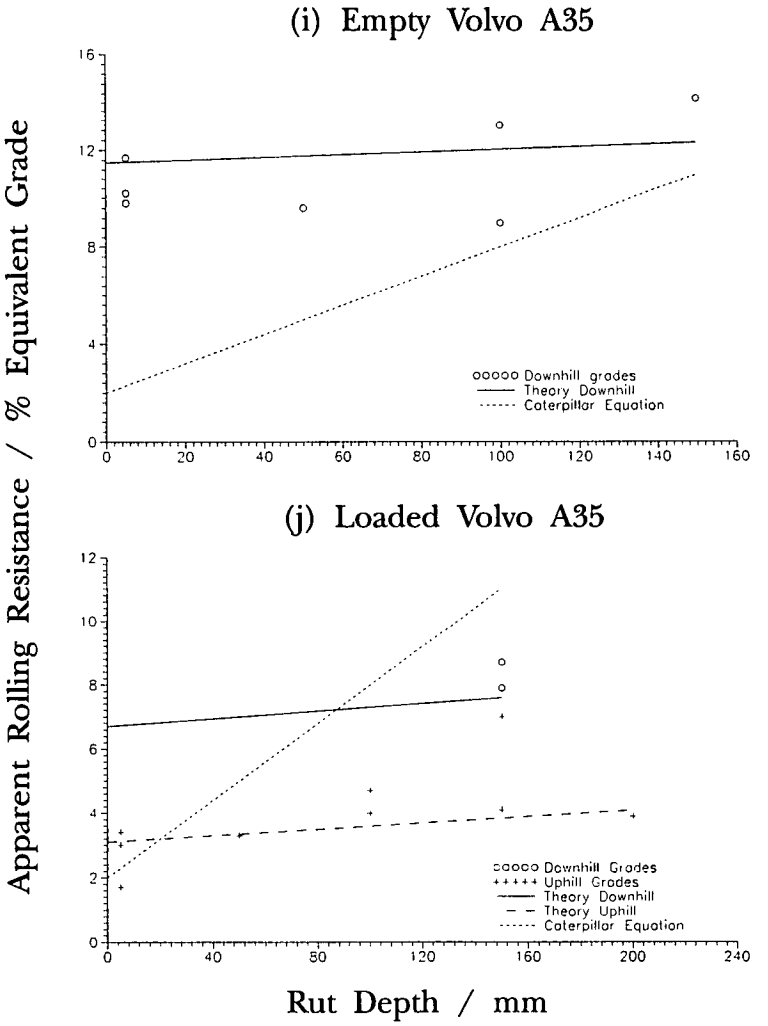

Figure 6.10 (i-j): Apparent Rolling Resistance versus Rut Depth Comparing Theory with Site Measurements

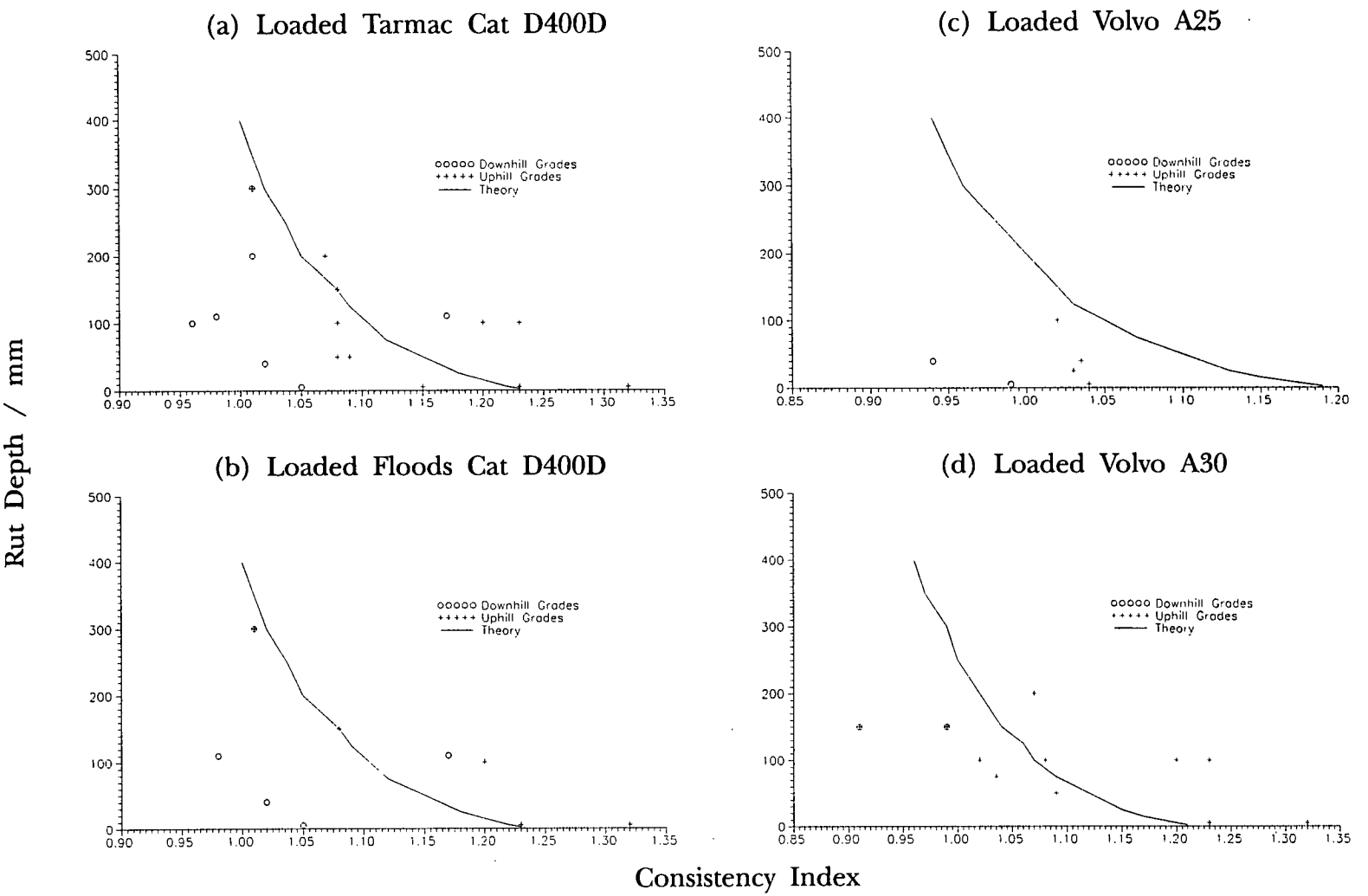

Figure 6.11 (a-d): Rut Depth versus Consistency Index Comparing Theory with Site Results

(e) Loaded Volvo A35

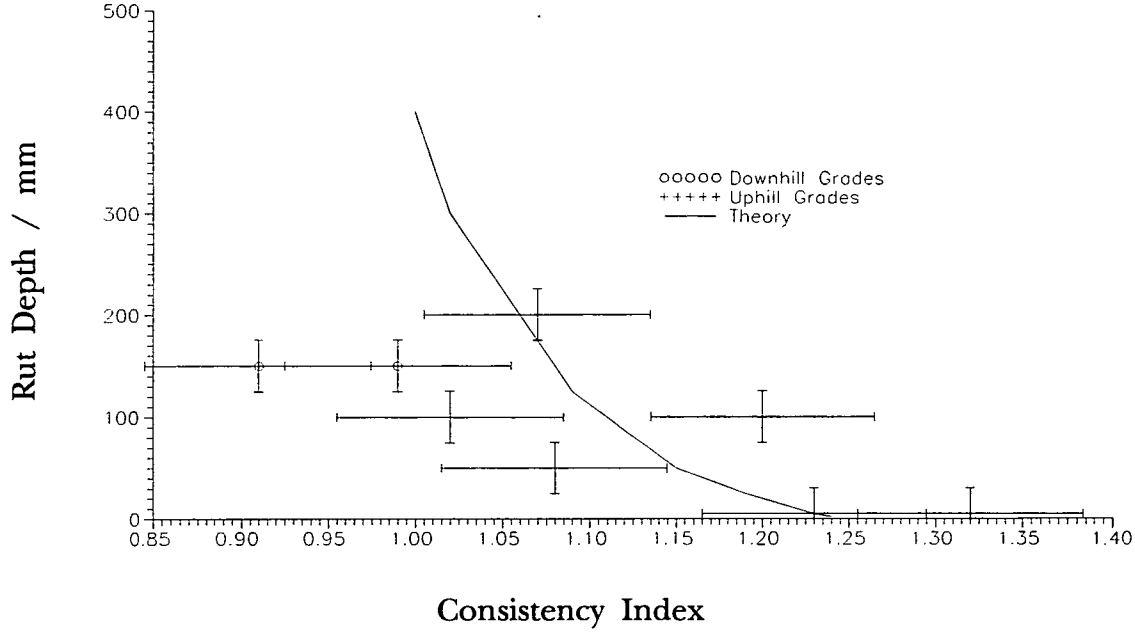

Figure 6.11 (e): Rut Depth versus Consistency Index
Comparing Theory with Site Results

Design Point	Factor 1	Factor 2	Factor 3	Factor 4	Response
1	0	0	0	0	R_1
2	1	0	0	0	R_2
3	0	1	0	0	R_3
4	1	1	0	0	R_4
5	0	0	1	0	R_5
6	1	0	1	0	R_6
7	0	1	1	0	R_7
8	1	1	1	0	R_8
9	0	0	0	1	R_9
10	1	0	0	1	R_{10}
11	0	1	0	1	R_{11}
12	1	1	0	1	R_{12}
13	0	0	1	1	R_{13}
14	1	0	1	1	R_{14}
15	0	1	1	1	R_{15}
16	1	1	1	1	R_{16}

Figure 6.12: Design Matrix for a 2^4 Factorial Design

Input Parameters

Levels	Wheel Constant		Normal Load Constant	Poisson's Ratio	Tangential / Max Normal Stress
- (Lower)	mass diameter width	46000kg 1.95m 0.75m	1	0.5	0.4
+ (Upper)	mass diameter width	64300kg 1.7m 0.6m	1.5	0.4	0.9

Design Matrix **Response**

Design Point	Wheel Constant Factor 1	Normal Load Constant Factor 2	Poisson's Ratio Factor 3	Tang./ Max Norm Stress Factor 4	Rolling Resistance at 100mm Rut / %
1	-1	-1	-1	-1	8.05
2	1	-1	-1	-1	6.98
3	-1	1	-1	-1	7.35
4	1	1	-1	-1	6.18
5	-1	-1	1	-1	7.95
6	1	-1	1	-1	6.88
7	-1	1	1	-1	7.25
8	1	1	1	-1	6.05
9	-1	-1	-1	1	7.15
10	1	-1	-1	1	5.98
11	-1	1	-1	1	6.45
12	1	1	-1	1	5.28
13	-1	-1	1	1	7.15
14	1	-1	1	1	5.88
15	-1	1	1	1	6.35
16	1	1	1	1	5.18

Effect no.	Effect on Average Rolling Resistance / %
e1	-1.16
e2	-0.74
e3	-0.09
e4	-0.91
e12	-0.02
e13	-0.02
e14	-0.03
e23	-0.02
e24	0.02
e34	0.02
e123	0.01
e124	0.04
e134	-0.01
e234	-0.01
e1234	0.02

Figure 6.13 Input Parameters, Design Matrix, Response, and Effects for the Four Factorial Design

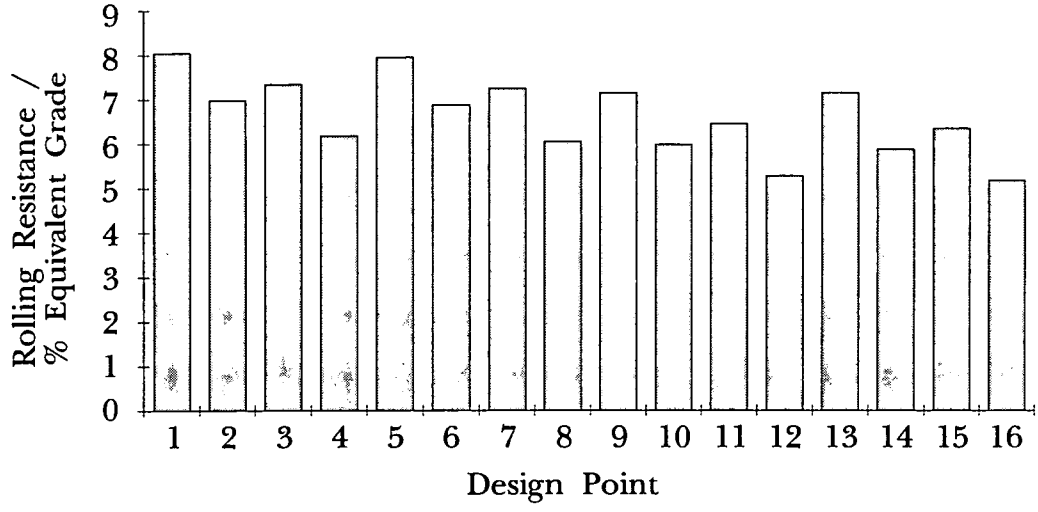

Figure 6.14: Rolling Resistance versus Design Point for 2^4 Factorial Design

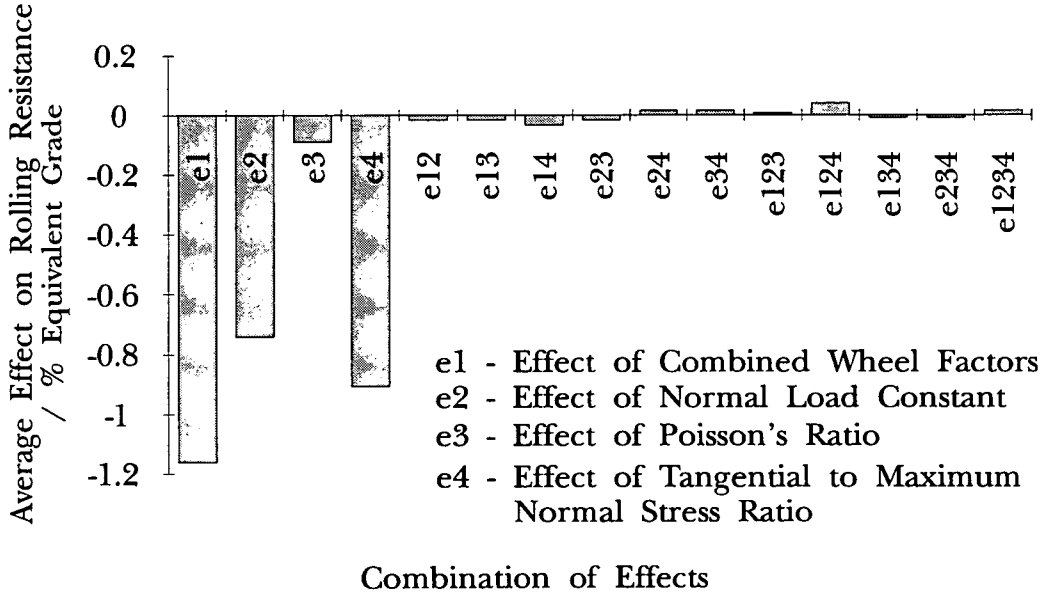

Figure 6.15: Average Effect on Rolling Resistance by Main and Interaction Effects for 2^4 Factorial Design

Input Parameters

Levels	Mass / kg	Diameter / m	Width /m
- (Lower)	46000	1.95	0.75
+ (Upper)	64300	1.7	0.6

	Design Matrix			Response
Design Point	Factor 1 Mass	Factor 2 Diameter	Factor 3 Width	Rolling Resistance at 100mm rut / %
1	-1	-1	-1	7.15
2	1	-1	-1	6.45
3	-1	1	-1	6.88
4	1	1	-1	6.28
5	-1	-1	1	6.65
6	1	-1	1	6.05
7	-1	1	1	6.48
8	1	1	1	5.78

Effect no.	Effect on Average Rolling Resistance / %
e1	-0.65
e2	-0.22
e3	-0.45
e12	0.00
e13	0.00
e23	0.00
e123	-0.05

Figure 6.16 Input Parameters, Design Matrix, Response, and Effects for the Three Factorial Design

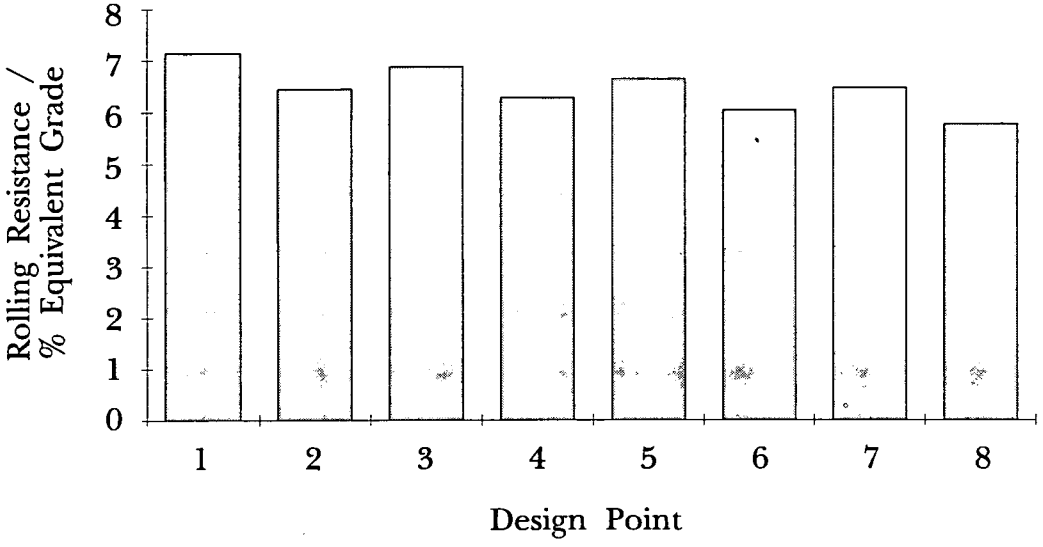

Figure 6.17: Rolling Resistance versus Design Point
For 2^3 Factorial Design

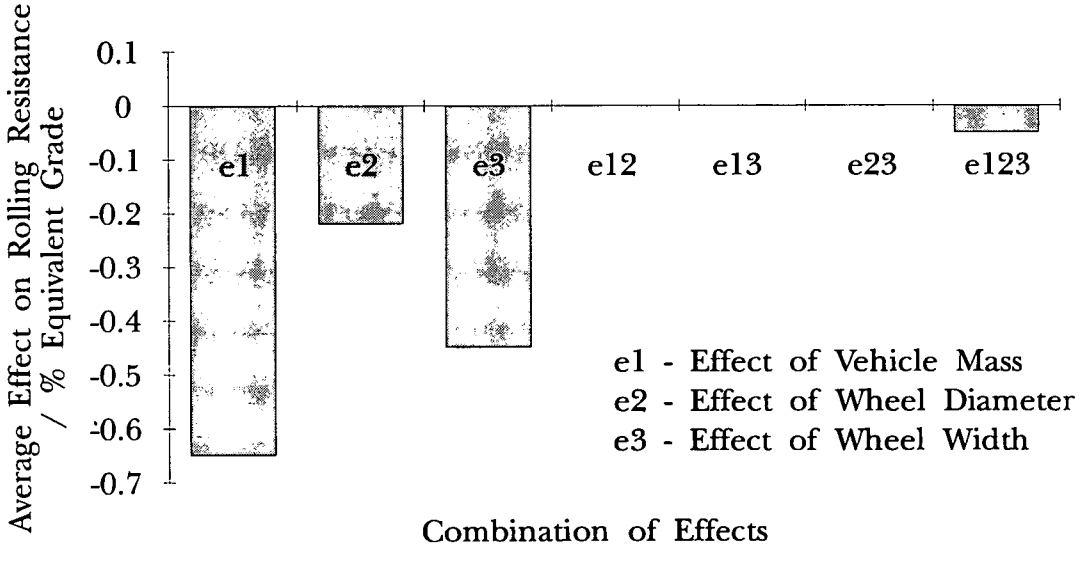

Figure 6.18: Average Effect on Rolling Resistance by Main and Interaction Effects
For 2^3 Factorial Design

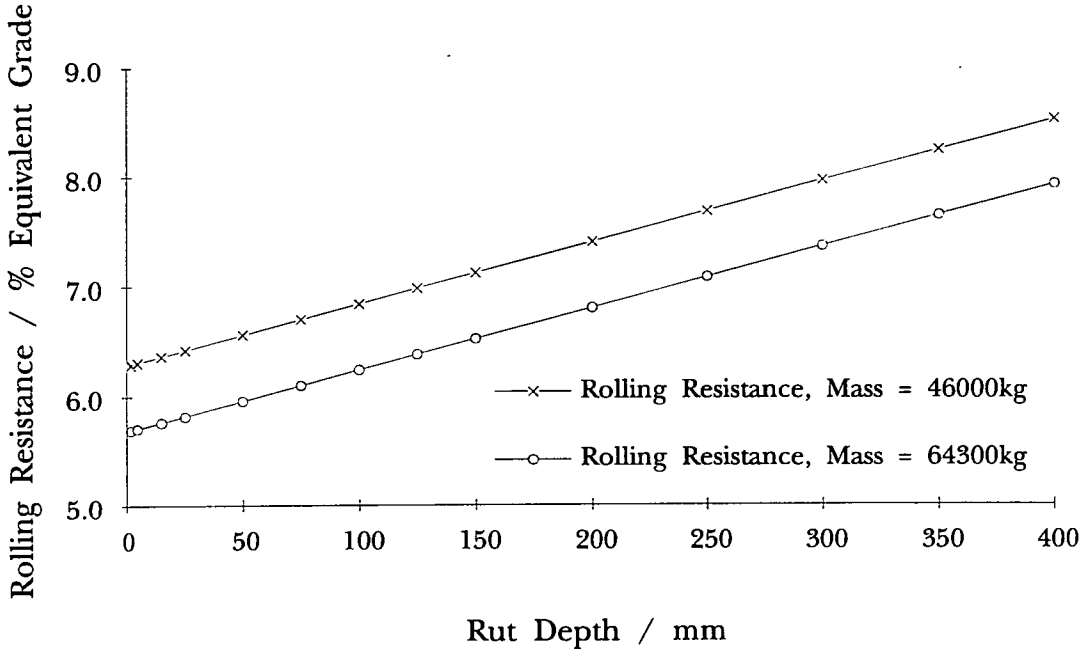

Figure 6.19: Rolling Resistance versus Rut Depth from Theory

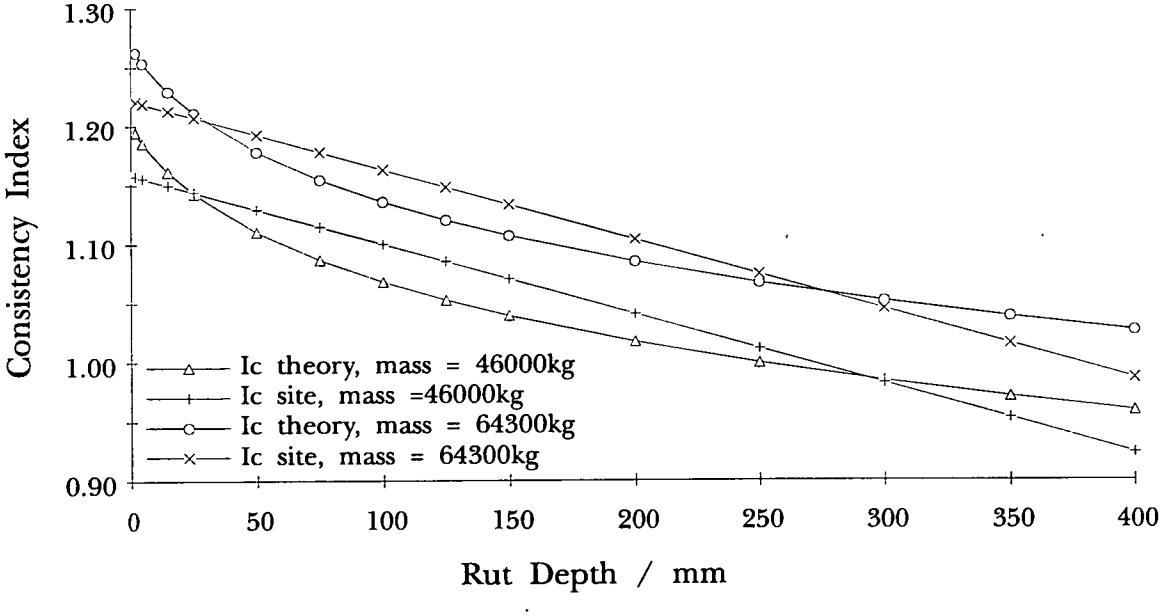

Figure 6.20: Consistency Index versus Rut Depth from Theory

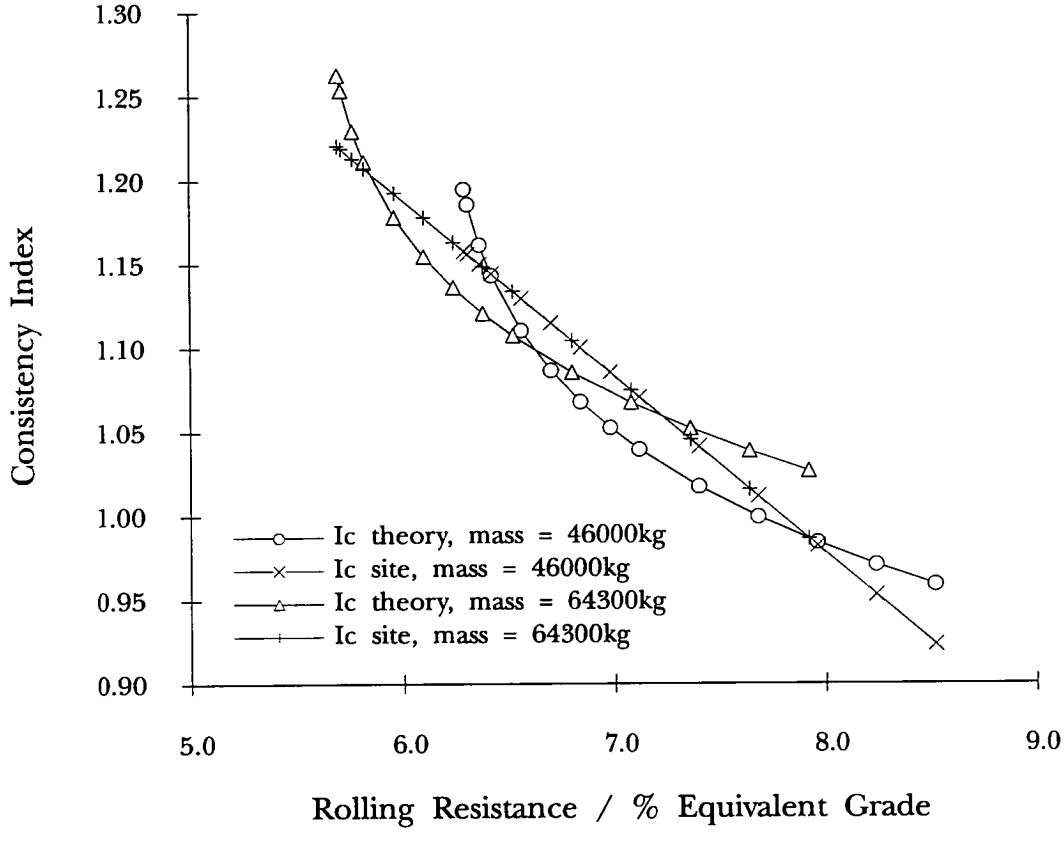

Figure 6.21: Consistency Index versus Rolling Resistance from Theory

Apparent Rolling Resistance in Terms of Tyre Penetration, (TP) / cm.

	Loaded		Empty	
	Downhill	Uphill	Downhill	Uphill
Tarmac Cat D400D	5.8 + 0.055TP	4.3 + 0.042TP	10.1 - 0.021TP	8.2 - 0.033TP
Floods Cat D400D	6.2 + 0.035TP	5.4 + 0.100TP	10.8 - 0.044TP	8.2 + 0.013TP
Volvo A25	7.0 - 0.0105TP	3.06 + 0.0005TP	12.5 + 0.130TP	5.5 + 0.180TP
Volvo A30	6.4 + 0.055TP	3.5 + 0.050TP	11.0 + 0.050TP	-
Volvo A35	6.7 + 0.060TP	3.1 + 0.050TP	11.5 + 0.055TP	-

Table 6.1: Amended Rut Depth, Rolling Resistance Equations for Various Vehicles

	Cat D400D	Volvo A25	Volvo A30	Volvo A35
Loaded Mass / kg	55232	33775	40250	48400
Empty Mass / kg	28000	16900	20000	24400
Wheel Diameter / m	1.86	1.50	1.50	1.68
Number of Wheels	6	6	6	6
Contact Width / m	0.66	0.61	0.65	0.61

Table 6.2: Input Vehicle Parameters for Spreadsheet, Figure 5.3

Factor Description	Lower Bounds	Upper Bounds	Standard Levels
Vehicle Mass /kg	46000	64300	55232
Wheel Diameter / m	1.95	1.70	1.86
Wheel Width / m	0.75	0.60	0.66
Normal Load Constant	1.0	1.5	1.2
Poisson's Ratio	0.50	0.40	0.45
Tangential to Maximum Normal Stress Ratio	0.40	0.90	0.65

Table 6.3: Upper and Lower Bounds for Sensitivity Analysis as well as Standard Values for a Loaded Cat D400D Articulated Dump Truck.

Chapter 7 Investigation Into the Effect of Pore Water Pressure Increase

7.1 Introduction

Whilst monitoring the plant on site it was observed that the condition of the haul road deteriorated as the operation progressed through the morning, but the condition stayed relatively constant throughout the latter part of the day. The quality of the haul roads were maintained by a grader. The effect of grading the haul road had no long term effect on the quality of the haul roads and rutting fully reappeared after subsequent passes. It was considered that with the continual passage of the plant, the pore water pressure was increasing, decreasing the effective stress, thus effectively weakening the material. One explanation for the ruts not increasing throughout the day is that the pore water pressure would reach a steady value, where the pore water pressure dissipation between vehicle passes would match the increase after each pass.

In order to investigate this hypothesis it was decided to cyclically load a confined sample of soil and monitor the pore water pressure at a depth below the surface. Three tests were carried out on fully saturated, normally consolidated, cohesive samples at different moisture contents. Skempton's pore water pressure parameters (Skempton, 1954) were omitted because for a saturated soil $B=1$ and for the condition of zero lateral strain $A \rightarrow 1$. Any errors in this assumption would be expected to be small compared to the rise in pore water pressure.

It should be noted that the rise in pore water pressure may not be the only possible mechanism for increased rutting, others include: large plastic strains leading to a remoulding of the material, high shear stresses at the running gear / soil interface, and localised redistribtuion of the pore pressures.

7.2 Theory

The theory presented is based on classical soil mechanics and is assumed to hold for any saturated fine grained material, of low permeability, having a Mohr-Coulomb failure criterion as described by equation 7.1.

$$\tau = c + \sigma.\tan \phi \qquad (7.1)$$

where: τ shear strength (kN/m^2)
c apparent cohesion (kN/m^2)
σ total normal stress (kN/m^2)
ϕ angle of shearing resistance.

In accordance with Terzaghi's fundamental concept of effective stress (Terzaghi, 1923, 1943):

$$\tau = c' + \sigma'.\tan \phi' \qquad (7.2)$$

where: c' and ϕ' are the shear strength parameters in terms of effective stress
σ' is the effective normal stress as defined in equation 7.3.

$$\sigma' = \sigma - u \qquad (7.3)$$

where: u is the pore water pressure in the sample, (kN/m^2).

For a remoulded soil, it can be assumed that $c'=0$, thus equation 7.2 can be simplified to:

$$\tau = \sigma'.\tan \phi' \qquad (7.4)$$

Assuming that the initial effective stress, prior to the first loading is defined by equation 7.5 and the stress associated with the wheel loading is equal to ΔW, then the effective stress at the wheel-soil boundary, σ_{1P}', during the passage of the vehicle, can be calculated using equation 7.6, as instantaneously all the vehicle load is carried by the pore water.

$$\sigma'_0 = \sigma_0 - u_0 \qquad (7.5)$$

$$\sigma'_{1P} = (\sigma_0 + \Delta W)-(u_0 + \Delta W) \qquad (7.6)$$

Once the vehicle has passed over the section the excess pore pressure would start to dissipate. The rate of dissipation would depend on the magnitude of the pore pressure and the permeability of the material. Prior to the second pass the excess

pore pressure may not have fully dissipated, thus the residual effective stress immediately before the second pass would be defined as in equation 7.7.

$$\sigma'_{1R} = \sigma_0-(u_0 + a_{1,0}.\Delta W) \quad (7.7)$$

where: $a_{1,0}$ is a factor describing the degree of dissipation between the first and second passes of the vehicle.

On the second pass, when the wheel again passes over the section of soil:

$$\sigma'_{2P} = (\sigma_0 + \Delta W)-(u_0 + a_{1,0}.\Delta W + \Delta W) \quad (7.8)$$

It is clear from equations 7.7 and 7.8, that the effective stress just before and during the passage of the vehicle are identical. In the interval between passes a proportion of the excess pore water pressure will again dissipate and immediately before the third passage the effective stress would be:

$$\sigma_{2R}' = \sigma_0-(u_0 + a_{1,0}.a_{1,1}.\Delta W + a_{2,0}.\Delta W) \quad (7.9)$$

where: $a_{1,1}$ is the degree of dissipation from the first passage of the vehicle between the second and third passes

$a_{2,0}$ is the degree of dissipation from the second passage of the vehicle between the second and third passes.

On the n^{th} pass of the vehicle the generic equation for effective stress would be:

$$\sigma_{nP}' = (\sigma_0+\Delta W)-(u_0+a_{1,0}.a_{1,1}\ldots a_{1,n-1}.\Delta W+a_{2,0}.a_{2,1}\ldots a_{2,n-2}.\Delta W+\ldots+a_{n-1}.\Delta W+\Delta W) \quad (7.10)$$

and prior to the $(n+1)^{th}$ pass the generic equation for the residual effective stress would be:

$$\sigma_{nR}' = \sigma_0-(u_0 + a_{1,0}.a_{1,1}\ldots a_{1,n}\Delta W + a_{2,0}.a_{2,1}\ldots a_{2,n-1}.\Delta W+\ldots+a_{n,0}.\Delta W) \quad (7.11)$$

The generic effect of the build up in pore water pressure and the resulting decrease in effective stress can be seen diagramatically in figures 7.1 and 7.2 respectively. With continual trafficking it is evident from equation 7.4 that there would be a reduction in the apparent undrained shear strength. On site, this decrease in shear strength would manifest itself in an increase in rut depth. The most effective remedy for this problem would be to allow the excess pore water pressure to dissipate, unfortunately this could take days to achieve depending on the permeability of the material.

7.3 Experimental Verification

A laboratory testing program was initiated to observe the increase in pore water pressure, at some depth below the surface of a saturated clay sample, during cyclic loading. The test work was conducted not to derive any firm relationships, or to aid in the prediction of apparent rolling resistance, but to verify the hypothesis of the above theory. For this reason the testing procedure did not necessarily have to mimic the field conditions.

Three tests were carried out in order to establish if the moisture content of the sample, hence the undrained shear strength, would have a significant effect on the development of excess pore water pressures under a regular cyclic load.

7.3.1 Test Material

The soil used for testing was from the A1/M1 link, contract 2, near Market Harborough. The material was typically a dark grey silty CLAY, with a particle size distribution as in figure 7.3, with 92% passing the 425μm sieve. The particle size distribution was established by wet sieving and hydrometer techniques as per BS1377 (BSI, 1990) was employed for the fraction less than 63μm in diameter. Liquid and plastic limits for the material were 51% and 21% respectively. All tests were carried out in accordance with BS1377 (BSI, 1991). A ϕ' value of 30° was used for this soil, as per the site investigation data.

The material for the test was prepared by passing it through a 2.36mm sieve, oven drying it, then mixing it to the required moisture content. In order that the material would be fully saturated and be in full contact with the pore pressure probe the sample was mixed to a slurry, with a moisture content of 75%, plate 7.1, rather than compacted. The volume of the sample was such that, once consolidated to a moisture content close to the plastic limit, the sample would be approximately 220mm high.

7.3.2 Test Apparatus

For logistical reasons it was decided to confine the sample and perform the tests in a computer controlled compression testing machine, rather than a triaxial rig. The

machine used for cyclically loading the sample was a Lloyd instrument LR 30K, plate 7.2. This machine is computer controlled and allows the stress pulse to be defined. A 100mm diameter bronze cylinder, figure 7.4 and plates 7.1, 7.2, and 7.3 was manufactured for confining the specimen. The cylinder was constructed in sections, enabling the height of the cylinder to be reduced as the sample consolidated. Each section of the cylinder had an 'O'-ring seal to prevent water egress, figure 7.4. A hole was drilled 100mm up from the base of the cylinder, to allow access for the pore water pressure probe, plate 7.3. The hole around the tubes was subsequently sealed with a silicone compound sealant. This sealant allowed the probe to move slightly during the consolidation stage of the experiment. The base plate had two 'O'-ring seals fitted to prevent drainage at the base of the cylinder, figure 7.4. The pore water pressure probe was connected to a 7 bar pressure transducer, which in turn was wired to a digital display, figure 7.4.

7.3.3 Pore Water Pressure Measurement

The pore pressure probe, plate 7.1, having a permeable ceramic tip, 10mm diameter and 15mm long, attached to small bore steel tubes, could be connected directly to a pressure transducer. To calibrate the system the probe was connected to a triaxial chamber outlet tap, via a short length of thick walled plastic tubing. The triaxial cell was then filled and the system flushed with de-aired water, the cell pressure was then increased in stages up to 110kN/m^2, reduced back down to zero, and repeated. The transducer output was correlated against the cell pressure, figure 7.5, giving a correlation coefficient of 0.99.

7.3.4 Test Procedure

Once the sample had been prepared, as in section 7.3.1, it was allowed to equilibrate for 24 hours. It was then poured into the bronze cylinder to a height just below the pore water pressure probe. The probe was then flushed with de-aired water, to ensure full saturation and the remainder of the sample poured into the cylinder. Several layers of filter paper were placed on the top of the sample which was left to consolidate under self weight, for 24 hours. The consolidation pressure was steadily increased until a pressure of 100kN/m^2 was achieved. The load was applied to the sample as per figure 7.6. The concentric rings were placed

on top of the sample to ensure a constant degree of consolidation across the sample.

Once the sample had been fully consolidated and the pore water pressure had equilibrated, the sample was placed in the testing rig and repeatedly subjected to the test pulse as in figure 7.7, until the excess pore water pressure, measured prior to each loading pulse, equilibrated. The shape of the pulse was limited by the accuracy of the equipment and the duration is known to be excessive. The 150 second delay between pulses represents a typical time lag between vehicle passes.

Once each test had been completed a sample was taken for moisture content determination. The sample was then consolidated to a higher pressure. Two further tests were carried out at consolidation pressures of 125 and 150kN/m^2. As the aspect ratio of the sample was small, it was considered that the consolidation pressure at the level of the pore water pressure probe would not be identical to that at the surface, due to stress distribution and wall friction effects. This problem was not considered to be serious for the reasons explained in section 7.3.

7.4 Experimental Results

The results of pore water pressure versus number of passes for the three tests are shown in figure 7.8. This figure shows that the pore water pressure does not increase above the initial value until approximately the tenth cycle. Also that as the moisture content of the sample decreases, the increase in excess pore water pressure reduces. The corresponding decrease in effective stress can be calculated using equation 7.3. Figure 7.9 shows the effect that the number of cycles has on effective stress. The shape of this figure compares reasonably well with the hypothesised generic graph of figure 7.2.

It is evident from figure 7.9 that the decrease in effective stress increases as the moisture content of the sample increases. The total reduction in effective stress, hence effective shear strength, would be of more interest to the site engineer than the decrease between individual passes, therefore the generic equations, equation 7.10 and 7.11, have been reduced to the form:

$$\sigma'_{100} = \sigma_0 - (u_0 + a_{100}\Delta W) \qquad (7.12)$$

where: σ'_{100} effective stress before or on the hundredth pass

a_{100} pore water pressure dissipation parameter between the first and hundredth pass

The value of a_{100} can be calculated for the three experimental cases and plotted against consistency index, figure 7.10. This figure in conjunction with equation 7.12 allows an approximation to be made of decrease in effective stress, hence shear strength, from a knowledge of the consistency index of the soil. The equation of the best fit line in figure 7.10, by the method of least squares, is:

$$a_{100} = 813e^{(-10.451_c)} \tag{7.13}$$

To see the effect the excess pore water pressure had on the shear strength of the material, an estimate of the initial shear strength had to be made. This was achieved by converting the corrected moisture content to consistency index, using equation 5.1, then to shear strength by the relationship derived, in section 5.5.2. Knowing the initial shear strength, the decrease in effective strength is calculated using equation 7.4. The effect of the cyclic loading on shear strength is plotted in figure 7.11. From this figure, it is evident that the percentage decrease in shear strength, as a function of the initial shear strength, increases as the moisture content of the sample decreases. For the three experiments carried out, the percentage decreases in shear strength were, 6, 17, and 38%, at moisture contents of 24, 26, and 28%, (consistency indices 0.90, 0.83, and 0.77) respectively. The overall decrease in effective strength can be calculated by combining equations 7.4, 7.12, and 7.13, as in equation 7.14.

$$\tau_{100} = \left[\sigma_0 - \left(u_0 + 813e^{(-10.451_C)}\Delta W\right)\right]\tan\phi' \tag{7.14}$$

Clearly these reductions in shear strength could have serious implications on the performance of plant on the haul roads, (Staples et al., 1992).

7.5 Discussion

The full effect of excess pore water pressure increases may not be realised, as only the vertical component of tyre loading has been investigated, the tyre shearing mechanism not being taken into account. However it should be noted that this was not an objective of the experiment. The excess pore water pressure in these experiments was measured at a single depth of approximately 120mm below the rut base. It is therefore unknown what value the pore water pressure would achieve at the surface and to what depth an increase in the pore water pressure would propagate. Nevertheless, the results from this experiment do show a distinct trend and are in agreement with the hypothesised theory outlined in section 7.2, thus confirming site observations that weaker soils deteriorate faster than drier ones.

It should be noted that the consistency indices measured in the field were higher than those calculated in the experiments. For a consistency index of unity extrapolating from equation 7.13 would yield a_{100} equal to 0.02. This would result in a minimal reduction in shear strength. It is therefore evident that pore water pressure effects at this depth would have a minimal effect on the apparent rolling resistance of articulated dump trucks on relatively firm operating conditions.

Although the experiments were carried out on confined saturated samples, the results still have practical implications: the operating effective shear strength on site could be lower than that extracted from the site investigation report, and the current practice of using graders to maintain the quality of haul roads may do relatively little to improve the long term condition of the haul road. Grading temporarily improves the running surface by smoothing the operational surface, but due to the loose state of the graded material observations indicate that the full depth of rut returns within a few number of passes. The only way to improve the quality of a relatively weak haul road in the long term would be to allow any developed excess pore water pressures to dissipate. This could be achieved by utilising the full width of the carriageway or on larger contracts varying the operation sequence. Unfortunately, these solutions may be impractical in the real world where time is money.

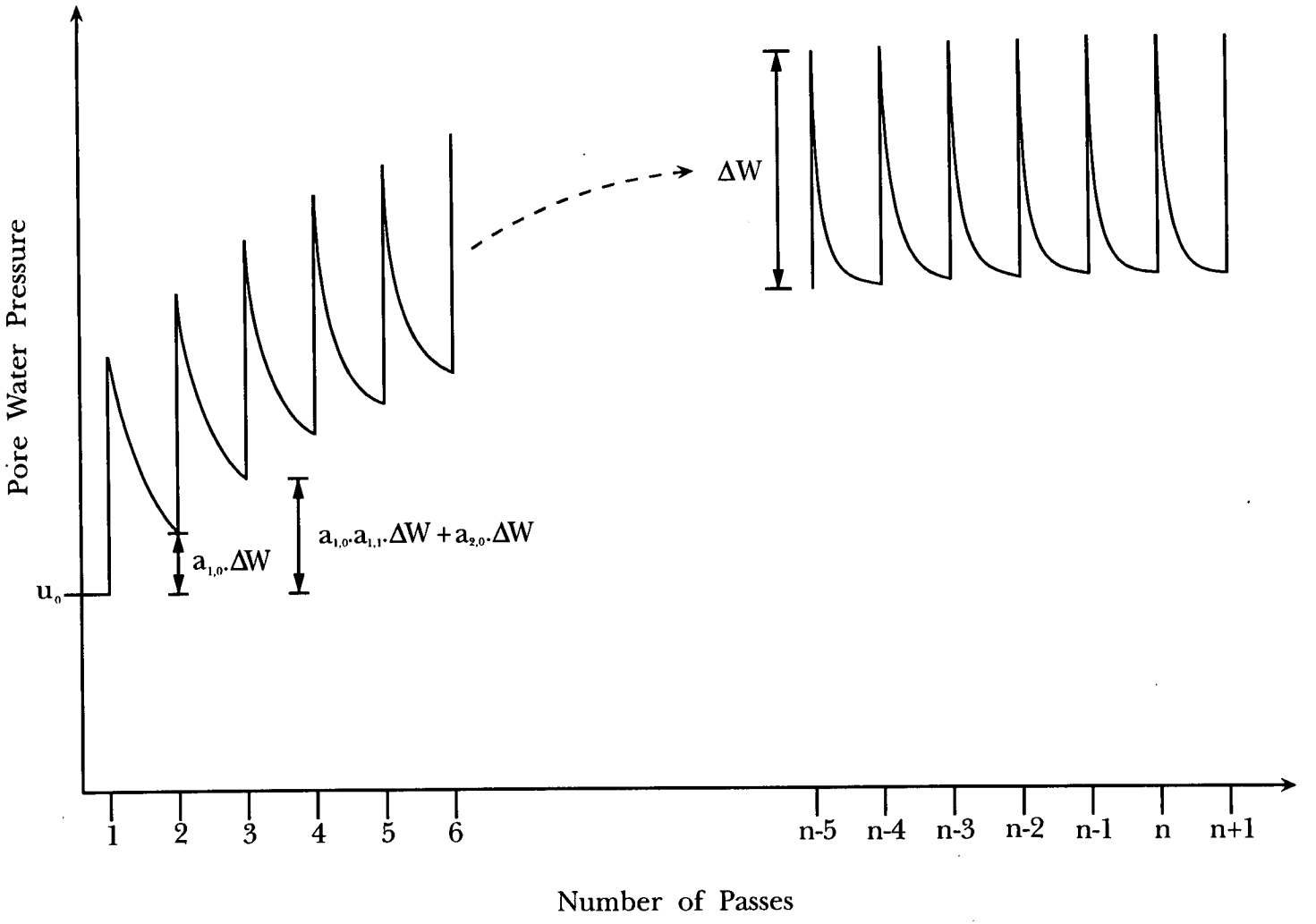

Figure 7.1: Diagramatic Effect of the Number of Passes on the Pore Water Pressure

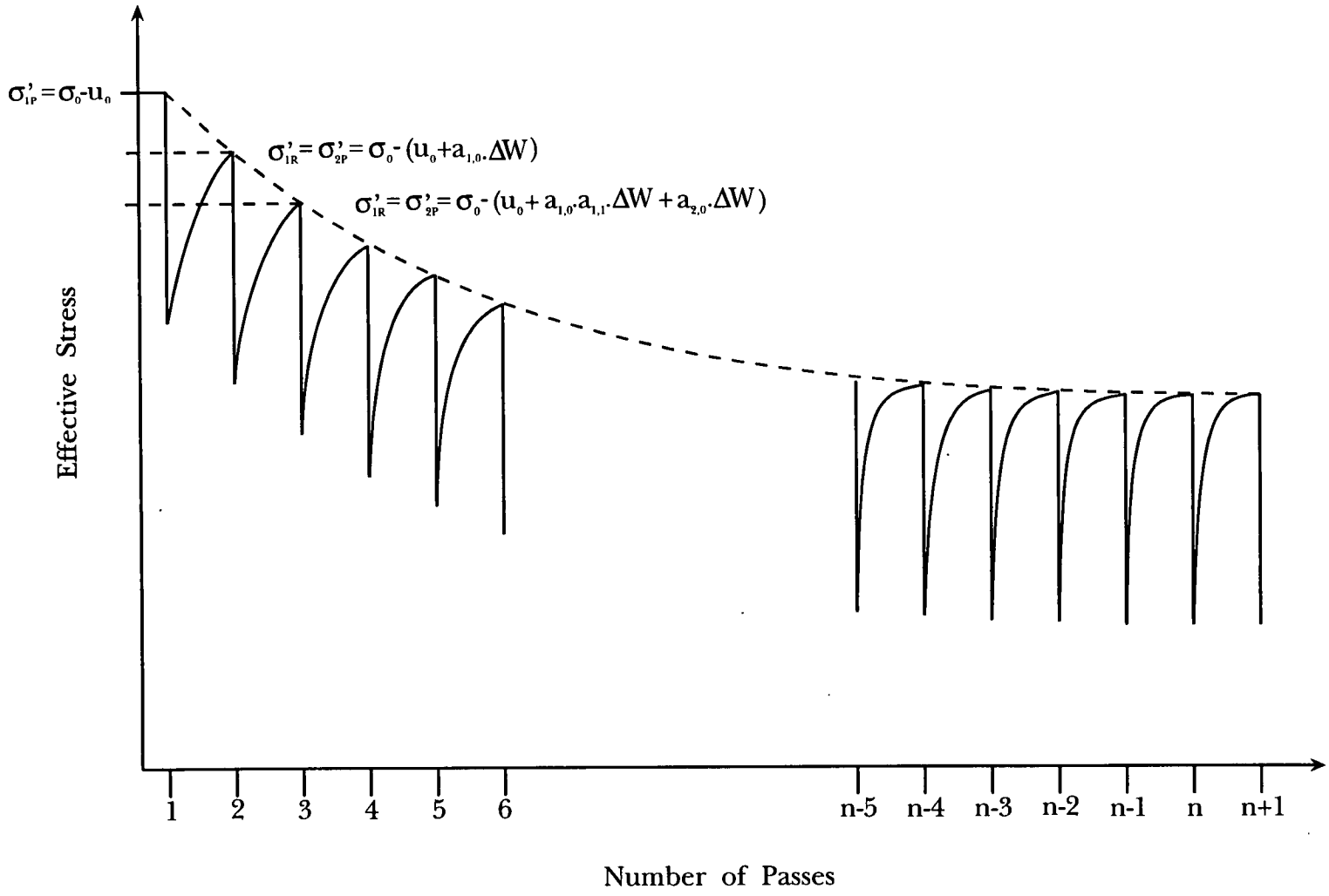

Figure 7.2: Diagramatic Effect of the Number of Passes on the Effective Stress

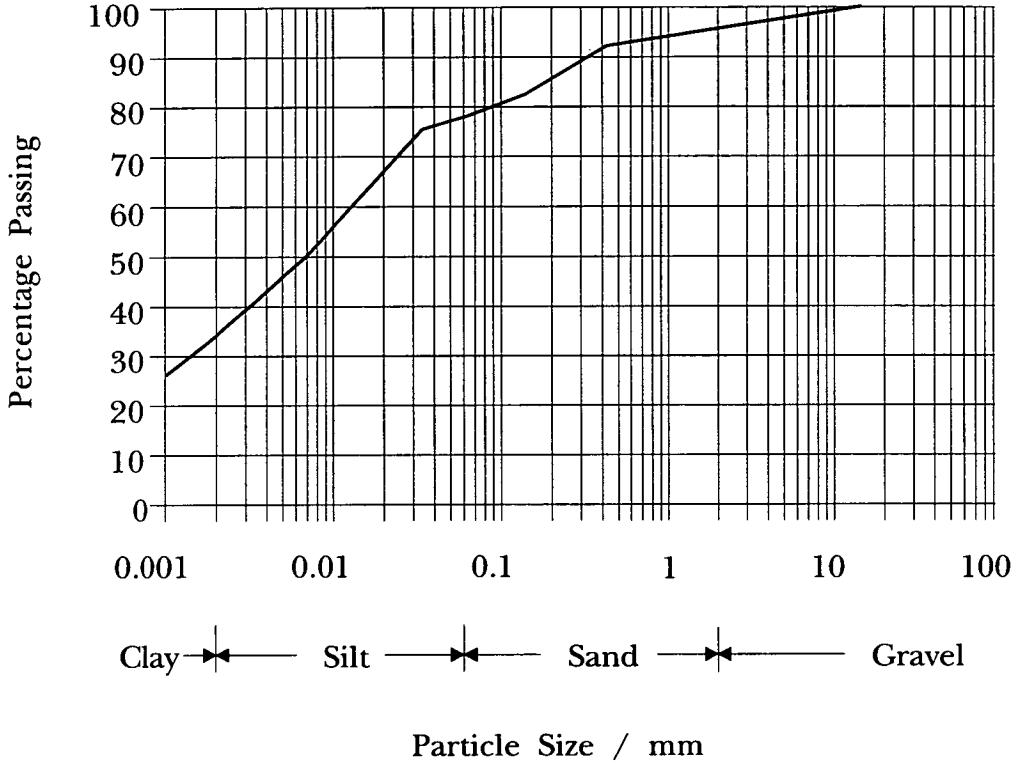

Figure 7.3: Particle Size Distribution for the Soil Sample used for Pore Water Pressure Experiments

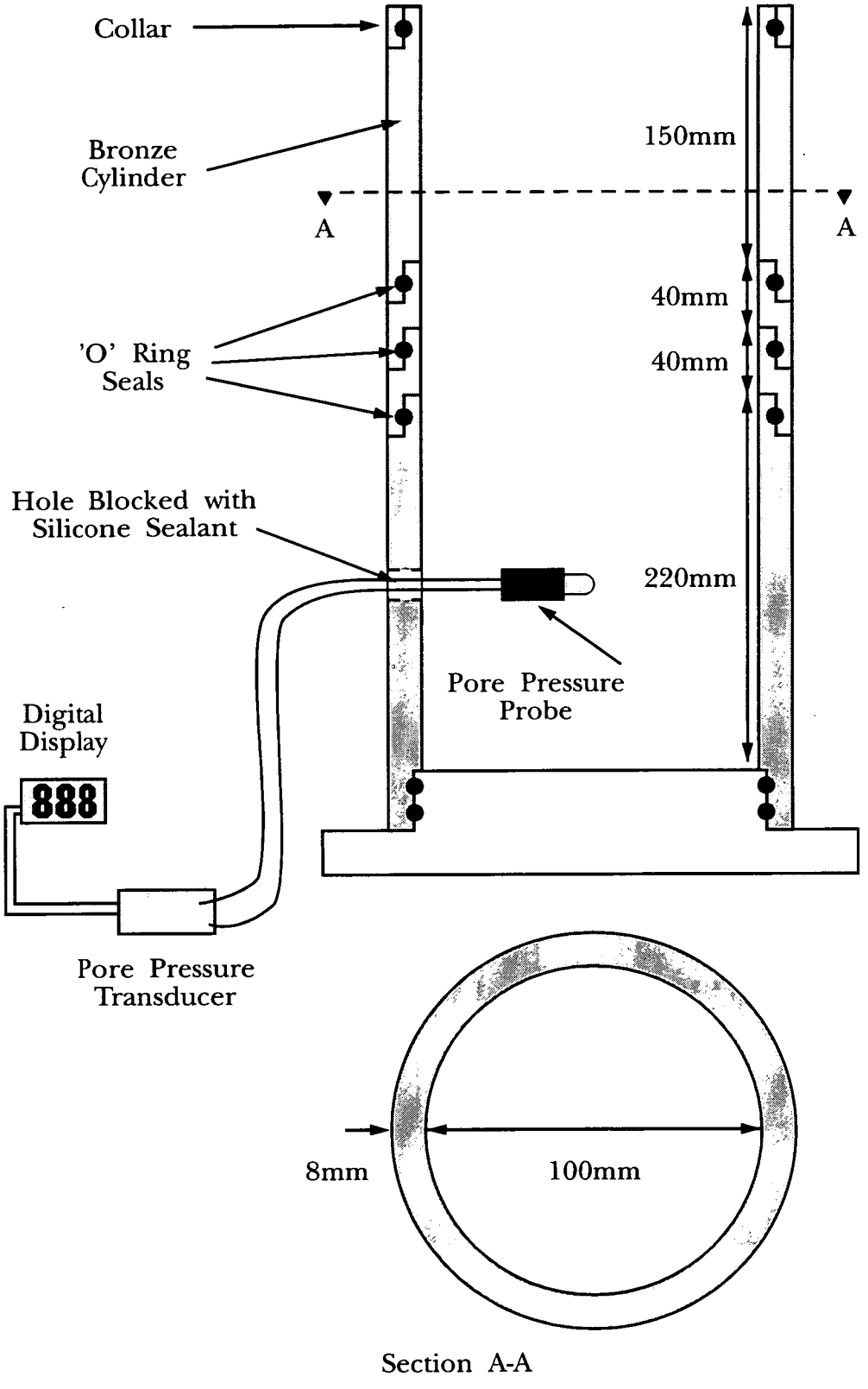

Figure 7.4: Apparatus for Pore Water Pressure Experiments

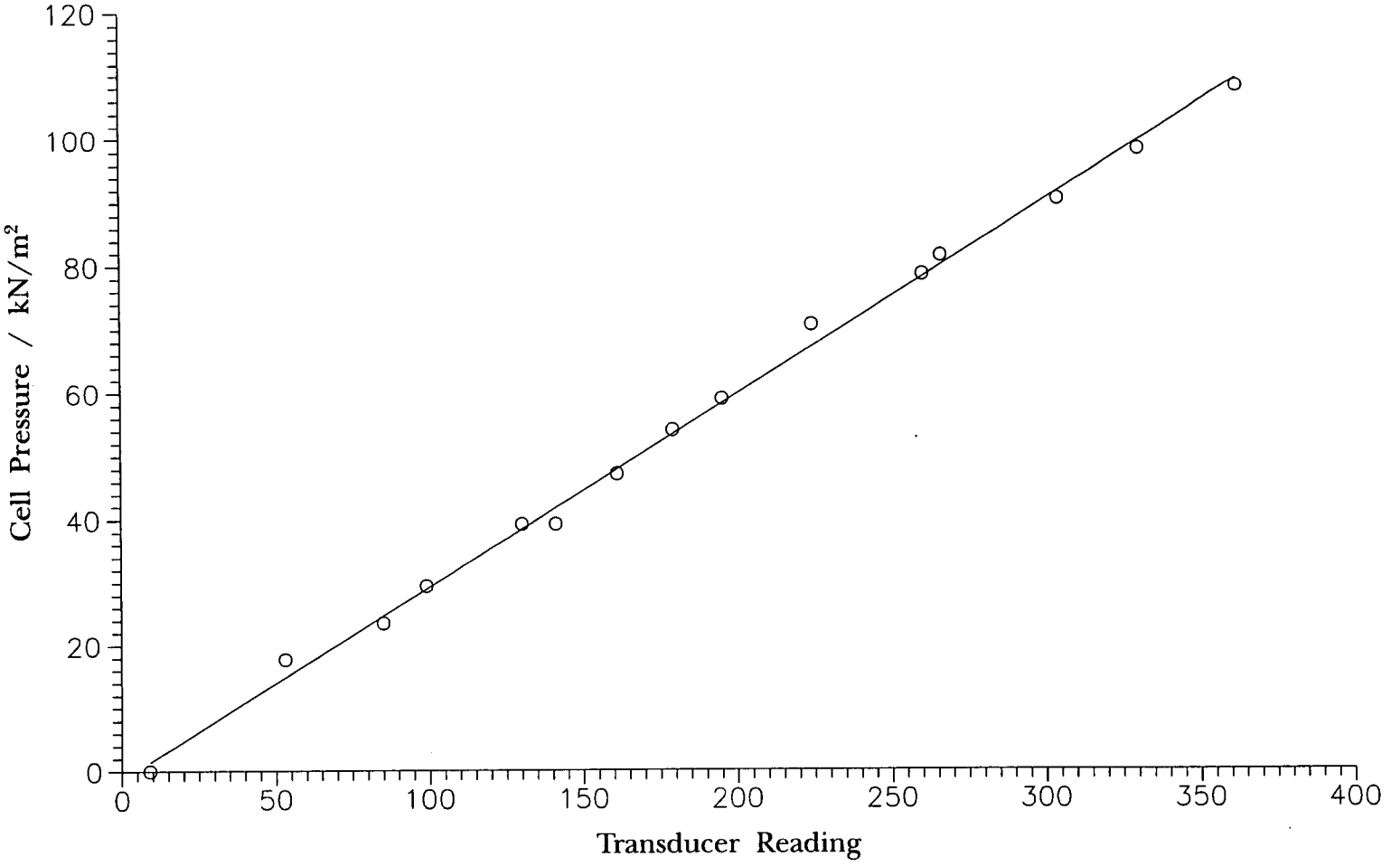

Figure 7.5: Calibration Curve for the Pore Water Pressure Probe and Transducer

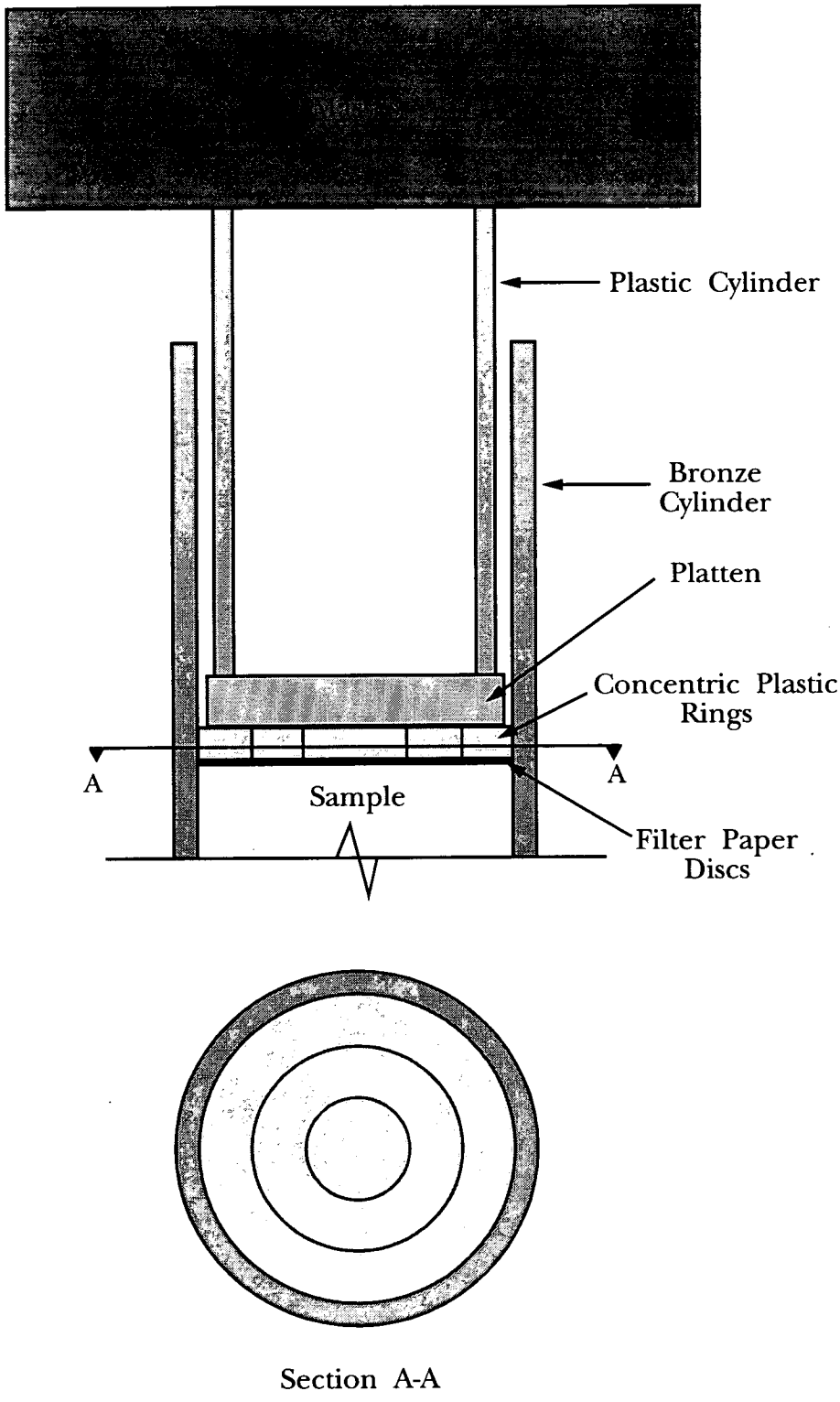

Figure 7.6: Schematic View of Loading Arrangement for Consolidation (not to scale)

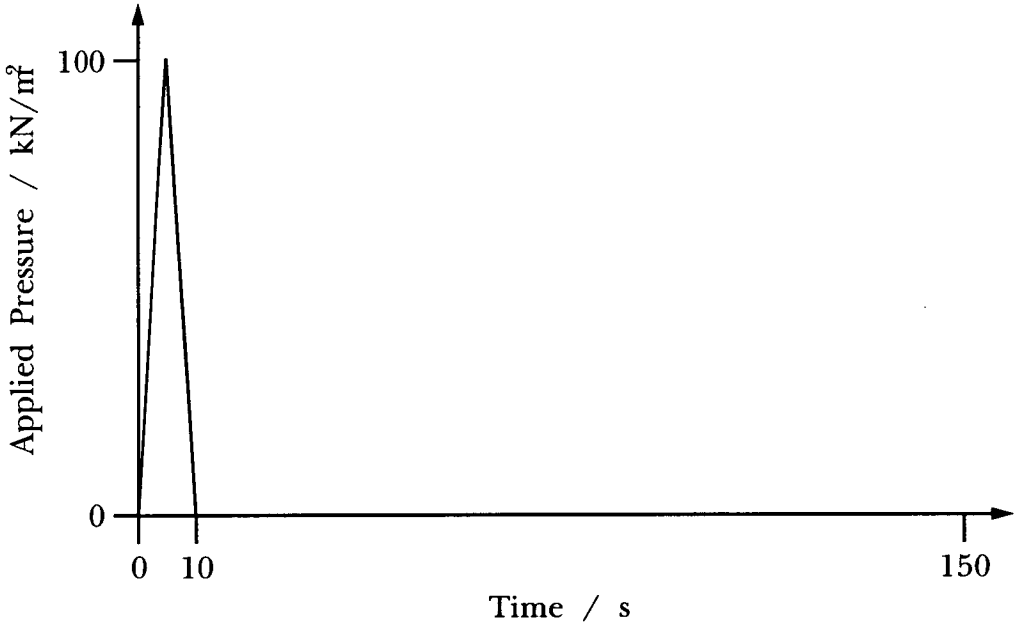

Figure 7.7: Loading Pulse

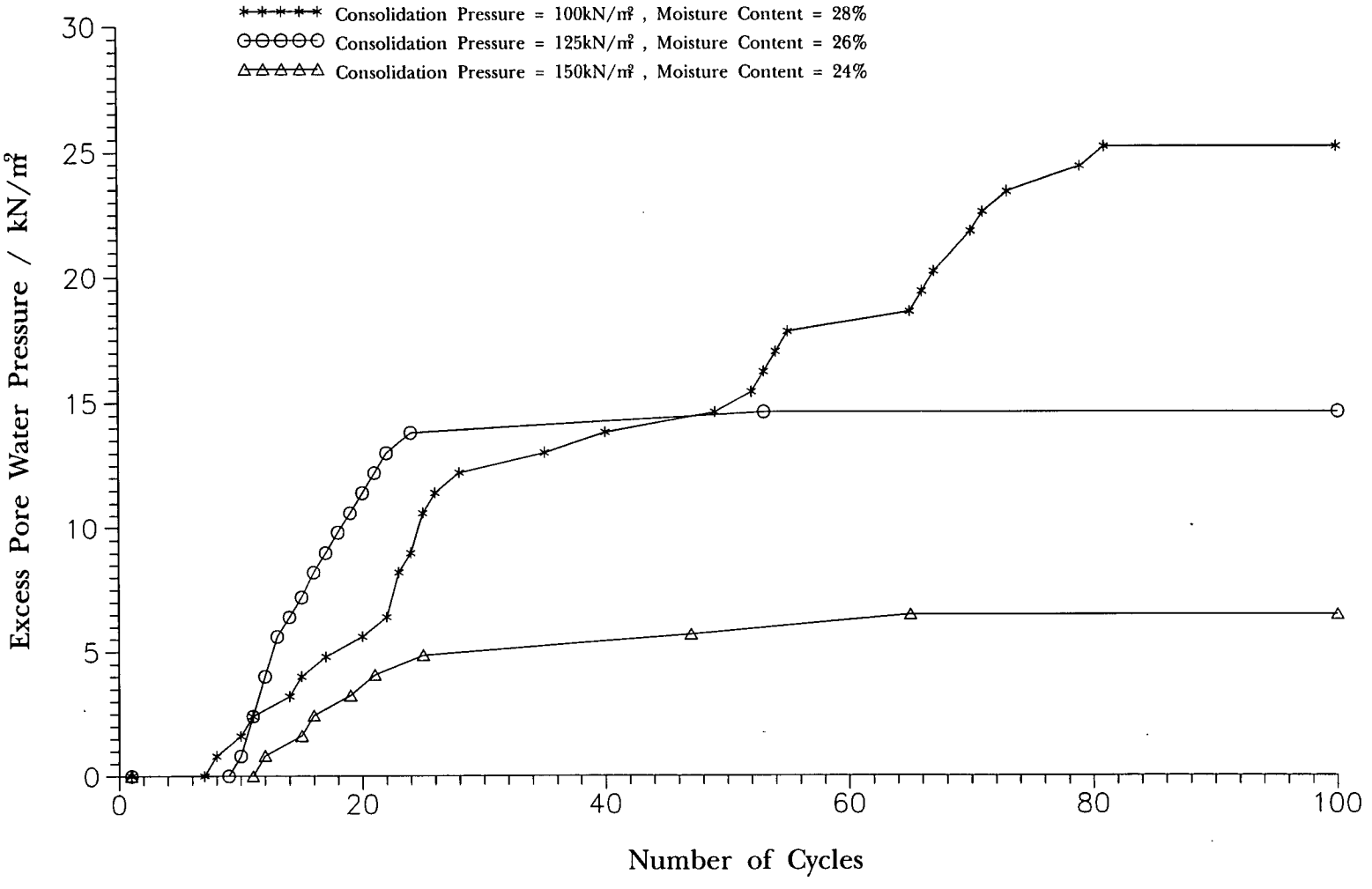

Figure 7.8: Excess Pore Water Pressure versus Number of Cycles

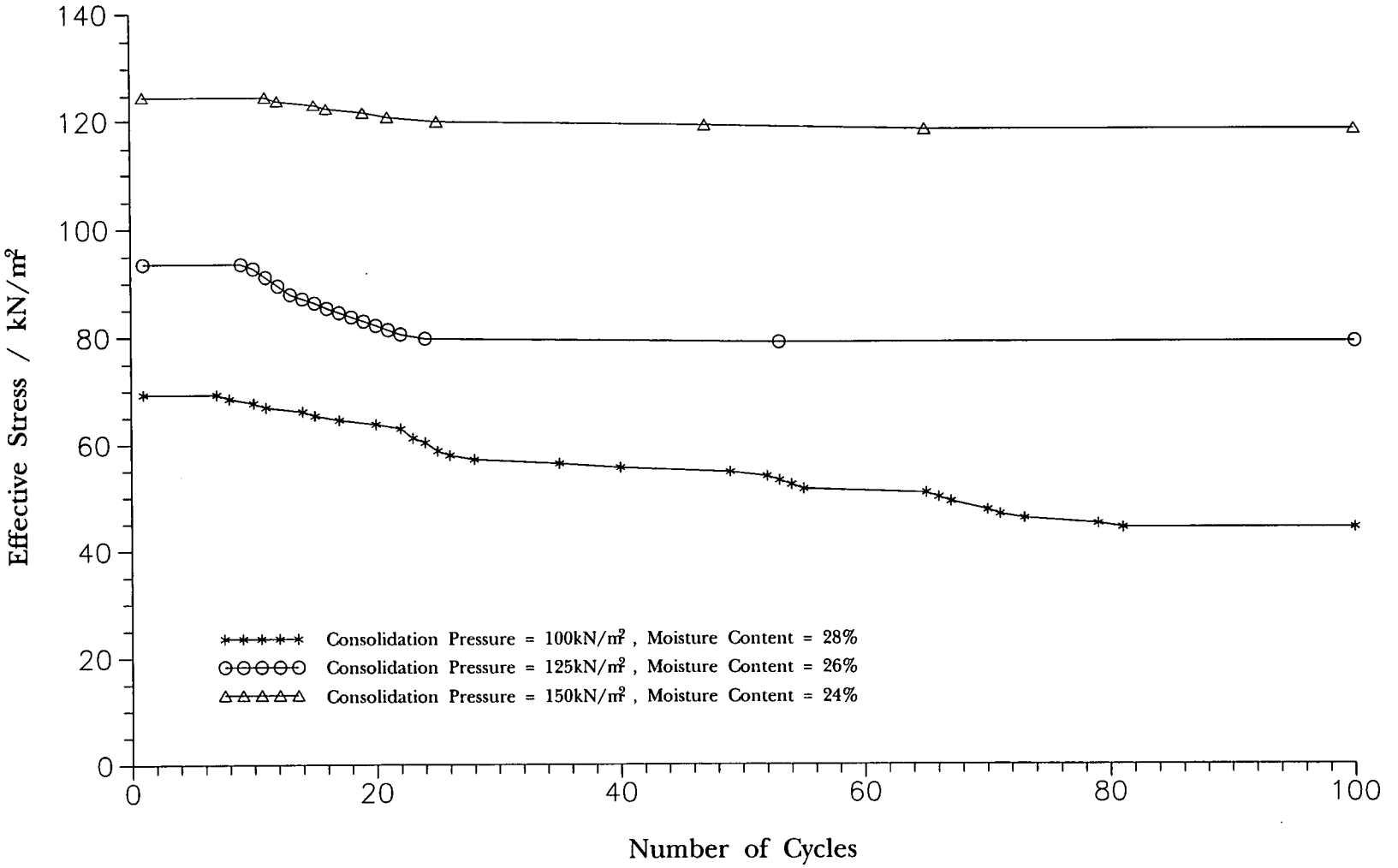

Figure 7.9: Effective Stress versus Number of Cycles

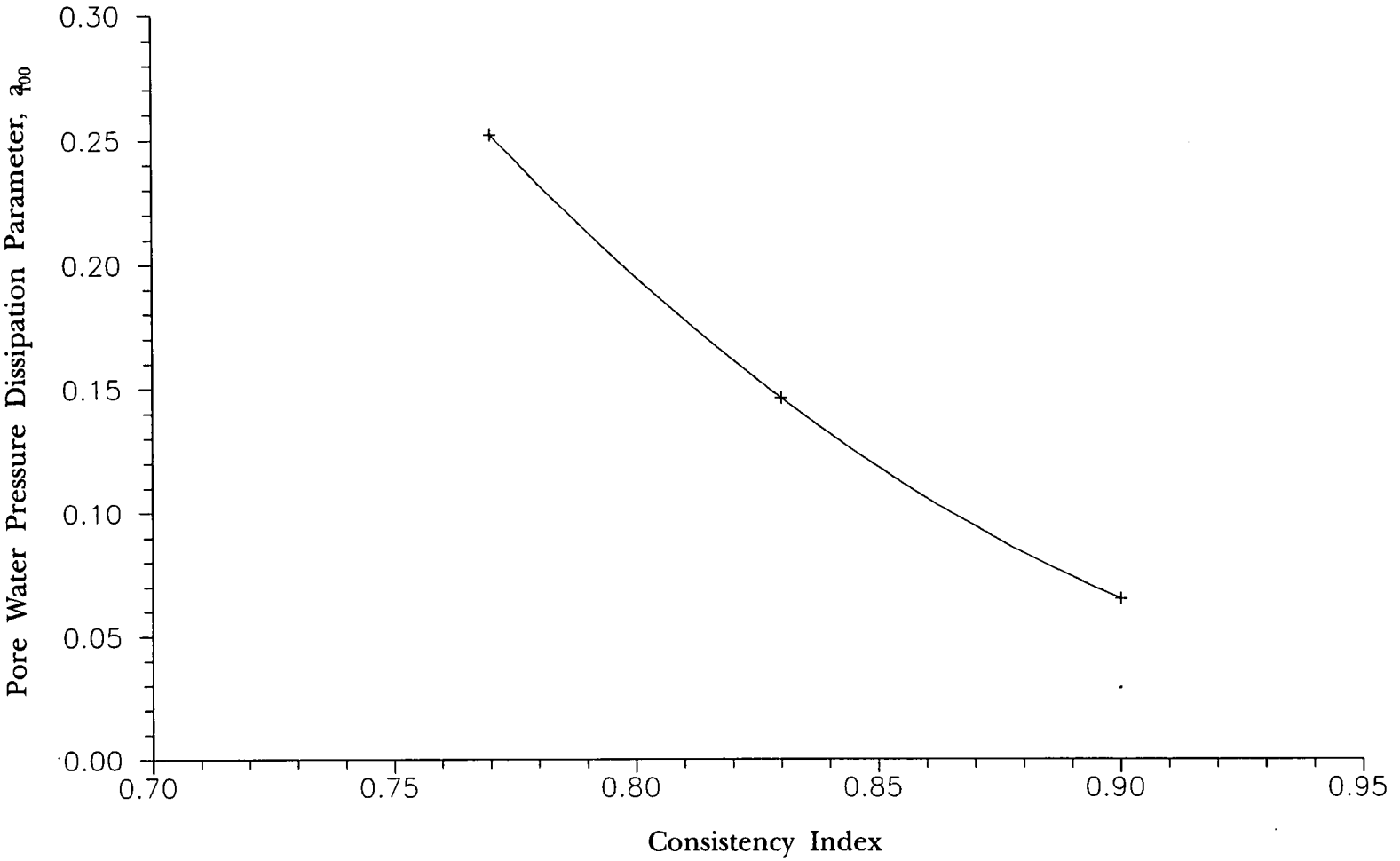

Figure 7.10: Pore Water Pressure Dissipation Parameter, a_{100} versus Consistency Index

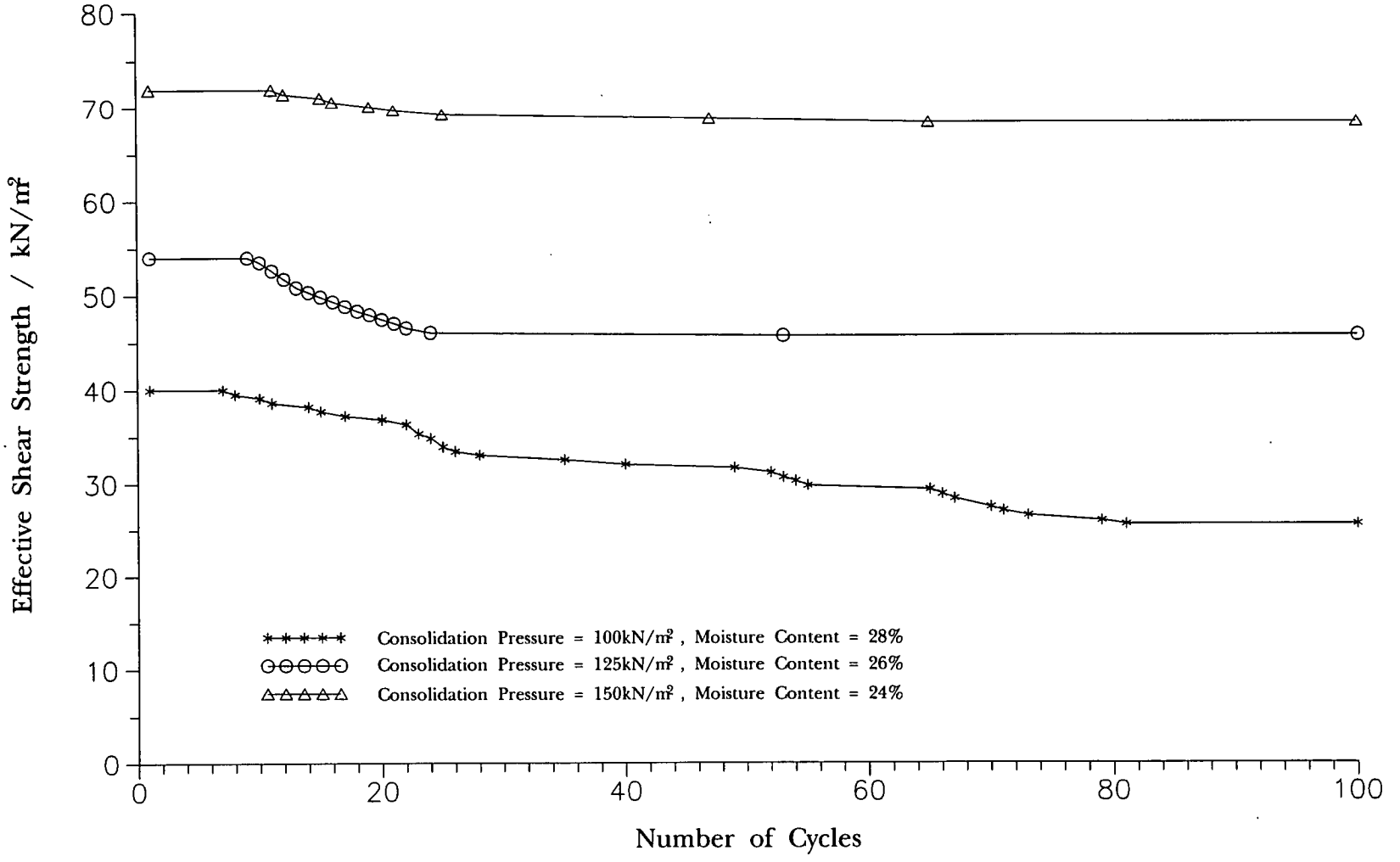

Figure 7.11: Effective Shear Strength versus Number of Cycles

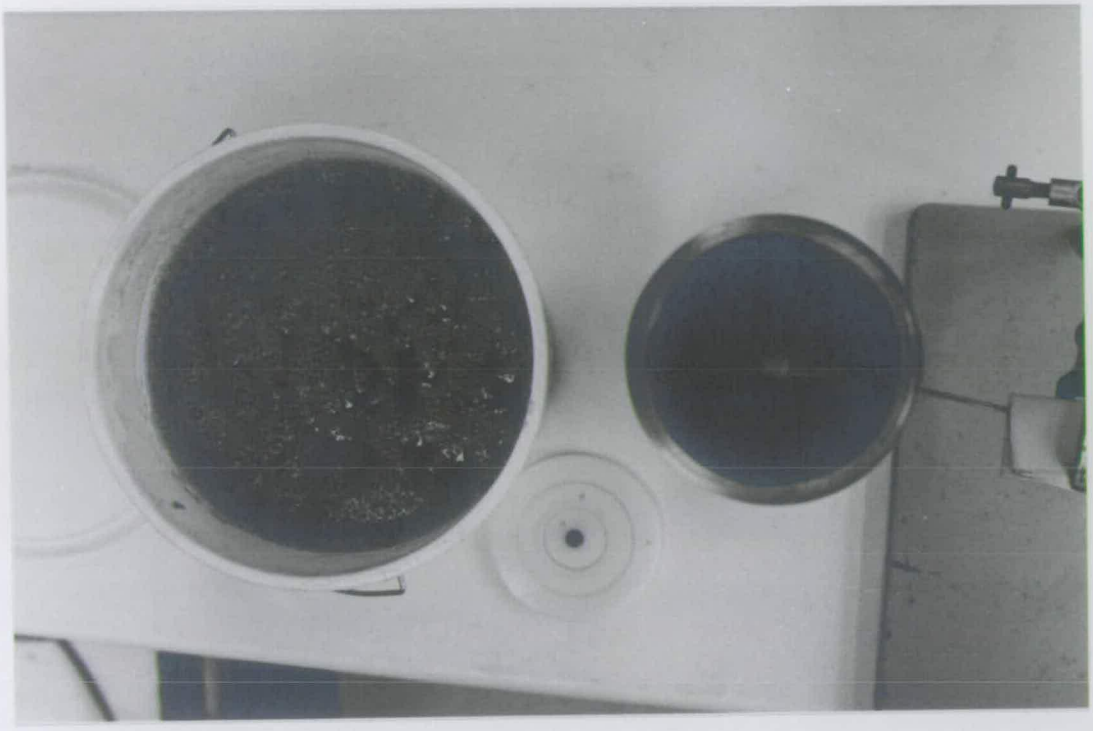

Plate 7.1

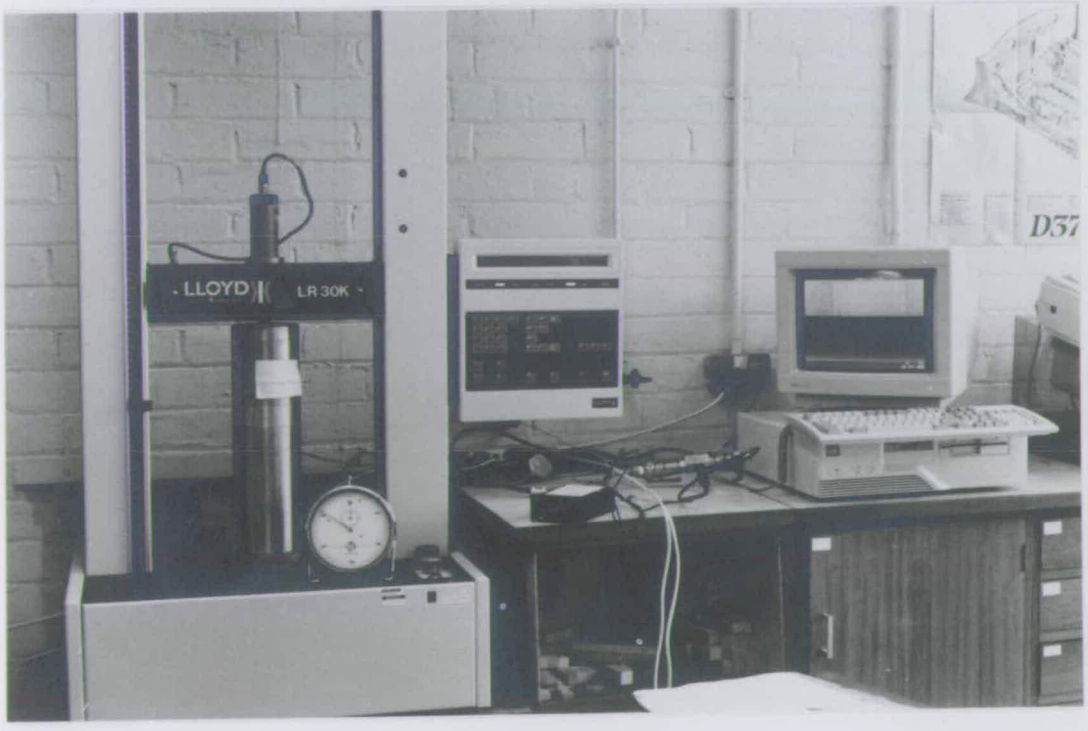

Plate 7.2

Plate 7.3

Chapter 8 Conclusions

8.1 Overall Conclusion

The overall conclusion to be drawn from this project is that the estimation of the rolling resistance of articulated dump trucks in an off-road situation is exceptionally complicated and depends on many factors including: soil type, moisture content, condition of the haul road, gradient, wheel load, and the driver. The geotechnical findings in site investigation reports can be used to estimate the apparent rolling resistance of the vehicle-terrain system, but the information contained within them must be accurate.

8.2 Literature

Many different solutions to the mobility problem have been put forward, but from the literature reviewed, it is evident that there is no unique theory for determining the rolling resistance of a vehicle, operating in an off-road situation. The majority of the work has been carried out by military and agricultural engineers and lacks a strong soil mechanics foundation. The inherent complexity of the driver-vehicle-terrain system forces the engineer to ignore analytical approaches, such as finite element methods, as they require too many unknown input parameters. Thus empirical techniques are employed for the determination of rolling resistance. The current method of estimating the productivity of a hauling team is from the length of the haul road. The main disadvantages of empirical techniques are: they cannot be extrapolated with confidence outwith the observed operational environment, and the more parameters incorporated into the theory the greater the financial burden on implementation.

8.3 Empirical Rolling Resistance

At the present time a value of rolling resistance, expressed as percent equivalent grade, is found by looking up tables provided by the vehicle manufacturers at the required condition of the haul road. This method does not allow an estimate of the rolling resistance at the tender stage of a contract. Manufacturers' specification

sheets and two computer programs, Vehsim and Accelerator, were also available for back analysing the rolling resistance. The specification sheets were discarded as they only deal with maximum velocity and do not allow for productivity estimation. The Accelerator program was chosen for use in the thesis as Vehsim took no account of the vehicle retarder when travelling downhill.

8.4 Site Monitoring

Studies of site operations of articulated dump trucks have never been previously reported in great detail and no information was available on the performance of these vehicles on chalk. The monitoring technique was to observe the speed of the plant, convert to apparent rolling resistance using the Accelerator software, then relate apparent rolling resistance to the soil and physical conditions of the haul road. For accurate monitoring on a section of haul road a minimum of ten time recordings should be taken. Observations of the performance of the plant in various working environments were also noted and recommendations for a more efficient working practice have been outlined.

8.4.1 Chalk

Apart from visual inspection, gradient was the only estimator of rolling resistance on the chalk haul roads, as no standard soils tests could be used on such a firm surface. The results showed that the gradient of the haul road has a secondary effect on the rolling resistance of the driver-vehicle-terrain system. When descending, the driver artificially slows the vehicle down to avoid the vehicle running out of control and to keep the engine temperature low. The effect of this is to increase the apparent rolling resistance. The apparent rolling resistance of articulated dump trucks travelling uphill on chalk decreases slightly as the gradient increases, because the drivers know they must attack the hill at maximum power.

Chalk will degrade to a slurry if its cellular structure is broken down. For this reason care should be taken when constructing haul roads, avoiding: steep ramps between benches, bottlenecks, and obstructions. By keeping the ramps smooth, a decrease in travel time, in excess of 10%, through the ramp could be achieved. If

the cellular structure remains intact, the haul roads will stay in excellent condition and the graders will only have to remove debris that has fallen out of the truck body. On no condition should an intact chalk haul road be graded, as this will lead to puttification of the chalk.

8.4.2 Clay

Compared to the chalk, monitoring on the clay site went into much greater detail, with apparent rolling resistance being related to five parameters: gradient, consistency index, moisture condition value, hand vane shear strength, and rut depth. The best method of predicting apparent rolling resistance was by using a five factor linear regression, giving an average correlation coefficient of 0.84. Simpler regression equations were given as all the information required may not be available at the time of tender. The equations have been validated by results not included in the regression analysis. These equations will allow the estimator to predict the apparent rolling resistance of an articulated dump truck at the time of tender and to monitor the operation throughout the duration of the contract. The on site estimation of apparent rolling resistance requires the timing of at least ten passes of a vehicle type.

8.5 General Observations of Site Practice

To maximise productivity on all sites the following practices should be employed where possible. Firstly, to prevent bunching, the utilisation of different types of plant on the same haul should be avoided. If bunching occurs then the faster vehicles should be allowed to overtake. Secondly, articulated dump trucks loaded with a backhoe excavator should be filled radially, not perpendicularly. Thirdly, the prime mover should be in operation for the majority of the time. Finally, the number of obstructions on the haul road should be kept to an absolute minimum.

8.6 Theory of Rolling Resistance

Previously developed American theories and equations have been shown to be inadequate for describing the relationship between rut depth and apparent rolling resistance, for British conditions of off-road hauling. The developed theory, utilising classical soil mechanics, has been shown to match site data well. Practically, the theory enables the engineer to estimate the maximum rut depth that will be encountered on site, from a knowledge of the vehicle and ground conditions. This rut depth can then be incorporated into the regression equations to estimate the apparent rolling resistance and be used as an indication of how much maintenance the haul roads are likely to require.

8.7 Pore Water Pressure Increase

Observations on both the chalk and clay sites, indicated that the condition of haul roads deteriorated as the operation progressed, led to the conclusion that the effective stress of the material was decreasing, possibly due to continual trafficking increasing the pore water pressure. A series of laboratory experiments were carried out to verify this hypothesis, by cyclically loading a confined sample. The results of this investigation proved that the weaker the initial state of the soil the more susceptible it will be to a decrease in effective stress. This indicates that the effective strength of the soil on site, after repeat trafficking, may be less than that indicated by the site investigation report. Extrapolation of the results to consistency indices encountered on site indicated that there would be a minimal decrease in effective strength. Other possible explanations for the increase in rut depth with time include: large strain effects, localised redistribution of the pore pressure in the soil, and remoulding of the soil structure.

The only remedy to the possible problem of increasing rut depths on site is to allow the excess pore water pressure to dissipate. Unfortunately, for financial reasons, any solution allowing for this on a site would be impractical.

Chapter 9 Recommendations for Future Work

9.1 Predicting Rolling Resistance

This thesis has concerned itself solely with the performance of articulated dump trucks on two ground conditions: chalk and firm clay. The first recommendation would therefore be to expand the research to frictional soils and weak cohesive soils, also to verify the derived equations on cohesive soils with a different plastic range and particle size distribution. As only one vehicle type has been studied it would be pertinent to develop a similar predictive tool for the other common types off-road earthmoving equipment: scrapers, rigid dump trucks, and other designs of articulated dump truck. There is no reason why the findings outlined in this thesis should not be used, or incorporated into, the predictive tools of other engineers interested in this aspect of the mobility problem.

To use the predictive equations the input information must be as accurate as possible. Some research has been carried out on the repeatability and reproducibility of the various tests, but this should be extended to all tests and printed with the site investigation report. Notoriously, the plastic limit test yields the greatest discrepancy and a new test, whether it be extrusion or cone penetrometer, should be incorporated into the standards.

9.2 Other Site Considerations

Site monitoring by either the contractor or research body should become a standard. Only by continual observation and the modification of design equations can the accuracy of estimates be improved. Other site factors that should be investigated are: whether graders are the best method for maintaining the quality of haul roads, how an obstruction influences productivity, and the effect of rainfall on the quality of the haul road and when the vehicles should stop, and restart, operating. It has been shown that the driver dictates the speed of the vehicle when travelling down steep inclines, other occasions where external factors cause the driver to reduce speed, e.g. tight corners and surfaces causing cab vibration, should be investigated.

9.3 Materials Testing

Some fundamentals properties of soils are not fully understood which could have a direct effect on the prediction of rolling resistance. Fundamental research should be carried out into: how a clay with a large coarse fraction should be corrected for moisture content, when does the percentage of fines in a sample become significant, and the correlation of quick on-site tests to controlled laboratory experiments.

It has been shown via a series of experiments that the pore water pressure in a sample increases to a constant level as the number of loading cycles increases. The experiments were conducted by normally loading a confined saturated soil cyclically and measuring the pore water pressure at a single depth. As difficulty was experienced in consolidating the sample it is recommended that a sample having a greater diameter to height ratio be used in subsequent tests. Simple expansion of this work could involve: determining the pore water pressure profile with depth, altering the loading pulse, and establishing how different soils will react to cyclic loading.

References

Accelerator, *Accelerator Vehicle Performance Software User's Guide*, Version 1.17, Accelerator, Inc., Fort Myers, Florida, 1987.

Alcock R. and Wittig V., An Empirical Method of Predicting Traction, *J. Terramechanics*, Vol.29, No.5, pp.381-394, 1992.

Anderson, W.F., The use of Multi-Stage Triaxial Tests to Find the Undrained Strength Parameters of Stony Boulder Clays, *Proc. Inst. Civ. Engrs.*, Vol.57, Part 2, pp.367-372, June 1974.

Anon., M40 Earthworks Contractor Solves Problems Posed by Chiltern Chalk, *Highways Design and Construction*, Vol.40, Dec. 1972.

ASAE, Soil Cone Penetrometer. American Society of Agricultural Engineers, Standard S313.2, 1985.

Ayers, P.D., and Perumpral, J.V., Moisture and Density Effects on Cone Index, *Trans. Am. Soc. Agric. Engrs.*, Vol.25, No.5, pp.1169-1172, 1982.

Bekker, M.G., Relationship between Soil and a Vehicle, *Soc. Auto. Engrs. Quarterly Trans.*, Vol.4, No.3, pp.381-396, July 1950.

Bekker, M.G., *Theory of Land Locomotion*, The University of Michigan Press, Ann Arbor, Michigan, 1956.

Bekker, M.G., *Off-Road Locomotion: Research and development in Terramechanics*, The University of Michigan Press, Ann Arbor, Michigan, 1960.

Bekker, M.G., *Introduction to Terrain-Vehicle Systems*, The University of Michigan Press, Ann Arbor, Michigan, 1969.

Bernstein, R., Probleme zur experimentellen Motorpfugmechanik, (Problems of Experimental Mechanics for Motor Ploughs), *Der Motorwagen*, Vol.16, pp.199-227, 1913.

Bjerrum, L., Problems of Soil Mechanics on Construction on Soft Clays, *Proc. 8th Int. Conf. S.M.F.E.*, Moscow, Vol.3, 1973.

Black, M., The Constitution of Chalk, *Proc. of the Geo. Soc. of London*, No.1499, 1953.

Blockley, D.J., Uncertain Ground: on Risks and Reliability in Geotechnical Engineering, *Proc. Conf. Risk and Reliability in Ground Engng.*, Instit. Civ. Engrs., London, 1993.

Boonsinsuk, P. and Yong, R.N., Soil Compliance Influence on Tyre Performance, *Proc. 8th Int. Conf. Int. Soc. Terrain-Vehicle Systems*, Cambridge, England, Vol.1, pp.61-80, 1984.

B.S.I., British Standards Institution, *Methods of Test for Soils for Civil Engineering Purposes*, BS 1377, Parts 1-9, London, 1990.

Burt, E.C. and Bailey, A.C., Load and Inflation Pressure Effects on Tires (sic), *Trans. Am. Soc. Agric. Engng.*, Vol.25, No.4, pp.881-884, 1982.

Burt, E.C., Wood, R.K. and Bailey, A.C., A Three-Dimensional System for Measuring Tire (sic) Deformation and Contact Stresses, *Trans. Am. Soc. Agric. Engng.*, Vol.30, No.2, pp.324-327, 1987a.

Burt, E.C. and Wood, R.K., Three-Dimensional Tire (sic) Deformation on Deformable Surfaces, *Trans. Am. Soc. Agric. Engng.*, Vol.30, No.3, pp.601-604, 1987b.

Carter, L.M., Portable Recording Penetrometer Measures Soil Strength Profiles, *Agric. Engng.*, Vol.46, No.6, pp.348-349, 1967.

Carter, L.M., Integrating Penetrometer Provides Average Soil Strength, *Agric. Engng.*, Vol.50, No.10, pp.618-619, 1969.

Casagrande, A. and Wilson, S.D., Effect of Rate of Loading on the Strength of Clays and Shales at Constant Water Content, *Géotechnique*, Vol.2, pp.251-264, 1951.

Caterpillar, *Caterpillar Performance Handbook*, 23rd Edition, Caterpillar Inc., Peoria, Illinois, U.S.A., 1992.

Caterpillar, *Caterpillar Performance Handbook*, 24th Edition, Caterpillar Inc., Peoria, Illinois, U.S.A., 1993.

Caterpillar, *Vehsim - Vehicle Simulation Software User's Manual*, Version 2.21, Caterpillar Inc., Peoria, Illinois, U.S.A., 1987.

Chatfield, C., *Statistics for Technology*, Third Edition, Chapman and Hall, London, 1983.

Clayton, C.R.I., The Collapse of Compacted Chalk Fill, *Int. Conf. on Compaction*, Vol.1, Paris, France, pp.119-124, 22-24 April, 1980.

Collins, H.J., and Hart, C.A., *Principles of Road Engineering*, Edward Arnold & Co., London, 1936.

Department of Transport, *Manual of Contract Documents for Highway Works, Vol.1, Series 600: Specification for Highway Works*, HMSO, Dec. 1991.

Department of Transport, *Earthworks, Design and Preparation of Contract Documents*, Highways Safety and Traffic Departmental Advice Note HA 44/91, 1991a.

Dwyer, M.J., Comely, D.R., and Evernden, D.W., The Field Performance of Some Tractor Tyres Related to Soil Mechanical Properties, *J. Agric. Engng. Res.*, Vol.19, pp.35-50, 1974.

Dwyer, M.J., Comely, D.R., and Evernden, D.W., Development of the N.I.A.E. Handbook of Agricultural Tyre Performance, *Proc. 5th Int. Conf. Int. Soc. Terrain-Vehicle Systems*, Detroit, Michigan, Vol.3, pp.679-700, 1975.

Dwyer, M.J., Tractive Performance of Wheeled Vehicles, *J. of Terramechanics*, Vol.21, No.1, pp.19-34, 1984.

Elbanna, E.B., and Witney, B.D., Cone Penetration Equation as a Function of the Clay Ratio, Soil Moisture Content and Specific Weight, *J. of Terramechanics*, Vol.24, No.1, pp.41-56, 1987.

Farrell, D.A., and Greacen, E.L., Resistance to Penetration of Fine Probes in Compressible Soils, *Aust. J. Soil. Res.*, Vol.4, pp.1-17, 1966.

Farrar, D.M., and Darley, P., *The Operation of Earthmoving Plant on Wet Fill*, TRRL Laboratory Report LR688, Transport Road and Research Laboratory, Crowthorne, 1975.

Forde, M.C., *Wet Fill for Clay Embankments*, unpublished PhD Thesis, University of Birmingham, 1975.

Freitag, D.R., *A Dimensional Analysis of the Performance of Pneumatic Tires (sic.) on Soft Soils*, Technical Report No.3-688, U.S. Army Engineering Waterways Experimental Station, Vicksburg, Mississippi, 1965.

Freitag, D.R., Green, A. and Murphy, N., *Normal Stresses at the Tire-Soil (sic) Interface in Yielding Soils*, Highway Research Record No.74, 1965.

Freitag, D.R., A Proposed Strength Classification Test for Fine-Grained Soil, *J. of Terramechanics*, Vol.24, No.1, pp.25-39, 1987.

Froehlich, O.K., *Druckverteilung im Baugrunde*, (Formulae of Boussinesq), Vienna, 1934.

Gee-Clough, D., The Bekker Theory of Rolling Resistance Amended to Take Account of Skid and Deep Sinkage, *J. of Terramechanics*, Vol.13, No.2, pp.183-188, 1976.

Gee-Clough, D., McAllister, M., and Evernden, D.W., Tractive Performance of Tractor Drive Tyres, II. A Comparison of Radial and Cross-ply Carcass Construction, *J. of Agric. Engng. Res.*, Vol.22, pp.385-395, 1977.

Gee-Clough, D., McAllister, M., Pearson, G., and Evernden, D.W., The Empirical Prediction of Tractor-Implement Field Performance, *J. of Terramechanics*, Vol.15, No.2, pp.81-94, 1978.

Goriatchkin, V.P., *Teoria i proisvodstov sielskohoziaÿnih mashin*, (Theory and Manufacturing of Agricultural Machines, collective works), Moscow, 1936.

Grez, J.M., Anegon, P.L., and Acillona, J.J., Analysis of Rolling Resistance with Driven Wheels, *Proc. 9th Int. Conf. Int. Soc. Terrain-Vehicle Systems*, Barcelona, Spain, Vol.1, pp.275-287, 1987.

Guy, D.G., Classification and Assessment of Chalk on the M25 Around the Gade Valley, Kings Langley, Hertfordshire, *Chalk*, Thomas Telford, London, pp.441-448, 1990.

Hart, M.B. and Carter, P.G., Some Observations on the Cretaceous Foraminifera of South East England, *J. of Foraminifera Res.*., Vol.5, No.2, pp.114-126, 1975.

Heatherington, J.G., and Littleton, I., The Rolling Resistance of Towed Rigid Wheels in Sand, *J. of Terramechanics*, Vol.15, No.2, pp.95-105, 1978.

Heatherington, J.G., Littleton, I., and Caws, I.M., The behaviour of Wheels with Rounded Profiles, *Proc. 7th Int. Conf. Int. Soc. Terrain-Vehicle Systems*, Calgary, Canada, 1981.

Heatherington, J.G., and Littleton, I., The Rolling Resistance of Towed Dual Wheel Conbinations in Sand, *Proc. 8th Int. Conf. Int. Soc. Terrain-Vehicle Systems*, Cambridge, England, Vol.1, pp.81-86, 1984.

Hegedus, E., Pressure Distributions under Rigid Wheels, *Trans. Am. Soc. Agric. Engng.*, Vol.8, pp.305-308, 1965.

Hendrick, J.G., Recording Soil Penetrometer, *J. of Agric. Engng. Res.*, Vol.14, No.2, pp.183-186, 1969.

Henry, F.D.C., *The Design and Construction of Engineering Foundations*, 2nd Edition, Chapman and Hall, London, 1986.

Hettiaratchi, D.R.P., and Liang, Y., Nomograms for the Estimation of Soil Strength from Indentation Tests, *J. of Terramechanics*, Vol.24, No.3, pp.187-198, 1987.

Horner, P.C., *Earthworks*, ICE Works Construction Guides, Thomas Telford, London, 1981.

Hurlbut, L.W., and Smith, C.W., Effect of Tractor Tire (sic) Size on Drawbar Pull and Travel Reduction, *Agric. Engng.*, Vol.18, No.2, pp.53-57, 1937.

Ingoldby, H.C. and Parsons, A.W., *The Classification of Chalk for use as a Fill Material*, TRRL Report LR806, Dept. of the Environment, Dept of Transport, Transport Road and Research Laboratory, Crowthorne, 1977.

Jakobsen, B.F., and Dexter, A.R., Prediction of Soil Compaction under Pneumatic Tyres, *J. of Terramechanics*, Vol.26, No.2, pp.107-119, 1989.

Jones, F.R., Tests in Texas of Pneumatic Tractor Tires (sic.), *Agric. Engng.*, Vol.15, No.2, pp.73, 1934.

Karafiath, L.L., and Nowatzki, E.A., *Soil Mechanics for Off-Road Vehicle Engineering*, Trans Tech Publications, Clausthal, Germany, 1978.

Knight, S.J., and Rula, A.A., Measurement and Estimation of the Trafficability of Fine Grained Soils, *Proc. 1st Int. Conf. Mech. of Soil-Vehicle Systems*, Turin, Italy, pp.371-386, 1961.

Knight, S.J., and Green, A.G., Deflection of a Moving Tire (sic.) on Firm to Soft Surfaces, *Trans. Am. Soc. Agric. Engng.*, Vol.5, pp.116-120, 1962.

Kogure, K., Ohira, Y, and Yamaguchi, H. Basic Study of Probabilistic Approach to Prediction of Soil Trafficability - Statistical Characteristics of Cone Index, *J. of Terramechanics*, Vol.22, No.3, pp.147-156, 1985.

Krick, G., Radial and Shear Stress Distribution Under Rigid Wheel and Pneumatic Tires (sic) Operating on Yielding Soils with Consideration of Tire (sic) Deformation, *J. of Terramechanics*, Vol.6, No.3, pp.73-98, 1969.

Larson, H.J., *Introduction to Probability Theory and Statistical Inference*, Third Edition, John Wiley and Sons, New York, 1982.

Law, A.M., and Kelton D.K., *Simulation Modelling and Analysis*, Second Edition, McGraw Hill Incorporated, New York, 1991.

L.C.P.C., (Laboratoire Central des Ponts et Chaussées), *Reccommandation pour les Terrassements Routiers*, facicules 1 à 4, 1976.

Masuda, S. and Tanaka, T., The Effect of Tire (sic) Tread on the Distribution of Ground Contact Pressure, *Proc. 2nd Int. Conf. Int. Soc. Terrain-Vehicle Systems*, Quebec City, Canada, pp.367-376, 1966.

McAllister, M., Reducing the Rolling Resistance of Tyres for Trailed Agricultural Machinery, *J. Agric. Engng. Res.*, Vol.28, pp.127-137, 1983.

McKibben, E.G., and Thompson, H.J., Transport Wheels for Agricultural Machines, I. Comparative Performance of Steel Wheels and Pneumatic Tires (sic.) on Two manure Spreaders of the Same Model, *Agric. Engng.*, Vol.20, No.11, pp.419-422, 1939.

McKibben, E.G., and Davidson, J.B., Transport Wheels for Agricultural Machines, II. Rolling Resistance of Individual Wheels, *Agric. Engng.*, Vol.20, No.12, pp.469-473, 1939b.

McKibben, E.G., and Davidson, J.B., Transport Wheels for Agricultural Machines, III. Effect of Inflation Pressure on the Rolling Resistance of Pneumatic Implement Tires (sic.), *Agric. Engng.*, Vol.21, No.1, pp.25-26, 1940.

McKibben, E.G., and Davidson, J.B., Transport Wheels for Agricultural Machines, IV. Effect of Outside and Cross-Section Diameters on teh Rolling Resistance of Pneumatic Implement Tires (sic.), *Agric. Engng.*, Vol.21, No.2, pp.57-58, 1940b.

McKibben, E.G., and Davidson, J.B., Transport Wheels for Agricultural Machines, V. Effect of Wheel Arrangement on Rolling Resistance, *Agric. Engng.*, Vol.21, No.3, pp.95-96, 1940c.

McKibben, E.G., and Davidson, J.B., Transport Wheels for Agricultural Machines, VI. Effects of Steel Wheel Rim Shape and Pneumatic Tire (sic.) Tread Design on Rolling Resistance, *Agric. Engng.*, Vol.21, No.4, pp.139-140, 1940d.

McKibben, E.G., and Hull, D.O., Transport Wheels for Agricultural Machines, VIII. Soil Penetration Tests as a Means of Predicting Rolling Resistance, *Agric. Engng.*, Vol.21, No.6, pp.231-234, 1940e.

Meyer, M.P., International Society for Terrain-Vehicle Standards, *J. of Terramechanics*, Vol.14, No.3, pp.153-182, 1977.

Meyerhof, G.G., The Ultimate Bearing Capacity of Foundation, *Géotechnique*, Vol.2, pp.301-332, 1951.

Mickelthwaite, E.W.E., *Soil Mechanics in Relation to Fighting Vehicles*, Military College of Science, Chertsey, 1944.

Montford, A.M., The Terrestrial Environment During the Upper Cretaceous and Tertiary Times, *Proc. Geo. Ass.*, Vol.81, part 2, p.18, 1970.

Montgomery, D.C., *Design and Analysis of Experiments*, Third Edition, John Wiley and Sons, New York, 1991.

Morgan, W.C., Private correspondence, 27th September 1993.

Mortimore, R.N., Roberts, L.D. and Jones, D.L. The Logging of Chalk for Engineering Purposes, *Chalk*, Thomas Telford, London, 1990.

Mulqueen, J., Stafford, J.V., and Tanner, D.W., Evaluation of Penetrometers for Measuring Soil Strength, *J. of Terramechanics*, Vol.14, No.3, pp.137-152, 1977.

N.I.A.E., *Test Reports. National Institute of Agricultural Engineering*, No.251, 1960.

Noel, D., Coccoliths Cretaces. La Companienne du Bassin de Paris, *CNRS*, Paris, 1970.

Norman, R., *The Effect of Wet Weather on the Construction of Earthworks*, C.E.R.A. Research Report No.3, October 1965.

Olsen, H.J., Electronic Cone Penetrometer for Field Tests, *Proc. 9th Int. Conf. Int. Soc. Terrain-Vehicle Systems*, Barcelona, Spain, Vol.1, pp.20-27, 1987.

Onafeko, O., Instrumentation for Measuring Radial and Tangential Stresses Beneath Rigid Wheels, *J. of Terramechanics*, Vol.1, No.3, pp.61-84, 1964.

Onafeko, O., Analysis of the Rolling Resistance Losses of Wheels Operating on Deformable Terrain, *J. Agric. Engng. Res.*, Vol.14, No.2, pp.176-182, 1969.

Onafeko, O. and Reece, A.R., Soil Stresses and Deformations Beneath Rigid Wheels, *J. of Terramechanics*, Vol.4, No.1, pp.59-80, 1967.

Parsons, A.W., *The Rapid Measurement of the Moisture Condition of Earthwork Material, Department of the Environment*, TRRL Report LR750, Transport Road and Research Laboratory, Crowthorne, 1976.

Parsons, A.W., *The Efficiency of Operation of Earthmoving Plant on Road Construction Sites, Department of the Environment*, TRRL Supplementary Report SR351, Transport Road and Research Laboratory, Crowthorne, 1977.

Parsons, A.W., *The Rapid Determination of the Moisture Condition of Earthwork Material, Department of the Environment*, TRRLReport LR750, Crowthorne, 1979.

Parsons, A.W., and Darley, P., *The Effect of Soil Conditions on the Operation of Earthmoving Plant, Department of Transport*, TRRL Laboratory Report LR1034, Transport Road and Research Laboratory, Crowthorne, 1982.

Parsons, A.W., and Toombs, A.F., *Pilot-Scale Studies of the Trafficability of Soil by Earthmoving Vehicles, Department of Transport*, TRRL Research Report RR130, Transport Road and Research Laboratory, Crowthorne, 1988.

Pavlics, F., Bevameter 100. A New Type of Field Apparatus for Measuring Locomotive Stress-Strain Relationships in Soils., *Proc. 1st Int. Conf. on Terrain Vehicle Systems*, Turin, Italy, 1961.

Perdok, V.D., A Prediction Model for the Selection of Tyres for Towed Vehicles on Tilled Soil., *J. Agric. Engng. Res.*, Vol.23, pp.369-383, 1978.

Peurifoy, R.L., and Ledbetter, W.B., *Construction Planning, Equipment and Mehods*, Fourth Edition, McGraw-Hill Book Company, New York, 1986.

Phillips, J., and Perumpral, J.V., Designing a Microcomputer Data logger for Soil Cone Penetrometer, *Agric. Engng.*, Vol.64, No.6, pp.13-14, 1983.

Prandtl, L., Spannungsverteilung in Plastischen Korpern, *Proc. 1st Int. Congress for Applied Mech.*, Delft, pp.43-54, 1924.

Prather, O.C., Hendrick, J.G., and Schafer, R.L., An electronic Hand-operated Recording Penetrometer, *Trans. Am. Soc. Agric. Engng.*, Vol.13, No.1, pp.385-386, 390, 1970.

Privett, K.D., Use of Thick Layers in Chalk Earthworks at Port Solent Marina, Portsmouth, UK, *Chalk*, Thomas Telford, London, pp.429-436, 1990.

Pugh, R.D., Private correspondence, 1st October 1993.

Quibel, A., Compaction of Chalk, *Chalk*, Thomas Telford, London, pp.437-440, 1990.

Rat, M. and Schaeffner, M., Classification of Chalks and Conditions of use in Embankments, *Chalk*, Thomas Telford, London, pp.425-428, 1990.

Rawitz, E., and Margolin, M., An Economical Hand-Held Recording Penetrometer, *Soil and Tillage Res.*, Vol.19, pp.67-75, 1991.

Reaves, C.A. and Cooper, A.W., Stress Distribution in Soils under Tractor Loads, *Agric. Engng.*, Vol.41, No.1, pp.20-21, 1960.

Reece, A.R., Theory and practice of Off-The-Road Locomotion, *J. and Proc. of the Inst. of Agric. Engrs.*, Vol.20, No.2, pp.82-90, 1964.

Reece, A.R., Principles of Soil-Vehicle Mechanics, *Proc. Auto. Div. Instn. of Mech. Engrs.*, Vol.180, Part 2A, No.2, 1965.

Reece, A.R., and Peca, J.O., An Assessment of the Value of the Cone Penetrometer in Mobility Prediction, *Proc. 7th Int. Conf. Int. Soc. Terrain-Vehicle Systems*, Calgary, Canada, Vol.3, pp.A1-A33, 1981.

Reina, P., M27 Muck-shifter to Claim £¼M, *New Civil Engr.*, April 24th 1975.

Rohani, B., and Baladi, G.Y., Correlation of Mobility Cone Index with Fundamental Engineering Properties of Soil, *Proc. 7th Int. Conf. Int. Soc. Terrain-Vehicle Systems*, Calgary, Canada, Vol.3, pp.959-990, 1981.

Sabey, B.E. and Lupton, G.N., *Photography of the Real Contact area of Tyres During Motion*, Ministry of Transport, RRL Report LR64, Road Research Laboratory, Crowthorne, 1967.

SDD, *The use and Application of the Moisture Condition Apparatus in Testing Soil Suitability for Earthworking*, Scottish Development Dept., Technical Memorandum SH7/83 amendment No.1, 1989.

Sela, A.D., On the Slip and Tractive Effort, *Proc. 1st Int. Conf. on Terrain Vehicle Systems*, Turin, Italy, 1961.

Skempton, A.W. and Northey, R.D., The Sensitivity of Clays, *Géotechnique*, Vol.3, pp.30-53,1952.

Smith, D.L.O., and Dickson, J.W., *The Compaction of a Sandy Loam by Wheels Supporting 1.73t at Four Different Ground Pressures*, S.I.A.E. Departmental note SIN/452, Scottish Institute of Agricultural Engineering, Bush Estate, Penicuik, UK 1985.

Soehne, W., Druckverteilung im boden und bodenverformung unter schlepperreifen (Distribution of pressure in the soil and soil deformation of tractor tyres), *Grundlagen der Landrechnik*, Heft 5, 1953.

Soehne, W., Fundamentals of Pressure Distribution and Soil Compaction under Tractor Tires (sic), *Agric. Engng.*, Vol.39, No.5, pp.276-681, 1958.

Staples, B.L., Wood, G.S., and Forde, M.C., Technical Evaluation of Earthworks Claims Under ICE Conditions of Contract 5th and 6th Editions, *Proc. of the Instn. of Civ. Engrs.*, Civil Engineering, Vol.92, pp.90-95, May 1992.

Taylor, D.W., *Fundamentals of Soil Mechanics*, John Wiley and Sons Inc., New York, 1948.

Taylor, J.H., Lug Angle Effect on Traction Performance of Pneumatic Tractor Tires (sic), *Trans. of the Am. Soc. Agric. Engng.*, Vol.16, pp.16-18, 1973.

Terex, *Production and Cost Estimating of Material Movement with Earthmoving Equipment*, Terex Corporation, U.S.A. 1981.

Terzaghi, K.,Die Berechnung der Durchlassigkeitsziffer des Tones aus dem Verlauf der hydrodynamischen Spannungserscheinungen, *Sitzbr. Akad. Wiss. Wien*, Abt.IIa, Vol.132, 1923.

Terzaghi, K., *Theoretical Soil Mechanics*, John Wiley and Sons Inc., New York, 1943.

Trabbic, G.W., Lask, K.V. and Buchele, W.F., Measurement of Soil-Tire (sic) Interface Pressures, *Agric. Engng.*, Vol.40, No.11, pp.678-681, 1959.

Turnage, G.W., *Performance of Soils under Tire (sic.) Loads; Application of Test Results to Tire (sic.) Selection for Off-Road Vehicles*, Technical Report No.3-666, Report 8, U.S. Army Engineer Waterways Experimental Station, Vicksburg, Mississippi, 1972.

Turnage, G.W., In-Soil Tractive Performance of Selected Radial- and Bias-Ply Tires (sic.), Paper No.76-1520, *Trans. Am. Soc. Agric. Engnrs.*, 1976.

Turnage, G.W., A Synopsis of Tire (sic.) Design and Operational Considerations Aimed at Increasing In-Soil Tire (sic.) Drawbar Performance, *Proc. 6th Int. Conf. Int. Soc. Terrain-Vehicle Systems*, Vienna, Austria, Vol.2, pp.757-810, 1978.

Turnage, G.W., Prediction of In-Tire (sic.) and Wheeled Vehicle Drawbar Performance, *Proc. 8th Int. Conf. Int. Soc. Terrain-Vehicle Systems*, Cambridge, England, Vol.1, pp.121-150, 1984.

Uffelmann, F.L., The Performance of Rigid Cylindrical Wheels on Clay Soils, *Proc. 1st Int. Conf. on Terrain Vehicle Systems*, Turin, Italy, pp.111-130, 1961.

Upadhyaya, S.K., Wulfsohn, D. and Jubbal, G., Traction Prediction for Radial Ply Tyres, *J. of Terramechanics*, Vol.26, No.2, pp.149-175, 1989.

Uphadyaya S.K., Prediction of Traction and Soil Compaction using 3D Soil-Tyre Contact Profile, *J. of Terramechanics*, Vol.29, No.6, pp.541-564, 1992.

Upadhyaya, S.K., Wulfsohn, D., Mehlschau, J., An Instrumented Device to Obtain Traction Related Parameters, *J. of Terramechanics*, Vol.30, No.1, pp.1-20, 1993.

U.S. Army, *Planning and Design of Roads, Airbases, and Heliports in the Theatre of Operations*, Chapter 9 - Soils Trafficability, Vol. II of Dept. of the Army Technical Manual, TM 5-330, 1968.

VandenBerg, G. E. and Gill, W.R., Pressure Distribution Between a Smooth Tire (sic) and the Soil, *Trans. Am. Soc. Agric. Engng.*, Vol.5, pp.105-107, 1962.

VandenBerg, G.E., and Reed, I.F., Tractive Performance of Radial-Ply and Conventional Tractor Tires (sic), *Trans. Am. Soc. Agric. Engng.*, Vol.5, pp.126-132, 1962.

VME, *Performance Manual Volvo BM Articulated Haulers*, Edition 2, Volvo Michigan Euclid, Växjö, Sweden, 1989.

Wakeling, T.R.M., A Comparison of the Results of Standard Site Investigation Methods Against the Results of a Detailed Geotechnical Investigation in Middle Chalk at Mundford, Norfolk, *Proc. of the Symp. on In-situ Investigations in Soils and Rocks*, BGS, London, pp.17-22, 1970.

Ward W.H., Burland, J.B. and Gallois, R.W., Geotechnical Assessment of a site at Mundford, Norfolk for a Large Proton Accelerator, *Géotechnique*, Vol.18, pp.399-431, 1968.

Whyte, I.L., Soil Plasticity and Strength - a New Approach Using Extrusion, *Ground Engng.*, Vol.15, No.1 pp.16-24, 1982.

Whyte, I.L., and Tonks, D.M., Project Risks and Site Investigation Strategy, *Risks and Reliabitity in Ground Engng.*, Thomas Telford Ltd., London, pp.100-112, 1994.

Wileman, R.H., Pneumatic Tires (sic.) vs. Steel Wheels for Tractors, *Agric. Engng.*, Vol.15, No.2, 1934.

Wills, B.M.D., Barrett, F.M., and Shaw, G.J., An Investigation into Rolling Resistance Theories for Towed Rigid Wheels, *J. Terramechanics*, Vol.2, No.1, 1965.

Wills, B.M.D., The Load Sinkage Equation of Theory and Practice, *Proc. 2nd Int. Conf. Int. Soc. Terrain Vehicle Systems*, Quebec, Canada, 1966.

Wismer, R.D., and Luth, H.J., Off-Road Traction Prediction for Wheeled Vehicles, Paper No.72-617, *Am. Soc. Agric. Engng.*, St. Joseph, Mich., Dec. 1972.

Wismer, R.D., and Luth, H.J., Off-Road Traction Prediction for Wheeled Vehicles, *J. of Terramechanics*, Vol.10, No.2, pp.49-62, 1973.

Wismer, R.D., and Luth, H.J., Off-Road Traction Prediction for Wheeled Vehicles, *Trans. Am. Soc. Agric. Engnrs.*, Vol.17, pp.8-10, 1974.

Wong, J.Y., and Reece, A.R., Soil Failure Beneath Rigid Wheels, *Proc. 2nd Int. Conf. Int. Soc. Terrain Vehicle Systems*, Quebec, Canada, pp.425-455, 1966.

Wong, J.Y., and Reece, A.R.,Prediction of Rigid Wheel Performance based on the Analysis of Soil Wheel Stresses, *J. Terramechanics*, Vol.4, No.1, pp.81-98, 1967.

Wong, J.Y., Discussion on "Prediction of Wheel-Soil Interaction and Performance using the Finite Element Method", *J of Terramechanics*, Vol.14, No.4, pp.249-250, 1977.

Wong, J.Y., *Theory of Ground Vehicles*, John Wiley and Sons, Inc., New York, 1978.

Wong, J.Y., On the Study of Wheel-Soil Interaction, *J of Terramechanics*, Vol.21, No.2, pp.117-131, 1984.

Wong, J.Y., *Terramechanics and Off-Road Vehicles*, Elsevier, Amsterdam, 1989.

Wood, R.K. and Burt, E.C., Soil-Tire (sic) Interface Stress Measurements, *Trans. Am. Soc. Agric. Engng.*, Vol.30, No.5, pp.1254-1258, 1987.

Woodruff, D.W., and Lenker, D.H., A Handheld Digital Penetrometer, *Am. Soc. Agric. Engnrs.*, Paper No.84-1038, 1984.

Wulfsohn, D. and Upadhyaya, S., Prediction of Traction and Soil Compaction Using Three-Dimensional Soil-Tyre Contact Profile, *J. of Terramechanics*, Vol.29, No.6, pp.541-564, 1992.

Yong, R.N., and Fattah, E.A., Prediction of Wheel-Soil Interaction and Performance using the Finite Element Method, *J. of Terramechanics*, Vol.13, No.4, pp.227-240, 1976.

Yong, R.N., Boonsinsuk, P., and Fattah, E.A., Prediction of Tyre Performance on Soft Soils Relative to Carcass Stiffness and Contact Areas, *Proc. 6th Int. Conf. Int. Soc. for Terrain-Vehicle Systems*, Vienna, Austria, Vol.2, pp.643-676, 1978.

Zink, F.J., Barger, E.L., Roberts, J., and Martin, T.E., Comparative Field Tests in Kansas of Rubber Tires (sic.) and Steel Wheels, *Agric. Engng.*, Vol.15, No.2, pp.51-54, 1934.

Appendix 1 Publications

A1.1 Published Papers

Paper Title: **Technical Evaluation of Earthworks Claims Under ICE 5th and 6th Editions of Contract**

by: **B.L. Staples**
G.S. Wood, BEng
M.C. Forde, BEng, MSc, PhD, MICE, MIHT, FINDT

Published in: The Proceedings of the Institution of Civil Engineers, Civil Engineering, Vol.92, May, pp.90-95, 1992.

Abstract

The annual value of earthworks claims is estimated to run into millions of pounds per year in the UK alone. Yet the approach to their evaluation is at times uncertain and unsatisfactory. The uncertainty lies in evaluating the change in ground conditions and the influence of any change upon the cost of the earthworks. Clauses 11 and 12 of the ICE Conditions of Contract 5th and 6th editions are discussed in relation to site investigations and earthmoving geotechnical conditions.

A worked example has been undertaken on London Clay, illustrating how a reduction of 24% in site soil shear strength results in an increase of 39.4mm in rut depth and 7.8% in rolling resistance. From this, plant productivity is seen to reduce by 37% compared with tender estimates.

Introduction

A typical major motorway construction contract could be of the value of £20 million - £60 million over a 12 month period. The earthworks component of such a contract could be up to £10 million. Although claims and disputes arise on contracts for all manner of reasons, one of the areas most prone to dispute relates to earthworks.

The United Kingdom's major highway client, the Department of Transport, has made considerable strides in clarifying earthworks design criteria and earthworks specifications in order to reduce areas of ambiguity and potential dispute. This has been achieved through the publication of a comprehensive specification relating to earthworks[1] and in the publication of Highway Advisory Note 44/91, Earthworks.[2] At the same time, the Conditions of Contract have been revised by the Institution of Civil Engineers. The contract normally used for such highway works is either the ICE Conditions of Contract, 5th edition[3] or the new ICE Conditions of Contract, 6th edition.[4]

Notwithstanding the major advances made in specification and contractual terms in recent years, situations still remain where genuine disputes can occur as a result of ground conditions which could reasonably have been foreseen by an experienced contractor.

Tender Site Data

In general terms, the Contractor is expected to have satisfied himself as to the ground conditions pertaining to the site of the construction work so far as is reasonable, and the given information made available to him by the Engineer to the works. The relevant clause is Clause 11, relating to Inspection of Site and Sufficiency of Tender. In the ICE Conditions f Contract, 6th edition, Clause 11 has been modified by inclusion of a new Clause

11 (1) The Employer shall be deemed to have made available to the Contractor before the submission of the Tender all information on the nature of the ground and sub-soil including hydrological conditions obtained by or on behalf of the Employer from investigations undertaken relevant to the Works.
The Contractor shall be responsible for the interpretation of all such information for the purposes of constructing the Works and for any design which is the Contractor's responsibility under the Contract.

and a new sub-clause

(3) The Contractor shall be deemed to have
(a) based his Tender on the information made available by the Employer and on his own inspection and examination all as aforementioned

There are a number of implications arising from this change to Clause 11 of the Conditions of Contract, 6th edition.

(a) The Engineer has a clear responsibility to make all factual data available to the Contractor. This could present problems, as it has been shown that factual information is only revealed for the first time in the interpretative part of site investigation reports.
(b) The Contractor will not be able to allege that he has not been given all of the available information, because the interpretative has been withheld - provided that all of the factual information has been included in the factual report.
(c) In order to meet the above conditions, the quality of site investigation reports will have to improve, for example by removing any possible ambiguity over the relative status and interpretation of borehole water strike levels and piezometer readings.

Problems During Construction

There are many types of problem that can occur with respect to earthworks on a major highway scheme. However, for the purposes of this Paper an example will be given that relates to the changing shear strengths encountered on a haul road from the Tender site investigation data to that in the Contract. Specifically, the example relates to the performance of a twin-engined scraper on a clay haul road. The haul roads on a highway project are typically the cut-and-fill surface layers as the Works proceed.

In general terms it is necessary for the Contractor to identify a problem and then decide whether this problem could, in his view, have been reasonably foreseen by an experienced contractor or not. If not, and the Contractor intends to make a claim under Clause 12 of the ICE Conditions of Contract, then he must give due notice to the Engineer to enable contemporary records to be taken.

In the 6th edition of the ICE Conditions of Contract, Clause 12 has been modified and split into three separate Clauses. Clause 12(1) calls for the earliest possible written notification to the Engineer of a Clause 12 situation; Clause 12(2) requires separate (or simultaneous) notification of the Contractor's intention to claim additional payment or extension of time. Of particular relevance to an earthworks claim is the fact that Clause 12(3) requires the Contractor, when giving notice under either Clause 12(1) or 12(2), to give details of the anticipated effects, the measures he has taken or is proposing to take and their estimated cost, and the possible delay or interference with the execution of the Works.

Once a problem has been identified in principle, it must then be carefully documented and quantified. In order to successfully make a claim under the ICE Conditions of Contract, 5th[5] and 6th editions it is essential that the Contractor puts forward a technically credible case demonstrating

the ground conditions which could reasonably have been anticipated at the time of tender, given the requirements of Clause 11, and then compare these conditions pertaining at the time of contract.[5] The Contractor must then demonstrate how the change in ground conditions affect the performance of the Contract, and in addition he must quantify the loss actually incurred as a result of these changing ground conditions. If the Contractor were to claim financing, then this would only be payable from the date that the loss was established. This could be many years after the money was spent if the dispute were to go to arbitration.[6]

It should be appreciated that in the above context the Contractor does not have to demonstrate that the material being encountered has changed from suitable to unsuitable, only that the material has changed in shear strength terms. Equally, the Contractor does not have to explain why the ground conditions have changed,[7] provided that he can demonstrate that the change is not 'due to weather conditions' which are specifically excluded from Clause 12.

Technical Quantification of a Claim

Quantification must be related to the changing ground conditions from the Tender stage to the construction phase in terms of the Contract. The example chosen for analysis relates to earthworks haul roads. Essentially, the Tender site investigation reports would have been carefully examined and the range of shear strengths relating to each of the areas to be excavated as cut for re-use as fill would have been identified. These shear strengths would then need to be related to Contract shear strength values. If there is a reduction in shear strength, which could not have been reasonably anticipated, then the Contractor would have to quantify the implications.

Case Example

Site Investigation and Contract Shear Strength Data

In order to illustrate the various points, the specific case example relates to the M25/M40 Interchange Contract at Denham. The earthworks were constructed during the 1983 summer earthmoving season using Terex TS-24 twin -engined scrapers of 1967 vintage. These machines were equipped front and rear with Detroit Diesel 8V-71N two-cycle diesel engines.[8]

The geotechnical conditions were principally the granular Reading Beds overlying brown weathered London Clay. Typical Atterberg limits for the London Clay were: w_L=70% and w_P=23%. The site investigation data was dated 1978.

Typically in a site investigation report, borehole data may be concentrated around bridge abutment sites. Thus it is necessary to estimate the 'missing' undrained shear strengths, c_u, from natural moisture contents and plasticity data. Shear strengths have been related to soil plasticity data by various workers.[9,10] In this context, consistency index has been found to be a useful normalising concept when relating moisture content to plasticity of the soil:

$$\text{Consistency Index} = I_c = \frac{w_L - w}{w_L - w_P}$$

It should be appreciated that the consistency index calculation should be carried out on the moisture content of the sample after adjustment for any fraction >425μm.[11] Care should be taken to take only the test results relating to the material that is actually to be moved. The full range of soil strengths encountered must be tested for the comparison to be valid.

For this site a graph was plotted of shear strength, c_u, against consistency index, I_c,-see Fig. 1. The correction for the fractional percentage >425μm was not necessary as the material was fine-grained

London Clay where almost 100% was finer than 425μm. Using this relationship between undrained shear strength and consistency index, it was now possible to take other data from the boreholes where only moisture content and liquid and plastic limits were available and then estimate the values of undrained shear strength. From these data it is possible to obtain a wider range of shear strengths for the site and plot a cumulative frequency graph at the time of Tender based on Denham (see Fig. 2).

At the time of Contract, the next step was to measure the in-situ shear strengths on first ass cut-and-fill material, prior to repeat trafficking by earthmoving plant. From these data it was possible to obtain a cumulative frequency plot of shear strength for the time of contract - also plotted on Fig. 2. The undrained shear strength data from the time of contract was obtained using a Pilcon hand vane. Additionally it was possible to develop a relationship between first pass undrained shear strength and the rut depth of the earthmoving plant - see Fig. 3. These shear strengths and rut depth relationships could then be used to evaluate Contract earthmoving performance. If a significant number of in-situ shear strengths were to prove $>130kN/m^2$, then triaxial samples would need to be taken above this figure as the pilcon hand vane is restricted to this upper shear strength measurement limit. At the Denham site this did not prove to be a significant problem.

From the cumulative frequency versus shear strength plots comparing Tender and site[9] measured shear strength, see Fig. 2, it can be seen that there is a 24% reduction in the average shear strength between that in the Tender site investigation report and site measurements. As a simplification, if one takes these mean values of shear strength it is possible to estimate the average rut depth at Tender as being 50.8mm and at Contract as being 90.2mm (see Fig. 3). All rut depths were measured after the passage of plant from the bottom of the rut to the top of the soil either side of the rut - no account was taken of transient elastic deformations which recovered. The relationship given in Fig. 3 yields lower rut depths for a give shear strength than reported by Farrer and Darley.[12] In practice, when evaluating an earthworks claim, one would build up a picture of the entire project. This would have to be undertaken systematically haul road by haul road and area by area - using specific shear strength data.

Timed Performance Analysis

A field performance analysis was carried out on a Terex TS-24 twin-engined over a specific length of haul road. The haul route under study was split into sections marked with distances and grades (see Fig. 4).

Back Analysis

From this field study carried out on the Terex TS-24 twin engined scraper over the haul road in Fig. 4, it was possible to perform a back analysis using the manufacturer's performance data and the vehicle's weight/power ratio in order to establish the performance of the plant over each section of the haul road (see Table 1).[13] The weight/power ratio refers to the average power delivered to the ground. The imbalance between the vehicle's motion producing forces and the roads and vehicles motion resisting forces determines the acceleration or deceleration of the vehicle. The process is simplified by expressing all of the motion resisting forces: rolling resistance, road grade, inertia, and air drag, as an equivalent percent grade.

From laboratory experimental work on London Clay and Cheshire Clay at a range of consistencies, it has been shown that there is a linear relationship between rolling resistance and sinkage for clay soils.[14,15] Therefore, if the site rolling resistance were 18.0% equivalent grade, as per the back analysis, then the rolling resistance at the time of Tender would have been 10.2% equivalent grade.

It was then demonstrated theoretically how the performance of the TS-24 would change as the rolling resistance of the haul road steadily increased. Fig. 5 shows the relationship between rolling

resistance and average speed. It is clear that the speed of the vehicle is most sensitive at lower values of rolling resistance, i.e. below 12%. Taking the average rolling resistance at the time of Tender (10.2%) and at the time of Contract (18%) it can be seen from Fig. 5 that there is a reduction of 37% in the average running speed of the vehicle. Fig. 6, depicting the relationship between rolling resistance and total payload per hour is clearly directly related to the average speed of travel. By using the above rolling resistance values one obtains a production reduction of 37%. Therefore, for a fixed volume of soil to be transported the decrease in average velocity results directly in an increase of 57.3% to the time required by the earthmoving plant during the Contract over the Tender estimates, assuming the same amount of plant is employed (see Table 1).

Figure 7 shows the effect rolling resistance has on the rate of fuel consumption for the Terex TS-24. By applying the above rolling resistance values to Fig. 7 it can be observed that there is a 50% increase in the amount of fuel used per trip over that which would have been estimated from the original site investigation data.

From a cost point of view it is apparent that the fuel bill will be a lot higher than that predicted from the Tender data. Adding this amount to the increased hire charge of the plant due to the prolonged duration of the earthmoving, the hiring of extra plant and the increased haul road maintenance costs due to increased rut depth, the total cost of the project will increase disproportionately to the decrease in shear strength from the Tender data to the site measured results.

The above example is simplified in a number of ways, but forms the basis for a more detailed analysis and evaluation of an earthmoving project.

Final Remarks

Areas of dispute in relation to earthworks problems have been identified and relevant differences between the 5th and 6th editions of the ICE Conditions of Contract have been highlighted in relation to Clauses 11 and 12.

A simplified analysis has been undertaken relating to a time trial on a haul road on a specific site on London Clay using twin-engined scrapers. It has been shown, in this simplified example, that a 24% reduction in average shear strength from the time of Tender to the time of Contract could yield a 57% increase in the time taken by the earthmoving plant to move the same quantity of material, together with a 55% increase in fuel used.

Acknowledgements

The authors wish to acknowledge the fieldwork undertaken and supervision given by C. Helm, J. Watts and P. Johns and the provision of facilities by Professor J.M. Rotter, Head of the Department of Civil Engineering, University of Edinburgh. The work was supported financially by Tarmac Construction Limited.

References

1. Department of Transport, *Specifications for Highway Works*, part 2, Series 600, Earthworks, 1986, HMSO, London.

2. Department of Transport, *Highway Advisory Note 44/91*, Earthworks, 1991, HMSO, London.

3. Institution of Civil Engineers et al., *ICE Conditions of Contract*, 5th Edition, ICE et al. London, 1986.

4. Institution of Civil Engineers et al., *ICE Conditions of Contract*, 6th Edition, ICE et al. London, 1991.

5. Institution of Civil Engineers et al., *ICE Conditions of Contract 5th and 6th Editions Compared*, Thomas Telford, London, 1991.

6. *McGregor (Contractors) Ltd. Versus Grampian Region*, Arbitration (1986).

7. *Sir Alfred McAlpineLtd. Versus Berkshire County Council*, Arbitration 1984.

8. Terex Ltd. *Terex TS-24 Performance Handbook, Form no.322*, Terex Limited, Motherwell, Scotland.

9. Skempton, A.W., and Northey, R.D., The Sensitivity of Clays, *Geotéchnique*, 1952, **3**, pp.30-53.

10. Whyte, I.L., Soil Plasticity and Strength - A New Approach Using Extrusion, *Ground Engineering*, 1982, **15**, No.1, pp.16-24.

11. Forde, M.C., Discussion, *Clay Fills*, ICE, London, 1979, pp.263-265.

12. Farrer, D.M., and Darley, P., *The Operation of Earthmoving Plant on Wet Fill*, Transport and Road Research Laboratory, Crowthorne, Berks., 1975, Report 688.

13. Pugh, R.D., *The Accelerator Vehicle Performance Software*, Accelerator Inc., Florida, 1987.

14. Forde, M.C., *Wet Fill for Highway Embankments*, University of Birmingham, PhD Thesis, 1975.

15. Gee-Clough, D., The Bekker Theory of Rolling Resistance Amended to Take Account of Skid and Deep Sinkage, *J. Terramechanics*, 1976, **13**, No.2, pp.87-105.

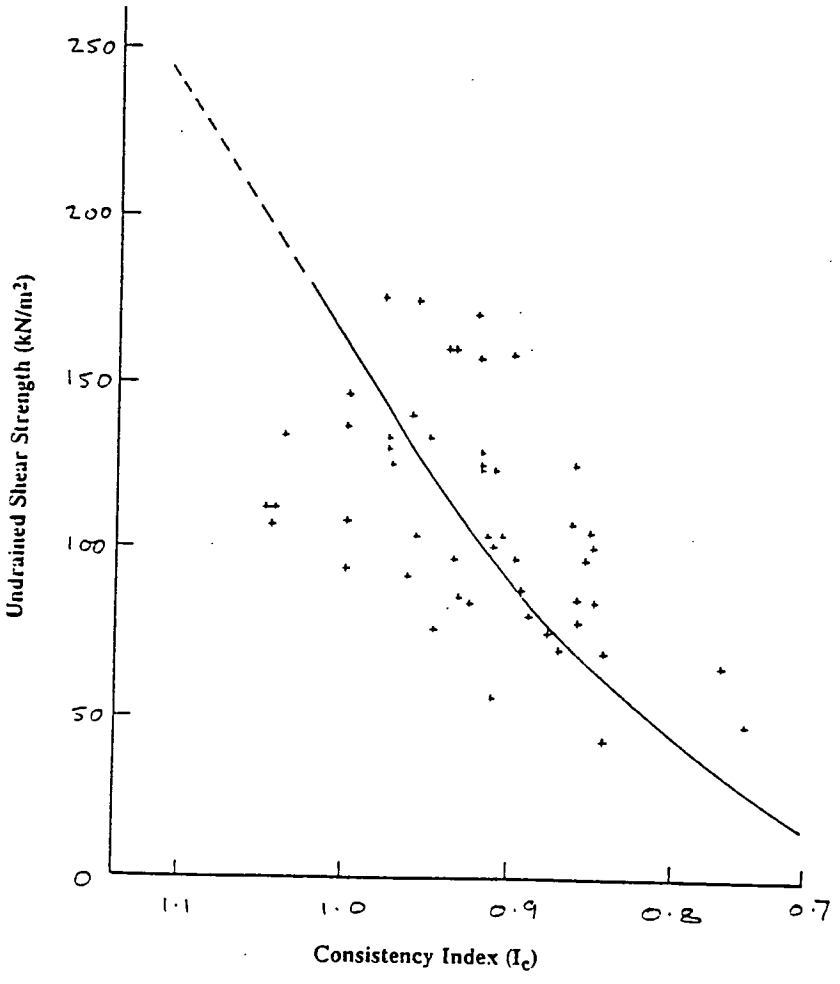

Figure 1

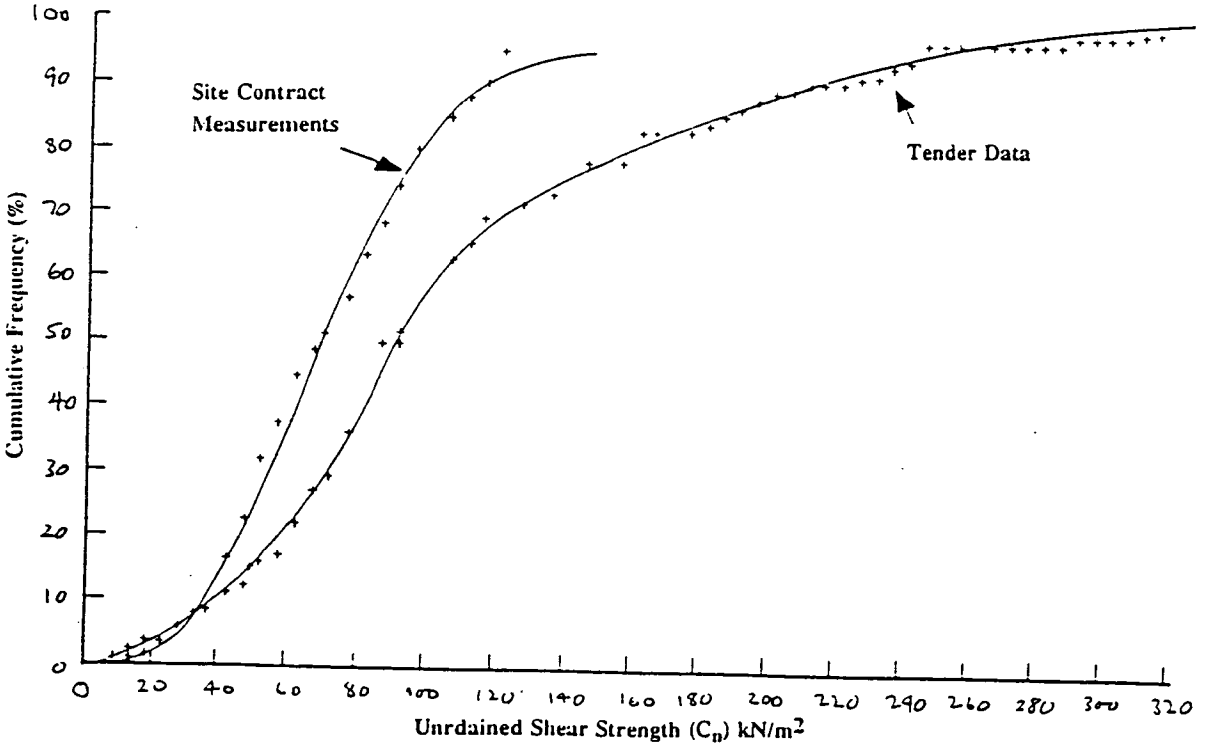

Figure 2

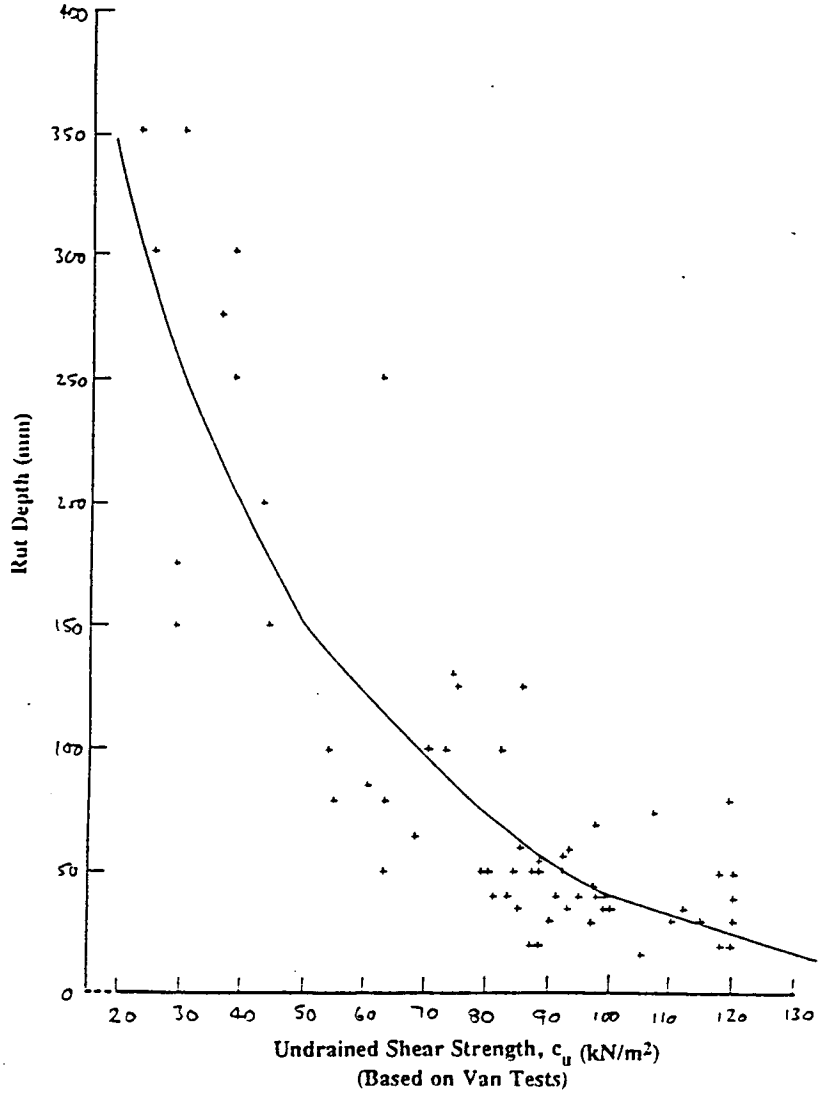

Figure 3

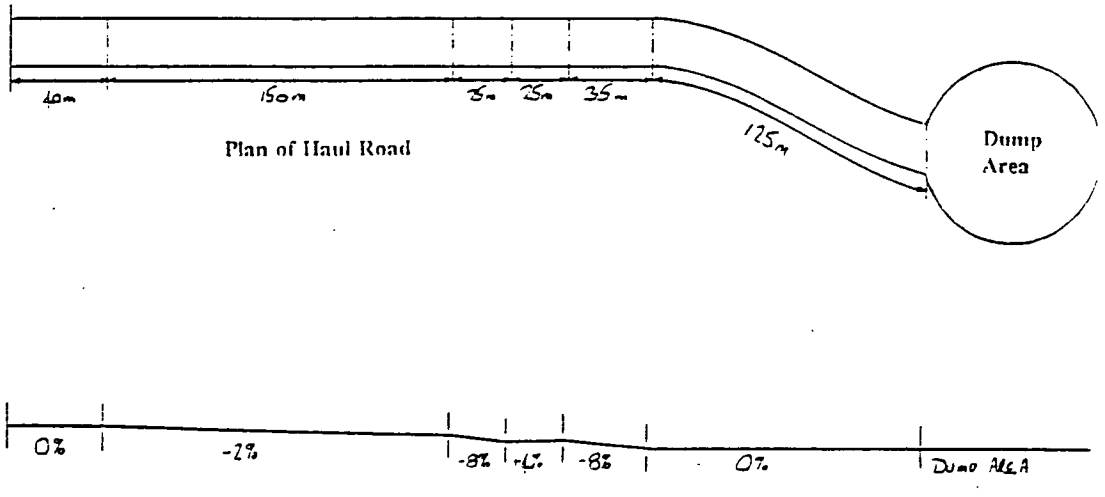

Cross-Section Showing Haul Gradients

Figure 4

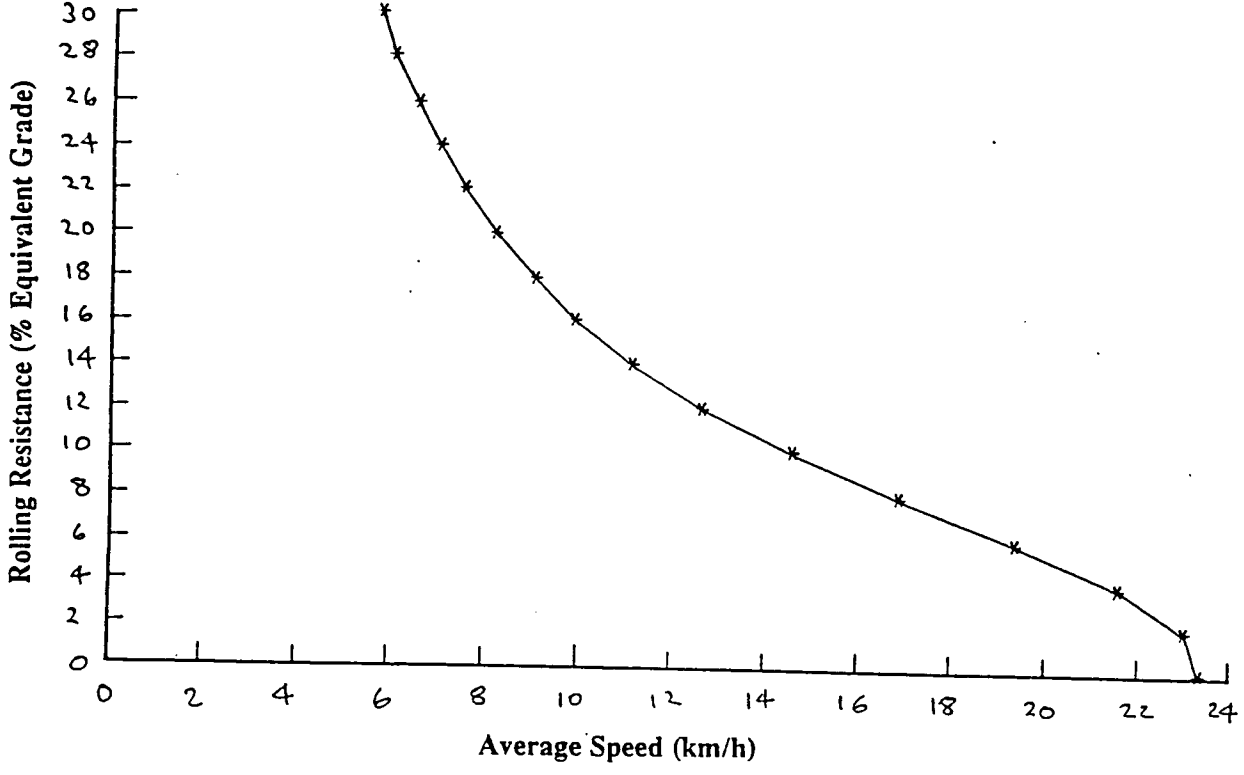

Figure 5

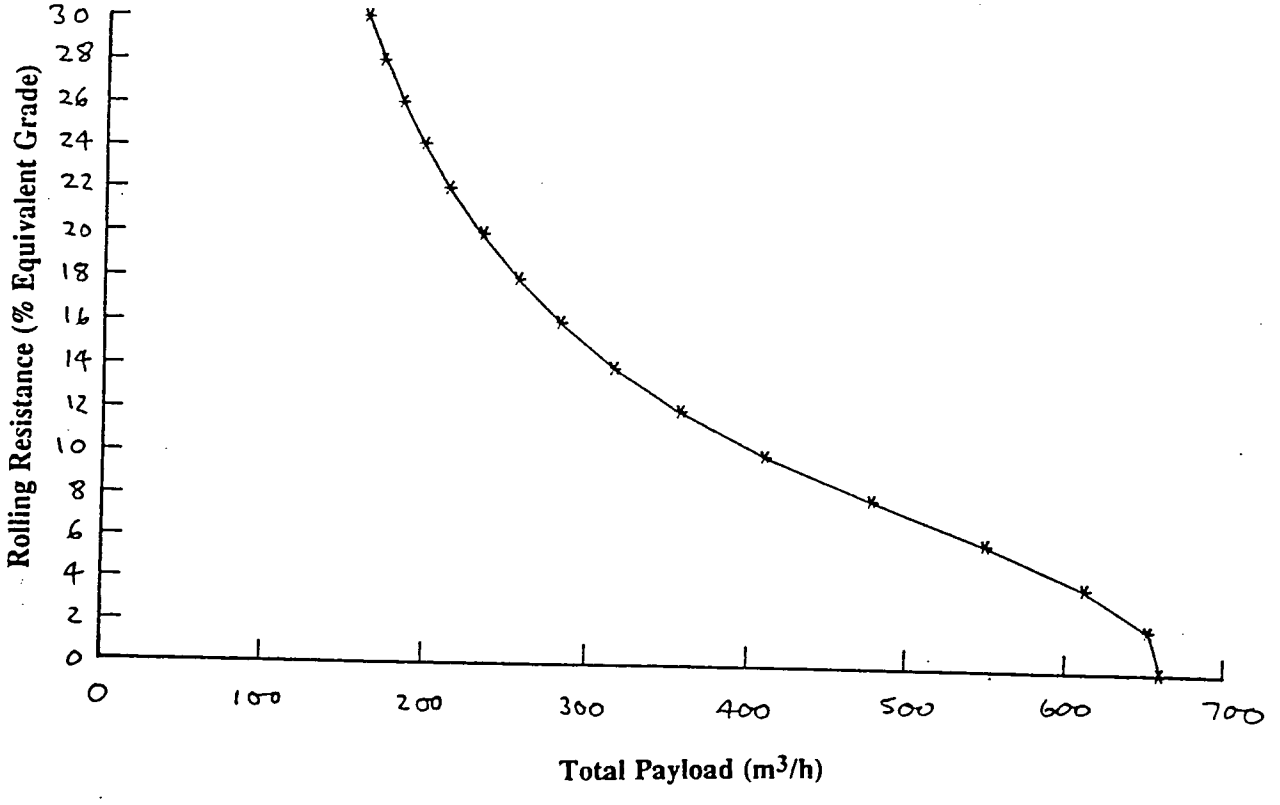

Figure 6

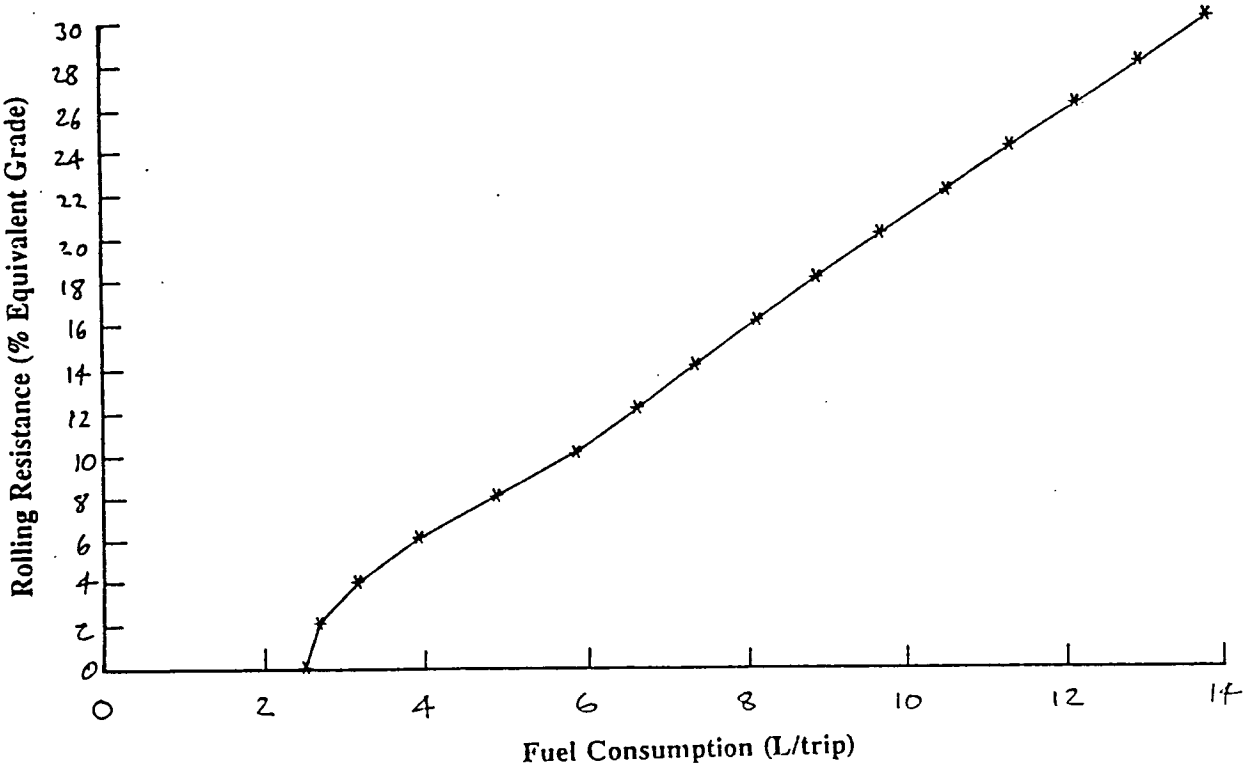

Figure 7

		Tender Site Investigation Analysis Rolling Resistance = 10.2%				Contract Analysis Rolling Resistance = 18%			
Section	Grade (%)	Entry Speed (km/h)	Top Speed (km/h)	Exit Speed (km/h)	Time (min)	Entry Speed (km/h)	Top Speed (km/h)	Exit Speed (km/h)	Time (min)
1 - Loaded	0	0.0	13.5	13.5	0.21	0.0	7.8	7.8	0.32
2 - Loaded	-2	13.5	17.0	17.0	0.55	7.8	8.7	8.7	1.03
3 - Loaded	-8	17.0	23.9	23.9	0.07	8.7	13.4	13.4	0.13
4 - Loaded	4	23.9	23.9	13.1	0.08	13.4	13.4	6.4	0.21
5 - Loaded	-8	13.1	24.5	24.5	0.11	6.4	13.6	13.6	0.18
6 - Loaded	0	24.5	24.5	0.0	0.51	13.6	13.6	0.0	0.96
7 - Dump	0	0.0	0.0	0.0	0.70	0.0	0.0	0.0	0.70
8 - Empty	0	0.0	25.2	25.2	0.35	0.0	14.6	14.6	0.53
9 - Empty	8	25.2	25.2	15.6	0.11	14.6	14.6	10.1	0.20
10 - Empty	-4	15.6	25.3	25.3	0.07	10.1	17.6	17.8	0.10
11 - Empty	8	25.3	25.3	17.2	0.07	17.6	17.6	10.1	0.13
12 - Empty	2	17.2	21.5	21.5	0.43	10.1	13.2	13.2	0.69
13 - Empty	0	21.5	23.1	0.0	0.16	13.2	14.6	0.0	0.20

Table 1

A1.2 Papers Accepted for Publication

Paper : **Soil Parameters for Estimating the Rolling Resistance of Earthmoving Plant on a Compacted Silty Cohesive Soil**

by: **G.S. Wood, B.Eng.***
J.R. Osborne, B.Sc., C.Eng., MICE†
M.C. Forde, B.Eng., M.Sc., Ph.D., C.Eng., MICE, MIHT, FINDT‡

Accepted by: The Journal of Terramechanics

Abstract

The performance of earthmoving plant is currently estimated through experience, often with no more than a limited inspection of the site investigation report. On site the absolute speed of the plant is seldom considered to be critical as long as the vehicles keep moving.

The different factors that affect the speed of the plant on the haul roads are discussed. The various soils tests that were carried out as well as how they relate to the apparent rolling resistance of the driver-vehicle-haul road system are discussed. Also the reasons why certain tests are inadequate for the estimation of the performance of earthmoving plant are discussed. It is shown that the speed of the plant can be estimated from the data contained within the site investigation report, and it can be continually monitored throughout the life of the contract, by using consistency index.

Introduction

The value of a typical motorway contract in Britain, generally runs at a value of approximately £2M / km, of which up to 20% can be attributed to earthmoving. Despite this, the costing of an earthmoving project in Britain is predominantly experience based utilising productivity information gained on previous sites with similar plant. This method of estimation is prone to error and does not enable the contractor to estimate the contract cost accurately enough at the time of tender or for a design and build type contract, or to quantify his losses easily in a claims situation[1].

Very little work has been carried out in the past relating the speed of the plant to soil conditions, with respect to civil engineering vehicles on haul roads. The majority of work has been carried out by the agricultural engineers on firm but uncompacted soils[2,3] and by the military engineers on virgin terrain[4]. Manufacturer's speed charts and various computer packages are available to the estimator to help estimate the speed of the plant on site. However they all rely on the parameter rolling resistance which is never defined accurately enough for general use and are lacking in data at the higher values of rolling resistance. Even the developers and professional users of the software gauge the value of rolling resistance through limited experience.

Rolling Resistance

Rolling resistance is a measure of the force that must be overcome to drive the wheels over the ground. Some of the factors that affect rolling resistance are:

---

* Research Student, Department of Civil Engineering, University of Edinburgh.
† Operations Director, Tarmac Structural Repairs, Wolverhampton.
‡ Tarmac Professor of Civil Engineering Construction, University of Edinburgh.

1. Soil type, a wheel will react differently in a clay or sand;
2. Condition of the haul road, a rutted road will cause a much higher rolling resistance than a smooth one;
3. Wheel loading, a loaded vehicle will have greater rolling resistance than an empty one;
4. Tyre and road flexing, this causes the vehicle to always be climbing out of a rut, the greater the flexing the larger the rolling resistance;
5. Internal friction any mechanical losses between the engine and the wheel will increase rolling resistance and finally;
6. Driver, if the operator is not wanting to drive as fast as the machine is capable, due to vibrations, health reasons, or because he will have to wait at the loader, then he will slow the vehicle down, giving an apparent rolling resistance which will be greater than the true rolling resistance.

This last effect is important as it is done subconsciously and cannot be accounted for at the estimating stage. It is therefore essential that the correct matching of plant on site is achieved, since it is better to slightly under resource than over resource an operation. An excellent discussion on motion resistance of tyres and tracks, and a review of some physical interpretations of motion resistance are given by Upadhyaya et al.[5].

Rolling resistance is expressed as a percentage of vehicle weight and can be added to grade resistance, uphill grade positive, to give total resistance. Total resistance is a useful parameter when working with manufacturers' rimpull - speed - gradeability curves, or with the various computer programmes.

Two computer programmes were initially used in this study to back analyse the rolling resistance, Vehsim[6], developed by Caterpillar and Accelerator[7]. Both can be used in the estimating of productivity for any earthmoving operation. Figure 1 shows the relationship between maximum attainable velocity and total resistance for a partially loaded Volvo BM A25 6x6 articulated dump truck, using both the Volvo handbook[8] and the two computer programmes. All the methods compare well when the vehicle is travelling uphill, but the Vehsim program has no provision in the software for the retarder on the machine, when travelling downhill. For this reason the Accelerator programme was used throughout the analysis of the results. Similar graphs can be constructed for other vehicles and for vehicles with varying payload.

Practical guidelines given by manufacturers on the value of rolling resistance is very scarce and comes in the form of a description of the haul road, which is unknown prior to the start of the operation, e.g.[9]

A dirt roadway, rutted or flexing under load, little if any maintenance, no water, 50mm tyre penetration or flexing	5%
Rutted dirt roadway, soft under travel, no maintenance, no stabilisation, 100mm tyre penetration or flexing	8%
Rutted dirt roadway, soft under travel, no maintenance, no stabilisation, 200mm tyre penetration and flexing	14%

The above classifications are all applicable to civil engineering type haul roads. Using these rolling resistances the range in speeds varies between 9 and 26km/h for a 75% rated payload Volvo BM A25 6x6 articulated dump truck, assuming a flat haul road, from figure 1, using the Accelerator program.

Earthworks Site Utilised

Monitoring and soil testing were carried out on the A1/M1 link contracts 2 and 3, during the 1992 earthmoving season and early into the 1993 season. The contracts were 28km in total length with a total volume of 3 million m^3 of soil to be moved. The earthworks were constructed using predominantly a backhoe/dump truck combination. The haulers were primarily a mixture of Cat D400D, Volvo BM A25 6x6, Volvo BM A30 6x6 and Volvo BM A35 articulated dump trucks.

The site investigation was carried out by five companies over a period of 11 years. Typically the material was a brown silty clay, with over 80% passing the 425μm sieve, figure 2. Average Atterburg limits were w_L = 47% and w_P = 22%. The haul roads were generally in good condition although flexing was apparent under most sections of the haul roads during trafficking. The material on the haul roads was generally dry of the plastic limit, remoulded and well compacted. Rut depths were minimal, but a layer of loose dry material accumulated on the surface with trafficking. Work was halted during prolonged periods of rain to preserve the condition of the haul roads and then left to dry adequately prior to re-trafficking.

Site Monitoring

All the site monitoring had to be undertaken from the side of the haul road as no instrumentation of, or interference with, the operation of the plant was possible. Timings of vehicles were taken over 60m sections of the haul road, where the vehicles could be assumed to be travelling at a steady velocity on a constant grade with no obstructions. Timings were averaged from at least 10 passes of a similar type of dump truck. Each section was surveyed to ascertain its length and gradient. Four soil samples were taken at 20m intervals along the section and the following soil tests were carried out at each point: moisture content; moisture condition value, MCV; cone penetrometer and shear vane. Along with these tests a series of plastic and liquid limits, particle size distributions and multistage triaxial tests were carried out on a representative sample of the material.

From the knowledge of the timings and gradients it was possible to use the charts developed using the Accelerator simulation, to back analyse the apparent rolling resistance for each section of the haul road.

Laboratory Soils Testing: Classification and Undrained Shear Strength

Soil Classification

From the soil samples taken on the haul roads the average plastic and liquid limits were 20% and 50% respectively, taken from a sample size of 46. Variation throughout the site was minimal and dependent on the depth of the haul road from the original ground level and to a lesser amount the position along the site. The envelope of particle size distributions is shown in figure 2, this was derived from 23 wet sieving and hydrometer tests, with a minimum of 88% passing the 425μm sieve. The particle size distribution again varied along the length of the haul road and also in vertical profile. The site investigation results indicate that the soil has a slightly narrower plasticity index, hence would be more susceptible to moisture content change. All tests were carried out in accordance with BS1377[10], 1990.

Multistage Undrained Triaxial Shear Tests

The multistage undrained triaxial shear tests were carried out using 100mm diameter remoulded samples. The tested samples can be assumed to replicate the field conditions as the haul roads have been heavily trafficked and maintained using a grader, thus causing severe disturbance to the surface of the haul road, followed by recompaction of the soil as the plant continues to traffic.

The test procedure involved the sample being broken up and sieved through a 5mm sieve and air dried before mixing to the required moisture content. It was then covered in polythene and allowed to equilibrate for at least 24 hours. The sample was then placed into a mould and extruded into a membrane for testing. The sample was then mounted in a triaxial cell. For testing the confining cell pressure was increased from 1 to 2 to 4kPa as the deviator stress-strain curve approached a constant. This method of testing yields three Mohr's circles on a sample with constant moisture content which is difficult to achieve with separate tests. The axial strain rate was held at 2%/min. The sample was assumed to be near saturated, and this is confirmed in that the maximum angle of internal friction was below 3°. Hand vane shear strengths were taken at each end of the sample after testing and four moisture contents were taken from the sample, one prior to the test and three after the test, one from each end and one from the centre, all of these values showed under 2% variation.

Shear strengths have been related to soil plasticity data by various workers [11,12]. In this context consistency index, equation 1 has been found to be a useful normalising concept when relating moisture content to the plasticity of the soil:

$$\text{Consistency Index, } I_C = \frac{W_L - W}{W_L - W_P} \quad (1)$$

where: W_L - liquid limit
W_P - plastic limit
W - corrected moisture content.

Where the corrected moisture content is the correction to the natural moisture content after adjustment for any fraction > 425μm, which is assumed to have a moisture absorption of 4%, equation 2.

$$W = \frac{W_N \text{ x } 100\% \text{ - } 4\% \text{ x } \% > 425\mu m}{\% < 425\mu m} \quad (2)$$

where: W_N - natural moisture content.

The results of the multistage triaxial tests, figure 3, show a curvilinear relationship between undrained shear strength and consistency index given by equation 3 with R^2 value of 0.97.

$$c_u = 0.79e^{(4.94I_c)} \quad (3)$$

This graph shows that the soil is very susceptible to changes in moisture content, dropping from a shear strength of 110kN/m^2 at the plastic limit, to a value of around 40kN/m^2 at a consistency index of 0.80. These results compare well with the findings of Whyte[12], whose equation relating undrained shear strength and consistency index, gives undrained shear strength values of 47kN/m^2 and 110kN/m^2 at consistency indices of 0.8 and 1.0 respectively.

The experimental relationship can be compared with similar site investigation data, figure 4. From this graph, showing the data from five commercial site investigation companies, it can be seen that there is considerable variation in the site investigation data.

The shift in emphasis towards design and construct projects may result in more detailed research quality site investigations making the above analysis more viable at the time of tender.

There is also a strong relationship between undrained shear strength and vane shear strength, taken in the sample after the completion of the test, figure 5. The shear vane is a quick and useful test to do at this stage as it can characterise the soil and be used in the field easily. The cluster of values at the high end of the graph is because the vane can only read to a maximum of 174kN/m².

Site Testing and Results in Relation to Rolling Resistance

Moisture Condition Value versus Rolling Resistance

The moisture condition value (MCV) test developed at TRRL[13,14] is being used extensively on road construction projects for determining the acceptability of fill material. The moisture condition apparatus works on the principle that there is a direct relationship between maximum bulk density, compactive effort and moisture content, and that shear strength is a measure of acceptability. The test is carried out by placing a 1.5kg sample of material, passing a 20mm sieve, in the mould. A fibre disc is placed on the top of the sample, the rammer is dropped through a height of 250mm onto the sample and the penetration into the mould is recorded. The process is then repeated with readings of penetration being recorded after a selected number of blows. The test is completed when the change in penetration between n and $4n$ blows is less than 5mm. The change in penetration is plotted against the initial number of blows and the best fit line drawn through the points. The moisture condition value is defined as 10 x log(n), where n is the number of blows at which the change in penetration equals 5mm, from the best fit line.

The benefits of this test are that it is relatively quick to complete and that it gives an almost instantaneous result, which would make the MCV an ideal method for estimating the speed of the plant both at the tender and construction stages of an operation. Figure 6 shows the relationship between rolling resistance and MCV for a loaded Cat D400D articulated dump truck split into both uphill and downhill grades. The graph indicates little to no trend in the data, except that as the MCV increases the rolling resistance decreases slightly and that uphill grades generally exhibit lower rolling resistances than corresponding downhill grades. At any single value of MCV the rolling resistance could vary by up to 4%. The explanation for the lower apparent rolling resistance uphill is that the driver is apt to utilise full throttle on the ascents, but will not accelerate when descending.

Several limitations can be noted about the MCV test on this silty clay, firstly there is no single value of MCV for an individual sample, MCV depends on how the sample is broken up and placed in the mould for testing. If the sample has bulked too much to fit in the mould then some initial compaction is required in order to fit the fabric disc to the top of the sample. If the sample is very dry then the test does not appear to be sensitive enough to pick up variations in the moisture content, which could relate to large decreases in shear strength.

Knowing there is a relationship between shear strength and consistency index, figure 7 was plotted, showing the relationship between MCV and consistency index. This figure shows the information both from the site investigation report and the work carried out on site. Both sets of results show that there is a distinct trend, but there is a large data spread, e.g. taking a consistency of 1.1, the MCV varies from 9.5 to 17 from laboratory data and from 9 to 20 from the site investigation data.

Cone Index versus Rolling Resistance

The hand held cone penetrometer[15] was developed by the American army to determine if an area of ground was passable for military vehicles. From its inception it has been used to predict the performance of vehicles in both frictional and cohesive materials[16,17]. Various sizes of cone exist, but the one used in this study was a 30° cone, 30mm high, see reference 15 for a description and measurement procedure. The cone gives outputs as in figure 8, showing the average cone index at four points along a section, each line is an average of six readings of similar variation. The data shows no constant trend and it was therefore considered impossible to try to predict the speed of the

plant from this data. The primary problem of the cone is that it is very small in comparison to a wheel. When encountering a stone the cone attempts to push it, thus shearing a far larger area of soil, reporting a far larger erroneous result.

Vane Shear versus Rolling Resistance

The shear vane also has the advantage of giving a rapid result. This method of determining the shear strength of the soil works by failing the soil along a specific plane. The vane was designed for calculating the undrained shear strength of clays and the theory for calculating the undrained shear strength of the soil is based on equation 4. It is assumed that for a clay the undrained angle of shearing resistance is zero therefore equation 4 can be simplified to equation 5.

$$\tau = c_u + \sigma \tan\phi_u \qquad (4)$$

where: τ - undrained shear strength
c_u - undrained cohesion
σ - normal stress
ϕ_u - undrained angle of shearing resistance

$$\tau = c_u \qquad (5)$$

As the vane is calibrated for a specific failure plane, therefore if there is any obstruction along the periphery of the shear plane the displayed resistance will be artificially high.

The vane used on site was a 19mm diameter, 38mm high shear vane, with a maximum reading of 174kN/m^2. This was used to measure the surface vane shear strength of the haul road. The rate of shear was kept constant at approximately 60°/s, the shear rate was kept high as it was more akin to wheel loading. At least three readings were taken at each point within the section and these were averaged to give an overall value for each section. The measured vanes were corrected in accordance with Bjerrum[18].

Figure 9 shows the relationship between rolling resistance and vane shear strength for a loaded Cat D400D articulated dump truck. The cluster of points at the high vane shear strengths is caused by the limitation of the apparatus, these points could all move to the right of the graph by some unknown amount. There is a clear split between the uphill and downhill grades, the uphill grades showing lower rolling resistances by approximately 2%. The reason for this split is unexplained, but is probably due to the fact that the driver will be psychologically more apt to maintain full throttle when travelling uphill. Figure 10 shows similar results for an empty machine, again the downhill grades show an increased apparent rolling resistance. In this case apparent rolling resistance has increased at the higher vane shear strengths making it almost independent of the vane shear strength. This may be due to the drivers not willing to travel faster than a certain speed, as doing so would cause uncomfortable vibrations for them in the cab.

The limitations of using this method to predict the speed of the plant are that very few hand vanes are performed at the site investigation stage, and that there is an upper limit restriction when using the vane.

Consistency Index versus Rolling Resistance

As shown previously in figure 3, consistency index can be a good measure of undrained shear strength. The difficulty in calculating the consistency index lies in the determination of the plastic limit. This test is carried out by rolling a thread of clay paste between the palm of the hand and a glass plate until it cracks when 3mm diameter. This is repeated on subsamples eight times to ensure the correct value is determined. The main problem with the test is that it is heavily operator

dependent, as every operator applies a different pressure and considers the sample to have failed at a different stage[19].

Figures 11 and 12 show the relationship between rolling resistance and consistency index for a loaded and empty Cat D400D articulated dump truck respectively. The downhill grades have a higher apparent rolling resistance than the uphill grades, for reasons explained previously.

Experimentally the consistency index has the advantage over the vane method in that there is no restriction on the size of the data range. Another advantage is that consistency indices can be calculated from the information given in the site investigation report, making prediction possible at the tender stage. The accuracy of any estimation relies wholly on accurate input, and as has been shown in figure 4 site investigation data can be misleading. For on site checking a value for the consistency index can be estimated from the corrected moisture content of the soil, as the Atterburg limits should not change considerably for a particular soil, which may have been tested previously.

Figure 12 shows that for an empty Cat D400D, as the consistency index increases, the soil becomes drier, the apparent rolling resistance increases slightly, which is contrary to what would have been expected. This increase in apparent rolling resistance represents a drop in speed from 28km/h to 21km/h, whereas a similar change in consistency index for a loaded machine would increase the speed from 18km/h to 28km/h. This increase in speed is far more important to the overall productivity, as the vehicle travels in a laden condition for a greater proportion of the complete cycle time, due to the lower speed of the laden vehicles.

Figures 13 and 14 compare the best fit relationships of rolling resistance and consistency index for three types of articulated dump truck Cat D400D, Volvo BM A30 6x6, and Volvo BM A35 6x6, in both the loaded and empty states. As would have been expected, all vehicles show similar characteristics in the loaded state, figure 13, especially on downhill grades where the apparent rolling resistances are almost identical. The Caterpillar machine shows the same trend as the Volvo machines on the uphill grades but at a slightly greater value of rolling resistance. The reasons for this are unclear as the machines or drivers cannot be instrumented. Unloaded there is no information available on the Volvo machines travelling uphill, but the trend would be expected to be parallel to the downhill grades, as in all the other cases, and about 2% lower. The Volvo machines experience a higher apparent rolling resistance at lower values of consistency index, but this decreases as consistency index increases, unlike the Caterpillar vehicle. This discrepancy is considered to lie in the different suspension methods between the two machines, causing two completely different dynamic responses at the driver.

Conclusions

It has been shown that the rolling resistance of a vehicle is related to the shear strength of the soil and is best displayed in terms of consistency index, as there is a limit on the maximum shear strength a hand shear vane can measure.

It is possible to estimate the speed of the plant from the site investigation report, as long as the results contained within the report are accurate.

The driver-vehicle combination reacts differently to gradients, going uphill at an apparently lower rolling resistance than downhill.

The apparent rolling resistance of an empty Caterpillar D400D articulated dump truck increases as the haul road increases in strength, but the corresponding increase in loaded speed would outweigh this effect.

The Volvo and Caterpillar machines have different types of suspension possibly contributing to variations in the performance of the vehicles.

Acknowledgements

The authors wish to acknowledge the laboratory work undertaken by Mr Colin Lambton and the provision of facilities by the University of Edinburgh. The work was supported financially by an SERC Case studentship and Tarmac Construction Limited, Wolverhampton.

References

1. Staples, B.L., Wood, G.S. and Forde, M.C., Technical Evaluation of Earthworks Claims Under ICE Conditions of Contract 5th and 6th Editions, Proc. of the Institute of Civil Engineers, Civil Engineering,Vol.92, pp.90-95, May 1992.

2. Wulfsohn, D. and Upadhyaya, S.K., Prediction of Traction and Soil Compaction using 3D Soil-Tyre Contact Profile, Journal of Terramechanics, Vol.29, No.6, pp.541-564, 1992.

3. Alcock R. and Wittig V., An Empirical Method of Predicting Traction, Journal of Terramechanics, Vol.29, No.5, pp.381-394, 1992.

4. Turnage G.W., Tire Selection and Performance Prediction for Off-Road Wheeled-Vehicle Operations, Proc. 4th Int. Conf. ISTVS, Vol.1, pp61-82, Stockholm, Sweden.

5. Upadhyaya, S.K., Chancellor, W.J., Wulfsohn, D. and Glancey, J.L., Sources of Variability in Traction Data, Journal of Terramechanics, Vol.25, No.4, pp.249-272, 1988.

5. Caterpillar, Vehsim - Vehsim Simulation Software User's Guide, Version 2.21, Caterpillar Inc., Peoria, Illinois, U.S.A., 1987.

6. Accelerator, Accelerator Vehicle Performance Software User's Guide, Version 1.17, Accelerator Inc., Fort Myers, Florida, U.S.A., 1987.

7. VME Performance Manual Volvo BM Articulated Haulers, Edition 2, Växjö, Sweden, 1989.

8. Caterpillar Performance Handbook, 24th Edition, 1993.

9. BS1377, Parts 1-9, BSI, 1990.

10. Skempton, A.W. and Northey, R.D., The Sensitivity of Clays, Geotechnique, Vol. 3, pp.30-53, 1952.

11. Whyte, I.L., Soil Plasticity and Strength - a New Approach Using Extrusion, Ground Engineering, Vol.15, No.1 pp.16-24, Jan. 1982.

12. Parsons, A.W., The Rapid Determination of the Moisture Condition of Earthwork Material, Dept. of the Environment, TRRL Report LR750, Crowthorne 1979.

13. The use and Application of the Moisture Condition Apparatus in Testing Soil Suitability for Earthworking, Scottish Development Dept., Technical Memorandum SH7/83 amendment No.1, 1989.

14. ASAE, Soil Cone Penetrometer. American Society of Agricultural Engineers, Standard S313.2, 1985.

15. Freitag, D. R., A Dimensional Analysis of the Performance of Pneumatic Tyres on Soft Soils, Technical Report No.3-688, U.S. Army Engineering Waterways Experimental Station, CE, Vicksburg, Mississippi, U.S.A., Aug. 1965.

16. Wismer, R.D., and Luth, H.J., Off-Road Traction Prediction for Wheeled Vehicles, Paper No.72-617 ASAE, St. Joseph, Michigan, U.S.A., Dec1972.

17. Bjerrum, L., Problems of Soil Mechanics on Construction on Soft Clays, Proc 8th Int. Conf. SMFE, Moscow, Vol.3, 1973.

18. Sherwood, P.T., The reproducibility of the results of soil classification and compaction tests, TRRL Report LR339, Crowthorne, 1970.

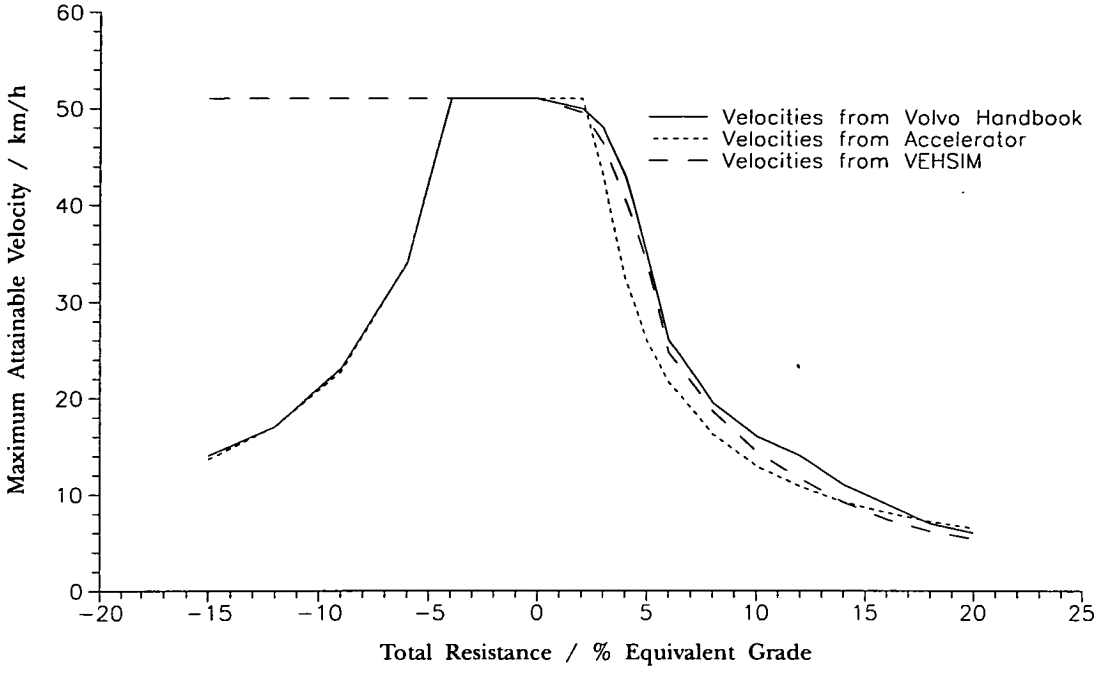

Figure 1: Maximum Attainable Velocity versus Total Resistance for a Partially Loaded (75%) Volvo BM A25 6x6 Articulated Dump Truck.

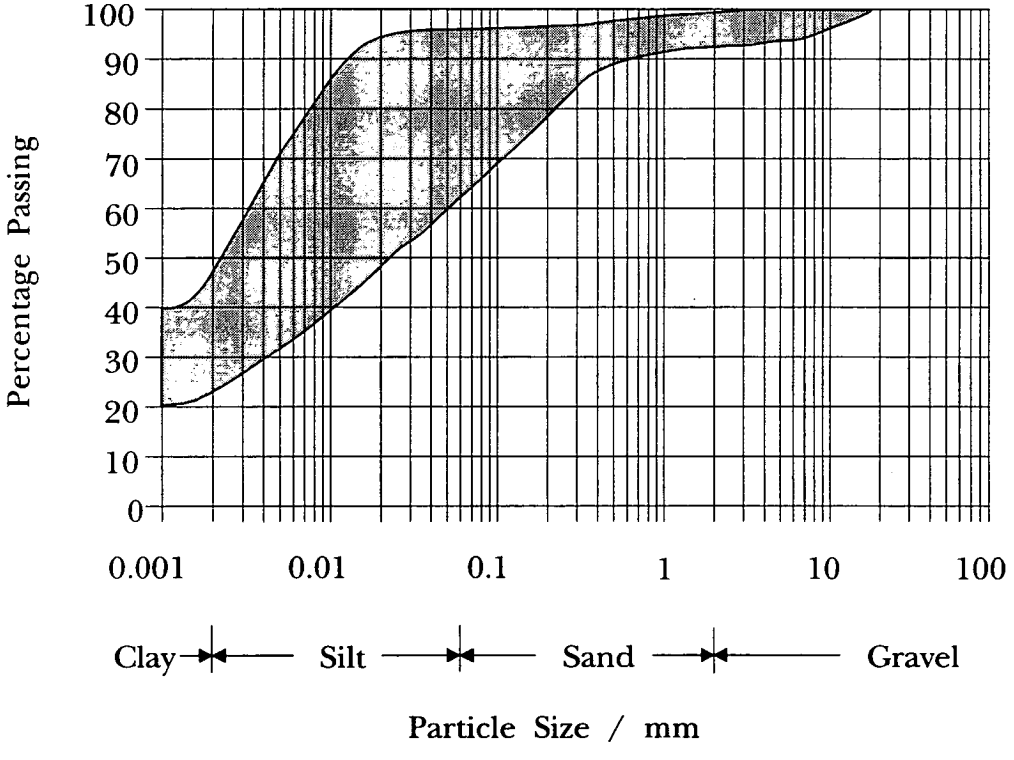

Figure 5.2: Particle Size Distribution Envelope for A1/M1 Link

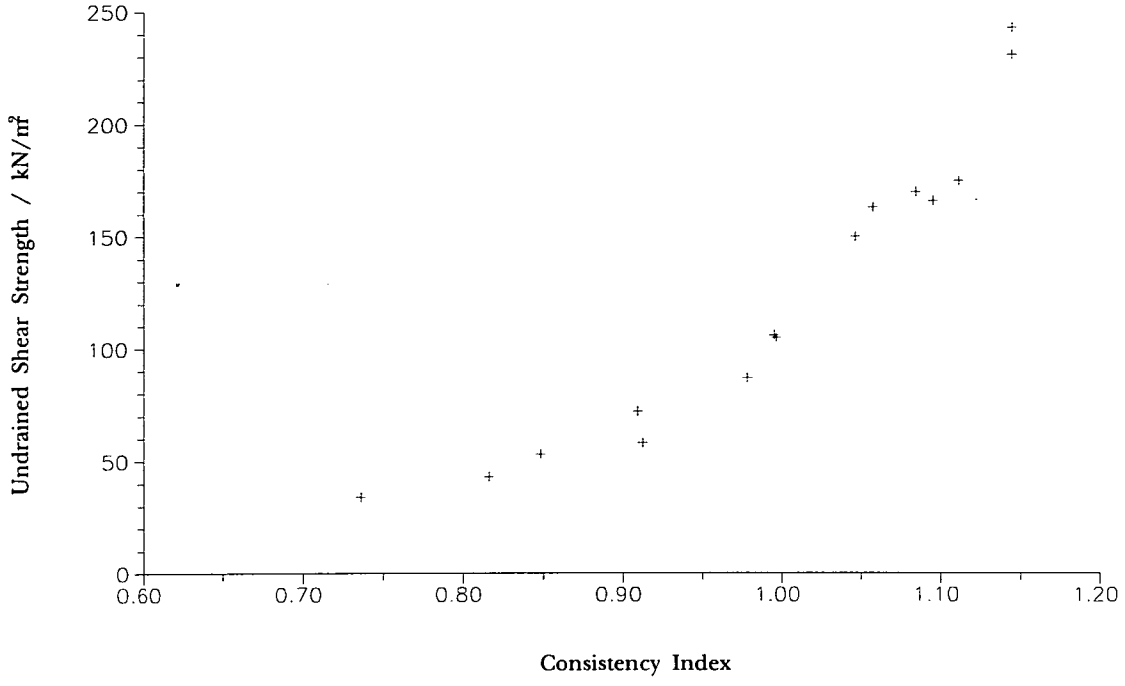

Figure 3: Undrained Shear Strength versus Consistency Index from Multistage Undrained Triaxial Tests.

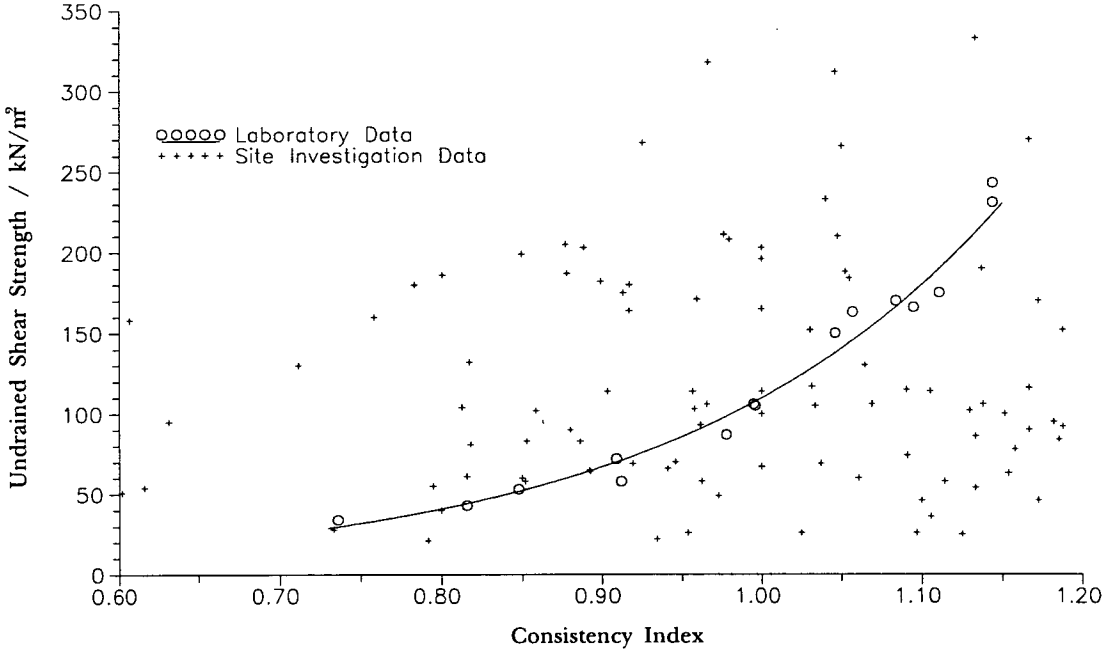

Figure 4: Undrained Shear Strength versus Consistency Index for the A1M1 Link, Comparing Site Investigation and Laboratory Data.

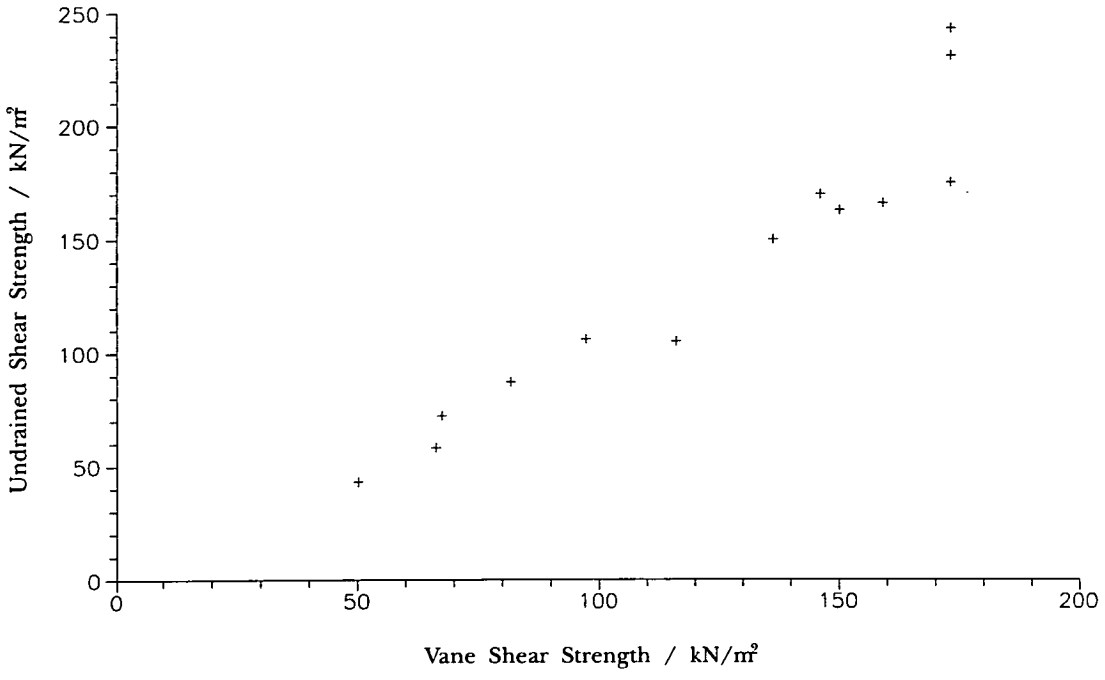

Figure 5: Undrained Shear Strength versus Hand Vane Shear Strength from Multistage Undrained Triaxial Tests.

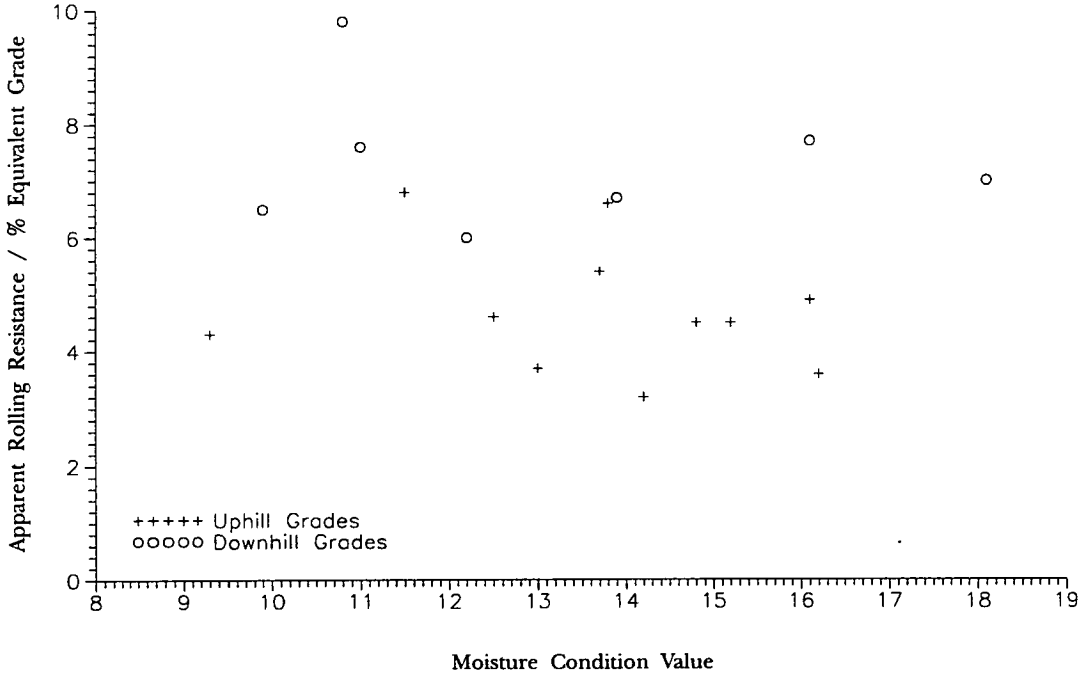

Figure 6: Apparent Rolling Resistance versus Moisture Condition Value for a Loaded Cat D400D Articulated Dump Truck.

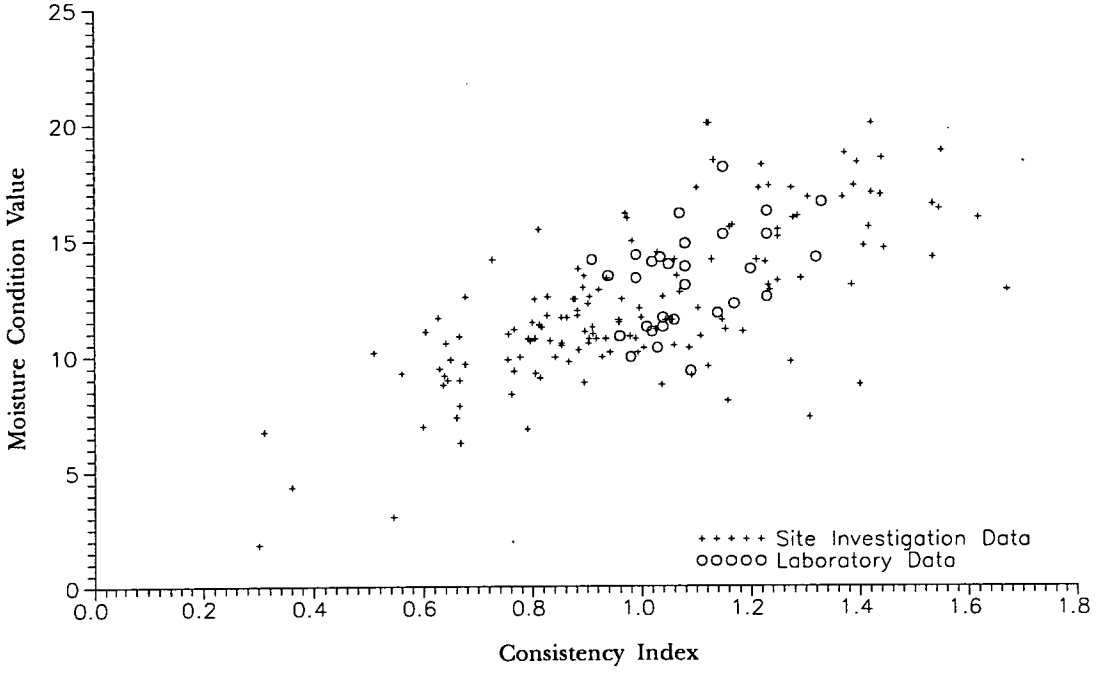

Figure 7: Moisture Condition Value versus Consistency Index for both Site Investigation and Laboratory Data from the A1M1 Link.

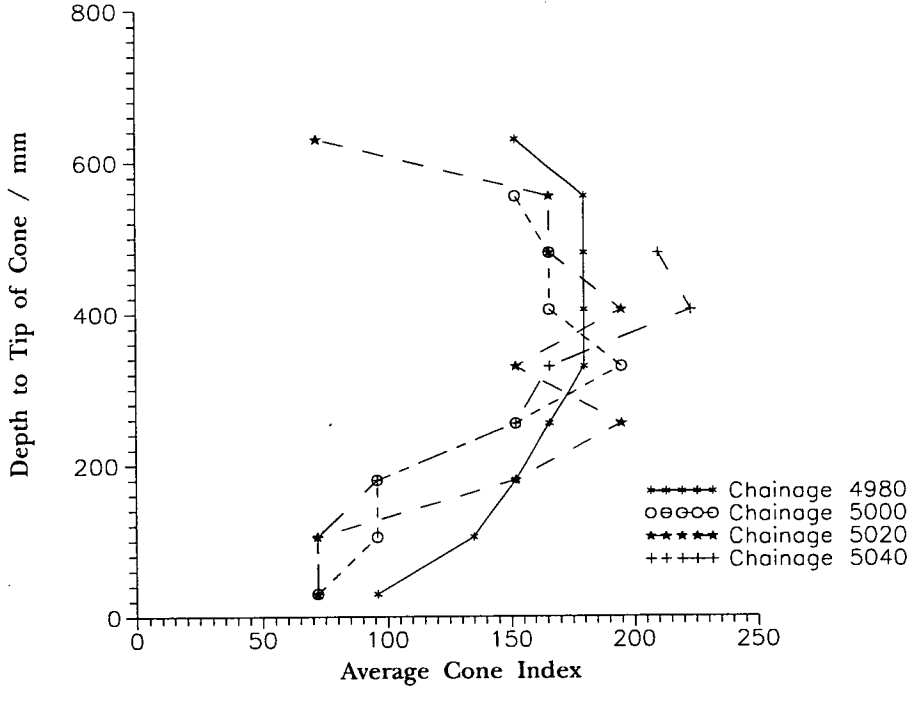

Figure 8: Depth versus Average Cone Index for a Typical Section on the A1M1 Link

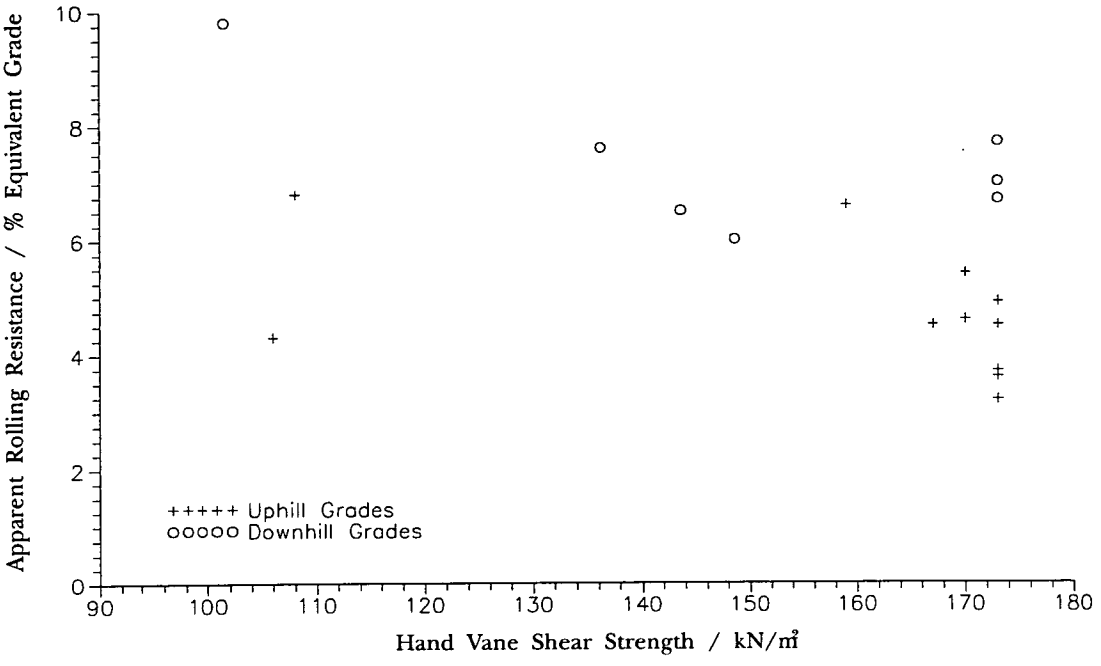

Figure 9: Apparent Rolling Resistance versus Hand Vane Shear Strength for a Loaded Cat D400D Articulated Dump Truck.

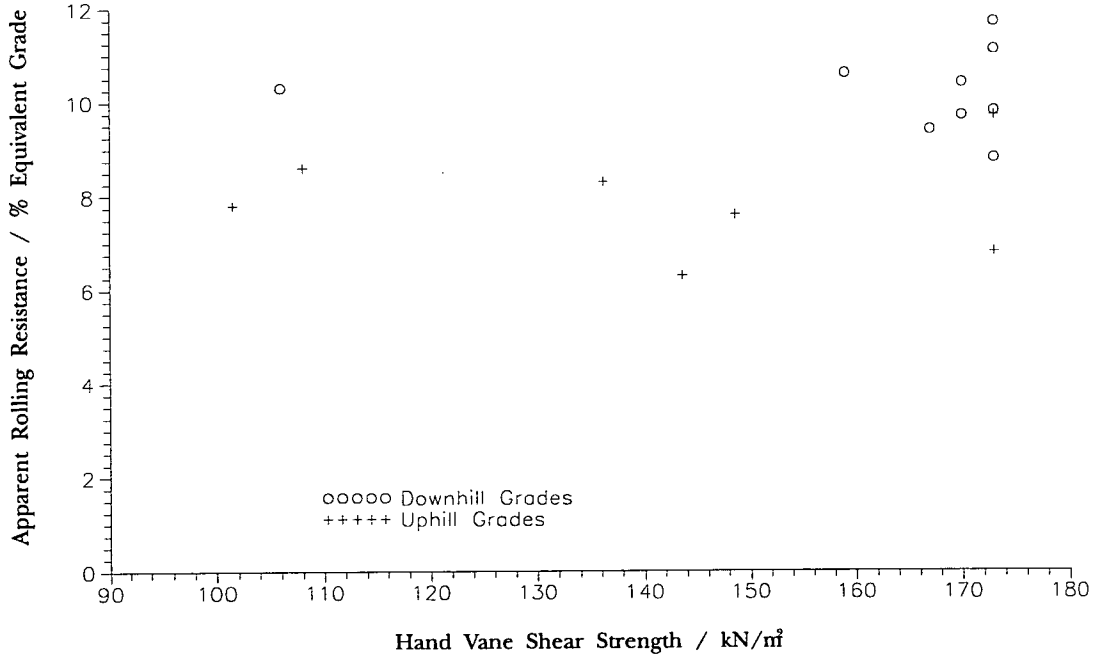

Figure 10: Apparent Rolling Resistance versus Hand Vane Shear Strength for an Empty Cat D400D Articulated Dump Truck.

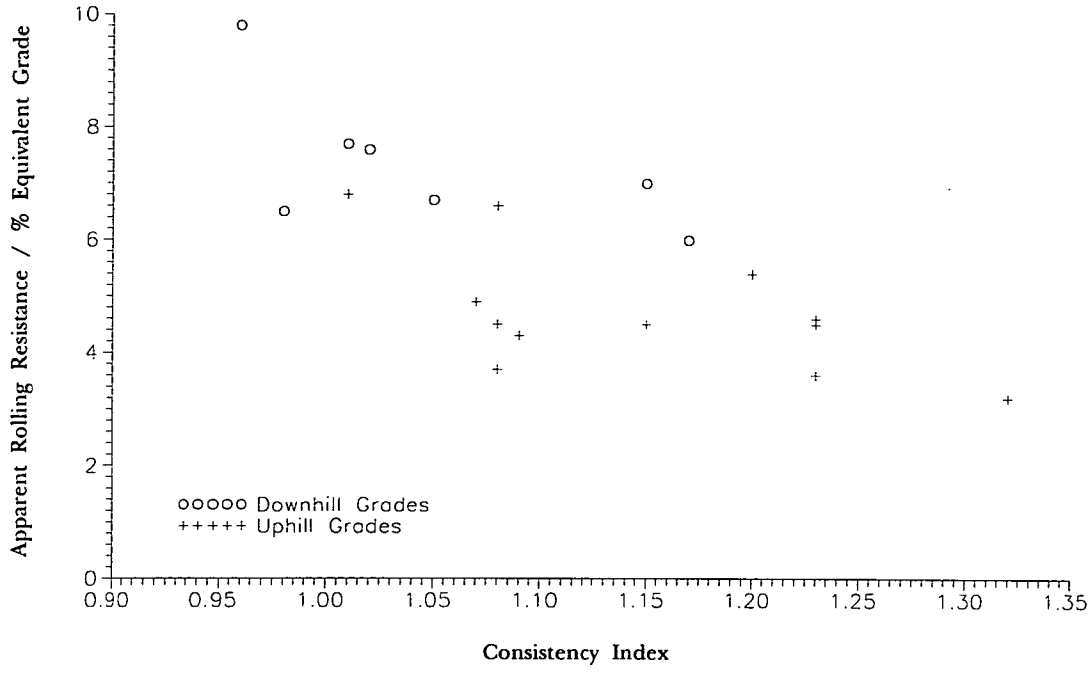

Figure 11: Apparent Rolling Resistance versus Consistency Index for a Loaded Cat D400D Articulated Dump Truck.

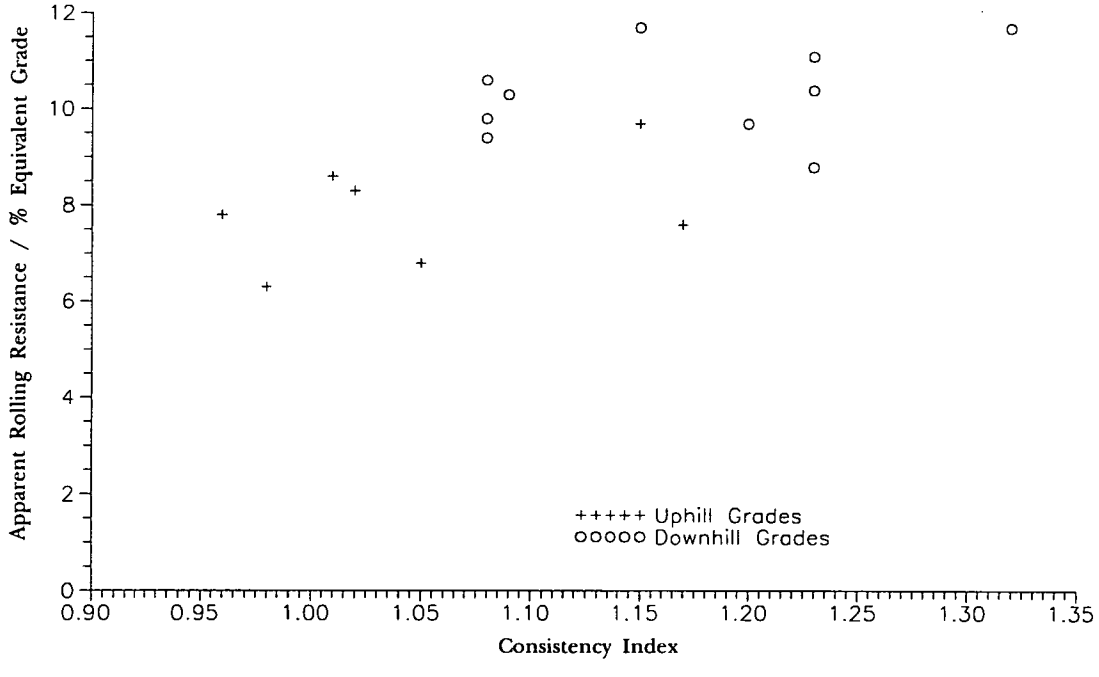

Figure 12: Apparent Rolling Resistance versus Consistency Index for an Empty Cat D400D Articulated Dunp Truck.

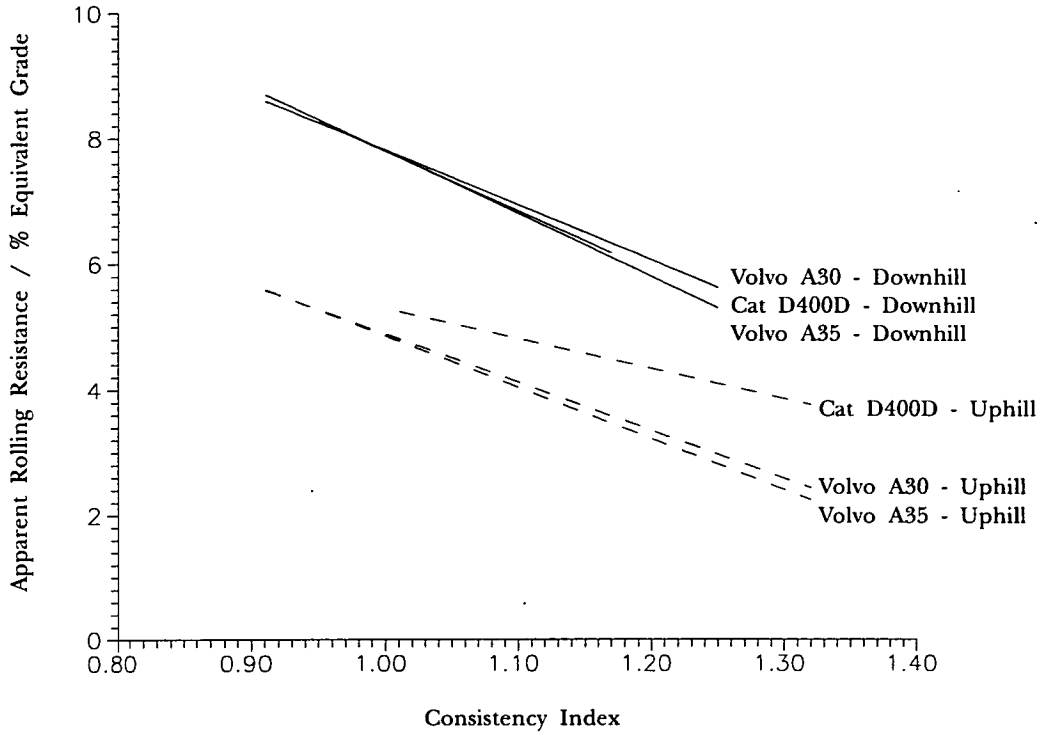

Figure 13: Apparent Rolling Resistance versus Consistency Index for Various Loaded Vehicles and Driving Conditions from A1M1 Link.

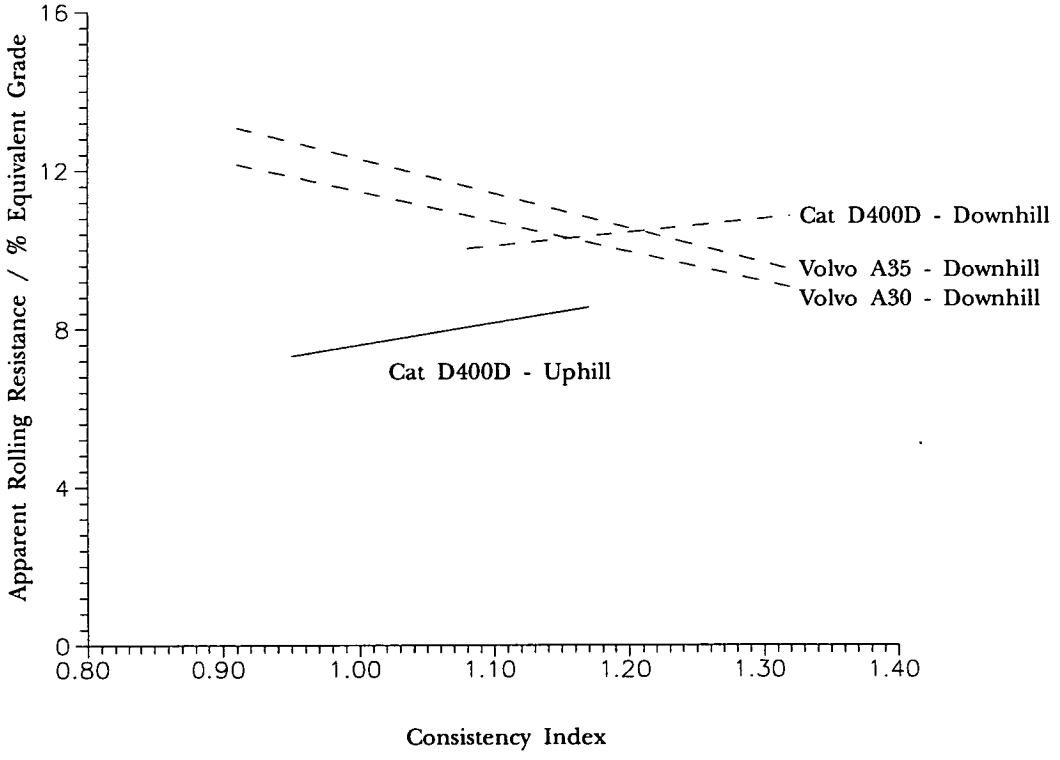

Figure 14: Apparent Rolling Resistance versus Consistency Index for Various Empty Vehicles and Driving Conditions from A1M1 Link.

A1.3 Papers Currently being Refereed

Paper Title:

Determination of the Rolling Resistance of Articulated Dump Trucks on Chalk

by: **G.S. Wood, B.Eng.***
J.R. Osborne, B.Sc., C.Eng., MICE†
M.C. Forde, B.Eng., M.Sc., Ph.D., C.Eng., MICE, MIHT, FINDT‡

Being Refereed at: The Institution of Civil Engineers

Abstract

The estimation of the performance of earthmoving plant is currently calculated through experience taking only limited account of the material the plant will be traversing. The performance of dump trucks on chalk haul roads has not been studied to any great extent, especially in relation to speed of dump trucks and trafficking of haul roads. The estimation of the performance of earthmoving plant on this material is important for the contractor and the client to ensure that the contract is completed efficiently and on time.

Various possible sources and solutions of degrading of the haul roads are investigated and discussed. The apparent rolling resistance of the driver-vehicle-terrain system is shown to be dependent on the grade of the haul road. The speed of the vehicles and therefore a more accurate estimation of the productivity of the plant on chalk can be calculated from a knowledge of the gradients of the haul road.

Introduction

The value of a typical motorway contract in Britain in the early 1990'S, generally runs at a value of approximately £2M/km, of which up to 20% can be attributed to earthmoving. Despite this, the costing of an earthmoving project is predominantly experienced based - utilising productivity information gained on previous sites with similar plant. This method of estimation is prone to error and does not enable the contractor to accurately estimate the contract production cost at the time of tender or quantify losses in a claims situation[1].

No records of the speed of earthmoving plant on chalk haul roads can be found in the literature. Manufacturer's performance charts and various computer programs are available to the estimator to help estimate the speed of the plant on site. However, all these methods rely on the parameter rolling resistance, which is never defined accurately enough for general use. Also published [2,3] are tables giving estimates of rolling resistance on various surfaces, but these do not include one for chalk.

Problems on Haul Roads

The quality of haul roads on chalk is generally very good, there are however certain areas where the contractor should take care not to cause unintentional deterioration of the haul road. These points occur where the machines accelerate and decelerate at the same position on each circuit: at the

* Research Student, Department of Civil Engineering, University of Edinburgh.
† Operations Director, Tarmac Structural Repairs, Wolverhampton.
‡ Tarmac Professor of Civil Engineering Construction, University of Edinburgh.

bottom of ramps between benches, before and after tight corners, in the loading and dumping areas, and at constrictions due to other works: plant crossings, or Bailey bridges. The deterioration of the chalk is caused by the breakdown of the cellular structure, releasing water into the particle matrix, being nearly saturated the silt sized material will be at a moisture content close to its liquid limit. As the material is continually trafficked excess pore water pressures can build up causing a decrease in the effective stress of the matrix, hence the shear strength.

Deterioration of Ramps Between Benches

On large excavations in any material, it is common to excavate in steps, called benches, figure 1. The height of each bench is usually in the region of 2.5-3m, depending on the size of excavator and the type of material being shifted. Normally ramps are constructed between benches at relatively steep grades of about 10-15%. Soft areas tended to appear towards the foot of the ramps between benches. These soft spots, once established, propagate in size and when quite large, 10-15m in length, a second soft spot would appear about 20m downhill from the first one on the horizontal portion of the bench, figure 1.

The formation of these soft areas occurs as follows: the vehicles are decelerated prior to reaching the top of the ramp, the driver then maintains a constant velocity down the ramp and accelerates away from the ramp. The chalk breaks down to its constituent silt sized particles through mechanical action as the vehicles accelerate from the bottom of the ramp. As the chalk is near saturation point the silt matrix will have a moisture content in the region of the saturated moisture content of the intact chalk, about 25-30%. The rate of change in gradient is important as the driver will approach the foot of a ramp slower if the rate of change of slope is great, and then accelerate away faster causing greater damage to the haul road. The driver on returning to the loading area will accelerate the vehicle into the ramp at a similar point as when accelerating from the ramp, hence the chalk is broken down by the vehicles travelling in both directions. As the chalk breaks down the surface of the haul road becomes wet and slippery around the soft spot, this causes the drivers to treat the section differently. The drivers when descending the ramp will keep the speed of the vehicle slow through the soft area then accelerate hard once clear of the section. Likewise going in the opposite direction the driver will break prior to the soft spot, to avoid skidding due to lack of traction. Again the points of acceleration and deceleration on the down side of the first soft spot will coincide causing the second weak spot, figure 1. Given time these two spots will enlarge merging into one another.

As the material breaks down the moisture in the chalk is released and causes the silt sized particles to take on the appearance of putty. As this is continually trafficked the pore water pressure in the silt matrix will increase with time, further reducing the effective stress in the matrix. This top layer of the haul road becomes useless as a supporting medium and the speed of the vehicles are dramatically reduced, as it is impossible to develop high traction for accelerating. The problem could be remedied in one of three ways, by surcharging the haul road with dry fines, constructing the ramp at a shallower grade, or by grading the surface putty chalk revealing a new, solid base for the haul road.

If dry fines are added to the putty chalk, the matrix moisture content will decrease, increasing the strength of the material. Fines will do this more effectively than a blockier material as they will mix easier through trafficking. Recently excavated chalk may not be suitable to use as a surcharging material as it will be near saturation, hence it will not reduce the moisture content of the putty chalk. This surcharge material will also degrade in time increasing the depth of the problem. Practically, depending on location, it may not be cost effective to import dry fines and the British climate does not lend itself to drying material on site.

Alternatively when the ramps are being constructed they can be built at a shallower angle with a longer transition zone. This would not be any more difficult for the excavator driver, but would take

a slightly longer period of time to construct. Solving the problem in this manner not only removes the weak material, but the vehicles operators will drive faster down a shallower ramp, increasing productivity.

If the problem of degradation is going to be solved by grading, the ramps must be smooth enough to allow the blade of the grader to reach all parts effectively, as the worst breakdown of material occurs near the point of greatest curvature on the ramp. To avoid disturbing the solid material under the putty chalk the grader driver has to be continually altering the depth of the blade, this is a difficult operation to complete accurately.

Deterioration due to Manoeuvring

The loading and unloading areas rut quite badly as the vehicles are continually manoeuvring into position under the loader, or preparing to dump in the fill area. The constant demand for high traction to overcome the initial friction causes large shear forces in the chalk that cause the material to degrade badly in these areas.

Remedial work in the loading area is very difficult to achieve effectively, as interference from other pieces of plant congests this area very quickly. This has the effect of dramatically reducing productivity, therefore utilising graders in this situation is impractical. Maintaining the area during breaks is probably the most effective solution, another is to keep altering the section being excavated. On site, the latter option is generally impractical as the travel time for the excavator between benches would result in a greater loss in productivity than the potential gain.

The dumping area is another zone where the degrading of the chalk can cause major problems, not only from an earthmoving point of view but from a long term structural standpoint. It is hard to generalise as the layout of dumping areas varies from site to site, nevertheless most dumping areas have a common point of entry and turning section for the dump trucks. As in the case of the loading area, the constant manoeuvring of machines in a constricted area causes the chalk to break up faster than on the body of the haul road, where the vehicles are travelling at a reasonably constant velocity. The continually manoeuvring compacting machinery is also present in the dumping area, therefore the chalk is being very heavily trafficked. Care must also be taken not to over compact the soil as this could lead to temporary instability of the embankment, resulting in deep rutting caused by the plant. Compaction of chalk is outwith the scope of this paper, but several publications have dealt with this topic[4,5,6].

Other Problem Areas

Any other place on the haul road where vehicles are perpetually accelerating or breaking has the possibility of degrading. These points may occur at plant crossings, constrictions on the haul road due to other works, or at Bailey bridges. If these bottlenecks cannot be avoided then the best remedy is to keep trimming the haul road with a grader to remove putty chalk. Graders on chalk should have very little to do except maintain these problem areas and remove any large blocks that have fallen off a dump truck. When grading, the blade of the machine should not penetrate into the solid chalk underlying the putty chalk, as this will roughen the surface by displacing and breaking up the chalk blocks, increasing the likelihood of putty chalk in the future.

The presence of graders on narrow haul roads causes obstructions for the haulers which can travel at greater velocities, especially on steep grades, dramatically affecting the productivity of the hauling team.

Full - Scale Monitoring

A chalk site was monitored through the 1993 earthmoving season - the final section of the M3 from Bar End to Compton, through Twyford Down. This 5km stretch of motorway contains 2.7Mm³ of earthmoving, the majority of which is in a single cut. The earthworks were entirely constructed using a backhoe-dump truck combination, as scrapers are not allowed to be used for transporting grade 3 material[7], unless directed by the engineer. The excavators on the site were Cat 245's loading a mixture of Volvo BM A35 and Cat D400D articulated dump trucks. The majority of the loaded hauling was downhill and maximum grades on the ramps were 25%. All monitoring of the vehicles took place on the cut sections of the haul road.

From the site laboratory data the average dry density and natural moisture content of the blocks were 1.63Mg/m³ and 23.8% respectively, taken from a sample size of 500. The dry density ranges between 1.38 and 2.01Mg/m³ with a standard deviation of 0.14 and the natural moisture content ranges between 9 and 29% with a standard deviation of 4.5. The natural moisture contents of the tested blocks were all at least 90% of the corresponding saturated moisture content. All tests were carried out in accordance with the relevant sections of BS1377[8], 1990. No classification system exists for predicting the effect of dump trucks on chalk haul roads. Two classification systems that are currently employed on chalk are: the Mundford scale[9,10], and the TRRL classification scheme[11]. The Mundford scale[9,10], figure 2, is based on the visual inspection of chalk and small deflections under loads, it is therefore considered inappropriate for the earthworks situation where the soil is subjected to large strains, nevertheless it is still used on earthmoving sites. The TRRL[11] classification scheme, figure 3, is used to classify chalk in relation to its behaviour as a freshly placed fill material. Although the haul roads monitored were not on fill material the classification scheme still gives an idea of the material encountered. Figure 3, shows the material to be predominantly class A with a small portion of class B, and the hardness[12] to be from medium hard to extremely soft. The fact that the material is class A/B only indicates that any form of excavation can be used and that instability of any resulting structure built from this material is unlikely. It should be noted in the TRRL method of classification that scrapers should not be used for excavating chalk[7], unless specified by the engineer.

On the main body of the haul roads there was no visible jointing between the blocks as this had been filled with chalk fines, that left after repeat trafficking an exceptionally smooth running surface. Localised degrading of the chalk had occurred at the foot of ramps, in the loading and dumping areas, and at plant crossings.

No instrumentation or interference with the operation of the plant was possible, therefore all timings had to be recorded from the side of the haul road. Vehicles were timed over complete sections of varying grade, as long sections of constant grade were not available on this site, a typical section is shown in figure 4. Timings were averaged from approximately 10 passes of similar plant. The length and grade of each section were ascertained by surveying the haul road with an electronic theodolite. All sections were assumed to have no obstructions and recordings that involved a vehicle that had been delayed by an external factor were removed from the analysis.

Rolling Resistance

Rolling resistance is a measure of the force that must bè overcome to drive the wheels over the ground. The deeper the tyres penetrate into the soil, the higher the value of rolling resistance. This can be thought of as the wheels having to continually climb out of a rut. Rolling resistance is affected by various factors including: soil type, the condition of the haul road, wheel loading, tyre and road flexing, internal friction, and the driver. The last effect is very important, if the driver is not driving the vehicle at optimum speed, due to vibrations, health reasons or because there is a queue at the loader, then the vehicle will be slowed down artificially giving a higher apparent rolling resistance.

Rolling resistance is expressed as a percentage of vehicle weight and can be added to grade resistance, uphill grade positive, to give total resistance, equation 1.

$$\text{Total Resistance} = \text{Rolling Resistance} + \text{Grade Resistance} \quad (1)$$

The Caterpillar handbook[2] gives descriptions of the haul road and quotes values of rolling resistance as:

> A hard, smooth, stabilised surfaced roadway without penetration under load, watered, maintained. 2%
>
> A dirt roadway, rutted or flexing under load, little maintenance, no water, 50mm tyre penetration or flexing. 5%.

From the descriptions above it could be assumed that the value of rolling resistance for the chalk haul roads encountered should lie between these two values.

Method of Calculating Rolling Resistance

The calculated rolling resistance for each individual section is back analysed using a computer package called Accelerator[13]. This program estimates the performance of the vehicles by using the weight to horse power ratio. This ratio is a measure of how much power is available to overcome motion resistance. Accelerator assumes that the available road power does not change significantly over the range of operating velocities. The average available road power is calculated from equation 2, by entering corresponding velocity and rimpull data, taken from manufacturer's specification sheets.

$$\text{Rimpull(kg)} = \frac{\text{constant x engine power(kW) x engine efficiency}}{\text{speed (km / h)}} \quad (2)$$

for this metric system of units the constant equals 367.

As rimpull is also defined as:

$$\text{Rimpull(kg)} = \frac{\text{GVW(kg) x Total Resistance(\%)}}{100} \quad (3)$$

where GVW is the gross vehicle weight, then the apparent rolling resistance can be calculated from equation 1.

Knowing power and velocity the accelerating force can be calculated from fundamental mechanics, equation 4, the vehicle acceleration is then calculated by dividing the accelerating force by the vehicle mass.

$$\text{Force(kN)} = \frac{\text{Power(kW)}}{3.6 \text{ x Velocity(km / h)}} \quad (4)$$

the constant on the denominator it to maintain consistency in the units.

As the vehicle accelerates, or the haul road profile varies, the vehicle's velocity will change, altering the available road power, hence the force available for acceleration, therefore the computer program must continually update the performance of the vehicle. Knowing the velocity of the vehicle from site measurements it is possible to use the software to back analyse the field situation and find the apparent rolling resistance of the driver-vehicle-terrain system.

The reason this package was used instead of other similar programs is because it takes account of the retarder on the earthmoving machine. The back analysed rolling resistances were assumed to be constant across each timed segment of the section. The varying gradient may have a secondary effect on the apparent rolling resistance of the section, but the effect of this cannot be quantified at this stage.

Results

Results for downhill grades tend to be more operator dependent than corresponding uphill grades. This is because on the uphill grades the speed of the vehicle is primarily governed by the output of the engine, whereas on steep downhill grades the vehicle will travel as fast as the driver is willing to let it, unless an automatic retarder is fitted. The severity of the grade also affects the variability of the timings. There are many factors outwith the scope of the project that could affect the speed the driver is willing to travel: amount of experience in the vehicle, health problems, and if the vehicle is not performing as per the specifications.

On this contract, the quality of the haul roads was in the majority very good, except at the foot of some ramps where the rate of change of curvature was severe, it was therefore expected that the back analysed rolling resistances would be correspondingly low, between 2-5%. Figures 5 and 6 show the relationship between back analysed rolling resistance and average grade resistance for the two types of hauler, Volvo BM A35 and Cat D400D articulated dump trucks. The abscissae in the figures are the average grade resistance for each timed section, any section that had a wide spread of grade resistance was omitted from the sample, for example sections 1-2 and 5-6, figure 4.

For a loaded Volvo BM A35 travelling down a steep slope, greater than 10%, figure 7, the apparent rolling resistance decreases linearly as the gradient becomes shallower. The value of rolling resistance is approximately 4% lower than the grade resistance, giving a constant total resistance of approximately 4%. As the slope becomes shallower the apparent rolling resistance stabilises at a value of between 3 and 6% and the total resistance rises linearly. This vehicle was never monitored travelling loaded uphill. When travelling uphill empty the apparent rolling resistance was constantly recorded below 6% and this value decreased slightly as the severity of the slope increased, as would be expected because the speed of the vehicle is becoming increasingly engine dependent. Similarly if the trucks were hauling uphill loaded then it would be expected that the apparent rolling resistance would lie in the 2 to 6% bracket. It is impossible however to predict the performance of the empty vehicles travelling downhill without further monitoring. These values are higher than the those expected from the description of the haul roads in the Caterpillar handbook.

Figure 6, showing the relationship between apparent rolling resistance and grade resistance for the Cat D400D articulated dump trucks, does not indicate as well defined a trend as that for the Volvo BM A35 in the previous figure. The majority of the points on the empty uphill portion of the graph lie below 6% apparent rolling resistance, but with a much wider spread. As the gradient becomes flatter and then downhill the rolling resistance increases indicating that the grade has a more marked effect on driver-vehicle performance. The loaded results show greater variability, but this can be partly explained by the inexperience of the drivers to a different and far steeper haul road. The two shaded areas in figure 6 lie out with a distinct trend, and these points relate to the sections of the haul road in figure 4. When monitoring took place this haul road had never been travelled by the

Cat D400D plant and the steep sections were longer and steeper than the drivers had previously encountered on this contract.

Figure 7 shows the relationship between maximum speed and total resistance, (the sum of grade and rolling resistance) and indicates that if the downhill grade is steep then as the rolling resistance increases the speed of the plant will increase until a value of grade resistance minus 2 to 3% is achieved, at this point the vehicle will be travelling at maximum velocity. Thus shaded area to the far left of figure 6 indicates that the vehicles are travelling slower than would have been anticipated, this could be due to the inexperience of the drivers in descending such severe slopes as mentioned in the previous paragraph, or the vehicle is slowed down to avoid overheating. The shaded area above and to the right of the expected trend shows that the vehicles are again travelling slower than would have been anticipated and is caused by the drivers slowing down in preparation for the next descent.

Figures 5 and 6 both show that steep downhill grades have the effect of increasing the apparent rolling resistance of the driver-vehicle-terrain system. From an estimating point of view this is exceptionally important as the vehicles are travelling at a significantly different velocity than would have been expected from the information available to date.

Figure 8 shows the same information as figure 5 for a loaded Volvo BM A35 articulated dump truck travelling, with 95% confidence and prediction intervals attached. These intervals would be used when estimating or monitoring a similar earthmoving operation. The confidence intervals would be used when estimating for numerous passes throughout the duration of an operation, whereas the prediction intervals would be used when a single pass of a vehicle was being monitored. Correlation between apparent rolling resistance and grade resistance for this situation gives an R^2 value of 88%.

Conclusions

- It is possible to estimate the rolling resistance of certain types of plant on strong, smooth haul roads on chalk simply from the gradient of the haul road, enabling better estimates of the time required to complete a contract to be made.

- Grade resistance has a secondary effect on the driver that slows the vehicle down more than expected.

- The apparent rolling resistance for empty machines travelling uphill on chalk is approximately 3%. Downhill the rolling resistance of the driver-vehicle-terrain system is dependent on the gradient of the haul road.

- Graders should not be used on chalk haul roads except to remove debris and to clear putty chalk from the surface without disturbing the underlying strong material.

- Ramps between benches should be as shallow as possible to avoid degrading the chalk at this point and to allow graders to clear the section easier.

Acknowledgements

The authors wish to acknowledge the support of Tarmac Construction Limited and Blackwells for allowing the research on the site and the provision of facilities by the University of Edinburgh. The work was supported financially by an SERC Case studentship and Tarmac Construction Limited, Wolverhampton.

References

1 Staples, B.L., Wood, G.S. and Forde, M.C., Technical Evaluation of Earthworks Claims under ICE Conditions of Contract 5th and 6th Editions, *Proc. Inst. Civil Engng.*, Civil Engineering, Vol. 92, May 1992, pp90-95.

2 Caterpillar, *Caterpillar Performance Handbook*, 24th Edition, Caterpillar Inc., Peoria, Illinois, U.S.A., 1993.

3 VME Performance Manual, *Volvo BM Articulated Haulers*, Edition 2, Växjö, Sweden, 1989.

4 Privett, K.D., Use of Thick Layers in Chalk Earthworks at Port Solent Marina, Portsmouth, UK, *Chalk*, Thomas Telford, London, 1990, pp.429-436.

5 Rat, M. and Schaeffner, M., Classification of Chalks and Conditions of use in Embankments, *Chalk*, Thomas Telford, London, 1990, pp.425-428.

6 Clayton, C.R.I., The Collapse of Compacted Chalk Fill, *Int. Conf. on Compaction*, Vol. 1, Paris, 22-24 April, 1980, pp.119-124.

7 Department of Transport, *Manual of Contract Documents for Highway Works*, Vol. 1, Series 600: Specifications for Highway Works, HMSO, Dec. 1991.

8 British Standards Institution, *Methods of Tests for Soils for Civil Engineering Purposes*, BS1377, Parts1-9, HMSO, London, 1990.

9 Ward W.H., Burland, J.B. and Gallois, R.W., Geotechnical Assessment of a site at Mundford, Norfolk for a large Proton Accelerator, *Géotechnique*, Vol. 18, 1968, pp.399-431.

10 Wakeling, T.R.M., A Comparison of the Results of Standard Site Investigation Methods Against the Results of a Detailed Geotechnical Investigation in Middle Chalk at Mundford, Norfolk, *Proc. Symp. on In-situ Investigations in Soils and Rocks*, BGS, London, 1970, pp.17-22.

11 Ingoldby, H.C. and Parsons, A.W., *The Classification of Chalk for use as a Fill Material*, TRRL Report LR806, Dept. of the Environment, Dept of Transport, Crowthorne, Berks., 1977.

12 Mortimore, R.N., Roberts, L.D. and Jones, D.L. The Logging of Chalk for Engineering Purposes, *Chalk*, Thomas Telford, London, 1990.

13 Accelerator, *Accelerator Vehicle Performance Software User's Guide*, Version 1.17, Accelerator Inc., Fort Myers, Florida, U.S.A., 1987.

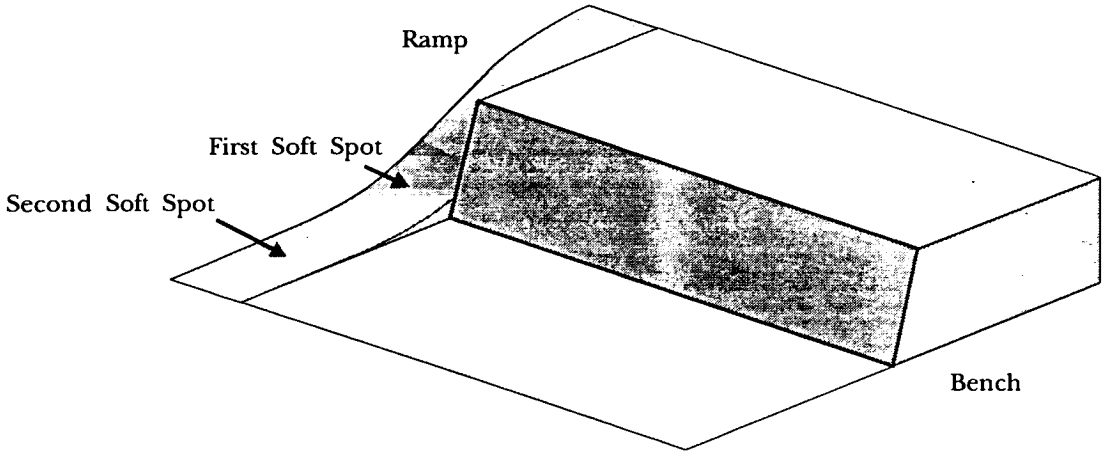

Figure 1: Cutting Bench and Ramp

Weathering Grade	Description	Approx. Range of Young's Modulus / kN/m²	Bearing Stress causing "yield" / kN/m²	SPT	Creep Properties
I	Hard, brittle chalk with widely spaced tight joints	> 50 x 10^5	> 1000	> 35	Negligible Creep for stresses of at least 400 kN/m²
II	Medium hard to hard chalk with widely spaced tight joints	20 x 10^5 - 50 x 10^5	> 1000	25 - 35	Negligible Creep for stresses of at least 400 kN/m²
III	Medium to hard rubbly to blocky chalk closely spaced, slightly open joints	10 x 10^5 - 20 x 10^5	400 - 600	20 - 25	For stress not exceeding 400 kN/m² creep is small and terminates in a few months
IV	Friable to rubbly chalk with open joints often infilled with soft remoulded chalk	5 x 10^5 - 10 x 10^5	200 - 400	15 - 20	Exhibits Significant Creep
V	Structureless remoulded chalk containing lumps of intact chalk	< 5 x 10^5	< 200	8 - 15	Exhibits Significant Creep
VI	Extremely soft structureless chalk containing small lumps of intact chalk	< 5 x 10^5	< 200	< 8	Exhibits Significant Creep

Figure 2: Amended Mundford classification correlating grade and the mechanical properties of chalk (after Wakeling, 1970)

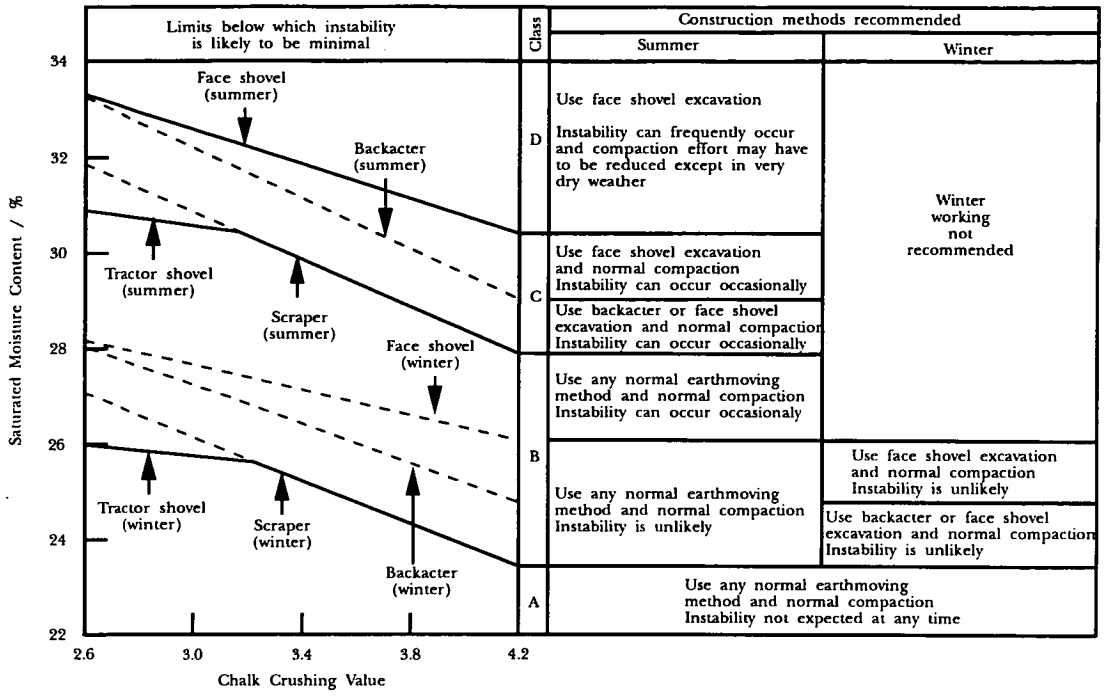

Figure 3: TRRL chalk classification scheme with measures required to avoid or minimise instability. (Ingoldby et al., 1977)

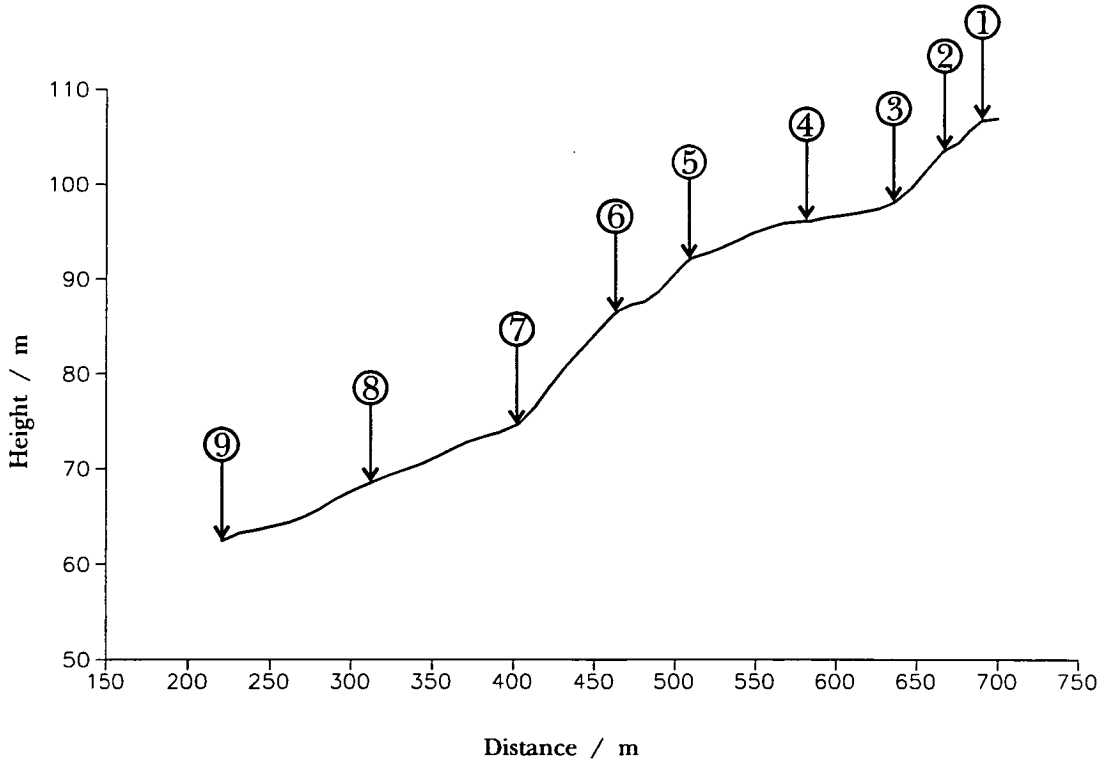

Figure 4: Surface Profile for a Section on the M3 with Timing Markers.

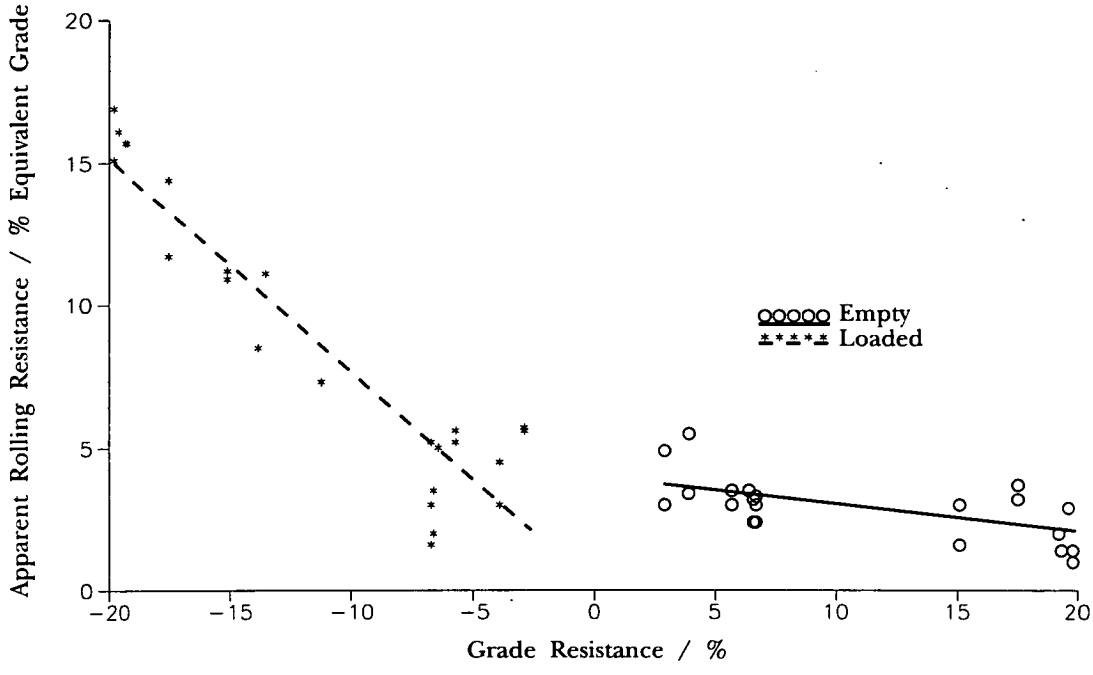

Figure 5: Apparent Rolling Resistance versus Grade Resistance for Volvo BM A35 Articulated Dump Trucks on Chalk

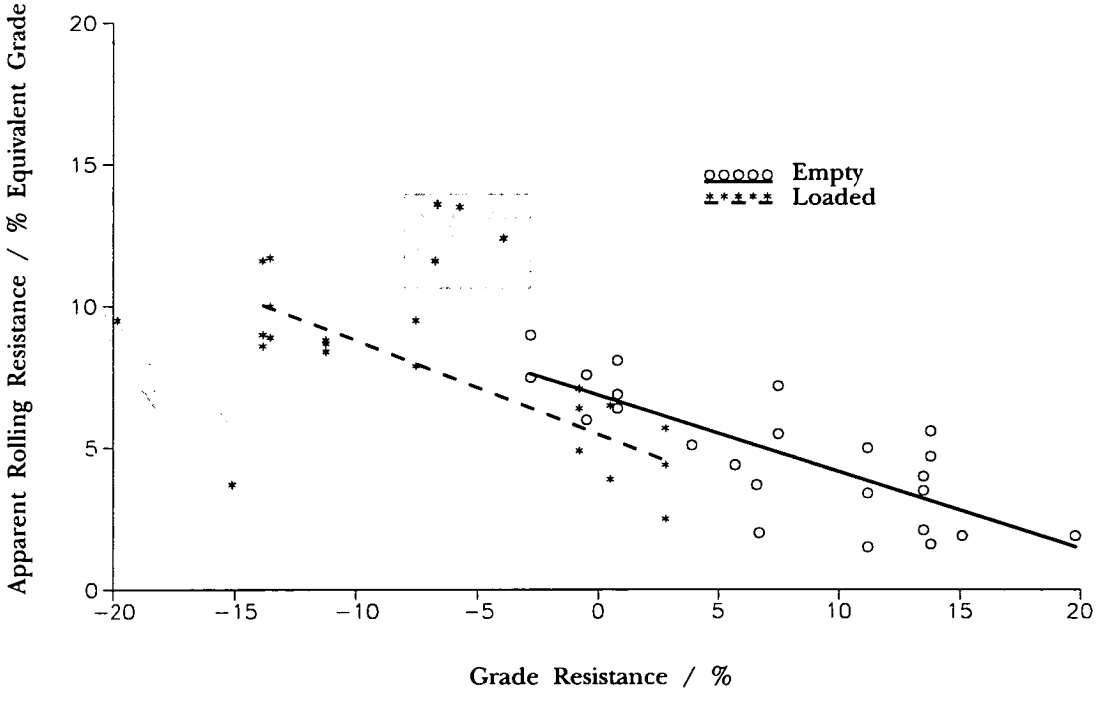

Figure 6: Apparent Rolling Resistance versus Grade Resistance for Cat D400D Articulated Dump Trucks on Chalk

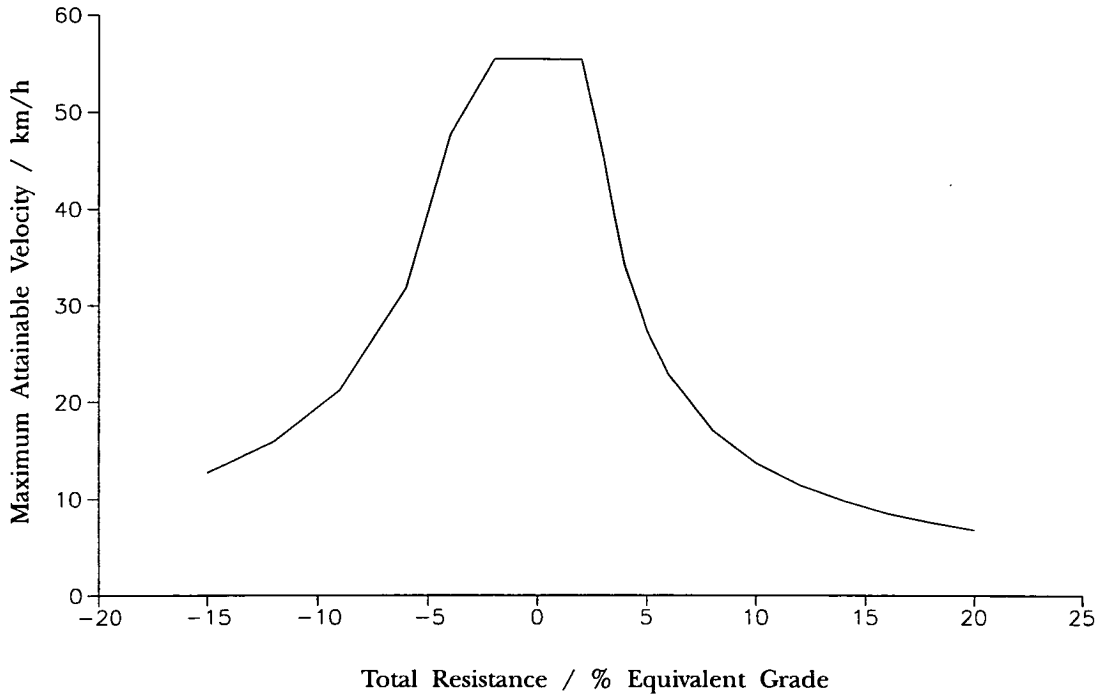

Figure 7: Maximum Velocity versus Total Resistance for a Loaded Cat D400D Articulated Dump Truck

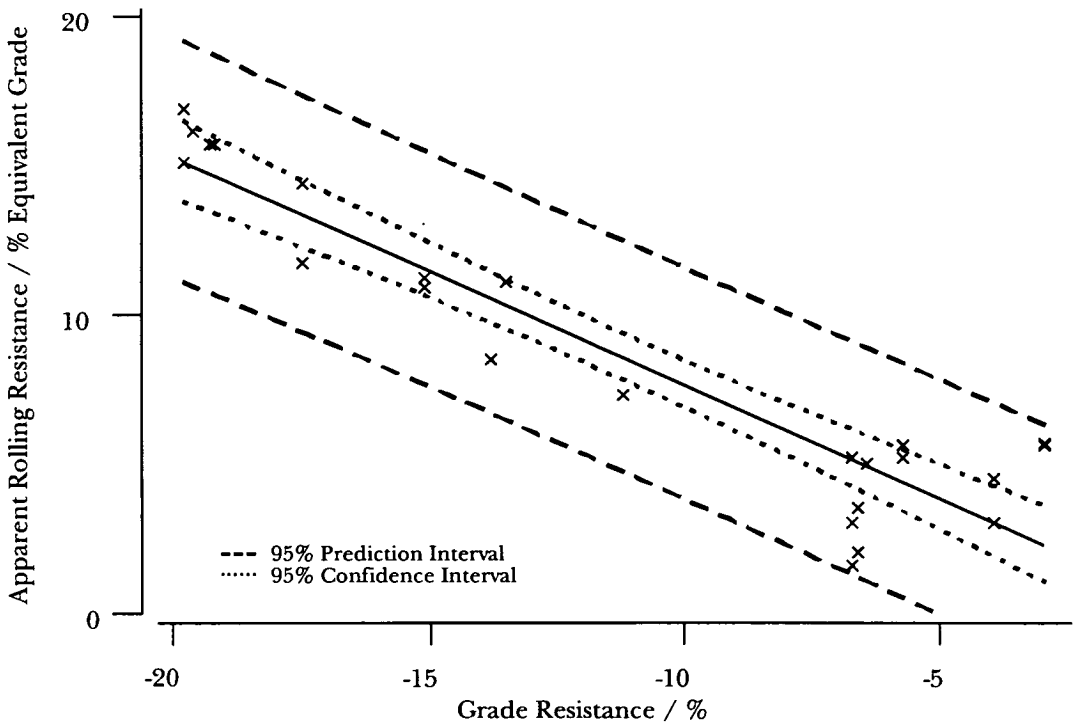

Figure 8: Apparent Rolling Resistance versus Grade Resistance for a Loaded Volvo BM A35 Articulated Dump Truck Travelling Downhill, Showing 95% Confidence and Prediction Intervals

Paper Title: **The Effect of Excess Pore Water Pressure on Haul Road Condition**

by: **G.S. Wood, B.Eng.**[1]
J.R. Osborne, B.Sc., C.Eng., MICE[2]
M.C. Forde, B.Eng., M.Sc., Ph.D., C.Eng., MICE, MIHT, FINDT[3]

Being Refereed at: American Society of Civil Engineers

Abstract

The deterioration of haul roads under repeat trafficking has generally been attributed to the remoulding of the soil. A theory has been developed, based on the principles of effective stress, to show that the decrease in shear strength is at least partly due the increase in pore water pressure. These decreases in effective shear strength could result in large reductions in plant productivity and therefore should be considered at the time of tender and planning of a project.

A series of normal cyclic loading experiments have been carried out on a saturated clay material. It has been shown that the percentage decrease in shear strength for samples at moisture contents of 24%, 26%, and 28%, were 6%, 17%, and 38% respectively.

Introduction

The deterioration of clay haul roads with repeat trafficking of earthmoving plant is a common occurrence. Observations made on site indicated that the depth of rut on a haul road, where the soil could be considered to be in a remoulded state, would initially increase as the earthmoving operation progressed, before reaching a constant depth. Wetter soils would deteriorate at a faster rate than drier ones. Subjectively, site production managers have indicated that wetter soils seem to deteriorate proportionately more than drier soils. Thus if a saturated clay soil encountered on site were wetter and weaker than anticipated from the pre-tender site investigation report, then the wetter soil would not only be weaker initially, but would exhibit a higher percentage reduction in shear strength under repeat trafficking.

The running surface of the haul roads is generally maintained by graders. The effect of grading a haul road provides a short term respite as the ruts fully reappear after only a few subsequent passes. It was considered that with the continual passage of the plant, the pore water pressure in the soil was increasing, thereby decreasing the effective stress, thus apparently weakening the material below that indicated in the site investigation report. An explanation as to why the condition of the haul road would not deteriorate further is that the excess pore water pressure would reach a constant level, where the pore water pressure dissipation between vehicle passes would equal the increase after each pass.

In order to investigate this hypothesis it was decided to cyclically load a confined sample of soil and monitor the pore water pressure at a depth below the surface. Three tests were carried out on fully saturated cohesive samples at different consolidation pressures.

---

[1]Research Student, Department of Civil Engineering, University of Edinburgh.
[2]Operations Director, Tarmac Structural Repairs, Wolverhampton.
[3]Tarmac Professor of Civil Engineering Construction, University of Edinburgh.

Theory

The theory presented is based on classical soil mechanics and is assumed to hold for any saturated fine grained material, of low permeability, having a Mohr-Coulomb failure criterion as described by equation 1.

$$\tau = c + \sigma.\tan\phi \qquad (1)$$

where: τ shear strength (kN/m^2)
c apparent cohesion (kN/m^2)
σ total normal stress (kN/m^2)
ϕ angle of shearing resistance.

In accordance with Terzaghi's fundamental concept of effective stress (Terzaghi, 1943),

$$\tau = c' + \sigma'.\tan\phi' \qquad (2)$$

where: c' and ϕ' are the shear strength parameters in terms of effective stress
σ' is the effective normal stress as defined in equation 3.

$$\sigma' = \sigma - u \qquad (3)$$

where: u is the pore water pressure in the sample, (kN/m^2).

For a remoulded soil, it can be assumed that $c'=0$, thus equation 2 can be simplified to;

$$\tau = \sigma'.\tan\phi' \qquad (4)$$

Assuming that the initial effective stress, prior to the first loading is defined by equation 5 and the incremental stress due to the wheel loading is equal to ΔW, then the effective stress at the wheel-soil boundary, σ_{1P}', during the passage of the vehicle, will be as in equation 6, as instantaneously all the vehicle load is carried by the pore water.

$$\sigma'_0 = \sigma_0 - u_0 \qquad (5)$$

$$\sigma'_{1P} = (\sigma_0 + \Delta W)-(u_0 + \Delta W) \qquad (6)$$

Once the vehicle has passed over the section the excess pore pressure will start to dissipate. The rate of dissipation will depend on the magnitude of the pore pressure and the permeability of the material. Prior to the second pass not all the excess pore pressure will have dissipated, thus the residual effective stress just before the second pass will be as defined in equation 7.

$$\sigma'_{1R} = \sigma_0-(u_0 + a_{1,0}.\Delta W) \qquad (7)$$

where: $a_{1,0}$ is a factor describing the degree of dissipation between the first and second passes of the vehicle.

On the second pass, when the wheel load is again passing over the section of soil,

$$\sigma'_{2P} = (\sigma_0 + \Delta W)-(u_0 + a_{1,0}.\Delta W + \Delta W) \qquad (8)$$

It is clear from equations 7 and 8, that the effective stress just before, and during the passage of the vehicle are identical. In the interval between passes, a proportion of the excess pore water pressure will again dissipate and shortly before the third passage the effective stress will be;

$$\sigma_{2R}' = \sigma_0-(u_0 + a_{1,0}\cdot a_{1,1}\cdot\Delta W + a_{2,0}\cdot\Delta W) \quad (9)$$

where: $a_{1,1}$ is the degree of dissipation from the first passage of the vehicle between the second and third passes
$a_{2,0}$ is the degree of dissipation from the second passage of the vehicle between the second and third passes.

On the n^{th} pass of the vehicle the generic equation for effective stress will be;

$$\sigma_{nP}'=(\sigma_0+\Delta W)-(u_0+a_{1,0}\cdot a_{1,1}\cdots a_{1,n-1}\cdot\Delta W+a_{2,0}\cdot a_{2,1}\cdots a_{2,n-2}\cdot\Delta W+\ldots+a_{n-1}\cdot\Delta W+\Delta W) \quad (10)$$

and prior to the $(n+1)^{th}$ pass the generic equation for the residual effective stress will be;

$$\sigma_{nR}' = \sigma_0-(u_0 + a_{1,0}\cdot a_{1,1}\cdots a_{1,n}\Delta W + a_{2,0}\cdot a_{2,1}\cdots a_{2,n-1}\cdot\Delta W+\ldots+a_{n,0}\cdot\Delta W) \quad (11)$$

The generic effect of the built up in pore water pressure and the resulting decrease in effective stress can be seen diagramatically in figures 1 and 2 respectively. With continual trafficking it is evident from equation 4 that the apparent undrained shear strength will reduce, if there is an excess pore water pressure. On site this decrease in shear strength will manifest itself as an increase in rut depth as the operation continues. The most effective remedy to the problem would be to allow the excess pore water pressure to dissipate. Unfortunately, this would not be fiscally viable, in the majority of cases, until the degree of rutting was very severe.

Experimental Verification

A testing programme was initiated to observe the increase in pore water pressure, at some depth below the surface of a saturated clay sample, during cyclic loading. The test work was conducted to verify the hypothesis of the above theory. The simplified testing procedure did not reproduce the stress pattern at the tyre-soil interface as shear stresses were ignored.

Three tests were carried out in order to establish if the consolidation pressure and hence the moisture content of the sample, had a direct effect on the development of excess pore water pressures under a regular cyclic load.

Test Material

The soil used for testing was from the A1\M1 link, contract 2, near Market Harborough, England. The material was a dark grey silty CLAY, with a particle size distribution as in figure 3, with 92% passing the 425μm sieve. The particle size distribution was established by wet sieving, for the coarse fraction, and the hydrometer technique was employed for the fraction less than 63μm in diameter. Liquid and plastic limits for the material were 51% and 21% respectively. All tests were carried out in accordance with BS1377 (BSI, 1991). A value of $\phi'=30°$ was used for this soil, as per site investigation data, (Soil Mechanics Ltd., 1988).

The material for the test was prepared by passing it through a 2.36mm sieve, oven drying it, then mixing it to the required moisture content. In order that the material would be fully saturated, the sample was mixed to the consistency of a slurry, with a moisture content of 75%. The volume of

the sample was such that, once consolidated to a moisture content close to the plastic limit, the sample would be approximately 220mm high.

Test Apparatus

For logistical reasons it was decided to confine the sample and perform the tests in a computer controlled compression testing machine, rather than a triaxial rig. The machine used for cyclically loading the sample was a micro computer controlled loading rig. A bronze cylinder, figure 4, was manufactured for confining the 100mm diameter specimen. The cylinder was constructed in sections, enabling the height of the cylinder to be reduced as the sample consolidated and to ensure that it would fit into the testing apparatus. Each section of the cylinder had an 'O'-ring seal to prevent water egress, figure 4. A hole was drilled 100mm up from the base of the sample, to allow access for the pore water pressure probe. The hole around the tubes was subsequently sealed with a silicone compound sealant. This sealant allowed the probe to move slightly during the consolidation stage of the experiment. The base plate was specially fabricated to fit the loading rig and had two 'O'-ring seals fitted to prevent drainage at the base of the cylinder, figure 4. The pore water pressure probe was connected to a 7 bar pressure transducer, which in turn was wired to a digital display, figure 4.

Pore Water Pressure Measurement

The pore water pressure probe, figure 4, has a permeable ceramic tip, 10mm diameter and 15mm long, attached to small bore steel tubes that can be connected directly into a pressure transducer. To calibrate the system the probe was connected to a triaxial chamber outlet tap, via a short length of thick walled plastic tubing. The triaxial cell was then filled and the system flushed with de-aired water, the cell pressure was then increased in stages up to 110kN/m^2, reduced back down to zero, then repeated. The calibration coefficient was ascertained by correlating the transducer output with the cell pressure, figure 5, giving a correlation coefficient of 0.99.

Test Procedure

Once the sample had been prepared, as described above, it was allowed to equilibrate for 24 hours, it was then poured into the bronze cylinder, to a height just below the pore water pressure probe. The system was then flushed with de-aired water, to ensure full saturation of the probe tip and the remainder of the sample poured into the cylinder. Three layers of filter paper were placed on the top of the sample and left to consolidate under self weight for 24 hours. The consolidation pressure was steadily increased until a target pressure of 100kN/m^2 was achieved. The load was applied to the sample as per figure 6. The concentric rings were placed on top of the sample to ensure a constant rate of consolidation across the whole diameter. The target consolidation pressure was chosen to mimic the field conditions. It was considered that a semi-prepared haul road would be in a remoulded state after the top soil strip and then would be compacted under the continual trafficking of site vehicles, the largest of which apply a ground pressure in the region of 100-130kN/m^2 (VME, 1989).

Once the sample had consolidated fully and the pore water pressure had equilibrated the sample was placed in the testing rig and repeatedly subjected to a hundred test pulses, as in figure 7, until the excess pore water pressure equilibrated. As mentioned previously the loading pulse does not exactly match the pulse applied by an articulated dump truck, as the shearing component could not be incorporated, but the pulse does apply a similar vertical pressure to that of a dump truck. The time delay between pulses represents a typical lag between vehicle passes. The pore water pressure was noted prior to each loading pulse.

Once each test had been completed a sample was taken from the surface for moisture content determination. The sample was then consolidated to a higher pressure. Two further tests were carried out at consolidation pressures of 125 and 150kN/m^2.

Experimental Results

The results of pore water pressure versus number of passes for the three tests are shown in figure 8. This figure shows that the pore water pressure, at a depth of approximately 130mm does not increase above the initial value until approximately the tenth cycle, also that as the moisture content of the sample decreases, the increase in excess pore water pressure reduces. The corresponding decrease in effective stress can be calculated using equation 3. Figure 9 shows the effect of the number of cycles on the effective stress. The shape of this figure compares well with the generic graph of figure 2.

The decrease in effective stress increases as the moisture content of the sample increases. The total reduction in effective stress is of more interest to the site engineer than the reduction between individual passes therefore the generic equations, equations 10 and 11, have been reduced to the form:

$$\sigma'_{100} = \sigma_0 - (u_o + a_{100}\Delta W) \qquad (12)$$

where: σ'_{100} = effective stress before or on the 100th pass

a_{100} = the degree of pore water pressure increase between the first and hundredth pass

The value for a_{100} can be calculated for the three cases and plotted against consistency index, figure 10. This figure allows an estimation to be made for the value of a_{100} from a knowledge of the consistency index of the material, equation 14. The best fit line for a_{100} in terms of consistency index, as per figure 10 is given in equation 13. Knowing the value of a_{100} it is possible to estimate the decrease in effective stress using equation 12.

$$a_{100} = 813e^{(-10.45 I_{c_M})} \qquad (13)$$

To see the effect the excess pore water pressure had on the shear strength of the material, an estimate of the initial shear strength had to be made. This was achieved by converting the corrected moisture content to consistency index, equation 14, then to undrained shear strength by equation 16, proposed by Whyte (1982) developed from data presented by Skempton et al. (1952). Equation 16 has been verified by a series of multistage undrained triaxial tests carried out on this material, figure 11.

$$I_{c_M} = \frac{w_L - w_M}{w_L - w_P} \qquad (14)$$

where: I_{c_M} = consistency index based on corrected moisture content

w_L = liquid limit

w_P = plastic limit

w_M = corrected moisture content, corrected as per equation 15, assuming the coarse fraction has a moisture content of 4%

$$w_M = \frac{100 \text{ x } w_N - 4\% \text{ x } \% > 425\mu m}{\% < 425\mu m} \quad (15)$$

where: w_N = natural moisture content

$\% > 425\mu m$ = percentage of soil greater than $425\mu m$

$\% < 425\mu m$ = percentage of soil less than $425\mu m$

$$c_u = 1.6e^{(4.23 I_{c_M})} \quad (16)$$

where: c_u = undrained shear strength

Thus knowing the initial shear strength the gradual decrease in shear strength can be calculated by combining equation 4 with the generic equation 10 or 11.

The effect of the cyclic loading on shear strength is plotted in figure 12. From this figure, it is evident that the percentage decrease in shear strength, as a function of the initial shear strength, increases as the moisture content of the sample increases. For the three experiments carried out, the percentage decreases in shear strength were, 6, 17, and 38%, at moisture contents of 24, 26, and 28% respectively. The overall decrease in effective strength can be calculated by combining equations 4, 12, and 13, as in equation 17.

$$\tau_{100} = \left[\sigma_0 - \left(u_0 + 813e^{(-10.45 I_{c_M})}\Delta W\right)\right]\tan\phi' \quad (17)$$

Clearly these reductions in shear strength could have serious implications on the performance of plant on the haul roads, (Staples et al., 1992).

Discussion

The full effect of excess pore water pressure increases may not be realised, as only the vertical component of tyre loading has been investigated, the tyre shearing mechanism not being taken into account. However it must be noted that this was not an objective of the experiment. The excess pore water pressure in these experiments was measured at a single depth of approximately 130mm. It is therefore unknown what value the pore water pressure would achieve at the surface and to what depth an increase in the pore water pressure would propagate. Nevertheless, the results from this experiment do show a distinct trend and are in agreement with the theory outlined above, confirming site observations that weaker soils deteriorate at a faster rate than drier ones.

Although the experiments were carried out on confined saturated samples, the results still have practical implications: the operating effective shear strength on site will be lower than that extracted

from the site investigation report, and the current practice of using graders to maintain the quality of haul roads does nothing to improve the long term condition of the haul road. Grading temporarily improves the running surface by smoothing ruts, but due to the loose state of the graded material the full depth of rut returns within a relatively few number of passes.

The only way to improve the quality of the haul road in the long term, is to allow any developed excess pore water pressures to dissipate. This could be achieved by running the vehicles in different lanes if possible. Unfortunately, the majority of road sites are narrow and letting the excess pore water pressures dissipate becomes impractical for financial reasons.

Conclusions

- A numerical relationship for the determination of undrained shear strength due to the build up in pore water pressure is given in terms of effective stress parameters.
- Under a normal cyclic load the pore water pressure at a certain depth in a saturated clay sample, will increase to a constant level.
- The amount of pore water pressure increase depends on the initial moisture content of the sample.
- Knowing the consistency index of the sample it is possible to approximately indicate the decrease in effective stress, hence shear strength.
- The operating shear strength on site could be significantly lower than the value extracted from the site investigation report.

Acknowledgements

The authors wish to acknowledge the assistance of Mr R. Paton and the provision of facilities by the University of Edinburgh. The work was supported financially by an SERC case studentship and Tarmac Construction Limited, Wolverhampton.

References

B.S.I., British Standards Institution, Methods of Test for Soils for Civil Engineering Purposes, BS 1377, Parts 1-9, HMSO, London, 1991.

Skempton, A.W., and Northey, R.D., The Sensitivity of Clays, Geotechnique, Vol.3, pp.30-53, 1952.

Soil Mechanics Ltd., Ground Investigation Report and Factual Information, Boreholes and Trialpits, M1-A1 Link Road, Catthorpe to Rothwell, Contract 2, Part 3, 1988.

Staple, B.L., Wood, G.S., and Forde, M.C., Technical Evaluation of Earthworks Claims under ICE Conditions of Contract 5th and 6th Editions, Proc. Inst. Civil Engrs., Civil Engng, Vol.92, pp.90-95, 1992.

Terzaghi, K., Theoretical Soil Mechanics, John Wiley and Sons Inc., New York, 1943.

VME, Performance Manual Volvo BM Articulated Haulers, Edition 2, Volvo Michigan Euclid, Växjö, Sweden, 1989.

Whyte, I.L., Soil Plasticity and Strength - a New Approach Using Extrusion, Ground Engineering, Vol.15, No.1 pp.16-24, 1982.

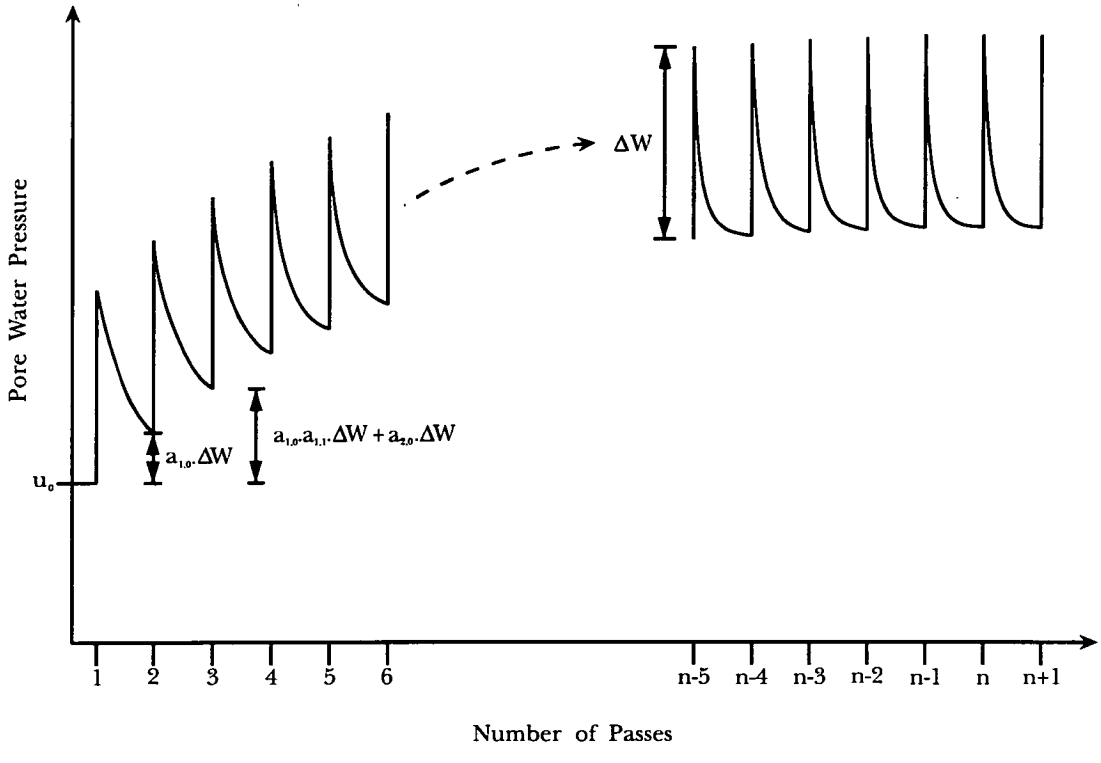

Figure 1: Diagramatic Effect of the Number of Passes on the Pore Water Pressure

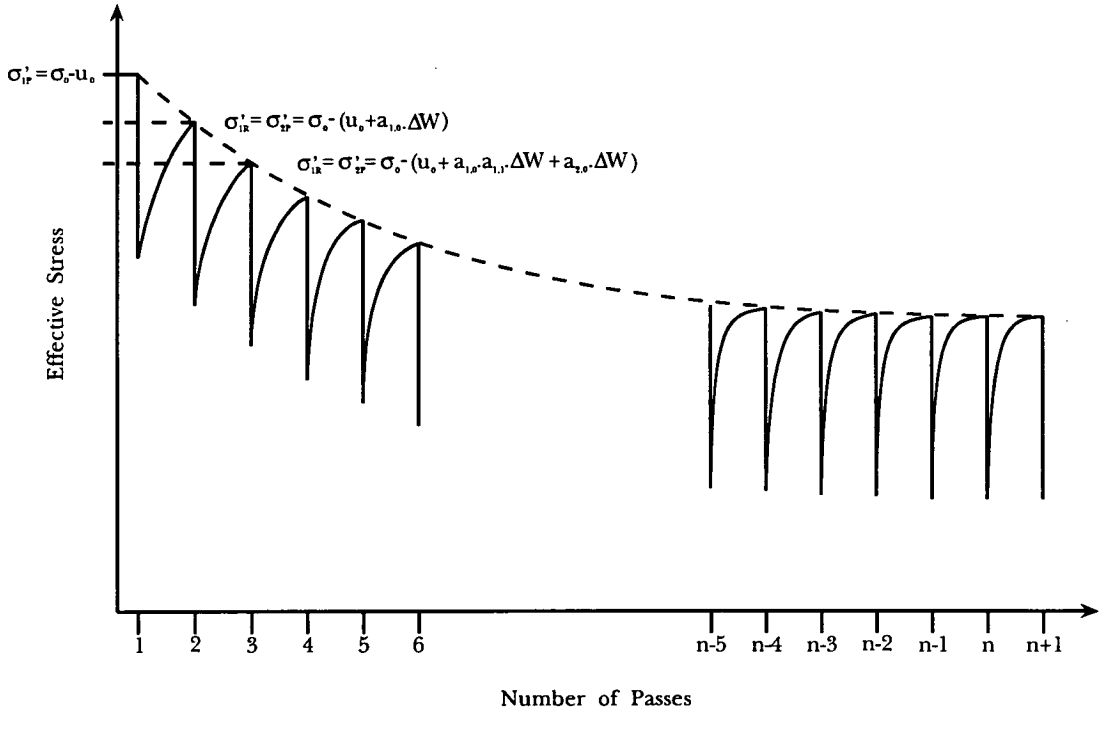

Figure 2: Diagramatic Effect of the Number of Passes on the Effective Stress

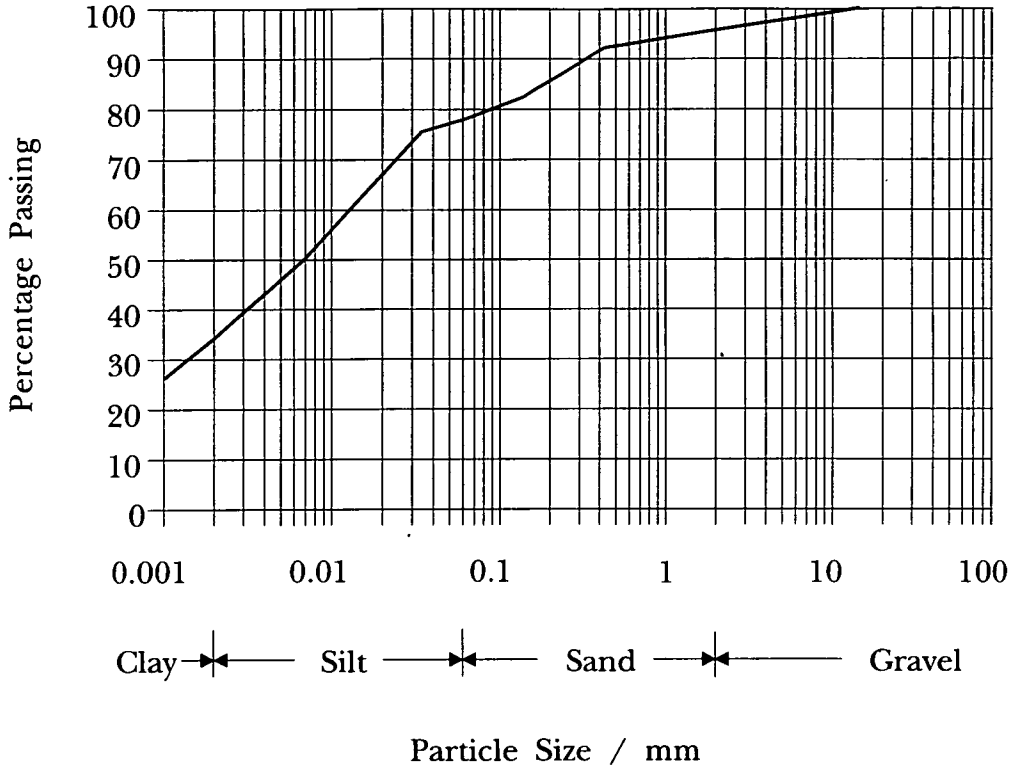

Figure 3: Particle Size Distribution for the Soil Sample used for Pore Water Pressure Experiments

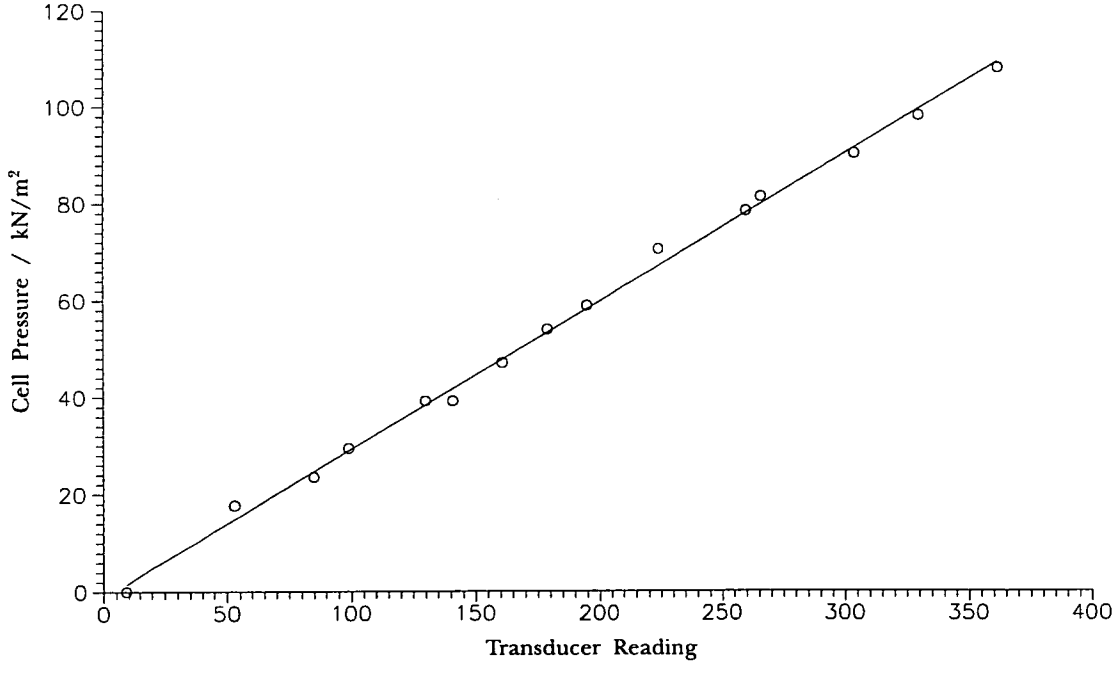

Figure 5: Calibration Curve for the Pore Water Pressure Probe and Transducer

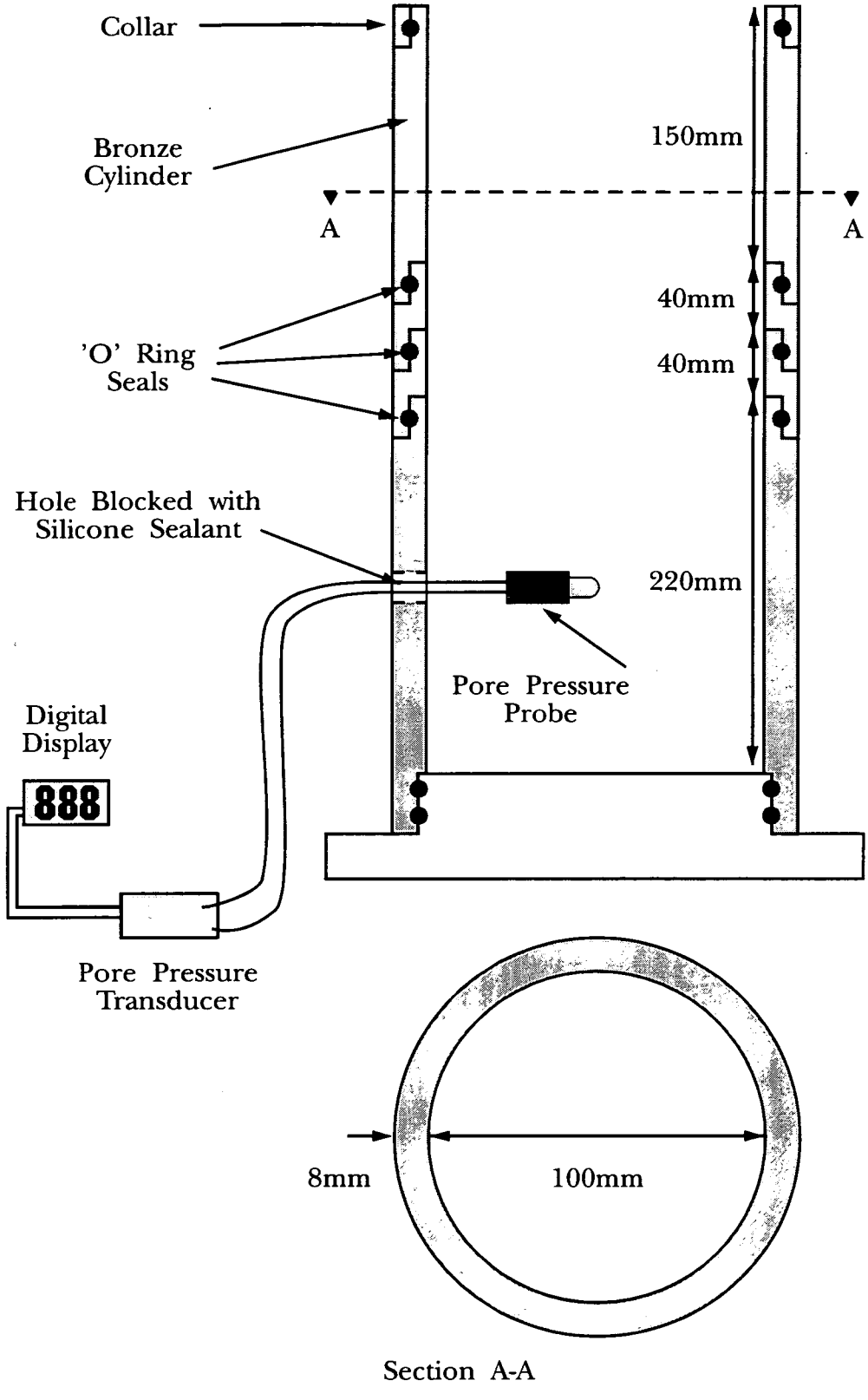

Figure 4: Apparatus for Pore Water Pressure Experiments

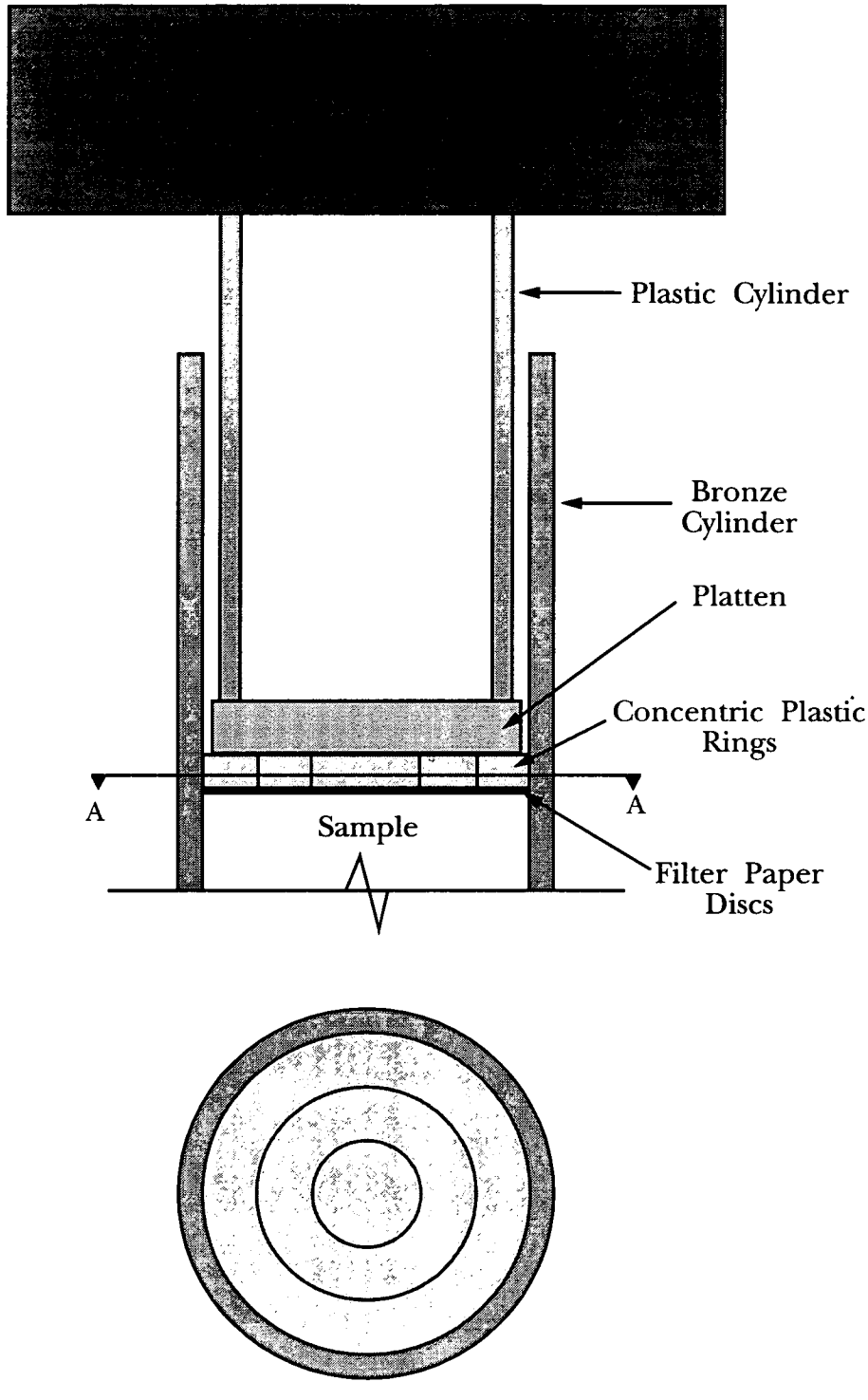

Figure 6: Schematic View of Loading Arrangement for Consolidation (not to scale)

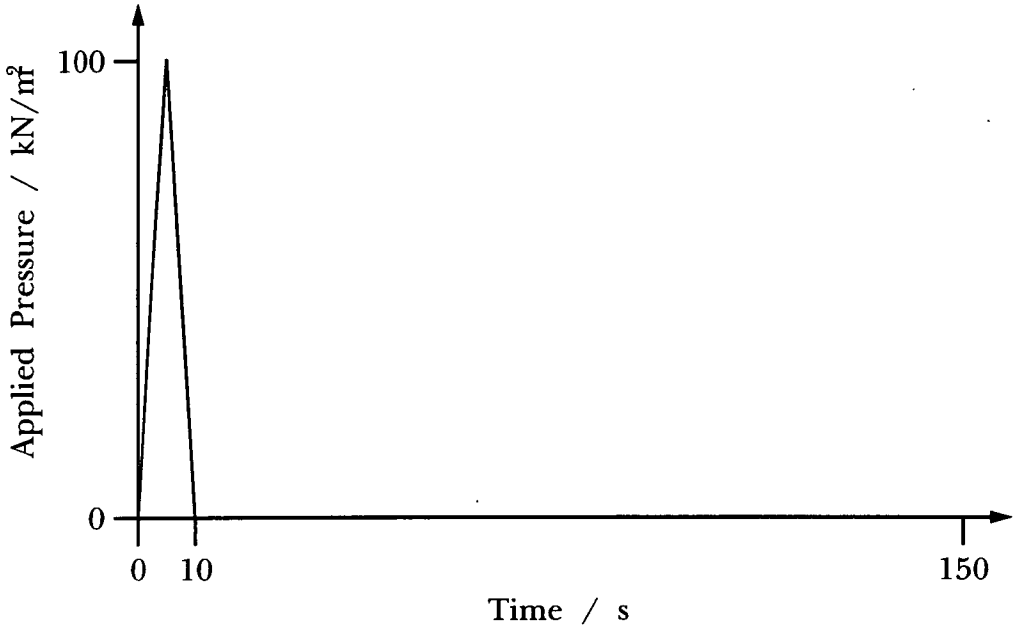

Figure 7: Loading Pulse

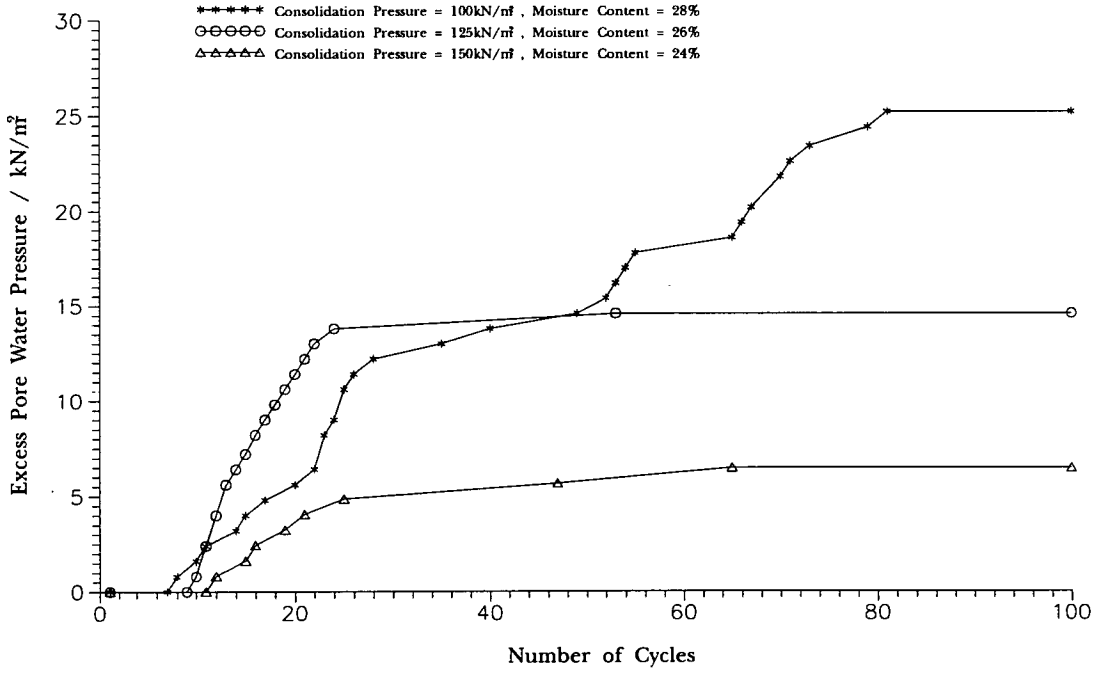

Figure 8: Excess Pore Water Pressure versus Number of Cycles

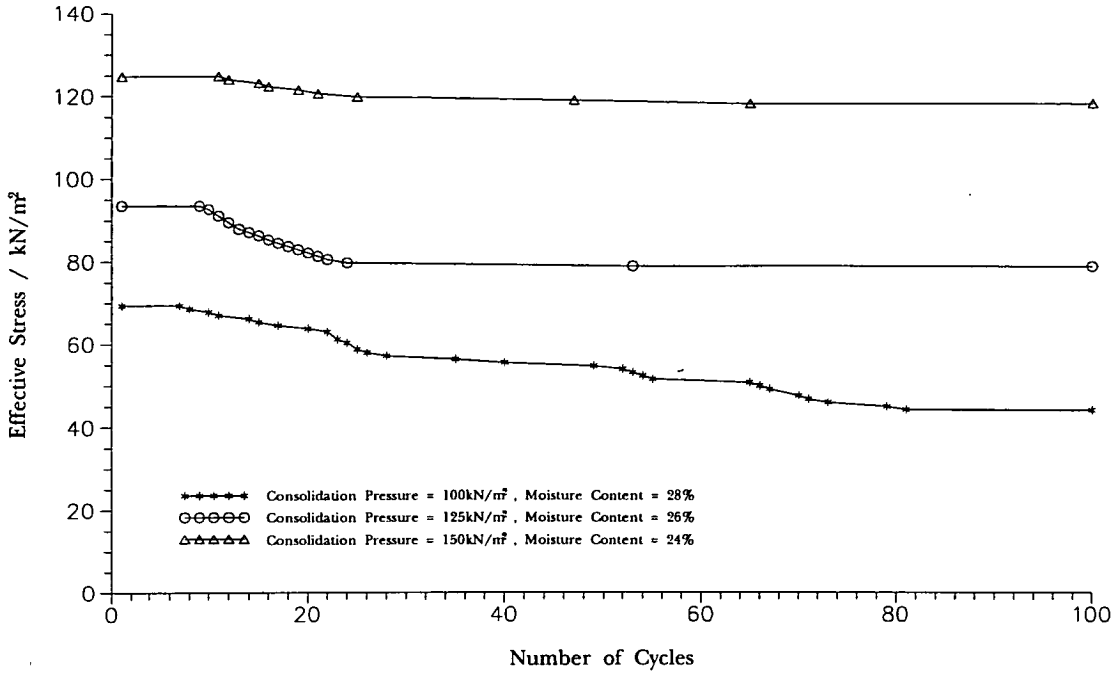

Figure 9: Effective Stress versus Number of Cycles

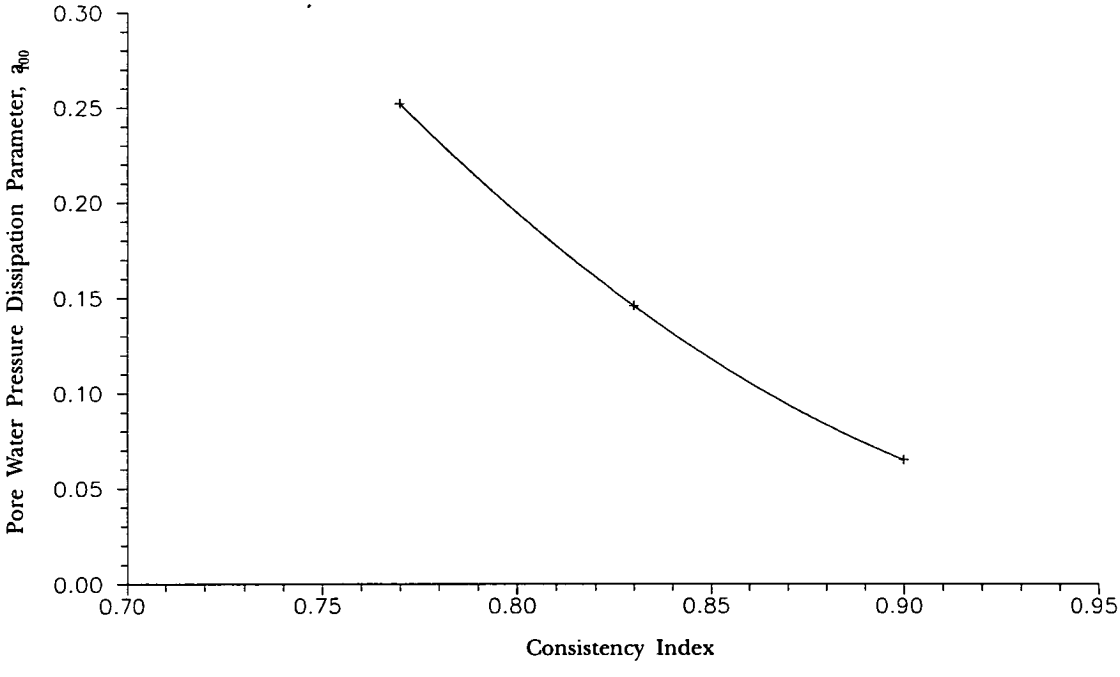

Figure 10: Pore Water Pressure Dissipation Parameter, a_{00} versus Consistency Index

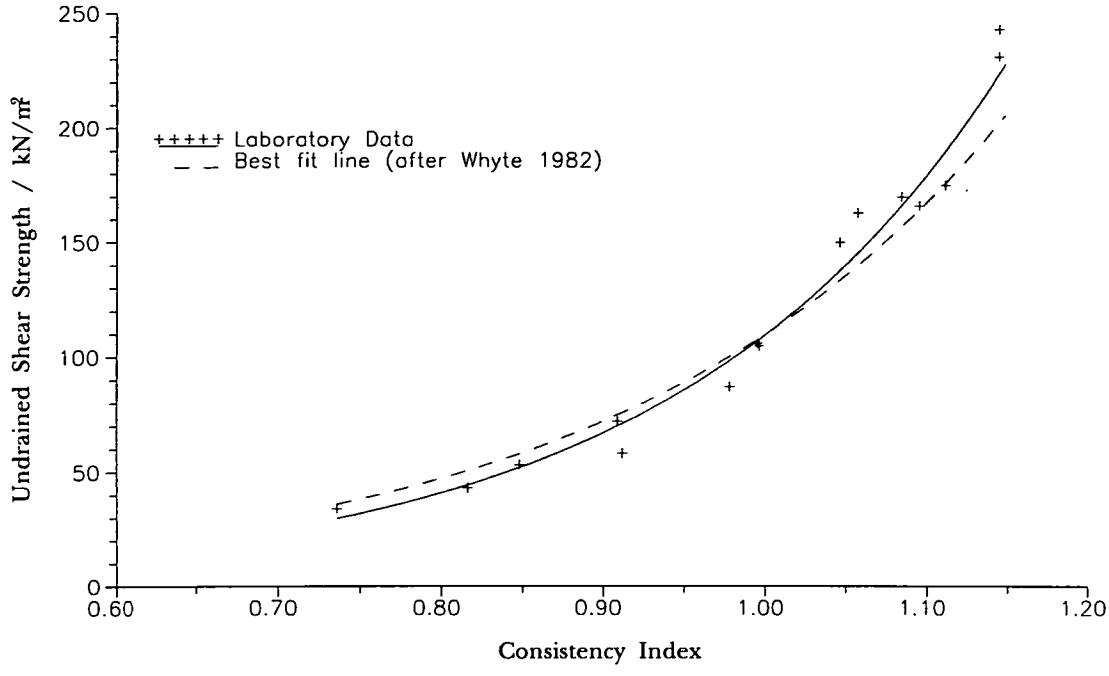

Figure 11: Undrained Shear Strength versus Consistency Index, Comparing the A1/M1 Data with that of Whyte, 1982.

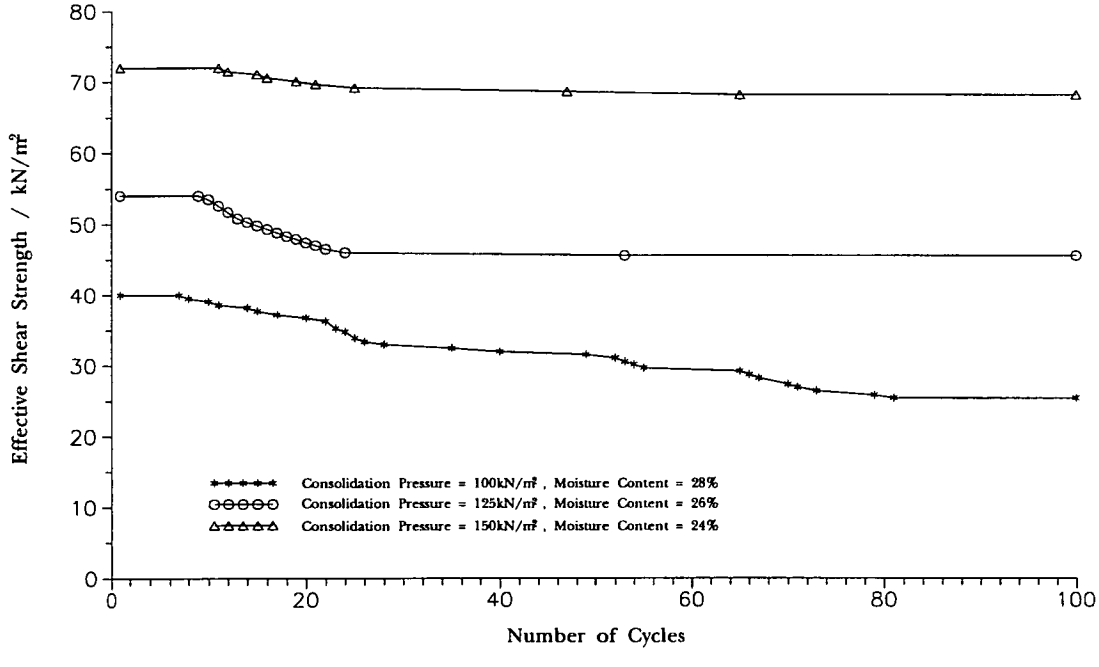

Figure 12: Effective Shear Strength versus Number of Cycles

Paper Title: **Rolling Resistance Coefficients for Articulated Dump Trucks on Civil Engineering Haul Roads**

by: **G.S. Wood, B.Eng.***
J.R. Osborne, B.Sc., C.Eng, MICE†
M.C. Forde, B.Eng., M.Sc., Ph.D., C.Eng., MICE, MIHT, FINDT‡

Being refereed at: Journal of Terramechanics

Keywords: rolling resistance, articulated dump trucks, clay, chalk, estimation.

Abstract

The performance of earthmoving vehicles on haul roads is currently estimated through experience, often with only a limited inspection of the material to be trafficked. Once the contract has been started the absolute speed of the plant is seldom considered to be critical as long as the vehicles keep moving. This could be critical to the contractor, who may not realise the full financial implications of the vehicles travelling at a slightly lower than anticipated velocity.

Different methods of calculating the rolling resistance of the plant are discussed. Two different types of haul road materials have been monitored: chalk and clay. The apparent rolling resistance of the vehicles are related to the various soil and physical properties. For the clay site the equations have been verified to an acceptable degree of accuracy. It is also shown that the velocity of the vehicles can be estimated from the data contained within the site investigation report, and can be continually monitored throughout the duration of the contract as long as a sufficient number of timings are recorded.

Introduction

For a civil engineering contractor working in earthmoving the estimation of the productivity of an earthmoving fleet is critical to the efficiency of an operation. Currently, productivity estimations are carried out on a knowledge of the length of the haul road and the productivity of plant on previous operations, taking little account of ground conditions or the gradient of the road. This method of estimation is prone to error and does not allow the contractor to determine accurately the cost of the project at the time of tender, or to quantify his losses in a claims situation[1].

Little work has been carried out by civil engineers in relating the performance of earthmoving plant to the conditions of the haul road. The majority of work in the past has been carried out by the agricultural engineers on firm but uncompacted soils[2,3], or by the military engineers on virgin terrain[4]. Practically, two empirical methods are available to the estimator for determining the velocity of the plant on site: manufacturers' performance charts, and computer programs. However these predictive tools all rely on the input parameter rolling resistance, which currently cannot be accurately defined at the time of tender, and lacks detail at the higher values of rolling resistance. Even the developers and professional estimators gauge the value of rolling resistance through limited experience.

Methods of Calculating Rolling Resistance

Rolling resistance, the sum of internal and external resistance to motion, has many definitions[5]. A good description of motion resistance of tyres and tracks, and a review of some physical interpretations of motion resistance are given by Upadhyaya et al.[6]. Rolling resistance for civil engineering haul roads is generally calculated using empirical tables[7,8], table 1. These give a description of the haul road condition and a corresponding value of rolling resistance, expressed in terms of percent equivalent

* Research Student, Department of Civil Engineering, University of Edinburgh
† Operations Director, Tarmac Structural Repairs, Wolverhampton
‡ Tarmac Professor of Civil Engineering Construction, University of Edinburgh

grade. For the estimator these charts are relatively useless, as the condition of the haul road is unknown at the time of tender.

By measuring the velocity of the vehicles in the field two methods of back-calculating apparent rolling resistance were available for this study : manufacturers' specification sheets, and the computer programs: Vehsim[9], developed at Caterpillar Inc., Peoria, and Accelerator[10], Accelerator Inc., Fort Myers.

The manufacturers' specification sheets[7,8], give basic information on the vehicle including a rimpull and retardation chart which relates total resistance to the maximum speed of the vehicle, via the mass of the machine. The retardation chart is used when the vehicle is travelling on long steep negative slopes, exceeding 5% total resistance. The major drawback of the rimpull and retardation charts is that only the maximum attainable velocity is ascertained, therefore the acceleration characteristics of a vehicle cannot be determined easily. This makes the estimation of travel time and productivity exceptionally difficult.

Two computer programs: Accelerator[9], and Vehsim[10], were available for estimating vehicle performance. These two programs have essentially the same input parameters, but calculate the acceleration of the vehicle in different ways. Vehsim uses computerised rimpull charts, whereas Accelerator calculates the vehicle performance from the weight to power ratio. Figure 1 shows the relationship between maximum attainable velocity and total resistance for a partially loaded Volvo BM A25 articulated dump truck, using both the Volvo handbook and the two computer programs. As can be seen, all the methods compare well when the vehicle is travelling uphill, but the Vehsim program has no provision for the vehicle retarder when travelling downhill. For this reason the Accelerator program was used throughout the analysis. Graphs for other vehicles with various payloads can be constructed in a similar manner. From these graphs knowing the velocity of the plant the total resistance of the plant can be estimated, assuming the trucks are working at maximum performance.

From table 1, the rolling resistance for a civil engineering haul road could easily lie in the range of 5-14% equivalent grade. The range in speed associated with these rolling resistances is 26-9km/h respectively, for a 75% loaded Volvo BM A25 6x6 articulated dump truck, assuming a flat haul road, using the Accelerator software.

Experimental Procedure

All site monitoring had to be undertaken from the side of the haul road as no instrumentation of, or interference with, the operation of the plant was possible. Vehicles were timed, wherever possible, over 60m sections of haul road having constant gradient, if the haul road varied in gradient then timings were made at recognisable positions. Sections were chosen with no obstructions such that the plant was operating at near maximum performance. An average of at least ten timings was taken for each type of dump truck on each section of haul road. All gradients were measured using an electronic theodolite.

On the clay site soil samples were taken at 20m intervals and the following soil tests were carried out on each sample: moisture content, moisture condition value[11,12] (MCV), cone penetrometer[13] and vane shear. As well as these tests a series of plastic and liquid limits, particle size distribution, and multistage triaxial undrained shear tests[14] were carried out on a representative sample of the material. All tests were carried out in accordance with BS1377[15].

From the knowledge of the timings and gradients, it was possible to use the Accelerator computer program to back analyse the apparent rolling resistance of each section of the haul road.

Chalk

Chalk is a soft fine-grained limestone made up of tiny hollow shell fragments and generally has a high void ratio. Any mechanical disturbance of the cellular structure releases pore water from the near saturated cells. Excess pore water causes dilatency of the silt sized chalk particles creating a material called putty chalk. This process is facilitated by chalk's low plasticity index and lack of absorbency. Drying of putty chalk results in recementation and generally increases the shear strength. For this reason haul roads on chalk are very strong and have an excellent running surface. The only way to deteriorate the surface is to traffic the haul road when wet or to excessively traffic a specific point.

The chalk site monitored was the final section of the M3, through Twyford Down, in the south of England. This 5km stretch of motorway contained 2.7Mm^3 of earthmoving, the majority in a single cut, therefore most of the loaded hauling was downhill, the maximum gradient being approximately 20%. The earthworks were constructed using a backhoe-dump truck combination. The excavators were Cat 245's and the haulers were a mixture of Cat D400D and Volvo A35 articulated dump trucks.

No physical tests were carried out on the chalk, the surface was too strong to use the shear vane or the cone penetrometer and no laboratory testing of the material was undertaken as all the tests carried out on chalk require a 300-500ml lump of chalk, which is difficult to obtain due to the surface being covered in dried putty chalk. Since no physical tests were carried out on the chalk the apparent rolling resistance of each section was related to the gradient of the haul road. As the quality of the haul roads was so good, the analysis on this material would be similar to that carried out on any non-rutting surface.

Figures 2 and 3 show the relationship between back analysed rolling resistance, calculated using the Accelerator software, and average gradient over each section, for the two types of hauler, Volvo BM A35 and Cat D400D articulated dump trucks respectively. These figures show clearly that the gradient of the haul road has a secondary effect on the apparent rolling resistance of the vehicles.

For a loaded Volvo BM A35 travelling down a steep slope, greater than 10%, figure 2, the apparent rolling resistance decreases linearly as the gradient becomes shallower, contradicting the expected outcome. The value of rolling resistance in this portion of the graph, is approximately 4% lower than the grade resistance, giving a constant total resistance of approximately 4%. As the slope becomes shallower the apparent rolling resistance stabilises at a value of between 3 and 6% and the total resistance rises linearly. The equation of the linear best fit line shown in figure 2, equation 1, has a R^2 value of 88%.

$$\text{Apparent Rolling Resistance} = 0.11 - 0.79 \times \text{Grade Resistance} \quad (1)$$

This vehicle was never monitored travelling loaded uphill, as the dumping areas were at the bottom of the cut. When travelling uphill empty the apparent rolling resistance was constantly recorded below 6%, this value can be seen to decrease slightly as the severity of the slope increases. The linear best fit line for the unloaded portion of the graph is given in equation 2 and has a R^2 value of 40%. This value of R^2 is much lower than that for the loaded vehicles due to the inherent variability in the unloaded travel time.

$$\text{Apparent Rolling Resistance} = 4.05 - 0.10 \times \text{Grade Resistance} \quad (2)$$

The performance of empty vehicles is more variable depending on the resourcing of the operation. If the haul is over-resourced then the vehicles will return to the loader slowly: to avoid queuing at the prime mover, and to reduce the strain on the engine. However, when travelling up steep inclines the vehicles must be driven at maximum power. For this reason it would be expected that the apparent rolling resistance for loaded vehicles travelling uphill would lie in the 2 to 6% bracket. It is impossible however to predict the performance of empty vehicles travelling downhill without further monitoring.

These values are in the majority higher than the those expected from the description of the haul roads in the Caterpillar handbook.

Figure 3, shows the relationship between apparent rolling resistance and grade resistance for the Cat D400D articulated dump trucks. This graph does not indicate as good a relationship as for the Volvo BM A35 in the previous figure. The majority of the points on the empty uphill portion of the graph lie below 6% apparent rolling resistance, the linear best fit line is given in equation 3 with a R^2 value of 64%. As the gradient becomes flatter and then downhill the rolling resistance increases indicating that the grade has an effect on driver-vehicle performance.

$$\text{Apparent Rolling Resistance} = 6.86 - 0.22 \times \text{Grade Resistance} \quad (3)$$

The loaded results again show that grade resistance has a secondary effect on apparent rolling resistance. The linear best fit line through the data is given by equation 4 and has a R^2 value of 78%. Again the degree of correlation is superior for the loaded vehicles over the empty vehicles, for similar reasons as explained earlier.

$$\text{Apparent Rolling Resistance} = 5.48 - 0.33 \times \text{Grade Resistance} \quad (4)$$

Both figures 2 and 3 show that steep downhill grades have the effect of increasing the apparent rolling resistance of the driver-vehicle-terrain system. From an estimating point of view this is exceptionally important as the vehicles are travelling significantly slower than could have been expected from any information available to date.

Table 2 gives a résumé of the apparent rolling resistance equations with respect to grade resistance, the degree of correlation, and the range of gradients for the vehicles tested.

Clay

Vehicle monitoring on clay haul roads took place on the A1/M1 link contracts 2 and 3. The contract was a total of 28km long with a total of $3Mm^3$ of soil to be moved. Again the earthworks were constructed using a backhoe / articulated dump truck combination. The haulers were primarily a mixture of Cat D400D, Volvo BM A25 6x6, Volvo BM A30 6x6, and Volvo BM A35 6x6 articulated dump trucks.

The site investigation was carried out by five companies over a period of 11 years. Typically the material was a brown silty clay, with over 80% passing the 425μm sieve, figure 4. Average Atterburg limits were w_L = 47% and w_P = 22%. The haul roads were generally in good condition although flexing was apparent under most sections of the haul roads during trafficking. The material on the haul roads was generally dry of the plastic limit, remoulded and well compacted. Rut depths were minimal, but a layer of loose dry material accumulated on the surface with trafficking. Work was halted during prolonged periods of rain to preserve the condition of the haul roads and then left to dry adequately prior to re-trafficking.

Apparent rolling resistance was calculated as for the chalk roads and linearly correlated with the parameters: moisture condition value, hand vane shear strength, consistency index, grade resistance, and rut depth. The first three parameters were discussed in a previous paper[16]. Continuing from this a multiple regression analysis was carried out to establish equations for apparent rolling resistance in terms of the five input variables. All possible combinations of these five input factors were considered. Initially the analysis dealt with individual types of vehicle travelling in the four main driving conditions: loaded uphill, loaded downhill, empty uphill, and empty downhill, but it was discovered that there was an insufficient number of points to carry out the analysis satisfactorily. It was therefore decided to simplify the analysis by combining all the vehicle types together. Hence six driving conditions were defined for all vehicles: all empty, all empty uphill, all empty downhill, all loaded, all

loaded uphill, and all loaded downhill. These conditions were regressed against all possible combinations of the five input variables.

The regression analysis showed that the multiple regression with the highest R^2 value was the five factor interaction, with an average value of 70% for all six driving conditions. The coefficients for each of the five parameters, the constant term, and the R^2 values are shown in table 3, e.g. the equation for any truck travelling uphill empty would be as in equation 5:

$$R_O = 12.3\text{-}0.588G\text{-}1.30Ic+0.300MCV\text{-}0.0335V\text{-}0.00648R. \quad (5)$$

where: R_O - Apparent Rolling Resistance (% Equivalent Grade)
G - Grade Resistance (%, uphill grades positive)
Ic - Consistency Index
MCV - Moisture Condition Value
V - Hand Vane Shear Strength (kN/m^2)
R - Rut Depth (mm)

It should be noted at this point that it would be dangerous to extrapolate outwith the data limits used to develop these equations[16].

For estimating purposes the primary drawback of this formula is that at the time of tender the rut depth on the haul road is unknown. For this reason the four factor regression equation, omitting the factor rut depth, have been calculated and are shown in table 4. As site investigation reports seldom hold all of this information at any single point, tables 5-8 give regression equations for all two factor regressions containing grade, except rut depth, and the single factor regression with just grade. The equations with grade are the most important for the estimator as this parameter will normally be known. The coefficients do not always have the expected sign, for example the coefficients for moisture condition value have a positive sign that would indicate that as the moisture condition value increased, the ground becomes drier, the apparent rolling resistance would increase. This is caused by the somewhat flat nature of the apparent rolling resistance versus moisture condition value graphs[16]. The other anomalies in the regression analysis are most likely a function of considering all the vehicles and interactions at once, and where a single stray result can completely alter the relationship.

For an estimator, it would be useful to know the range of average apparent rolling resistances for a given set of input conditions. Using the average values for each of the five parameters, on the six driving conditions, 95% confidence intervals were calculated for each of the regression equations and are shown in table 9. When monitoring an individual operation for a short period of time the spread in data will be greater than the average for the complete operation. Prediction intervals have been calculated for the various regression analyses and the results can be seen in table 10. Both tables 9 and 10 show the range in confidence and prediction intervals to be similar for all the different regression equations, at the average values. As mentioned previously care must be taken not to extrapolate outwith the data limits.

Relating the confidence and prediction intervals to the velocity of the vehicle shows how accurate the prediction would be. For example an empty vehicle travelling downhill, and using the five factor regression, with average input values, has a 95% confidence interval for apparent rolling resistance of 10.4-11.2%. This range in apparent rolling resistance corresponds, for a Volvo BM A25 6x6 articulated dump truck, to a range in maximum speed from 26 to 29km/h. The corresponding prediction interval for apparent rolling resistance is 8.4-13.2%, which relates to a maximum velocity range of 22.5-36km/h. These intervals have a greater accuracy than the current method of estimating the velocity of earthmoving plant.

Validation of Regression Equations

When the regression equations were calculated three sets of data were omitted from the analysis as there were only a few data values for each of the vehicle types. The makes of vehicles had all been incorporated into the analysis, but the vehicles came from different subcontractors. These vehicles generally worked in conjunction with the various other subcontractors on the operations. The input parameters for the five factor regression analysis for these extra sections are given in table 11. The predicted apparent rolling resistances were calculated using the relevant equations from table 3, and the results are given in table 12.

Comparing the predicted rolling resistances with the actual rolling resistances, as measured on site, shows excellent correlation between the two, table 12. The majority of the predicted values lie within the 95% confidence interval, and all the estimated rolling resistances lie within the 95% prediction interval. The corresponding velocities for both the predicted and actual apparent rolling resistances can also be seen in table 12. These show the expected results, with the sections on uphill grades having lower velocities than the downhill grades.

The percentage differences in the velocities expressed as a percentage of the predicted velocity can be seen in table 13. This table also shows the number of timings taken to formulate the average, and the number of different operator-vehicle combinations. The large percentage changes in velocity are related to the number of timings taken to calculate the average, figure 5. This shows that as the number of readings increases the accuracy of the estimation improves. At the lower number of time recordings there is still the possibility of a reasonable correlation, but the probability is much lower. Therefore when monitoring the vehicles on site it is recommended that a minimum of ten recordings should be taken before calculating the average.

The number of vehicles used in the estimation also effects the average, for example if there is only one operator-vehicle combination in operation, then the recorded average is statistically less likely to be similar to the average, for a number of drivers over the same section of haul road. For this reason the predicted value of rolling resistance for the single Volvo A35, Fleet 2, has the greatest inaccuracy of all the validation vehicles. Increasing the number of vehicles used to determine the average travel time generally increases the accuracy of the estimation.

Even for the limited number of results used to validate the five factor regression equation, it is clear that the equations work well for the conditions tested.

Conclusions

Grade resistance has a secondary effect on the driver, which increases the apparent rolling resistance, especially on steep grades.

It is possible to estimate the apparent rolling resistance of articulated dump trucks on a non-flexing roadway by the gradient.

On clay regression equations have been developed to express apparent rolling resistance in terms of: grade resistance, consistency index, moisture condition value, vane shear strength, and rut depth. These equations have been verified on different vehicles, enabling a prediction of the speed of the plant to be made from the site investigation report, as long as the data contained within the report are accurate.

For site monitoring, a minimum of ten time readings should be made for each type of vehicle on each section of the haul road tested.

References

1. Staples, B.L., Wood, G.S. and Forde, M.C., Technical Evaluation of Earthworks Claims Under ICE Conditions of Contract 5th. and 6th. Editions, *Proc. Inst. of Civil Engrs.*, Civil Engineering, Vol.92, pp.90-95, May 1992.

2. Wulfsohn, D. and Upadhyaya, S.K., Prediction of Traction and Soil Compaction using 3D Soil-Tyre Contact Profile, *J. Terramechanics*, Vol.29, No.6, pp.541-564, 1992.

3. Alcock R. and Wittig V., An Empirical Method of Predicting Traction, *J. Terramechanics*, Vol.29, No.5, pp.381-394, 1992.

4. Turnage G.W., Tire Selection and Performance Prediction for Off-Road Wheeled-Vehicle Operations, *Proc. 4th. Int. Conf. Int. Soc. Terrain Vehicle Systems*, Vol.1, pp.61-82, Stockholm, Sweden, 1972.

5. Plackett, C.W., A Review of Force Prediction Methods for Off-Road Wheels, *J. Agric. Engng. Res.*, Vol.31, pp.1-29, 1985.

6. Upadhyaya, S.K., Chancellor, W.J., Wulfsohn, D. and Glancey, J.L., Sources of Variability in Traction Data, *J. Terramechanics*, Vol.25, No.4, pp.249-272, 1988.

7. Caterpillar, *Caterpillar Performance Handbook*, 24th. Edition, Caterpillar Inc., Peoria, Illinois, U.S.A., 1993.

8. VME, *Performance Manual Volvo BM Articulated Haulers*, Edition 2, Volvo BM Haulers, Växjö, Sweden, 1989.

9. Caterpillar, *Vehsim - Vehsim Simulation Software User's Guide*, Version 2.21, Caterpillar Inc., Peoria, Illinois, U.S.A., 1987.

10. Accelerator, *Accelerator Vehicle Performance Software User's Guide*, Version 1.17, Accelerator Inc., Fort Myers, Florida, U.S.A., 1987.

11. Parsons, A.W., *The Rapid Determination of the Moisture Condition of Earthwork Material*, Dept. of the Environment, TRRL Report LR750, Crowthorne 1979.

12. The use and Application of the Moisture Condition Apparatus in Testing Soil Suitability for Earthworking, Scottish Development Dept., Technical Memorandum SH7/83 amendment No.1, 1989.

13. ASAE, *Soil Cone Penetrometer*, American Society of Agricultural Engineers, Standard S313.2, 1985.

14. Anderson, W.F., The use of Multi-Stage Triaxial Tests to Find the Undrained Strength Parameters of Stony Boulder Clays, *Proc. Inst. Civil Engrs.*, Vol.57, Part 2, pp.367-372, June 1974.

15. B.S.I., British Standards Institution, *Methods of Test for Soils for Civil Engineering Purposes*, BS 1377, Parts 1-9, HMSO, London, 1991.

16. Wood, G.S., Osborne, J.O., and Forde, M.C., Soil Parameters for Estimating the Rolling Resistance of Earthmoving Plant on a Compacted Silty Cohesive Soil, *J. Terramechanics*, to be published.

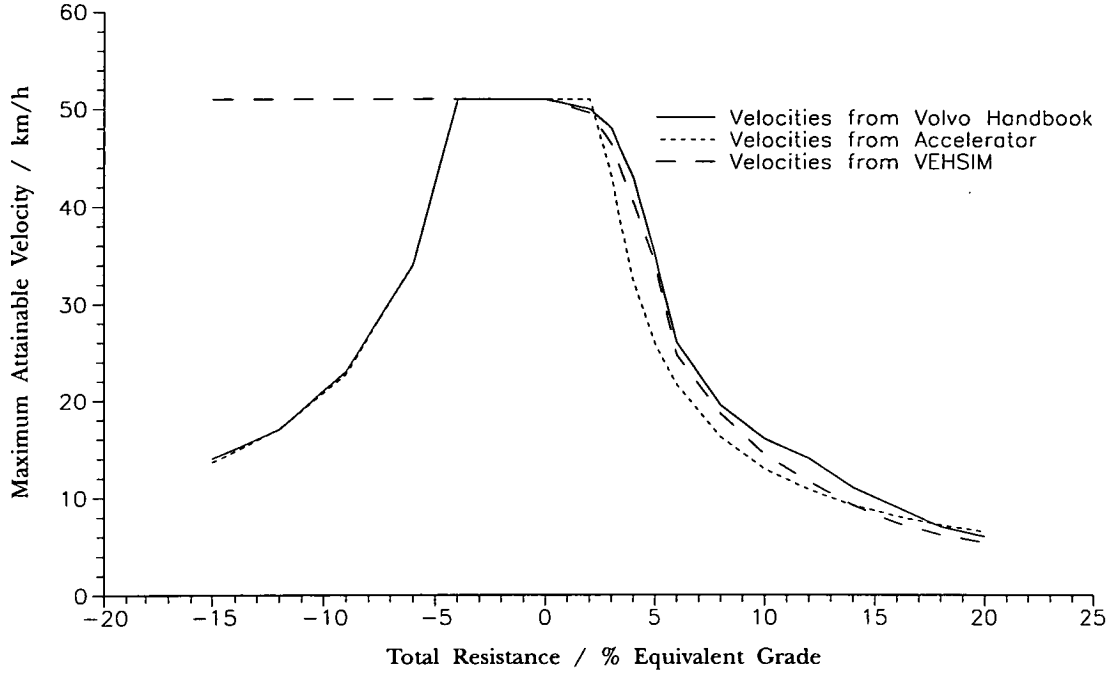

Figure 1: Maximum Attainable Velocity versus Total Resistance for a Partially Loaded (75%) Volvo BM A25 6x6 Articulated Dump Truck.

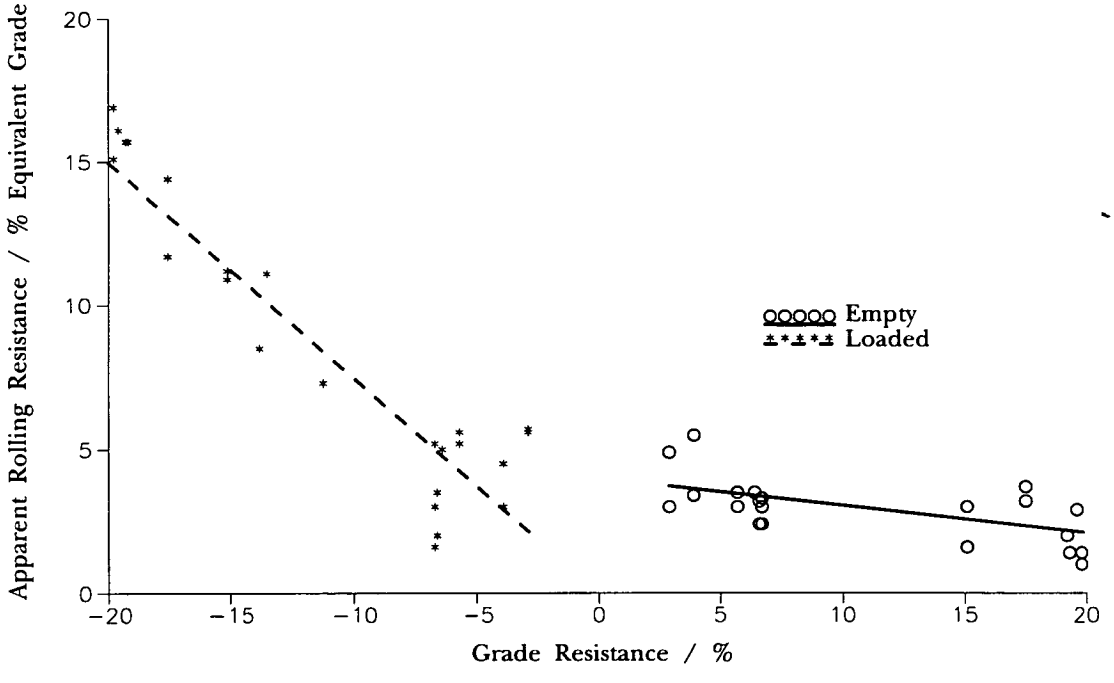

Figure 2: Apparent Rolling Resistance versus Grade Resistance for Volvo BM A35 Articulated Dump Trucks on Chalk

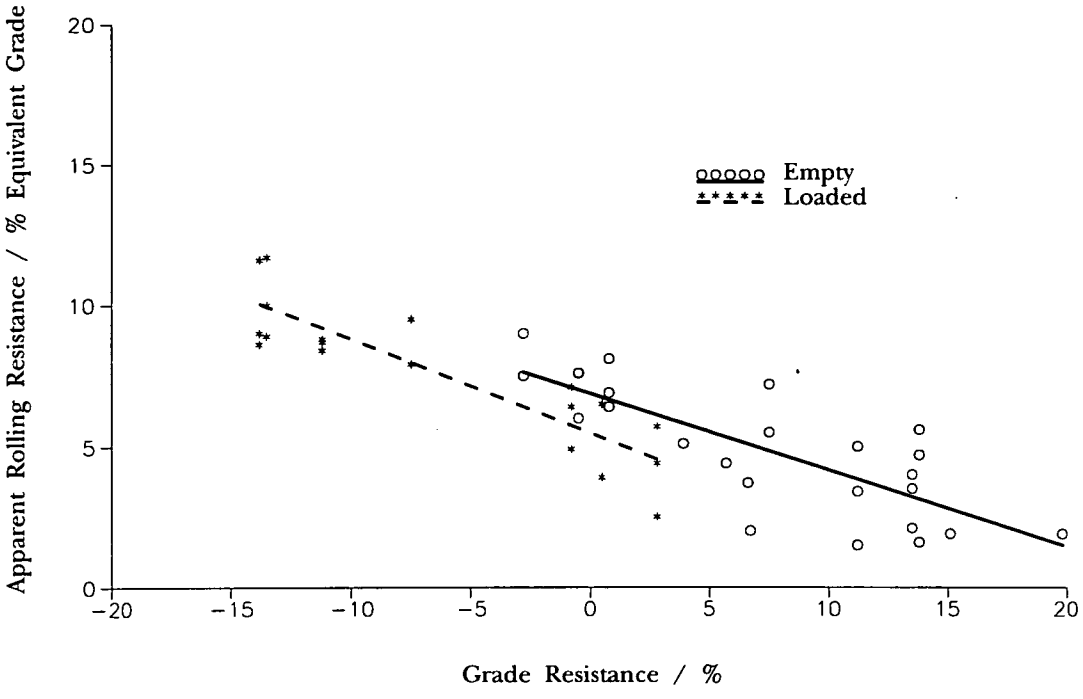

Figure 3: Apparent Rolling Resistance versus Grade Resistance for Cat D400D Articulated Dump Trucks on Chalk

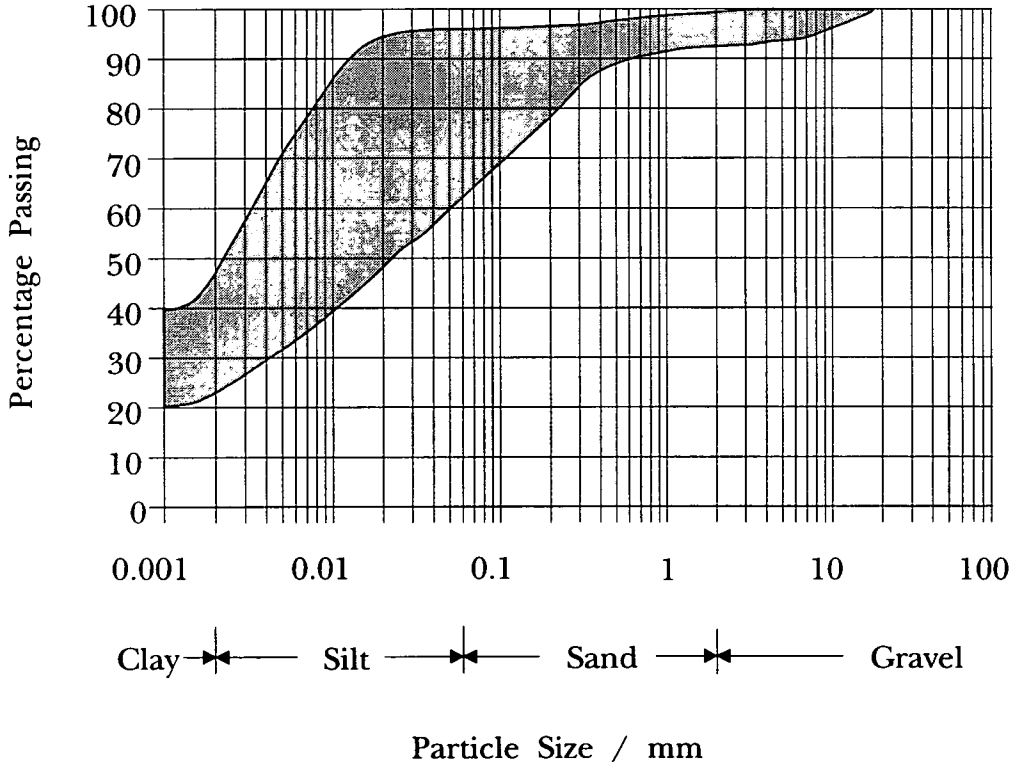

Figure 4: Particle Size Distribution Envelope for A1/M1 Link

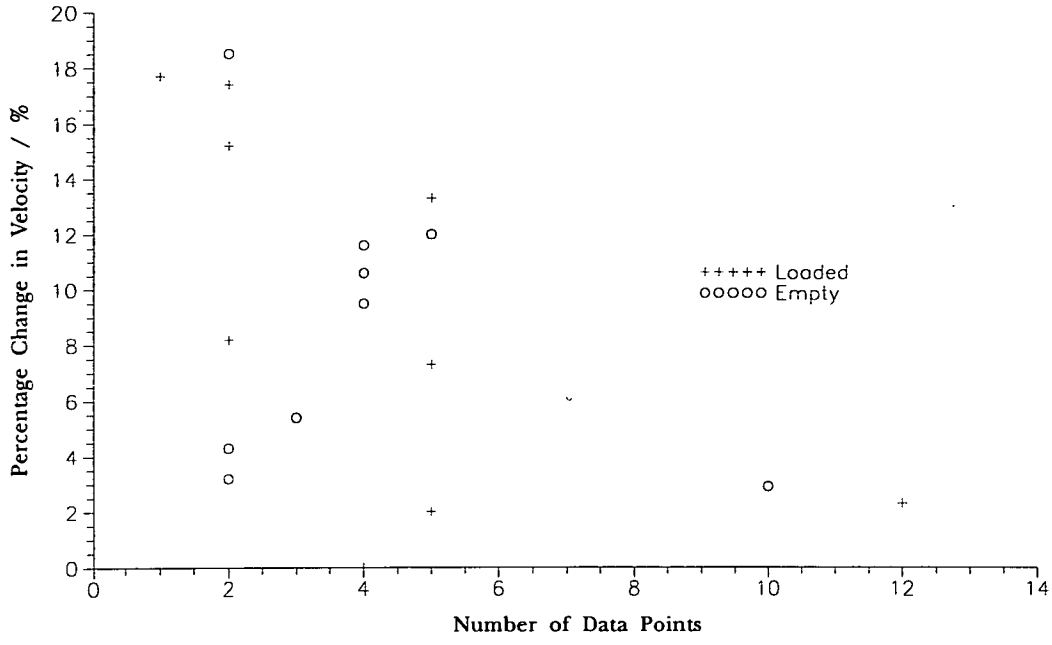

Figure 5: Percentage Change in Velocity versus Number of Points for the Various Vehicles used in the Validation of the Five Factor Regression Equations.

Surface Condition	Rolling Resistance / % Equivalent Grade
A very hard, smooth roadway, concrete, cold asphalt or dirt surface, no penetration or flexing.	1.5
A hard smooth stabilised surfaced roadway without penetration under load, watered, maintained.	2.0
A firm, smooth rolling roadway with dirt or light surfacing, flexing slightly under load or undulating, maintained fairly regularly, watered.	3.0
A dirt roadway, rutted or flexing under load, little maintainance, no water, 25mm penetration or flexing.	4.0
A dirt roadway, rutted or flexing under load, little maintainance, no water, 50mm penetration or flexing.	5.0
Rutted dirt roadway, soft under travel, no maintainance, no stabilisation, 100mm tyre penetration or flexing.	8.0
Loose sand or gravel.	10.0
Rutted dirt roadway, soft under travel, no maintainance, no stabilisation, 200mm tyre penetration or flexing.	14.0
Very soft, muddy, rutted roadway, 300mm tyre penetration, no flexing.	20.0

Table 1: Caterpillar Table of Rolling Resistance (after Caterpillar, 1993)

Vehicle	Loaded / Empty	Equation	Gradient Range		R^2
			Min.	Max.	
Volvo BM A35	Loaded	$R_o = 0.11 - 0.76 \times G$	-19.8	-2.9	88
	Empty	$R_o = 4.05 - 0.10 \times G$	2.9	19.8	40
Cat D400D	Loaded	$R_o = 5.48 - 0.33 \times G$	-13.8	2.8	78
	Empty	$R_o = 6.86 - 0.27 \times G$	-2.8	19.8	64

R_o - Apparent Rolling Resistance
G - Grade Resistance

Table 2: Equations of Apparent Rolling Resistance for Chalk

Driving Condition	Coefficients for the Parameters						R^2 /%
	Constant	Grade	Consistancy Index	Moisture Condition Value	Vane Shear Strength	Rut Depth	
All Empty	12.7	-0.637	-2.30	+0.287	-0.0281	-0.00359	74.3
All Empty Up	12.3	-0.588	-1.30	+0.300	-0.0336	-0.00648	56.8
All Empty Down	11.5	-0.615	-0.35	+0.385	-0.0446	+0.00254	47.6
All Loaded	9.11	-0.477	-4.84	+0.117	-0.0027	+0.00797	82.3
All Loaded Up	6.3	-0.43	-3.87	+0.060	+0.0102	+0.01130	68.4
All Loaded Down	12.5	-0.599	-2.99	+0.197	-0.0409	-0.00023	88.4

Table 3: Coefficients for the Parameters in the Five Factor Regression Analysis Relating Apparent Rolling Resistance to Grade, Consistency Index, Moisture Condition Value, Vane

Driving Condition	Coefficients for the Parameters					R^2 /%
	Constant	Grade	Consistancy Index	Moisture Condition Value	Vane Shear Strength	
All Empty	11.20	-0.625	-1.62	+0.266	-0.0236	73.2
All Empty Up	7.48	-0.294	+1.27	+0.252	-0.0239	52.2
All Empty Down	12.60	-0.587	-1.38	+0.349	-0.0396	47.3
All Loaded	12.60	-0.447	-7.36	+0.212	-0.0113	76.6
All Loaded Up	12.40	-0.576	-9.09	+0.234	+0.0019	48.4
All Loaded Down	12.40	-0.602	-2.92	+0.196	-0.0408	88.4

Table 4: Coefficients for the Parameters in the Four Factor Regression Analysis Relating Apparent Rolling Resistance to Grade, Consistency Index, Moisture Condition Value, and V

Driving Condition	Coefficients for the Parameters			
	Constant	Grade	Consistancy Index	R^2 /%
All Empty	14.70	-0.647	-4.92	64.6
All Empty Up	16.70	-0.728	-6.67	57.2
All Empty Down	14.40	-0.579	-4.43	44.7
All Loaded	12.20	-0.446	-6.07	71.9
All Loaded Up	14.20	-0.451	-7.79	42.1
All Loaded Down	8.22	-0.623	-2.57	51.4

Table 5: Coefficients for the Parameters in the Two Factor Regression Analysis Relating Apparent Rolling Resistance to Grade, and Consistency Index.

Driving Condition	Coefficients for the Parameters			
	Constant	Grade	Moisture Condition Value	R^2 /%
All Empty	8.95	-0.603	+0.0278	68.8
All Empty Up	7.38	-0.487	+0.1260	42.2
All Empty Down	10.40	-0.631	-0.0840	35.2
All Loaded	5.42	-0.531	+0.0236	59.4
All Loaded Up	4.41	-0.320	+0.0530	9.5
All Loaded Down	6.42	-0.673	-0.0710	44.7

Table 6: Coefficients for the Parameters in the Two Factor Regression Analysis Relating Apparent Rolling Resistance to Grade, and Moisture Condition Value.

Driving Condition	Coefficients for the Parameters			
	Constant	Grade	Vane Shear Strength	R^2 /%
All Empty	10.70	-0.621	-0.0089	69.8
All Empty Up	9.10	-0.451	-0.0014	34.6
All Empty Down	12.30	-0.636	-0.0185	41.0
All Loaded	7.39	-0.512	-0.0105	60.6
All Loaded Up	6.25	-0.264	-0.0078	10.4
All Loaded Down	9.97	-0.763	-0.0310	77.0

Table 7: Coefficients for the Parameters in the Two Factor Regression Analysis Relating Apparent Rolling Resistance to Grade, and Vane Shear Strength.

Driving Condition	Coefficients for the Parameters		
	Constant	Grade	R^2 /%
All Empty	9.40	-0.579	55.2
All Empty Up	10.00	-0.774	39.1
All Empty Down	8.96	-0.720	36.0
All Loaded	5.71	-0.529	58.0
All Loaded Up	4.96	-0.268	7.4
All Loaded Down	5.69	-0.608	44.8

Table 8: Coefficients for the Parameters in the Single Factor Regression Analysis Relating Apparent Rolling Resistance to Grade.

	95% Confidence Interval for the Average Values					
Driving Condition	Five Factor	Four Factor	Two Factor Grade and Consistency Index	Two Factor, Grade and Moisture Condition Value	Two Factor, Grade and Vane Shear Strength	Single Factor
All Empty	9.6 - 10.2	9.5 - 10.2	9.6 - 10.3	9.5 - 10.2	9.5 - 10.2	9.5 - 10.3
All Empty Up	7.3 - 8.7	7.1 - 8.5	7.6 - 9.0	7.3 - 8.4	7.3 - 8.4	7.5 - 9.0
All Empty Down	10.4 - 11.2	10.4 - 11.2	10.2 - 11.1	10.4 - 11.2	10.4 - 11.2	10.2 - 11.2
All Loaded	5.1 - 5.6	5.1 - 5.6	5.0 - 5.6	5.0 - 5.7	5.0 - 5.7	5.0 - 5.6
All Loaded Up	4.0 - 4.6	3.4 - 4.6	3.9 - 4.6	3.9 - 4.8	3.9 - 4.8	3.8 - 4.7
All Loaded Down	7.2 - 7.8	7.2 - 7.7	7.0 - 7.8	6.9 - 7.8	7.1 - 7.6	7.0 - 7.8

Table 9: 95% Confidence Intervals for the Regression Analyses Given in Tables 3-8, all Intervals are Calculated on Average Values.

	95% Prediction Interval for the Average Values					
Driving Condition	Five Factor	Four Factor	Two Factor Grade and Consistency Index	Two Factor, Grade and Moisture Condition Value	Two Factor, Grade and Vane Shear Strength	Single Factor
All Empty	7.7 - 12.0	7.7 - 12.0	7.4 - 12.4	7.5 - 12.1	7.6 - 12.1	7.1 - 12.7
All Empty Up	5.7 - 10.2	5.6 - 10.0	5.4 - 11.1	5.7 - 10.0	5.6 - 10.1	5.0 - 11.5
All Empty Down	8.4 - 13.2	8.4 - 13.1	8.1 - 13.3	8.3 - 13.3	8.4 - 13.2	7.9 - 13.4
All Loaded	3.6 - 7.1	3.3 - 7.4	3.1 - 7.5	2.7 - 8.0	2.7 - 7.9	2.7 - 7.9
All Loaded Up	2.5 - 6.1	2.0 - 6.6	2.0 - 6.6	1.4 - 7.3	1.4 - 7.3	1.4 - 7.2
All Loaded Down	6.5 - 8.5	6.5 - 8.4	5.6 - 9.2	5.5 - 9.2	6.2 - 8.5	5.6 - 9.3

Table 10: 95% Prediction Intervals for the Regression Analyses Given in Tables 3-8, all Intervals are Calculated on Average Values.

	Loaded Grade /%	Empty Grade / %	Consistency Index	Moisture Condition Value	Vane Shear / kN/m²	Rut Depth / mm
Cat D400D	-3.0	3.0	1.02	11.0	136	40
	-2.7	2.7	1.05	13.9	173	5
	-2.6	2.6	0.98	9.9	144	110
	0.2	-0.2	1.08	13.8	158	150
Volvo A35 (Fleet 1)	3.0	-3.0	0.91	14.1	157	150
	5.4	-5.4	1.02	14.0	160	100
Volvo A35 (Fleet 2)	-1.5	1.5	1.17	12.2	149	110
	3.5	-3.5	1.04	14.2	167	75
	5.4	-5.4	1.02	14.0	172	100

Table 11: Input Parameters for Vehicles not Included in the Regression Analysis

		Rolling Resistance / % Equivalent Grade		Velocity / km/h		95% Confidence Interval for Rolling Resistance / % Equivalent Grade	95% Prediction Interval for Rolling Resistance / % Equivalent Grade
		Predicted	Actual	Predicted	Actual		
Loaded	Cat D400D	7.8	7.7	24.4	24.9	7.4 - 8.2	6.8 - 8.8
		6.6	6.9	30.1	27.9	6.1 - 7.1	5.5 - 7.6
		7.1	7.0	26.0	26.6	6.7 - 7.6	6.1 - 8.2
		6.2	7.4	18.3	15.4	5.5 - 6.8	4.3 - 8.1
	Volvo A35 (Fleet 1)	5.6	4.3	14.1	16.6	4.9 - 6.4	3.7 - 7.5
		3.6	5.0	13.5	11.7	3.0 - 4.3	1.7 - 5.5
	Volvo A35 (Fleet 2)	6.2	5.5	25.8	30.3	5.6 - 6.7	5.1 - 7.3
		4.1	4.8	15.9	14.6	3.7 - 4.6	2.3 - 6.0
		3.7	3.8	13.3	13.2	3.1 - 4.4	1.8 - 5.7
Empty	Cat D400D	7.7	8.8	25.2	22.8	6.7 - 8.7	5.3 - 10.1
		7.7	9.1	25.9	22.8	6.5 - 8.9	5.2 - 10.1
		7.0	7.3	28.0	27.2	5.9 - 8.0	4.6 - 9.3
		9.9	9.6	27.7	28.6	8.8 - 10.9	7.3 - 12.4
	Volvo A35 (Fleet 1)	11.8	10.9	31.8	35.5	10.8 - 12.8	9.3 - 14.4
		13.0	13.9	36.9	33.0	11.9 - 14.0	10.4 - 15.5
	Volvo A35 (Fleet 2)	7.9	7.5	29.8	31.1	6.4 - 9.3	5.3 - 10.5
		11.5	11.1	35.0	36.9	10.8 - 12.2	9.0 - 13.9
		12.4	14.0	40.0	32.6	11.3 - 13.5	9.8 - 15.0

Table 12: Comparison of Actual Measured Rolling Resistance and Predicted Values from the Five Factor Regression Analysis.

		Velocity / km/h		Percentage Change in Velocity / %	Number of Different Vehicles in Calculating Average Travel Time	Number of Timings to Calculate Average Travel Time
		Predicted	Actual			
Loaded	Cat D400D	24.4	24.9	+2.0	3	5
		30.1	27.9	-7.3	3	5
		26.0	26.6	+2.3	4	12
		18.3	15.4	-15.2	2	2
	Volvo A35 (Fleet 1)	14.1	16.6	+17.7	1	1
		13.5	11.7	-13.3	2	5
	Volvo A35 (Fleet 2)	25.8	30.3	+17.4	1	2
		15.9	14.6	-8.2	1	2
		13.3	13.2	-0.8	1	4
Empty	Cat D400D	25.2	22.8	-9.5	3	4
		25.9	22.8	-12.0	4	5
		28.0	27.2	-2.9	4	10
		27.7	28.6	+3.2	1	2
	Volvo A35 (Fleet 1)	31.8	35.5	+11.6	2	4
		36.9	33.0	-10.6	2	4
	Volvo A35 (Fleet 2)	29.8	31.1	+4.3	1	2
		35.0	36.9	+5.4	1	3
		40.0	32.6	-18.5	1	2

Table 13: Percentage Change in Velocity, as a Function of the Predicted Velocity, the Number of Vehicles and Individual Timings to Calculate the Average Travel Time for the Vehicles used in the Regression Validation.

Appendix 2 Site Monitoring Procedure

On arrival on site the section of haul road that is to be monitored must be identified. This was done by watching the plant operating on the haul road until a section, of approximately 60m length of relatively constant gradient, was observed where the vehicles were considered to be travelling at a constant velocity.

Having identified the section the vehicles were timed between two markers. This was done utilising two people, one started timing when the nose of the vehicle passes the first marker and the other signalling when the nose of the vehicle passes the second marker. The vehicle type, identification number, and time were also noted for each passage.

The gradient and length of the section were measured using an electronic theodolite. Several points were taken along the length of the section, also prior to and after the section, to ensure that the gradient remained constant. The surveying data from the theodolite was downloaded into a simple spreadsheet which calculated the gradient from the eastings, northings, and heights of each portion of the section.

Once the vehicles had been timed and the section surveyed, soil samples were taken at 20m intervals along the section and in-situ tests were performed. In-situ soil tests on the clay haul roads were: cone penetrometer, and hand shear vane. These two tests were carried out at least four times at 20m intervals along the section to determine an average. The samples were taken back to the on site laboratory where moisture condition value, and moisture content were determined for each sample. These tests had to be completed soon after sampling in order that the in-situ values are recorded. The residue of the samples were taken back to Edinburgh where the remainder of the tests were completed: liquid and plastic limit determination, multi-stage triaxial testing, and cyclic loading.

The average velocity can calculated easily from a knowledge of the length of the section and the average time to pass through the section. From this the apparent rolling resistance can be back-analysed using the Accelerator software.

Rut depths were also recorded at 20m intervals along the section. This was completed by placing a straight edge across the rut and measuring down to the foot of the rut using a steel rule. This method of determining rut depth does not account for elastic recovery or lateral soil heave.

Appendix 3 Tabulated Results

The following tables tabulate the data for the A1/M1 contract. The moisture condition value, average velocity, hand shear vane, rut depth and grade were measured on site or in the site laboratory, whereas the liquid and plastic limits, and the back analysed rolling and total resistances were calculated at the University of Edinburgh. These data should allow all the graphs in Chapter 5 to be reproduced and theories developed further.

					Back Analysed Resistances											
					Rolling				Total							
Loaded		Plastic	Liquid		loaded		unloaded		loaded		unloaded		Measured	Measured Uncorrected	Average Velocity Loaded	Average Velocity Unloaded	Measured
Grade	Machine	Limit	Limit	Ic	accel	vsm	accel	vsm	accel	vsm	accel	vsm	Average MCV	Average Vanes	/km/h	/km/h	Average Rut / mm
-4.6	Cat D400(T)	50	22	1.01	7.7	8	-	-	3.1	3.4	-	-	16.1	140	38.4	-	200
-3.3	Cat D400(T)	53	23	0.96	9.8	10.3	7.8	9.1	6.5	7	11.1	12.4	10.8	82	18.3	24.5	100
-3.0	Cat D400(T)	56	26	1.02	7.6	8.5	8.3	9.5	4.6	5.5	11.3	12.5	11	110	25.4	24.3	40
-2.7	Cat D400(T)	50	19	1.05	6.7	7.8	6.8	8.3	4	5.1	9.5	11	13.9	140	28.3	28	5
-2.6	Cat D400(T)	58	22	0.98	6.5	7	6.3	7.6	3.9	4.4	8.9	10.2	9.9	116	30.2	30.4	110
-2.4	Cat D400(T)	45	20	1.15	7	7.8	9.7	8.6	4.6	5.4	12.1	11	18.1	140	26.5	28	50
-1.5	Cat D400(T)	57	23	1.17	6	6.9	7.6	9	4.5	5.4	9.1	10.5	12.2	120	26.4	29.9	110
0	Cat D400(T)	58	23	1.01	6.8	8	8.6	9	6.8	8	8.6	9	11.5	87	17.3	31.2	300
0.2	Cat D400 (T)	41	22	1.09	4.3	5.2	10.3	11.8	4.5	5.4	10.1	11.6	9.3	86	26.4	26.4	50
0.2	Cat D400(T)	51	20	1.08	6.6	7.8	10.6	12	6.8	8	10.4	11.8	13.8	128	17.6	26.4	150
0.4	Cat D400(T)	53	28	1.04	11.2	11.5	15	15.2	11.6	11.9	14.6	14.8	11.2	75	10.3	19.1	300
1.4	Cat D400 (T)	58	25	1.08	4.5	5.2	9.4	9.4	5.9	6.6	8	8	14.8	135	19.9	34	100
1.6	Cat D400(T)	40	21	1.15	4.5	5.1	11.7	13.3	6.1	6.7	10.1	11.7	15.2	140	19.3	26.5	5
1.7	Cat D400(T)	52	23	1.23	3.6	4.4	8.8	9.3	5.3	6.1	7.1	7.6	16.2	140	22.2	32.3	5
2.2	Cat D400(T)	52	24	1.2	5.4	6.9	9.7	9.8	7.6	9.1	7.5	7.6	13.7	137	15.3	35.5	100
2.3	Cat D400 (T)	54	23	1.23	4.6	6	10.4	10.4	6.9	8.3	8.1	8.1	12.5	137	16.6	33	100
2.3	Cat D400(T)	54	23	1.32	3.2	3.9	11.7	13.1	5.5	6.2	9.4	10.8	14.2	84	21.8	28.9	5
2.3	Cat D400(T)	56	25	1.23	4.5	5.8	11.1	12.3	6.6	7.1	8.8	10	15.2	140	18	30.9	5
2.6	Cat D400(T)	47	21	1.08	3.7	4.3	9.8	10.1	6.3	6.9	7.2	7.5	13	140	18.5	37.4	50
4.6	Cat D400(T)	50	22	1.07	4.9	5.9	-	-	9.5	10.5	-	-	16.1	140	12.2	-	200
-3	Cat D400(F)	56	26	1.02	7.9	8.8	7.8	9.3	4.9	5.8	10.8	12.3	11	110	24.1	25.1	40
-2.7	Cat D400(F)	50	19	1.05	7.1	8	9.1	9.1	4.4	5.3	11.8	11.8	13.9	140	26.7	26.8	5
-2.6	Cat D400(F)	58	22	0.98	7.2	8.2	7.1	8.7	4.6	5.6	9.7	11.3	9.9	116	26.3	28.2	110
-2.4	Cat D400(F)	45	20	1.15	6.6	7.1	7.4	8.8	4.2	4.7	9.8	11.2	18.1	140	29	28	50
-1.5	Cat D400(F)	57	23	1.17	6.4	7.3	8	9.8	4.9	5.8	9.5	11.3	12.2	120	24.2	28.3	110
0	Cat D400(F)	58	23	1.01	8.5	10	9.6	11.5	8.5	10	9.6	11.5	11.5	87	13.7	28.2	300
0.2	Cat D400(F)	51	20	1.08	6.9	8.3	10	11.6	7.1	8.5	9.8	11.4	13.8	128	16.2	27.5	150
0.4	Cat D400(F)	53	28	1.04	11.3	11.6	14.8	14.8	11.7	12	14.4	14.4	11.2	75	10.2	19.6	300
2.2	Cat D400(F)	52	24	1.2	5.6	7.2	9.9	9.9	7.8	9.4	7.7	7.7	13.7	137	14.9	34.7	100
2.3	Cat D400(F)	54	23	1.32	3.2	4	11.7	13.1	5.5	6.3	9.4	10.8	14.2	84	21.6	28.9	5
2.3	Cat D400(F)	54	23	1.23	4.5	5.8	11.1	12.3	6.8	8.1	8.8	10	15.2	140	17.7	30.9	5
-0.4	TS-24(G)	54	25	1.04	8.5	7.8	13.1	12.2	8.1	7.4	13.5	12.6	11.2	99	17.1	19.9	-
0.3	TS-24(G)	48	19	1.14	8.6	7.5	17.8	16.8	8.9	7.8	17.5	16.5	11.8	132	15.9	15.2	-
1.1	TS-24(G)	53	24	1.01	8	8	18.2	17.2	9.1	9.1	17.1	16.1	11.2	107	15.6	15.5	-
-2.4	Cat D400(J)	45	20	1.15	5.8	6	4.7	5.2	3.4	3.6	7.1	7.6	18.1	140	36	38	50
-3	Cat D400(M)	56	26	1.02	7.7	8.6	8.8	9.9	4.7	5.6	11.8	12.9	11	110	25	23.2	40
-2.7	Cat D400(M)	50	19	1.05	6.9	7.9	9.1	9.1	4.2	5.2	11.8	11.8	13.9	140	27.5	26.9	5
-2.6	Cat D400(M)	58	22	0.98	7	8	7.3	9	4.4	5.4	9.9	11.6	9.9	116	27.1	27.2	110

Loaded Grade	Machine	Plastic Limit	Liquid Limit	Ic	Back Analysed Resistances								Measured Average MCV	Measured Uncorrected Average Vanes	Average Velocity Loaded /km/h	Average Velocity Unloaded /km/h	Measured Average Rut / mm
					Rolling				Total								
					loaded		unloaded		loaded		unloaded						
					accel	vsm	accel	vsm	accel	vsm	accel	vsm					
0.2	Cat D400(M)	51	20	1.08	7.4	8.8	9.6	10.9	7.6	9	9.4	10.7	13.8	128	15.5	29	150
-0.4	TS-24(T)	54	25	1.04	9.5	9.3	15.8	13.6	9.1	8.9	16.2	14	11.2	99	15.1	16.1	-
0.3	TS-24(T)	48	19	1.14	8.8	8.8	17.1	16.1	9.1	9.1	16.8	15.8	11.8	132	15	15.9	-
1.1	TS-24(T)	53	24	1.01	8.3	8.2	17.2	15.7	9.4	9.3	16.1	14.6	11.2	107	14.8	16.2	-
-6.1	Volvo A25(T)	46	20	0.94	9.4	10.4	6.3	7.9	3.3	4.3	12.4	14	13.4	132	33.4	21.2	40
-3.6	Volvo A25(T)	42	17	0.99	6.6	8	6.1	7.5	3	4.4	9.7	11.1	13.3	139	36.7	27.3	5
3.5	Volvo A25(T)	41	21	1.035	3.6	4.5	11	12.6	7.1	8	7.5	9.1	14.2	135	13.5	35	40
4.1	Volvo A25(T)	44	21	1.03	2.3	3.1	13.2	14.3	6.4	7.2	9.1	10.2	10.3	88	17.5	28.2	25
4.1	Volvo A25(T)	44	21	1.04	2.1	2.9	11.8	13.5	6.2	7	7.7	9.4	10.3	104	18	33.8	5
5.4	Volvo A25(T)	45	18	1.02	4.2	5	12.5	14.3	9.6	10.4	7.1	8.9	14	129	11.8	36.7	100
1.8	Volvo A25(B)	-	-	-	1.3	2.3	8.3	9.6	3.1	4.1	6.5	7.8	-	-	36.1	40.7	-
3.1	Volvo A25(B)	-	-	-	1.9	2.9	9.6	10.9	5	6	6.5	7.8	-	-	22.4	40.5	-
1.4	Volvo A25(B)	-	-	-	2.1	3.1	6.7	5.5	3.5	4.5	5.3	4.1	-	-	32.9	49.1	-
-0.7	Volvo A25(B)	44	21	0.77	7.3	8.3	13.3	14.7	6.6	7.6	14	15.4	-	-	17	18.7	-
0.8	Volvo A25(B)	40	23	1.56	3.1	4.1	6.1	4.8	3.9	4.9	5.3	4	-	140	28.8	37.9	-
-1.2	Volvo A25(B)	-	-	-	4.1	5	6	7.8	2.9	3.8	7.2	9	-	-	38.9	36.1	-
-1.3	Volvo A25(B)	-	-	-	7.2	8.3	5.1	6.2	5.9	7	6.4	7.5	-	-	40.3	41.3	-
2.6	Volvo A25(B)	-	-	-	2	2.9	8.8	10	4.6	5.5	6.2	7.4	-	-	24.4	42.3	-
-0.7	Volvo A25(B)	44	21	0.76	5.3	6.1	10.9	12.1	4.6	5.4	11.6	12.8	-	116	24.6	22.4	-
2.2	Volvo A25(B)	-	-	-	2.6	3.6	7.9	8.1	4.8	5.8	5.7	5.9	-	-	23.5	46	-
-3.6	Volvo A30(B)	38	15	0.99	7.9	9	-	-	4.3	5.4	-	-	14.3	139	24.9	-	150
-3	Volvo A30(B)	45	20	0.91	8.6	9	-	-	5.6	6	-	-	14.1	110	20	-	150
0.2	Volvo A30(B)	41	22	1.09	3.7	4.8	9.7	11.2	3.9	5	9.5	11	9.3	86	26.2	25.9	50
1.4	Volvo A30(B)	58	25	1.08	4.2	5	8.9	10.3	5.6	6.4	7.5	8.9	14.8	135	19.1	33	100
2.2	Volvo A30(B)	52	24	1.2	3.8	5	11.4	12.8	6	7.2	9.2	10.6	13.7	137	17.3	27	100
2.3	Volvo A30(B)	54	23	1.32	1.2	2	10.1	11.5	3.5	4.3	7.8	9.2	14.2	84	30.8	31.5	5
2.3	Volvo A30(B)	54	23	1.23	2.9	3.7	-	-	5.2	6	-	-	15.2	140	20.6	-	5
2.3	Volvo A30(B)	56	25	1.23	4	5	8.8	9.9	6.3	7.3	6.5	7.6	12.5	137	17	37.2	100
3	Volvo A30(B)	45	20	0.91	4.1	5	13.5	14.9	7.1	8	10.5	11.9	14.1	127	15.3	24	150
3.5	Volvo A30(B)	41	21	1.035	5.4	7.1	9.9	11	8.9	10.6	6.4	7.5	14.2	135	12	37.8	75
3.6	Volvo A30(B)	38	15	0.99	5.8	7.8	-	-	9.4	11.4	-	-	14.3	140	12.8	-	150
4.6	Volvo A30(B)	50	22	1.07	5	7	-	-	9.6	11.6	-	-	16.1	140	12.5	-	200
5.4	Volvo A30(B)	45	18	1.02	4.6	6.8	12.8	14.1	10	12.2	7.4	8.7	14	129	10.3	33.4	100
-4.6	Volvo A35(H)	50	22	1.01	10.1	11.4	-	-	5.5	6.8	-	-	16.1	140	20	-	200
-3.6	Volvo A35(H)	38	15	0.99	7.8	8.9	-	-	4.2	5.3	-	-	14.3	139	26	-	150
-3	Volvo A35(H)	45	20	0.91	8.2	9.2	-	-	5.2	6.2	-	-	14.1	110	19.3	-	150

					Back Analysed Resistances											
					Rolling				Total							
Loaded		Plastic	Liquid		loaded		unloaded		loaded		unloaded		Measured	Uncorrected	Average Velocity	Average Velocity	Measured
Grade	Machine	Limit	Limit	Ic	accel	vsm	accel	vsm	accel	vsm	accel	vsm	Average MCV	Average Vanes	Loaded /km/h	Unloaded /km/h	Average Rut / mm
3	Volvo A35(H)	45	20	0.91	4.3	6.3	10.9	13	7.3	9.3	7.9	10	14.1	127	15.2	31.3	150
3.6	Volvo A35(H)	38	15	0.99	4.8	6.9	-	-	8.4	10.5	-	-	14.3	140	13	-	150
4.6	Volvo A35(H)	50	22	1.07	4.8	6.9	-	-	9.4	11.5	-	-	16.1	140	11.9	-	200
5.4	Volvo A35(H)	45	18	1.02	5	7.1	13.9	15.9	10.4	12.5	8.5	10.5	14	129	10.4	29.9	100
-3.6	Volvo A35(K)	38	15	0.99	7.9	9	-	-	4.3	5.4	-	-	14.3	139	25.3	-	150
-3	Volvo A35(K)	45	20	0.91	8.7	10.2	-	-	5.7	7.2	-	-	14.1	110	19.3	-	150
1.7	Volvo A35(K)	52	23	1.23	3	4	9.8	12.4	4.7	5.7	8.1	10.7	16.2	140	23.2	28.5	5
2.2	Volvo A35(K)	52	24	1.2	4.7	6.6	9	10.6	6.9	8.8	6.8	8.4	13.7	137	15.9	36.4	100
2.3	Volvo A35(K)	54	23	1.32	1.7	2.9	11.7	13.5	4	5.2	9.4	11.2	14.2	84	27	27	5
2.3	Volvo A35(K)	54	23	1.23	3.4	4.8	10.2	12.3	5.7	7.1	7.9	10	15.2	140	19.5	31.3	5
2.6	Volvo A35(K)	47	21	1.08	3.3	4.9	9.6	11.1	5.9	7.5	7	8.5	13	140	18.6	35.4	50
3	Volvo A35(K)	45	20	0.91	7	9	14.2	15.8	10	12	11.2	12.8	14.1	127	11	22.4	150
3.6	Volvo A35(K)	38	15	0.99	4.1	6.3	-	-	7.7	9.9	-	-	14.3	140	14.2	-	150
4.6	Volvo A35(K)	50	22	1.07	3.9	5.5	-	-	8.5	10.1	-	-	16.1	140	12.8	-	200
5.4	Volvo A35(K)	45	18	1.02	4	6	13	14.8	9.4	11.4	7.6	9.4	14	129	11.5	33.4	100
-1.5	Volvo A35(T)	57	23	1.17	5.5	6.8	7.5	9.5	4	5.3	9	11	12.2	120	26.4	28	110
3.5	Volvo A35(T)	41	21	1.035	4.8	6.8	11.1	13	8.3	10.3	7.6	9.5	14.2	135	13.1	32.6	75
5.4	Volvo A35(T)	45	18	1.02	3.8	5.8	14	16	9.2	11.2	8.6	10.6	14	129	12.2	28.9	100
-4.6	Volvo A35(P)	50	22	1.01	10.9	12.6	-	-	6.3	8	-	-	16.1	140	17.6	-	200
-3.6	Volvo A35(P)	38	15	0.99	8.3	9.3	-	-	4.7	5.7	-	-	14.3	139	23.7	-	150
-3	Volvo A35(P)	45	20	0.91	7.5	8.6	-	-	4.5	5.6	-	-	14.1	110	24.6	-	150
3	Volvo A35(P)	45	20	0.91	4.6	6.6	-	-	7.6	9.6	-	-	14.1	127	14.5	-	150
3.6	Volvo A35(P)	38	15	0.99	5.2	7.2	-	-	8.8	10.8	-	-	14.3	140	12.7	-	150
4.6	Volvo A35(P)	50	22	1.07	3.8	5.4	-	-	8.4	10	-	-	16.1	140	13	-	200